The evolution of the Sacramento River during the Late Quaternary and the influence of an “inherited” topography on modern floodplain sedimentation rates

Submitted by **Mathias Will** to the University of Exeter

as a thesis for the degree of

Doctor of Philosophy in Geography

in September 2015

I certify that all material in this thesis which is not my own work has been identified and that no material has previously been submitted and approved for the award of a degree by this or any other University.

Abstract

This study investigates the evolution of the Sacramento River since the late Quaternary, and the influence of this “inherited” topography on last century’s floodplain deposition by analysing and dating fluvial deposits at one of the key sites in the Sacramento River flood network. This thesis investigates older deposits and also modern (last-century) depositional history as means of interpretation.

Take home message 1: This study provides an extensive time constraint on Late Quaternary fluvial sediments in the Western US. It indicates a link between Late Quaternary climate instability and fluvial deposition and erosion in the research area. The main periods of deposition are around 77 ± 25 ka, between 33 and 22 ka, and after 6 ka, with a period of surface stability on indicated by the development of a soil between 22 and 6 ka Llano Seco Terrace. The floodplain channels are of Holocene age and origin, potentially the result of an incomplete avulsion.During the period around ~ 75 ± 25 ka, the progradation of the Stony Creek fan system towards the centre of the valley (represented by vast gravel deposits of Coast Range origin), relocated the Sacramento River to the ~ 4 – 6 km east of its current position. Between ~ 33 ka and ~ 22 ka, shallow (1 – 2 m) fluvial sands were deposited covering large parts of the floodplain. After 22 ka soil development suggests a stable surface in the eastern part of the research area. This indicates the existence of an incised Sacramento River around the Last Glacial Maximum in the vicinity of the recent channel. In the early Holocene a meandering system is established, covering the soil of the Llano Seco terrace with fine-grained overbank deposits. Different meander generations have been dated, because a westward movement of the Sacramento River has been observed. The oldest (easternmost) dated meander dates to 2.4 ± 0.1 cal PB. At least 2 older generations of meanders are topographically visible that have not been dated. The prominent ephemeral floodplain channel systems in the research area have developed almost exclusively in sediments of Holocene age and origin. They are therefore interpreted as the product of a Holocene avulsion that remains incomplete, because the Sacramento River is not able to incise in the underlying gravel deposits.

Take home message 2: XS ^{210}Pb profile analysis used tool to investigate the influence of sedimentation and land use on XS ^{210}Pb activity profiles, withthe CIRCAUS/CNAXS dating technique further enhanced for anthropogenically influenced landscapes.

Take home message 3: Using high-resolution XS ^{210}Pb analysis it was possible to reconstruct sedimentation rates, sometimes frequency of deposition, as well as identify the influence of land-use on XS ^{210}Pb profile development. Results showed that the floodplain channels along the Sacramento River are an excellent conveyor of sediments and are able to disperse ~ 33 % of the average annual suspended sediment load over longer timeframes (50% of each biannual flood) to the distal parts of the floodplain. The main controlling factor for sediment deposition in the research area is the distance from the main river channel. But a total of 60 % of the suspended sediment load is transported more than 500 m away from the main stem Sacramento River and removed from areas that are frequently reworked.

Acknowledgements

Many people have supported me in my quest to complete this thesis in the past years, by providing scientific, laboratory, and field support. First I want to thank my supervisors Rolf Aalto, Richard Jones, Chris Turney, and the Department / School of Geography / College of Life (or whatever else it was called during my time of study at the University of Exeter for the opportunity to investigate the late Quaternary history of the Sacramento River. I am grateful for the opportunity and the support presented by the faculty.

I owe huge thanks to Markus Fuchs (JLU Giessen) and the University of Bayreuth, who provided the resources for OSL dating. I want to thank Markus not only for his scientific support, but also for his open door policy and his general supportiveness that got me through a couple of rough spots.

I want to thank the laboratory staff at the University of Exeter, especially Diane Fraser, Jim Grapes and Sue Franklin for their patients with my continuous streak of questions and request. I also have to thank Manfred Fischer from the luminescence laboratory in Bayreuth for the same patients and for creating time slots in an already overflowing luminescence detector schedule. Thanks also to the countless other lab minions in Exeter and Bayreuth that were in one way or the other involved in helping me to cope with my workload.

I could not have done the fieldwork without the support of the management and workers of Rancho Llano Seco, so thank you. Special thanks goes to Shannon Samuelson for his ground breaking work with the excavator that created the nice and shady profile pits that were not only the basis for my stratigraphic work, but also provided highly appreciated shadow in the Californian summer heat. His wealth of knowledge on the recent history of the area was priceless and helped me in avoiding some (scientific) pitfalls. I have to thank Joe Silveira for his help in kind of everything I did out there in California, and of cause for sharing his recipe for the (in)famous Frogwater Blitz. I am also indebted to all the people from the Nature Conservancy and the Soil Office in Chico, for providing a roof over my head during the field seasons, and for sharing their knowledge on locals soils.

My time in Exeter has been enriched by so many academics, fellow postgraduates, and friends that it is hard to single out individual people. Of the many people I've met along the way, I want to mention and thank the few who had to deal with my continuous moaning and complaints during the not-so-good times, and for all the good time that we've wasted having good times. So thanks to Jordan, Julia, and Sabine for their friendship, patience, and encouragements. I also want to thank (in no particular order) Agathe, Bruno, Emilie, Hannah, Jalal, John, Joy, Laura, Michael, Olafur, Rebecca, Stephanie, Steve, Suzanne, Tom, and so many others that have also enriched my time in Exeter, and still enrich my life after, throughtheir general kindness, support, and friendship.

Last, but most importantly I want to thank my parents, and my family for their continuous love and support.

Table of Contents

List of Figures

List of Tables

List of Abbreviations

^{14}C	Radiocarbon
^{210}Pb	Lead 210 (Dating)
^{210}Po	Polonium 210
a.s.l.	above sea level
BP	Radiocarbon years before present
cal BP	Calibrated radiocarbon years before 1950
CICCS	Constant Initial Concentration Constant Sedimentation (^{210}Pb)
CIRCA	Constant Initial Reach Clay Activity (^{210}Pb)
CIRCACS	Constant Initial Reach Clay Activity Constant Sedimentation (^{210}Pb)
CIRCAUS	Constant Initial Reach Clay Activity Unknown Sedimentation (^{210}Pb)
CNAXS	Clay-Normalized Adsorbed Excess (^{210}Pb)
conc	Concentrated (Acid)
GISP	Greenland Ice Sheet Project
HCl	Hydrochloric Acid
ka	10^3 years
HNO_3	Nitric Acid
LGM	Last Glacial Maximum
N	Normality (of a solution)
North-GRIP	North Greenland Ice Core Project
ODP	Ocean Drilling Programme
OSL	Optically Stimulated Luminescence
SPECMAP	Mapping Spectral Variability in Global Climate Project
SST	Sea Surface Temperature
U-Th	Uranium-Thorium Dating
XS ^{210}Pb	Excess (unsupported) ^{210}Pb (not derived from natural fallout)

1. INTRODUCTION

The project site was chosen because Sacramento River floodplains in most of the research area have experienced limited alterations of its topographical features – while not pristine, it is one of the few areas in the developed Central Valley where the surface structure of the floodplain is largely unchanged since its first "discovery" by European Americans. This relative lack of floodplain alterations preserved a largely undisturbed topography that can provide insight into the Late Quaternary evolution of the Sacramento River, as well as add to the knowledge of depositional behaviour of floodplains along large rivers. For the research of past and present floodplain development, the vicinity of Rancho Llano Seco (River Mile[1] (RM)174 – RM184) is particularly interesting. It contains the least disturbed part of a network of large ephemeral (palaeo? / floodplain) channels (Olmsted & Davis 1961; Helley & Harwood 1985; Robertson 1987; Dunne & Aalto 2013) preserved in an active floodplain in California.

The Sacramento River and its floodplain channel system also provide the opportunity to investigate the influence of an "inherited" topography on modern fluvial deposition and erosion along a large Mediterranean river system. The questions this thesis tries to answer in this landscape are: 1) How did this landscape evolve in response to the climate alterations during the Late Quaternary? (including: How and when did the floodplain channel systems in the research area evolve?) 2) Is CIRCAUS/CNAXS ^{210}Pb dating a suitable tool to investigate floodplain deposition in agriculturally impacted landscapes? 3) What is role of these 'active palaeo'-channel networks in regards modern sediment dispersal?

Due to its proximity, the Stony Creek megafan, fan deposits are likely to have influenced the evolution of the research area as well. Earlier extension of the Stony Creek and other coast range fans across the Sacramento Valley have

[1] The River Mile classification of the Sacramento River specifies the distance along the course of the river from the mouth of the Sacramento River at Collinsville (confluence with the San Joaquin River in the vicinity of the San Francisco Bay Estuary = RM0). This classification has been established by the US Army Corps of Engineers by 1964, and does not denote distance along the river center line anymore, but River Miles are used as place names along the Sacramento River (e.g. Larson & Greco 2002; Larson et al. 2006b).

been reported during the Pliocene (Olmsted & Davis 1961; Helley & Harwood 1985). And at least 5 separate fluvial terraces are recorded for the Pleistocene Stony Creek and its fan system (Steele 1980). Also, it has been argued by Meyer & Rosenthal (2008) that the Stony Creek fan extended to the east of Llano Seco during the late Quaternary. But even though the general setup of the geologic formations in the Northern Sacramento River Valley is known, little is known of the environmental conditions these sediments have been deposited under. One of the reasons for this lack of knowledge is the lack of numeric dating evidence of the Quaternary stratigraphy in California that would link these stratigraphic units to records of environmental conditions.

Not only the timing and origin of the stratigraphic units are lacking proper chronologic control, also the timing of the evolution of many of the topographic features is still unknown. The most prominent example of topographic floodplain features In the Sacramento Valley are the Sacramento River floodplain channel systems. Their evolution has been discussed and classified controversially (Olmsted & Davis 1961; Helley & Harwood 1985; Robertson 1987; Dunne & Aalto 2013), but timing and processes involved in their development still remain unclear. The floodplain channels systems of the Sacramento River have been investigated employing aerial photography and the cross correlation of soil profiles (Robertson 1987). Robertson (1987) interpreted the channel features of the Sacramento River floodplain as anastomosing and braiding stages of the Sacramento River during the Quaternary and therefore as relic Pleistocene landforms. The floodplain and floodplain channel units were roughly estimated as dating to ~ 260 ka, with the age constrained between 140 ka and 450 ka using cross correlation of soils (Robertson 1987), linking them stratigraphically to the Riverbank formation. Robertson (1987) does not interpret the floodplain channel features as directly connected to climate driven fluvial change, but argues that unstable environmental conditions due to either tectonic, volcanic or glacial conditions are responsible for the development of the floodplain channel features. This contradicted prior age estimates, which proposed that all the floodplain channel complexes of this region are of Holocene age (Olmsted & Davis 1961; Helley & Harwood 1985). Dunne & Aalto (2013) recently linked the change in fluvial style to changes in runoff and sediment supply at the end of the last glacial period. While Robertson's (1987) and Dunne & Aalto's (2013) interpretation would imply that the ephemeral floodplain channel systems are

long-term stable landscape features and thus are not receiving significant amounts of sediment from the main stem Sacramento River, even though they are the main conveyors of flood runoff to Butte Sink, while the interpretations by Olmsted & Davis (1961) and Helley & Harwood (1985) would imply that the floodplain channels are active Holocene landscape elements.

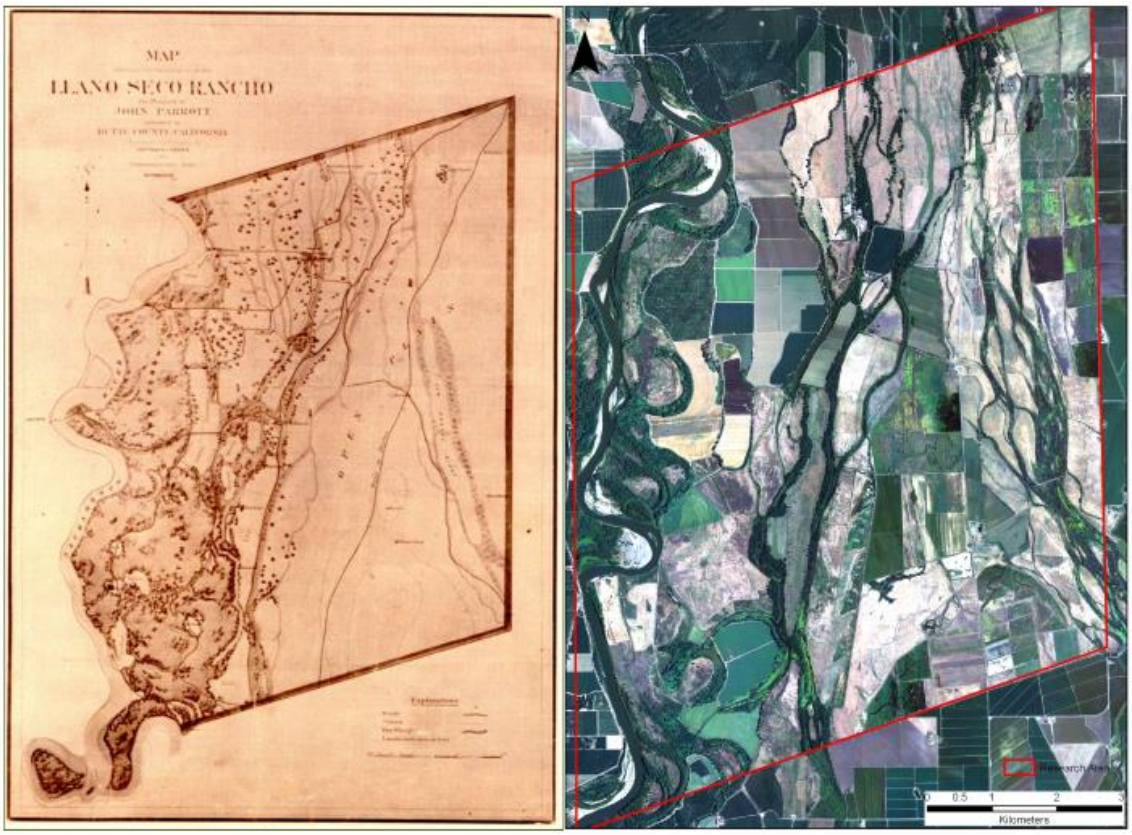

Figure 1 First detailed map of the Sacramento River floodplain channel systems at Rancho Llano Seco (left) produced by John Parrott (1874, reprint from Jostes 1972), showing the presence of floodplain channels that are still present in today's topography (right) indicating that alterations to the surface topography has been limited since the arrival of European Americans. Even though land cover has been influenced by human activity (reprint from Jostes 1972).

The main regional focus in this study is on the least disturbed floodplains within Rancho Llano Seco (Figure 1, RM175 – RM184), a ~ 80 km^2 tract that is one of the last Spanish Land Grants in California remaining as a whole. The premise was originally granted to Sebastian Keyser in 1845, acquired by John Parrott between 1860 and 1875, and owned by a single family since (CVJV 2013).

The research area shows an unique setup regarding the contemporary use of its (relic) fluvial features (Robertson 1987). While elsewhere anastomosing or braided channels are inactive, buried or preserved as terrace deposits and are remnants of past fluvial activity, the floodplain channels observed along the Sacramento River are active during floods and play an

important role in its present day flood conveyance. The limited floodplain alterations preserved a largely undisturbed topography that can provide insight into the depositional behaviour of distal floodplains along large rivers.

This fact necessitates the rather holistic approach of this thesis, covering the long-term evolution of the system, as well as its recent evolution. A short introduction into the relevant research will be given to produce an overview over the field of study. The two major fields of research that need to be facilitated in this study are 1) the evolution of (large) river systems during the late Quaternary reconstructed from stratigraphic records, and 2) the modern fluvial deposition and erosion on the floodplain.

In palaeo-environmental studies it has been argued that changes in climate often have major impacts on fluvial dynamics. Especially major climate changes – e.g. changes from full glacial to post glacial conditions - are often associated with valley incision and changes in fluvial style, and planform patterns (e.g. Blum & Valastro 1994; Knox 1995; Vandenberghe 1995; Huisink 1997; Huijzer & Vandenberghe 1998; Tebbens et al. 1999; Blum & Törnqvist 2000; Huisink 2000; Houben 2003; Jain & Tandon 2003; Kasse et al. 2005; Rittenour et al. 2005; Blum & Aslan 2006; Leigh 2006; Houben 2007; Rittenour et al. 2007; Garvin 2008; Kesel 2008; Leigh 2008; Vandenberghe 2008; Blum et al. 2013), often leading to the development of terrace staircases over several glacial/interglacial cycles (e.g. Penck and Brückner 1909; Anders et al. 2005; Boenigk & Frechen 2006; Bridgland & Westaway 2008). However, there is a large variety in the style and timing of river response to environmental signals (Vandenberghe 2003). The changes in climate at the transition between glacial and interglacial periods are often marked by changes in fluvial planform, leaving stratigraphic evidence of these changes. Bridgland & Westaway (2008) proposed a conceptual model for evolving terrace staircases for different incision scenarios at the transitions between warm-cold cycles. This model illustrates the individual stratigraphic records for evolving terraces that enable to reconstruct past fluvial change from stratigraphic records. Notwithstanding the insight that not one, but a variety of climate related factors are driving fluvial history, but also tectonic and base level changes are known to play a major role in fluvial dynamics (Blum & Törnqvist 2000; Vandenberghe 2003).

Changes in river hydrology are triggered by climate and environmental changes, tectonic movements, or base level changes. Several attempts have been made to quantify driving factors that cause the formation of different river channel planforms. Leopold and Wolman 1957 emphasised slope (s) and (bankfull) discharge (Q_{bf}) as influencing factors on channel pattern ($s=0.012Q_{bf}^{-0.44}$). Instead of focusing on bankfull discharge Lane 1957 used slope (s) and mean annual discharge (Q) to establish thresholds for braiding and meandering in sand bed rivers (Braiding Threshold: $s = 0.0007Q^{-0.25}$, Meandering Threshold: $s = 0.004Q^{-0.25}$). In addition to mean annual discharge and slope, Henderson 1963 introduced median grain size d_{50} as an important factor for the threshold between braiding and meandering ($s = 0.0002d_{50}^{1.15}Q^{-0.44}$). Schumm 1981 grouped channel types by the characteristic calibre of its sediment load. Knighton & Nanson's (1993) continuum concept acknowledges the slope and discharge relations as well established, but argued that sharp thresholds should be replaced by gradual transitions. According to Knighton and Nanson's (1993) continuum concept, channel patterns depend on hydraulic factors (flow strength), bank erodibility, and relative sediment availability. This concept is using an ordinal scale (Low – Medium – High) to describe the influencing factors on channel pattern. Church (2006) argues that the governing processes in the development of a fluvial planform are sediment supply, sediment calibre, channel gradient, and channel stability, all modulated by the scale of the channel (Church 2006). Arguing on basis of rather conceptual models (e. g. Knighton & Nanson 1993; Church 2006) seems to be more suitable for arguments concerning the long term reconstruction of planform dynamics, because of the uncertainties in the reconstruction of environmental factors (e.g. climate change, slope development, tectonic), and its subsequent influences on the regional and local hydrology.

Of special interest to this study are the prominent ephemeral floodplain channel systems that originate north of Chico / Hamilton City (~ RM210, Figure 2), but become more prominent downstream of River Mile 195. These features are located between 2 and 10 km east of the Sacramento River, parallel to its modern meander belt, and terminate in the backswamps of Butte Sink (Figure 2). These floodplain channels are largely ephemeral (with the exception of the channel of Little Chico Creek) and only active during floods, and play an

important role in the Sacramento River flood web. Existing hypotheses on the origin of these channels have been described above.

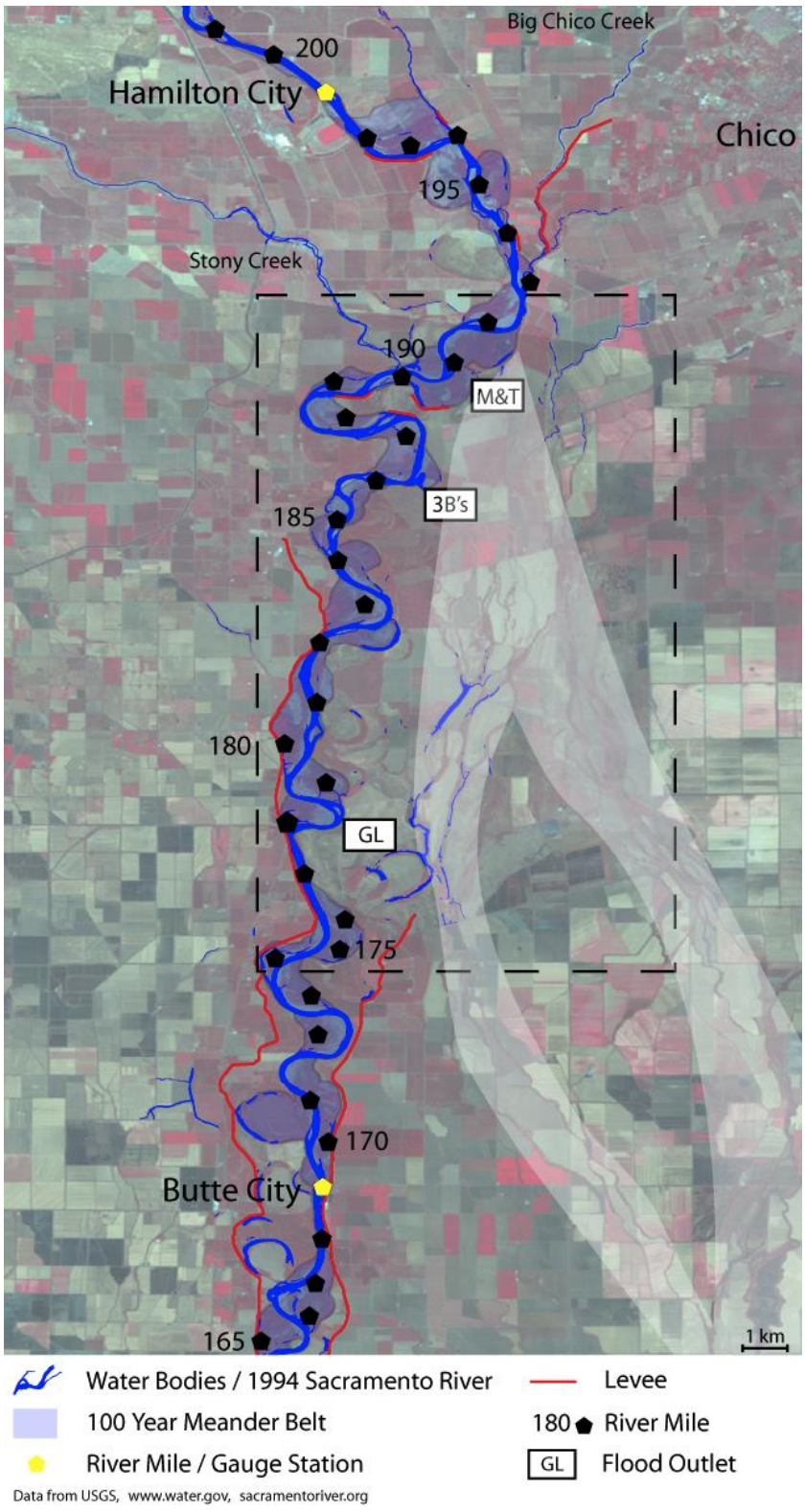

Figure 2 Location of the research area within the adjacent flood web, including the 100 year meander belt, the artificial levees of the Sacramento River flood protection system, and the natural and artificial flood outlets in the research area. Also shown are the gauge stations at Butte City and Hamilton City. The the floodplain channel systems are outlined in white.

This thesis aims to reconstruct the evolution of the Sacramento River and its floodplains / floodplain channels during the late Quaternary since ~ 50 ka on a short reach between River Mile 174 and 194 (including the premise of

Rancho Llano Seco), and a width of the modern floodplain of ~ 10 km, in response to late Quaternary climate and environmental change.

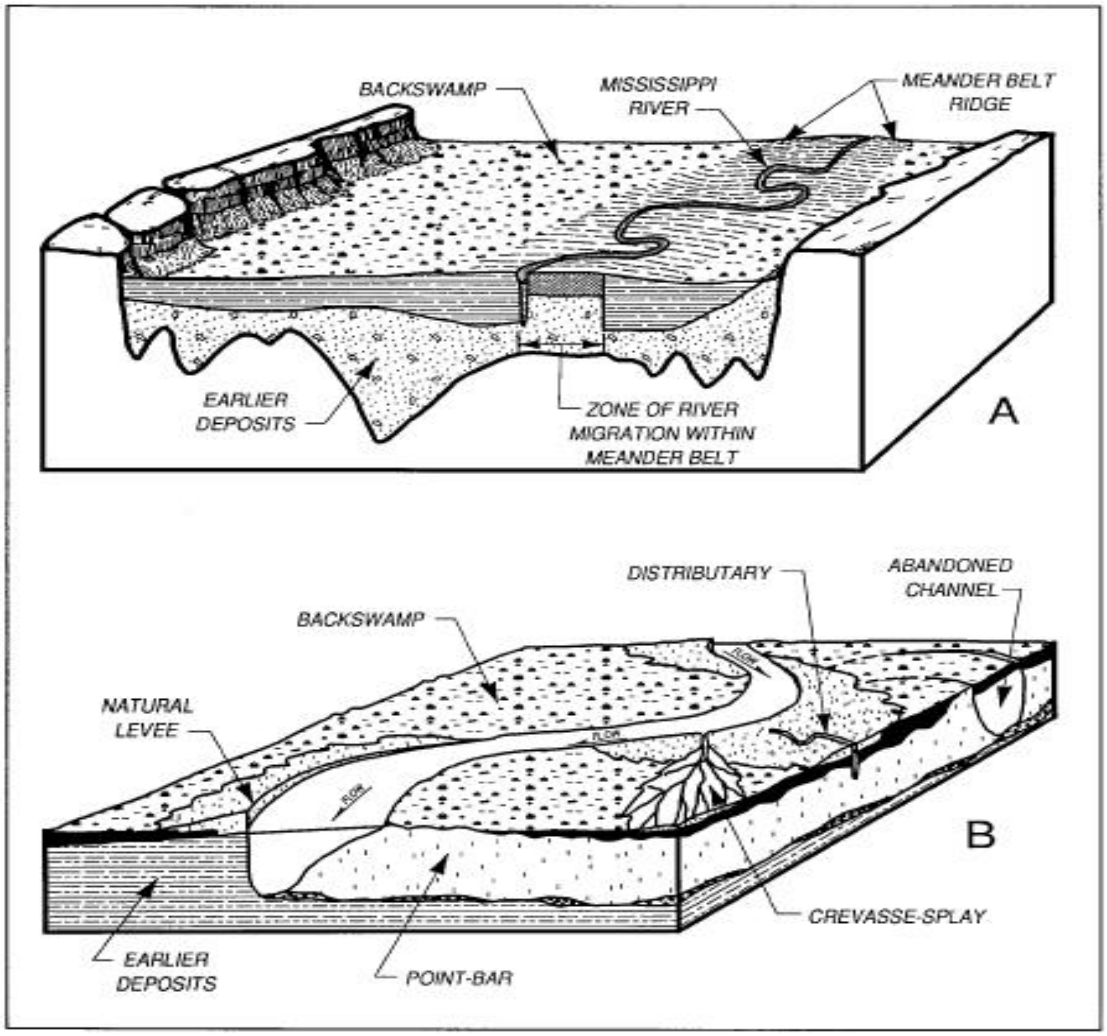

Figure 3 The Mississippi floodplains with its depositional environments including the migrating river bars, natural levees (as proximal elements) and backswamps (as distal element). Adapted from Saucier (1994).

But not only the long-term evolution represented by the stratigraphic units in deep profiles, but also the distribution of deposition and erosion of sediment during the last century in this landscape are focus of this thesis. The floodplain channels of the Sacramento River provide the link between long term evolution and modern sedimentation. This thesis aims to understand how those ephemeral channels have been formed, and how these features influence modern day sedimentation and erosion. The Sacramento River floodplain channels are likely to act as major conveyors of overbank discharge during floods, and are therefore likely to show some degree of fluvial activity. The questions that this thesis tries to answer in respect to modern day sedeimentation are, 1) how does this heterogeneous floodplain function in comparison with other (large) river floodplains in different environments and 2)

what are the driving factors for floodplain deposition and erosion reconstructed from XS ^{210}Pb activity profiles?

Floodplains of meandering rivers are constructed by lateral migration of the channel and by the dispersal of suspended material across the floodplain (summarised by e.g., Dunne & Aalto 2013). These floodplains – at least the ones along large meandering rivers - show several different topographic units that show different sedimentation processes and tendencies. Following Saucier (1994) large meandering river floodplains can be differentiated in: 1) The channel with its bars constructed by the lateral migration of the channel. 2) Natural levees formed by sediment deposited immediately after floodwater leaves the channel during floods. 3) Crevasse splay deposits that are transporting even coarser (sandy) material over large distances away from the main stem. 4) Distal floodplains with backswamps and lakes that are receiving few and fine grained sediment during floods. Additional (smaller) units that exist are e.g. abandoned channels, and units that connect the distal parts of a floodplain with the more proximal areas (e.g., Saucier 1994, Figure 3).

Sedimentation rates are generally higher at the channel edge decreasing with distance from the channel building the topographic ridges of the natural levees over time. The deposition of (suspended) sediment is initiated immediately after the sediment-laden water leaves the channel. Hereby flow depth decreases and the surface roughness increases by vegetation, therefore a decrease in flow velocity leads to a reduced transport capacity of the floodwater as the shear velocity of the flow drops below the settling velocity of the transported particles (summarised e.g. in Julien 2010). In the process of the construction of natural levees an average of 85 % of the total sediment entering the floodplain along the Amazon River is deposited (Mertes 1994). Especially coarser components like sand drop out early creating the natural levees that show a steep increase in relative elevation near the channel slowly decreasing in height away from the channel (e.g., summarized in Dunne & Aalto 2013). Walling & He (1998) observed deposition along 5 rivers in the UK and showed a slow and variable decline of sedimentation rates from the river channels along all researched rivers, constructing natural levees. Further from the main channel Walling & He (1998) point out the importance of depressions in the floodplain for sediment accumulation in these smaller floodplains. Along two tributaries of

the River Rhine, Thonon et al. (2007) observed an exponential decrease in deposition rates with distance from the main channel, creating natural levees along reaches without artificial flood protection. Thonon et al. (2007) argued that along theses reaches, secondary channels play a major part in the transport and dispersal of sediment away from the main channel. These smaller channels are sometimes more important for sediment delivery to a site than the main channel. Additionally to the importance of different order channels, Thonon et al. (2007) showed that sedimentation is highly dependent on the floodplain topography and inundation patters during floods at certain reaches of the River Waal and Ijsel River. But areas close to the main river are not just sediment sink preventing sediment from entering the distal part of a floodplain, but also source for sediment by scouring of the surface. Sediment scours occur where channel banks turn away from the downstream flow path, and the surface water is super-elevated. At these locations the flow is leaving the channel following its original direction and is creating a zone of high sheer stress on the floodplain surface. Scours occur at these locations if undergrowth is missing, creating chute cut-offs along the Sacramento River (Constantine et al. 2010). The same process can lead to scours that provide sediment for further dispersal to the distal parts of the floodplain. Processes like levee formation and scouring occur proximal to the main channel. During floods, areas more than 1 – 2 km away from the main channel generally receive little sediment by overbank flow, because low water pressure and vegetation leading to the deposition of most the suspended sediment before reaching the distal part of the floodplain. These distal parts of floodplains are often long term existing features in large river floodplains. Their topographic position is often lower than the present river, and swamps and lakes are common features. Their sediments commonly consists of fine clays or peats indicating low deposition rates with potential layers of sand transported by floodplain channels and as a result of large scale crevasse splays (Dunne & Aalto 2013). Nevertheless, along large tropical floodplains at the Strickland River (Papua New Guinea) - Swanson et al. (2008) observed highly variable deposition rates decreasing with distance from the channel, but also showed that sediment is transported from the main stem to the distal part of the floodplain.

Comparing this result with other studies, Swanson et al. (2008) found similar trends in deposition rates along the Brahmaputra-Jamuna River (Allison

et al. 1998) and the Beni River in Bolivia (Aalto et al. 2003), but not so much at the Fly River (Papua New Guinea) that is showing a rapid decrease in sedimentation rates after the flood water leaves the channels (Day et al. 2008). This rapid decrease in deposition rates seems to be an exception and a slower decrease in deposition rates seems to be present at most of the above described sites, indicating that the transport of sediment to more distant parts of floodplains by overland flow is a common process along large river systems.

Of great importance to fluvial transport processes in floodplain settings seems to be the pre-existing topography of a floodplain – in the case of the research area the floodplain channel systems - as the blueprint for the modern fluvial processes and the dispersal of sediment over a floodplain. For large river floodplains in the lower Pánuco basin (Mexico), Hudson & Colditz (2003) showed that an increase in the complexity of the floodplain topography results in an increase in the complexity of the inundation patterns and subsequently the sediment dispersal during floods. The importance of the floodplain topography for sediment dispersal was also observed along several other rivers in different environments (e.g., Walling & He 1998; Thonon et al. 2007; Day et al. 2008). As pointed out by Thonon et al. (2007) and Day et al. (2008), floodplain channels are an important factor for the sediment transport to more distal parts of a floodplain. Day et al. (2008) found that channels are the major conveyor of sediments to distal floodplain locations on tropical floodplains in aggregating lowland basins in Papua New Guinea. Day et al. (2008) observed an exponential relationship, between the distance from the (floodplain) channel and the deposition rate. This observed trend was independent of the order of the channel. For the Fly River, the transport away from these channels to the rest of the floodplain is very limited (Day et al. 2008). Responsible for the gross of the sediment transport away from the main channel in Day et al.'s (2008) study of the Fly River (Papua New Guinea) are two distinct types of floodplain channels (Dietrich et al. 1999). Dietrich et al. (1999) summarises them for the floodplains of Papua New Guinea as 1) tie channels with a general width of ~ 10 % of the main stem, delivering water and sediment to oxbow lakes, and blocked valley lakes (e.g., Rowland et al. 2005), and 2) low gradient tributary channels (Dietrich et al. 1999; Day et al. 2008). These channels create a sedimentary web in the tropical floodplains in Papua New Guinea.

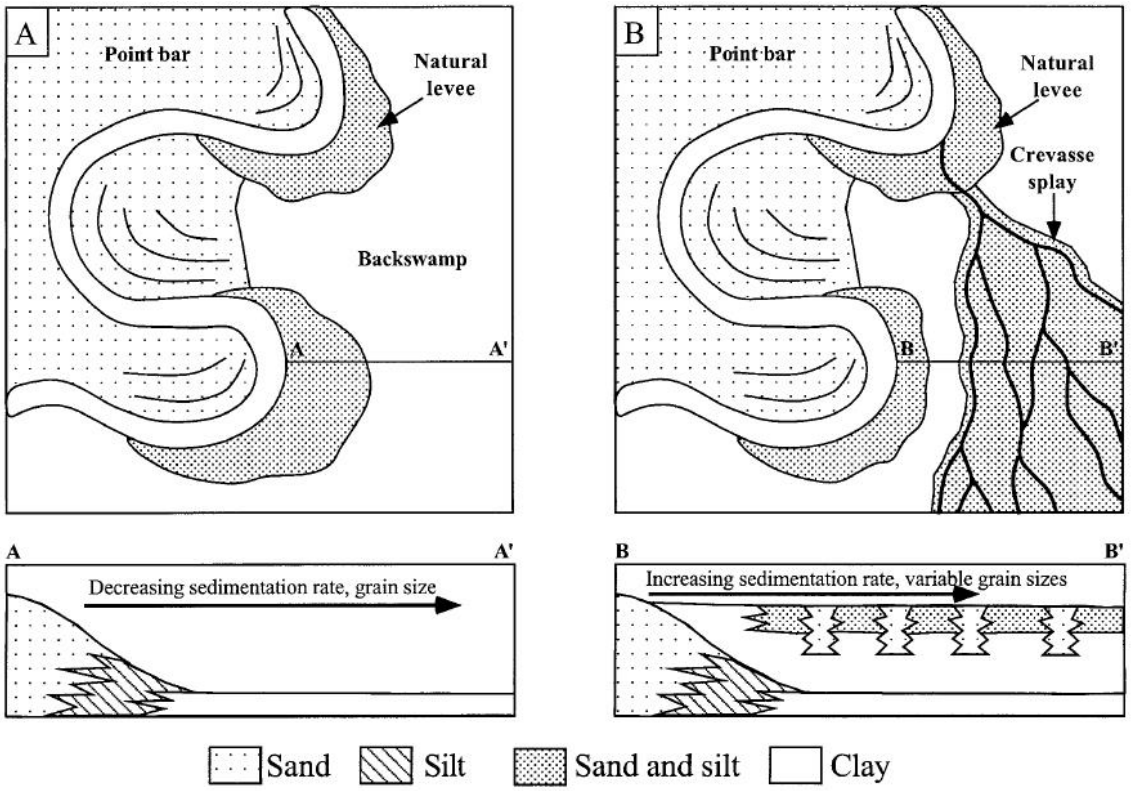

Figure 4 Conceptual model of sedimentation processes and their stratigraphic records. (A) shows deposition along a large river by overbank deposition. (B) shows deposition and its stratigraphic records created by avulsion and crevassing. Adapted from (Aslan & Autin 1999).

Additional to floodplain channels, avulsions are responsible for the transport of large quantities of sediment away from the parent channel onto the floodplain. These processes are observed to play an important role in the long-term development of floodplains (Slingerland & Smith 2004; Blum & Aslan 2006). Slingerland & Smith (2004) use a broad definition for avulsions and classify avulsions as (any) diversion of flow from the parent channel. This diversion has not to be permanent, but also the temporal diversion of flow is defined as avulsion. This definition would also include crevasse splays (Smith et al. 1989) that are observed to deposit large lenses of sediment on the floodplain in the Amazon Basin (Aalto et al. 2003). Aslan & Autin (1999) show that along the Mississippi River overbank deposition during large floods are only responsible for a small percentage of floodplain deposition. They argue that distal floodplain depressions are filled rapidly and continuously during episodes of crevassing and avulsion. After a depression is filled, later avulsions relocate the focus of deposition to different parts of the river, subsequently filling the Holocene flood basin, making avulsions the most effective driver of aggradation along the Mississippi River (Aslan & Autin 1999, Figure 4).

All these studies indicate that the existing topography has a large influence on the distribution of sediments during floods. Especially floodplain channels seem responsible for the transport of sediment to the distal parts of the floodplain. This study aims to contribute to this discussion by analysing a floodplain, and floodplain channels in an environment that differs from the previously researched tropical and temperate environments, and to investigate the importance of floodplain channels on sediment dispersal.

Aims and Objectives

This thesis aims to improve the understanding of the late Quaternary history of the Sacramento River in the vicinity of the Quaternary megafan of Stony Creek. This area is of special interest, because its surface structure has been interpreted controversially (see above). These surface features are used by modern day processes, and are one of the few areas in the Central Valley that has not undergone significant alterations of the floodplain topography. The thesis aims to understand how, and when these floodplain cannels evolved in relation to local late Quaternary evolution of the Sacramento River. It also tries to investigate how the existing topography of the floodplain channels is influencing modern (last centurie's) sedimentational behaviour.

This thesis aims to solve three objectives

(1) To analyse and date the subsurface stratigraphic units, and link their evolution to past climate and environmental changes.
(2) To investigate the potential of CIRCAUS/CNAXS dating in an agriculturally used landscape, and to date modern deposition events using XS ^{210}Pb along the Sacramento River.
(3) To investigate the spatial distribution of sediment deposition and erosion reconstructed from XS ^{210}Pb dating on the Sacramento River floodplain.

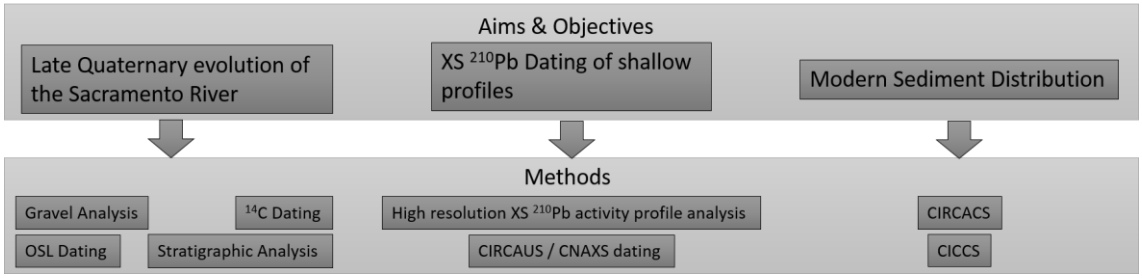

Figure 5 Study design of the thesis and the methods used to achieve each of the goals.

Objective 1: The dating of the stratigraphic units is necessary to shed light on the evolution of the Sacramento River. In order to understand the driving factors for the long-term evolution of the Sacramento River, the age of the present stratigraphic units has to be established. This knowledge will potentially enable the author to link depositional units to environmental conditions in the past. The knowledge of the development of the present underlying topography will also help to understand the modern processes present. The age of topographical features, especially if these features that have developed by erosional processes, is hard to quantify, and is therefore discussed on the basis of hypotheses, supported by dating evidence provided by OSL dating of the surrounding sediments. To achieve this goal a combination of OSL and radiocarbon dating has been applied to several sediment profiles in the vicinity of Llano Seco. The surface structures along the Sacramento valley have been controversially discussed in the past (Olmsted & Davis 1961; Helley & Harwood 1985; Robertson 1987; Dunne & Aalto 2013) and dating the subsurface stratigraphic units can possibly shed light on the age and origin of the stratigraphy of the Sacramento River. The findings will be discussed using regional environmental changes as denominator for changes in runoff or sediment supply.

Objective 2: Studies suggested that XS ^{210}Pb is a reliable mean to date deposition events in silt rich sediments of tropical rivers (Aalto et al. 2003, Aalto & Dietrich 2005; Aalto & Nittrouer 2012). However, even though CIRCAUS/CNAXS has been applied to Sacramento River sediments (Singer et al. 2008; Singer & Aalto 2009) it has yet to be thoroughly tested in a low deposition, agriculturally impacted environment. This study aims to investigate the potential of XS ^{210}Pb dating in an agriculturally influenced area, and the potential problems caused by equifinality of land use induced changes in XS ^{210}Pb activity profiles.

Objective 3: In large river floodplains sedimentation is distributed unevenly, depending on topographical and hydrological factors (Mertes et al. 1994; Allison et al. 1998; Walling & He 1998; Aalto et al. 2003; Hudson & Codiz 3003; Thonon et al. 2007; Day et al. 2008; Swanson et al 2008). This area with its limited alterations of floodplain topography and its large ephemeral floodplain channels provides an excellent opportunity to empirically research natural

sediment dispersal on a large floodplain in an otherwise heavily altered landscape.

2. SETTING OF THE RESEARCH AREA IN THE GENERAL GEOLOGIC AND (PALAEO)CLIMATOLOGIC CONTEXT, AND THE IMPORTANCE OF THE STUDY REACH IN THE SACRAMENTO RIVER FLOOD WEB

2.1. Geology and climate of the Sacramento River catchment

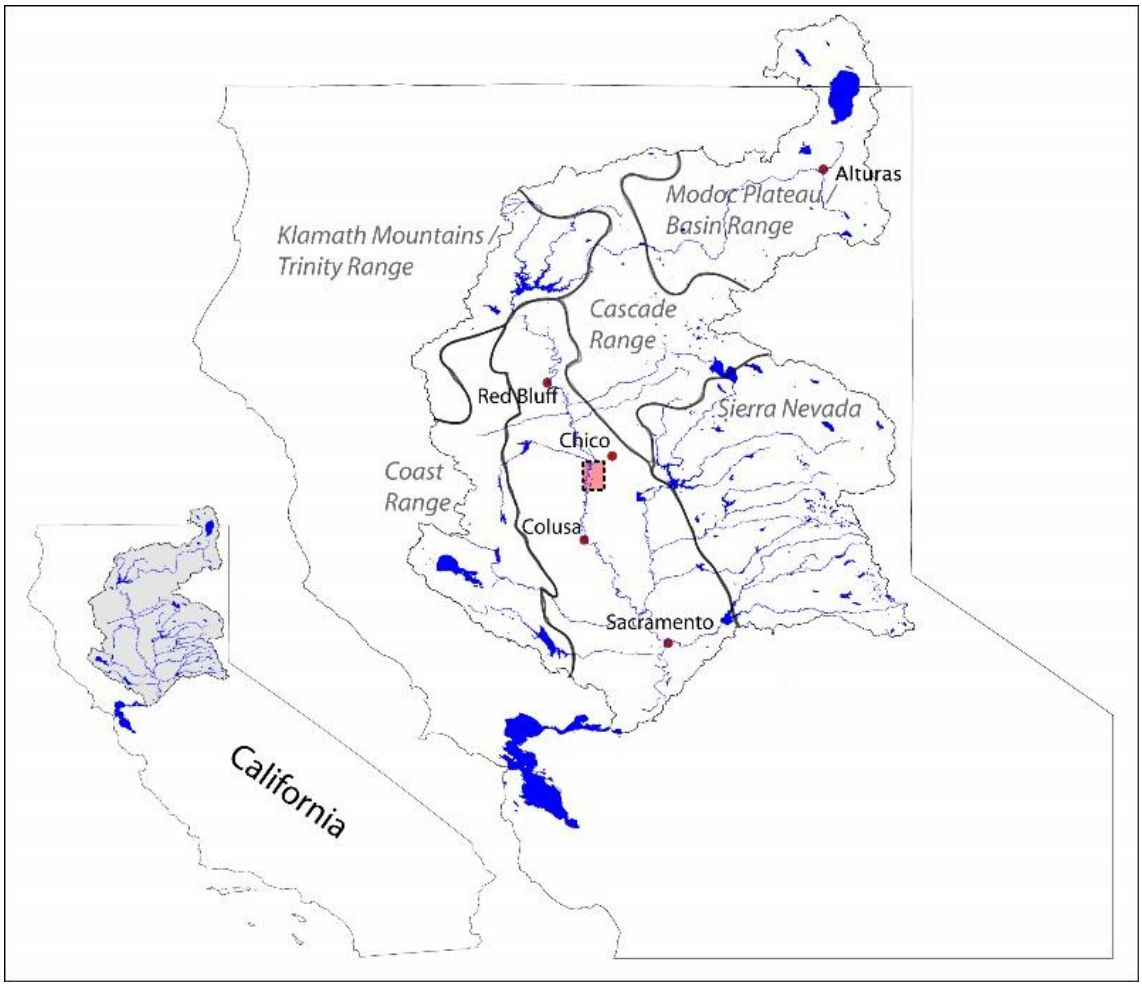

Figure 6 General geographic setting of the Sacramento River catchment (research area red rectangle). Including the main geologic units the catchment. Geologic landscape units after Jenkins (1938). Further map data www.sacramentoriver.org, www.cencus.gov, www.water.gov).

The research area is located along the Sacramento River, the largest river in California that drains with its 68000 km^2 catchment large parts of Northern California (~ 30000 km^2 upstream of the research area). The Sacramento River originates near Mount Shasta (Sacramento River), with tributaries entering the Sacramento River upstream of the research area originating on the Modoc Plateau (Pit Fork tributary), the Cascade Range (e.g. Big Chico Creek), the Klamath Mountains, the Trinity Range and the Coast Range (e.g. Stony Creek) (Jenkins 1938; Helley & Harwood 1985, Figure 6).

The Sacramento River enters the structurally controlled basin of the Central Valley south of the Shasta Dam near Red Bluff (RM246, Helley & Harwood 1985) approximately 80 km north of the research area.

Several different geologic provinces are contributing sediment to the Sacramento River catchment. The different provinces are fundamentally different in their abundance of geologic units (Figure 6, Figure 7). The northern and eastern geologic units of the catchment are dominated by volcanic rocks (Modoc Plateau, Cascade Range), or by volcanic and metamorphic (crystalline) rocks (Sierra Nevada, Trinity Mountains, and Klamath Mountains). The Coast Range in the west is dominated by sedimentary rocks such as sandstones, mudstones and conglomerates (USGS 1966**,** Figure 7). These differences in geology enable to distinguish between the influences of different tributaries to the local river gravel composition along the Sacramento River. Clear indication for Modoc Plateau or Cascade Range influence would be volcanic rocks like andesite, while silt- and sandstone and other sedimentary rocks would be indicative for Coast Range influence.

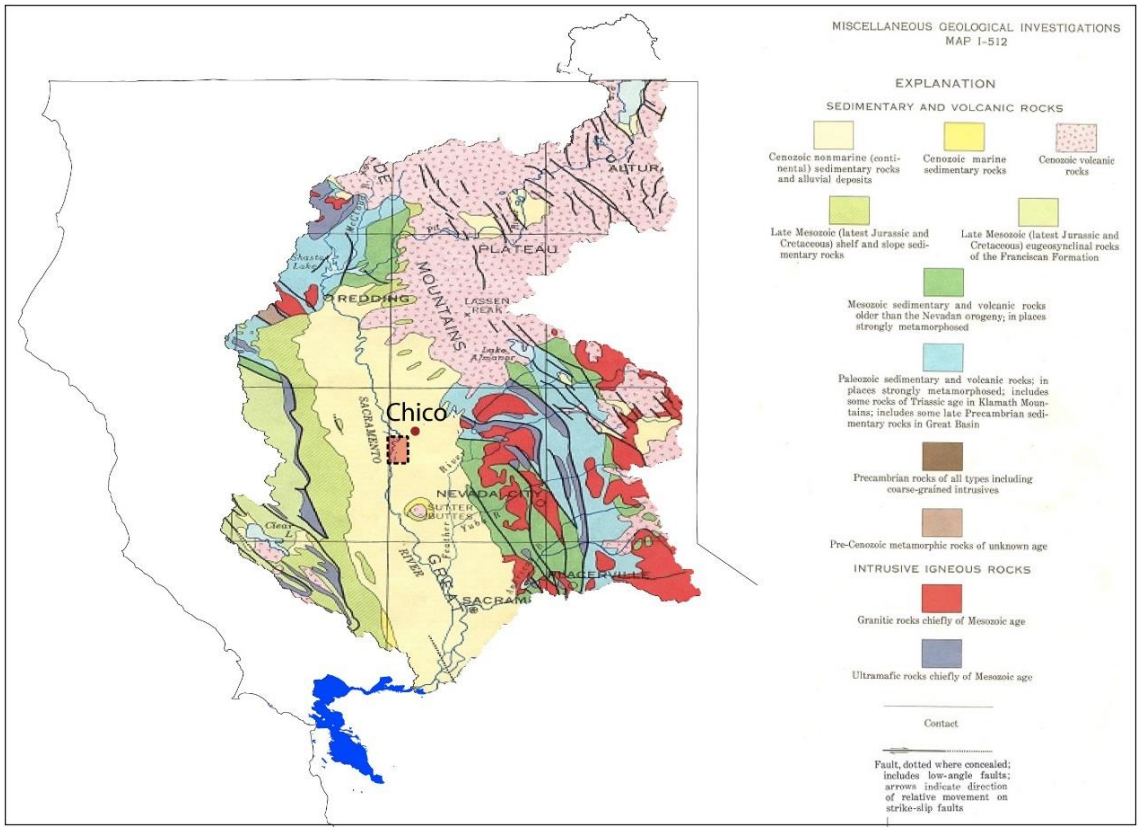

Figure 7 Simplified geologic map of California showing clear differences in geology between the northern and eastern mountain ranges supplying volcanic, and crystalline rocks, whereas the Coast Range supplying sedimentary rocks. (Research area red rectangle) (Adapted and modified from, (USGS 1966), further data www.cencus.gov, www.sacramentoriver.org, www.water.gov).

The youngest Pliocene sediments in the Northern Sacramento Valley on top of which the Quaternary sediments have been deposited is the Pliocene fluvial Tehama Formation (Olmsted & Davis 1961; Helley & Harwood 1985), or the also Pliocene Tuscan Formation that mostly consist of volcanic mudflows (Olmsted & Davis 1961; Lydon 1968; Helley & Harwood 1985). Both formations are of similar Late Pliocene age and probably extent into the Pleistocene. The oldest Pleistocene formation in the Northern Sacramento Valley is the Red Bluff Formation that consist of thin (1 – 11 m) floodplain deposits (Olmsted & Davis 1961; Helley & Harwood 1985) that cover a pediment surface that was dated to a Mid-Pleistocene age of 1,08 ka – 450 ka (Helley & Harwood 1985; Helley & Jaworowski 1985). The Riverbank formation overlies the Red Bluff Formation with a thickness of 1 – 60 m (Helley & Harwood 1985). It consisting of fluvial gravel, sands and silts and was deposited between 450 ka – 130 ka (Marchand & Allwardt 1981). The youngest Pleistocene Formation in the Northern Sacramento Valley is the Modesto Formation that consists of a Lower and an Upper Member. Both Members comprise of fluvial gravel, sands and silts with a total thickness between 3 m and 60 m (Helley & Harwood 1985). The Lower Member Modesto Formation has been dated to a minimum age of 29.5 - 45.5 ka (Marchand & Allwardt 1981; Helley & Harwood 1985). The Upper Member Modesto Formation is described as sandy fluvial deposits at the type location (Marchand & Allwardt 1981) and with vast deposits present in the foothills of the Sierra Nevada (Helley & Harwood 1985). Its suggested age range is between 10 ka and 17 ka (Marchand & Allwardt 1981), even though a slightly earlier start of the Upper Member Modesto Formation is possible (Marchand & Allwardt 1981). The Modesto Formation is covered by the Holocene Alluvium in the Sacramento River floodplain (Helley & Harwood 1985).

Because of the active tectonic setting the Sacramento River is likely to be influenced by tectonic activities - in the long-term confining it to the structurally controlled basin of the Great Central Valley between the Coast Ranges and the Sierra Nevada (Fisher 1994). The structure of the basin in the north is mainly controlled by two large fault systems, the Chico Monocline (east) and the Willows and Corning Faults (west) (Harwood & Helley 1987; WET 1990, Figure 8). These large tectonic faults control the general geologic and topographic setup of the northern part of the Sacramento River valley, but smaller tectonic structures are likely to have an impact on the (recent) position

of the Sacramento River itself (WET 1990). This can be observed at several sites throughout the system, e.g. upstream of the research area, the Sacramento River is closely following the course of the Los Molinos Syncline (RM245 – RM233, Figure 8). A similar trend can be observed along the Glenn Syncline upstream (RM205 – RM200) and in the vicinity of the research area (RM197 – RM173) (WET 1990). At the instances where the river follows the geosynclinal structure, the active channels / meander belts are widening (in comparison to reaches where the river runs independent of tectonic structures) (WET 1990, Figure 8). This westward trend potentially impacted the position of the Sacramento River in the research area over millennial time scales (WET 1990; Harwood & Helley 1987), but the speed and timing of this gradual westward movement is still unknown.

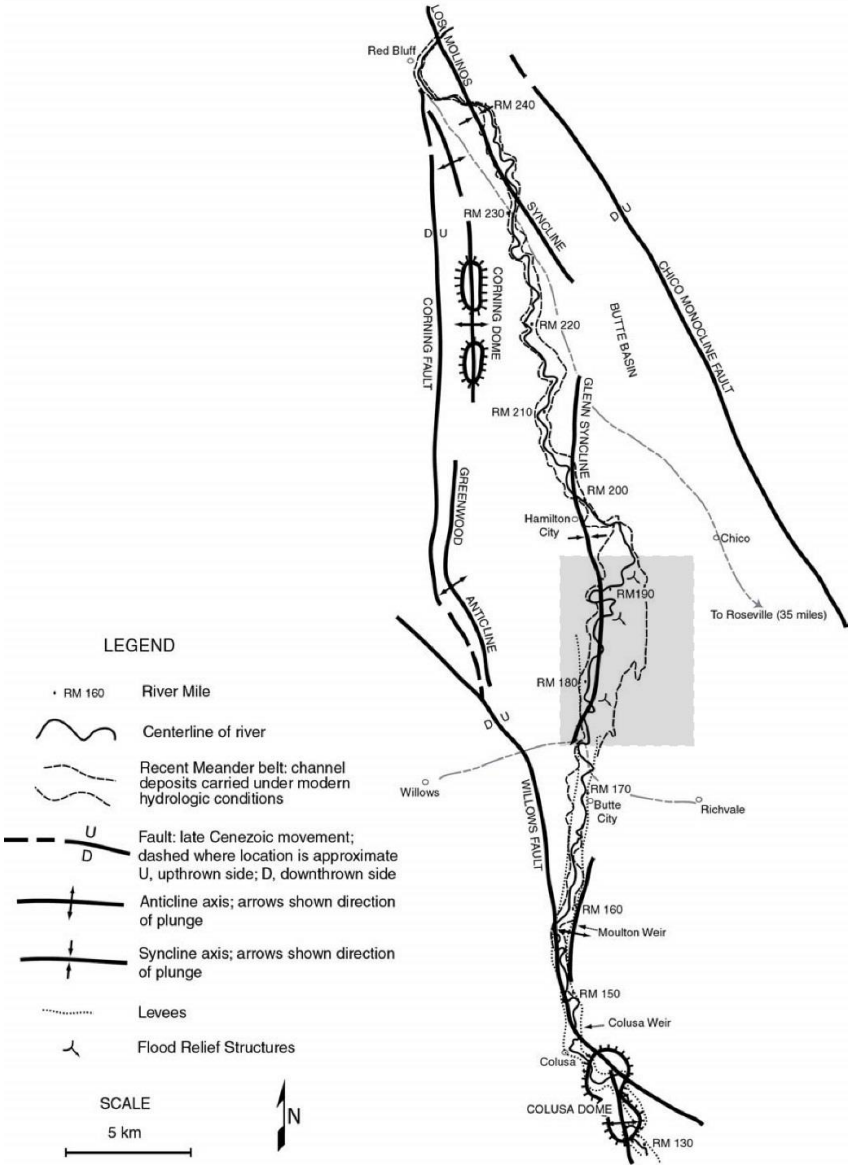

Figure 8 Geologic structures of the northern Sacramento River Valley (Red Bluff to Colusa). The research area is shaded grey. Adapted and modified from Larsen et al. (2002) (from Harwood & Helley (1982) after Fisher (1994))

Late Quaternary climate of Northern California

Modern precipitation rates in the Sacramento River catchment are highly variable. The mountain ranges in Northern California show high precipitation rates (1500 – 3200 mm/a) with peaks in precipitation in the northern Cascade Range (Figure 9). Within the Californian Central Valley, and the plateau positions in Northern California and Southern Oregon precipitation rates drop to a minimum of 250 – 330 mm/a (PRISM Climate Group 2014, Figure 9). The annual precipitation distribution is typical for Mediterranean climate with a peak in precipitation during the winter month. The largest reported floods in Northern California are often associated with several day precipitation events known as “atmospheric rivers” or “pineapple expresses” where relatively warm atmospheric moisture is transported from the Pacific Ocean to the continent and precipitated over the mountain ranges of California (e.g. Weaver 1962; Higgins et al. 2000; Dettinger 2004 2011; Ralph & Dettinger 2011; Lund 2012).

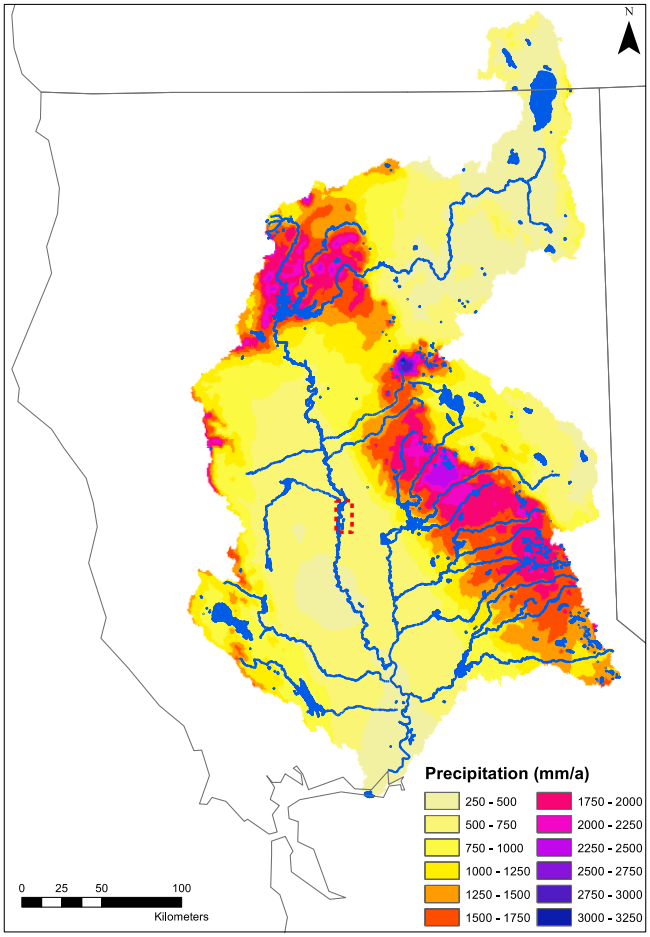

Figure 9 Average precipitation rates (PRISM Climate Group 2014) for the research area (reference period 1961 – 1990). Note high precipitation rates in the mountain ranges to the north and northeast of the research area (red rectangle) and low precipitation rates in the Sacramento Valley and in the Modoc Plateau (Pit Fork Catchment) (map data: ESRI, sacramentoriver.org).

While last century's temperature and precipitation is well recorded, historic records of climate data are limited to the last two centuries due to the lack of prior European American occupation and therefore missing continuous observations of climate. The palaeoclimate of the research area has been reconstructed in this thesis from marine, lacustrine and terrestrial records from Oregon, Nevada and Northern-, and Central California (Figure 10). The palaeoclimate is well established for the postglacial period in Northern California (e.g., Daniels et al. 2005), but records are sparser and the results of these records show a greater variability in environmental signals for the Last Glacial Maximum and before (see below).

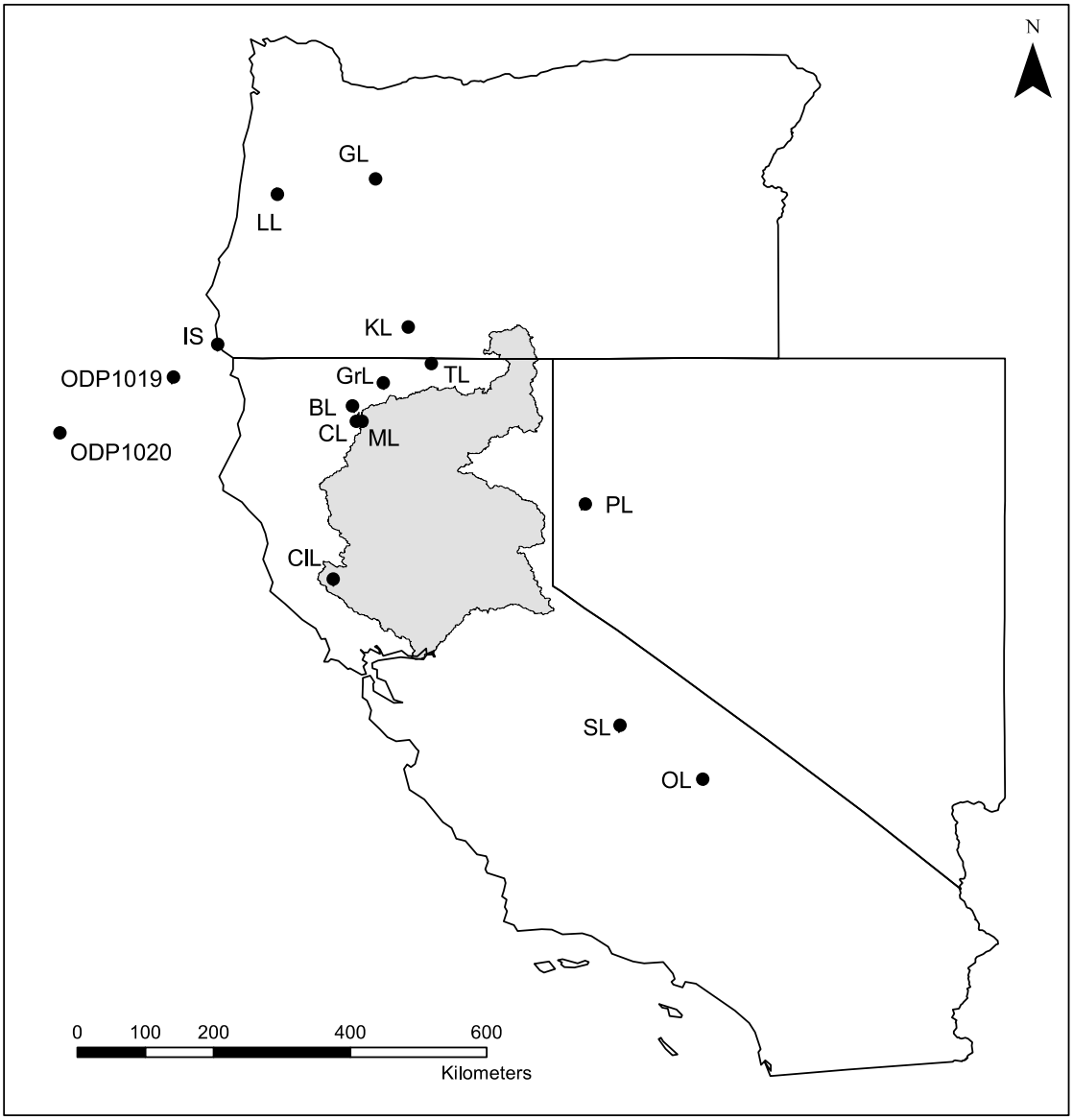

Figure 10 Map shows palaeoenvironmental studies covering the Late Quaternary in the vicinity of the research area used to reconstruct climate trends in this thesis. ODP = Ocean Drilling Programme site, IS = Indian Sands, LL = Little Lake, KL = Upper Klamath Lake, PL = Pyramid Lake, SL = Swamp Lake, OL = Owens Lake, ClL = Clear Lake, TL = Tule Lake, GL = Gordon Lake, GrL = Grass Lake, BL = Bluff Lake, CL = Cedar Lake, ML = Mumbo Lake, LS = Lake Surprise. (Map data ESRI, sacramentoriver.org)

Temperature reconstructions of the late Pleistocene for Northern California and surrounding areas generally reflect worldwide trends (Herbert et al. 2001; Barron et al. 2003). Changes in Sea Surface Temperatures (SST) that have been observed along the California Current reflect worldwide changes in SST, as well as local phenomena along the California Current, and correlate well to climate changes on land (Herbert et al. 2001).

Temperatures in California during the last glacial cycle were considerably lower than today. Herbert et al. (2001) observed a drop in SST by ~ 5 – 6° C along the California Current. For terrestrial archives, environmental reconstructions show a drop in temperature by 7 – 8° C (Adam & West 1983). Especially during the Last Glacial Maximum the precipitation regime in Northern California has been heavily influenced by the southward displacement of the polar jet stream (Bartlein et al. 1998, Figure 11). This displacement lead to generally wetter conditions in Central California, reflected by for example lake level maxima of the pluvial lakes in the Great Basin from ~ 30 – 20 ka (e.g., Benson et al. 1995; Bacon et al. 2006).

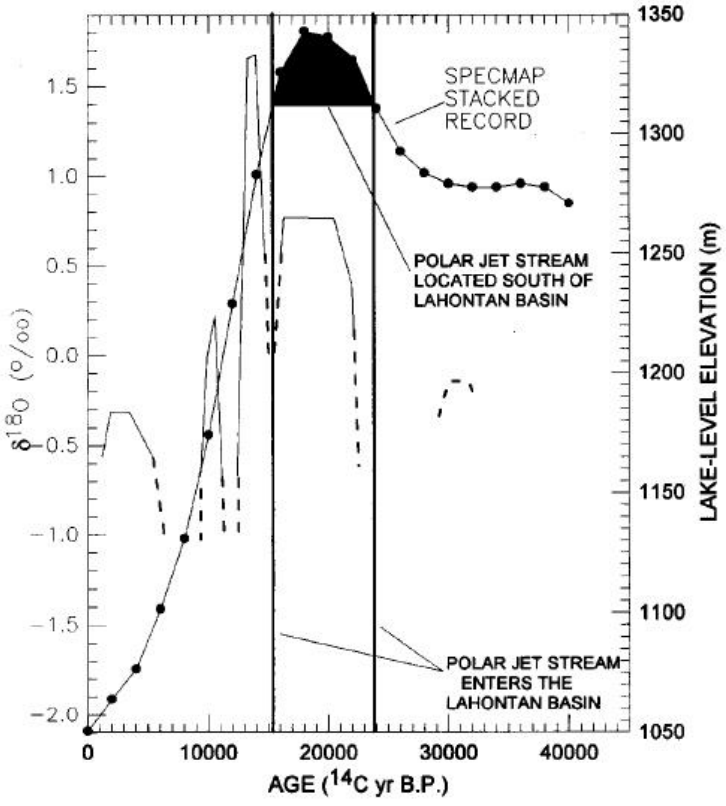

Figure 11 Comparison of SPECMAP δ ^{18}O data with Lahontan Basin lake level records, showing the time and duration of the southward displacement of the polar jet stream south of the Lahontan Basin (Central California) (Benson et al. 1995).

While Central California experienced an increase in moisture, climate has been cool and moderately dry but non-glacial before 30 ka during the last glacial cycle in northern California and Oregon (Worona & Whitlock 1995). Sea Surface Temperature reconstructions for this period show relatively cold climate

for Northern California and a further decrease in temperature ~ 28 ka (Herbert et al. 2001). In Southern Oregon climate shifts between cold non-glacial and glacial conditions occurred between 45 and 23 ka, before turning into full glacial conditions after 23 ka (Bradbury et al. 2004). Before 30 ka Adam & West (1983) reconstructed wet conditions for the Coast Range from Clear Lake pollen compositions (~ 4-fold increase in comparison to modern precipitation rates). Even though Adam & West (1983) argue that precipitation reconstructions from pollen are associated with high error margins, it can be assumed that there was a substantial increase in precipitation rates in the Coast Range before 30 ka. Around 30 ka cal BP climate shifted to cooler and dryer (glacial) conditions in Coastal Oregon, after a period of cooler and wetter but non-glacial conditions before 30 ka cal BP (Worona & Whitlock 1995). This shift in climate resulted in the formation of dunes along the coastline of Oregon from 29 ka to at least 23 ka (Davis 2006). Sea Surface Temperature reconstructions for this period show relatively cold climate for Northern California with a drop in temperature at around 28 ka (Herbert et al. 2001). In the Klamath Mountains the extent of the glaciation was low but variable until 25 ka, before glaciers significantly advanced (Rosenbaum & Reynolds 2004a). For the Cascade Range (Washington) the age constrain of glacier advances is rather weak but it can be argued that glaciers retreated before ~ 30 ka. No glacial deposits were mapped between ~ 30 ka and ~ 25 ka, with the largest advance following from ~ 25 ka – 18 ka (Clark & Bartlein 1995). In Southern Oregon climatic shifts between stadial and interstadial conditions occurred between 45 ka and 23 ka before turning into full glacial conditions after 23 ka (Bradbury et al. 2004). Hakala & Adam (2004) reconstructed an opening of the forest vegetation in Southern Oregon and on the Modoc Plateau from 32 ka. From 30 ka – 19 ka an open sagebrush steppe was dominating, indicating an overall reduction in precipitation. Hakala & Adam (2004) also reported an increase in sand accumulation in Grass Lake during this cold interval. Conditions were generally dry from 25 ka at Tule Lake (Northern California), with short wet intervals (Bradbury 1992). Grigg et al. (2001) find higher variability in moisture and vegetation cover post 28 ka in Little Lake pollen records (Southern Oregon) indicating the opening of the landscape and the establishment of a relatively open forest vegetation after 25 ka with several major erosion events post 24 ka under generally cold conditions with a brief warm period from 25 ka – 22 ka. Dry

conditions are also reported from Modoc Plateau between 30 ka to 21 ka (Hakala & Adam 2004). This dry climate in Northern California coincides with a period of lake level high stands in Central California before 20 ka (Bacon et al 2006) and low δ 18O value for Owens Lake also indicate relatively moist conditions between 30 ka and 20 ka in the Central Californian region (Benson et al. 2002, Figure 57). The differences in climate signals between Northern and Central California can be explained by a southward displacement of the jet stream during the late Quaternary (Bartlein et al. 1998, Figure 11) that is responsible for opposing moisture regimes in late Quaternary California.

Sea surface temperatures remained cool throughout the Last Glacial Maximum, and started to increase from 18 ka (Herbert et al. 2001). Precipitation simulations by Kim et al. (2008) showed generally wetter conditions for the Last Glacial Maximum at 21 ka for the West Coast of the United States. Ibarra et al 2014 reconstructed a low increase in precipitation rates (2 – 18% compared to modern values) during the Last Glacial Maximum at Lake Surprise (Northern California / Nevada), with a strong increase in precipitation (~ 75% compared to modern values) between ~ 17 and 13 ka. Worona & Whitlock (1995) reported an increase in precipitation in coastal Oregon from 20 ka cal BP to 16 ka cal BP, as do Hakala & Adam (2004) for the Modoc plateau between 21 ka and 18 ka. Grigg et al. (2001), on the other hand, find the coldest and driest condition between 21 ka and 17 ka in Coastal Oregon, and at Tule Lake (Northern California) conditions remained cold and dry until 15 ka (Bradbury 1992). In Central California a rapid drop in lake levels occurred after 20 ka with increasing lake levels after 16 ka (Baconet al 2006). Low lake levels are also represented by a hiatus in the δ 18O record from ~ 18 ka to ~ 16 ka (Benson et al. 2002). Daniels et al. (2005) also report dryer conditions than today until 13 ka in Northern Californian and Southern Oregon lake records (Figure 11). Significant glaciation in the Klamath Mountains occurred from 25 ka with a peak between 19.2 – 17.8 ka before a rapid decrease in glacier extent around 16 ka (Rosenbaum & Reynolds 2004).

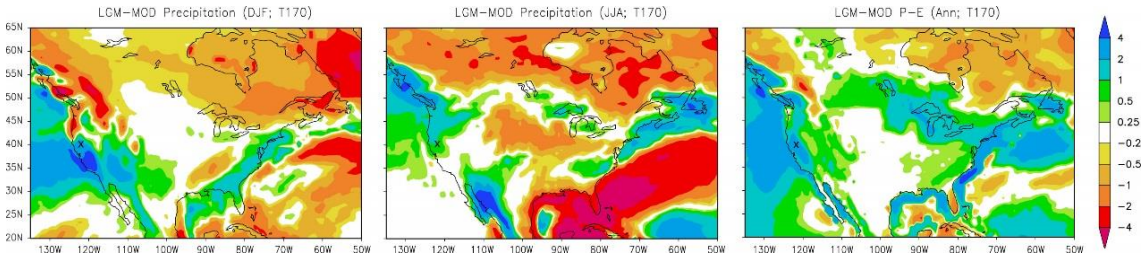

Figure 12 Modelled differences in precipitation between modern day rates and the Last Glacial Maximum at 21 ka in North America. Differences are modelled for winter precipitation (left), summer precipitation (middle), and annual-mean precipitation minus evaporation (right). The position of the research area is indicated on the map by an (x). Adapted and modified from (Kim et al. 2008).

Sea Surface Temperatures dropped again between 13 ka – 11.5 ka along the Northern Californian coast (Herbert et al. 2001; Barron et al. 2003). Records all over Northern California show a cool and wet period starting 15 –16 ka and lasting until 11 ka – 11.5 ka (Daniels et al. 2005). Western Oregon experienced increased precipitation and moderately cool conditions from ~ 15 ka to 11.5 ka (Grigg & Whitlock 1998). After this brief cooler interval SST rapidly recovered and reached modern temperatures (~ 12° C) between 11.5 ka and 10 ka (Herbert et al. 2001; Barron et al. 2003). By that time terrestrial records in Southern Oregon and Northern California have reached Holocene conditions as well (e.g. Benson et al. 2002).

Due to a lack of suitable archives for environmental reconstructions in the Central Valley itself, little is known about past environments within the Sacramento River Valley. The location of the research area between the dry conditions in Northern California and the relatively wet conditions in Central California during the Late Quaternary potentially suggests highly variable precipitation rates and vegetation in the research area.

During the Pleistocene major alpine glaciation influencing the Sacramento River system were only reported for the Sierra Nevada tributaries (e.g. Gillespie & Zehfuss 2004; Ehlers et al 2011). In Northern California only smaller mountain glaciers are reported for the Lassen Volcano, Mount Shasta, Medicine Lake Volcano, the Castle Crags, the Trinity Alps and in the Coast Ranges (Wahrhaftig & Birman 1965; Bateman & Wahrhaftig 1966). While the alpine glaciations in the Sierra Nevada influenced the Feather River, and its tributaries, this large glaciation had little influence on the research area. Glaciers in the northern part of the Sacramento River catchment that were potentially influencing the research area during the last glacial cycle, remained comparatively small (Bateman & Wahrhaftig 1966; Dyke 2004; Meyer 2013),

and their influence on the hydrology of the Sacramento River in the Central Valley was probably limited due to the small size of the glaciers.

2.2. The Research Area

The research area is characterised by three major active fluvial features: 1) the modern perennial meandering river, 2) small perennial tributaries to Butte Sink (Little Chico Creek), and 3) a set of large ephemeral floodplain channels (Figure 13). The channel systems have been thoroughly mapped and described using aerial photography and historic maps (Robertson 1987; Greco & Alford 2003a; Greco & Alford 2003b). While the modern river shows meandering patterns (sinuosity 1.64), little is known of its behaviour in the past. Robertson (1987) interpreted the ephemeral channel patterns as relic Sacramento River channels. These floodplain channel features show a significant difference in channel geometry, channel slope and sinuosity to the modern Sacramento River (Table 1). Robertson (1987) argues that the eastern channel system resembles a braided river system in their channel geometry and the western channels rather resembles an anaostomosing system.

The floodplain channel systems have been correlated to similar sedimentary units using soil description and weathering indices and were cross-correlated to soil units with ages between 140 ka – 450 ka (Robertson 1987), but no in depth description of floodplain profiles and on site dating has been done using modern geochronological techniques. Therefore the true age of the fluvial features, the timing of the channel evolution and involved processes remains unclear.

Table 1 Fluvial Morphology of the Sacramento River and its Floodplain Channel Systems

	Holocene Meanders	Western Channel Systems	Eastern Channel Systems
Slope (m/m)	0.0004	0.0005	0.0005
Sinuosity	1.64	1.10	1.06

Geologically the entire research area is described as Quaternary alluvium and consists preliminary of reworked fluvial material (Helley & Harwood 1985). Closest to the river, different generations of abandoned channels can be found of which the most recent channels have been investigated thoroughly for their century-scale migration rates (Brice 1977; Greco & Alford 2003a; Greco & Alford 2003b; Larsen 2007; Constantine & Dunne 2008; Constantine et al. 2010; Michalcovál et al. 2011; Micheli & Larsen

2011), with longer-term migration rates and evolution still unknown. The channel evolution and fluvial stratigraphy are complicated by tectonic influences from nearby active tectonic faults and synclines that are deemed to be responsible for a gradual westward shift of the Sacramento River to its current position (Harwood & Helley 1987), counterbalancing a potential eastward disposition of the Sacramento River by prograding fans from Coast Range tributaries (Robertson 1987). While for other parts of the Sacramento River large natural levees are reported (Robertson 1987; Fischer 1994; Singer et al 2008; Singer 2015 in press), these natural levees, and alluvial splays caused by levee failures are missing in the research area (Figure 13).

The research area was chosen for; a) its nearly natural flooding conditions, due to its location upstream of the start of the continuous levees of the Sacramento River flood control system (Figure 2), ensuring regular, and partly naturally distributed flooding, b) its position within the Sacramento River flood web as the first opportunity for water leaving the channel to reach the distal floodplains of Butte Sink, c) its lack of significant alteration in topography, and d) its accessibility – being owned by a family that actually grands access to their property. The fact that the floodplain topography has not been significantly levelled in comparison to most other locations along the Sacramento River, provides a mostly undisturbed topography providing insight into the depositional history and behaviour of the distal floodplains. Special focus is directed to the most significant floodplain features of this area, two sets of large floodplain channels (Figure 13) formerly controversially interpreted as either relic Pleistocene landforms (Robertson 1987; Dunne & Aalto 2013) or Holocene floodplain alluvium (Olmsted & Davis 1961; Helley & Harwood 1985).

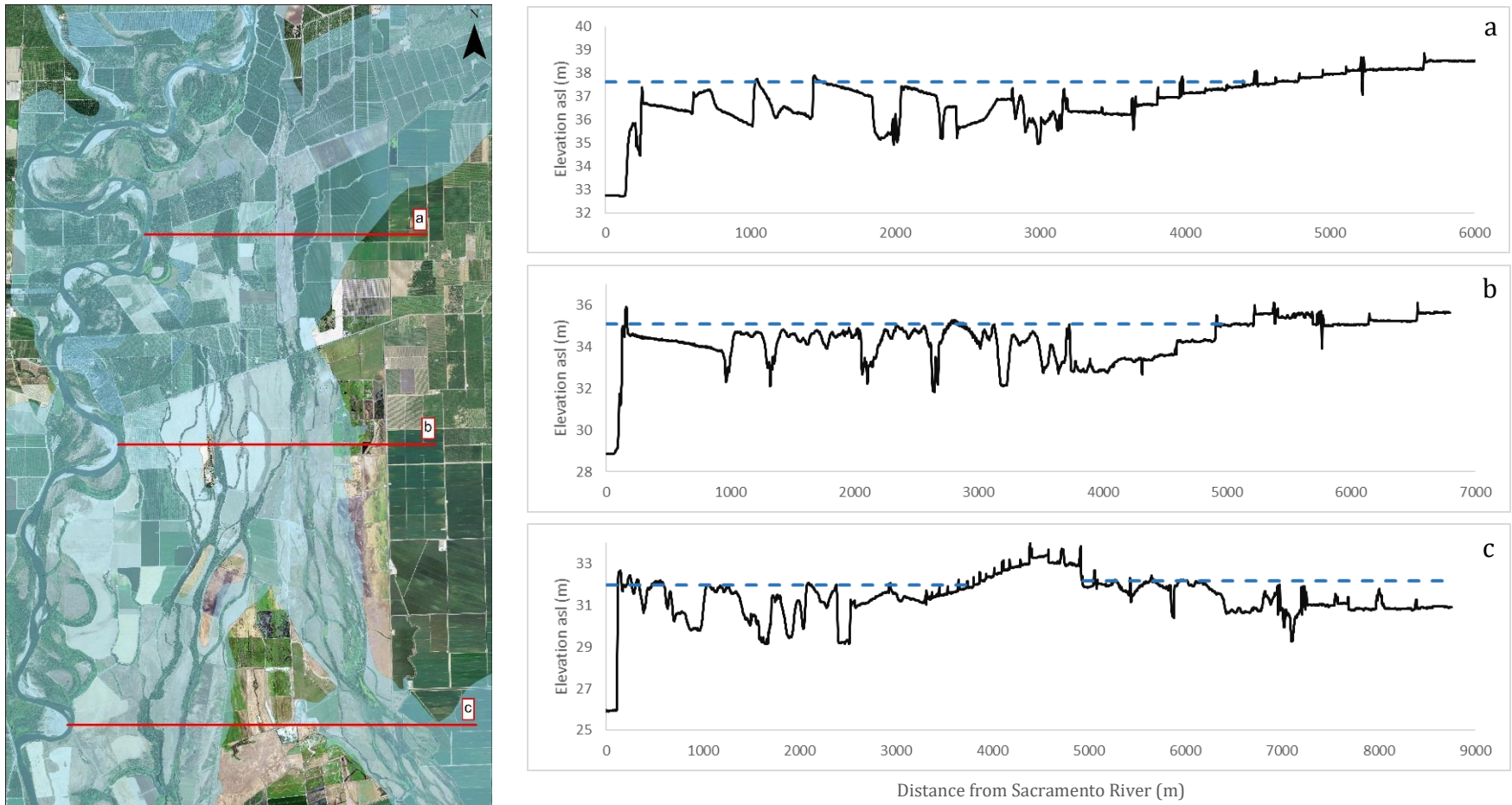

Figure 13 Topographic profiles of the Sacramento River floodplain at the research area. Locations of the cross-sections are marked red. FEMA 100 year flood extent is depicted as shaded area on the map (FEMA) and, 100 year flood elevations are shown as dotted blue lines in the topographic profiles. The natural levees that are reported for the Sacramento River downstream of this reach (Robertson 1987, Fischer 1994, Singer et al 2008, Singer 2015 in press) are missing and flooding is just limited by smaller training levees or roads that function like small levees, but are not part of the Sacramento River flood control system (data: FEMA, seamless.gov, Nature Conservancy).

The research area is located along the Sacramento River in the northern part of the Central Valley of California, just south of Chico and Hamilton City (Figure 2). The Sacramento River's banks and natural levees are readily overtopped during flooding events in this area (WET 1994). It includes one of the last remaining quasi-pristine sections of the Sacramento River in terms of floodplain topography and flood flow control (continuous artificial levees of the SR flood control system start at the lower end of the research area approximately at RM176).The study area itself is located south of Hamilton City between RM175 and RM193, where the Sacramento River frequently leaves its channel during floods. From here the water flows down-valley into Butte Sink, a large natural flood basin located north of Sutter Buttes and east of the Sacramento River. The research focus is on the less disturbed floodplains within Rancho Llano Seco (RM175 – RM184), an ~ 80 km^2 tract that is the only Spanish Land Grant remaining as a whole in California, owned by a single family since 1861.

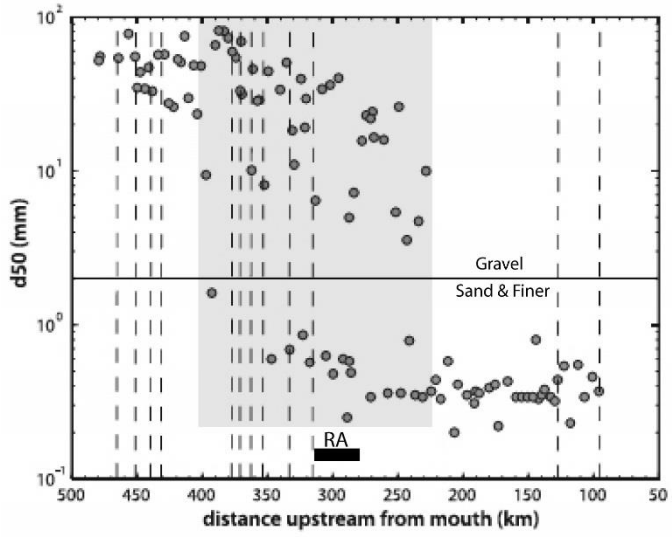

Figure 14 Average grain sizes aggregated within cross sections within the channel along the Sacramento River. Grey shaded box marks the transitional zone from gravel-bed to sand-bed river. The thick black line labelled RA marks the position of the research area within this transition. Dotted vertical lines mark tributaries of the Sacramento River. Adapted and modified from (Singer 2008).

The Sacramento River in the Central Valley is a gravel-bed river that slowly transitions into a sand-bed river (Singer 2008, Figure 14). The research area is located within this 180 km long transition zone, downstream of the last larger tributary (Stony Creek) for more than 150 km (Singer 2008). Singer (2008) shows that these tributaries have little effect on the modern grain size distribution of the bed material. But tributaries like Stony Creek – the second largest Coast Range tributary to the Sacramento River – probably had greater impact on the main stem and the research area in the past (Meyer & Rosenthal 2008). Little is known about the scale of the potential extend of the Late

Quaternary Stony Creek megafan in today's floodplain. A greater influence of the Stony Creek on the Sacramento River Valley in the past can probably be inferred from the existence of its vast (gravel) fan complex deposited throughout the Pliocene and Pleistocene (Helley & Harwood 1985).

One of the attractions of the research area is a network of ephemeral channels parallel to the main stem that transport most of the Sacramento River overbank discharge during floods (Figure 1, Figure 13, Figure 15). The origin of these floodplain channels is still not fully understood, but it has been argued that the floodplain cannels represent relic channel systems of the Sacramento River, representing differing stages of the evolution of the Sacramento River during the Quaternary (Robertson 1987).

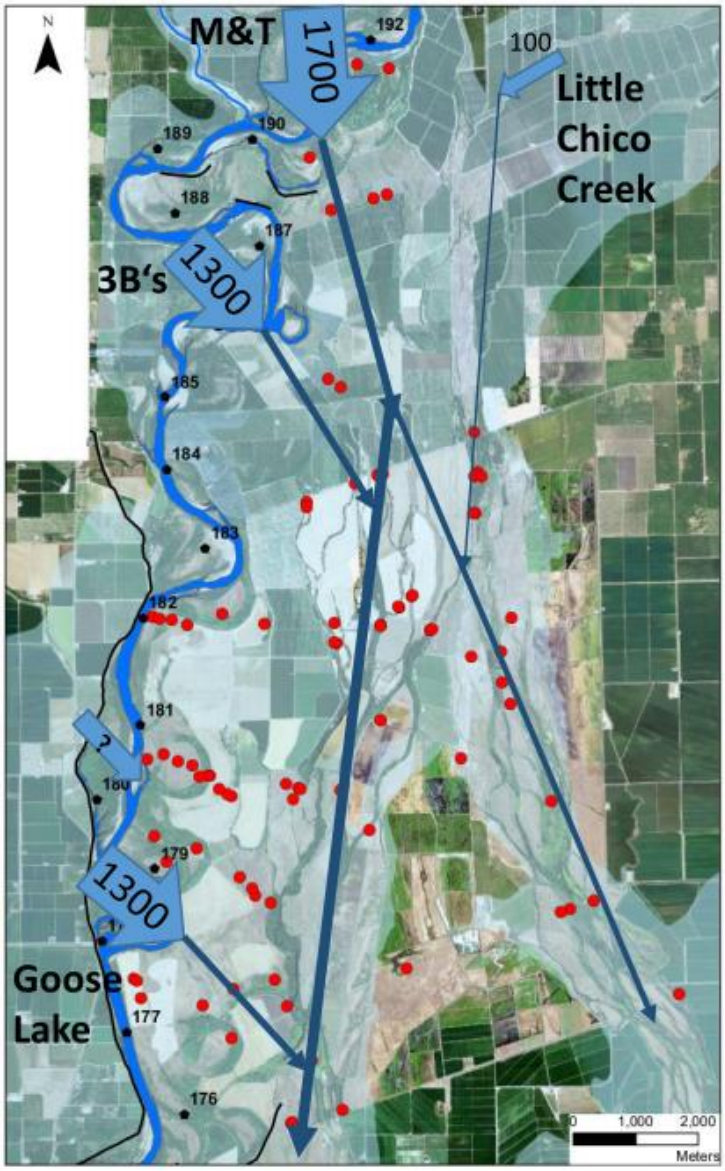

Figure 15 Flooded areas using the FEMA 100 year flood outlines (shaded) for the research area. Map includes levees (black lines), river miles (black numbers), and the 1997 river channel (blue), and sample sites (red dots). Features influencing the movement of water are the artificial levees of the Sacramento River flood protection system, and the natural and artificial flood outlets in the research area). Arrows indicate the overflow points, were water is leaving the Sacramento River channel and the flow (in m^3/s) that is potentially diverted at these locations (Larsen et al 2002). The positions of the flood outlets (indicated by blue arrows) are later used as source for floodwater when calculating windowed distance from the nearest flood source (Map Data: FEMA, seamless.usgs.gov, sacramentoriver.org).

Modern river discharge in this area is highly variable with a clear peak during winter precipitations and snowmelt. Local gauge records are only available since the late 19th century and many have been discontinued between 1980 and 2000. Nevertheless, gauge records are available upstream of the research area for Hamilton City (RM199) from 1945 – 1980, and further upstream for Bend Bridge (USGS gauge number 11377100, RM258) from 1891 – present. For periods during which Hamilton City Gauge was inactive the discharge rates have been reconstructed from Bend Bridge Gauge station records. The average annual discharge of the Sacramento River at the closest upstream gauge station (Hamilton City gauge, River Mile 199, 1946 – 1980) is ~ 350 m^3/s, with an average flood discharge of ~ 2510 m^3/s and maximum discharge up to 4276 m^3/s. Flood discharge is heavily reduced in comparison to the natural conditions that preceded the construction of Shasta Dam in 1943, with average pre-dam flood discharge of ~ 3850 m^3/s and maximum discharge of ~ 9900 m^3/s. Even though some of the study area is inundated annually, generally it is just the larger events that are visible within water loss estimates that can be reconstructed from upstream and downstream gauge records.

Even though the floodplains of the research area are inundated during winter floods most years (as reported in interviews with farm workers), large scale water loss of the Sacramento River to Butte Sink in the vicinity of the research area is only reported for floods with discharge exceeding ~ 2250 m^3/s at Hamilton City Gauge (USGS gauge number 11383800) (Blodgett & Steihr 1974; Larsen et al. 2002), flooding large parts of the research area (Figure 13, Figure 15). Major floods with substantial water loss over bank, diverting an average of ~ 30 % of the total maximum flood flow to Butte Basin (Larsen et al. 2002). The highest annual discharge on the Sacramento River is reported during the winter month (December – March), with only few exceptions of annual discharge maxima reported at other times of the year (< 1 % in November, < 5 % in April).

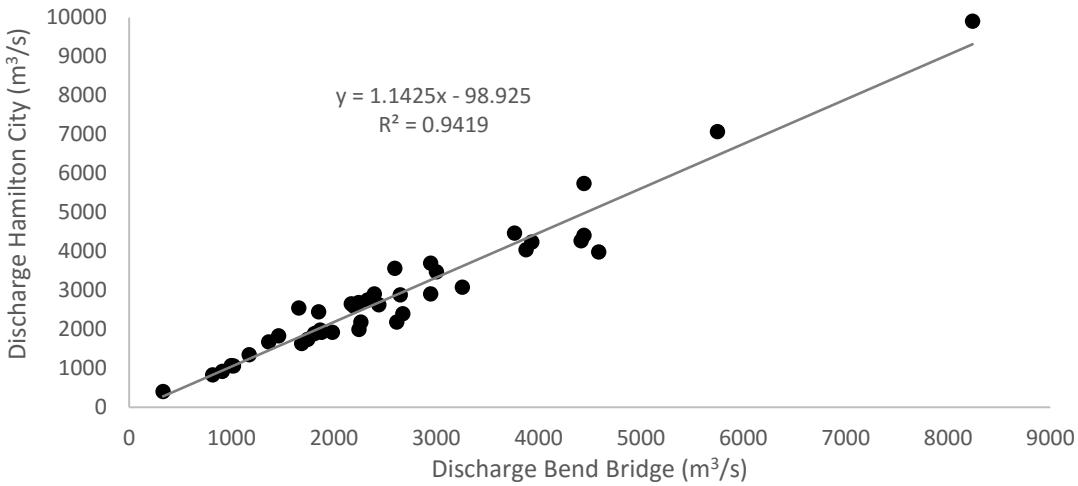

Figure 16 Maximum flood discharge (m^3/s) at Hamilton City (RM199) compared with maximum flood discharge at the upstream gauge station at Bend Bridge (RM258). Records are in good agreement (r^2=0.9419) for the observation period between 1940 – 1980. Shasta Dam has been constructed from 1943 – 1945, but flow relationship at the site have been reconstructed since the beginning of flow records at the site, because this change upstream of both gauge stations should not influence the flow relation between the stations. (Flow data USGS gauge station number 11383800 and 11377100).

Bend Bridge discharge records show a very close correlation to Hamilton City discharge (r^2 = 0.9419 from 1940 – 1980, Figure 16), so Bend Bridge records were used to extend the record of discharge at Hamilton City until today. Additionally, discharge records are available for Big Chico Creek (USGS gauge number 11384000, confluence at RM193, Figure 2) from 1931 – 1986 and Stony Creek (CDEC station ID STC, confluence at RM190, Figure 2) from 1955 – 1990, enabling the reconstruction of river discharge for the Sacramento River at the research area. Downstream of the research area, discharge records are available for Butte City (USGS gauge number 11389000, RM169, Figure 2) from 1938 – 1995. Records from gauge stations further downstream are not suitable for reconstructing flow at Butte City by extending the recorded discharges through a calibration. The nearest gauge station with longer records (1921 – present) is located at Colusa (USGS gauge number 11389500, RM144) but between these two stations there is substantial flow diverted into Butte Basin at Moulton Weir (CLSC1, RM159) and Colusa Weir (CLAC1, RM146), and records of flow diverted are limited to the period 1943 – 1977 and 1943 – 1980, respectively, as are records for water loss at both weirs.

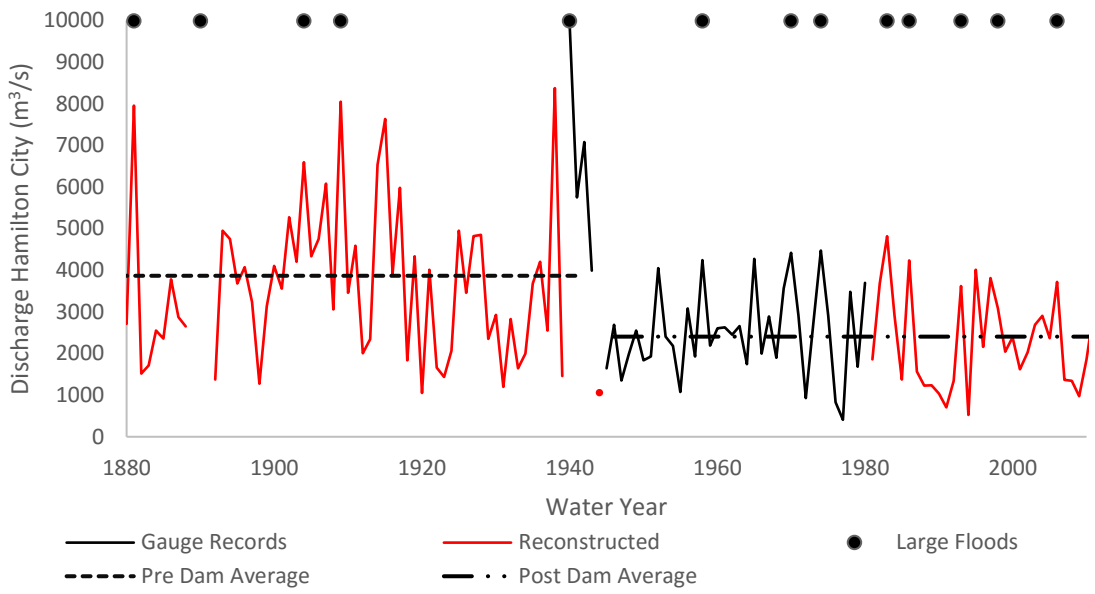

Figure 17 Maximum flood discharge for the Sacramento River at Hamilton City, recorded at Hamilton City Gauge (1945 – 1980) and reconstructed from Bend Bridge Gauge records (1879 – 1944, 1981 – 2011, Hamitlon City flow = 1.1425 * Bend Bridge flow – 98.925). Dots show exceptional large floods at least partly originating from the Sacramento River upstream of the Feather River confluence affecting the research area (Simpson 1978; USACE 1998).

The lack of locally recorded data prior to 1943 does not affect this study, because the focus of this research is on the last 50 – 70 years of erosion and infilling, with the pre-dam flood regime of lesser importance. The large floods within the past 30 – 40 years are therefore of the greatest interest for this study's research. Large floods originating in and affecting the Sacramento River have been reported in 1964, 1974, 1983, 1986, 1993, 1997, and 2006 (USACE 1998, Figure 17). Flood frequency analysis showed that Llano Seco is flooded by floods from an exceedance probability of 1.96 years (flow >~ 2250 m^3/s at Hamilton City Gauge (USGS gauge number 11383800) (Blodgett & Steihr 1974; Larsen et al. 2002). 10 largest floods after the construction of Shasta Dam directly affecting the research area occurred in 1983, 1974, 1970, 1965, 1986, 1958, 1952, 1956, 1997, and 2006.

Modern peak flood discharge is heavily reduced in comparison to the natural conditions that preceded the construction of Shasta Dam in 1943 (Figure 18, Singer 2007). This impoundment of half the runoff area has resulted in a period of lower flood flows and especially a decrease in the magnitude of large floods after 1940 (Larsen et al. 2002). Prior to the construction of Shasta Dam large floods have been reported for the Sacramento River for 1862, 1867, 1881, 1890, 1904, 1909 and in the early 1940s with the largest flood for this period reported in 1940. The largest floods after the construction of Shasta Dam

occurred in the water years 1958, 1970, 1974, 1983, 1986, 1993, 1997 (Simpson 1978; USACE 1998), and 2006 (Figure 17). The average pre-dam flood discharge has been recorded as ~ 3850 m^3/s with a maximum discharge of ~ 9900 m^3/s in 1940 (Figure 17). Time to peak is longer for moderate and long floods for post dam Stony Creek. At low exceedance probabilities time to peak is shorter at Bend Bridge after the construction of Shasta Dam, except for the largest flood since dam construction (Singer 2007). Stony Creek shows a significantly longer drawdown time for post dam completion floods, while Bend Bridge shows shorter drawdown times after floods (Singer 2007).

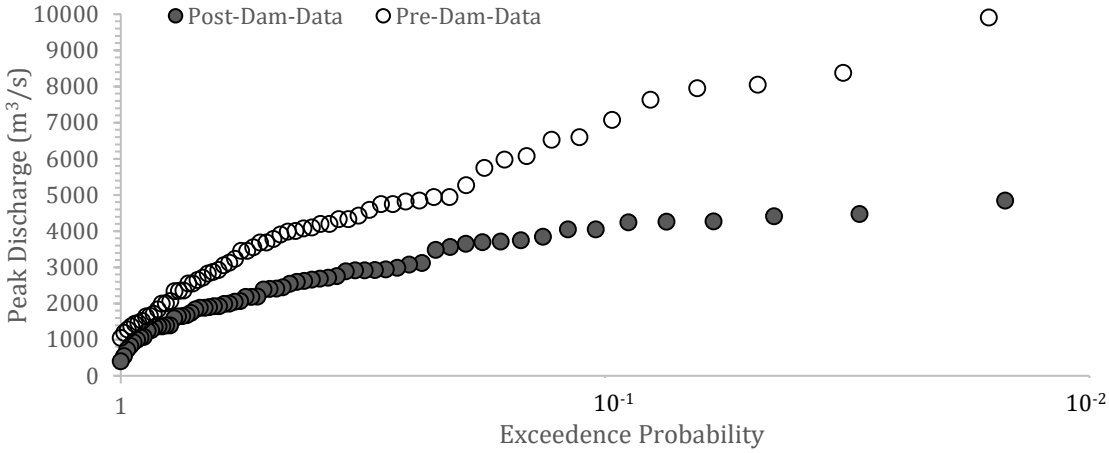

Figure 18 Annual peak flow probability at Hamilton City Gauge for pre-dam and post-dam peak flows.

During floods sediment laden flood water leave the Sacramento River within the study reach at three main outlets that feed into the research area, M&T Bend (RM191, M&T), 3B's natural overflow (RM186.5, 3B's) and Goose Lake (RM179, GL) (Figure 15, WET 1994). While 3B's is a natural overflow area M&T Bend and Goose Lake are at least partly engineered structures, in the sense that flood water is leaving the channel at these points naturally, but flow is slightly restricted by the position of elevated roads and other engineered structures. These floodwaters are initially conveyed by the existing floodplain channels (that are able to convey up to ~ 283 m^3/s (Simpson 1978), but flooding covers the entire floodplain at larger floods, when up to ~ 3000 m^3/s of flow are diverted from M&T Bend and 3B's overflow (Larsen et al 2002). Of these 3000 m^3/s approximately 1700 m^3/s are diverted at M&T Bend and additionally 1300 m^3/s are diverted at 3B's. Goose Lake overflow at RM179 affects the downstream end of the research area where it is able to contribute ~ 1300 m^3/s to the total potential diverted flow of 4300 m^3/s entering Butte Basin through the

research area (Larsen et al. 2002). Additionally to the sediment that is entering the research area from the Sacramento River localised scours provide additional sediment for the distribution by the floodplain channels. Harmon (1994) reported two scour holes at RM 190.8 that have been caused by the 1986 flood, and referred to written communication with the Department of Water Resources that 12000 tons of rock and 382280 m^3 sediments were required to refill these scour holes.

The floodplain channels

While the Sacramento River is a meandering river with a sinuosity of 1.64 and a slope of 0.0004 (m/m), the western and eastern channel systems show a slightly steeper slope (0.0005 m/m) and a rather straight geometry (sinuosity of 1.10 and 1.06 respectively). The floodplain channels also show multiple threads for each system, with larger – for the lack of a better word – bars in the western system. The channels in the research area show an average depth of ~ 2 m and an average width of ~ 10 – 30 % of the main stem Sacramento River. While the western channels are deeper (2 – 3 m) and less wide (~ 50 – 100 m), the eastern channels are wide (average ~ 200 m) and shallow (~ 1 m). The eastern channels show a high width-depth ratio of approximately 270, the western channels a moderate width depth ratio of ~ 34. According to the discharge slope relationship by Leopold & Wolman (1957) and using 2250 m^3/s as bankfull discharge (Blodgett & Steihr 1974; Larsen et al. 2002) the modern Sacramento River planform is very vulnerable to changes in discharge. Only a slight increase in bankfull discharge could result in a change of planform towards a braided type river (Robertson 1987).

Land use and topographic units

The research area can be divided into several land use types and topographic units. The most basic separation can be done by classifying the research area in channel and non-channel locations. The channel locations can be subdivided into partially filled channel scars of the main stem Sacramento River, narrow western floodplain channels and shallow eastern floodplain channels. The non-channel locations are represented by sites proximal to the Sacramento River (< 1 km from main stem Sacramento River), low fields and

grassland, low orchards and woodlands, and elevated floodplains at the lower end of Llano Seco (Figure 19).

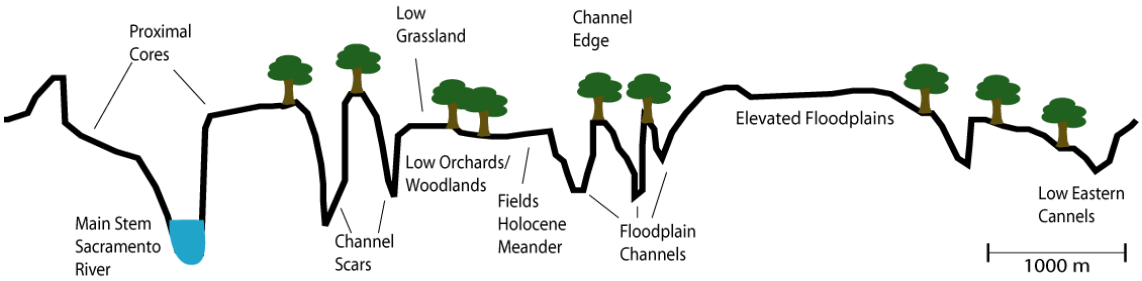

Figure 19 Schematic overview over the landscape units along the Sacramento River.

The four main land use types can be classified as woodlands, natural grasslands, pasture, fields and floodplain channels and subdivided into pristine sites (Figure 20) and agricultural sites (Figure 21). The pristine sections of the research area are woodlands (mainly open valley oak woodlands and riparian forests), natural grasslands proximal to the river and unimproved pastures as well as different types of floodplain channels described by Robertson (1987). Undisturbed sites must not have undergone ploughing or other surface alterations. To ensure a “pristine” state of the soil profiles, interviews with the local farmers and land managers have been conducted and undisturbed sites have been identified.

Figure 20 Unimproved environments along the Sacramento River with undisturbed channels and woodlands (left) and unimproved pasture (right).

Agriculturally used areas are different types of orchards (mainly walnut and peach), fields that include all ploughed areas within the research area, and improved pastures that are disced with a disc harrow on a regular basis. In this campaign it was not possible to sample most of the orchards within the setting of the research area because property access was restricted, thus knowledge on the influence of orchards on XS ^{210}Pb activity profiles remain unclear.

Figure 21 Examples for managed landscapes in the research area, ploughed fields (left) and improved pasture (right).

3. METHODS

This thesis tries to bridge millennial scale evolution of the fluvial system with decadal to century scale floodplain development, therefore a combination of dating methods has been applied to account for the different timescales involved. To reconstruct the long-term evolution of the system a combination of radiocarbon (^{14}C, half-life 5730 ± 40 years), and Optically Stimulated Luminescence dating (dating range 0.1 ka – 100 ka) has been used on samples from deep pits (2 – 5 m). For last century's deposition and erosion different ^{210}Pb (half-life 22.3 years) dating models have been applied to short (< 1 m) cores.

The methods chapter follows the following outline. In chapter 3.1. the general sampling strategy and the sample distribution throughout the research area is described.

In chapters 3.2. and 3.3. the methods that are applied to investigate the late Quaternary evolution of the Sacramento River are presented. In chapter 3.2. the basic principles of optically stimulated luminescence dating are described. In chapter 3.3. the basics of radiocarbon dating are outlined. These dating methods in combination with stratigraphic records of the research area are used to reconstruct the long term evolution of the Sacramento River and link the recorded stratigraphic units to palaeoenvironmental conditions, answering questions about the long term evolution of the Sacramento River.

In chapter 3.4. the fundamentals of ^{210}Pb dating are outlined. In this context the used CICCS, CIRCAUS-CNAXS, and CIRCA models are described. Also problems with ^{210}Pb dating in agriculturally used landscapes are discussed. This is used to research whether XS ^{210}Pb dating is a suitable tool to investigate the spatial, and temporal distribution of sediments in this environment. After determining the applicability of the method, XS ^{210}Pb dating is used to calculate sedimentation rates throughout the research area, as well as implemented to date single events in suitable cores.

3.1. Sample Distribution and Strategy

A total of 15 detailed stratigraphic profiles were taken at select locations across the floodplain. Five of these profiles are located in the distal part of the floodplain (T2P1, T1P9, TEP7, TEP8, TEP15), further ten profiles (T1P2, T1P3, T1P4, T1P5, T1P6, T2P12, T2P13, T2P14, T3P10, T3P11) were obtained within the modern meander belt (Figure 22, Figure 23) to reveal the late Quaternary and Holocene development within the different old floodplain channel systems. Additionally, 78 shallow cores have been collected to reveal the deposition history of the past ~ 70 years.

The deep profiles (blue, Figure 22, Figure 23) that were used to reconstruct the long-term evolution of the Sacramento River are located at elevated positions on the floodplain to avoid the potential loss of stratigraphic evidence through erosion, and consequently to get a more complete picture of the late Quaternary. The deep profile pits within the Holocene meander belt were placed at subsequent channel scars throughout the research area to investigate the timing of the westward movement of the Holocene meander belt.

Short cores (< 1 m) for XS ^{210}Pb analysis were collected at the sites of deep profiles as well. Additionally, cores for XS ^{210}Pb analysis were collected at sites that are likely to be undisturbed and that provided a high chance to provide suitable profiles with preserved and datable events within the research area. Not a criteria for choosing XS ^{210}Pb cores was its suitability for the reconstruction of sediment distribution and dispersal throughout the system.

18 cores have been collected prior to this thesis by Rolf Aalto and Mike Singer, of which 4 (LSL1, LSL2, LSF-T, MSLSF32) have been prepared and measured by Rolf Aalto (Singer & Aalto unpublished). Additional 4 have been partially prepared and measures by Rolf Aalto (LSD 1 – 4). The 10 remaining cores collected prior to this study, and all cores collected during this study have been prepared and measured by the author. The interpretation of all but one core (LSF-T) has been carried out in this study. A table of which method is used at which site can be found in table 1, appendix A.

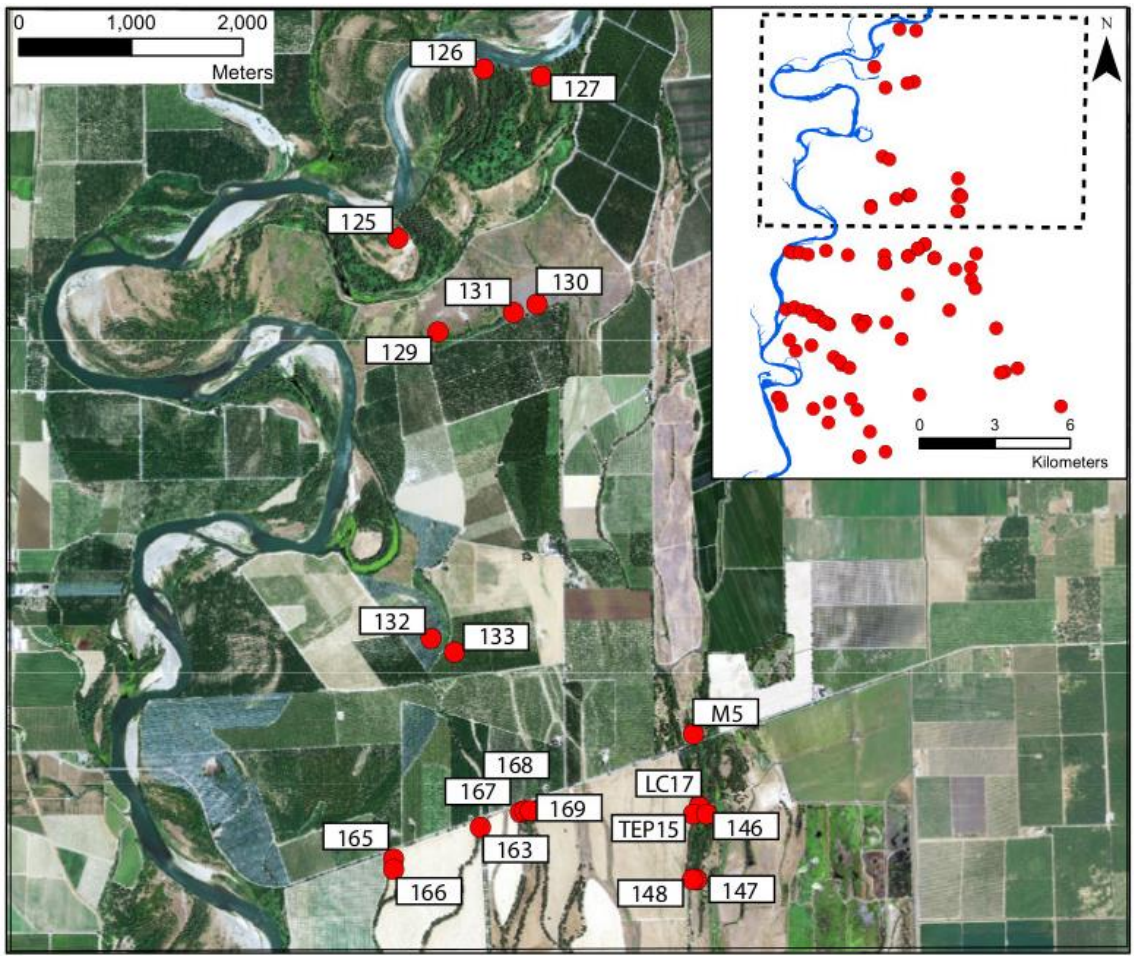

Figure 22 Sample Locations in the Northern Part of the research area (image: googleEarth).

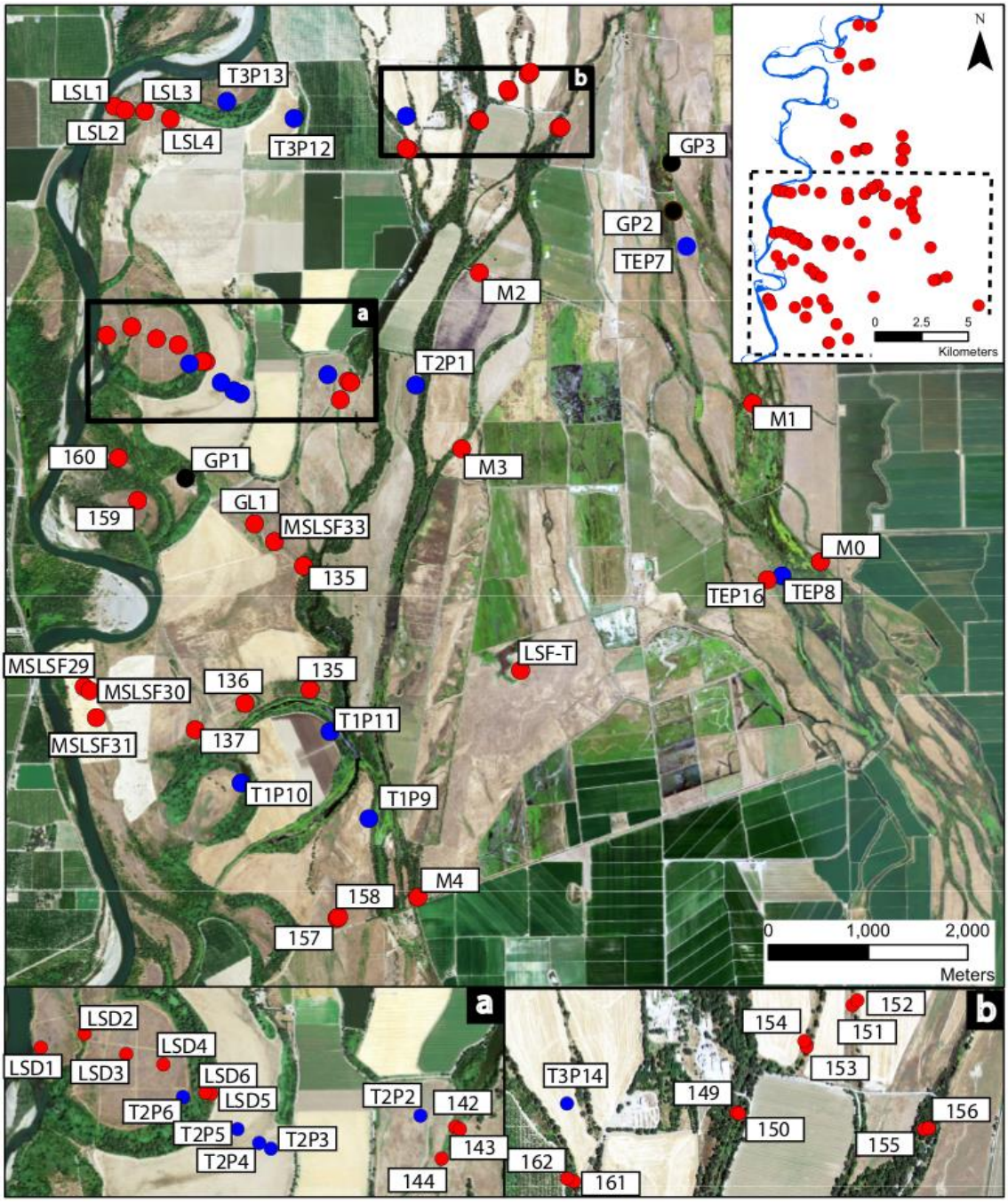

Figure 23 Sample Locations in the southern part of the catchment. Shallow cores were taken at locations marked with red dots, deep pits and cores were sampled at sites marked with blue dots, and gravel pits were sampled at sites marked with black dots. Samples for ^{210}Pb analysis have been collected at all sites, radiocarbon and OSL dating has been conducted on samples collected at deep pits (blue). If possible sample for gravel analysis have been collected in deep pits (blue) and gravel pits (black) (images: googleEarth).

3.2. Optical stimulated luminescence dating

The phenomenon of luminescence of rocks has been known since the time of Ancient Greece, and was already described by Aristotle (Harvey 1957). Since the 1950s Luminescence dating is one of the standard methods for the dating of archaeological samples, and Quaternary sediments (e.g. Aitken 1998; Wagner 1998; Preusser et al. 2008). Optical stimulated luminescence has first been applied with green laser stimulation in the 1980s (Huntley et al 1985). The most commonly used aspects of luminescence in geoscience are thermo- (heat) and optically stimulated luminescence, while the use of other aspects of luminescence is less common, or still in development (e.g. Post IR-IRSL, radioluminescence) (e.g. Preusser et al. 2008; Yukihara & McKeever 2011).

Luminescence dating employs the ability of crystals to act as a quasi radiometer. Luminescence uses the imperfections in a crystal for energy to be stored in electron holes. This energy for the excitation of electrons in a crystal is provided by ionising radiation from radioactive decay of the surrounding material and gamma radiation. Optical stimulated luminescence (OSL) dating dates the last incident a grain of Quartz or Feldspar mineral was exposed to light and buried thereafter during its last reworking cycle. During the exposure to the stimulant (light or heat) the luminescence signal of a crystal is removed (bleached). After the now bleached grains are covered and shielded from light the signal recharges due to the surrounding radiation. A more complete overview on luminescence dating can be found for example in Aitken (1998), Wagner (1998), Preusser et al. (2008), and Yukihara & McKeever (2011).

The burial age or luminescence age [3.1.] is calculated by dividing the energy the collected by the sample (palaeodose D_E*[Gy]*) by the energy emitted by the surrounding sediment plus gamma radiation (dose rate $\dot{D}$*[Gy/ka]*).

$$Luminescence\ Age\ (A)\ (ka) = \frac{D_E\ (Palaeodose)[Gy]}{\dot{D}\ (Natural\ Dose\ Rate)[Gy/ka]} \qquad [3.1.]$$

OSL has been applied to aeolian, colluvial, and fluvial archives and became one of the standard methods for dating Holocene and Late Quaternary sediments. It has been successfully proven in many prior studies of sedimentation within river system (e.g., Rittenour 2008; Fuchs et al. 2010;

Fuchs et al. 2011). Nevertheless, river sediments still provide a challenge for OSL dating, due to insufficient bleaching of the sediment potentially due to its transport position at the bottom of the water column. To account for the possibility of insufficient bleaching of material the method developed by Fuchs & Lang (2001) has been applied. This method implies that not all grains are (fully) bleached and the aliquots that show the lowest palaeodoses consist only or mostly of grains that have been bleached during the last transportation process and therefore are more likely to represent the burial age of the sample. These are the selected to reconstruct the palaeodose of the sample (Fuchs & Lang 2001). For sediments that were found to be insufficiently bleached, it was assumed that the obtained ages might be overestimating the real age of the dated sediment, and in that case these dates were treated as maximum ages.

There are several methods of detecting the luminescence signal, but the most commonly used method is the single aliquot regeneration-dose protocol introduced by Murray and Wintle (2000) that has been applied in this study. In this method all measurements are carried out on each aliquot of a sample. After recording the natural signal increasing amounts of radiation are applied to the aliquot. After measuring several of these regeneration dose points in a final step the lowest regeneration dose point is repeated to detect potential sensitivity changes during the repeated irradiation (Murray & Wintle 2000, 2003).

In this study the SAR protocol has been applied to the coarse grain fraction (90 – 200 µm) of quartz minerals, and using small aliquots (~ 200 grains) to detect incomplete resetting of the OSL signal during the last cycle of sediment reworking (Fuchs & Wagner 2003). The equivalent dose for the method proposed by Fuchs & Lang (2001) was calculated using the luminescence package (Kreutzer et al. 2012) developed for the R© software. Ages were calculated using the ADELE OSL analysis software (Kulig 2005).

Sample Preparation and Measurement

In order to obtain undisturbed material for luminescence dating samples have been collected using either 5 cm diameter aluminium tubes, or during night time using subdued red illumination and transferring the samples to opaque bags for transport. Sample preparation was carried out using the standard laboratory procedure at the OSL laboratory in Bayreuth described in

Fischer (2009, unpublished) and Fuchs et al. (2010). In the laboratory, sample preparation for luminescence analysis was carried out under low intensity red illumination with a wavelength of 640 ± 20 nm. If samples were collected in aluminium tubes ~ 3 cm each side of the tube has been removed to account for possible light exposure. Samples have been wet sieved to extract the 90 – 200 µm (coarse grain) fraction. After sieving, the samples have been treated with 10 % HCl and 10 % H_2O_2, to remove carbonate and organic material. Between treatments, the samples have been thoroughly washed with deionised water. After the removal of carbonate and organic matter, the samples have been washed and subsequently dried in a drying oven at no more than 50° C. Quartz (density 2.65 g/cm^3) has been separated from feldspar and heavy minerals using litium-heteropolytungstate density liquid at 2.62 g/cm^3 and 2.75 g/cm^3 respectively (Mejdahl 1985). Between density separation runs, samples have been thoroughly washed with deionised water and dried at no more than 50° C. Following, the quartz sample has been etched for at least 45 minutes with 40 % HF in order to remove the remaining feldspar minerals and the alpha-irradiated outer layer of the quartz grains. After etching the sample with HF, the sample was treated with 10 % HCl to remove remaining fluorides and washed thoroughly again. After drying (max. 50° C) the sample is sieved with a 90 µm sieve to homogenise the remaining sample. The fraction > 90 µm of the samples are mounted on aluminium cups using silicon to fixate the sample (Fuchs et al. 2010).

The luminescence signal was measured using a Risø-Reader TL/OSL-DA-15, stimulating with blue LEDs (wavelength 470 ± 30 nm). The reader uses a Thorn-EMI 9235 photomultiplier in combination with a 7.5 mm U-340 Hoya filter with a detection window of 290 – 370 nm. For irritation a 90Y/90Sr β-source is used.

3.3. Radiocarbon Dating

Radiocarbon dating is one of the oldest and most established dating methods for Quaternary sediments (Libby et al. 1949). Atmospheric radiocarbon (^{14}C), formed in the upper atmosphere, is absorbed by living organisms and stored in their tissue. Uptake of ^{14}C ends as soon as the organism dies and the decay of ^{14}C starts. ^{14}C decays with a half-life of 5730 ± 40 years (Goodwin 1962) but in radiocarbon dating an earlier approximation of the half-life of 5568 ± 30 years is used (Arnold & Libby 1949), to ensure that radiocarbon ages produced before 1962 can be compared to later ages, even though Libby (1967) suggested that the half-life established by Goodwin (1962) would be more accurate.

The uptake of radiocarbon by living organisms is dependent on the presence of ^{14}C in their environment. The production and subsequent concentration of atmospheric ^{14}C was varying over time, thus ^{14}C years do not equal calendar years. The dating of dendrochronological dated samples has shown that radiocarbon ages are generally underestimating the correct age of the samples (e. g. Renfrew 1973; Pearson et al. 1986; Hajdas et al. 1993). Several correcting calibration curves have been developed by correlating ^{14}C ages to independently dated dendrochronological, annually laminated sediments, and speleothem records to account for the natural variations in atmospheric radiocarbon, and the error created by the use of the Libby radiocarbon decay rate, and present more reliable ages for dated samples (e.g. Bard et al. 1990; Stuiver et al 1998; Raimer et al 2004; Fairbanks et al 2005; Raimer et al 2009; Weninger & Jöris 2009; Raimer et al 2013). Radiocarbon ages are always presented in years before present (BP) or after calibration as calibrated years before present (cal BP), with “present” being represented by the year 1950 AD. Radiocarbon dating and its application is discussed in detail by e.g. Walker (2005), Hajdas (2008, 2009), and Olson (2009).

Samples for ^{14}C dating were mainly obtained from in situ burned layers or by using plant macro fossils (identified in the soil profiles) to minimise the possibility of dating reworked material first buried in a former deposition cycle. Following the assumption that older organic material might have been reworked

and incorporated in younger sediment, ^{14}C ages should be treated as maximum ages.

The radiocarbon dating was conducted by the NSF AMS-Facility in Arizona. Obtained radiocarbon ages as well as published and uncalibrated radiocarbon ages were calibrated with the software CALIB 6.1.0 (Stuiver et al. 2005) using the IntCal09 calibration curve (Reimer et al. 2009) to enable the comparison with published records, and ages obtained by other dating methods.

3.4. High-resolution XS ^{210}Pb activity profile analyses - a tool for sedimentation process and land-use reconstruction

3.4.1. The use of fallout ^{210}Pb in the detection of deposition and land-use, and its application in dating last century's deposition

Fallout radionuclides like ^{210}Pb (half-life 22.3 a) have been widely used as tracers for deposition and erosion in marine, lacustrine, fluvial and colluvial environments (e.g., Goldberg 1963; Krishnaswany et al. 1971; Koide et al. 1972; Walling & He 1998; Walling et al. 2003; Appleby 2008). To apply fallout radionuclides more efficiently and to a greater variety of archives several models have been developed to reconstruct erosion and deposition rates (e.g. Walling & He 1994; Caroll & Lerche 2003; Appleby 2008; Aalto & Nittrouer 2012). ^{210}Pb as a dating tool has mainly been used in marine and lacustrine environments (e.g. summary by Appleby 2008) before Walling & He (1994) (He & Walling 1996b) successfully applied the CICCS ^{210}Pb model to reconstruct sedimentation rates in fluvial environments.

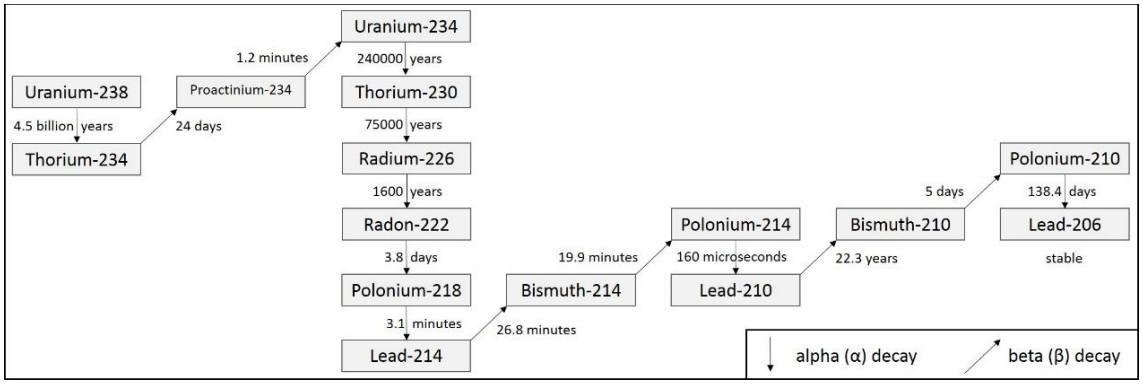

Figure 24 Uranium-238 decay chain with ^{210}Pb at the lower end of the decay chain with ^{210}Po just above the stable ^{206}Pb as the suitable element for α-detection.

Experiments have shown that 90 % of ^{210}Pb is adsorbed to the sediment within the first 3 cm of a given soil profile under laboratory conditions, while penetration depth is significantly higher under natural conditions (He & Walling 1997). The penetration depth in natural soil profiles can varying due to soil characteristics and the influence of bioturbation (e.g. He & Walling 1996; Mabit et al 2008; Resner et al 2011; Perreault et al 2012). When natural conditions prevail, ^{210}Pb penetrates up to 20 cm below surface. Up to 95 % of meteoric ^{210}Pb is deposited in the uppermost 10 cm of the profile (Mihailović et al. 2014;

Ötzdem et al. 2013; Vaaramaa et al. 2010; Doering et al. 2006; San Miguel et al. 2004).

Most of the studies focusing on ^{210}Pb analysis were designed to quantify sediment movements along slopes, on floodplains, or in lacustrine/marine environment and not specifically to analyse changes in XS ^{210}Pb activity profiles. The profile analyses in the study presented here were generally designed to distinguish between stable, eroding, and depositing sites and identify deposition events that can be used for CIRCAUS/CNAXS dating (Aalto & Nittrouer 2012) using XS ^{210}Pb inventories. However, farming activity in the area also made it necessary to account for potential influences of land use on XS ^{210}Pb activity profile development.

The chosen high-resolution sampling of XS ^{210}Pb will provide the necessary resolution, to distinguish between genuine deposition profiles and anthropogenically-influenced cores. It also enhances the ability to distinguish between individual depositions events in this low deposition environment (as compared to the more common 2 – 3 cm resolution). This is especially the case for environments where average deposition rates are rather lower than ~ 5 – 10 mm per year.

Sampling at 2 cm resolution works best for identifying accumulation events of > 4 – 6 cm (Aalto & Nittrouer 2012), but it still can be vulnerable to disturbance of the soil profile, e.g. by ploughing or intensive soil reworking by bioturbation (e.g., Walling & He 1994; Resner et al. 2011). Reducing core-sampling intervals to 1 cm enhances the ability to detect smaller deposition events (~ 3 cm) and enables the detection of profile disturbances more clearly. In some cases it might be possible to mathematically enhance the calculated size of deposition events to a sub-centimetre resolution.

Unsupported ^{210}Pb activity profiles have been analysed in different land use settings in floodplain and colluvial archives in the UK (He & Walling 1997). In this study clear differences between unimproved sites and ploughed fields were apparent. Unimproved sites showed a steep decrease in XS ^{210}Pb from the surface before reaching background levels of XS ^{210}Pb. Ploughed fields showed a constant level of XS ^{210}Pb from the surface to plough penetration depth and an immediate decline in XS ^{210}Pb activities below (He & Walling 1997,

Figure 25). Similar trends in XS ^{210}Pb activity profiles for unimproved and ploughed sites have been observed in other studies: in humid (He & Walling 1997; Wakiyama et al. 2010), in Mediterranean (Porto & Walling 2012; Gaspar et al. 2013) and in semiarid climates (Walling et al. 2003; Mabit et al. 2008; Kato et al. 2010; Benmansour et al. 2013; Damnati et al. 2013).

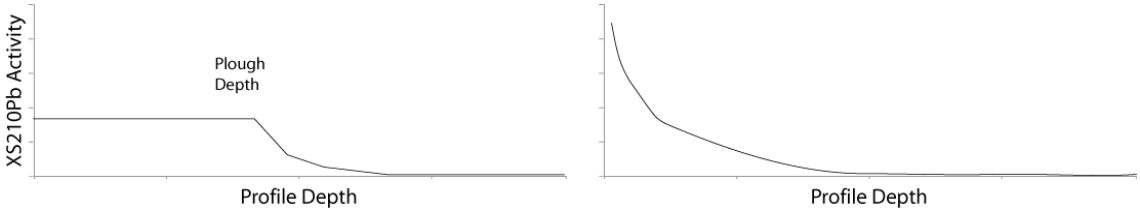

Figure 25 Simplified XS ^{210}Pb activity profiles for cultivated (left) and undisturbed profiles (right) summarized from He & Walling (1997), Walling et al. (2003), Mabit et al. (2008), Porto & Walling (2012), Benmansour et al. (2013), and Gaspar et al. (2013).

An influence that often cannot be accounted for, but is assumed to influence the shape the XS ^{210}Pb activity profile are burrowing animals (He & Walling 1997; Resner et al. 2011). Resner et al. (2011) reported a change in the general shape of the XS ^{210}Pb due to the invasion of non-native earthworms. In this study non-invaded soils showed a steeper decline and reached earlier background values than soils invaded by earthworms (Resner et al. 2011). Nonetheless, a deeper understanding of the influence of farming techniques and bioturbation on the shape of XS ^{210}Pb activity profiles as a potential source for misinterpretations caused by equifinality of deposition profiles and agricultural reworked profiles is missing.

The concept of equifinality in geomorphology describes the notion that there is a possibility that similar (land)forms can be the product of different (geo)morphological processes, and/or different initial conditions (e.g. Chorley 1962; Haines-Young & Petch 1983). In this study it is possible that several cores show similar XS ^{210}Pb activity profiles, but the processes involved in creating these XS ^{210}Pb activity profiles differ. This equifinality of sedimentation and land use signatures in XS ^{210}Pb activity profiles is one of the largest challenges of CIRCAUS/CNAXS ^{210}Pb profile analysis and dating in anthropogenically used landscapes. The shape of XS ^{210}Pb activity profiles is in general influence by at least 4 – 5 controlling factors. One controlling factor is the atmospheric deposition of ^{210}Pb on the surface that is affecting only near surface parts of the profile (He & Walling 1997). The 2nd controlling factor is sediment deposition that influences the profile by adding (potentially varying)

XS ^{210}Pb to the profile (e.g. Aalto & Nittrouer 2012). A third controlling factor is natural diffusion of ^{210}Pb by burrowing animals (e.g. Resner et al. 2011). A factor that has limited influence on larger scales but can impact profiles strongly locally are natural scours. The final and probably most influential factor controlling XS ^{210}Pb profiles in anthropogenically used areas are human activities that disturb the upper parts of a XS ^{210}Pb profile like ploughing, discing, and other earth movements (e.g. He & Walling 1997). Only deposition of sediment and atmospheric ^{210}Pb influences the depth integrated ^{210}Pb inventory, while other influences on XS ^{210}Pb profiles (bioturbation, and anthropogenic influence) are not influencing the XS ^{210}Pb inventory.

This issue has not been fully addressed in previous studies that apply CIRCAUS/CNAXS dating to pristine floodplains (Aalto & Nittrouer 2012). However, post sedimentary profile alterations have been reported by He & Walling (1997) and Resner et al. (2011) and other studies have been located in anthropogenically altered landscapes (Singer & Aalto 2009; Singer et al. 2008). If one acknowledges the potential of equifinality, an in depth investigation of the influence of different land-uses is important to differentiate between cores that have been influenced by anthropogenic surface reworking and cores that show natural processes. Given that the research area is or has been used for agricultural purposes, it is of critical importance to be able to identify and distinguish agricultural and sedimentary characteristics in XS ^{210}Pb profiles.

In order to differentiate between influences of different environmental / depositional settings and land use on depth distribution of XS ^{210}Pb, sediment cores were collected at sites that represent the four predominant recent land cover types in the research area (improved and non-improved pasture, woodland, and arable fields). For the selection of environments, the most common landscape features were identified by field mapping and discussions with local farmers. These different environments have been sampled at different topographic positions within the landscape, to avoid bias towards site-specific effects like anthropogenic alteration or bioturbation by earthworms and other burrowing animals. To account for land use practices and potential past-changes in these practices in the past, interviews were conducted with local farmers and farm workers, as well as areal images were studied to evaluate

changes in land use and the history of farming techniques used for the different types of land cover.

In the past ^{210}Pb detection has been relatively inaccurate due to the utilisation of gamma counting, therefore detailed in depth analyses of high-resolution cores was consequently difficult (Aalto & Nittrouer 2012). The analyses of activity depth profiles has so far been limited to environments showing homogenous grain size distribution because of the affinity of ^{210}Pb for clay particles that has been recognised by e.g. Nittrouer et al. (1979), He & Walling (1996), and Goodbred & Kuehl (1998). Additionally, the high error in ^{210}Pb measurements (30 – 50%) and large sample volumes (7 – 50 g) using Gamma Spectrometric detection of ^{210}Pb was limiting the potential of XS ^{210}Pb activity profile analyses (Zaborska et al. 2007; Aalto & Nittrouer 2012). Another benefit of Alpha Spectroscopy is the fact that only the activity of ^{210}Pb adsorbed to the sediment is measured, so only the geochronologically critical component of the ^{210}Pb activity is analysed, without having to account for the significant influence of sediment locked ^{210}Pb (Aalto & Nittrouer 2012).

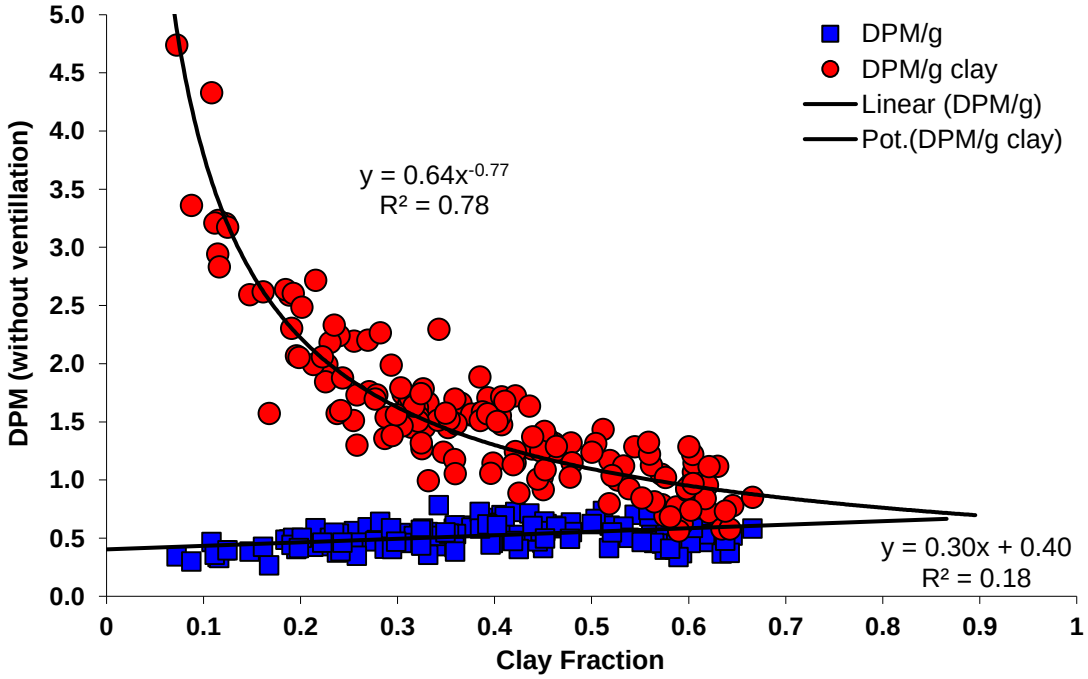

Figure 26 Site-specific asymptotes for supported ^{210}Pb derived from terrace and deep profile cores showing a strong correlation between XS ^{210}Pb activity and clay content.

The progress in the ^{210}Pb analyses of fluvial sediments using clay normalised ^{210}Pb activity profiles (He & Walling 1996; Goodbred & Kuehl 1998) and specific corrections for reach dependent sediment activity (Aalto & Nittrouer

2012) reduced the errors in XS ^{210}Pb activity determination and dating, and opened up more possibilities in XS ^{210}Pb analyses of cores. With the introduction of clay normalisation, higher resolution analysis of cores using primarily the clay-adsorbed ^{210}Pb component is now applicable. The resolution that can be obtained by using the described additions is now only limited by the sampling interval (Aalto & Nittrouer 2012). In this study XS ^{210}Pb activity depth profiles were analysed at a high resolution (1 – 2 cm) using the advantages of the low analytical errors (~ 3 %) of alpha detection (Aalto & Nittrouer 2012), to gain insights in the specific XS ^{210}Pb distributions of different sedimentation and mechanical reworking scenarios.

An additional issue that has been addressed is the strong correlation between soil organic matter and ^{210}Pb activity (e.g. Dorr & Munnich 1989; Aslani et al. 2005; Narayana et al. 2006; Vaaramaa et al. 2010; Ötzdem et al. 2013; Mihailović et al. 2014), however the extremely low organic matter content (< 2 %) in the soils in this area (see below) does not make it necessary to account for organic matter content separately.

Three models are applied to floodplain locations in this study, the CICCS model (Walling & He 1994; He & Walling 1996b) and the CIRCACS, CIRCAUS/CNAXS models developed by Aalto & Nittrouer (2012). Walling & He (1994) assumed a constant initial concentration of deposited sediment at a site and constant sedimentation in addition to a constant fallout rate of ^{210}Pb from the atmosphere. The CIRCAUS/CNAXS model (Aalto & Nittrouer 2012) assumes that sediment deposited within floodplains of large river systems has a constant reach dependent initial concentration of XS ^{210}Pb that is mainly adsorbed and transported by clay particles ($A_{CIRCA\text{-}XS}$, Figure 26). If the surface is stable after deposition, meteoric fallout of ^{210}Pb leads to the development of a “meteoric cap” of XS ^{210}Pb in the profile. A meteoric cap of XS ^{210}Pb describes the decrease of XS ^{210}Pb activity with depth on top of an activity plateau (A_{cXSsed}, Figure 27).

The calculation of XS ^{210}Pb activity using alpha spectroscopy requires the external calculation of supported ^{210}Pb activity. For that Aalto & Nittrouer (2012) illustrated that the supported ^{210}Pb activity is dependent on the clay content of the sample. Therefore, the normalisation for clay content can be used to calculate XS ^{210}Pb activity from alpha spectroscopy using the CNAXS

(clay normalised adsorbed XS ^{210}Pb) model. In this approach it is assumed that only the grain size fraction < 4 µm is responsible for the transport of XS ^{210}Pb, and other fractions are not contributing to the transport of XS ^{210}Pb and can therefore be neglected (Aalto & Nittrouer 2012). This approach is feasible because XS ^{210}Pb is mainly adsorbed and transported by clay minerals (Walling et al. 1992; He & Walling 1996; Goodbred & Kuehl 1998; Aalto et al. 2008; Aalto & Nittrouer 2012). Local supported ^{210}Pb from in situ ^{226}Rn was calculated using samples collected below the significant influence of ^{226}Rn ventilation from sediment recovered from deep trenches, scour sites and the bottom regions of long cores. This approach creates a normalisation function to predict support activity as a direct function of clay content using these undisturbed samples (Aalto & Nittrouer 2012).

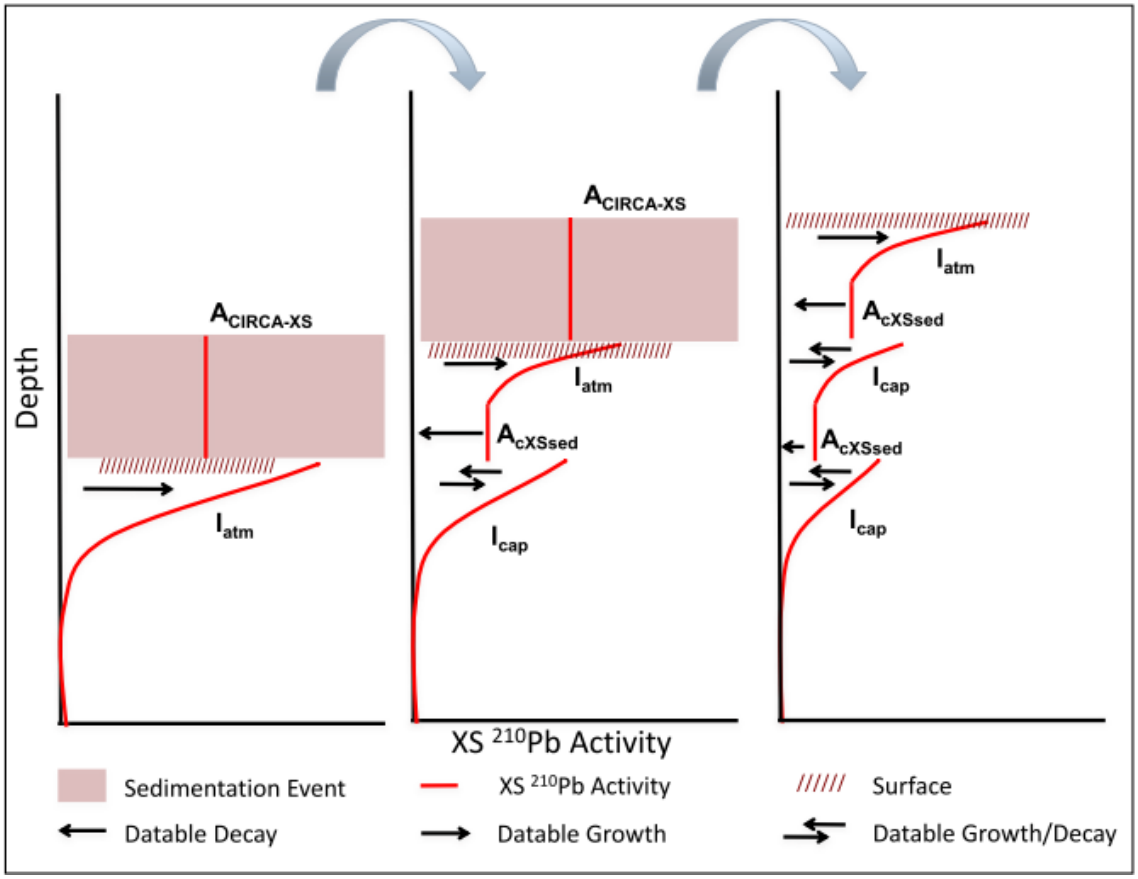

Figure 27 Schematics of episodic deposition of 2 sediment lenses on top of a long-term stable surface. $A_{CIRCA-XS}$ here is the clay-normalised activity of the incoming sediment. I_{atm} is the natural fallout inventory for an undisturbed stable profile. I_{cap} is the inventory of a XS ^{210}Pb cap on top of a XS ^{210}Pb activity plateau, A_{cXSsed} is the activity of said activity plateau.

To utilise the model developed by Aalto & Nittrouer (2012) a reach dependent clay normalisation has to be established to account for the variation in supported ^{210}Pb activity with clay content (Figure 26). After this has been established, the XS ^{210}Pb activity can be determined by subtracting the

supported activity from the measured total activity, and thereafter the growth time of caps and the decay of XS ^{210}Pb of deposited sediments can be dated. In a final step the radon ventilation has to be accounted for.

CICCS (Walling & He 1994; He & Walling 1996b) erosion and sedimentation rates assume that fallout of ^{210}Pb in an area is constant as well as the sedimentation of unsupported ^{210}Pb via floodplain sedimentation remains constant over time.

The natural fallout inventory was calculated by locating undisturbed sites outside the recently flooded area that are unlikely to have received any sediment within the last century from natural or anthropogenic processes. Three of these sites are within the research area (M2, TEP16, LSF-T) and one has been collected outside or the immediate research area (Cemetery). M2 and LSF-T are on the high part in the centre of Llano Seco and were collected at sites well outside the potential area of anthropogenic impact, and flooding. TEP16 is located on an elevated part of the floodplain at the far southern end of Llano Seco on an unimproved pasture. The core outside of Llano Seco was collected in an historic cemetery close to a 19th century gravestone. For this site it is assumed that the age of the grave is an indication that the side was probably not disturbed within the last century.

The sedimentation rate (R measured in cm/a) is calculated using the decay constant of ^{210}Pb (λ_{Pb} = 0.031a^{-1}), the content of unsupported ^{210}Pb deposited on the floodplain (C_i) and the catchment derived inventory (I_{ex}) (Walling & He 1994; He & Walling 1996b) [3.2.].

$$R = \lambda_{Pb} \frac{I_{ex}}{C_i} \qquad [3.2.]$$

For dating plateaus after Aalto & Nittrouer 2012 [3.3.] it is assumed that deposited sediment in a certain reach arrives with a stable XS ^{210}Pb activity, because the sediment is homogenised during transport. The clay-normalised activity of the incoming sediment at a certain river reach can be established from freshly deposited sediment lenses or clearly defined sediment plateaus with undisturbed caps ($A_{CIRCA\text{-}XS}$) and the clay-normalised average of a clearly visible plateau has to be calculated (A_{cXSsed}) (Figure 28). Then, the radioactive

decay of ^{210}Pb is calculated (using the decay constant for ^{210}Pb (λ_{Pb} = 0.031a^{-1})) to establish the sedimentation age by:

$$T_{sed} = -ln\frac{(A_{cXSsed})/(A_{CIRCA-XS})}{\lambda_{Pb}} \quad [3.3.]$$

The dating of caps with the CIRCAUS approach [3.4.] utilises the knowledge of the atmospheric fallout rates of ^{210}Pb in an area. This fallout is visible as cap on top of a plateau of similar XS ^{210}Pb activities. The growth age of this cap (T_{cap}) can be determined using the plateau as the baseline for this cap. Assuming the fallout rate is constant, the age can be calculated using the decay corrected relation between measured cap inventory (I_{cap}) and the inventory of the natural occurring fallout (I_{atm}) (Figure 28).

$$T_{cap} = -ln\frac{1-(I_{cap}/I_{atm})}{\lambda Pb} \quad [3.4.]$$

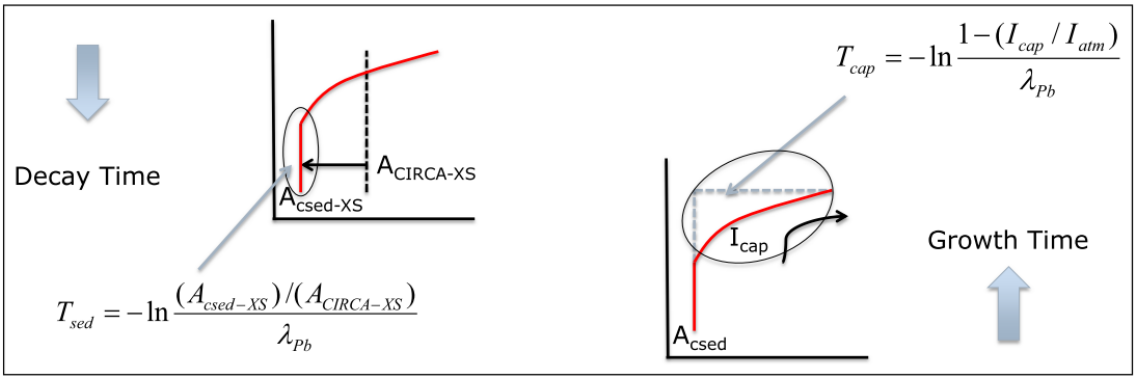

Figure 28 Components of the CIRCAUS dating model. On the left hand site is the process of ^{210}Pb decay depicted used to calculate the age of ^{210}Pb activity plateaus. Depicted on the right is the subsequent growth of a meteoric cap which inventory is used to date ^{210}Pb growth ages.

To date a deposition event (T_{sedn}) using buried caps [3.5.], the calendar age can be calculated using the sum of the age of the sediment plateau emplaced above the earlier deposition event, or burial age (T_{bur}) plus the age of the underlying cap within the depositional event (T_{cap}).

$$T_{sedn} = T_{bur} + T_{cap} = T_{bur} + [-ln\frac{1-(I_{cap}/I_{atm})}{\lambda Pb}] \quad [3.5.]$$

3.4.2. Sampling and sample preparation for high-resolution XS ^{210}Pb analyses

If one is to reliably use XS ^{210}Pb profiles to date deposition events it is of crucial importance that the XS ^{210}Pb activity profiles represent undisturbed sedimentation events, and are not influenced by post-sedimentational changes in the profile. Post-sedimentational changes include bioturbation, and anthropogenic activity like deliberate sediment redistribution or agricultural use of an area. To minimise land-use influences and the resulted XS ^{210}Pb variations and potential misinterpretations of individual cores, at least 3 cores were collected for each environment. The sediment cores were collected in clear 2.5 cm diameter tubes and sealed in the field to avoid profile disturbance and contamination. Cores were packed horizontally after collection and shipped to Exeter (UK) where they were stored in a cold store (4° C). In the laboratory the sediment cores were cut and sampled in 1 cm or 2 cm intervals. These intervals were chosen to best provide a suitably high-resolution XS ^{210}Pb activity profile, as well as to yield enough sample material for grain size analysis and alpha spectroscopy. The ^{210}Pb activity was measured indirectly using the detection of the alpha decay of the ^{210}Pb granddaughter nuclide ^{210}Po. This way sample size can be reduced to as little as 0.5 – 1.0 g and the precision of measurement can be greatly improved to ~ 3 % in comparison to 30 – 50 % using Gamma Spectroscopy (e.g., Aalto & Dietrich 2005; Aalto & Nittrouer 2012).

Samples were disaggregated and dried for approximately 24 hours at 50° C before they were weighed and dry mass was measured for each sample volume to calculate down profile density changes. Large organic matter and visible gravel were removed before the samples were homogenised and split for further analyses. 1 – 5 g were used for ^{210}Pb geochemistry and 3 – 5 g used for grain size analyses. Samples were analysed following the method elaborated in Aalto & Nittrouer (2012) using the α-decay of ^{210}Po – a daughter nuclide of ^{210}Pb. ^{210}Po was autoplated on silver discs for approximately 24 hours in a 0.3 N HCl solution produced from the sediment. This solution is produced by geochemical leaching of the sample using 12 N HNO_3 and 6 N HCl subsequently brought to near boiling point on a hotplate (e.g., Aalto & Nittrouer

2012). The air-dried silver discs were measured for 72 – 168 hours for α-decay to ensure to get at least 500 counts per sample using Ortec Ultra-AS counters.

The clay normalisation process was modified for distal floodplain cores in this study, because the informed estimate of the analytical error for grain size measurements using Micromeritics Sedigraphs (± 5 %)[2] exceeds the grain size variability within most of the cores in the distal part of the floodplain. For these areas of low grain size variability the clay content was measured for at least 3 locations per core profile, and if the grain size variability was lower than the analytical error the average grain size of the core has been used for clay normalisation. The obtained XS ^{210}Pb activity profiles were analysed and compared for representative activity/depth changes in each sedimentation and land use category and with representative profiles that have been created to visually illustrate profiles under certain sedimentation and land use conditions.

3.4.3. Adaption of ^{210}Pb dating for on-site conditions, and the advantages and applications of high-resolution sampling for XS ^{210}Pb analysis in a heterogeneous landscape

The following argument is based on the CIRCAUS (constant initial reach clay activity, unknown sedimentation)/CNAXS model proposed by Aalto & Nittrouer (2012).

The independent dating of meteoric caps and sediment of an individual event (after Aalto & Nittrouer 2012) can be used to test if the location is eroding or infilling after initial deposition of sediment. This approach only works at sites were post depositional sediment mixing can be excluded. For this the CIRCAUS/CNAXS approach developed by Aalto & Nittrouer (2012) can be modified comparing the CIRCAUS/CNAX cap age with the CIRCAUS/CNAX plateau age. For long-term stable and undisturbed sites the sediment age (T_{sed}) and the cap age (T_{cap}) would both result in be indefinable, for all other sites that have been stable for a prolonged period, but not long enough to have accumulated the total fallout inventory, the cap age would match the deposition age [3.6.].

[2] This estimate is based on the error of the used Micromeritics Sedigraph III and 5100 and an informed estimate for the error from incomplete soil homogenisation and biased splitting.

$$T_{sed} = T_{cap} \rightarrow \frac{T_{cap}}{T_{sed}} = 1 \qquad [3.6.]$$

Following this argument values > 1 indicate infilling tendencies at a given profile, due to the arrival of XS ^{210}Pb activity in deposited sediment and values < 1 indicating erosion tendencies due to the removal of XS ^{210}Pb at the profile. This should also be true for buried caps assuming that the burial age (T_{burn}) of a given cap equals the sedimentation age of the cap above, then:

$$T_{sedn} = T_{burn} + T_{capn} \rightarrow \frac{T_{burn} + T_{capn}}{T_{sedn}} = 1 \qquad [3.7.]$$

Using this assumption, changes (erosion or deposition) in a profile after deposition of a sediment lens and therefore changes in sedimentation style can be detected, if post sedimentation soil mixing can be excluded.

In addition to the dating of sediment lenses and the reconstruction of post deposition changes in sediment profiles it is also possible to reconstruct the thickness of single sedimentation events with higher precision than the sampling interval following the assumptions above. For the calculation of a mixing depth in a profile, at least two deposition events with well-defined and datable XS ^{210}Pb activity plateaus are needed. These plateaus have to be topped by meteoric fallout caps for both of the events (Figure 28, Figure 30). Between these two events one sample must exist that is clearly detectable as one that cannot be associated with either of these events (sample M, Figure 28, Figure 30). The activity of this sample has to be between the activity of the plateau above (Figure 28, *x1*, Figure 30, $A_{cXSed\ e1}$) and the maximum value of the cap below (Figure 28, Figure 29, *x2*).

$$M > x1 \text{ or } A_{cXSed\ e1} \quad \text{and} \quad M < x2$$

To be able to resolve cores below the resolution they were sampled in, certain preconditions are required to be fulfilled: At least two different sedimentation events are clearly detectable and an outlier (*M*), clearly identifiable as such, must be present between these two events (e1, e2). This is the case where a sample point showed increased values to the baseline of the younger sedimentation event (e1) between two distinct sedimentation events and decreased values to the maximum activity of the cap topping the older sedimentation event (e2). In this case assuming a) there has not been a

deposition event < 1 cm and b) bioturbation can be excluded (bioturbation was negligible in the profiles of this area) a simple mixing model can be used to calculate the boundary between both sedimentation events as well as increase the accuracy of the dating of event 1 and 2.

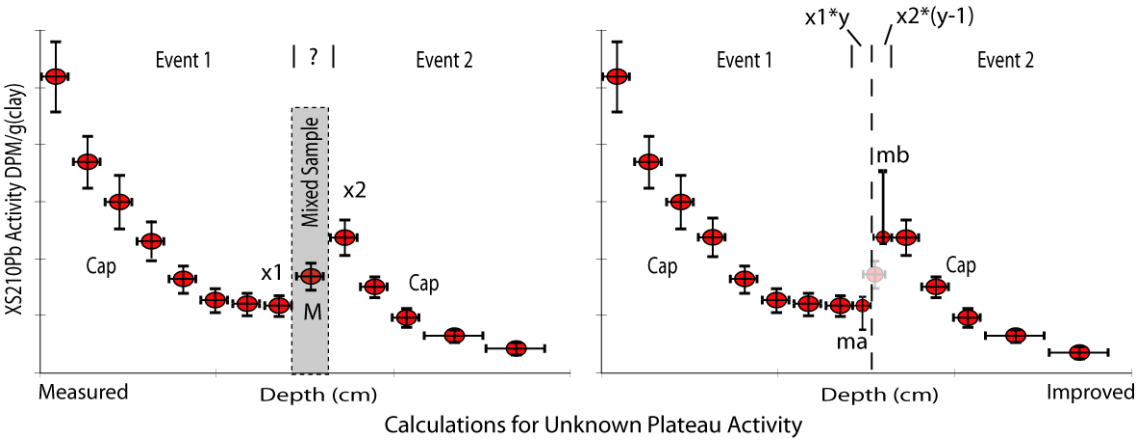

Figure 29 Calculation of mixing depth using a simple mixing model with well-defined caps and plateaus based on the assumptions by Aalto & Nittrouer (2012). Application of a simple mixing model used for profiles with not well defined activity plateaus. Formulas used to define the mixing depth are shown in [1.6] and [1.7].

Following this argument it can be assumed that the value of the upper fraction of the mixed sample (*M*) is equal or smaller than the value of the sample above (x_1) ($m_a \leq x_1$) and the lower part equal or larger than the value of the sample below (x_2) ($m_b \geq x_2$) therefore:

$$M = m_a + m_b \qquad [3.8.]$$

To determine the percentaged influence (y[0,1]) of the sediment below and above on the mixed sample, the assumptions discussed above dictate that $m_a = x_1 * y$ and $m_b = x_2 * (1 - y)$. Therefore, for profiles with poorly defined plateaus the following can be assumed:

$$M = x_1 * y + x_2 * (1 - y) \qquad [3.9.]$$

The method can be further refined for well-defined plateaus. To calculate the sediment mixing depth (in % influence [y] of the mixed sample) in well-defined profiles with higher accuracy, the formula can be improved using the assumptions of the CIRCAUS/CNAXS model described by Aalto & Nittrouer (2012).

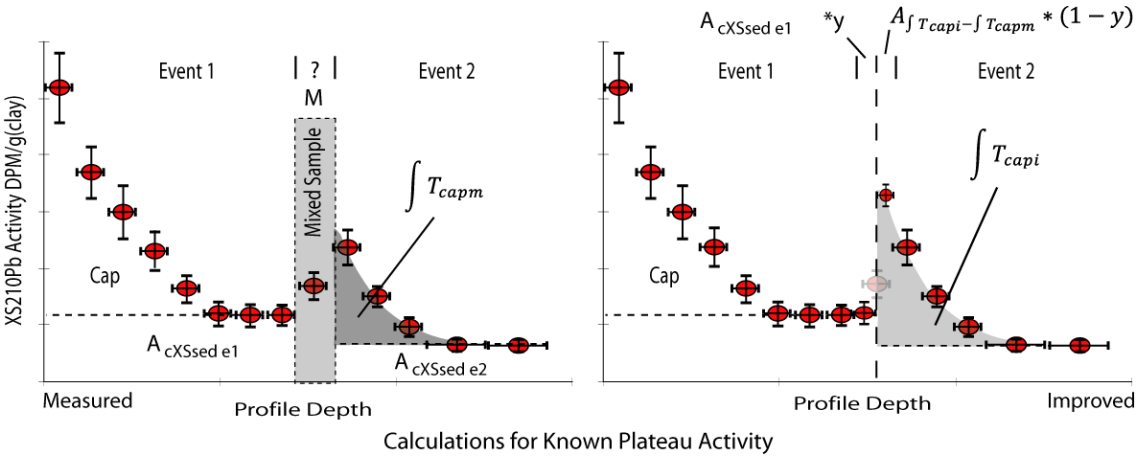

Figure 30 Calculation of mixing depth using a simple mixing model with well-defined caps and plateaus based on the assumptions by Aalto & Nittrouer (2012).

Following the argument above one fraction of the mixed sample (x_1) would match the averaged clay corrected activity of the plateau above the point identified as a mixed value ($A_{cXSsed\ e1}$). To calculate the second fraction of the mixed samples (x_2) the growth time for the cap would have to be calculated by subtracting the plateau age above ($T_{sed\ e1}$) from the plateau age below ($T_{sed\ e2}$). The ideal inventory for the cap can be calculated ($\int T_{capi}$) using the calculated cap age (T_{capi}). The activity attributed to the cap below can therefore be calculated by subtracting the measured inventory ($\int T_{capm}$) from the ideal inventory ($\int T_{capi}$). From that the ideal mixing depth in percent of the mixed sample (M) can be calculated replacing x_1 and x_2 with the calculated activity values:

$$M = A_{cXSsed\ e1} * y + [A_{\int T_{capi} - \int T_{capm}} * (1-y)] \qquad [3.10.]$$

The reconstruction of the ideal mixing depth is only possible/valid if no deposition or erosion occurred between the events sharing the mixed sample, therefore the percentaged influence of the mixing sample (y) has to be between 0 – 100 % (y[0,1]). If $y \neq [0;1]$. Sediment erosion or slow deposition must have happened before the upper deposition event (event 1, Figure 30) has buried the underlying meteoric cap of event 2. In this case it is not possible to calculate the mixing depth, because the ideal inventory of the cap cannot be calculated.

Using this method the thickness of deposition events in well-defined cores can be reduced to approximately ± 10 % of the sampling interval. This improvement of the method could resolve events in suitable cores to a millimetre rather than the original centimetre resolution. Even though this

method has been developed during the course of this thesis it has only been possible to apply this to one core in this study, because of the research area's lack of suitable cores that showed more than one datable activity plateau and meteoric cap.

3.5. Calculation of fluvial sediment transport parameters

For all calculations of distance from channel, distance from the channel is expressed as meters along the most probable flow path from the main stem of the Sacramento River. It is assumed that flow leaves the channel mainly at the allocated natural and artificial flood outlet points (Figure 15).

The elevation of each core has been extracted from a 1.2 m digital elevation model (curtesy to the Nature Conservancy, unpublished). Coordinates and elevations for each site can be found in appendix A. Inundation depth for each site has been calculated from FEMA 100 year flood maps overlain on the 1.2 m DEM. The mapped flood extend is not necessarily in agreement with modern topographical features and elevations. Therefore it was assumed that the extent of the FEMA flood map does not correspond with the exact flood extend and a horizontal error of ± 100 m was applied on cross section elevation data to calculate the flood elevation. From the extracted elevation data the mean, minimum, and maximum elevation values have been calculated and used (Figure 31).

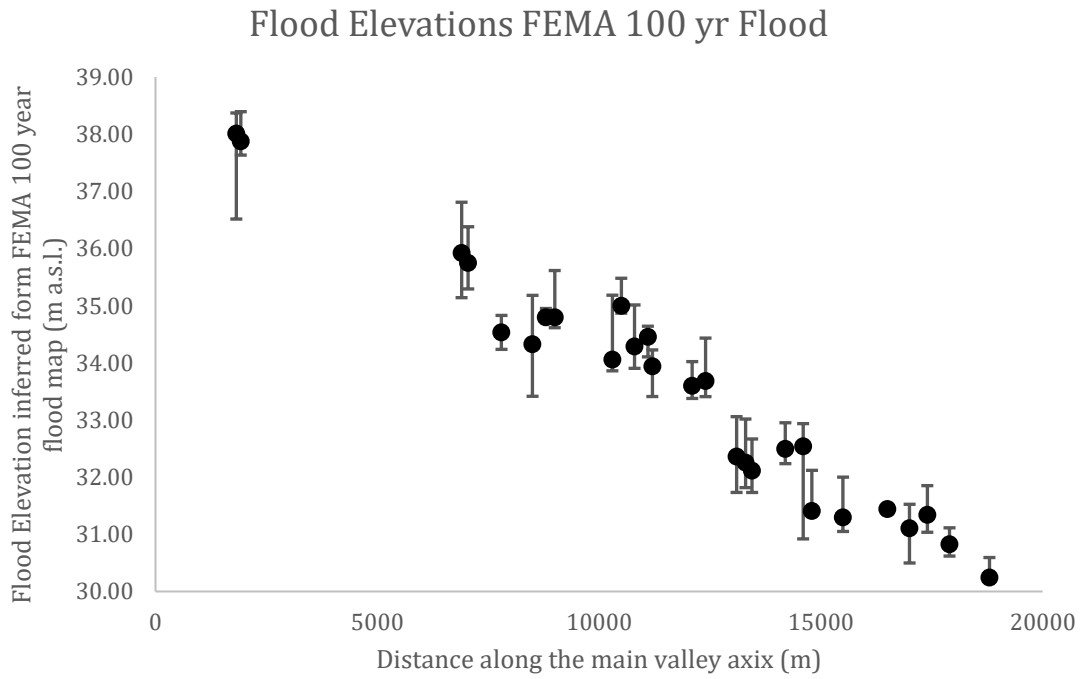

Figure 31 Flow depth of the sites along the main valley axis reconstructed from a 1.2 m DEM (curtesy The Nature Conservancy) and the map of the FEMA 100 year flood extent.

For sample profiles RASRF 125, 129, 130, 131 it was not possible to calculate flood elevation because they are located at the confluence with Little Chico Creek and reconstructed flow elevations would rather represent Little Chico Creek stages and not the flow elevation at the sites. For sample sites

RASRF127, RASRF128 flood elevation can be assumed as too low because these sites are located at a flood outlet with artificial levees preventing the flow to reach the lower elevations the that are shown as flood extend by the FEMA 100 year flood map. Flow reconstructions from the FEMA 100 year flood map have to be treated with caution because of the high uncertainties associated with them (Figure 32).

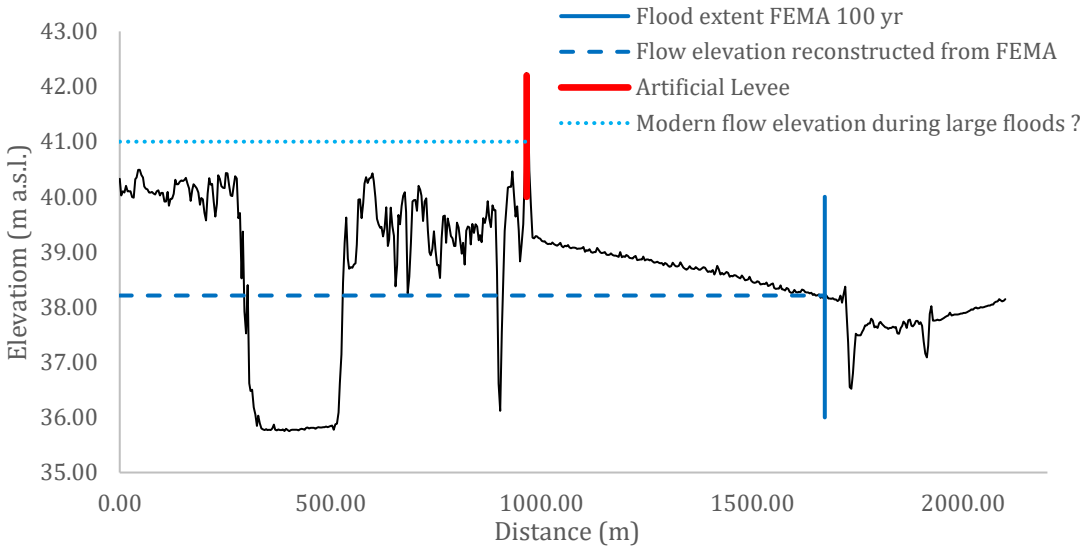

Figure 32 Cross section at RASRF126 illustrates the problems with reconstructing flood elevations from FEMA 100 year flood layer.

The average amount of sediment per flood has been calculated by calculating the area for each windowed distance from the closest upstream flood outlet and overlay these areas with the FEMA 100 year flood extent. It is assumed that the first 500 m from the main stem are flooded all along the Sacramento River. It is also assumed that not all surface areas have been flooded each flood, so an informed estimate of 80 % surface inundation has been chosen. These 80% of flooded surface have been multiplied with the average sedimentation rate for each windowed distance. Results have been multiplied by the average density of floodplain deposits in the research area (~ 1.59 t/m^3) to get an estimate for the amount of sediment deposited on the floodplain. It was also accounted for a biannual reoccurrence of floods that inundate the floodplains of the research area.

4. RESULTS

The first subchapter is presenting results that are concerning the long term evolution of the Sacramento River (4.1.). First the results from OSL and ^{14}C dating and gravel counts are presented (4.1.1., 4.1.2.) and subsequently are placed in the spatial, topographic, and stratigraphic context of the research area (4.1.3.). These results are there to support the discussion of the long term evolution of the Sacramento River.

Chapters 4.2.1. and 4.2.2 trying to determine the influence of land use on XS ^{210}Pb activity profiles that influences the interpretation and applicability of dating XS ^{210}Pb cores. In chapter 4.2.1. the natural fallout inventory of the research area is calculated and presented. In chapter 4.2.2. the general shape of XS ^{210}Pb activity profiles is presented for different environmental and processual settings. The analysing has been developed as part of this thesis and proved to be vital for XS ^{210}Pb dating in agriculturally used landscapes.

In chapter 4.3. CIRCAUS/CNAXS dating results are presented from suitable cores. The results from dating are compared with the Sacramento River flood records.

In chapter 4.4. the results concerning the spatial distribution of sedimentation along the Sacramento River floodplain is presented.

4.1. The late Quaternary evolution of the Sacramento River

4.1.1. Dating

The application of different dating methods proved to be vital for dating the floodplains along the Sacramento River. While some sediments lacked organic remains for radiocarbon dating, in other sediments the luminescence properties were poor due to insufficient bleaching during transport.

OSL ages range from 1.4 ± 0.2 ka in the modern meander belt to 33.7 ± 5.1 ka dating fluvial sands on the Pleistocene terrace. Almost all age determinations are aligned in stratigraphic order and only one age inversion has been observed (T2P1_200). Sample T2P1_200 is assumed to show insufficient bleaching and therefore is discarded, because 2 radiocarbon ages above and 3 OSL ages below are significantly younger than the discussed sample (Table 2).

Table 2 Results of the OSL and 14C dating campaign

Location	Profile	Depth	Lab Nr						Age (ka)
OSL				Paleodose (Gy)			Dose Rate (Gy/a)		
Eastern Channels	TE P7	100	BT792	8.04	±	0.81	1.44	± 0.25	**5.6 ± 0.8**
		135	BT881	5.93	±	0.61	1.41	± 0.28	**4.2 ± 0.7**
		270	BT882	19.22	±	1.93	1.39	± 0.22	**13.8 ± 1.7**
	TE P8	110	BT883	31.72	±	4.11	1.12	± 0.24	**28.2 ± 4.8**
Western Channels	T2 P1	200	BT855	76.37	±	8.73	2.27	± 0.43	**33.7 ± 5.1**
		340	BT869	48.10	±	4.93	1.89	± 0.35	**25.5 ± 4.0**
		380	BT870	43.51	±	6.65	1.84	± 0.42	**23.7 ± 4.0**
		420	BT868	40.52	±	4.12	1.80	± 0.29	**22.5 ± 2.8**
	T1 P9	145	BT864	10.51	±	1.10	1.78	± 0.33	**5.9 ± 0.9**
		195	BT865	48.31	±	6.47	1.87	± 0.40	**25.8 ± 4.3**
		395	BT876	59.63	±	6.64	1.78	± 0.41	**33.5 ± 6.8**
Modern Meander Belt	T1 P10	235	BT866	2.97	±	0.30	2.12	± 0.37	**1.4 ± 0.2**
Radiocarbon				Radiocarbon Age					Age cal BP (Reimer et al 2009)
Western Channels	T2 P1	120	AA88364	3520	±	160			**3823 ± 418**
		160	AA87461	4780	±	61			**5467 ± 143**
	T3 P14	145	AA87462	964	±	36			**863 ± 74**
		287	AA88367	5540	±	700			**6206 ± 1583**
Eastern Channels	TE P15	330	AA93275	3031	±	38			**3219 ± 138**
Modern Meander Belt	T1 P11	90	AA87464	312	±	58			**392 ± 108**
	T2 P3	295	AA87468	2390	±	110			**2449 ± 292**
	T2 P4	125	AA87467	225	±	34	modern		**210 ± 210**
		190	AA88366	92	±	58	modern		**136 ±136**
		250	AA88365	161	±	34	modern		**142 ± 142**
	T2 P5	380	AA87468	2001	±	38			**1962 ±91**
	T3 P12	105	AA87463	220	±	35	modern		**209 ±209**

4.1.2. Gravel Composition

Gravel samples have been collected at seven sites throughout the research area (T2P1, T2P3, TEP7, TEP8, GP1, GP2, and GP3) and in the bed of the modern Stony Creek. At the other sites it was not possible to collect samples, because gravel could not be reached or not retrieved in necessary quantity. The collected samples have been analysed for their geologic composition and provenance by emeritus Professor Ken Aalto. For each site at least 47 – 199 pebbles were analysed (appendix B). The most common geology in the samples is quartz and argillite associated with vein quartz with an abundance of 28 – 58 % (Figure 33). All gravel samples show at least 15 – 20 % silt and sandstones, indicating a strong influence of the Stony Creek tributary on the geologic composition of the gravel deposits in the research area. The third most common rock type is chert (red, green, gray) with an abundance of 12 – 34 %. While green chert is present in all samples, gray chert is missing in two locations (Stony Creek, GP3), and red chert is missing in profile TEP7. Greenstone is abundant in all sample locations varying from 3 – 31 %. Low concentrations of conglomerate were present in sample locations GP1, GP3, TEP8, and T2P3. Granite was detected in samples from site GP1, GP3, and T2P3. None of the collected samples showed any indication of Andesite, the characteristic geology for the Modoc Plateau and the Cascade Range, but missing in Coast Range gravel (Figure 7, Figure 30). In none of the gravel samples Andesite is present that would indicate the influence of Modoc Plateau or Cascade Range geology on the composition of fluvial gravel in the profiles.

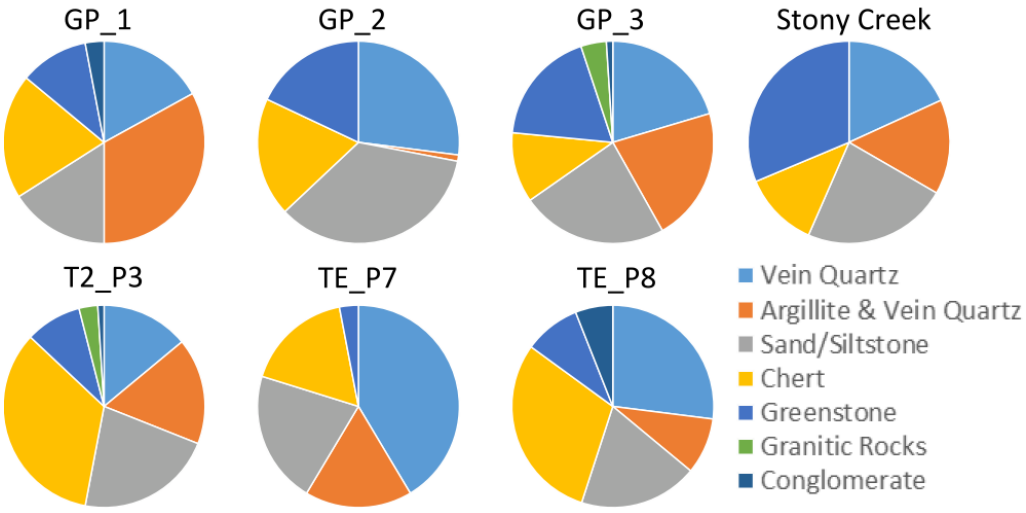

Figure 33 Distribution of rock abundance in gravel samples collected throughout the research area. There is no Andesite present in any of the samples that would indicate that some of the gravel collected are partially sourced from the Modoc Plateau or the Cascade Range.

4.1.3 Spatial Analysis of Stratigraphic Units

4.1.3.1 The Distal Channel Profiles

Three different sedimentary units that demarcate distinct changes in sedimentation style have been identified in exposed distal floodplain profiles. The base of each sedimentary sequence consists of a homogenous gravel deposit (Figure 34, Figure 35) with a lithology that shows characteristic of the Coast Range provenance (geologic analysis executed by emerit. Prof. Ken Aalto, appendix B). However, between the sample locations no clear trend of gravel distribution can be found (Figure 33).

The discussed sedimentary unit is overlain by fluvial sands. Clay- and silt-rich floodplain deposits without evident carbonate cover this sandy unit (Figure 34, Figure 35). At two locations within the eastern channel system (GP2, GP3), the sandy sediment is missing and the silty-clay unit is directly overlying gravel deposits, potentially separated by an erosional discontinuity but the archives did not show this conclusively. The existence of a soil developed atop the sandy deposit, and the presence of a buried petrocalic or duric layer within the upper part of the sands both indicate that stable conditions existed for a considerable amount of time before the initiation of the distal overbank deposition that emplaced the floodplain loams (Figure 34, Figure 35).

The sequence described above can be observed at many locations across the floodplains (T2P1, T1P9, TEP7, TEP8) of the research area, despite the fact that the upper limits of gravel deposits are located at different relative elevations and that sequences show differently strong soil development at different locations (Figure 34, Figure 35). The different elevations are likely to represent remnants of the palaeo-topography, for example different lobes of the Stony Creek fan system, but also later neo-tectonic movements cannot be excluded as a reason for the different relative elevations of the stratigraphic units.

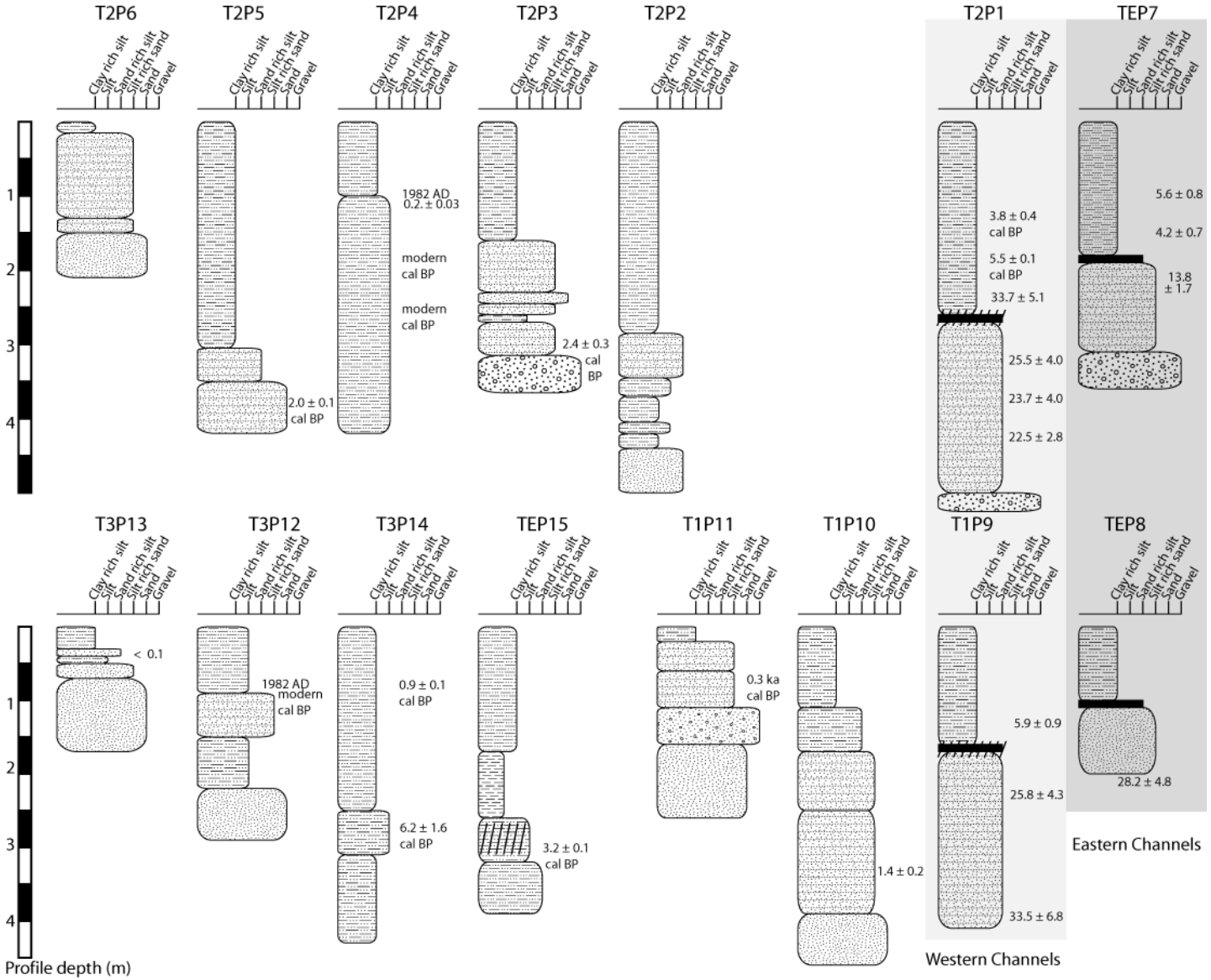

Figure 34 Schematic stratigraphic profiles of the Sacramento River floodplain. The profiles show grain size distributions and important soil layers. Dating results are presented in ka. Modern sediments that have been dated using a modern marker layer are presented as event year AD. Duric and petric layers are indicated by solid black lines. Soil development is marked by hatches.

Only one profile will be described in detail here but can be used as type location for the Llano Seco terrace. T2P1 the most extensively studied and most complete profile is located on an elevated floodplain in the centre of Llano Seco. It can be described as a type profile for the Llano Seco terrace. At the site 2 m of homogeneous floodplain loams with a sand content of < 5 % are deposited on top of a soil that is developed within sandy silts (>10 % sand, ~ 70 % silt). Within these 2.8 m of sandy silts layers with worm holes or small root canals as well as other indications of initial soil development at different depth. Below the sandy sediments. Below the sands at ~ 5 m below surface gravel can be found, but it was not possible to investigate these further at the site. Dating of the site infers a Holocene age of the floodplain loams, rapid deposition of the sandy sediment around 25 ka, with a stable surface after the initial deposition of the sandy loams. Nothing can be said about the transition between the gravel and sands at the site but other location suggest a rapid change in sediment size and thus sedimentation conditions.

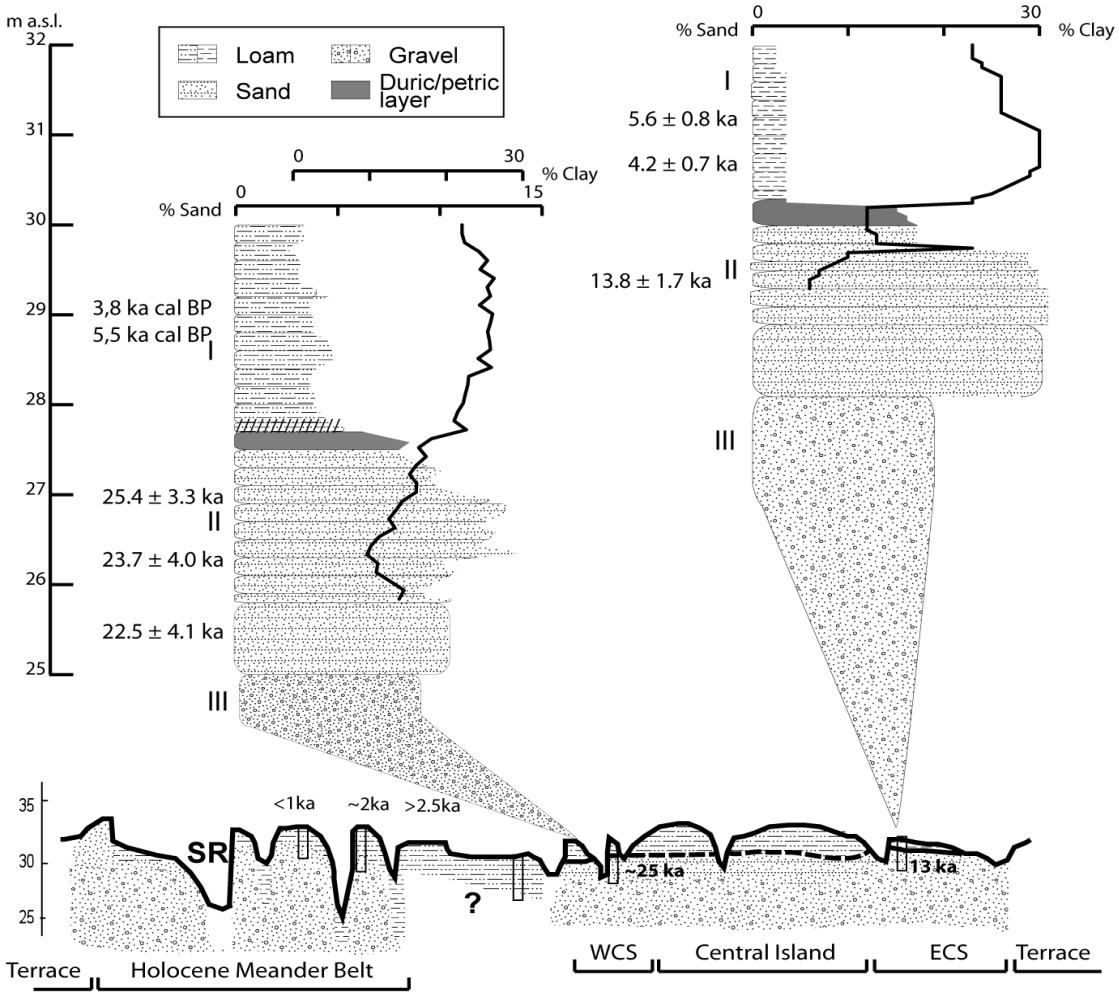

Figure 35 Comparison of stratigraphic profiles, between the eastern (TEP7) and the western (T2P1) channel systems. At another profile in the eastern channels the sands have been dated to 28.2 ± 4.8 ka, a similar age to the ages obtained in the western channels.

Summary

U/Th dating of calcite crusts around gravel (-121.926053; 39.604426) show early to middle Wisconsin ages (77 ± 25 ka) for the gravel deposits (Maher written communications 2012). It is possible that these ages overestimate the actual age of the gravel deposit, because it is possible that calcite crusts were deposited at an earlier time and that these inherited calcite crusts that developed prior to the last deposition event have been dated. Thus the age calculated from the calcite precipitation is treated as maximum age. Nevertheless the dated age fits well in the local stratigraphy.

OSL dating produced mainly pre to early Late Glacial Maximum ages (33.7 ± 5.1 ka to 22.5 ± 2.8 ka, Figure 35, Table 2) of the sandy sediments on top of the gravel deposits in the eastern part of Llano Seco. The narrow time frame of the OSL-ages indicates a relatively short period of sedimentation of the sandy deposits (Figure 34, Figure 35). The sedimentation of sandy deposits starts around 33.7 ± 5.1 ka in the southern part and around 25 ka in the northern part of Llano Seco (Figure 35, Figure 36). Only one sample was dated to a post-LGM age in the sandy deposits within the eastern channel system (13.8 ± 1.7 ka, TEP7). There is a lack of younger sandy deposits and a soil is developed on top of the sandy deposits in several parts of the floodplain channel system in Llano Seco (T1P1, T3P9, TEP7, TEP8) suggesting a stable surface after the deposition of the sandy sediments in parts of the research area.

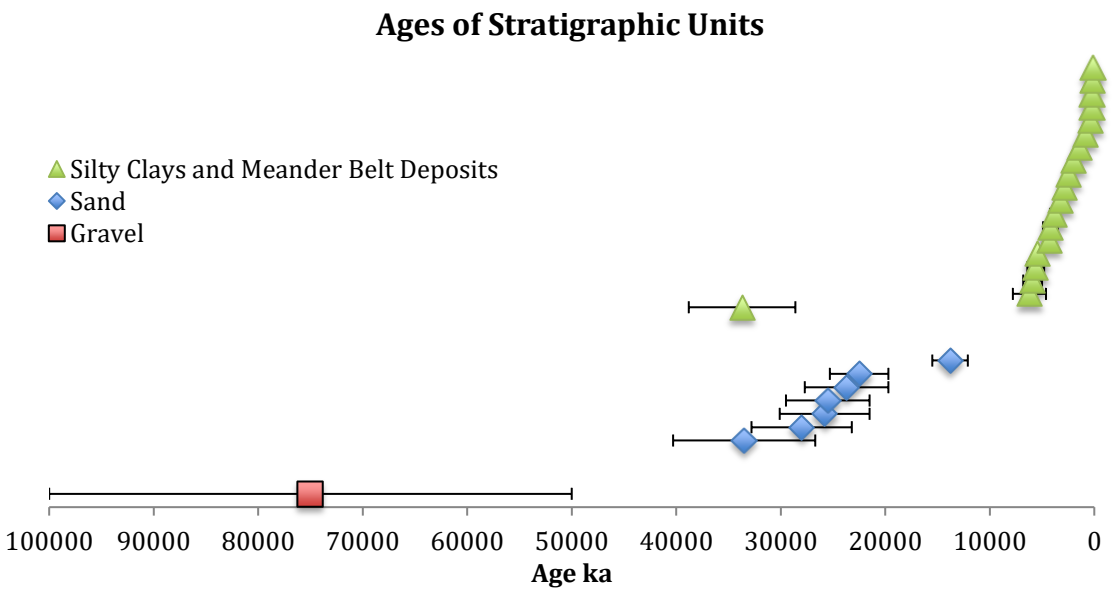

Figure 36 Age distribution of this study according to stratigraphic units. Only one age calculated is not in the general age range of the stratigraphic unit.

By the early Holocene slow overbank sedimentation had started across the floodplains. The onset of floodplain sedimentation is not dated because dating attempts at this crucial profile location repeatedly failed in profile T2P1, but the sedimentation of fines started probably in the early Holocene, because a sample within the floodplain loams ~ 1 m above the soil topping the sandy sediments was dated to 5.5 ka cal BP (T2P1, Figure 34, Figure 35). This onset of floodplain deposition is confirmed by two ages in different profiles dated to 5.9 ± 0.9 ka cal BP or 6.2 ± 1.6 ka cal BP respectively (T1P9, T3P14, Figure 34). These ages indicate that a meandering system was already established by at least 6.2 ± 1.6 ka cal BP, probably at the start of the Holocene. The floodplains along the eastern channels remained active or exhibited little sedimentation probably until the mid-Holocene. This observation is also supported by a wetland soil buried under 1.5 m of sediment in the northern part of the system that indicates wetter conditions and little sedimentation for the eastern channels at least until ~ 3.2 ka cal BP (TEP15, Figure 34).

4.1.3.2. The Holocene Meander Belt

The western part of the river system is dominated by the incised channel belt of the Sacramento River, which over the past several thousand years has gradually meandered across a zone that is approximately 1 – 2 km wide. In the Holocene a meandering river system was established in the western part of the research area, as indicated by a change of sedimentation towards fine silts and clay all over the floodplain (Figure 34, Figure 35). Infilling rates in the distal part stayed low without large variability during the whole Holocene (Figure 34).

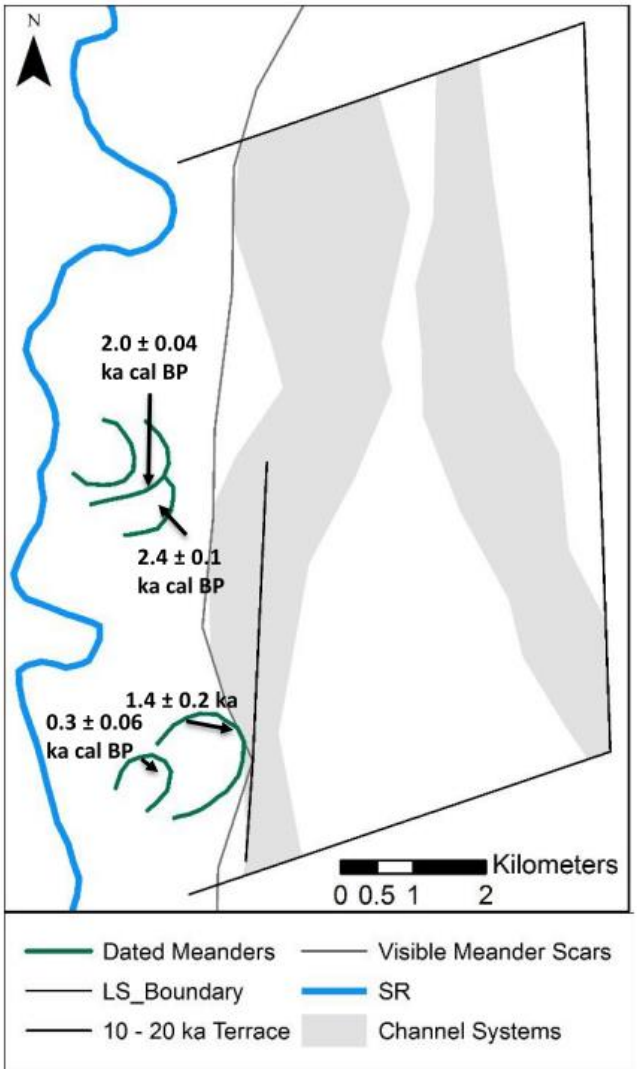

Figure 37 Dated Holocene meanders of the Sacramento River in the context of the known extend of the Holocene meander belt. Maximum eastward extend of the meander belt is the Pleistocene (10 – 20 ka) Llano Seco terrace, the maximum westward extend is often marked by the recent channel of the Sacramento River that is eroding Stony Creek fan material.

The Sacramento River's modern position is at the far west of its Holocene meander belt eroding older Stony Creek fan deposits. This westward migration has been observed in previous studies (Harwood & Helley 1987, WET 1990, Fischer 1994), but the timing of this migration has not been subject to these investigations. In this study the third oldest meander still visible in the topography along this reach of the Sacramento River is dated to 2.4 ± 0.1 ka cal BP, with other ages getting younger towards the west (Figure 37). This trend indicates a westward shift of the Sacramento River since at least 2.4 ± 0.1 ka cal BP. The onset of a westward movement of the active channel happened at least two meander generations earlier because two sets of topographically visible channel scars have been partially eroded by the channel active around 2.4 ± 0.1 ka cal BP. Additionally, the lack of a buried petrocalcic layer east of the topographically visible meander scars and west of the western channel systems outline the extend of the Holocene valley fill and the distance the Sacramento River presumably migrated to its current position during the

Holocene (Figure 35, Figure 37, Figure 37). The evidence indicates an earlier onset of a meandering river and a further extent of meanders to the east, followed by a westward shift of the Sacramento River.

4.1.3.3. Floodplain channels

The dominating topographic features of the Llano Seco floodplain are its prominent sets of ephemeral floodplain channels. Dating applied in this study showed that floodplain channels are almost exclusively developed in Holocene floodplain loams and hardly ever extend into older sedimentary units. The few instances sand or gravel were recorded at the bottom of these channels are at locations where scour occur downstream of bridge crossings, a process that started only recently (after the construction of these engineered structures) when concentrated flows started actively eroding older deposits. The gravel elevations within the research area have been compared with the surface elevations of recent topography (TEP7, Gravel Pit 2). These observations indicate that today's floodplain surfaces are independent from the underlying strata (Figure 38).

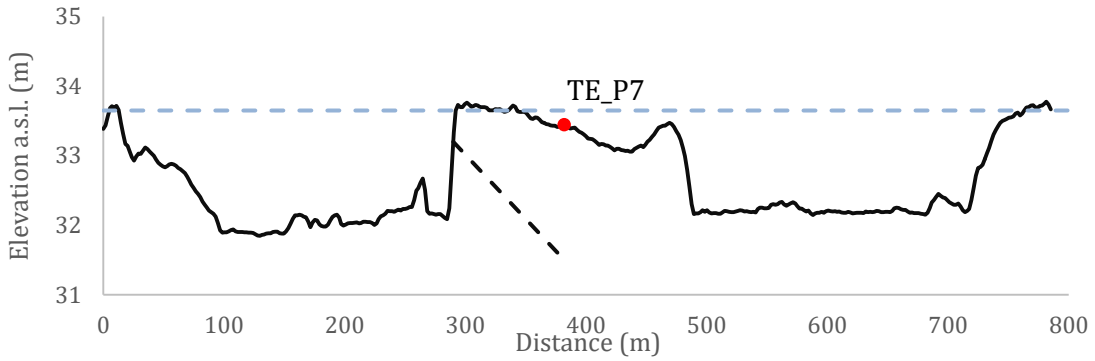

Figure 38 Topographical cross-section at profile location of TEP7. The solid black line shows the present surface, the dotted blue line shows the water surface during 100 a flooding events. The dotted black line connects known gravel elevations at an outcrop close to GP2 and the stratigraphic profile of TEP7. The large difference in elevation indicate that the surface is independent from the underlying strata.

Nonetheless, the ephemeral floodplain channels are not lateral stable features in this landscape, because slow natural lateral erosion of these channels can be observed at multiple locations (e.g. Figure 39), along with sediment erosion and deposition along the channel bottoms following large flood events (see below). This also suggests that these channels are still active landscape elements within an active Holocene floodplain, not an ancient (Mid Quaternary) relic part of the landscape reoccupied by today's processes as formerly assumed (Robertson 1987).

Figure 39 Exposed roots of a valley oak in one of the western floodplain channels in Llano Seco as indication for modern fluvial erosion.

4.2. XS ^{210}Pb Profile Analysis and dating in an agriculturally used landscape

The study was designed to date deposition events along the Sacramento River. During the interpretation process of the XS ^{210}Pb activity profiles it became apparent that land use has a greater influence on the distribution of XS ^{210}Pb activities in soil profiles than any other process. Thus, it became necessary to identify the influence of anthropogenic land use on the profile characteristics to distinguish between genuine deposition and post-deposition land use induced profile disturbance to identify cores that are suitable for dating. Therefore, sediment cores were grouped using land use as denominator to detect potential XS ^{210}Pb characteristic for the present land use types. Cores were collected in unimproved pasturelands from positions outside of potential flooding areas. They were also collected in pastures, woodlands and ephemeral channels with a high flooding frequency. The goal was to analyse down profile changes of XS ^{210}Pb under natural conditions, both for stable and for actively infilling environments.

4.2.1. Natural Distribution in XS ^{210}Pb Activity Profiles

To detect differences in sedimentation styles it is best to use undisturbed cores, because post deposition reworking can destroy potential caps or deposition plateaus (Aalto & Nittrouer 2012) by mixing material of different activities and thereby smoothing the key details from the XS ^{210}Pb activity curve.

Stable conditions

Stable conditions by Walling & He 1994 as well as in this thesis are defined as sites where the total CICCS inventory calculated after Walling & He 1994 matches the total natural fallout inventory of ^{210}Pb of the region, established by averaging cores of undisturbed sites located outside of the natural floodplains. Therefore, stable profiles for the research area are defined as sites with a total XS ^{210}Pb activity of 17.76 ± 0.77 DPM/cm^2 and a steady decrease in XS ^{210}Pb activity with depth.

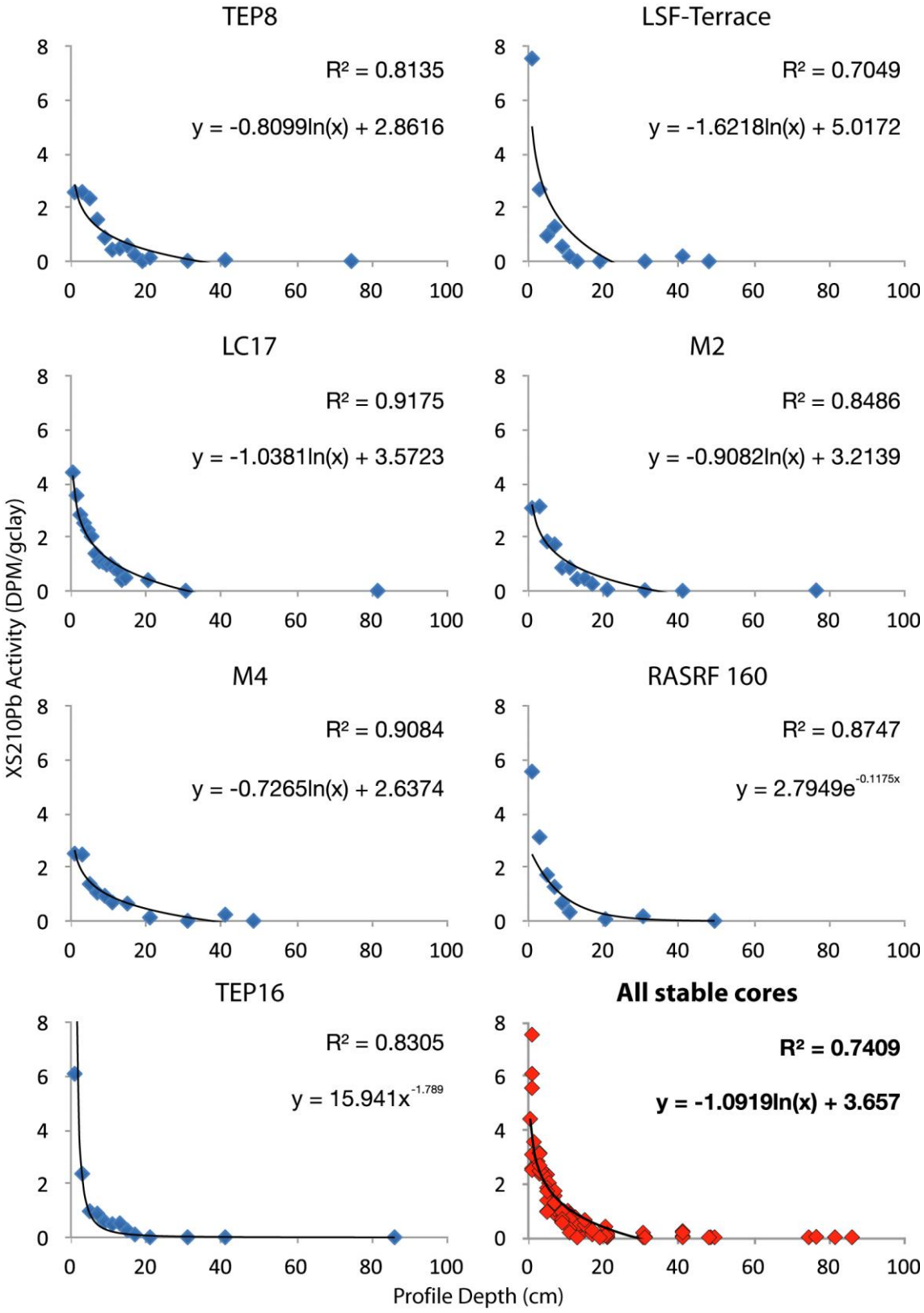

Figure 40 XS ^{210}Pb activities of all stable and not agriculturally impacted cores in the research area. In all stable cores a very clear trend in activities of a steep monotonic decline in XS ^{210}Pb activities can be observed. Additionally there is a distinct lack of activity inversions, both indicate little influence of mechanical reworking of the soil profile by bioturbation. No XS ^{210}Pb activity can be observed below 30 cm. Negative activity values that result from grain size correction and radon ventilation corrections have been assigned the value 0.001 DPM/g_{clay} for presentation purposes.

XS ^{210}Pb activity depth profiles of cores under stable conditions show a steep decline within the first 3 – 5 cm for soil profiles following a steep logarithmic trend. XS ^{210}Pb values are still detectable up until 20 – 25 cm of depth. Bioturbation or post-deposition soil reworking at sites classified as stable and non-infilling is not very intense or variable because the cores do show very similar distributions at each location, steady down core decline of activities and no significant extension of the XS ^{210}Pb activity profiles (Figure 40). CICCS inventories representative of stable conditions were observed at 10 sites within and outside of the natural flood boundaries of which 7 have been used (LSF-Terrace, LC17, M2, M4, RASRF160, TEP8, TEP16). 3 of these profiles showed indications of post-deposition profile modification (non-monotonic decrease in activity) and were not used in the description of stable profiles. All except for two of the collected stable cores show a logarithmic decrease in XS ^{210}Pb values with depth, the two other cores show an exponential decrease with depth (Figure 40).

Steady deposition

For sites that show sediment deposition, the total measured inventory of XS ^{210}Pb is larger than the regions specific fallout inventory of 17.76 ± 0.77 DPM/cm^2, and show a down-core decrease of XS ^{210}Pb activities. The average infilling rate was 0.38 ± 0.16 cm/a, for the 12 sites showing constant sedimentation. Minimum deposition rate for a site was 0.04 cm/a, maximum deposition rate is 0.72 cm/a (Figure 41) spanning a variety of depositional environments (channels, woodlands, pasture). Two profiles RASRF149 and T3P13 show very low deposition rates (0.04 cm/a and 0.06 cm/a) which might also indicate stable conditions, but were deemed to have potentially received minor amounts of sediment as well. The majority of the cores (9 cores = 75 %) with constant deposition showed a logarithmic decrease in XS ^{210}Pb activities within the top 40 – 50 cm with very high values within the first 2 – 4 cm of the core and a slow decrease until XS ^{210}Pb reaches background values between 30 and 80 cm. Just 3 cores reach background levels of XS ^{210}Pb activity within the first 30 cm below surface, with two of them showing the lowest sedimentation rates of the sampled sites (Figure 41).

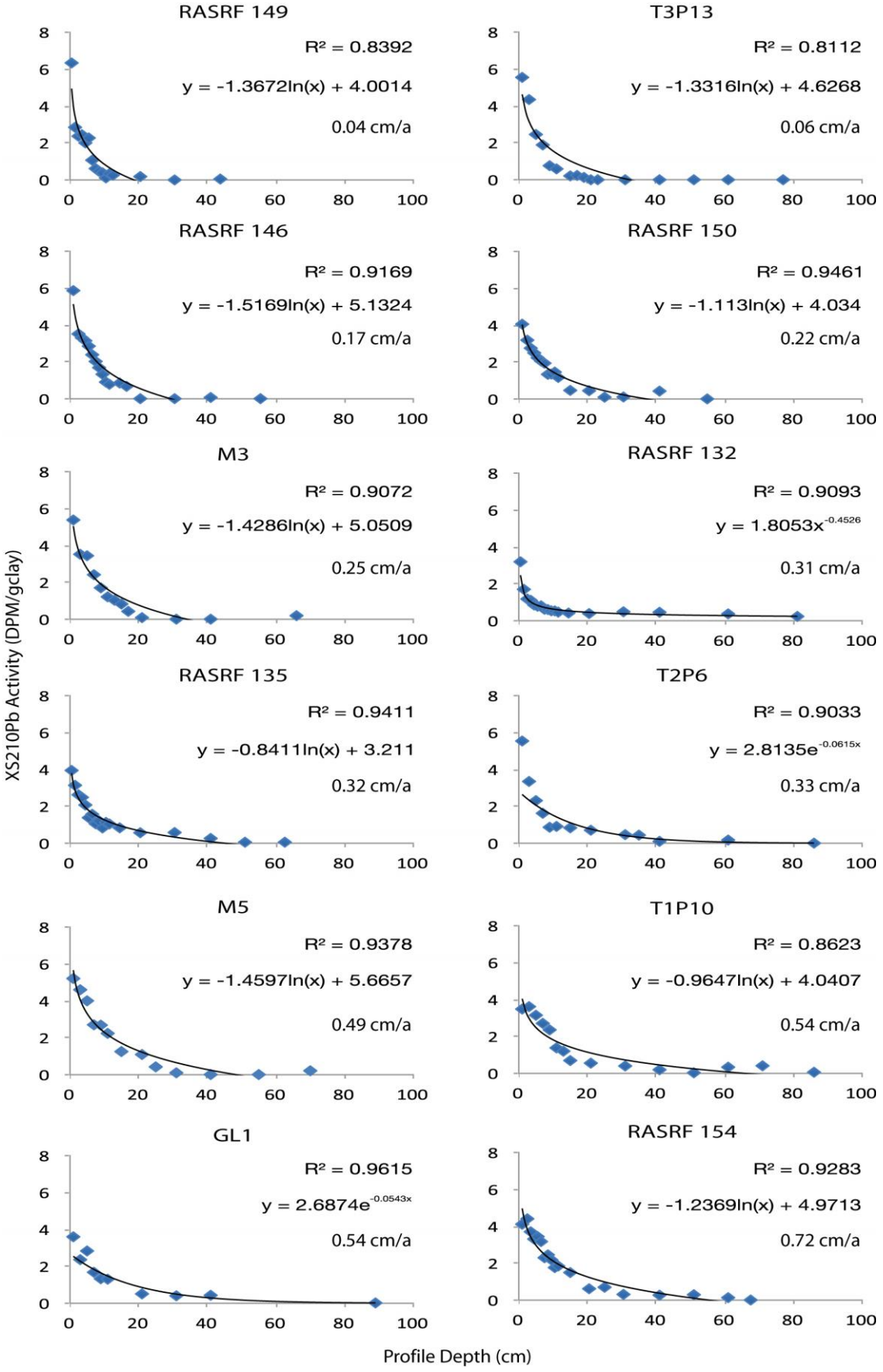

Figure 41 Summary of the activity profiles of all cores that are outside of cultivated areas and showing deposition. Sites are arranged for deposition rates from almost stable to fast sedimentation. XS ^{210}Pb profiles show a decrease in slope with the increase in deposition rates. Negative XS ^{210}Pb activity values that result from grain size correction and radon ventilation corrections have been assigned the value 0.001 DPM/g$_{clay}$ for presentation purposes.

Episodic deposition

Episodic sediment deposition events in the research area are defined as sedimentation events that occur infrequently but with a high magnitude or high volumes of sediments arriving at a certain location during one particular event. Episodic deposition events show a meteoric cap in XS ^{210}Pb activity that is clearly elevated above an XS ^{210}Pb activity plateau (Figure 42). This activity plateau can only consist a single value for not well-defined plateaus or several values for well-defined plateaus. The meteoric cap topping the plateau shows a rapid decrease in XS ^{210}Pb values below the uppermost XS ^{210}Pb activity of the cap. Its shape is not always as well defined as the meteoric caps in stable profiles, especially if the surface of an event is not exposed over an extended period of time. The dating of single deposition events is described in detail below.

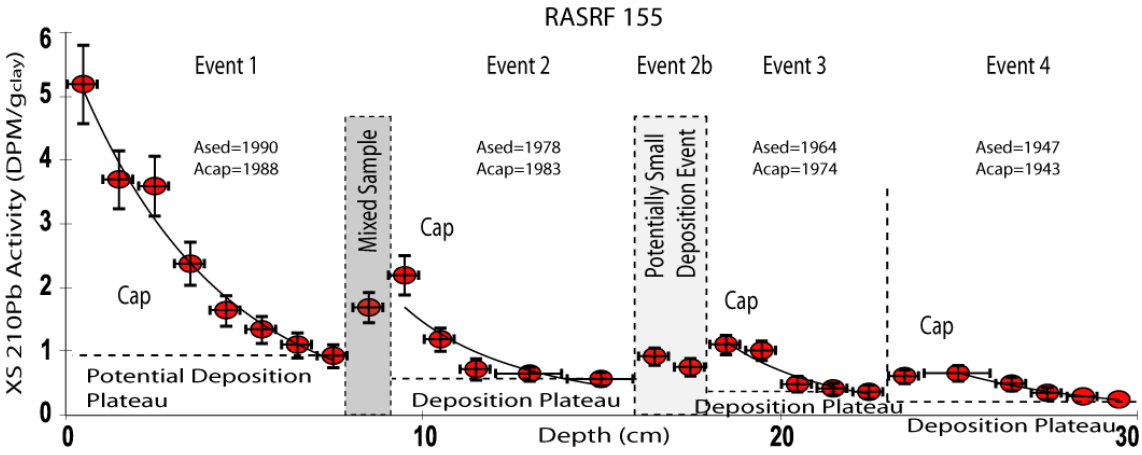

Figure 42 Core RASRF155 showing at least four (potentially 5) clearly recognizable deposition events with stable periods between the single events indicating episodic sedimentation at the site. All deposition events are represented by a clear cap on top of an activity plateau. The deposition ages calculated from the activity plateaus and meteoric fallout caps have been displayed in year AD without error ranges but errors range from ± 5 a for event 1 – 3, to ± 15 a at event 4. The high cap age at Event 3 likely suggests minor deposition after the event itself or sediment mixing of the uppermost sample of event 3 and the lowermost sample of undated event 2b.

Deposition in fluvial environments might vary over time and in accordance with the change in relative topographic position or flooding patterns. This may potentially change the amount of sediment deposited in a single event and the frequency of deposition at a site. The approach discussed above also enables to detect changes in sedimentation styles / patterns. If there are clear detectable and datable plateaus and the age of the cap above the dated plateau significantly overestimate or underestimate the plateau age (Figure 43) there must have been a change in sedimentation frequency or quantity per event, as observed at four sites (RASRF136, RASRF152, RASRF153, RASRF169).

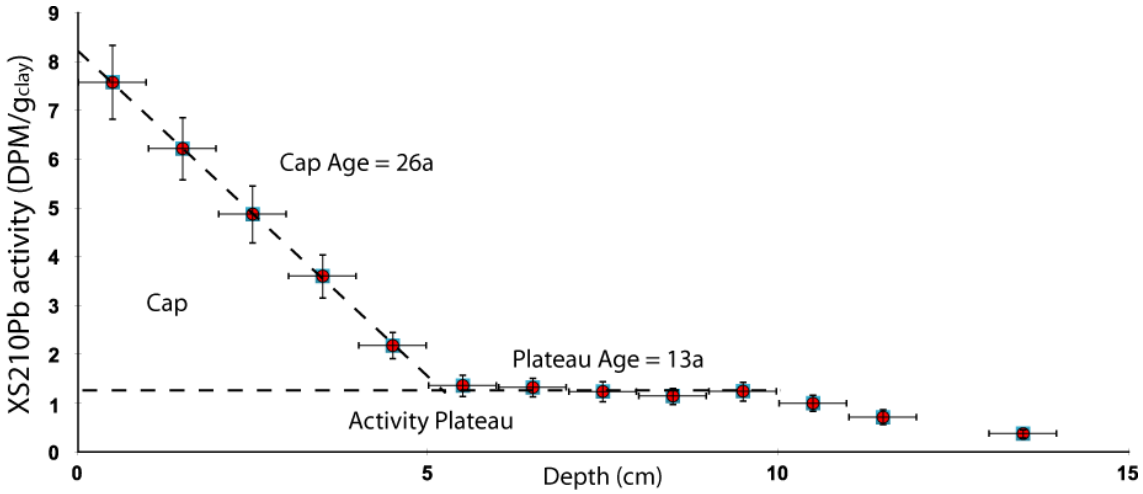

Figure 43 At site RASRF152 a change from episodic (or high deposition) to rather continuous sedimentation can be observed. The cap age (26 a) at this site highly exceeds the age of the underlying plateau (13 ± 4 a) of a large sediment package, therefore smaller amounts of sediments must have been deposited after the arrival of a large stack of sediment creating the plateau. Additional XS ^{210}Pb from sediment deposition is necessary to increase the inventory of the meteoric cap that would reflect the calculated age. Given that the deposition of the additional XS ^{210}Pb is not visible in the XS ^{210}Pb activity profile it has to be deposited in rather small quantities over a longer period.

Undisturbed sites showing erosion

There were sites with very minor (< 1 mm/a) erosion rates within the research area, and sites where scour have been occurring but no sites with constant moderate erosion rates. Sites with low erosion rates show the same trends as stable sites with an exponential decline in XS ^{210}Pb activity profiles. The sites, where reported scour occurred in the past also show a very clear cap with a very steep decline in XS ^{210}Pb activities for the first 2 – 6 cm, with very low or background activity below (Figure 44). Two profiles (RASRF157, RASRF158) belong to the same scour and show very similar XS ^{210}Pb inventories, a steep decline in XS ^{210}Pb activity and XS ^{210}Pb activities reach background values within the first 10 cm. The third profile (RASRF134) shows a slightly higher XS ^{210}Pb inventory and showed similar XS ^{210}Pb activities for the top 6 cm and a steep decline thereafter (Figure 44).

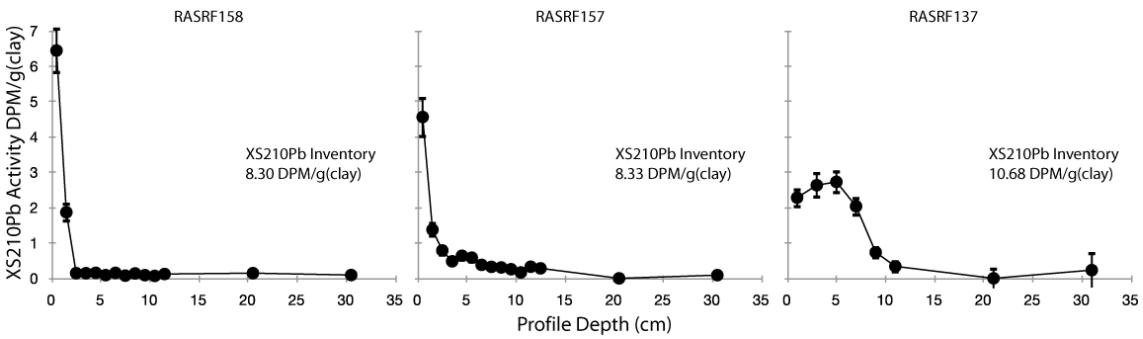

Figure 44 Profiles RASRF158, RASRF157, and RASRF137 collected at sites of reported scour. Cores show a decreased XS ^{210}Pb inventory (Full inventories would show 17.76 ± 0.77 DPM/g$_{clay}$) and reduced infiltration of XS ^{210}Pb in comparison to stable sites (Figure 40).

4.2.2. XS ^{210}Pb Activity Profile Development at agriculturally used Sites Cultivated Fields, and Pastures

In an intensely anthropogenically used landscape it is important to be able to distinguish between XS ^{210}Pb activity profiles that have been caused by natural deposition processes and post-depositional redistribution of sediment. Thus high-resolution analysis of XS ^{210}Pb activity profiles is used to investigate the influence of land use processes on profile development in cultivated areas. This is necessary to be able to detect cores that are suitable for CIRCAUS/CNAXS dating. Cultivated areas in the research area are - fields and pastures - that are ploughed and or disced on a more or less annual basis, mechanically reworking the material close to the surface and redistributing soil particles over the upper couple of centimetres to decimetres. Further it will be distinguished between fields that are ploughed and disced on a regular basis and a special form of pastures that are disced but not ploughed (for pastures that have not been disced see above).

Ploughed and disced fields

4 cores were collected at ploughed fields (T2P3, T2P4, T2P5, T3P14, Figure 45). In contrast to the cores from undisturbed pasture and woodlands, ploughed and disced fields showed a homogenous distribution or a slow monotonic decline of XS ^{210}Pb values in the upper part of the core, especially within the uppermost 10 cm. Profiles that are ploughed and disced on a yearly basis showed low or highly reduced surface XS ^{210}Pb activities compared to pristine profiles in the research area.

Three (T2P3, T2P4, T3P14) out of four cores collected at fields that are ploughed show almost stable XS ^{210}Pb activities for the upper 8 – 15 cm (Figure 45). Only one core shows a clear decrease in XS ^{210}Pb activity for the top 30 cm of the core (Figure 45, T2P5). One core shows a fresh sediment lens at 0 – 4 cm (Figure 45, T2P4) and homogenous distribution of XS ^{210}Pb activities from 8 – 16 cm below surface and slightly decreasing activities below. This core also shows the highest infilling rates in the research area (3.3 cm/a), reconstructed from an absolutely dated layer at 95 – 100 cm below surface dating to 1980 – 1981. This age has been calculated from an in situ burned layer that can be linked to the clearing of the natural oak forests at the site and the subsequent

burning of the tree stumps and roots in 1980 – 1981 (oral communication with resident Mr Shannon Samuelson, Dec 2011). The only stable site shows an even distribution of XS ^{210}Pb from 0 – 8 cm with increased activities up to 15 cm (Figure 45, T3P14).

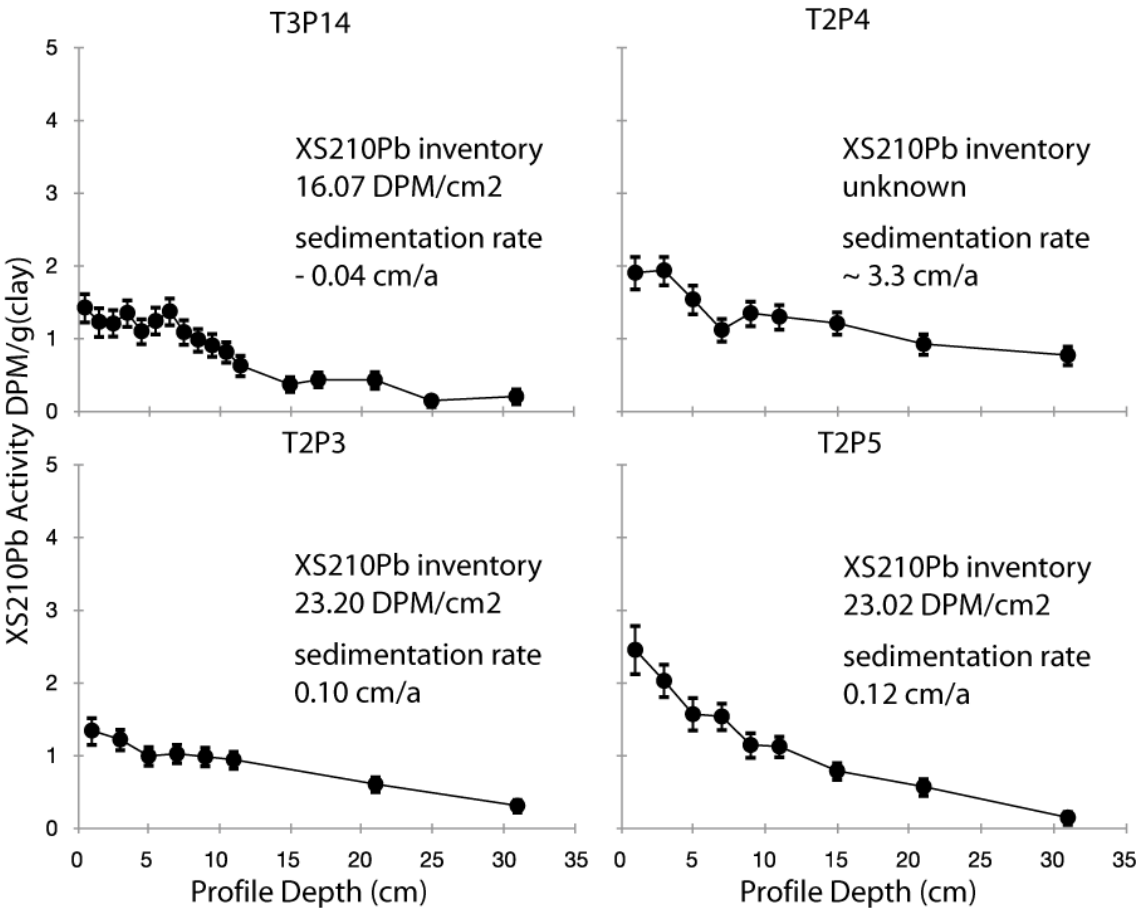

Figure 45 Cores T2P3, T2P4, T2P5, and T3P14 collected at ploughed fields showing well mixed profiles for the upper part of the profiles as well as at actively deposition (T2P3 – T2P5), as at stable sites (T3P14). The core at the stable site shows homogenous XS ^{210}Pb activity in the top 8 cm, and decreasing activities below. Cores collected at sites showing active deposition do show incomplete homogenisation of the XS ^{210}Pb activities throughout the top 30 cm with constantly decreasing XS ^{210}Pb activities.

Disced Pasture

A practice of agricultural surface modification in this area is the annual discing of pastures using a disc harrow, a tool to disaggregate the uppermost part of the soil profile. Sediment cores from pasture sites where no ploughing but discing occured show a very different distribution of XS ^{210}Pb with depth to cores that are ploughed and disced. The distribution of XS ^{210}Pb activities within these cores is more or less dependent on the prior land use. At undisturbed sites(Figure 46, RASRF129, TEP7) itshows high surface values and a steep decline within the first couple of centimetres (Figure 46). In sediment profiles from disced pasture sites a slight increase in XS ^{210}Pb can be observed at 10 –

12 cm. This increase in XS ^{210}Pb activity does occur on sites that have been ploughed prior to a change in land use to discing as well (Figure 46, T2P1, T2P2) with otherwise typical features of ploughed fields. Three out of four cores show reduced XS ^{210}Pb inventories indicating erosion, even though the topographic locations suggested stable conditions.

Site T2P2 (Figure 46) has a more complex land use and sedimentation history with a change from ploughed fields to disced pasture prior to core collection and 0.1 cm/a accumulation. All this history is present in the XS ^{210}Pb activity profile and can potentially be reconstructed form the profile, depending on further development of the method. The XS ^{210}Pb activity profile shows the development of a cap between 0 – 5 cm and increased values at 12 – 14 cm, slightly below the maximum depth of discing.

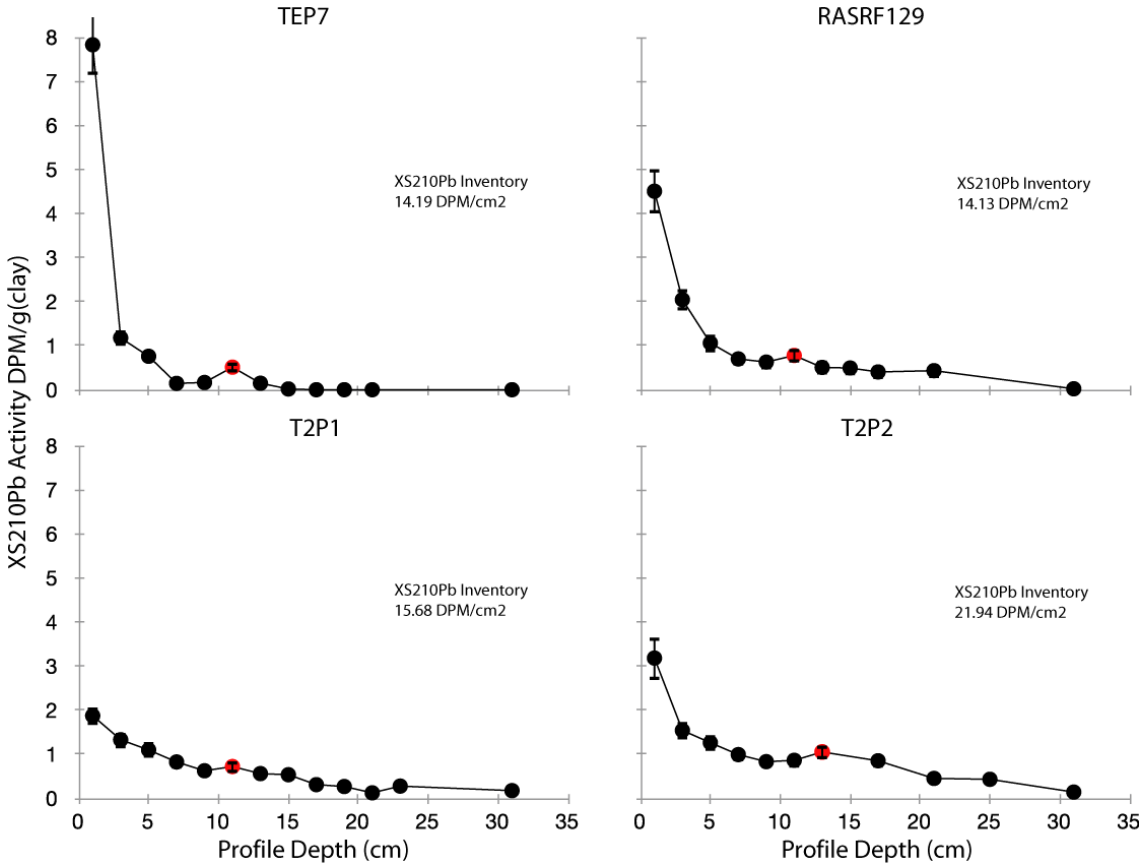

Figure 46 Cores T1P1, T2P2, TEP7, and RASRF129 collected in disced pasture show elevated XS ^{210}Pb activities from 10 – 12 cm in each core. TEP7 and RASRF129 both have just been disced in the past whereas T2P1 and T2P2 have more complex land use histories. Site T2P1 has been ploughed until recently and showed a high grazing pressure and therefore no proper cap is present. Site T2P2 has a highly variable land use history with a change from ploughed field to disced pasture and the occurrence of sedimentation. Nevertheless the characteristic increase of XS ^{210}Pb activity for disced sites at 12 – 14 cm below surface can be observed.

Suspected land use history

Unknown and uncertain land use histories are often common in undeveloped countries or densely populated areas. In most industrial countries the procession of land use and changes in land use is well recorded or known for most of the agriculturally used areas. However, there are still cases where land use is unknown or the boundaries of areas where certain practices were applied in the past cannot exactly be located. In these cases, only a high spatial resolution might help with the detection of human or natural influences on the development of XS ^{210}Pb activity profiles. In the research area several sites indicating episodic deposition of sediments have been found. While many of them seem genuinely episodic sedimentation, some are more likely to be the product of anthropogenic influences.

One prime example for uncertain land use histories are the cores collected at the sites LSD1 – LSD4, all located in grassland proximal to the river. This grassland shows some small bushes and appears undisturbed by agricultural land use. The cores are located between ~ 50 m and ~ 800 m away from the main stem Sacramento River, and showed CICCS sedimentation and erosion rates of - 0.16 cm/a to + 0.59 cm/a. All cores of LSD 1 – LSD 4 showed 2 plateaus and peaks in XS ^{210}Pb activity with peaks located at 8 – 10 cm and 18 – 20 cm below surface in each core (Figure 47). This homogeneous distribution of the depth of the peaks at very different topographical positions is likely to indicate a different cause of the distribution of the XS ^{210}Pb activity peaks other than natural sedimentation.

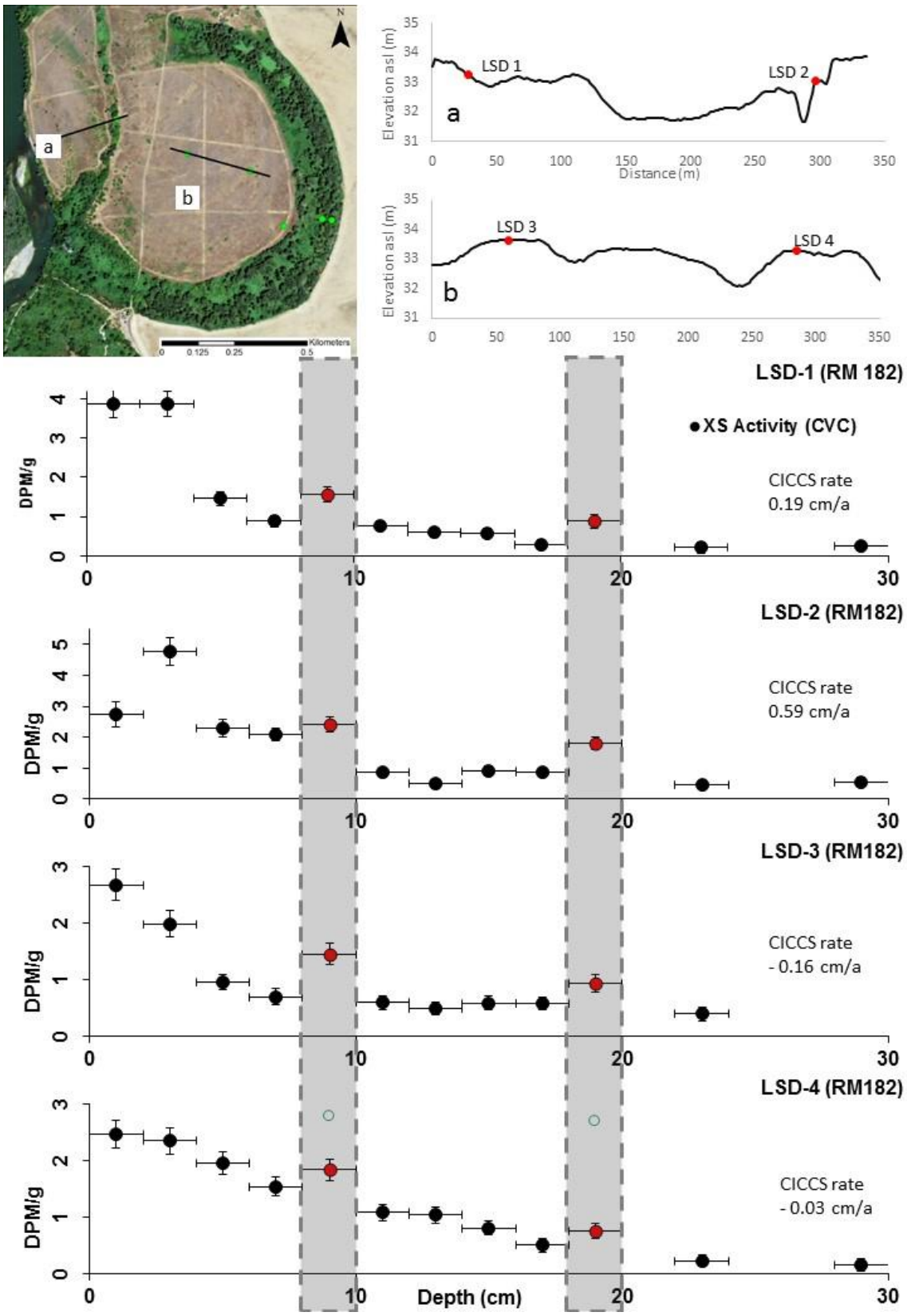

Figure 47 Cores LSD1 – LSD4 that are located in the same field, showing the same general trends in XS ^{210}Pb activity depth profiles (LSD-1 – LSD-4), but are located in very different topographic positions (a, b), and show very different CICCS sedimentation rates (LSD-1 – LSD4).

4.2.4. Dating of Flooding Events using XS ^{210}Pb

Of the collected cores only 19 showed clear plateaus and peaks in their XS ^{210}Pb activity. Of these 8 were likely influenced by anthropogenic activity (see above), and only 11 proved suitable for CIRCAUS/CNAXS dating (Table 3). In these 11 cores, it was possible to date a total of 16 deposition events. Additionally, 4 cores were suitable to date erosion events. In only 7 of the 16 dated deposition events the age of the dated activity plateau is in agreement with the age of the dated caps (Table 3). At the other sites it was assumed that the age of the activity plateau represents the deposition age and the alteration of the cap age is the result of additional deposition or erosion after initial sedimentation of the plateau.

Table 3 Age of dated accumulation and erosion events using the CIRCAUS/CNAXS method

Core	*Event*	*Event Thickness (cm)*	*Cap Age (AD)*	*Sediment Age (AD)*	Error (a)	Notes
RASRF 134		14	1987	1989	± 4	
RASRF 136		~20	2004	1994	± 4	Episodic deposition, later constant sedimentation
RASRF 137			1983		± 4	Erosion, complete removal of XS ^{210}Pb cap
RASRF 147		8	2007	2008	± 4	
RASRF 148	1	**5**	2007		± 4	Just cap datable
	2	5		1990	± 5	
RASRF 152		10	1967	2000	± 4	Sedimentation event, cap eroded
RASRF 153		9	1965	2002	± 4	Sedimentation event, cap eroded
RASRF 155	1	8.7	1988	1990	± 4	Calculated using linear mixing model
	2	5.3	1983	1978	± 5	Calculated using linear mixing model
	3	5	1974	1964	± 5	Pot. Change in deposition process
	4	7	1943	1946	± 7	Too old -> error too high to match with flood record
RASRF 157			1990		± 4	Erosion, complete removal of XS ^{210}Pb cap
RASRF 158			1990		± 4	Erosion, complete removal of XS ^{210}Pb cap
RASRF 163			1984		± 4	Erosion/Deposition
RASRF 165		**3**		1985	± 4	
RASRF 168		12	1988	1977	± 4	
RASRF 169	1	6	2007		± 4	
	2	~9	2003	1990	± 4	Episodic deposition, later constant sedimentation
T2 P6		~20	1979	1985	± 4	

Only three profiles showed more than one datable deposition event (RASRF148, RASRF155, RASRF169), and only one of these showed more than two events (RASRF155). Four cores have been included even though they

are located in environments that potentially have experienced post depositional soil reworking due to their proximity to agriculturally used areas (RASRF152, RASRF153) or in young reforestation sites (RASRF134, RASRF136). The average thickness of a sediment deposition event is ~ 9 cm with a maximum of sediment deposition in a single event of ~ 20 cm (Figure 48). In one core it was possible to increase the accuracy of the sediment thickness of two separate events to 8.7 and 5.3 cm respectively using a simple linear mixing model (described above). Acknowledging these limitations, the largest flooding events still seem coordinated temporally with the depositional dates determined for sediment lenses. Nevertheless, a deposition/erosion event (1990) within a period of < than 2 year exceedance probability flooding (1987 – 1992) that are associated with an absence of substantial water loss to Llano Seco seems to be correlated with the largest number of datable deposition/erosion events across the floodplain (~ 1990, Table 3).

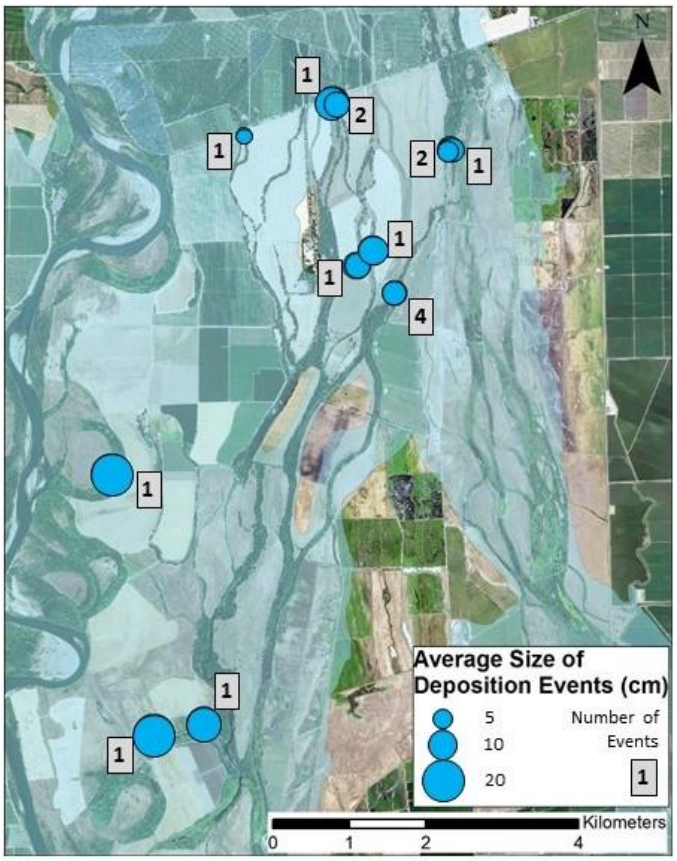

Figure 48 Average size and frequency of datable deposition events in XS ^{210}Pb activity profiles in the research area.

The dating of arriving sediment lenses indicates a culmination of events in the mid-70s, mid 80s, and around 1990, with less deposition recorded thereafter (Table 3). The low number of datable sediment lenses inhibits further assumptions on the potential influence of flooding events on sediment

accumulation and erosion, so additional research would be necessary to overcome these limitations.

4.2.3. Calculation of sedimentation rates

Sedimentation rates of the profiles in the research area have been calculated using CICCS (Walling & He 1994, He & Walling 1996) and CIRCACS (Aalto & Nittrouer 2012) respectively. For sediment cores that showed no XS ^{210}Pb at the bottom of the core CICCS sediment dating has been applied. For cores that showed XS ^{210}Pb throughout the core, sedimentation rates have been calculated using CIRCACS sediment dating. For these cores CIRCACS rates were compared with CICCS sedimentation rates. The comparison of both showed clearly the expected discrepancy (Aalto & Nittrouer 2012) between the two calculation methods.

For the calculation of sedimentation rates the natural meteoric influx of ^{210}Pb to the region has to be established. The chosen reference sites are all located outside the area of flooding and not impacted by agricultural surface alterations (M2, TEP16, LSF-T, and Cemetery). All reference profiles showed the highest XS ^{210}Pb at the surface with a monotonic decline in below. All reference cores reach background values within the first 20 cm. For these reference sites the unsupported ^{210}Pb inventories calculated. Natural fallout inventory was calculated from the average inventory of the four undisturbed reference profiles to 17.76 ± 0.77 DPM/cm^2. Cores with CICCS inventories below or above that activity are deemed eroding or infilling, respectively.

The campaign revealed significant differences in the spatial distribution of overbank deposits. High-resolution XS ^{210}Pb analyses, CIRCAUS/CNAXS dating and CICCS/CIRCACS sedimentation rate calculation was applied to a total of 78 cores. Additionally, sedimentation rates were calculated by 1) comparing core depth as indicator for minimum deposition rates to reconstructed time of channel abandonment and 2) using the thickness of sediment above known independent soil marker layers. In this study, mainly CICCS sedimentation rates have been used to calculate sediment distribution. In cases where the profiles could possibly be interpreted as episodic (independent of topographic proxies) it was apparent that CICCS sedimentation rates significantly underestimate sedimentation rates calculated by the CIRCACS model (Figure 49). In at least 22 cores it is likely that the CICCS

rates are underestimating the real sedimentation rates because background XS ^{210}Pb activities were not reached at the bottom of the cores (Walling & He 1994), or the sites have been mapped as active Sacramento River channel positions within the past 50 years. For these sites, even though episodic deposition can be expected predominantly, constant sedimentation rates were assumed and CIRCACS sedimentation rates were calculated. For the compared sites, using the CIRCACS method 17 of the 18 calculated samples sedimentation rates are considerably higher than rates calculated using the CICCS method (Figure 49). In 3 cases the CICCS approach would render negative sedimentation rates (=erosion) at sites where an active channel has been present less than 50 years ago. Only one of these cores show elevated XS ^{210}Pb activities at the bottom of the core. For these cores both of the approaches underestimate real sedimentation at proximal locations. Therefore, sedimentation rates are treated as minimum rates.

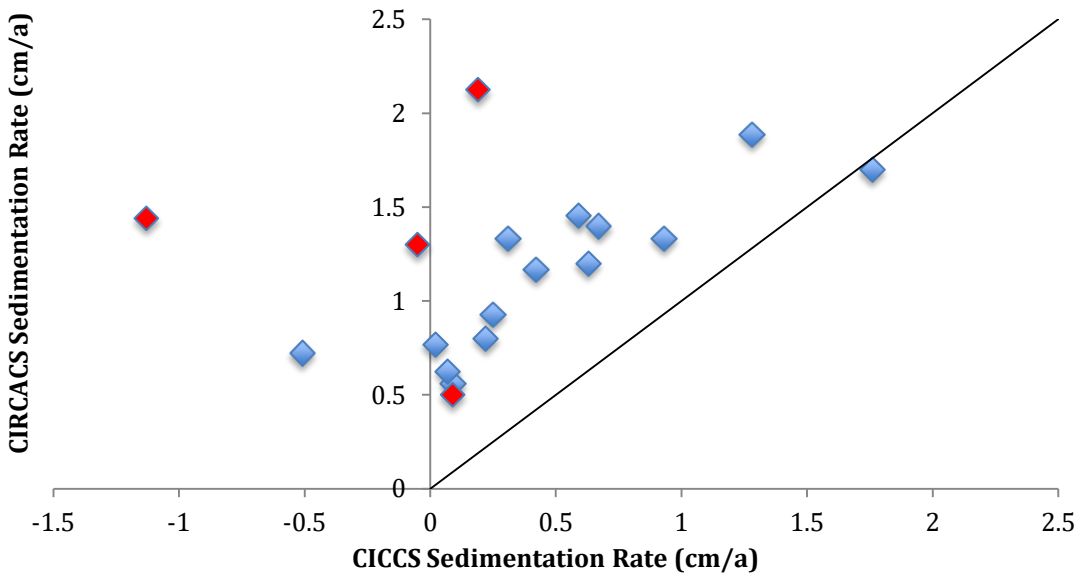

Figure 49 Relationship between deposition rates calculated using the CICCS and the CIRCACS methods. Red symbols show rates calculated using core depth and abandonment age of the channel. All ages have to be treated as minimum ages.

In the analyses of spatial distribution of deposition rates, processes determination and XS ^{210}Pb dating a total of 78 cores were analysed. Of all analysed cores, 3 cores had to be excluded from further analysis and the calculation of CICCS sedimentation rates. In these cores visible profile disturbances due to anthropogenic influences where apparent. One cores were collected outside of the research aera and to calculate a fallout inventory for stable sites. For this calculation additional two cores within the research area were collected outside of the flooded areas adding up to four cores in the

calculation of the regional natural fallout inventory (17.76 ± 0.77 DPM/cm^2 / 296 ± 13 mBq/cm^2). Of the collected cores, 7 have not received notable sedimentation or erosion over the past ~ 70 – 100 years. These cores were exclusively located in the distal part of the floodplain. Using the CICCS model 19 of the sites show reduced inventories suggesting erosion. Of these sites at least 3 have received a significant amount of sediment indicated by the position at a site recently abandoned by the channel at the coring location (e.g. RASRF126, Figure 50) or by the elevated XS ^{210}Pb activities at the bottom of the core. Additional deposition events are visible in XS ^{210}Pb activity profiles even though the cores show erosion in their fallout inventories. At least 3 sites experienced the total removal of the meteoric cap due to scouring and remain stable thereafter. At the remaining 47 sampling locations deposition occurred with a maximum average sedimentation rate of 2.13 cm/a. Of these sites, 23 showed clear evidence for episodic deposition, 9 sites show indications for episodic deposition, but the activity profiles of these profiles could potentially be explained by land-use or bioturbation as well. At 9 sites no evidence for episodic processes could be detected, therefore, constant deposition is likely. At 16 sites deposition rates were reconstructed from XS ^{210}Pb inventories but anthropogenic profile reworking obscured the nature of the deposition (chapter 4.4.2).

Proximal cores or cores within the first kilometre of the main stem show signs of episodic sedimentation, as so cores located proximal to the smaller floodplain channels -- especially in the western part of the system. However, not all sites receiving a significant amount of sediment exhibit this sedimentation clearly in either the CICCS / CIRCACS inventory or the XS ^{210}Pb activity profile. This is especially apparent at several sites that have been abandoned by the Sacramento River channel since the 1960s, where no well-defined meteoric fallout caps have been established yet and the sites' fallout inventories suggest erosion within the past 50 – 70 a. For these erosional sites XS ^{210}Pb activity profiles were either inconclusive or they suggested some minor sedimentation events, but not to the extent of sedimentation that would be expected for a site that has been an active channel position within the past 70 years.

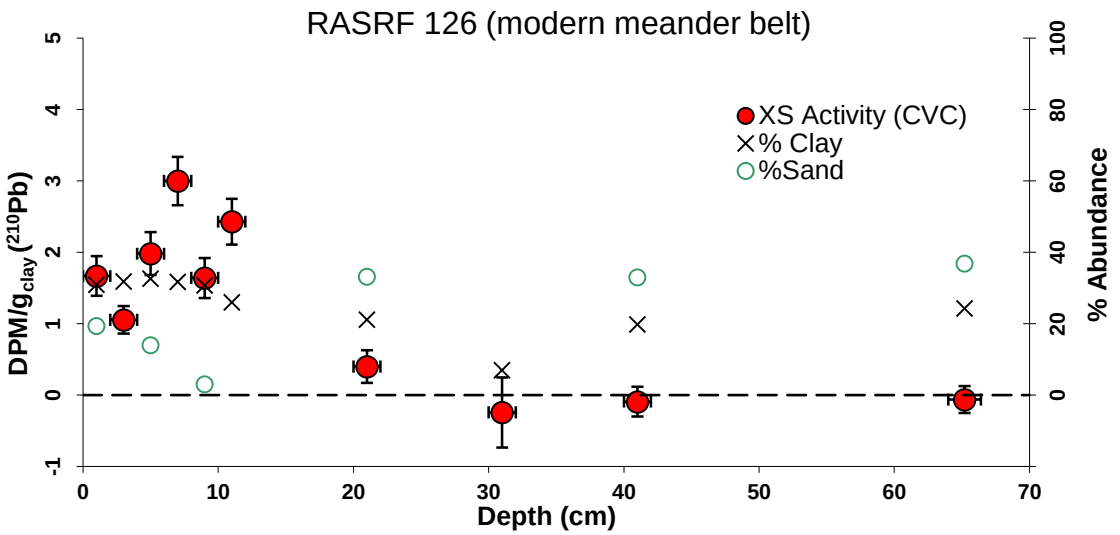

Figure 50 XS ^{210}Pb profile of core RASRF126 collected at a former channel position abandoned 1960-1964 showing negative CICCS sedimentation rates (- 0.05 cm/a). The profile shows no clear cap but variable XS ^{210}Pb activities up to 12 cm below surface. This variability in XS ^{210}Pb activities could be interpreted as signature of minor deposition events. The lack of elevated XS ^{210}Pb activities below 30 cm in addition to the CICCS sedimentation rate would suggest almost stable or eroding conditions for the past 100 years. This is in contrast with the topographical information that the location was at the location of the active channel of the Sacramento River.

4.3. Spatial Distribution of Deposition along the Sacramento River and its Floodplain Channels

The sedimentation and erosion rates along the Sacramento River decrease with distance from the main stem (r^2=0.2341, P<0.00001, significant at p < 0.01, Figure 51, Figure 52, Table 4) but remain highly variable until ~ 2.5 km away from the closest potential concentrated flood outlet (Z= -2.7568, p = 0.00578, significant at p≤ 0.05, Figure 51, Figure 52). Further than ~ 3 km away from the channel, the sedimentation is limited to floodplain channels and their immediately adjacent banks, whereas high floodplains receive little sediment (-0.03 ± 0.02 cm/a), and are more prone to erosion (statistically not significant in comparison with floodplain channels (0.26 ± 0.41 cm/a), Z=1.2474, p=0.2113, not significant at p≤ 0.05, U=18, critical U (p≤ 0.05) = 11, not significant at p≤ 0.05). None of the median sedimentation rates along the Sacramento River significantly differs from all other windowed distances (n=76, H=13.19838639, P = 0.280557033, not significant at p < 0.05). Sand in the system is mainly deposited within the first 500 m from the main stem Sacramento River (Figure 51, Z=-3.393596, p= 0.000690, significant at p≤ 0.05).

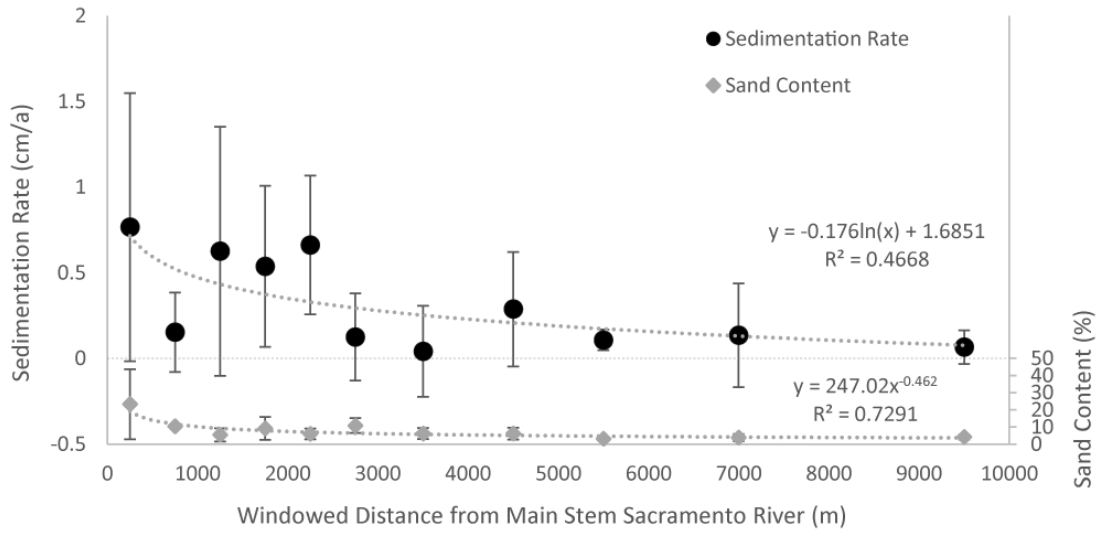

Figure 51 Sedimentation rates and sand content grouped by windowed distance from the nearest flood outlet point in the direction of flow. Sedimentation rates show a significant decline with distance from the nearest flood outlet for the research area (r^2=0.4668, P=0.029426 significant at p < 0.05). Sand content declines steeper than sedimentation rate with windowed distance from the main stem Sacramento River (r^2=0.7291, p=0.00001, significant at p < 0.01).

This decrease with distance is valid for most of the floodplain locations higher in topography. Exceptions are floodplain depressions left from abandoned channels, scours, and other floodplain channels. In these cases, large meander scars accumulate sediment at a higher rate than the surrounding floodplains (Z = -3.1543, p = 0.00164, significant at p≤ 0.05; U = 0, critical U (p≤ 0.05) = 12, significant at p≤ 0.05. Also, scours located in the direction of the main flood are exceptions from this observation, because they remove large quantities of sediment during their formation relatively independent of their individual distance to the main channel (not enough data for reliable statistics, but scour -0.21 ± 0.1 cm/a, channel edges 0.17 ± 0.22 cm/a). Additional exceptions are smaller ephemeral floodplain channels that show varying sedimentation and erosion (0.26 ± 0.41 cm/a) transporting sediments over vast distances away from the main stem, but show no significant difference to the surrounding areas (0.11 ± 0.21 cm/a, Z = -0.78, p = 0.4354, not significant at p≤ 0.05; U = 77.5, critical U (p≤ 0.05) = 52, not significant at p≤ 0.05).

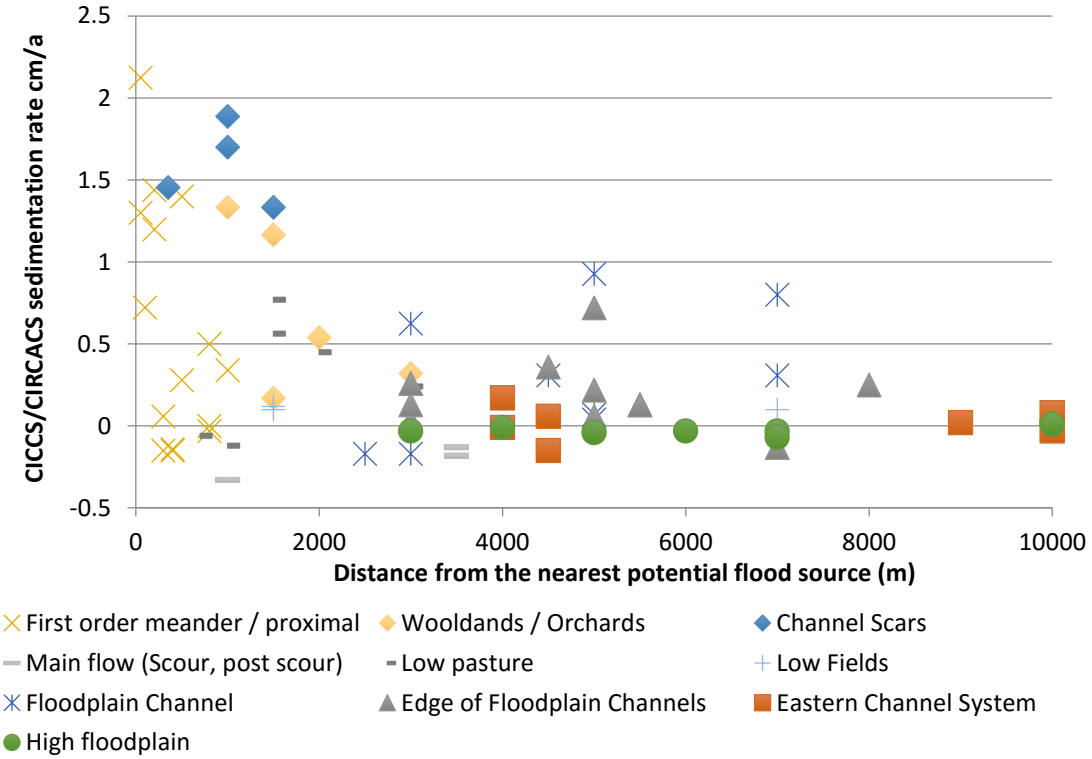

Figure 52 The distribution of CICCS/CIRCACS deposition and erosion rates (cm/a) along the Sacramento River in relation with the distance to the main channel in the direction of flow from the nearest flood outlet point. General sedimentation rates decrease from the main stem (r^2=0.2341, P<0.00001, significant at p < 0.01). Different symbols represent the environment the cores have been collected in. While sediment accumulation is present in all landscape units within the first 3 km from the main stem, deposition is limited to the floodplain channels and their banks for sites further than 3 km distance from the main stem Sacramento River.

From these smaller channels, sediment gets transported to the surrounding areas (r^2=0.0794, p=0.09108, significant at p≤ 0.1) and deposited within the first 80 m of these channels with 2 exceptions showing a significant amount of deposition of up to 140 m away from the nearest floodplain channel. Erosion rates do not show great changes up to 135 m away from the nearest floodplain channel. This is only true for the small floodplain channels and does not include sites with the Sacramento River main stem as nearest channel (Figure 52).

Flow depth has been calculated for each site from the FEMA 100 year flood layer and the DEM provided by the Nature Conservancy (unpublished). The results indicate that flow depth is not correlated with deposition in the research area. The calculated flow depth would result in an r^2 = 0.0055 with p = 0.536176, not significant at p < 0.05 (Figure 53).. This lack of correlation with the additional parameter flow depth could have several causes: a) an erroneous extent of the FEMA 100 year flood layer that is indicated by the location of the flood boundaries on downward slopes or low points in the DEM (this could also

be due to changes in the topography since the mapping of the flood layer) b) the assumption that the flow is allocated equally across the floodplain that does not consider that flow might be distributed unevenly by the separating islands in the floodplain topography, c) inaccuracies in the digital elevation model (including errors that can occur during the conversion of different underlying projections), d) a combination of more than one factor, because cores that clearly receive sedimentation according to XS ^{210}Pb profile analysis and CICCS rates, are located above the flow level reconstructed from FEMA 100 yr flood extend, or e) they are in fact not correlated in the research area and other factors have a larger influence on sedimentation rate.

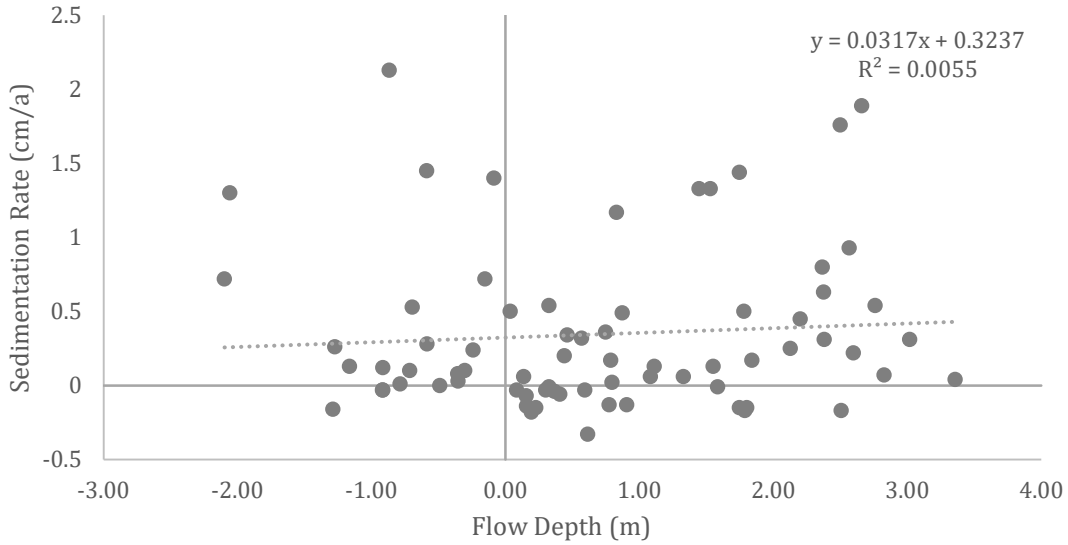

Figure 53 There is no correlation between sedimentation rate and flow depth (r^2 = 0.0055) in the research area. Potential reasons for this phenomenon are discussed above.

The average amount of sediment per flood has been calculated from area per windowed distance (80% of the total area) and the average deposition rate in each window. In flood years an average amount of 0.75 ± 0.87 Mt/flood of sediment is deposited on the floodplains in the research area. Of these approximately 40% remain within the first 500 m of the channel while 0.45 ± 0.57 Mt/flood are transported more than 500 m away from the active channel.

Table 4 Sedimentation rates for windowed distances from the closest potential flood source, including the total flooded areas for each windowed distance for FEMA 100 yr flood extend. At the bottom sedimentation rates for channel locations are shown.

Windowed Distance (m)	n	Sedimentation Rate (cm/a)				
		Mean	Median	Maximum	Minimum	Flooded area FEMA (km^2)
0 - 499	12	0.77	0.96	2.13	- 0.15	15.13
500 - 999	6	0.15	0.14	0.50	- 0.16	2.56
1000 - 1499	10	0.63	0.45	1.89	- 0.33	5.12
1500 - 1999	4	0.54	0.33	1.33	0.17	6.06
2000 - 2499	4	0.66	0.54	1.33	0.24	6.65
2500 - 2999	8	0.13	0.08	0.63	- 0.17	6.51
3000 - 3999	4	0.04	- 0.07	0.49	- 0.18	13.28
4000 - 4999	10	0.29	0.24	0.93	- 0.15	8.51
5000 - 5999	6	0.11	0.10	0.22	0.00	7.03
6000 - 7999	7	0.14	- 0.03	0.80	- 0.13	10.90
8000 - 11000	5	0.07	0.02	0.25	- 0.03	8.21
Environment						
Channel Scars	5	1.55	1.45	1.89	1.30	
Floodplain Channels	10	0.26	0.19	0.93	- 0.17	
Scour Scars	3	- 0.21	- 0.18	- 0.13	- 0.33	
Channel Edge	13	0.17	0.13	0.72	- 0.18	
High Floodplain	6	- 0.03	- 0.03	0.01	- 0.04	

4.3.1. Floodplain Processes

Of the 78 cores/sites that were analysed, 18 did not shown enough evidence to distinguish between deposition processes, because disturbances in the XS ^{210}Pb profile at these locations made it impossible to determine a reliable interpretation of the sedimentation processes involved. The majority of profiles within this research area showed episodic erosion or deposition (n = 27), or non-ideal profiles that showed indications for episodic processes, but that could also be explained by other processes involved in the XS ^{210}Pb profile development (n = 12). In contrast, profiles indicating constant processes were relatively rare (n = 11), and only 7 sites exhibited fully undisturbed natural fallout inventories. At 3 sites fluvial erosion is unlikely, because of the site's topographic positions and land-use, therefore wind erosion was the most plausible interpretation of the profiles present (see "High Floodplains" below).

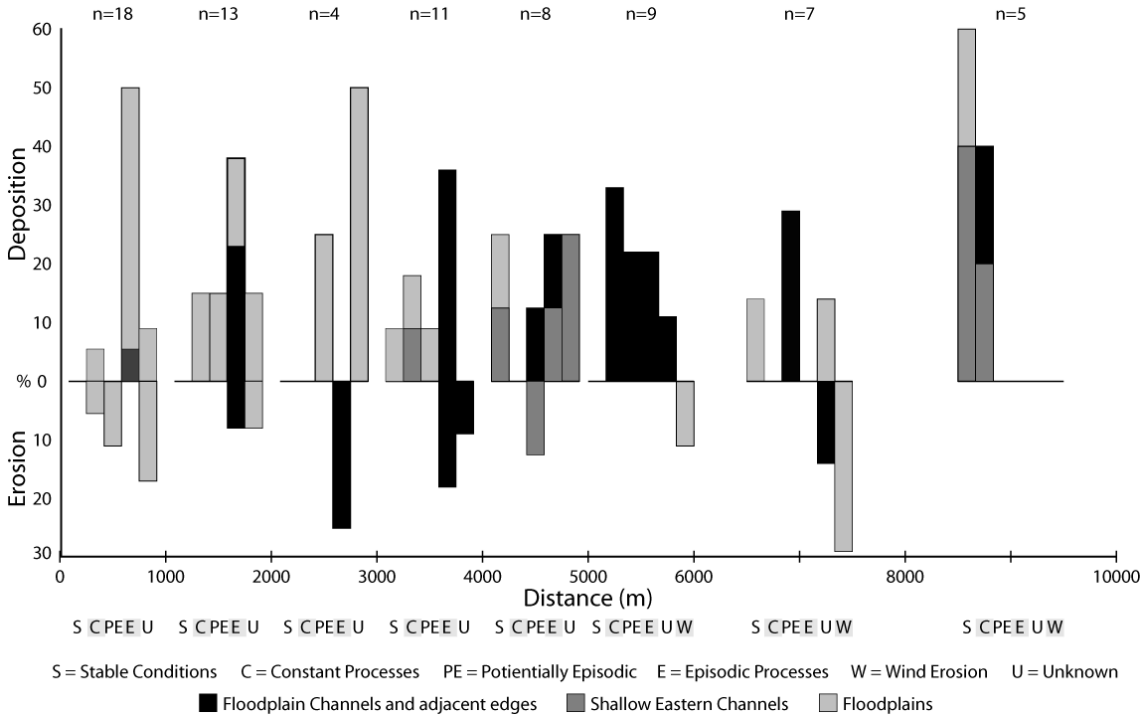

Figure 54 Processes involved in the construction of the floodplain along the Sacramento River depending on distance. Stable conditions indicate the lack of sedimentation or erosion within the detection period. Constant processes indicate the presence of slow deposition or erosion below the detection ability of separate events. Episodic processes are defied here as larger deposition or erosion events detectable in the XS ^{210}Pb activity profile or visible in the topography. Potentially episodic are cores that are not clearly interpreted as episodic in the XS ^{210}Pb profile with plateaus and caps, but show indications of episodic processes. Unknown are cores that have undergone post sedimentation profile reworking, so the original sedimentation process cannot be inferred from the XS ^{210}Pb profiles. Wind erosion is the most likely process for cores on high floodplains within cores that shows a reduced XS ^{210}Pb activity, but are outside of the area of natural flooding. Colours illustrate the information on the environmental position in the floodweb. A trend is visible from predominantly episodic to predominantly constant processes dominating deposition and erosion.

The first kilometre from the main stem is dominated by episodic processes in all environments (Figure 54). After 1 km distance from the Sacramento River, episodic processes are mainly limited to floodplain channel positions and their immediate adjacent banks/edges. The influence of fluvial processes is therefore greatly reduced for distal floodplain locations, with surface stability and wind erosion dominating the higher floodplains of the Llano Seco area (Figure 54).

Still, within the first 4 km from the main stem of the Sacramento River, episodic processes are clearly the dominant process (> 60%). Episodic processes remain prevalent for floodplain channel banks/edges located up to 6 km from the main stem, but cease thereafter. Moving away from these channel-proximal positions leads to a clear decrease in activity, with erosion and deposition more constant or near zero.

4.3.2. The Influence of "Topographic Environments" on Deposition along the Sacramento River

Along the Sacramento River, different environments have very similar distributions of sedimentation rates and processes. Samples were collected from 7 different fluvial environments, of which 4 were genuine floodplain locations and 3 were ephemeral channel environments within this floodplain setting. The environments not only show variations in their sedimentological behaviour with distance from the channel, but also behave differently between environments.

Depressions within the floodplain

There are three fundamentally different types of topographic depressions present in the floodplains of the research area. They are all of fluvial nature but differ in their evolution and the transport mechanisms present. These depressions can be classified as abandoned channels or meander scars created by the main stem Sacramento River, scours that are actively eroding forms, created by and following the course of the main overbank flow, and existing floodplain channels that are maintained by focused flow. These environments show the highest activity of all researched environments with the highest erosion rates, the highest deposition rates, and the highest variability in sedimentation rates on the floodplains of the Sacramento River. All these sites are actively evolving and none of the sites showed surface stability over the detection period.

Channel scars

Channel scars in this area are relatively frequent phenomenon, especially south of RM200 and east of the modern Sacramento River between RM174 and RM194. Limited data were obtained, but in general these environments have high infilling rates for the floodplains along this reach of the Sacramento River with 1.54 cm/a ± 0.25 cm/a for 5 profiles (LSD2, LSD5, LSD6, T2P4, Packer Lake (Sullivan 1982)) (Figure 55). Even though sedimentation rates might not be fully represent the actual extend of sedimentation, given the low number of samples, the failure to reach background levels of XS ^{210}Pb within any of the cores plus the mixed nature of infilling at one of the sites

(T2P4) both indicate that accumulate rates are very high. Because all the sites do not reach background level for XS ^{210}Pb, the CIRCACS approach must be used to avoid underestimation of the deposition rates present. One site shows different mechanisms of sediment delivery with a change in land use from woodland to fields ~ 1978 – 1982, resulting in the onset of farming activities and ploughing of the fields leading to colluvial relocation of sediment - therefore results from this site are likely to overestimate the natural deposition from fluvial transport. The infilling rates calculated for this site range between ~ 0.64 cm/a (CICCS / underestimated), 1.33 cm/a (CIRCACS / potentially underestimated), and ~3.4 cm/a (averaged from a 1980 marker horizon / overestimated for flood deposits) (T2P4). For the calculation of average infilling rates, additional values have been included from published studies in this area, with Packer Lake (RM168) showing an sedimentation rate of 1.3 cm/a since 1860 and ~ 0.94 cm/a for the pre-modern period (Sullivan 1982). Minimum sedimentation rates are used for the calculation of averages rates, because cores that can just be calculated by the CICCS method are not reaching background XS ^{210}Pb activity and must therefore represent minimum infilling rates. Also CIRCACS rates are known to underestimate the total amount of sedimentation under certain circumstances (see above). Average infilling rates for channel scars are 1.54 cm/a ± 0.25 cm/a, with a minimum sedimentation rate of at least 1.3 cm/a for modern sedimentation (CIRCACS), making the channel scars the most active accumulating fluvial feature in the research area (Figure 55). Overall, the sediment accumulation can be described as quasi-episodic because deposition is happening on a regular basis, but accumulation events are large enough that single deposition layer can be distinguished.

Floodplain channels

Within the floodplain channels in the research area 9 cores (RASRF142, RASRF144, RASRF149, RASRF151, RASRF153, RASRF161, RASRF163, RASRF165, RASRF167) have been collected to investigate the functioning of the channels in terms of sediment transport, erosion and deposition. The floodplain channels are not an exclusively eroding or depositing feature, but have a high variability in deposition records (Figure 55). Two of the cores collected, show erosion and seven show deposition in their CICCS inventories, and only one of the sites was stable. Additional sites have been observed

during the field campaign where active erosion of the underlying gravel deposits is evident. Lateral erosion was observed during the field campaigns, with the frequently exposed roots of large oak trees along these channels indicating slow lateral movement (see above), but the migration or lateral erosion rates of the ephemeral floodplain channel in the research are could not be quantified using orthoimagery, due to the extremely slow nature of this process. Otherwise, erosion seems to be more present in the upper part of the catchment. In several cases the erosion might be triggered by a change in flow velocity downstream of roads (2 erosion, one deposition sites) and bridges (1 erosion, 1 deposition site), whereas further downstream it appears that sediment get deposited more quickly.

Scour Sites

The scour sites along the Sacramento River were still topographically visible and formed along the main flood pathways, and were sampled at M&T and Goose Lake. At these locations the CICCS method suggests erosion rates of 0.21 cm/a ± 0.10 cm/a (RASRF137, RASRF157, RASRF158) (Figure 55). Topographic evidence shows the formation of several-meter deep scours and the initiation of floodplain channels (RASRF158) as evidenced by the removal of the meteoric cap, which in turn indicates the removal of sediment. These scours appear to occur episodically, forming a stable surface after initial removal of sediment (see above). These profiles show decreased XS ^{210}Pb inventories for the three analysed sites, and no indications for erosion or deposition after the initial erosion event took place. Erosion rates calculated for these sites are to be viewed as minimum erosion rates because it was impossible to reconstruct the additional amount of sediment removed after the removal of the initial meteoric cap using ^{210}Pb activities. Erosion at these sites could amount to several meters of sediment removal during the scour. The meteoric caps topping these sediments can be used to date the timing of the removal of the prior atmospheric cap.

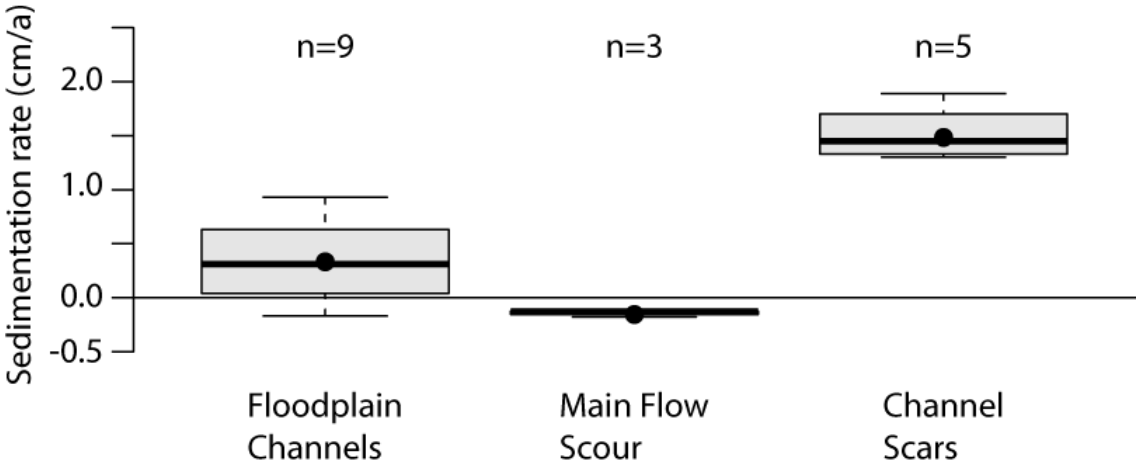

Figure 55 Sedimentation rates for different topographic depressions showing clear differences in average sedimentation rate as well as in minima and maxima.

Low eastern channels

The eastern channels are wide, relatively shallow and, in their centre often filled with water. No samples have been collected in the centre of these channels because access was restricted, or the channels were too deep to collect samples. The 7 cores included in the analyses have average sedimentation rates of 0.02 cm/a ± 0.1 cm/a, varying from moderate erosion – 0.15 cm/a to low sedimentation 0.15 cm/a. Overall 9 cores (RASRF146, RASRF147, RASRF148, LC17, TEP8, TEP15, M0, M1, M5) were sampled at edges of these channels, focusing on the central part of the research area (because of access limitations at its northern and southern ends). Of the sampled sites, two profiles were excluded from the calculation of average deposition rates, one of them was likely to be disturbed because the profile showed similar high XS ^{210}Pb activities throughout the core and was located between the edge of an artificial channel and an intensely used field, indicating anthropogenic soil deposition within the last century (TEP15). The second core excluded (M5) has been collected upstream of a bridge that showed evidence of ponding of flow during floods and is likely influenced by this local anthropogenic disturbance. The processes present at the sites are heterogeneous: 3 stable sites, 2 sites eroding and 2 showing deposition. Two sites show constant and two show episodic processes (Figure 54).

Floodplains

There are several different floodplain environments showing different infilling trends and processes based on topographic location. These topographic locations are mainly explored in terms of their qualitative characteristics that can be clearly distinguished in the field. Following “topographic location” is used as a conceptual framework that shows differences in flooding processes and deposition rates.

High floodplains

These high floodplains in the distal part of the channel are structurally older than the Holocene meander belt and slightly elevated in comparison to the rest of the floodplain, but they are still largely inundated on an annual basis. The 8 cores (LSF-T, M2, M4, T2P1, TEP7, T1P9, T3P14, TEP16) collected at these locations show stable profiles or often minor erosion. Even though these areas are inundated on a regular basis, no sediment deposition could be observed in the collected cores (appendix A). The documented erosion is unlikely to be of fluvial nature, because during the flooding season little of the landscape is under agricultural use and therefore vulnerable to erosion. However, grazing pressure and agricultural use of these areas are likely to cause minor aeolian erosion during summer months when either cattle is kept on these pastures or the fields are disced (Figure 56).

Edges of floodplain channels

11 cores (RASRF143, RASRF150, RASRF152, RASRF154, RASRF155, RASRF156, RASRF162, RASRF166, RASRF168, RASRF169) have been collected along the edges of the two ephemeral floodplain channel systems. The edges of channels mainly show deposition, with 10 depositing cores and one eroding. Two of the cores are inconclusive, 2 sites are likely to show episodic processes, 4 cores show episodic processes and 3 show constant processes (Figure 54). The samples show relatively high sedimentation rates, averaging at 0.20 cm/a ± 0.22 cm/a with high variability in values between -

0.13 cm/a and 0.72 cm/a (Figure 56). Deposition rates are mostly consistent with the deposition rates in the adjacent channel.

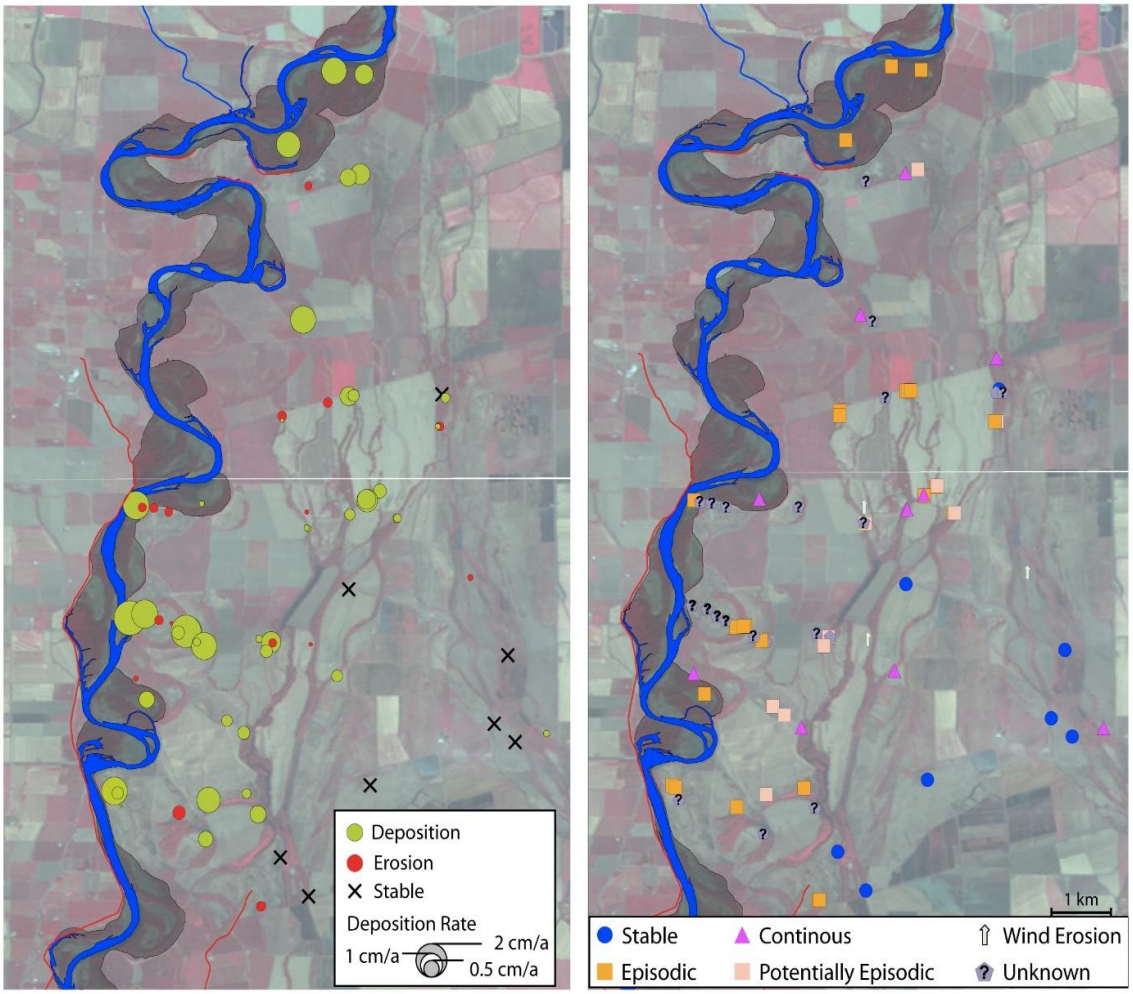

Figure 56 Distribution of sedimentation / erosion rates and floodplain processes along the Sacramento River. (Sources for imagery and data: www.sacramentoriver.org, www.water.gov, seamless.usgs.gov)

5. DISCUSSION

5.1. Late Quaternary Climate in Northern California and its influence on the Sacramento River

This study presents extensive geochronological controls on the stratigraphic units of the floodplains of the Sacramento River between RM192 and RM175. Chronologic controls on Quaternary units are sparse for the region and many interpretations are based on relative stratigraphic positions or soil parameters (Steele 1980, Robertson 1987) but are still representing the only sources for late Quaternary landscape evolution in the region. The only prior attempts to date the fluvial features of the Sacramento River in the study area, resulted in dates and paleo-environmental conclusions (Robertson 1987; Aalto & Nittrouer 2012) that do not agree with the Holocene age and evolution of the system determined by Olmsted & Davis (1961) and Helley & Harwood (1985). The dates presented in this study show that Olmsted & Davis (1961) and Helley & Harwood's (1985) interpretations of a Holocene age and origin of the floodplain channels are likely to be more accurate. The east side of Llano Seco shows stratigraphic evidence that it is a late Quaternary terrace position that is re-occupied by Holocene processes, therefore the eastern part of the research area will be referred to as Llano Seco (LS)-Terrace.

This study has shown a complete lack in characteristic gravel of non-Coast Range origin (Andesite) (Figure 7), what could be seen as indication that Stony Creek, the largest local supplier of Coast Range sediment along the Sacramento River, is the most likely source for most of the gravel deposits in LS-terrace. For the eastern part of Llano Seco, Robertson (1987) described gravel deposits with up to 40% abundance of Andesite on the east side of the research area originating in the Modoc Plateau / Klamath Mountains. This gravel body could potentially mark the intertwining area of the Sacramento River and the Stony Creek fan system gravel bodies. Following the interpretations above, the gravel deposits found in this study in Llano Seco can be interpreted as a Late Quaternary maximum extend of the Stony Creek megafan system that is preserved in this terrace deposits. This is in agreement with Meyer and Rosenthal's (2008) interpretation of the Llano Seco gravel

deposits that suspected a further extend of the late Quaternary Stony Creek fan, but did not provide evidence fort their hypothesis.

The Late Pleistocene

The resulting ages correlate the gravel deposits of LS-terrace with the Artbuckle terrace of the Stony Creek (Steele 1980). The lower fan and terrace formations along the western side of the Sacramento River, including the Stony Creek fan Artbuckle Terrace (Steele 1980) have been linked to the Lower Member Modesto Formation with minimum ages of 29.5 ka – 45.5 ka (Marchand & Allwardt 1981; Helley & Harwood 1985, Figure 57). However, more extensive numerical dating evidence is still missing. Steele (1980) estimated the age of the Artbuckle terrace ~ 30 ka due to the intensity of the soil development on this terrace. This is in coarse agreement with an U/Th age provided by Kate Maher (UC Sanford, previously published in an internal memo, but not publically available, used with consent of Kate Maher, written communication 05.05.2012) dating calcite crusts using SHRIMP series dating (Maher et al. 2007) forming on gravel deposits in the research area to 77 ka ± 25 ka. It is possible that this age overestimates the factual deposition age of the gravel, because it is possible that prior calcite crusts have not been destroyed and inherited calcite crusts were dated that developed prior to the last transportation deposition event.

Gravel mobilisation and transport in these deposits may be relatively limited, given that Llano Seco is located close to the confluence of the Stony Creek megafan and the palaeo-Sacramento River course. This is indicated by the dominance of Coastal Range gravel on the east side of the valley, with local tributaries sources in a different geology, making the nearby Stony Creek the most likely source for the deposited gravel. Thus, the age calculated from the calcite precipitation is treated as maximum age. Therefore, even though only one sample for age control is available and the age constrain is associated with a high uncertainty, we can interpret the gravel that start at ~ 2 – 5 m below surface as a maximum extent of the late Quaternary Stony Creek megafan system during the deposition period of the Artbuckle terrace. This in turn, indicates a greater influence of the Coast Range tributaries during the last glacial period, with the expanded fan likely diverting the Sacramento River east of its current position (potentially outside of the research area). This hypothesis,

of an increase in fluvial activity and expansion of the Stony Creek fan, is supported by climate data presented by Adam & West (1983) who reconstructed a substantial (~ 4-fold) increase in precipitation from Clear Lake pollen compositions. This substantial increase in precipitation was likely to increase runoff and therefore transport capacity in the Coast Range tributaries during the last glacial cycle.

Oregon and Northern California showed relatively cold and dry climates with shifts between non-glacial and glacial conditions before 23 ka (Worona & Whitlock 1995; Herbert et al. 2001; Bradbury et al. 2004). Hakala & Adam (2004) reconstructed the opening of the forest vegetation in Southern Oregon and on the Modoc Plateau from 32 ka. From 30 – 19 ka an open sagebrush steppe was dominating, indicating an overall reduction in precipitation. Little Lake pollen records (Southern Oregon) suggest higher variability in moisture and vegetation cover post 28 ka and indicated the opening of the landscape and the establishment of a relatively open forest vegetation after 25 ka with several major erosion events post 24 ka under generally cold conditions with a brief warm period from 25 – 22 ka (Grigg et al. 2001). Generally dry conditions with short wet intervals are reported from 25 ka at Tule Lake (Northern California) (Bradbury 1992). The shift in climate during full glacial conditions could have triggered a change in the balance between the Stony Creek and the Sacramento River, represented by a decrease in the influence of the Stony Creek fan system (and a strong decrease in younger Stony Creek fan gravel) and by an increase in the prevalence of finer (sandy) sediments in the research area. This culminated in the relatively rapid accumulation of shallow (< 3 m) fluvial sands between 33 ka and 22 ka, probably triggered by an increased sediment input to the fluvial systems in Northern California, where sediment was mobilised after a decrease in vegetation cover (Grigg et al. 2001) and an increase in the mobility and subsequent deposition of sands that was observed in lake sediments (Hakala & Adam 2004). Additionally, the remobilisation of dunes as observed in coastal Oregon (Davis 2006) indicate dryer conditions and an opening of the landscape. The dryer conditions that were observed throughout Southern Oregon and Northern California could have been responsible for the remobilisation and transportation of sediment to the floodplains, providing sediment for fluvial transport in the river systems of the adjoining areas. This intake of sands and a reduction in runoff due to generally

dryer conditions, potentially led to the development of a system that rapidly accumulated sands. Stratigraphically, this sandy unit observed in LS-Terrace can potentially be linked to the Upper Member of the Modesto Formation described as sandy fluvial deposits at the type location in Southern California (Marchand & Allwardt 1981) and with vast deposits present in the foothills of the Sierra Nevada (Helley & Harwood 1985). The difference in timing of the type location and the Llano Seco deposits can either be explained by the lack of ages produced in the original study at the type location (Marchand & Allwardt 1981), the advances in dating Quaternary sediments, or if there is indeed a difference in deposition age, the observed opposing trends in moisture regimes during the late Quaternary between Southern/Central and Northern California. Steele (1980) links the Yolo terrace of the Stony Creek to the Upper Member Modesto formation, but estimates its age to approximately 10 ka. Thus, either the sandy deposits on the Sacramento River floodplain are not linked to the Yolo terrace or the age estimate by Steele 1980 is underestimating the age of Yolo terrace. Contrasting to Steele (1980), Shlemon & Begg (1974) (written communication in Steele 1980) link the Stony Creek alluvial fan level 2 to an age of 10 – 30 ka what would correlate with the age of LS-Terrace in this study.

While Sea Surface Temperatures remained relatively low, they started to increase from 18 ka (Herbert et al. 2001, Figure 58). Precipitation increased in coastal Oregon and the Modoc Plateau from ~ 21 ka to ~ 16 ka (Worona & Whitlock 1995; Hakala & Adam 2004), even though some records show cool and dry conditions until ~ 17 – 13 ka (Bradbury 1992; Grigg et al. 2001; Daniels et al. 2005).

The general wetter conditions in Oregon and Northern California potentially lead to an increased vegetation cover that stabilised the surface and reduced sediment transport from the slopes to the fluvial system (e.g. Lian & Hickin 1996; Zolitschka & Negendank 1998; Brathauer et al. 1999; Harvey 2002; Hakala & Adam 2004; Cammeraat et al. 2005; Dreibrot et al. 2010) enabling concentrated flow and erosion to take place in the Sacramento River. This process resulted in a lower topographic position of the Sacramento River, with parts of the former fluvial system remained as a terrace, protected from erosion and deposition accompanied by soil formation processes at these terrace locations (Figure 58). Given its active tectonic history and the influence of Glenn Syncline on the current position of the Sacramento River (Helley &

Harwood 1985; WET 1990; Fisher 1994), an influence of the Glen Syncline on the late Quaternary Sacramento River is also likely, but cannot be reconstructed on the basis of the data collected in this study. Whether the influence of the Glen Syncline was important enough to cause sudden and substantial incision of the Sacramento River to establish the 10 – 20 ka terrace that was reconstructed from stratigraphic evidence, cannot be verified. Potentially a combination of climate and environmental changes in combination with tectonic movements could explain the shift and incision of the Sacramento River after ~ 20 ka.

The Pleistocene Holocene Transition

Records for Northern California and Western Oregon show a cool and wet period starting 15 – 16 ka and lasting until 11 – 11.5 ka (Grigg & Whitlock 1998; Herbert et al. 2001; Barron et al. 2003; Daniels et al. 2005, Figure 57).In Central California lake levels dropped after 13 ka and recovered by 11 ka (Bacon et al. 2006, Figure 58). This brief period of increased precipitation might be responsible for reworking of material in the eastern part of the research area. Additionally, James et al. (2002) observed a rapid ice retreat in the North-western Sierra Nevada around ~ 14 ka probably leading to an additional increase in runoff for Sierra Nevada and Klamath Mountain tributaries during that time the from melting glaciers. This probably resulted in the reworking of fluvial sands in the eastern part of the research area. This episode remains speculative, because this hypothesis is based on only one OSL age and limited knowledge on North-western Sierra Nevada paleohydrology.

The Holocene

After this short cold event temperatures rapidly recovered and reached modern values between 11.5 and 10 ka (e.g. Herbert et al. 2001; Benson et al. 2002; Barron et al. 2003, Figure 58). This shift to modern temperatures and precipitation rates likely lead to hydrologic conditions that are similar to the ones observed today and the establishment of a single thread meandering river in the early Holocene represented by the onset of the deposition of silt rich floodplain deposits analogous to Holocene developments worldwide (e.g., Knox 1995). This establishment of a meandering system is confirmed by three ages dating silt rich floodplain deposits to the Mid-Holocene (6.2 ± 1.5 ka cal BP, 5.9 ± 0.9

ka, 5.5 ± 0.1 ka cal BP) or older. This has to be assumed as a minimum age, because none of the dates are from the base of the floodplain loam strata of the profiles. In two cases, it was impossible to sample the bottom of the strata, because it was either not reached (T3P14) or submerged by water (T1P9). For T2P1 3 dating attempts produced ages that have all been discarded because they do not fit in the chronology of the profile that has been well established by 5 ages that are aligned in stratigraphic order.

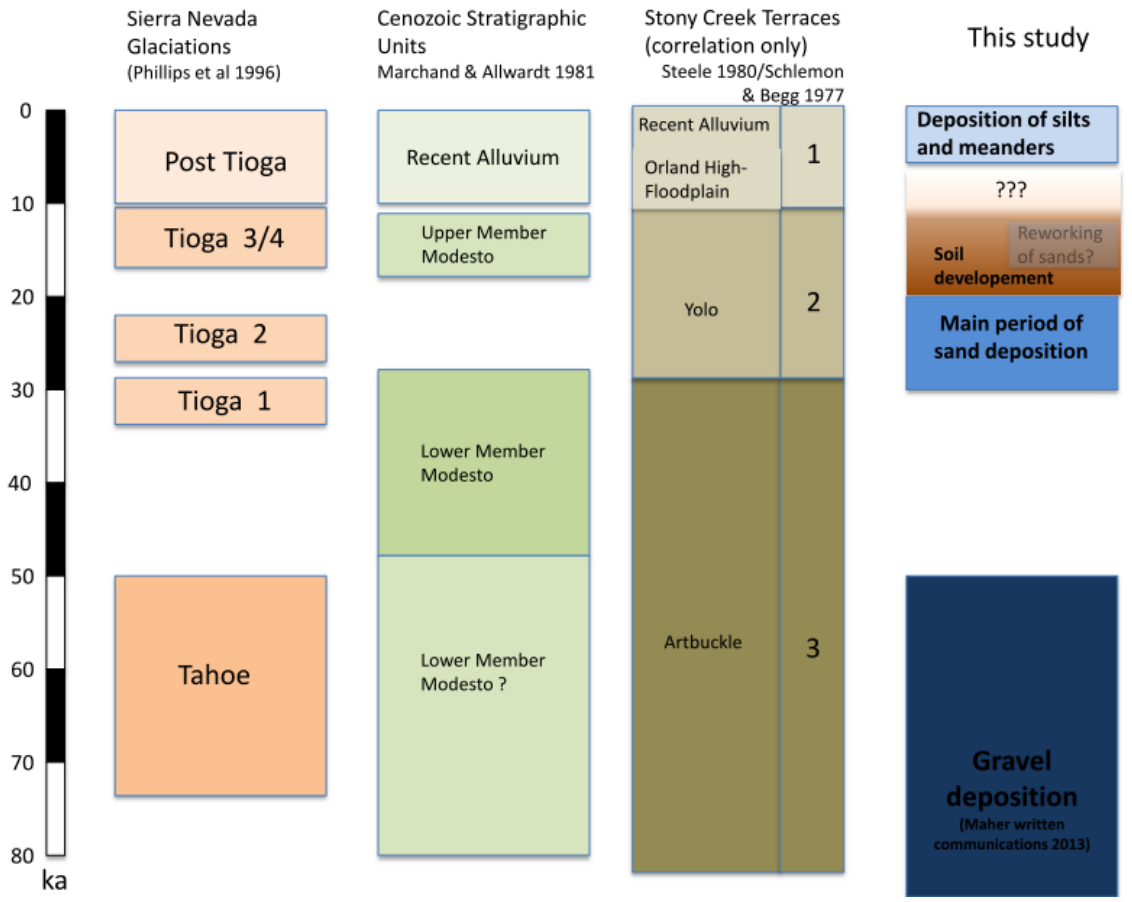

Figure 57 Linking the stratigraphic units in the research area to regional stratigraphies. The local deposits have stratigraphically linked to the stages of the Sierra Nevada glaciations (Phillips et al. 1996), Stony Creek terraces (Steele 1980), and the regional geologic formations (Marchant & Allward 1981).

5.1.1. The influence of local tectonic faults on the position of the Sacramento River

Prior studies highlighted the influence of tectonic features on the morphology and position of the Sacramento River (Harwood & Helley 1987; WET 1990; Fischer 1994; Singer & Dunne 2001; Singer & Dunne 2004). While Harwood & Helley (1987), WET (1990), and Fischer (1994) discussed the influence of tectonic faults on the lateral position of the Sacramento River at the

research area, Singer and Dunne (2001, 2004) focused on the influence of tectonic features on the longitudinal profile of the Sacramento River. The influence of tectonic movements that influence longitudinal profile of the Sacramento River on the research area cannot be reconstructed due to the study design.

In this study the established meander chronology has been used to reconstruct the timing of the westward movement of the Sacramento River. The oldest dated meander in this study shows an age 2.4 ± 0.1 ka cal BP with older meanders reported by Sullivan (1982) and Robertson (1987) and visible in historic aerial photos. Within the research area, the active channel is located at the westernmost position within its tectonically widened Holocene meander belt (Harwood & Helley 1987; WET 1990; Fischer 1994). The results of this study indicate a westward movement of the Sacramento River since at least 2.4 ka cal BP plus 2 meander generations. The resulting configuration of oxbow lakes and channel scars shows a remarkable resemblance with the (modelled) response of meanders to lateral tilting (e.g., Peakall et al. 2000). WET (1990) observed that the Sacramento River is following smaller synclinal structures in the Central Valley at several instances. While following these structures, the active meander belt of the Sacramento River is significantly widening in comparison to other reaches of the river (WET 1990). In the vicinity of the research area, the Holocene meander belt is ~ 2 – 4 km wide, and the current position of the Sacramento River closely follows the Glenn Syncline. Both observations are indicating the influence of this tectonic structure on the position of the river within the basin (Harwood & Helley 1987; Robertson 1987; WET 1990). The movement of the river to the west, the general widening of the Holocene meander belt (WET 1990), the river's position relative to the geosynclines, and the resemblance to results from studies modelling the influence of lateral tilting on meander migration (Peakall et al. 2000), all support the hypothesis that the modern, western position of the Sacramento River is probably largely influence by lateral tilting processes along Glenn Syncline (Helley & Harwood 1985; WET 1990; Fischer 1994). Additionally, changes in sediment productivity of the Stony Creek could potentially modulate the influence of the Glenn Syncline on the position of the Sacramento River in the vicinity of the confluence, by providing a surplus in gravel that could potentially translocate the position of the Sacramento River further to the east. The

relatively young channel scars (2.4 ka cal BP) in an eastern position within the Holocene meander belt possibly indicate a relatively recent onset of the westward movement of the Sacramento River (Figure 37).

5.12. The evolution of Sacramento River floodplain channel system

Contradicting the hypothesis of Robertson (1987) and Dunne & Aalto (2013), the dating of the floodplain sediments in this study showed that the floodplain channels are not relic Pleistocene landforms. This study supports Olmsted & Davis (1961) earlier hypothesis of a Holocene age and origin of the floodplains, that of a more recent (potentially Holocene) development of the floodplain channel systems – because the floodplain channels are almost exclusively present in Holocene sediments and rarely extend into older deposits, and are also independent from the underlying gravel and sand topography (Figure 38).

Similar floodplain topography has been observed during the initial stages of avulsions, with diverted flow creating an anastomosing channel geometry (Slingerland & Smith 2004; Makaske 2001; Smith et al. 1989). Therefore, the stable anabranching patterns of the Sacramento River floodplain channels could potentially be classified as the result of an incomplete avulsion. Aslan et al. (2005) showed for avulsions along the Mississippi River that a steeper slope gradient of the floodplain is a necessary condition for the occurrence of avulsions, but the substrate composition and the channel geometry are of greater importance for the completion of the avulsions. In the case of the research area, the channel geometry of the Sacramento River between River Mile 190 – 193, the bed aggradation forced by the extensive gravel deposits of Stony Creek, and the resulting flood runoff diverted from the Sacramento River (especially during large floods) probably initiated the avulsion and the creation of the floodplain channel by the concentration of flow along the main down-valley flow path. The the gravel contents of the modern Sacramento River (and as a layer under the Holocene floodplain deposits) and its resistant Pleistocene terrace deposits (e.g. Modesto Formation, Fischer 1994) are probably prohibiting the completion of the avulsion that would permanently relocate the main stem of the Sacramento River.

Besides substrate, the low difference in slope between the Sacramento River and the floodplain channels (0.04 and 0.05 respectively) might have some influence on the stability of these channels. Miall (2014) observed that elevated levees that can be breached with high energy to create crevasse channels are another important requirement for stable avulsions. Such elevated levees are missing along this reach of the Sacramento River (Figure 13), which could be an influencing factor prohibiting the completion of the avulsion. The channel geometry of the Sacramento River therefore probably favours the maintenance of a stable flow diversion of a high amount of annual flood runoff, supporting the maintenance of the floodplain channel network. Consequently, the floodplain channel systems provide a permanent transport pathway for water and suspended sediment from the Sacramento River to the Butte Sink, maintaining shallow floodplain channels that supply the distal parts of the floodplain with fresh sediment without progressing to a full avulsion.

Artificial levees did not influence the initial development of the Sacramento River, because the floodplain channels did already exist before the construction of the Sacramento River levee system. Today's influence of artificial levees on the channels must be relatively minor, because they don't exist along the left bank of the Sacramento River for most of the research area (Figure 13). The role that the right bank levees might play in forcing more floodwater towards the research area can only be speculated, but it is likely only a secondary effect because there are not many floodplain channels to the west.

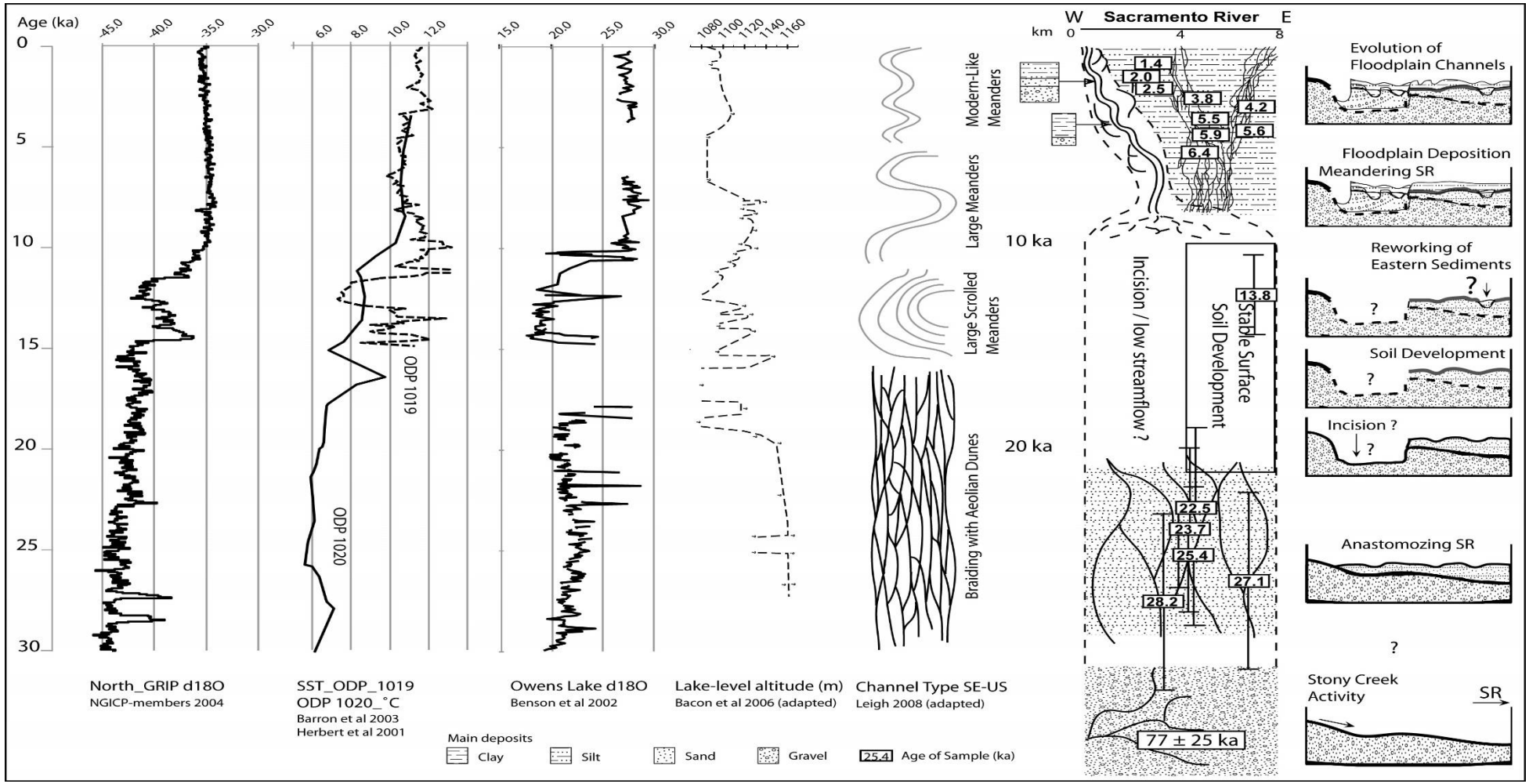

Figure 58 Response of the Sacramento River to Late Quaternary climate change illustrated by northern hemisphere climate reconstructions from Greenland (NGCIP-members 2004), local sea surface temperatures along the Californian coast (Herbert et al. 2001; Barron et al. 2003), climate records from Central California with δ ^{18}O records from Owens Lake (Benson et al. 2002), lake level altitude changes in Central California (Bacon et al. 2006), and changes in fluvial planform throughout the Pleistocene-Holocene transition in the American East (Leigh 2008).

5.2. The influence of agriculture on the ^{210}Pb dating potential applying the CIRCAUS/CNAXS approach

More traditional analyses of unsupported or excess ^{210}Pb (utilising large sample volumes and Gamma Spectrometry) were in some cases able to apply a high-resolution sampling strategy that could distinguish differences in XS ^{210}Pb activity profiles between different regions and land use types within one region in fluvial and colluvial settings (e.g., He & Walling 1997; Walling et al. 2003; Mabit et al. 2008). These studies showed specific properties of XS ^{210}Pb activity depth profiles for pastures and ploughed areas (e.g., He & Walling 1997) as well as for infilling and stable sites in both fluvial and colluvial settings (e.g., Walling & He 1997; Walling et al. 2003).

The obtained XS ^{210}Pb activity depth distributions presented here show clear evidence that land use, land use changes and different sedimentation scenarios are reflected in the specific shapes of the XS ^{210}Pb activity depth distributions. XS ^{210}Pb activity profiles of undisturbed cores in the research area are similar to undisturbed profiles in humid (e.g., He & Walling 1997; Wakiyama et al. 2010; Walling & He 1994) as well as in Mediterranean (Porto & Walling 2012; Gaspar et al. 2013) and semi-arid environments (e.g., Kato et al. 2010; Mabit et al. 2008). This common trend is an indication for the accumulation of adsorbed fallout XS ^{210}Pb at the surface with little and post sedimentation redistribution of XS ^{210}Pb under stable conditions (He & Walling 1997).

Comparing XS ^{210}Pb activity profiles at sites showing no sedimentation and sites showing constant sedimentation, several differences become apparent that are not only dependent on total inventories, even though total inventories differ significantly. Surface values are similar in both scenarios but there is a steeper decline in XS ^{210}Pb activities for stable sites between 0 – 6 cm, with XS ^{210}Pb activities reaching background levels at 22 – 30 cm whereas sites experiencing deposition hardly (3 out of 12) reaching background levels within the first 30 cm. At this depth only one core under stable conditions show elevated XS ^{210}Pb activities (Figure 40, Figure 59). The constant supply of sediment and XS ^{210}Pb buries sediment that is showing elevated XS ^{210}Pb activities. Activities remain increased until XS ^{210}Pb has fully decayed and only supported ^{210}Pb is present (Figure 59).

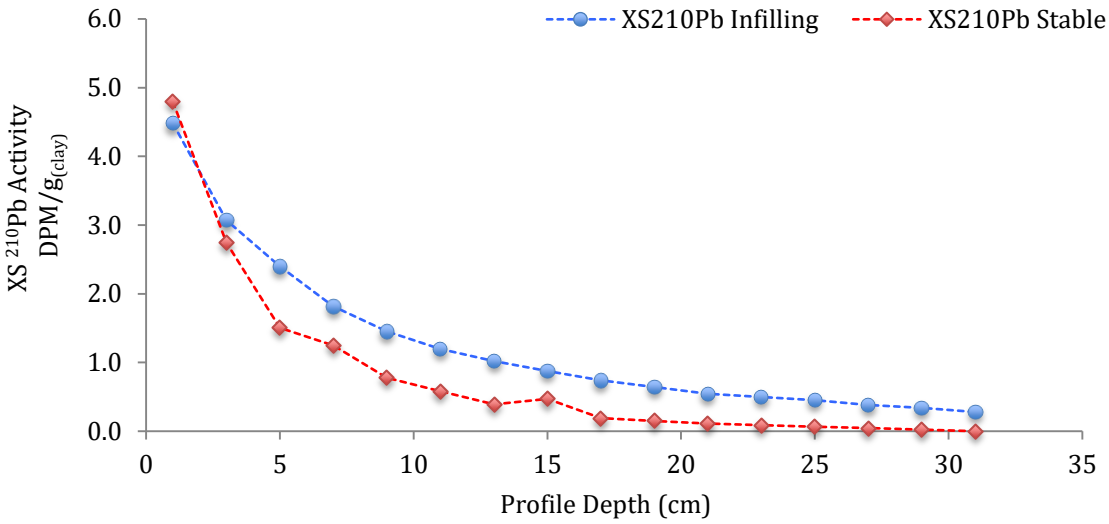

Figure 59 Comparison of the average XS ^{210}Pb activity profiles of infilling and stable sites showing the steeper decline in XS ^{210}Pb activities in stable profiles.

Even though the general trends are different (Figure 59), it is impossible to distinguish between stable sites and sites showing deposition on shape alone. CICCS inventories are essential to distinguish between stable sites and sites showing constant deposition because the shape of single activity profiles can be similar between both environments. (Figure 40, Figure 41, Figure 60).

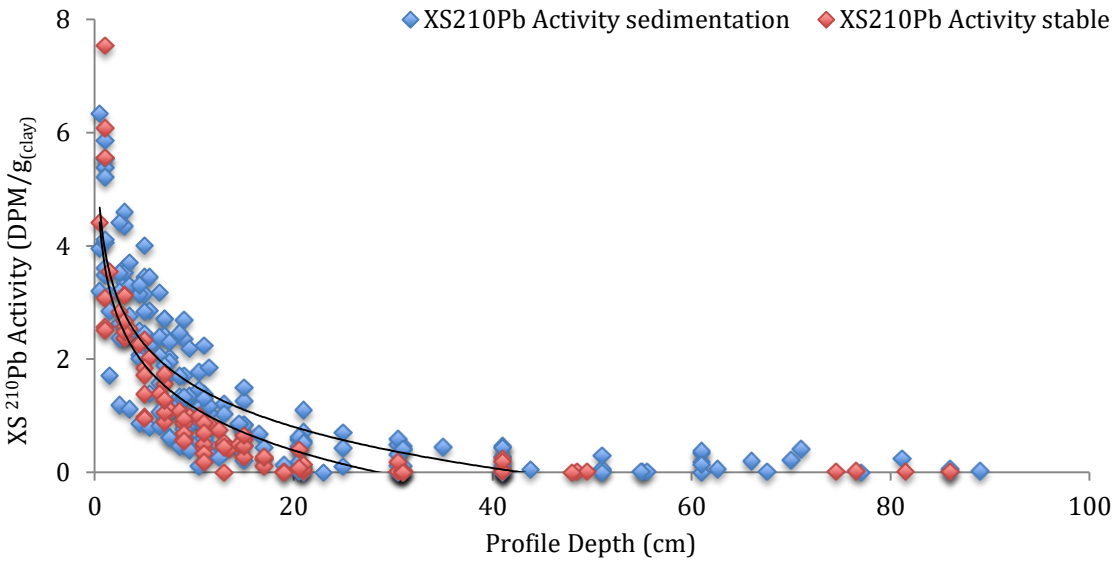

Figure 60 XS ^{210}Pb activities for stable sites and sites showing constant sedimentation, showing clear differences in infiltration depth and the slope of XS ^{210}Pb activity decrease but also an overlap of the activity profiles.

This study also shows that the detection of episodic deposition is possible in a medium to low deposition environment as shown by Singer & Aalto (2009). For this detection, two main conditions are required: a) for one sediment packages have to be larger than twice the sample interval or it would not be recognisable as single event, and b) no significant post-sedimentation reworking by cultivation (e.g., He & Walling 1997) or bioturbation (Resner et al.

2011) must have occurred, because mechanical soil movements would destroy event signatures. Using the developed high-resolution (1 cm) approach, larger sedimentation events (> 4 – 5 cm deposition/event) are well datable (Aalto & Nittrouer 2012), but even small deposition events (2 – 4 cm deposition/event) are detectable and therefore the sedimentation style and changes in this style over the detection period are possible to determine and date.

All cores collected at agricultural sites show clear indications of mixing and homogenisation of the top portion of the cores due to mechanical reworking by ploughing, discing and potentially sowing with all machines breaking up the surface and redistributing surface material to locations further down in the soil profile. The tendency of post deposition redistribution of XS ^{210}Pb by agricultural use of a landscape has been shown in prior studies (e.g., He & Walling 1997; Walling et al. 2003; Mabit et al. 2008; Porto & Walling 2012; Benmansour et al. 2013; Gaspar et al. 2013), but this study is the first to show differences in profile shape for different types of agricultural land use, and how this is affecting the potential for CIRCAUS/CNAXS dating in this environment.

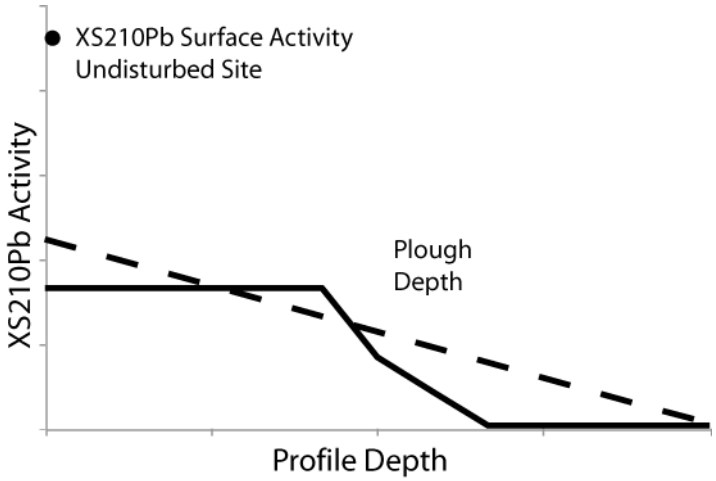

Figure 61 Idealised activity depth profiles for ploughed sites. Solid line marks a ploughed profile under stable conditions. Dashed line marks a ploughed profile under infilling conditions showing sediment mixing but lack of complete homogenisation.

At ploughed sites mechanical redistribution of XS ^{210}Pb as shown in several other studies (e.g., He & Walling 1997) leads to a significant reduction in surface activity of XS ^{210}Pb. The transport of XS ^{210}Pb further down the profile results in increased XS ^{210}Pb activities at depth below 10 cm. Complete mixing seems to be dependent on the lack of active sedimentation at the site, so more than one mixing cycle is necessary to create an even distribution of the XS ^{210}Pb activities in a profile, as observed for other radionuclides by Meisel et al.

(1991) - because only stable sites or sites with low erosion rates show even distributions of XS ^{210}Pb activities (Figure 45, Figure 61). At depositional sites, a slight down profile decrease in XS ^{210}Pb activities can be observed indicating incomplete homogenisation at infilling sites under ploughing. This might be due to high deposition rates with a plateau formation needing several ploughing cycles to completely homogenise the ploughed part of the profile (He & Walling 1997; Meisel et al. 1991, Figure 45).

Pastures that are disced with a disc harrow generally show an increase in XS ^{210}Pb at maximum disc depth (in this case 10 – 12 cm) (Figure 62). The fact that this increase in XS ^{210}Pb at 10 – 12 cm can be found at sites that are disced on an annual basis indicates that this distribution is a product of the use of a disc harrow. This indicates post fallout transport of XS ^{210}Pb in a non-diffusive manner with a resulting emplacement of an increased concentration of XS ^{210}Pb at the disc depth. This characteristic shape changes in XS ^{210}Pb activity profiles are harder to determine in areas where sediment accumulates. In these environments, the increase in XS ^{210}Pb activity associated with discing depth can be mistaken for a deposition event in an area showing episodic sedimentation - the increase in XS ^{210}Pb activity resembles an XS ^{210}Pb cap at sites showing episodic deposition (Figure 62). Sites that have been disced also show reduced average XS ^{210}Pb activities indicating erosion. The reduction in XS ^{210}Pb may have been caused by wind erosion following the discing process or due to cattle farming during the summer month with high grazing pressure reducing the surface cover and trotting cattle breaking up soil aggregates enabling XS ^{210}Pb bearing clay minerals to be eroded. For high-resolution profile analyses anthropogenically undisturbed sites are therefore essential, especially for processes that cause only minor changes in the activity profiles.

Previous studies indicate that deposition styles and large-scale land use are detectable in several different environments (e.g., He & Walling 1997; Aalto & Nittrouer 2012). However, Resner et al. (2011) observed that factors like bioturbation play a major role in XS ^{210}Pb profile development and might limit the potential to detect less prominent profile changing activities like discing in other environments.

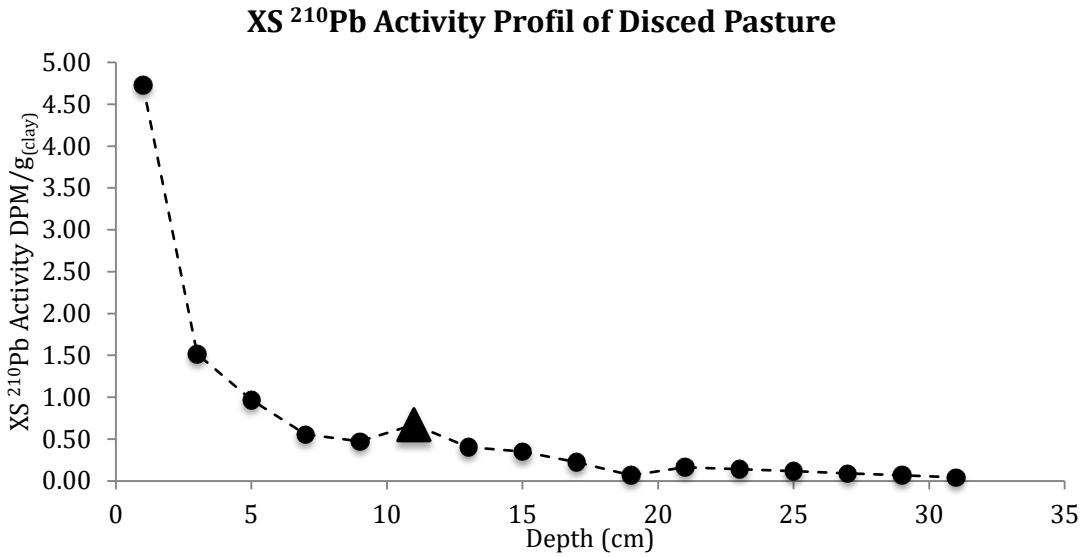

Figure 62 XS ^{210}Pb activity profile for pastures that have been disced or are disced on a regular basis show increased XS ^{210}Pb activities at disc penetration depth (10 – 12 cm).

Deposition events

In this study it was investigated where and how sediment deposition has occurred along the Sacramento River. Aalto et al. (2003) were able to correlate deposition events with runoff and climate phenomena in the Amazon Basin using XS ^{210}Pb dating. In the case of the Sacramento River, linking sedimentation events dated with XS ^{210}Pb to runoff or precipitation events islimited bythe restriction of the dating potential of XS ^{210}Pb dating of specific events to the past ~ 40 years by the low fallout rates of ^{210}Pb in the region. Additionally, the error of approximately ± 4 a for this period is making it difficult to correlate deposition events with runoff data from the Sacramento River. Also, the lenses of sediment deposited within a single event are rather thin (~ 5 cm), and the dating of deposition / erosion events was limited to 17 events in 14 cores. This low number of datable events complicates the correlation with flooding, inundation rate, or other hydrologic proxies. Nevertheless deposition events can sometimes be correlated to large floods (1984/1986, 1997). However, other periods of low flow (with little inundation) show event like characteristics as well (1990). This can especially be observed at ~ 1990, when the most commonly detected episodic event occurred, a year that is also located within a fairly prominent period of below average flood runoff (from 1987 – 1992). The reason for the distribution of dated deposition / erosion events is still unclear and could be an artefact of the sampling distribution that is further accentuated by the low number of total dated events or even a genuine

increase in fluvial activity. However, to prove deposition trends in this area, more research and core dating are needed.

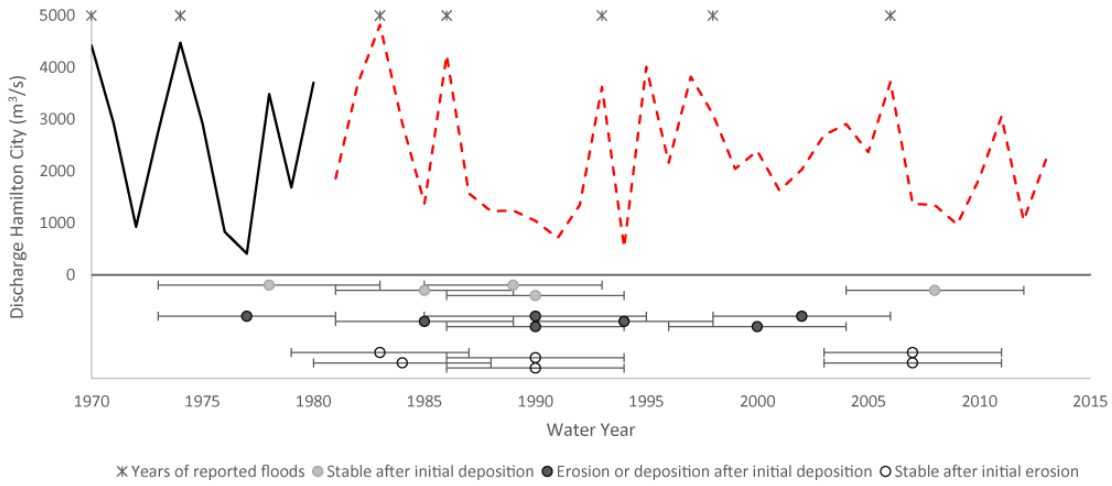

Figure 63 Graph showing flow and water loss at Llano Seco including deposition/erosion events. Apparent are the high number of dated events between 1985 and 1990. There are just two events dated to the time before 1970, so they've not been included in the graphic.

There seems to be a decrease in datable episodic events after the mid-90s. The dating of arriving sediment stacks showed that there is a culmination of events in the mid-1970s, mid 1980s and around 1990. Especially, the 1990 event is fairly prominent mainly due to erosion in 3 cores in the lower part of the floodplain. This event of high deposition and erosion probably happened during the only larger flooding event during a period of low flows and decreased water loss to Llano Seco (1987 – 1992, Figure 63).

It is likely that large floods are responsible for the largest suspended sediment concentration along the Sacramento River (Singer & Dunne 2001), and therefore for the largest deposition events on the floodplain. The source of suspended sediment in rivers is highly variable but and dependent on the position within the system. The majority of suspended sediment is sourced on the slopes of the river system, even though bank erosion is likely to play a larger role in large river systems (Walling 1999, Walling 2005).

According to the empirical flood frequency analysis 34 of the past 67 floods (~ 50 %), went overbank (Figure 18). The largest 10 floods occurred in 1983, 1974, 1970, 1965, 1986, 1958, 1952, 1956, 1997, and 2006. None of the flooding events that occurred in the 1950s and 1960s could be found in the collected profiles. There are 2 dated events in the late 1970s. Whether one or both of the large flooding event in 1970 and 1974 is responsible for the stacks

of sediment dated to 1977 ± 4 / 1978 ± 5 is not clear, because these events are at the edge of the error ranges of the dating method. There are 3 dated events in the 1980s represented in the cores that could easily represent either one of the large flooding events in 1983 or 1986. With the error of the method it is not possible to determine which one of these events is responsible for the deposited sediment. There is none of the largest 10 flooding events within the dating error of the largest accumulation of deposition/erosion events (1989 – 1990). The only larger flood with a 5 year exceedance probability within the dating error occurred in 1993. This flood or the 1994 flood (3 year exceedance probability) is potentially responsible for the sediment deposit dated to 1990 ± 4. Even though it is likely that larger floods lead to larger sediment dispersal on the floodplain, the dating in this study does neither confirm nor rebut this hypothesis.

There is a multitude of reason for this: 1) a rather low number of dated events, 2) the relatively large error of the used dating method, and 3) the high reoccurrence interval of flood flow entering the floodplain (2 years). But not only problems in the dating method might have caused this weak correlation of dated events with individual floods, because the largest number of dated events falls in the centre of a 7-year period of below average flood flows. This could either be explained by declaring the dating method as useless, or not only very large floods are responsible for floodplain surface alterations, but factors that differ from discharge forcing play a role in floodplain erosion and deposition processes.

Even though it is possible to date single events along the Sacramento River, the CIRCACS/CNAXS approach (Aalto & Nittrouer 2012) seems not to be as well applicable as in other systems (e.g. Aalto et al 2002). In the research area less than 20 % of all collected cores can be used for dating individual events, even though the coring locations have been specifically targeted potentially undisturbed sites in one of the least intensely used areas in the Sacramento River Valley. This indicates an important limitation to the applicability of CIRCACS/CNAXS dating in agriculturally used areas.

5.3. Quantification of sedimentation rates using XS ^{210}Pb

Along the Sacramento River, sedimentation can be traced and deposition rates can be quantified using the CICCS approach (Walling & He 1994; He & Walling 1996). However, these results are underestimating sedimentation rates in certain environments (Aalto & Nittrouer 2012). This is especially the case for sites close to the modern main stem, located along the main flood pathways and within channel scars, where sedimentation rates are high. Wherever sedimentation occurs infrequently or the site is too young to develop the full natural fallout inventory, the CICCS approach does not render reliable sedimentation rates (Aalto & Nittrouer 2012). In cases where the background activity of XS ^{210}Pb cannot be reached by the bottom of the core or grain size is highly variable, the CIRCACS method is likely to produce more accurate results (Aalto & Nittrouer 2012). Nevertheless, episodic events can only be translated to sedimentation or erosion rates for periods of deposition while the amount of eroded sediment often can't be reconstructed, because a high amount of erosion might erode more than the natural fallout cap of the sediment, making it impossible to calculate the real erosion rate (Aalto & Nittrouer 2012). Generally, in this study the CICCS and CIRCACS rates are used to calculate approximate sedimentation rates. In one case, a reliable marker horizon was present. At this location the sedimentation rate was reconstructed using the CIRCACS method, the results significantly underestimated the sedimentation rate calculated from the independent marker horizon (T1P4). This indicates that the calculation of high sedimentation rates using any of these methods is not necessarily accurate – ultimately, results from both CICCS and CIRCACS dating have to be treated as minimum sedimentation rates. Especially for the case of extremely high deposition rates and/or sandy sediments, neither approach is able to render reliable results, leaving much room for improvement of ^{210}Pb dating (Aalto & Nittrouer 2012). Nevertheless, the combination of CIRCACS and CICCS sedimentation rates provides reasonable constraint on sedimentation and deposition along the Sacramento River.

Singer & Dunne (2001) identified eroding and depositional reaches of the Sacramento River by analysing the average suspended sediment load and identify the study reach as eroding. In this study the total amount of sediment

deposited on the floodplain was calculated. This study found that approximately 0.75 Mt of sediment are stored during average floods (on a biannual basis). For this calculation an informed estimate for floodplain inundation of the FEMA 100 year flood extend of 80 % has been used. This estimate is depending on varying discharge rates so an 80 % floodplain inundation rate can only be used as an approximation and has to be treated with caution. Considering the variability of sedimentation rates throughout the system the uncertainty of total deposition would amount to more than 100 %. Assuming the calculated 0.75 Mt/flood of sediment deposition are relatively reliable, approximately 33 % of total suspended sediment load (Hamilton City gauge, Singer & Dunne (2001)) are transported to and deposited within the research area during average discharge floods. This amount equals the net divergence of suspended sediment between Hamilton City and Butte City gauge (0.75 Mt/yr, Singer & Dunne 2001) in average flood years. Of the sediments transported to the floodplain ~ 60 % are removed from areas easily reworked by the Sacramento River and stored in long term stable sinks on the distal floodplain.

Deposition trends (Crevasse splays)

The deposition along the Sacramento River is driven by deposition proximal to the main river channel (~ 40 % of total floodplain sedimentation within the first 500 m), and flow and sediment dispersal via ephemeral channels that are supplied by natural and man-made flood outlets with long-term fixed positions (Figure 15). The existence of stable and maintained flood outlets leads to a lack of last century's levee failures and crevasse splay deposits in the research area. While Aalto et al. (2002) argued that crevasse splays and sheet sands are the main driver of floodplain aggregation along some rivers in the Amazon Basin, no recent crevasse splays can be observed along the Sacramento River between RM174 and RM194. The main reason for the contrasts in driving depositional processes, besides the obvious difference in size, climate, and land-use between the river systems, might be the fact that the Sacramento River has developed a permanent flood avulsion pathway (present at least since the 1874, Figure 1) that is acting as a natural flood release system, with the floodplain channels readily conveying the flow and sediment from the main stem to Butte Sink basin. This and the additional anthropogenic flood outlet structures (Singer et al 2008) reduce the pressure on natural and

anthropogenic levees downstream of the research area, thereby preventing or minimizing levee failures and therefore the emplacement of major crevasse splays.

Deposition trends

Day et al. (2008) documented an exponential decrease in sedimentation rates for floodplains along tropical rivers in Papua New Guinea. Here, the rates depend on the distance from the closest channel, with sediment transport independent of the channel type and solely dependent on distance to the adjacent channel. Similar trends, in respect to the main stem have been reported by Middelkoop & Asselman (1998) along the River Rhine and also in respect to the long-term evolution of a floodplain in relation to its channel belt by Törnqvist & Bridge (2002) along the River Rhine and the Mississippi River. The results of this study differ significantly from the results presented by Middelkoop & Asselman (1998); Törnqvist & Bridge (2002); and Day et al. (2008). The deposition within the research area generally shows only a slow decrease from the main stem, with highly variable sedimentation rates up to 8 km from the main stem of the Sacramento River (Figure 51, Figure 52). It is possible that these sediments originate from local sources, however, the high transport capacity of the floodplain channels at least do not exclude the possibility of long distance transport of sediments in these channels. Especially since all grain sizes measured in the cores are potentially transported as wash load in the channels. Within the first 3 km of the main stem, the erosion and deposition rates are highly variable, and the floodplain channels serve to transport sediment to the distal part of the floodplain, resulting in a very slow decrease in the documented deposition rates. This slow decrease of average deposition rates might be partially a product of the sampling strategy that was chosen to target undisturbed locations, to detect and date flooding events, rather than document the spatial distribution of erosion and deposition rates throughout the research area. The resulting distribution of sample sites is following closely the course of the smaller floodplain channels, because most of the undisturbed sites are located in the vicinity of these channel features (Figure 22, Figure 23). Therefore, samples have not been collected in transects away from the described channel features as practised in other studies (e.g., Middelkoop & Asselman 1998; Törnqvist & Bridge 2002; Day et al. 2008). On the other hand,

it is observable that the low rates of the decline in sedimentation rates away from the main stem are an observable feature of this landscape – and the prevalence of these small floodplain channels presents a viable mechanism for this observation. It is important to note that the floodplain channels in question are much more shallow, ephemeral, and not connected to the main stem in comparison to the tie-cannels investigated by Day et al. (2008). The difference in depositional trends might potentially be influenced by the difference in surface cover and other natural and anthropogenic topographical factors between the densely forested reaches of the tropical Fly River (Day et al. 2008), the fully agricultural reaches of the River Rhine (Middelkoop & Asselman 1998), and the heterogeneous vegetation cover along the Mediterranean Sacramento River. The difference in deposition rates could also be influenced by the high variability of landscape units, the anthropogenic creation of sinks and the limitation of flood release to three long term topographically stable locations along the Sacramento River, channelling the diverted flow along certain pathways, and therefore limiting deposition to certain areas of the floodplain.

The trend observed along the Sacramento River is rather similar (on a larger scale) to the results Swanson et al. (2008) report for deposition rates along the tropical Strickland River (Papua New Guinea) that show high variability in deposition rates for the first kilometre from the channel bank. The greater distance that sediment is transported away from the Sacramento River could be a result of the limited presence of dense riparian forests at the flood outlets that exhibit few trees and little undergrowth at these sites. Enabling the transport of sediment along efficient flow path to the distal part of the floodplains, in comparison to the dense forests along the tropical Strickland River in Papua New Guinea.

Deposition trends (floodplain channels)

Sedimentational trends in different types of channels that are visible in the topography of the floodplain often correlate with their morphological history and connectivity. Scour scar channels seem to create stable surfaces after their initial incision as observed at all three sites located within these scour channels (RASRF 137, 157, 158). Channel scars, the remnants of former meanders show the highest infilling rates of all floodplain cores. These high sedimentation rates

are likely the result of the high connectivity with the main channel (Cabezas et al. 2010).

Focusing on the transport within the floodplain channels and excluding deposition associated with 1) the main stem Sacramento River and 2) deposition within smaller channels and channel scars, the deposition rates do decline rather quickly as you move away from the floodplain channels. This drop is again not as pronounced as reported for the more established floodplain channels in tropical environments by Day et al. (2008), but the sediment is generally deposited within 100 m of these channels.

The difference in the influence of floodplain channels on sediment transport to distal parts of the floodplain between the Sacramento River and the observations e.g. by Day et al. (2008) could lie in the different nature of the channels that orchestrate the transport processes for both river systems. The channels discussed by Day et al. (2008) – the main channel, tie and tributary channels – are deep conduits that are permanently connected to the main stem, whereas floodplain channels along the Sacramento River are separated from the main stem by a strip of elevated floodplain, and start up to 1 km from the main channel. This configuration for floodplain channels exiting along the Sacramento River is likely to reduce the hydrologic connectivity between both channel systems, and therefore it is likely to affect the sediment load delivered to the floodplain (Cabezas et al. 2010). The sediment load transported by the floodplain channels away from the Sacramento River has therefore to be heavily reduced in respect to the original sediment load of the main stem, in response to deposition occurring during changes in flow depth and velocity. Therefore, the floodplain channels along the Sacramento River carry and disperse only a substantially reduced sediment load for an expansive floodplain, located up to 10 km away from the closest flood outlet of the main stem Sacramento River. Consequently, the distal floodplain accumulation rates must therefore remain lower along the floodplain channels than those along the main stem or in areas with a higher connectivity between floodplain channels and main stem. Therefore, deposition and erosion along the Sacramento River floodplain channels does not follow the exponential model proposed by e.g., Day et al. (2008), but rather a linear trend away from floodplain channels similar to the trends observed by Walling & He (1998) or Swanson et al. (2008).

However, these channels are not exclusively depositional environments, because they are also slowly reworking the existing floodplain. Erosion was observed at several locations along both of the floodplain channel systems, but seems to be a less important process. It often appears to be associated with human influences (post-bridge/-road scours) and tree roots, but further investigations would be necessary to verify or falsify this hypothesis.

Environmental influences

Even though sedimentation trends seem to be highly variable with distance from the channels, similar environments seem to have similar sedimentation trends independent of their relative distance to the sediment source. Nevertheless, there is a general trend with the highly variable and generally more active environments closer to the river, exhibiting similar high sedimentation rates. This is in contrast to rather uniform and lower infilling rates, documented further away from the channels and main stem. This is not as obvious in absolute distance to channels, but rather for the relative position within the flood web. Especially, some of the environments have very low variability (e.g. channel scars, low fields, high floodplains). The similarities between the environments are potentially linked to similar land use / vegetation cover, runoff, or general position in the flood web. The environments with the lowest variability seem to have the most similar environmental and flow conditions. While e.g. proximal locations with variable flow and variable topography show a high variability in deposition rates and processes, high floodplains have a low flow, a low variability of flow, and very similar environments and topography show very little difference in deposition rates and processes. In low fields, some of the low variability is potentially caused by some type of homogenisation due to the removal of topographic differences in ploughed fields. This observation might be biased by the relative large number of cores taken in some environments and comparatively fewer cores taken in other environments. The sampling strategy of the whole project was mainly designed to sample undisturbed locations to detect deposition events and not necessarily to track deposition rates, therefore this studies' insights to sedimentation patterns is limited by its design.

According to theory, the sedimentation processes in the floodplain are dependent on flow, inundation, topography and sediment availability (e.g.,

Walling & He 1998; Thonon et al. 2007). At proximal locations, the fluvial activity is higher due to a higher the flow velocity and in parallel a higher sediment load. Deposition can happen episodically during floods, leading to the construction of natural levees (e.g., summarised by Dunne & Aalto 2013). Further from the main stem, the limitation to 3 flood outlets leads to a concentration of flow, and scours that can occur in the main path of the flow. In depression areas, where water is collected and more stagnant, larger amounts of sediment are deposited, and at more frequent episodes (similar to that observed by Walling & He (1998) along several rivers in the UK). Floodplain channels transport water and sediment at a higher velocity than the surrounding floodplains, so the potential for a higher fluvial transport capacity and therefore episodic processes is increased. At locations that are most distal to the water and the sediment sources in the main stem, the local flow velocity and inundation is decreased enough that fluvial activity is limited. The same happens at sites where the inundation is limited in height and frequency, especially in elevated positions located in the distal part of the floodplain. At sites like this, fluvial processes during the winter floods are less likely to be responsible for soil removal under vegetation cover than aeolian processes under intensive agricultural pressure during summer season.

Summary

The main take-home messages for each of the research questions are (Figure 64):

Q1: The late Quaternary evolution of the Sacramento River is closely linked to the climate conditions of the Coast Range, the Klamath Mountains, and the Modoc Plateau. The main periods of deposition are 77 ± 25 ka, between 33 and 22 ka, and after 6 ka, with a period of surface stability on Llano Seco Terrace represented by the development of a soil between 22 and 6 ka. The floodplain channels are of Holocene age and origin, potentially the result of an incomplete avulsion.

Q2: CIRCAUS/CNAXS ^{210}Pb dating of sediments is possible in this low deposition environment, but low deposition rates have to be accounted for by

smaller sample intervals. Analysing cores for signs of agricultural influences on the XS ^{210}Pb activity profile is vital for CIRCAUS/CNAXS dating.

Q3: Approximately 33 % of the total suspended sediment load are transported and deposited on the Sacramento River floodplain with each flood. Sedimentation rates are dependent on distance from the nearest flood outlet, but floodplain channels convey sediment across the floodplain.

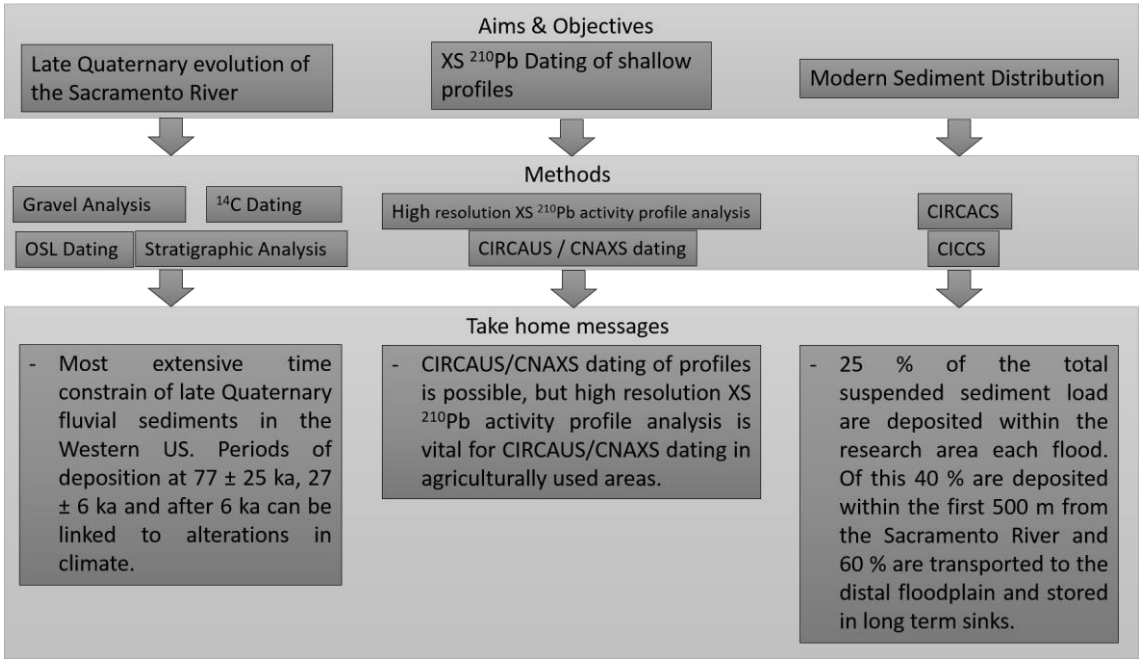

Figure 64 Take home messages from this thesis in relation to the research questions this thesis tried to answer.

6. CONCLUSION

Late Quaternary Evolution

In this study, the combination of numeric dating methods (^{14}C, OSL, U/Th) provided the geochronological framework for the establishment of the first in situ chronology for the late Quaternary stratigraphy of the Sacramento River, as well as the most extensive time constrain on Late Quaternary fluvial sediments in the region, yet. Dating of the fluvial sediments along the Sacramento River showed that the floodplain sediments and features in the Sacramento River floodplain are younger than some authors suggested previously (Robertson 1987, Dunn & Aalto 2013). The results of this study further emphasize the importance of numeric age control for the understanding and interpretation of past processes. The late Quaternary evolution of the Sacramento River is a result of the interactions of climate, and precipitation alterations in different parts of its catchment as well as local tectonic movements.

Around 77 ± 25 ka the Stony Creek fan system had a greater influence on the Sacramento River, relocating the course of the Sacramento River east of its current position to an unknown location. Gravel compositions presented in Robertson (1987) showing an abundance of up to 40 % of Andesite in the samples from pits on the eastern edge of Llano Seco, indicating that the confluence of the Stony Creek fan and the Sacramento River was probably located in the eastern part or just east of the premises of Rancho Llano Seco. From ~ 33 ka to 22 ka the deposition of shallow fluvial sands (< 2 m) indicates the presence of a system with shallow channels. From 22 ka the development of a soil on top of the fluvial sands indicates the incision of the Sacramento River into the Stony Creek fan system in the western part of the research area, preserving parts of the research area as terraces in the process. During the Younger Dryas the eastern tributaries potentially showed increased activity presented by the reworking the sands on the terrace. To confirm this hypothesis more dating would be necessary. The modern meandering Sacramento River was established between 14.2 and 6.2 ka - the last dated deposition sandy sediment and the first dated deposition of silty overbank deposits.

The current position of the Sacramento River is likely to be influenced by neo-tectonic movements in the Central Valley (Helley & Harwood 1985; Robertson 1987; WET 1990; Fisher 1994). The eastward movement of the channels started at least 2 meander generations before 2.4 ka.

It can be argued that the floodplain channels in the vicinity of Llano Seco are landforms of Holocene age and origin, due the fact that they are exclusively established in Holocene sediments, and independent from the underlying topography of the Pleistocene sand and gravel units. This indicates that these channels have actively evolved during the Holocene in response to the high discharge and sediment transport that is occurring during large floods of the Sacramento River.

^{210}Pb Dating of Sacramento River sediments

XS ^{210}Pb activity profile analysis is a very useful tool, not just for dating sediments, but also to analyse different mechanical mixing processes occurring in the sediment column due to land use and bioturbation. The study confirmed that the accuracy of the detection method and the chosen sampling interval are what limits the potential detection and characterisation of sedimentation and mixing processes (Aalto & Nittrouer 2012). Using Alpha Spectroscopy and high-resolution XS ^{210}Pb activity profile analyses it is possible to resolve a higher number of different sedimentation and land use scenarios in comparison to the more traditional approach using Gamma Spectroscopy (Aalto & Nittrouer 2012). The present research investigates using this approach at high sampling resolution of 1 cm intervals. Cores that are generally undisturbed by intense post-deposition reworking all showed a trend towards the development of a clearly visible meteoric cap on top of an interval of homogenous activity values.

The distribution of XS ^{210}Pb in undisturbed activity depth profiles in the research area is mainly dependent on atmospheric fallout processes, with high values on tops of the exposed soil profile, then a steep decline in XS ^{210}Pb to 3 – 5 cm depth, and finally the absence of XS ^{210}Pb below 15 – 20 cm. Similar trends have also been observed in other environments (e.g., He & Walling 1997). In environments where slow deposition is the main factor, the XS ^{210}Pb activity is still mainly depending on XS ^{210}Pb fallout from the atmosphere, but the input of XS ^{210}Pb with deposition of sediment starts playing a significant role.

The contribution of XS ^{210}Pb input from deposition increases with an increase in sedimentation rates. This change in XS ^{210}Pb delivery dynamics is reflected in XS ^{210}Pb activity profiles with a decrease in the steepness of the XS ^{210}Pb activity curve that occurs directly due to increasing sedimentation rates – from rapid and exponential declines at stable sites to more gradual and linear shaped curves at sites with higher infilling rates. If there is a lack of deposition over a certain period of time or deposition events generally occur episodically with large sediment packages arriving in infrequent intervals, the resulting soil profiles tend to show multiple XS ^{210}Pb plateaus and caps that can be utilised to date these events (Aalto & Nittrouer 2012).

Major post-fallout reworking of XS ^{210}Pb is only common in locations where mechanical processes (land use, high rates of bioturbation) are present. This physical mixing allows particles with adsorbed XS ^{210}Pb to be relocated vertically within the profile, rearranging the “natural” XS ^{210}Pb activity profiles. This study was able to show that different types of land use do have different signatures, and that high-resolution XS ^{210}Pb activity profile analyses is a suitable tool to determine and potentially track these changes. Equifinality between undisturbed cores and cores that have undergone agricultural activity indicate that the knowledge of current and prior land use is crucial to CIRCAUS/CNAXS dating. More research is needed further explore whether XS ^{210}Pb profiles are a robust tracing tool for determining deposition processes and land-use impacts in a wider range of varying environments than are investigated here.

Distribution of sediments throughout the system

This study has shown that XS ^{210}Pb analysis is a useful method for calculating deposition and erosion rates and processes within the heterogeneous environments of the research area. During floods 33 % of the total suspended sediment load are transported to the floodplains of the research area. Of these sediments ~ 60 % are transported to distal parts of the floodplain. Erosion and deposition rates generally decrease with increasing distance from the main stem of the Sacramento River. However, erosion and deposition rates remain highly variable until ~ 3 km from the main stem. Erosion and deposition rates on floodplains decline > 3 km from the main stem. From ~

3 km and beyond, sedimentation and erosion is limited mainly to the floodplain channel features and the immediate surrounding banks. Floodplain channels are responsible for the dispersal of sediment to the distal floodplain locations along the Sacramento River, and are able to readily dispersing even fine sands as wash load, but are much less efficient conveyors than floodplain channels documented in other environments (e.g., Day et al. 2008).

Episodic processes are mainly limited to the proximal parts of the floodplain, nearest the main flow path and floodplain channels. Whereas distal parts of the floodplain including channel locations and higher floodplain locations – even though inundated on an annual basis – are dominated by slower deposition processes or surface stability (no sediment accumulation or erosion). Along the Sacramento River deposition and erosion events can be detected and dated using XS ^{210}Pb analyses but the applicability of CIRCAUS/CNAXS dating is limited temporally due to the low deposition rates and low natural ^{210}Pb fallout.

APPENDICES

APPENDIX A – Profile Locations and Topography

In the following section a table of methods used on sites and a table on profile locations, sedimentation rates, elevations, and other features are given.

Figure 1: List of cores and profiles with the analysis executed and persons involved in the analysis in the samples. Gravel counts have been done by emerit prof Dr Ken Aalto.

		^{210}Pb Analysis					
Site	Core Collected by	Core Processed by	Core Counted by	Interpretation	^{14}C	OSL	Gravel Counts
LSL-1	Aalto & Singer	Franklin	Aalto	This Thesis			
LSL-2	Aalto & Singer	Franklin	Aalto	This Thesis			
LSL-3	Aalto & Singer	Will	Will	This Thesis			
LSL-4	Aalto & Singer	Will	Will	This Thesis			
LSD-1	Aalto & Singer	Franklin/Will	Aalto/Will	This Thesis			
LSD-2	Aalto & Singer	Franklin/Will	Aalto/Will	This Thesis			
LSD-3	Aalto & Singer	Franklin/Will	Aalto/Will	This Thesis			
LSD-4	Aalto & Singer	Franklin/Will	Aalto/Will	This Thesis			
LSD-5	Aalto & Singer	Will	Will	This Thesis			
LSD-6	Aalto & Singer	Will	Will	This Thesis			
LSF-T	Aalto & Singer	Franklin	Aalto	This Thesis			
GL1	Aalto & Singer	Will	Will	This Thesis			
MSLSF29	Aalto & Singer	Will	Will	This Thesis			
MSLSF30	Aalto & Singer	Will	Will	This Thesis			
MSLSF31	Aalto & Singer	Will	Will	This Thesis			
MSLSF32	Aalto & Singer	Franklin	Aalto	This Thesis			
MSLSF33	Aalto & Singer	Will	Will	This Thesis			
LC 17	Will	Will	Will	This Thesis			
T2_P1	Will	Will	Will	This Thesis	X	X	
T2_P2	Will	Will	Will	This Thesis			
T2_P3	Will	Will	Will	This Thesis	X		X
T2_P4	Will	Will	Will	This Thesis	X		
T2_P5	Will	Will	Will	This Thesis	X		
T2_P6	Will	Will	Will	This Thesis			
TE_P7	Will	Will	Will	This Thesis		X	X
TE_P8	Will	Will	Will	This Thesis		X	X
T1_P9	Will	Will	Will	This Thesis		X	
T1_P10	Will	Will	Will	This Thesis		X	
T1_P11	Will	Will	Will	This Thesis	X		
T3_P12					X		
T3_P13	Will	Will	Will	This Thesis			
T3_P14	Will	Will	Will	This Thesis	X		
TE_P15	Will	Will	Will	This Thesis	X		
TE_P16	Will	Will	Will	This Thesis			
M-0	Aalto	Will	Will	This Thesis			
M-1	Aalto	Will	Will	This Thesis			
M-2	Aalto	Will	Will	This Thesis			

M-3	Aalto	Will	Will	This Thesis	
M-4	Aalto	Will	Will	This Thesis	
M-5	Aalto	Will	Will	This Thesis	
RASRF125	Will	Will	Will	This Thesis	
RASRF126	Will	Will	Will	This Thesis	
RASRF127	Will	Will	Will	This Thesis	
RASRF129	Will	Will	Will	This Thesis	
RASRF130	Will	Will	Will	This Thesis	
RASRF131	Will	Will	Will	This Thesis	
RASRF132	Will	Will	Will	This Thesis	
RASRF133	Will	Will	Will	This Thesis	
RASRF134	Will	Will	Will	This Thesis	
RASRF135	Will	Will	Will	This Thesis	
RASRF136	Will	Will	Will	This Thesis	
RASRF137	Will	Will	Will	This Thesis	
RASRF142	Will	Will	Will	This Thesis	
RASRF143	Will	Will	Will	This Thesis	
RASRF144	Will	Will	Will	This Thesis	
RASRF146	Will	Will	Will	This Thesis	
RASRF147	Will	Will	Will	This Thesis	
RASRF148	Will	Will	Will	This Thesis	
RASRF149	Will	Will	Will	This Thesis	
RASRF150	Will	Will	Will	This Thesis	
RASRF151	Will	Will	Will	This Thesis	
RASRF152	Will	Will	Will	This Thesis	
RASRF153	Will	Will	Will	This Thesis	
RASRF154	Will	Will	Will	This Thesis	
RASRF155	Will	Will	Will	This Thesis	
RASRF156	Will	Will	Will	This Thesis	
RASRF157	Will	Will	Will	This Thesis	
RASRF158	Will	Will	Will	This Thesis	
RASRF159	Will	Will	Will	This Thesis	
RASRF160	Will	Will	Will	This Thesis	
RASRF161	Will	Will	Will	This Thesis	
RASRF162	Will	Will	Will	This Thesis	
RASRF163	Will	Will	Will	This Thesis	
RASRF165	Will	Will	Will	This Thesis	
RASRF166	Will	Will	Will	This Thesis	
RASRF167	Will	Will	Will	This Thesis	
RASRF168	Will	Will	Will	This Thesis	
RASRF169	Will	Will	Will	This Thesis	
Cementery	Aalto & Singer	Will	Will	This Thesis	
LSF-T	Aalto & Singer	Franklin	Aalto	Aalto	
GP1					X
GP2					X
GP3					X
Stony Creek					X

Core	Coordinates		Elevation a.s.l.	Flow depth (FEMA)	CICCS rate cm/a	XS ^{210}Pb inventory DPM/g(clay)	Used CICCS / CIRCACS rate cm/a	Distance closest potential source (m)	Distance Nearest Channel (m)	Environment	Erosion/deposition style	Notes
	Lat	Long										
GL_1	-121.9773	39.5673	29.24	2.76	0.54	38.82	0.54	2500			Potentially Episodic	close to training levee
LC17	-121.932067	39.625605	34.00	0.33	-0.01	17.47	-0.01	4000	10	ECS	Stable	
LSD1	-121.994336	39.584513	33.23	-0.87	0.19	22.39	2.13	50	50	Proximal	Episodic	1964-1969
LSD2	-121.991345	39.585226	32.95	-0.59	0.59	35.11	1.45	350		CS	Episodic	Depression
LSD3	-121.98852	39.584129	33.65	-1.29	-0.16	13.70	-0.16	600	250	Proximal	if deposition episodic	
LSD4	-121.98599	39.583558	33.28	-0.92	-0.03	16.97	-0.03	800	160	Proximal	if deposition episodic / stable	
LSD5	-121.98275	39.582	29.75	2.50	1.76	93.40	1.76	1000		CS	Episodic	minimum
LSD6	-121.983133	39.58205	29.59	2.66	1.28	76.43	1.89	1000		CS	Episodic	minimum
LSL1	-121.993082	39.605217	32.54	1.75	-1.13	7.64	1.44	200	200	Proximal	Episodic	1960-1964, episodic deposition likely
LSL2	-121.991852	39.604846	34.06	0.23	-0.15	14.76	-0.15	300	300	Proximal	Unknown	1923-1935, likely erosion after initial deposition
LSL3	-121.989548	39.604727	32.54	1.75	-0.15	13.58	-0.15	400	400	Proximal	Unknown	genuinely eroding
LSL4	-121.986577	39.603998	34.13	0.16	-0.14	13.91	-0.14	400	400	Proximal	Unknown	genuinely eroding
M0	-121.91119	39.563292	31.65	-0.36	0.08	22.26	0.08	10000	15	ECS	Constant	
M1	-121.918898	39.577665	31.70	0.80	0.02	18.63	0.02	9000	10	ECS	Stable	potentially soil mixing in the past due to rice farming
M2	-121.95066	39.589781	33.38	0.30	-0.03	17.43	-0.03	6000		HF	Stable	Stable site outside flooded area
M3	-121.952972	39.57386	30.37	2.13	0.25	28.26	0.25	8000		CE	Constant	
M4	-121.958675	39.533374	28.66	1.58	-0.01	16.46	-0.01	4000	13	HF	Stable	
M5	-121.932585	39.631392	33.66	0.87	0.49	37.02	0.49	3500	7	ECS	Constant	Pre-Bridge damming of flood flow, outlier minimum
MLSLF29	-121.997403	39.552716	31.38	-0.09	0.67	27.66	1.4	500		Proximal	Episodic	
MLSLF30	-121.996733	39.552359	31.88	-0.59	0.28	27.16	0.28	500		Proximal	Episodic	
MLSLF31	-121.996023	39.549938	31.93	-0.49	0	17.84	0	800		Proximal	Unknown	Sedimentation rate potentially higher because increased XS ^{210}Pb values up to 40cm
MLSLF33	-121.974958	39.565666	31.65	-0.24	0.24	25.77	0.24	3000		Low pasture	Potentially Episodic	
PL					1.3		1.3			CS	Episodic	Sullivan 1987, long-term average
RASRF 125	-121.962704	39.67152	38.66		0.63	30.60	1.2	200	200	Proximal	Episodic	1960-1964, potentially >60cm

126	-121.953569	39.685045	40.07	-2.06	-0.05	16.60	1.3	50	50	Proximal	Episodic	1960-1964 profile suggests 10-30cm recent sedimentation but meander age suggests higher deposition rates
127	-121.947621	39.684402	39.97	-2.10	-0.51	9.68	0.72	100	100	Proximal	Episodic	1923-1935 potentially <30cm deposition
129	-121.958701	39.663932	38.38		-0.12	14.13	-0.12	1000	135	Low pasture	Unknown	
130	-121.948326	39.666082	37.54		0.02	18.83	0.77	1500	76	Low pasture	Potentially Episodic	
131	-121.950771	39.665456	37.73		0.09	21.82	0.56	1500	58	Low pasture	Constant	
132	-121.959763	39.639351	34.39	1.53	0.31	31.79	1.33	1000	130	Wooldands	Constant	minimum
133	-121.957357	39.638211	35.31	0.44	0.2	27.68	0.2	1500	107	Wooldands	Unknown	anthropogenic/discarded
134	-121.971045	39.552261	29.60	1.84	0.17	24.35	0.17	1500	19	Wooldands	Episodic	
135	-121.971608	39.563438	30.84	0.57	0.32	30.67	0.32	3000	35	Wooldands	Constant	potentially disturbed
136	-121.978625	39.551084	30.61	0.83	0.42	33.98	1.17	1500	50	Wooldands	Potentially Episodic	minimum / potentially disturbed
137	-121.984511	39.548743	30.49	0.62	-0.33	10.68	-0.33	1000	48	Scour	Episodic	Removal of several meter
142	-121.966143	39.580084	29.75	2.37	0.22	27.76	0.8	7000		FC	Potentially Episodic	Surface disturbance by cow prods
143	-121.965841	39.579966	31.21	0.91	-0.13	11.76	-0.13	7000	23	CE	Unknown	Potentially ~8cm deposition on eroded cap or soil mixing
144	-121.967085	39.578421	29.70	2.38	0.31	30.96	0.31	7000		FC	Potentially Episodic	Surface disturbance by cow prods
146	-121.93134	39.624967	33.54	0.79	0.17	24.52	0.17	4000	20	ECS	Unknown	
147	-121.932488	39.619712	32.99	1.80	-0.15	10.53	-0.15	4500	15	ECS	Potentially Episodic	
148	-121.932873	39.619723	33.71	1.08	0.06	20.22	0.06	4500	48	ECS	Episodic	
149	-121.950539	39.603559	30.93	3.36	0.04	19.54	0.04	5000		FC	Constant	
150	-121.950422	39.603528	31.69	2.60	0.22	28.71	0.22	5000	4	CE	Constant	
151	-121.944681	39.60766	31.98	3.02	0.31	29.99	0.31	4500		FC	Episodic	
152	-121.944436	39.607857	34.25	0.75	0.36	31.06	0.36	4500	7	CE	Potentially Episodic	Either episodic or ploughed in the past with minor sedimentation after
153	-121.946985	39.606085	31.49	2.57	0.25	27.94	0.93	5000		FC	Episodic	minimum
154	-121.947103	39.606305	34.21	-0.15	0.72	40.37	0.72	5000	6	CE	Constant	
155	-121.941175	39.60283	32.90	1.55	0.13	27.12	0.13	5500	5	CE	Episodic	
156	-121.940915	39.602865	33.34	1.11	0.13	22.42	0.13	5500	10	CE	Potentially Episodic	

157	-121.9682	39.531529	30.05	0.19	-0.18	8.33	-0.18	3500		Scour	Episodic	
158	-121.967969	39.53164	29.47	0.77	-0.13	8.26	-0.13	3500		Scour	Episodic	total removal of cap
159	-121.990954	39.569537	30.76	1.78	0.09	21.24	0.5	800	130	Proximal	Episodic	1960 -1964, minimum, potentially stable since 1964
160	-121.993121	39.573382	32.09	0.41	-0.06	15.79	-0.06	700	90	Low pasture	Constant	
161	-121.95873	39.600972	31.11	2.83	0.07	21.27	0.07	5000		FC	Potentially Episodic	
162	-121.959059	39.601079	32.61	1.33	0.06	19.83	0.06	5000	1	CE	Unknown	
163	-121.954857	39.624114	33.01	1.79	-0.17	9.91	-0.17	3000		FC	Unknown	Post bridge, slow erosion
165	-121.963932	39.621634	32.29	2.51	-0.17	8.21	-0.17	2500		FC	Episodic	Post bridge, hard to interpret but likely erosion with minor sedimentation after
166	-121.963941	39.620817	35.15	-0.35	0.03	19.16	0.03	3000	10	CE	Episodic (slow)	Post bridge
167	-121.950682	39.625281	31.95	2.38	0.07	20.32	0.63	3000		FC	Episodic	minimum, Post bridge
168	-121.950233	39.625407	35.49	-1.16	0.13	22.03	0.13	3000	29	CE	Episodic	Post bridge
169	-121.949667	39.62539	35.60	-1.27	0.26	24.00	0.26	3000	10	CE	Episodic	Post bridge
T2P1	-121.964287	39.540515	33.03	-0.91	-0.03	15.68	-0.03	7000	73	HF	Pot Wind Erosion	
T2P2	-121.958267	39.579668	32.42	-0.30	0.1	21.94	0.1	7000	60	Low Fields	Unknown	
T2P3	-121.968522	39.580702	32.83	-0.71	0.1	23.20	0.1	1500	60	Low Fields	Unknown	
T2P4	-121.978741	39.579059	30.67	1.45	0.64	52.38	1.33	1500		CS	Episodic	minimum
T2P4	-121.979519	39.579355			3.33		3.33			CS		discarded, maximum, Reconstructed from known horizon but multiple processes involved
T2P5	-121.98098	39.580109	33.03	-0.91	0.12	23.02	0.12	1500	140	Low Fields	Unknown	
T2P6	-121.984678	39.581835	31.79	0.46	0.34	30.76	0.34	1000	56	Proximal	Episodic	
TEP7	-121.926392	39.59194	33.44	0.16	-0.07	14.19	-0.07	7000	115	HF	Pot Wind Erosion	
TEP8	-121.915713	39.562016	30.70	0.59	-0.03	16.56	-0.03	10000	2	ECS	Stable	
T1P9	-121.964287	39.540515	30.74	0.08	-0.03	16.66	-0.03	3000	54	HF	Stable	Potentially slight erosion with 2cm recent deposition
T1P10	-121.968768	39.548443	30.78	0.33	0.54	38.85	0.54	2000	10	Low pasture	Unknown	
T1P11	-121.979197	39.543862	29.14	2.20	0.45	36.43	0.45	2000	32	Low pasture	Unknown	
T3P12	-121.97213	39.603939	34.25	0.04	0.33		0.33	800		Low Fields		maximum anthropogenic/discarded
T3P13	-121.979992	39.605502	33.92	0.14	0.06	19.67	0.06	300	80	Proximal	Constant	1896-1908

T3P14	-121.959026	39.603984	33.92	0.37	-0.04	16.07	-0.04	5000	73	HF	Pot Wind Erosion	
TEP15	-121.932673	39.624987	35.02	-0.69	0.53	36.50	0.53	4000	20	ECS	Unknown	anthropogenic/discarded
TEP16	-121.917435	39.561706	32.08	-0.79	0.01	18.15	0.01	10000	48	HF	Stable	
Cemetery*						18.60						Stable site outside flooded area
LSF-T*	-121.946372	39.553769	31.94			16.87						Stable site outside flooded area

Figure 2: Coordinates, elevation, flow depth, CICCS, used sedimentation rate, XS ^{210}Pb inventory, distance to the closest flood outlet, distance to the nearest channel, environment, deposition style, and additional notes for each location. Environment is divided into 10 different environments: channel scars (CS), floodplain channels (FC), scour, channel edge (CE), high floodplain (HF), eastern channel system (ECS), proximal (< 500 m from the main stem Sacramento River), low pasture, low fields, woodlands.

APPENDIX B – Profile Descriptions and Gravel Counts

In the following section the profile drawings of the described profiles are presented. Additionally we present gravel counts from selected profiles.

The collected gravel samples have been analysed by emeritus Professor Ken Aalto.

Profile Descriptions

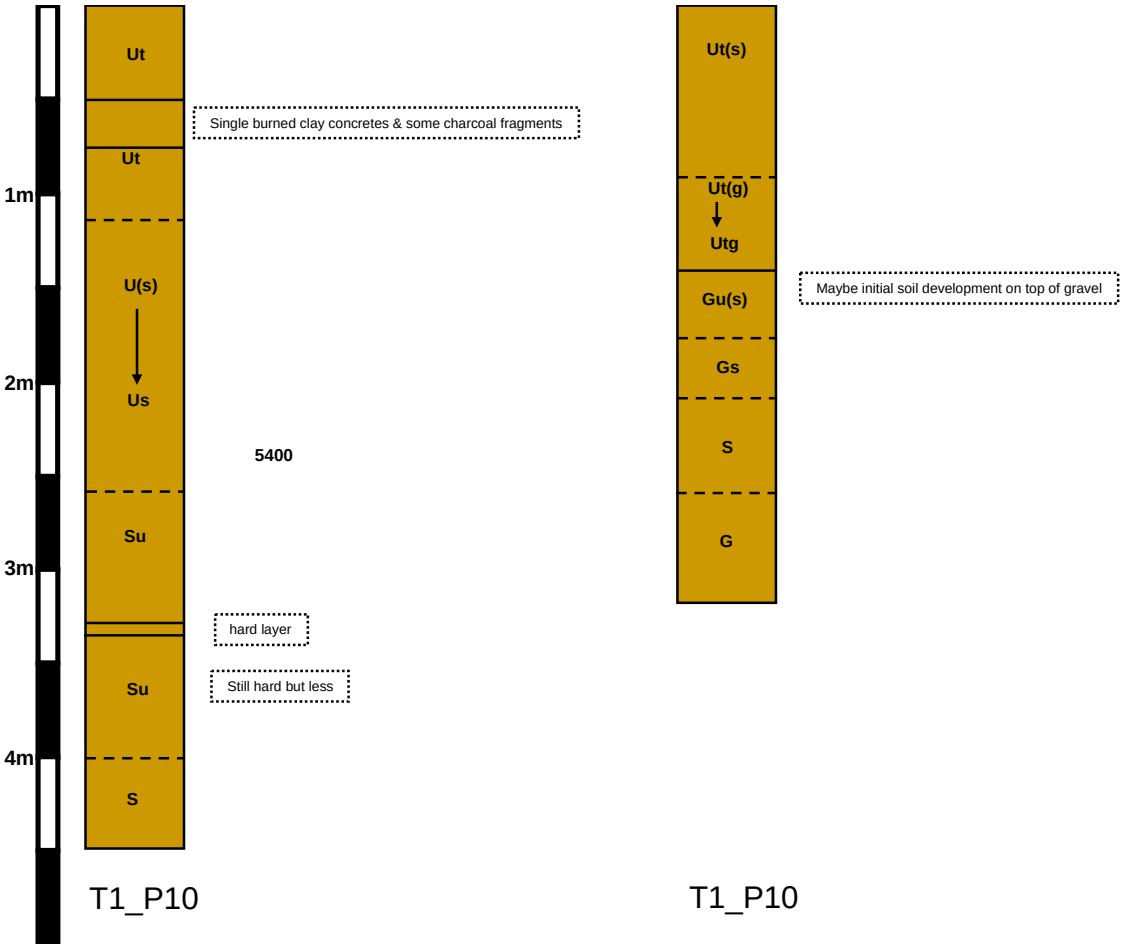

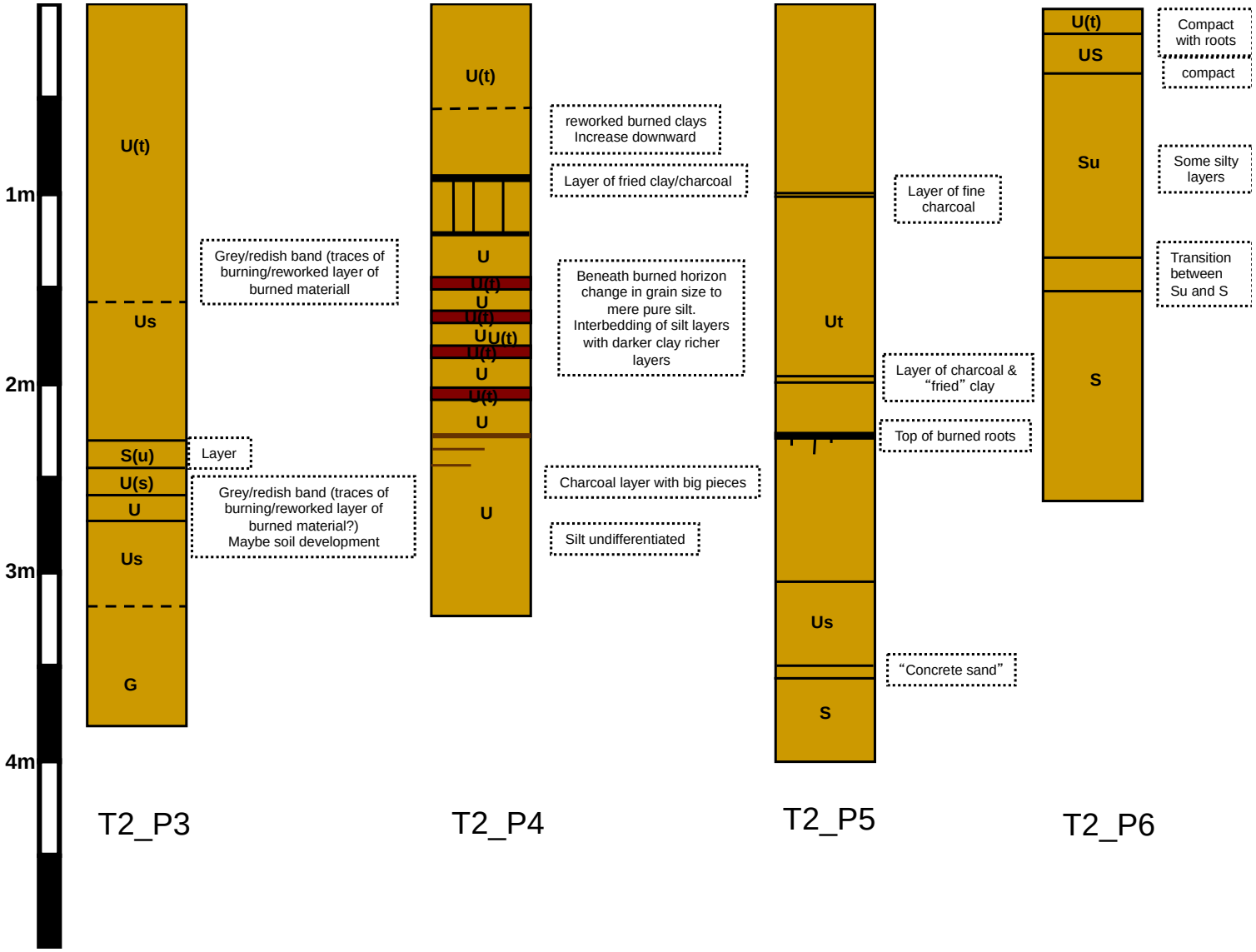
1m
2m
3m
4m
U(t)
Us
S(u)
U(s)
U
Us
G
Grey/redish band (traces of burning/reworked layer of burned materiall
Layer
Grey/redish band (traces of burning/reworked layer of burned material?)
Maybe soil development
T2_P3
U(t)
U
U(t)
U
U(t)
U
U(t)
U
U(t)
U
U
reworked burned clays
Increase downward
Layer of fried clay/charcoal
Beneath burned horizon change in grain size to mere pure silt.
Interbedding of silt layers with darker clay richer layers
Charcoal layer with big pieces
Silt undifferentiated
T2_P4
Ut
Us
S
Layer of fine charcoal
Layer of charcoal & “fried” clay
Top of burned roots
“Concrete sand”
T2_P5
U(t)
US
Su
S
Compact with roots
compact
Some silty layers
Transition between Su and S
T2_P6

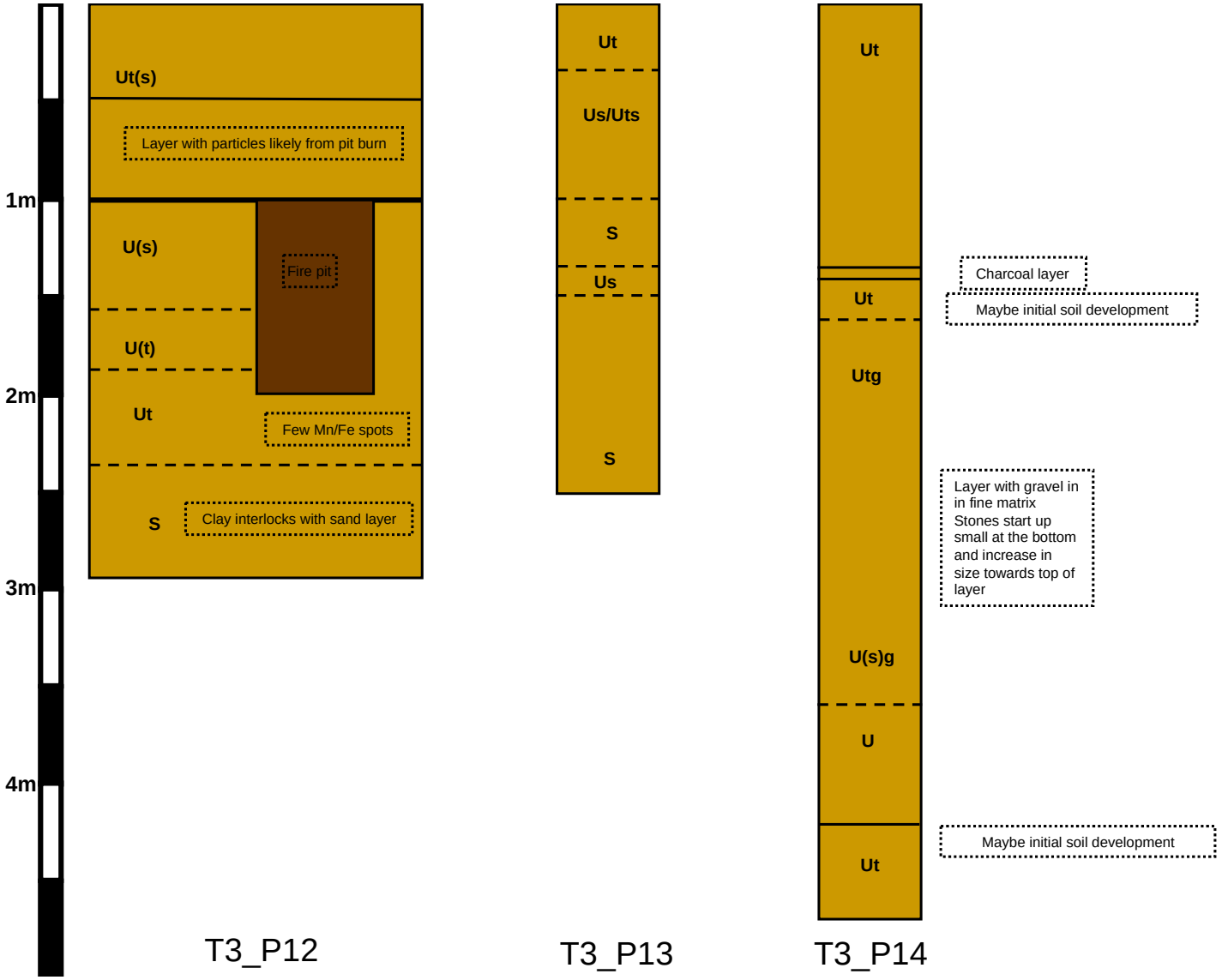
1m
2m
3m
4m
Ut(s)
Layer with particles likely from pit burn
U(s)
Fire pit
U(t)
Ut
Few Mn/Fe spots
S
Clay interlocks with sand layer
T3_P12
Ut
Us/Uts
S
Us
S
T3_P13
Ut
Charcoal layer
Ut
Maybe initial soil development
Utg
Layer with gravel in in fine matrix Stones start up small at the bottom and increase in size towards top of layer
U(s)g
U
Ut
Maybe initial soil development
T3_P14

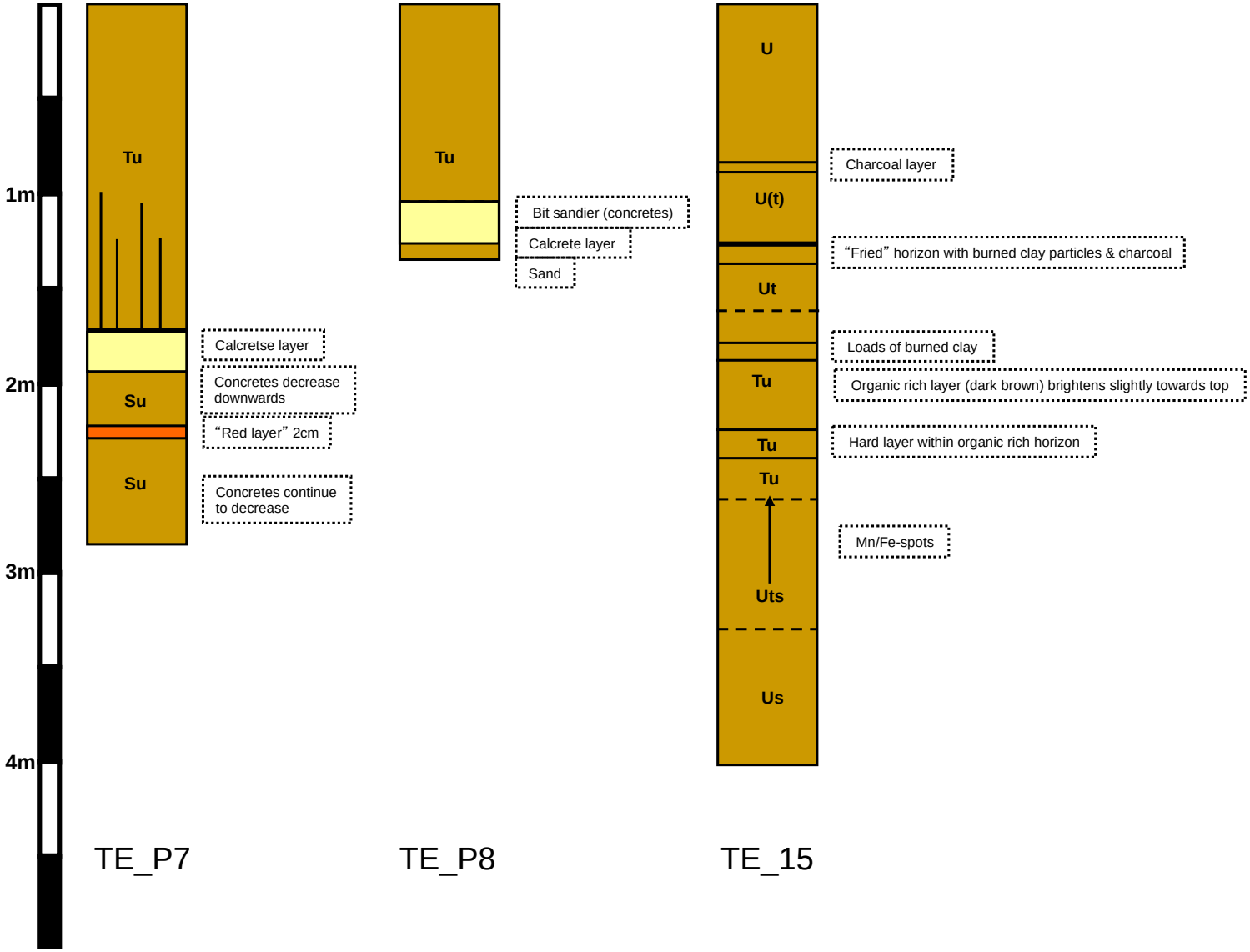
1m
2m
3m
4m
Tu
Calcretse layer
Su
Concretes decrease downwards
"Red layer" 2cm
Su
Concretes continue to decrease
TE_P7
Tu
Bit sandier (concretes)
Calcrete layer
Sand
TE_P8
U
Charcoal layer
U(t)
"Fried" horizon with burned clay particles & charcoal
Ut
Loads of burned clay
Tu
Organic rich layer (dark brown) brightens slightly towards top
Tu
Hard layer within organic rich horizon
Tu
Mn/Fe-spots
Uts
Us
TE_15

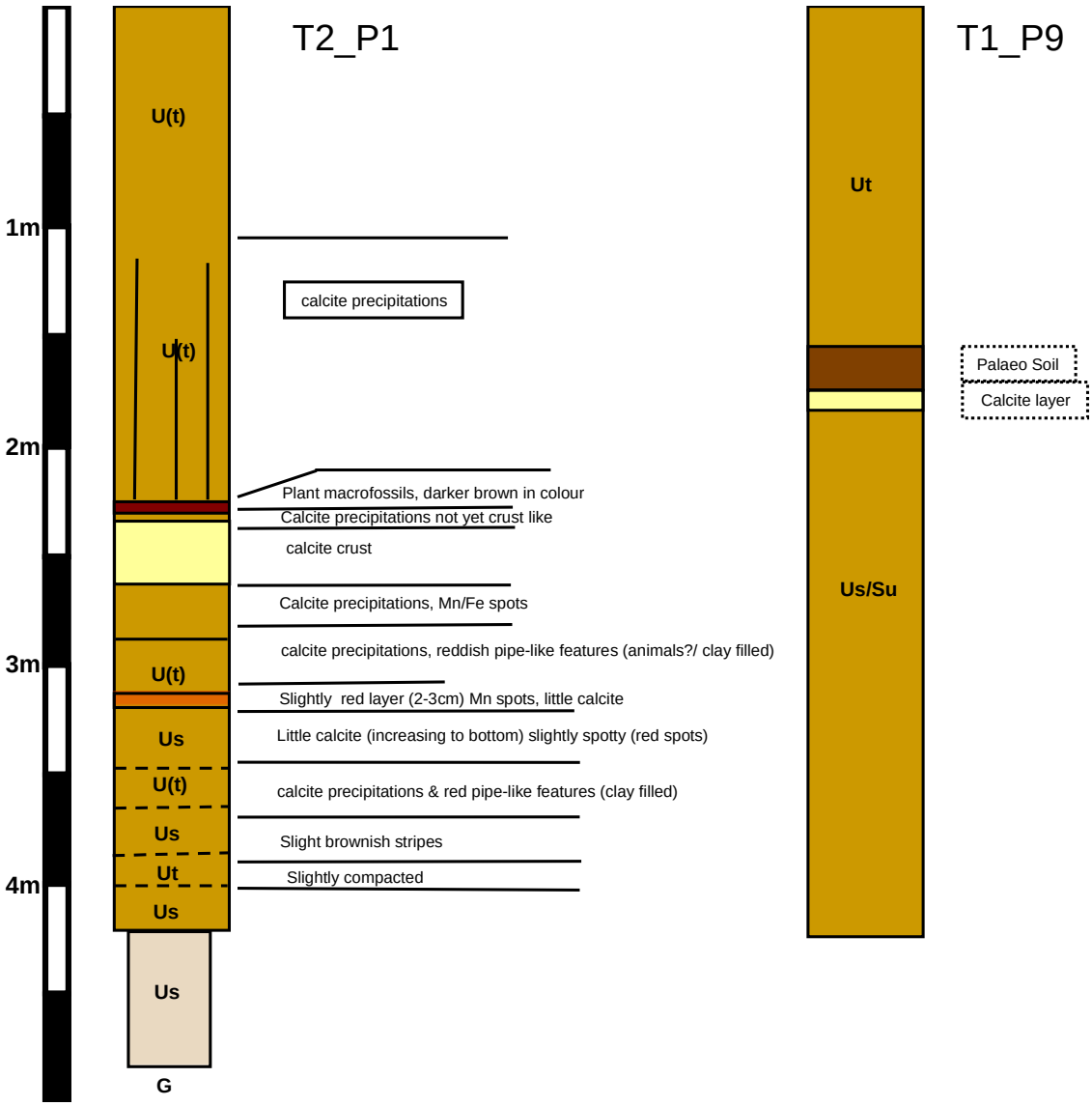
T2_P1
T1_P9
1m
2m
3m
4m
U(t)
U(t)
U(t)
Us
U(t)
Us
Ut
Us
Us
G
Ut
Us/Su
Palaeo Soil
Calcite layer
calcite precipitations
Plant macrofossils, darker brown in colour
Calcite precipitations not yet crust like
calcite crust
Calcite precipitations, Mn/Fe spots
calcite precipitations, reddish pipe-like features (animals?/ clay filled)
Slightly red layer (2-3cm) Mn spots, little calcite
Little calcite (increasing to bottom) slightly spotty (red spots)
calcite precipitations & red pipe-like features (clay filled)
Slight brownish stripes
Slightly compacted

Gravel Counts

sample:	~size	vein qtz	arg.+ qtz	red chert	tan/green chert	gray-black chert	sand/siltst one	conglomerate	greenstone	granitic	count total:
Gravel Pit 1	pebbles	34	66	10	26	4	31	6	21	1	199
Modern SR		17%	33%	5%	13%	2%	16%	3%	11%	Tr	
Eastern Channels	peb/cobble	22	1	1	13	1	29	0	15	0	82
northern gv pit 2		27%	1%	1%	16%	1%	35%		18%		
Eastern Channels	pebbles	22	23	6	9	0	25	1	20	4	110
southern gv pit 3		20%	21%	5%	8%		23%	1%	18%	4%	
Stony Creek	pebbles	27	22	5	14	0	35	0	46	0	149
		18%	15%	3%	9%		23%		31%		
TE_P7 ~3m	pebbles	38	16	0	12	4	19	0	3	0	92
Eastern Channels		41%	17%		13%	4%	21%		3%		
TE_P8, 2+m	peb/cobble	13	4	2	7	5	9	3	4	0	47
Eastern Channels		27%	9%	4%	15%	11%	19%	6%	9%		
T2_P3	pebbles	13	16	9	15	9	21	1	9	3 aplite [2]	96
Modern SR		14%	17%	9%	16%	9%	22%	1%	9%	3%	

Notes: 1) White vein quartz and the argillite plus vein quartz mix are likely genetically associated and grade into one another. Provenance: low-med. Grade metasedimentary rock.

2) Siltstone grades into fine sandstone; fine conglomerate rich in chert and quartz pebbles

3) Greenstone can be uniformally aphanitic, vesicular, amygdular or porphyrytic

4) Granitic clasts range from dioritic to aplitic in appearance

Holocene Meander Belt

Gravel Pit 1

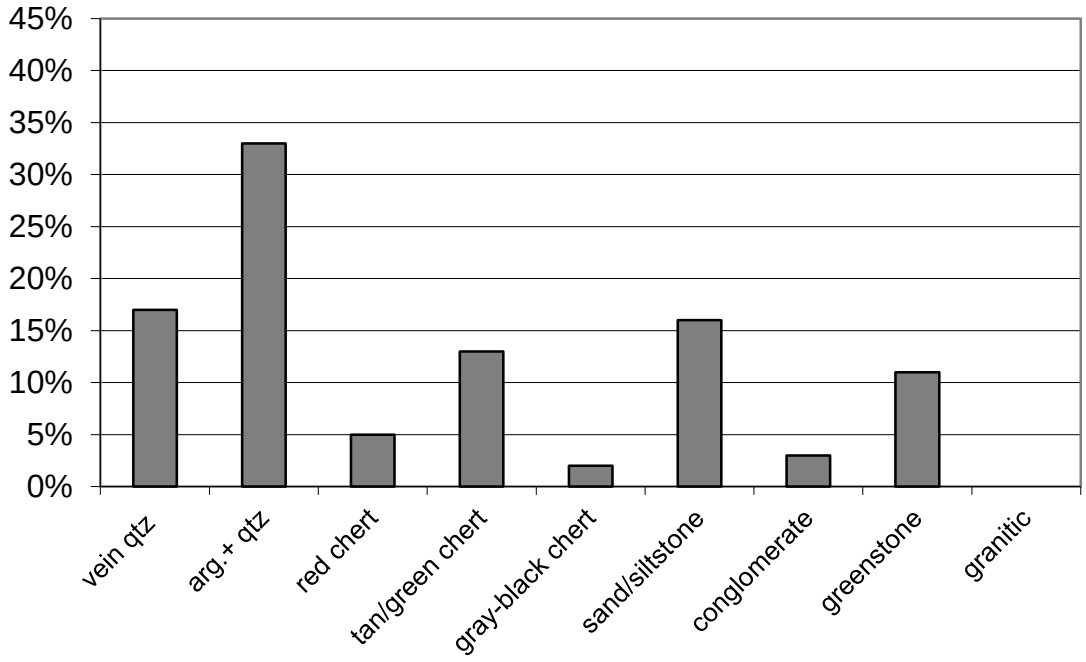

T2_P3

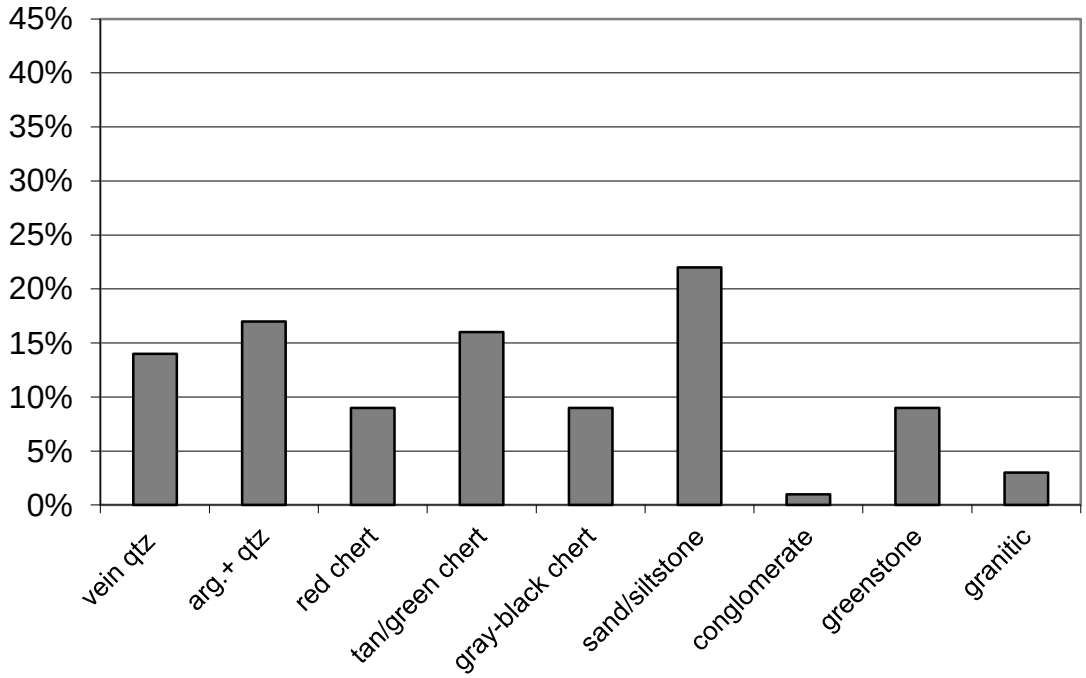

Eastern Channel System

Northern Gravel Pit 2

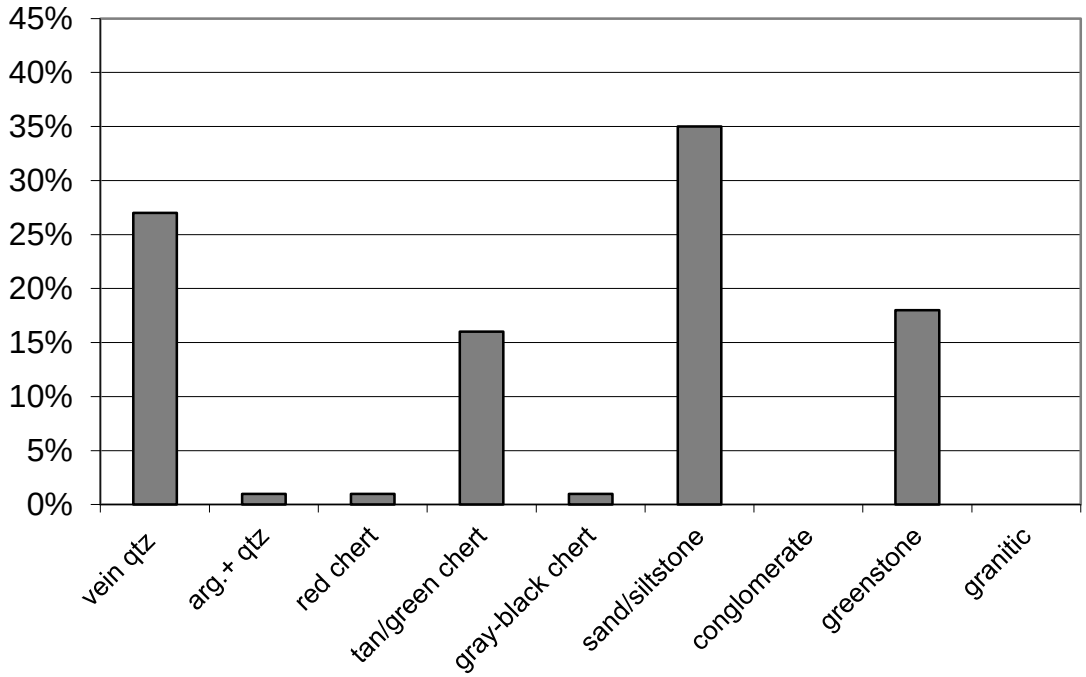

TE_P7

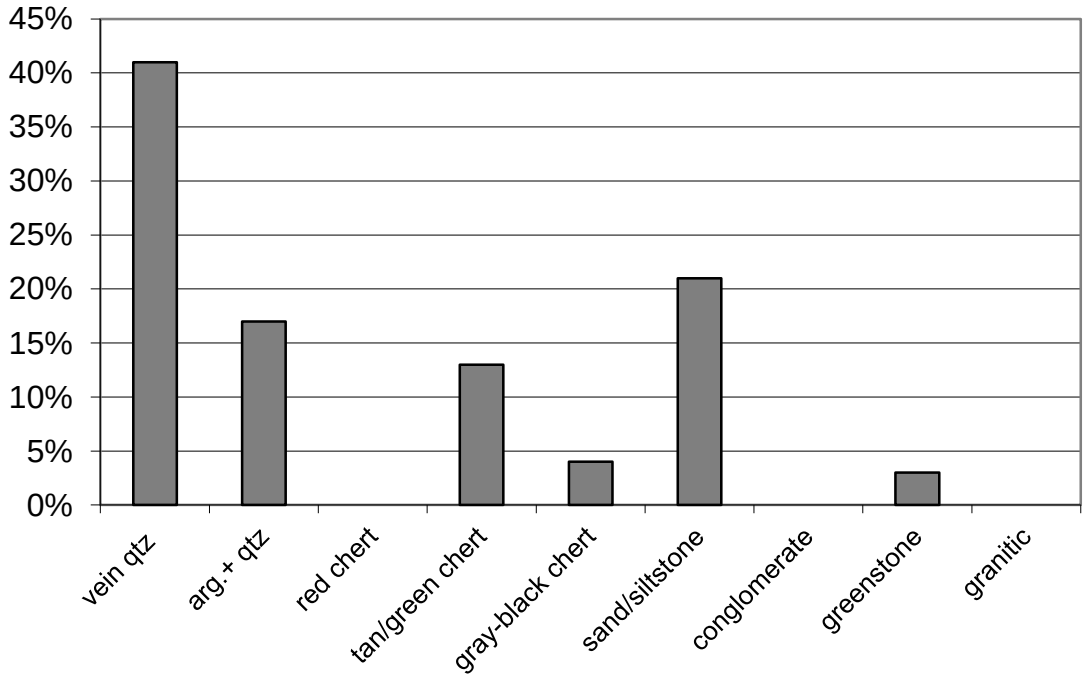

Southern Gravel Pit 3

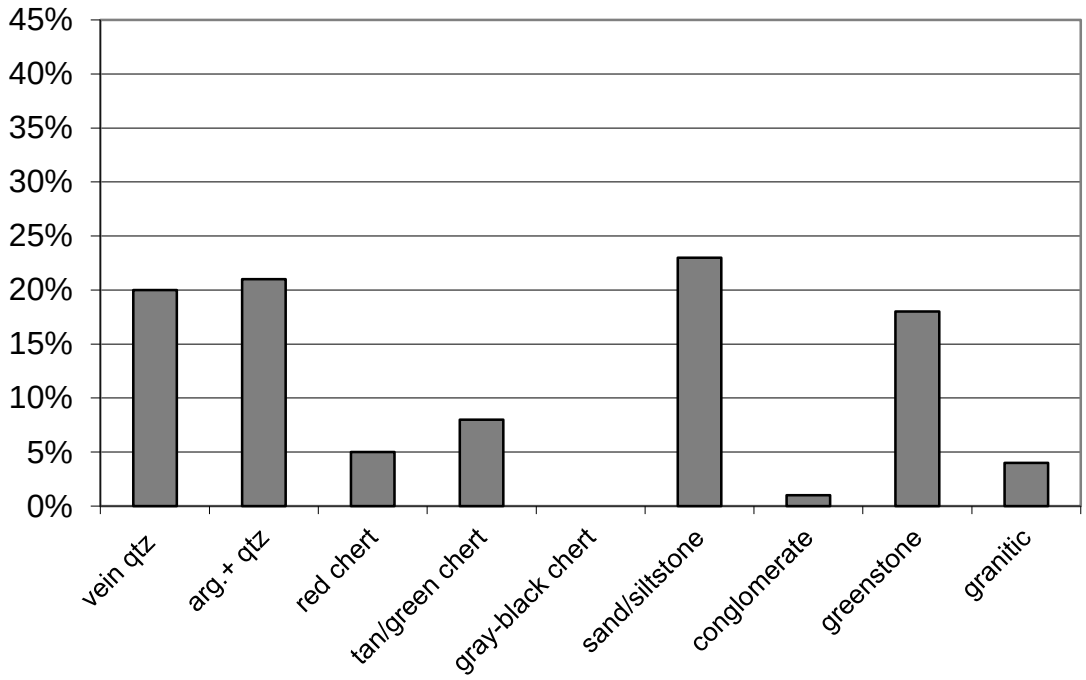

TE_P8

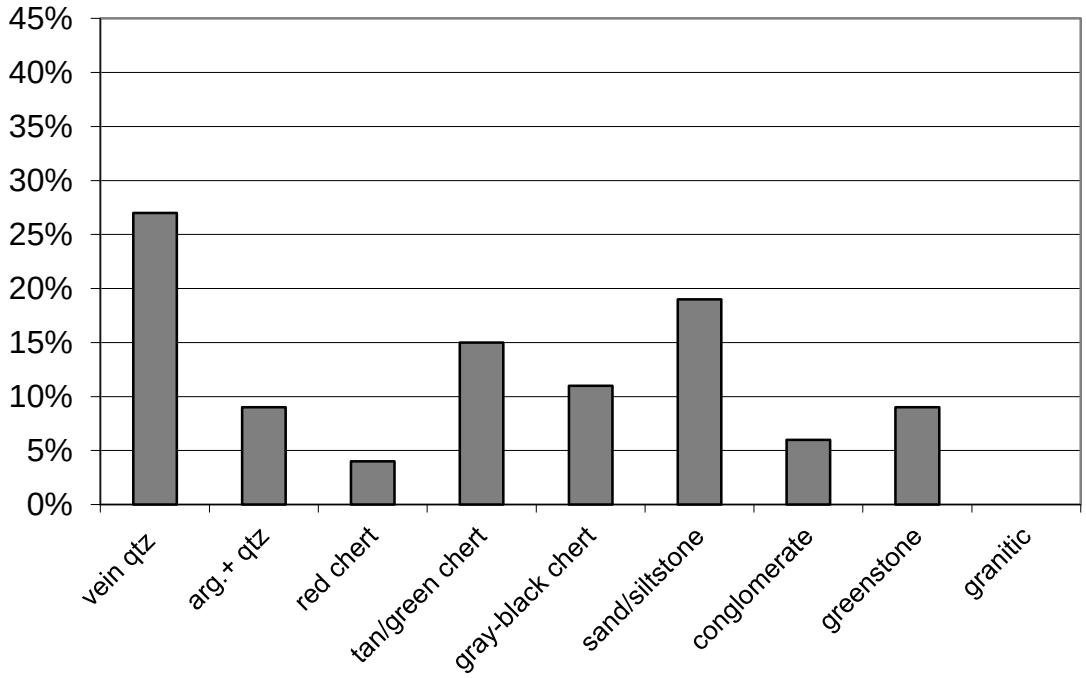

Stony Creek

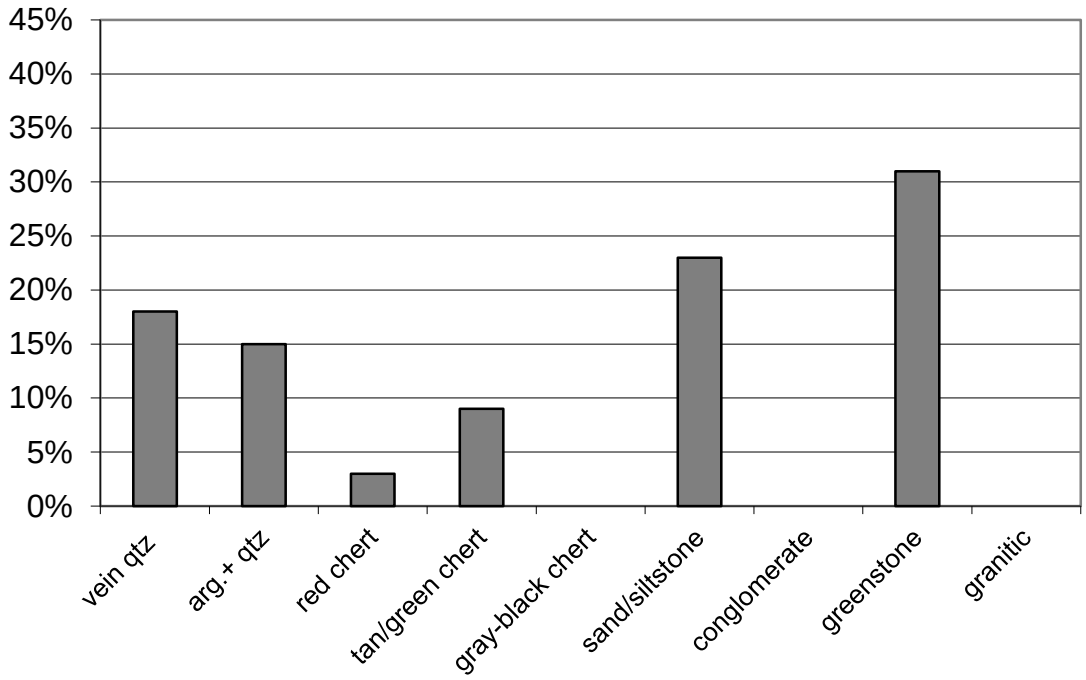
45%
40%
35%
30%
25%
20%
15%
10%
5%
0%
vein qtz
arg.+ qtz
red chert
tan/green chert
gray-black chert
sand/siltstone
conglomerate
greenstone
granitic

APPENDIX C – Dating Results

In the following section the results of the OSL and Radiocarbon dating are presented. The radiocarbon samples have been analysed by the NSF-Arizona AMS Laboratory. The OSL samples have been prepared and analysed by the author at the University of Bayreuth. The final results are presented in Table 2 of the main document, in this section the data of the measurements itself are presented.

Radiocarbon Dating

AA #	Sample ID	Material	d13C	F	14C age BP
AA88364	LS_T2_P1_120	charcoal	-20.7	0.645 ± 0.013	3520 ± 160
AA87461	LS_T2_P1_160	charcoal	-25.3	0.5516 ± 0.0042	4780 ± 61
AA87468	LS_T2_P3_295	charcoal	-24.7	0.7426 ± 0.0098	2390 ± 110
AA87467	LS_T2_P4_125	charcoal	-26.3	0.9723 ± 0.0041	225 ± 34
AA88366	LS_T2_P4_190	charcoal	-26	0.9886 ± 0.0072	92 ± 58
AA88365	LS_T2_P4_250	charcoal	-26.2	0.9802 ± 0.0041	161 ± 34
AA88369	LS_T2_P5_380	charcoal	-24.1	0.7795 ± 0.0036	2001 ± 38
AA87464	LS_T1_P11_90	charcoal	-22.6	0.9619 ± 0.007	312 ± 58
AA87463	LS_T3_P12_105	charcoal	-26.7	0.973 ± 0.0043	220 ± 35
AA87462	LS_T3_P14_145	charcoal	-27.4	0.8869 ± 0.0039	964 ± 36
AA88367	LS_T3_P14_287	charcoal	-27.8	0.502 ± 0.044	5540 ± 700
AA93275	LS_TE_P15_330	soil (bulk)	-26	0.6857 ± 0.0032	3,031 ± 38
AA93276	LS_TE_P7_90	gravel *	-28.2	0.0998 ± 0.0053	18,510 ± 430

Samples have been analysed by the NSF-Arizona AMS Laboratory

* Calcite crust around gravel, likely overestimates age because of reservoir effect, accidently analysed.

OSL Dating

Dose Recovery Test

Labor-Nr.	TE_P7_100 (BT790) (applizierte Dosis = 500s auf Moritz)							
PreHeat	180°C		200°C		220°C		240°C	
	DE	±	DE	±	DE	±	DE	±
Aliquot 1	540.56	39.5	531.33	32.85	440.05	12.54	541.37	39.04
Aliquot 2	447.73	20	499.85	11.03	513.6	34.69	424.76	20.37
Aliquot 3	525.55	19.35	470.51	16.96	518.78	29.43	528.85	22.82
mean	504.61	49.83	500.56	30.42	490.81	44.04	498.33	64.02

Labor-Nr.	BT 790 Recuperation			
PreHeat	180°C	200°C	220°C	240°C
Aliquot 1	1.26	2.34	3.57	2.83
Aliquot 2	3.73	3.36	4.98	4.65
Aliquot 3	6.82	1.85	1.43	1.63
mean	3.937	2.517	3.327	3.037

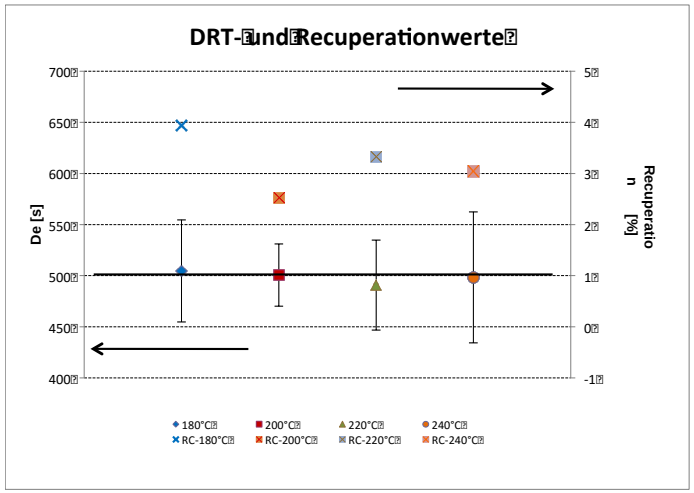

Labor-Nr.	T2_P1_200 (BT)855 (applizierte Dosis = 500s auf Moritz)							
PreHeat	180°C		200°C		220°C		240°C	
	DE	±	DE	±	DE	±	DE	±
Aliquot 1	546.12	15.63	490.42	22.65	515.47	33.28	492.91	26.43
Aliquot 2	510.25	27.46	486.61	14.12	502.6	18.4	520.2	12.01
Aliquot 3	498.71	23.78	500.38	25.05	492.84	16.72	485.28	16.37
mean	518.36	24.72	492.47	7.11	503.64	11.35	499.46	18.36

Labor-Nr.	BT 855 Recuperation			
PreHeat	180°C	200°C	220°C	240°C
Aliquot 1	3.49	0.98	4.5	0.66
Aliquot 2	3.92	8.6	1.4	1.19
Aliquot 3	1.62	1.83	2.08	1.05
mean	3.010	3.803	2.660	0.967

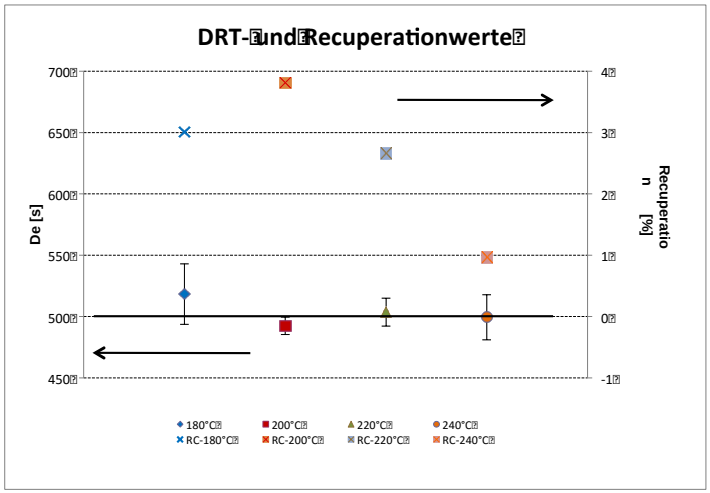

Labor-Nr.	T1_P9_145(BT864) (applizierte Dosis = 300s auf Moritz)							
PreHeat	180°C		200°C		220°C		240°C	
	DE	±	DE	±	DE	±	DE	±
Aliquot 1	291.86	15.48	305.93	7.43	324.87	15.94	287.45	5.7
Aliquot 2	310.02	10.49	262.3	10.07	311.03	9.66	262.47	5.79
Aliquot 3	267.49	11.95	301.27	6.95	257.18	10.2	270.52	12.22
mean	289.79	21.34	289.83	23.96	297.69	35.76	273.48	12.75

Labor-Nr.	BT 864 Recuperation			
PreHeat	180°C	200°C	220°C	240°C
Aliquot 1	0.5	1.55	1.55	1.41
Aliquot 2	2.15	2.73	0.52	2.8
Aliquot 3	3.24	0.28	5.97	3.34
mean	1.963	1.520	2.680	2.517

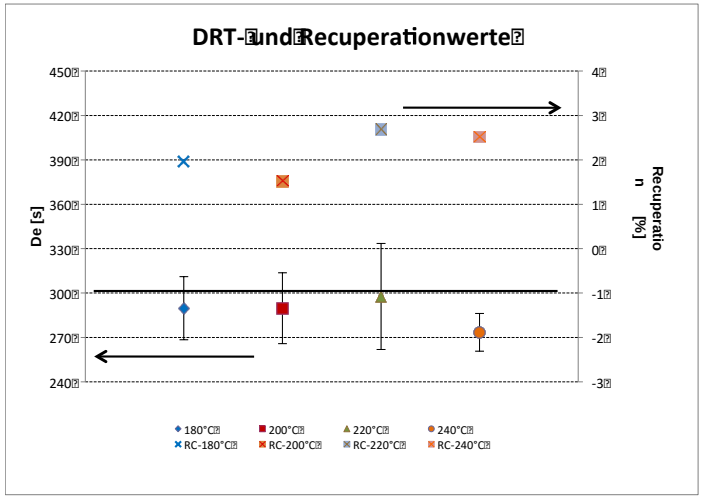

Labor-Nr.	T1_P10_235 (BT866) (applizierte Dosis = 300s auf Moritz)							
PreHeat	180°C		200°C		220°C		240°C	
	DE	±	DE	±	DE	±	DE	±
Aliquot 1	292.46	31.55	286.95	10.7	245.69	17.39	314.35	12.65
Aliquot 2	317.21	16.75	298.7	9.96	316.69	18.01	239.16	14.45
Aliquot 3	298.44	23.05	258.03	15.64	265.15	19.06	377.26	22.46
mean	302.70	12.91	281.23	20.93	275.84	36.69	310.26	69.14

Labor-Nr.	BT 866 Recuperation			
PreHeat	180°C	200°C	220°C	240°C
Aliquot 1	0.69	8.99	1.56	3.26
Aliquot 2	5.11	1.47	3.32	7.66
Aliquot 3	1.36	3.84	4.49	1.93
mean	2.387	4.767	3.123	4.283

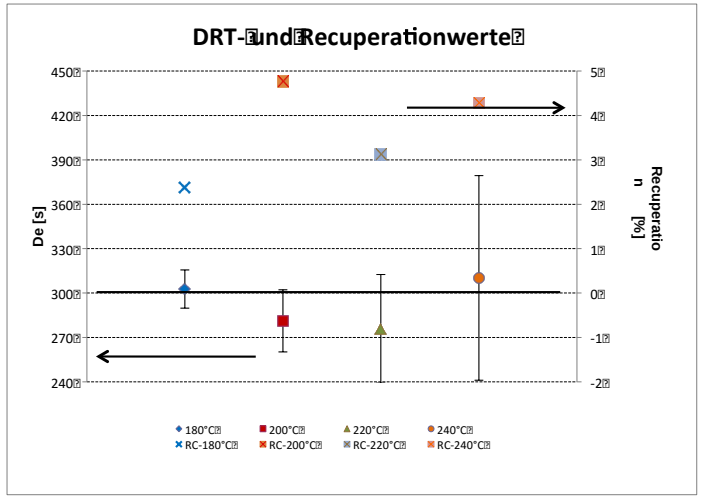

Labor-Nr.	T2P1_340 (BT869) (applizierte Dosis = 500s auf Moritz)							
PreHeat	180°C		200°C		220°C		240°C	
	DE	±	DE	±	DE	±	DE	±
Aliquot 1	460.29	41.58	529.99	29.55	422.21	32.68	478.83	46.06
Aliquot 2	515.33	50.97	543.77	41.28	523.2	27.62	597.71	68.66
Aliquot 3	540.91	75.63	455.24	71.68	498.21	39.65	627.73	78.71
mean	**505.51**	**41.20**	**509.67**	**47.64**	**481.21**	**52.60**	**568.09**	**78.75**

Labor-Nr.	BT 869 Recuperation			
PreHeat	180°C	200°C	220°C	240°C
Aliquot 1	2.13	6.13	1.94	6.02
Aliquot 2	1.11	0.1	1.86	1.82
Aliquot 3	1.84	1	6.31	5.05
mean	1.693	2.410	3.370	4.297

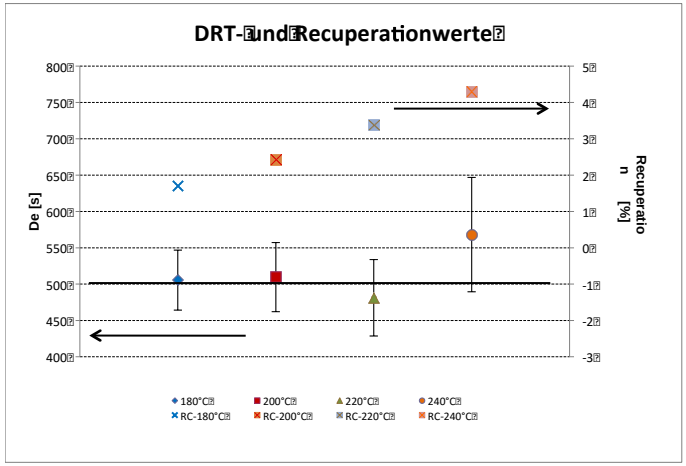

Labor-Nr.	TE_P7_135 (BT881) (applizierte Dosis = 300s auf Moritz)							
PreHeat	180°C		200°C		220°C		240°C	
	DE	±	DE	±	DE	±	DE	±
Aliquot 1	304.17	7.08	289.88	5.31	276.78	6.21	262.34	6.34
Aliquot 2	307.37	4.61	267.23	5.98	290.55	10.97	264.3	5.26
Aliquot 3	310.09	4.35	284.25	7.74	293.96	11.76	293.61	7.46
mean	**307.21**	**2.96**	**280.45**	**11.79**	**287.10**	**9.10**	**273.42**	**17.52**

Labor-Nr.	BT 881 Recuperation			
PreHeat	180°C	200°C	220°C	240°C
Aliquot 1	2.2	3.96	2.22	4.4
Aliquot 2	1.91	0.64	3.14	2.74
Aliquot 3	2.6	1.85	1.01	2.46
mean	2.237	2.150	2.123	3.200

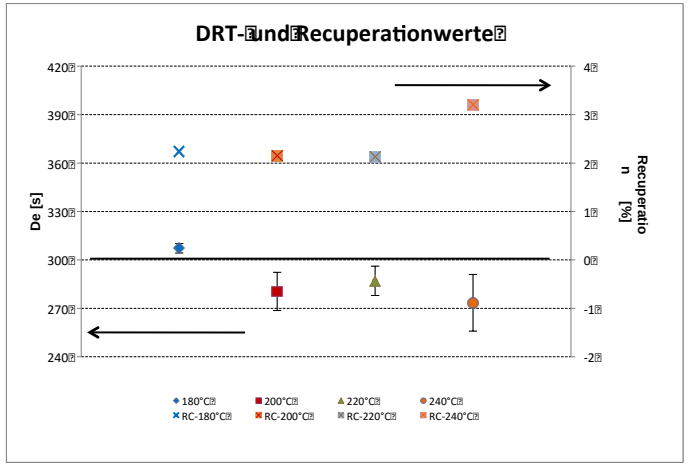

Labor-Nr.	BT 883 (applizierte Dosis = 500s auf Moritz)							
PreHeat	180°C		200°C		220°C		240°C	
	DE	±	DE	±	DE	±	DE	±
Aliquot 1	543.87	23.78	536.75	10.49	370.79	50.75	558.64	72.04
Aliquot 2	572.79	40.99					460.41	36.89
Aliquot 3			496.09	12.25	490.26	34.39	416.55	13.18
mean	558.33	20.45	516.42	28.75	430.53	84.48	478.53	72.76

Labor-Nr.	BT 883 Recuperation			
PreHeat	180°C	200°C	220°C	240°C
Aliquot 1	0.88	1.14	2.66	5.82
Aliquot 2	5.8			8.09
Aliquot 3		0.77	2.75	5.37
mean	3.340	0.955	2.705	6.427

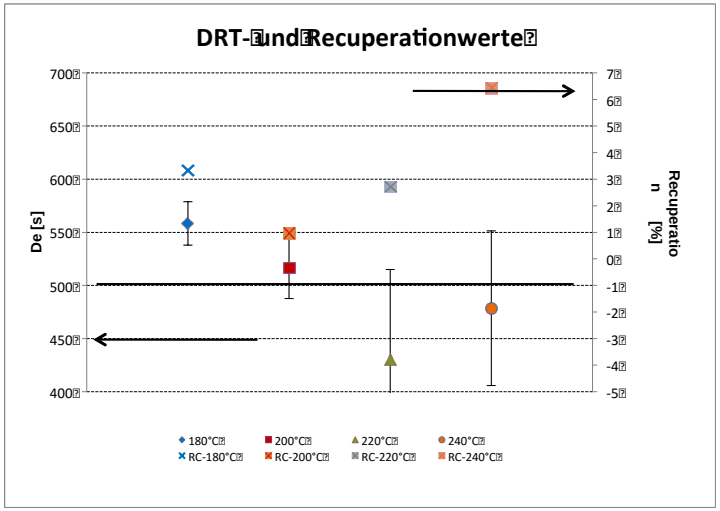

Calculation of the Equivalent Dose

T2_P1_200 (BT855)

	Natural Signal		Regeneration Points											Recycling					
	OSL	IRSL	1	2	3	4	1 Rep	ED	ED Error	N-Signal	BG-Signal	Test Signal	Residual Signal	Test Si	Ratio	Error	Ln/Tn	**ED / Gray**	**ED (error)**
1	17784	48	10457	14725	22370	26221	12951	2299	126.55	17784	380	2601	1134	1.14	1.12	0.05	8.44	84.15	4.63
2	8589	46	6038	7888	11295	13611	7540	1887	150.34	8589	481	1710	1085	1.05	1.12	0.07	6.91	69.06	5.50
3	139832	311	55826	72280	102890	119637	57367	5360	370.16	139832	980	9646	3164	0.89	1.06	0.02	16.08	196.17	13.55
4	20752	240	12805	17683	26777	32440	16199	2236	136.21	20752	315	2519	891	1.16	1	0.04	9.52	81.84	4.99
5	16609	50	7759	10383	15258	18931	10821	2994	325.3	16609	198	1704	494	1.08	1.04	0.06	11.2	109.57	11.91
6	22202	59	11670	13855	17266	20110	13659												
7	25615	59	24660	29530	38852	46530	25173	992	66.77	25615	763	6049	7090	0.82	1.22	0.04	4.84	36.31	2.44
8	26186	136	10432	14065	21144	25677	11746	3792	270.51	26186	366	1976	647	1.04	1	0.05	16.39	138.79	9.90
9	39525	60	28831	36658	50279	62468	33837	1412	58.61	39525	1160	7178	6344	0.87	1.16	0.03	6.43	51.70	2.15
10	12879	34	7999	10076	13408	15079	9200	1827	142.82	12879	348	1923	826	0.96	1.01	0.06	7.97	66.85	5.23
11	16426	48	6943	9381	12646	14335	8900	2909	437.4	16426	299	2024	501	0.91	1.03	0.06	9.42	106.46	16.01
12	19559	56	8685	11562	17445	20776	10332	3996	415.92	19559	313	1855	724	1.03	0.99	0.05	12.34	146.24	15.22
13	30681	1271	18939	26023	39248	49272	23227	1931	66.97	30681	729	7524	2203	1.01	1.09	0.03	4.69	70.68	2.45
14	26458	239	14407	20394	34633	46193	20537	1923	56.95	26458	323	6415	1220	1.08	1.17	0.03	4.56	70.39	2.08
15	54747	64	43704	50450	63270	69585	31969	1255	39.05	54747	2944	18488	7162	0.55	1.11	0.02	3.32	45.94	1.43
16	29497	427	15596	22299	36136	46679	22419	2700	93.39	29497	774	5759	2176	1.28	1.01	0.03	6.28	98.82	3.42
17	36051	622	15885	21524	33792	41779	20238	3105	116.44	36051	433	6081	1212	1.05	0.99	0.03	6.5	113.65	4.26
18	45834	212	20579	27951	40411	47974	24305	3144	120.25	45834	453	7342	1441	0.96	1.04	0.03	6.82	115.07	4.40
19	20390	62	10076	13424	19465	24291	13116	3629	242.19	20390	673	4310	1638	1.12	0.91	0.03	5.96	132.81	8.86
20	19779	784	11479	16538	26647	34793	16356	2088	86.97	19779	536	4740	1406	1.22	0.99	0.03	5.03	76.40	3.18
21	19544	677	9996	14084	22165	26525	11939	2502	91.18	19544	599	4081	1348	0.99	1.05	0.04	5.62	91.59	3.34
22	40291	266	19161	26416	38670	45890	23345	2973	118.67	40291	789	6981	1983	1	1	0.03	6.57	108.79	4.34
23	62861	359	33056	43102	63896	80145	41949	2521	77.3	62861	2204	12596	7150	1	1.06	0.02	5.98	92.26	2.83
24	24236	324	19548	24041	28936	32672	17984	1204	63.43	24236	815	9180	2996	0.72	1.21	0.03	2.99	44.08	2.32

T2_P1_340 (BT869)

	Natural Signal		Regeneration Points											Recycling					
	OSL	IRSL	1	2	3	4	1 Rep	ED	ED Error	N-Signal	BG-Signal	Test Signal	Residual Signal	Test Si	Ratio	Error	Ln/Tn	**ED / Gray**	**ED (error)**
1	4491	172	1987	3448	4730	5531	1973	433	33.08	4491	120	1209	368	0.97	1.09	0.07	4.15	52.41	4.01
2	1577	179	704	1383	2249	3007	939	363	37.59	1577	104	475	209	1.21	1.08	0.13	3.98	43.98	4.55
3	2257	203	887	1463	2565	3189	992	416	42.24	2257	129	562	158	0.99	0.92	0.1	4.8	50.41	5.12
4	2361	97	1337	2210	3387	3995	1352	279	24.32	2361	393	1137	432	0.8	0.97	0.1	2.51	33.73	2.95
5	909	95	358	681	1140	1394	396	327	44.73	909	90	305	88	0.8	1.21	0.23	3.74	39.64	5.42
6	3196	131	1329	2193	3029	3751	1420	579	94.84	3196	139	915	243	1.11	0.87	0.07	3.96	70.13	11.49
7	3219	187	825	1438	2155	2641	856												
8	2443	55	679	1142	1673	1938	652												
9	3120	288	856	1719	3216	4108	985	527	58.64	3120	206	544	191	1.01	1.07	0.15	8.05	63.82	7.10
10	3880	104	851	1598	2382	2816	870	834	122.19	3880	120	585	138	0.86	1.13	0.13	7.87	100.94	14.80
11	4385	395	1654	3140	5148	6320	1905	355	21.84	4385	180	1191	258	0.92	1.15	0.08	4.19	43.02	2.64
12	18210	353	3577	6113	9674	11812	3624												
13	868	63	361	564	919	1278	414	616	110.09	868	111	266	162	1.11	0.68	0.15	4.64	74.56	13.33
14	6884	141	2727	4349	5937	6915	3003												
15	2911	137	1015	1897	2765	3616	1265	410	37.47	2911	126	789	191	0.98	1.38	0.13	4.23	49.67	4.54
16	4738	355	1814	3914	7222	9184	2246	374	17.69	4738	198	1239	273	1.09	1.09	0.07	4.28	45.25	2.14
17	3298	208	735	1515	2452	3239	843	633	50.66	3298	98	483	133	0.98	1.19	0.13	8.23	76.66	6.13
18	4855	1045	3432	6903	13236	18225	4469	176	7.52	4855	438	2194	688	1.07	0.97	0.05	2.41	21.33	0.91
19	1698	73	537	969	1537	1841	602	986	319.33	1698	142	363	164	0.99	1.2	0.19	6.68	119.37	38.67
20	1796	106	664	1108	1824	2359	754	449	61.95	1796	148	492	147	0.91	1.03	0.13	4.44	54.33	7.50
21	6538	51	1689	2693	4032	4849	1667												
22	2707	141	794	1576	2675	3247	933	591	71.55	2707	122	526	157	1.02	1.13	0.13	6.32	71.54	8.66
23	15753	91	2973	4956	6719	7347	2113	1170	81.23	15753	160	1794	350	0.7	0.96	0.06	9.61	141.68	9.84
24	2150	97	774	1335	2177	2651	851	497	62.08	2150	124	537	177	1.01	0.73	0.09	4.98	60.23	7.52
25	2872	167	1267	2262	3704	4806	1446	402	29.76	2872	133	875	300	1.05	1.16	0.1	4.05	48.70	3.60
26	4050	226	1476	2720	4460	5500	1711	443	33.34	4050	353	1233	305	0.91	0.99	0.08	3.91	53.62	4.04
27	2012	65	700	1267	1983	2377	796	549	76.26	2012	114	477	156	1.01	1.08	0.14	5.14	66.45	9.24

T2_P1_380 (BT870)

	Natural Signal		Regeneration Points											Recycling					
	OSL	IRSL	1	2	3	4	1 Rep	ED	ED Error	N-Signal	BG-Signal	Test Signal	Residual Signal	Test Si	Ratio	Error	Ln/Tn	**ED / Gray**	**ED (error)**
1	7917	122	3709	5415	7707	9159	4173	2543	258.82	4919	218	1102	303	0.83	0.98	0.07	5.21	93.08	9.47
2	7655	172	3385	4682	6872	8178	3912	3097	480.91	4671	208	974	252	0.92	1.03	0.08	5.74	113.36	17.60
3	5102	470	4346	7277	13740	17748	6246	1107	56.92	3084	164	1132	459	1.28	1.03	0.06	2.97	40.52	2.08
4	1647	160	1161	1899	3055	3689	1610	1730	342.08	978	105	310	234	1.44	0.77	0.14	4.26	63.30	12.52
5	2954	314	2495	4113	7295	9457	3802	1114	90.88	1748	93	572	241	1.53	0.98	0.08	3.43	40.78	3.33
6	5499	118	2249	3111	4792	5885	2602												
7	7040	160	3535	4988	7902	9666	4188	2446	272.9	4338	105	838	290	1.07	0.94	0.07	5.76	89.53	9.99
8	1601	78	747	975	1473	1709	907												
9	4171	364	2874	4766	8879	11456	4597	1708	139.76	2538	77	634	502	1.8	1.01	0.09	4.57	62.53	5.12
10	1524	512	3530	6184	11392	14760	5098	341	28.95	864	106	744	446	1.59	1.04	0.08	1.2	12.49	1.06
11	8738	168	3305	4574	7379	8925	3771	2862	332.8	5411	91	814	176	1	0.94	0.07	7.22	104.76	12.18
12	1996	106	1317	2184	3783	5210		1555	184.89	1169	67	375	253	1.62	0.95	0.12	3.72	56.93	6.77
13	1044	4793	6304	22878	37799	51776	13362	150	15.65	664	37	1019	752	2.36	1.07	0.05	0.65	5.48	0.57
14	4080	353	3048	4889	7161	9376	3054	2274	211.16	2588	88	496	163	1.36	1.1	0.1	6.3	83.24	7.73
15	2756	401	1204	2919	4107	5190	1517	2263	277.85	1583	93	303	108	1.09	0.99	0.14	6.65	82.82	10.17
16	259077	43797	98045	34944	39650	614177	120104	1942	20.83	143271	4093	20213	3979	0.87	1.01	0.01	7.92	71.09	0.76
17	2298	463	1849	3934	5658	6991	2313	1085	104.28	1332	68	398	120	1.09	1.04	0.11	3.74	39.72	3.82
18	1585	118	1001	2127	2797	3493	1308	1828	276.65	995	53	283	95	1.07	1.25	0.17	4.04	66.90	10.13
19	681	45	378	771	1001	1121	475	1736	654.79	408	33	115	50	1.13	1.11	0.3	4.26	63.54	23.97
20	6636	1232	5971	13289	20106	26360	7749	874	44.94	3513	390	1631	778	0.99	1.18	0.07	2.33	31.98	1.64
21	3167	512	1582	3631	5323	6955	2083	2221	288.67	1921	56	327	127	1.47	0.96	0.12	6.78	81.28	10.57
22	2688	419	1514	3598	5187	6573	2139	1852	190.17	1518	59	349	175	1.36	0.97	0.11	4.98	67.79	6.96

T2_P1_420 (BT868)

	Natural Signal		Regeneration Points												Recycling					
	OSL	IRSL	1	2	3	4	1 Rep	ED	ED Error	N-Signal	BG-Signal	Test Signal	Residual Signal	Test Si	Ratio	Error	Ln/Tn	**ED / Gray**	**ED (error)**
1	3015	410	1626	2494	4138	4880	1997	2890	250.82	3015	159	895	305	1.18	0.95	0.07	3.89	105.78	9.18
2	1801	330	1334	2083	3275	3898	1873	1776	157.55	1801	182	908	438	1.3	0.94	0.08	2.25	64.99	5.77
3	11482	535	6036	10501	20447	29752	13266	2786	123.68	11482	260	3194	2358	2.11	1.01	0.04	4.07	101.96	4.53
4	2876	475	1603	2453	3971	4883	1960	2238	169.51	2876	218	932	380	1.07	1.04	0.09	3.65	81.92	6.20
5	2851	545	2092	3529	6714	8622	2635	1474	74.84	2851	273	1304	350	1.07	1.04	0.06	2.41	53.95	2.74
6	2270	420	1407	2154	3643	4496	1858	2077	179.06	2270	257	876	393	1.1	1.11	0.1	3.06	76.02	6.55
7	2662	420	2187	3475	5835	7372	3251	1492	106.59	2662	295	1295	732	1.36	1	0.07	2.29	54.62	3.90
8	17955	15170	29907	56020	111308	150842	47963	608	8.95	17955	1356	14298	5036	1.59	1.01	0.02	1.28	22.25	0.33
9	1484	370	1098	1878	3575	4410	1789	1708	158.11	1484	171	651	464	1.53	1.03	0.11	2.71	62.51	5.79
10	2697	705	2455	4212	7210	9108	3149	1130	45.55	2697	150	2127	332	1.14	1.1	0.05	1.29	41.37	1.67
11	4320	245	2063	3049	4779	5866	2415	2492	193.29	4320	565	1587	411	0.8	1.04	0.08	3.23	91.22	7.07
12	2947	265	2017	3125	5103	6083	2583	1658	116.49	2947	237	1252	488	1.17	1.15	0.08	2.67	60.67	4.26
13	2529	245	809	1324	2474	3216	926	3420	266.95	2529	87	468	80	0.85	1.06	0.11	6.15	125.16	9.77
14	1603	207	939	1374	2426	2972	1037	1978	153.52	1603	113	721	157	0.92	0.95	0.09	2.47	72.39	5.62
15	2455	175	1328	1913	2899	3701	1536	2344	229.33	2455	163	771	215	1.02	1.06	0.1	3.7	85.78	8.39
16	2168	174	961	1578	2476	3073	1107	3054	270.98	2168	138	577	136	1.02	1	0.09	4.26	111.76	9.92
17	848	178	792	1339	2438	3147	1238	1547	157.39	848	78	433	237	1.52	1.05	0.11	2.21	56.61	5.76
18	1308	242	1077	1780	3361	4469	1428	1251	99.53	1308	114	681	134	1.15	0.91	0.08	2.15	45.77	3.64
19	2005	430	1953	3172	5242	7083	2801	1063	62.16	2005	130	1102	275	1.33	1.07	0.06	1.95	38.92	2.28
20	4115	266	1838	2804	4301	5325	2148	2681	171.36	4115	127	1172	213	0.94	1.07	0.07	3.78	98.12	6.27
21	2877	456	2158	3504	6604	8883	2884	1472	90.28	2877	176	1225	283	1.24	0.9	0.05	2.51	53.86	3.30
22	1886	639	2925	5003	8737	12030	3600	638	27.14	1886	131	1674	324	1.26	0.98	0.05	1.14	23.36	0.99
23	1159	182	653	952	1704	2171	845	1945	208.51	1159	78	378	146	1.04	0.88	0.11	3.52	71.18	7.63
24	4161	348	4279	6790	11606	16077	6398	985	56.47	4161	950	2668	1772	1.22	1.02	0.06	1.75	36.04	2.07

T1_P9_145 (BT864)

	Natural Signal		Regeneration Points											Recycling				
	OSL	IRSL	1	2	3	4	1 Rep	ED	ED Error	N-Signal	BG-Signal	Test Signal	Residual Signal	Test Si	Ratio	Error	Ln/Tn	**ED / Gray**	**ED (error)**
1	100628	269	24105	33999	53469	65646	23958	932	15.18	100628	351	21037	1522	0.94	0.97	0.01	4.93	34.10	0.56
2	11622	125	7922	12188	19287	22901	9418	275	6.5	11622	469	7644	2536	1.1	1.1	0.03	1.69	10.07	0.24
3	46098	2784	21117	32212	50045	58893	21199	390	5.34	46098	2507	20921	4382	0.9	1.03	0.02	2.45	14.28	0.20
4	7471	40	4473	6364	9709	11107	4544	335	12.07	7471	457	4236	1438	0.96	1.04	0.05	2	12.26	0.44
5	6944	342	3935	6203	10036	12501	4751	320	9.99	6944	238	3752	972	1.14	1.02	0.04	2	11.71	0.37
6	19887	37	15965	23776	37152	42280	16486	213	4.35	19887	519	15670	3550	0.96	1.09	0.02	1.35	7.81	0.16
7	208223	34330	63957	101533	180846	224998	65776	574	4.09	208223	8437	54949	7121	0.94	0.99	0.01	4.14	21.01	0.15
8	50224	133	17850	26532	43798	54765	20359	508	7.07	50224	476	16018	2687	1.05	1.01	0.02	3.31	18.58	0.26
9	75850	5605	21308	32092	52325	65282	21321	657	8.36	75850	356	18406	1787	0.95	0.97	0.02	4.29	24.05	0.31
10	12582	251	8916	14064	22929	27904	10642	249	5.48	12582	302	8059	2409	1.13	1.07	0.03	1.67	9.12	0.20
11	14662	885	5014	7111	11107	13749	4886	515	13.82	14662	206	4727	817	0.86	0.97	0.04	3.37	18.86	0.51
12	51138	304	28986	42092	64828	73592	27479	325	4.15	51138	1541	24739	6245	0.88	1.05	0.02	2.23	11.90	0.15
13	25376	54	4586	6648	10076	11717	4541	2409	147.06	25376	227	11507	1124	0.87	1.03	0.03	2.29	88.17	5.38
14	58903	39	5909	8202	12947	15435	5444												
15	13105	28	6485	10111	17004	20414	8481	403	8.82	13105	322	13532	1541	1.19	1.07	0.03	1.03	14.73	0.32
16	7970	36	2972	4068	7011	9090	3280	515	12.63	7970	168	6535	635	1.04	0.91	0.03	1.28	18.84	0.46
17	3047	44	1722	2747	4971	6503	2763	382	14.9	3047	166	3599	822	1.58	1.07	0.05	0.9	13.96	0.55
18	6901	31	3627	5382	8654	10970	4438	331	8.1	6901	138	8868	989	1.05	1.13	0.04	0.81	12.10	0.30
19	11074	4113	14049	26892	54047	75444	30039	163	2.69	11074	1065	28147	11967	2.18	1.04	0.02	0.4	5.97	0.10
20	3239	145	2130	3269	5520	6592	2637	285	8.64	3239	148	4896	795	1.1	1.07	0.05	0.68	10.44	0.32
21	5198	41	2915	4440	7318	8624	3615	362	10.71	5198	224	7429	1152	1.02	1.18	0.05	0.75	13.27	0.39
22	3455	59	2604	4118	6247	7036	3092	219	8.38	3455	142	7247	989	0.9	1.21	0.05	0.49	8.00	0.31
23	10142	1090	6856	12308	23002	31365	11112	268	4.82	10142	215	15111	1689	1.62	1.06	0.02	0.69	9.82	0.18
24	4759	31	1844	2703	4707	6067	2408	541	17.94	4759	100	4063	460	1.29	1.03	0.05	1.26	19.79	0.66

T1_P9_195 (BT866)

	Natural Signal		Regeneration Points											Recycling					
	OSL	IRSL	1	2	3	4	1 Rep	ED	ED Error	N-Signal	BG-Signal	Test Signal	Residual Signal	Test Si	Ratio	Error	Ln/Tn	**ED / Gray**	**ED (error)**
1	6457	175	3765	6224	11785	15581	5139	1678	125.21	6457	169	743	259	1.43	0.99	0.07	11.05	61.41	4.58
2	19143	45	6704	8613	13112	16059	8233												
3	4907	39	3036	4051	5334	6323	2997	1431	127.61	4907	163	959	431	0.87	0.95	0.08	6.35	52.38	4.67
4	2717	18	1393	2053	2846	3344	1587	2201	423.33	2717	188	516	319	1.06	0.83	0.13	8.11	80.55	15.49
5	7373	27	8148	9662	12102	14176	7614	491	55.09	7373	203	2971	1731	0.73	1.36	0.06	2.71	17.98	2.02
6	5304	66	3429	4856	7998	9849	3888	1222	75.97	5304	285	1335	708	0.98	0.93	0.06	5.01	44.72	2.78
7	3560	20	2106	2722	3811	4337	2427	3084	1017.41	3560	142	559	265	1.21	1.03	0.09	8.2	112.86	37.24
8	12487	41	3265	4279	6266	6964	2841												
9	13861	43	4657	6460	9599	11750	4768	3053	250.17	13861	125	1114	207	0.85	1.05	0.07	14.16	111.74	9.16
10	26767	18	10010	11402	13201	14552	9779												
11	26490	30	35104	44536	58858	68522	38198	250	55.59	26490	1224	9158	15583	0.81	1.24	0.03	3.18	9.16	2.03
12	1185	18	791	1082	1675	2063	888	1625	332.11	1185	122	280	212	1.15	1.03	0.2	6.99	59.49	12.16
13	8289	75	2873	4901	6319	7377	2684	5505	1856.07	8289	136	772	383	1.06	1.02	0.1	13.48	201.47	67.93
14	8981	31	3793	4996	6184	6979	3977	2548	540.37	8981	223	1622	418	0.85	0.95	0.06	6.31	93.27	19.78
15	1671	16	1082	1736	2473	3198	1315	1278	194.19	1671	167	415	314	1.09	1.22	0.21	6.06	46.76	7.11
16	29549	11	9468	14802	19599	23178	8100	3183	137.84	29549	194	2390	839	0.98	0.99	0.05	13.89	116.51	5.04
17	7126	38	3241	4587	6626	8743	3542	1902	207.16	7126	256	1363	595	1.06	1.07	0.1	7.54	69.60	7.58
18	27764	28	40876	57157	64184	70565	33251	282	19.51	27764	1250	11875	10620	0.73	1.09	0.02	2.51	10.34	0.71
19	7767	16	4857	7150	9264	9870	3918	1163	76.84	7767	305	1523	521	0.82	0.94	0.07	6.22	42.57	2.81
20	41485	60	13656	17827	23064	27795	12235	2494	145.11	41485	315	5165	1367	0.7	0.94	0.03	8.63	91.30	5.31
21	11240	49	4080	6061	8497	11267	3985	2692	215.92	11240	183	1314	509	1.01	0.95	0.07	10.34	98.52	7.90
22	23349	31	10690	17702	24313	30768	10995	2054	87.25	23349	330	3015	1179	1.16	1.02	0.05	10.35	75.18	3.19
23	5036	27	2871	4190	5632	6865	2960	2035	268.79	5036	407	1089	818	1.22	0.93	0.12	8.14	74.48	9.84
24	5813	26	7796	13509	18125	20772	8146	510	33.93	5813	287	2354	2062	1.19	0.94	0.04	2.79	18.68	1.24
25	1852	20	1742	2791	3860	4771	1738												
26	33244	36	11038	17340	22613	25593	11278	1200	149.48	1852	98	422	73	1.18	1.1	0.11	5.28	43.93	5.47
27	5535	115	7863	12785	16680	19155	7040	4728	656.78	33244	435	3131	70	0.92	0.94	0.04	12.76	173.04	24.04
28	4371	45	2184	3695	5142	6234	2393	315	10.7	5535	219	2642	228	0.66	1.01	0.05	2.23	11.51	0.39
29	18854	56	6354	9933	12325	14177	6479	1890	198.64	4371	101	648	74	1.13	0.86	0.08	8.16	69.16	7.27
30	4910	202	2801	4594	6262	7995	3496	2957	264.01	18854	240	2083	122	0.81	0.97	0.05	10.52	108.21	9.66

T1_P9_435 (BT876)

	Natural Signal		Regeneration Points											Recycling					
	OSL	IRSL	1	2	3	4	1 Rep	ED	ED Error	N-Signal	BG-Signal	Test Signal	Residual Signal	Test Si	Ratio	Error	Ln/Tn	**ED / Gray**	**ED (error)**
1	6046	43	2403	3650	4980	6137	2676	518	57.25	6046	439	1740	550	0.97	1.05	0.08	4.68	62.76	6.93
2	14378	48	3903	6344	9128	10635	3678	1045	123.02	14378	281	2483	503	0.88	0.94	0.05	6.6	126.58	14.90
3	28550	140	8293	12811	19102	24157	8465	653	34.03	28550	459	5332	873	0.87	0.96	0.03	5.96	79.04	4.12
4	46597	60	12085	19805	29895	38947	13173	927	37	46597	277	6082	650	1.02	1.02	0.03	8.33	112.27	4.48
5	16711	1270	10710	20157	32532	40307	12041	222	5.1	16711	382	5676	1675	0.98	1.04	0.03	3.2	26.88	0.62
6	40003	133	11483	17930	24851	29897	11694	1552	564.17	40003	495	6137	1065	0.91	1.05	0.03	7.36	187.95	68.32
7	15594	44	4702	7388	10412	12566	4927	925	87.89	15594	283	2768	547	0.9	1.04	0.05	6.31	112.02	10.64
8	12336	443	4688	8102	13477	17572	5792	436	17.39	12336	334	3043	791	1.04	1	0.05	4.76	52.81	2.11
9	10887	71	2810	4199	5838	6911	2670												
10	21932	119	15831	26501	34979	37228	13853	205	9.53	21932	435	10243	2940	0.68	1.24	0.03	2.28	24.79	1.15
11	14813	95	6063	9491	13032	15538	5737	459	20.2	14813	316	3385	961	0.87	0.99	0.04	4.92	55.60	2.45
12	31403	145	9802	14772	20581	25561	9519	802	42.04	31403	371	5562	1001	0.92	0.98	0.03	6.51	97.14	5.09
13	12981	24	4026	6201	8347	9598	3889												
14	139612	40	14449	24006	37554	48777	15128												
15	20215	82	5380	8238	11574	14181	5491	1449	436.85	20215	241	2972	461	0.87	1.05	0.04	7.57	175.52	52.90
16	20082	12575	25711	58618	115104	163925	37030	114	2.69	20082	743	10402	2095	1.4	0.98	0.02	2	13.84	0.33
17	36449	126	10902	16464	22736	26597	10616	1034	87.17	36449	416	5947	905	0.83	0.98	0.03	6.63	125.25	10.56
18	140869	57	36139	54740	80376	97409	37158	1040	50.28	140869	516	19702	1342	0.84	1.04	0.02	7.49	125.99	6.09
19	9529	64	3281	5620	8693	11177	3958	806	83.44	9529	604	2054	909	1.1	1.03	0.07	5.93	97.64	10.10
20	25209	49	8710	13626	19120	22178	9240												
21	16387	128	6084	9091	12143	14494	5952	650	42.55	16387	332	3544	876	0.87	1.06	0.04	5.11	78.77	5.15
22	64506	45	16534	25899	35728	40520	16079												
23	64456	28	14569	21548	29296	34905	12310												
24	20247	73	7635	11931	17489	21079	8040	556	25.85	20247	430	4546	1129	0.93	1.09	0.04	5.1	67.37	3.13
25	99171	53	22948	33349	43710	52683	20069												
26	19415	37	4797	7191	9695	10828	4577												

T1_P10_235 (BT866)

	Natural Signal		Regeneration Points												Recycling				
	OSL	IRSL	1	2	3	4	1 Rep	ED	ED Error	N-Signal	BG-Signal	Test Signal	Residual Signal	Test Si	Ratio	Error	Ln/Tn	**ED / Gray**	**ED (error)**
1	278	13	150	228	350	407	170	106	15.22	278	39	375	78	1	?	?	0.76	3.90	0.56
2	1842	13	803	1220	2134	2613	774	116	5.95	1842	122	1686	205	1.09	?	?	1.16	4.24	0.22
3	1221	19	580	901	1371	1769	717	140	8.61	1221	172	1210	501	1.13	?	?	1.24	5.12	0.32
4	356	18	219	288	517	590	164	87	8.27	356	51	477	81	0.87	?	?	0.75	3.18	0.30
5	111	17	132	129	213	295	113	48	16.35	111	65	176	62	1.26	?	?	0.42	1.77	0.60
6	173	10	117	123	194	257	123	96	25.15	173	58	178	85	0.93	?	?	1	3.53	0.92
7	1216	7	672	986	1785	2226	616	81	3.76	1216	113	2008	242	0.95	?	?	0.63	2.98	0.14
8	605	18	305	447	725	833	358	105	8.55	605	80	742	199	0.96	?	?	0.85	3.86	0.31
9	1751	9	901	1442	2490	3102	738	83	3.13	1751	83	2296	165	0.87	?	?	0.78	3.02	0.11
10	192	16	94	105	203	247	98	146	23.42	192	47	212	53	0.88	?	?	0.94	5.33	0.86
11	1374	13	431	778	1492	1880	409	121	5.76	1374	45	1249	92	1.09	?	?	1.15	4.43	0.21
12	2888	22	281	383	644	766	233	665	38.75	2888	108	653	119	0.91	?	?	5.36	24.35	1.42
13	864	29	604	789	1257	1677	627	72	6.18	864	219	1239	195	1.16	1.09	0.1	0.62	2.64	0.23
14	864	17	499	915	1460	1941	626	78	4.93	864	72	1276	171	1.19	1.01	0.1	0.71	2.85	0.18
15	225	20	169	283	458	503	244	58	8.9	225	53	494	130	0.97	1.48	0.37	0.46	2.12	0.33
16	348	20	221	343	550	699	290	89	9.27	348	55	438	148	1.03	0.96	0.22	0.84	3.24	0.34
17	2716	25	1100	1694	3200	3809	933	108	3.22	2716	63	2654	131	0.85	0.99	0.06	1.04	3.94	0.12
18	155	16	118	178	265	344	136	66	13.54	155	48	272	70	0.85	1.82	0.62	0.5	2.41	0.50
19	3333	20	1234	2011	3531	4345	1102	110	3	3333	71	3218	153	0.79	1.03	0.06	1.05	4.03	0.11
20	248	29	189	357	598	768	331	45	6.88	248	44	994	140	1.09	1.83	0.28	0.22	1.65	0.25
21	883	16	649	997	1725	2070	691	67	3.77	883	72	1487	205	1.09	0.95	0.09	0.65	2.47	0.14
22	551	22	277	405	697	823	344	122	10.91	551	86	688	208	0.97	1.22	0.23	0.87	4.45	0.40
23	298	19	245	361	509	609	362	92	13.58	298	94	463	207	1.27	1.04	0.37	0.67	3.35	0.50
24	531	21	295	456	785	884	312	119	10.73	531	94	602	176	1.27	0.91	0.17	0.97	4.35	0.39

TE_P7_100 (BT792)

	Natural Signal		Regeneration Points											Recycling					
	OSL	IRSL	1	2	3	4	1 Rep	ED	ED Error	N-Signal	BG-Signal	Test Signal	Residual Signal	Test Si	Ratio	Error	Ln/Tn	**ED / Gray**	**ED (error)**
1	19088	24	8804	13241	21390	27092	9355	244	5.37	13073	172	7684	994	0.88	1.09	0.03	1.77	**8.93**	**0.20**
2	7061	70	4532	7455	13237	17866	6089	174	5.55	4764	133	4695	658	1.04	1.25	0.05	1.06	**6.35**	**0.20**
3	20464	39	9345	14807	25299	32905	11180	266	5.69	13034	269	6292	1089	1.09	1.06	0.03	2.17	**9.75**	**0.21**
4	3554	39	2773	4511	7519	9883	3568	142	5.91	2378	114	2486	448	1.14	1.05	0.06	1.05	**5.20**	**0.22**
5	32081	267	12550	20656	35099	48392	14996	292	4.45	21796	209	9814	1021	1.09	1.04	0.02	2.32	**10.70**	**0.16**
6	34130	92	14653	21444	33763	44916	13787	248	3.93	22947	199	10374	676	0.91	0.98	0.02	2.28	**9.06**	**0.14**
7	14440	32	6613	10803	18909	25127	7124	224	5.15	9587	94	5056	347	0.98	1.03	0.03	1.99	**8.20**	**0.19**
8	9530	64	5492	7918	12702	16654	5599	195	5.43	6380	177	4106	579	0.92	0.93	0.04	1.68	**7.15**	**0.20**
9	12682	69	8029	13139	23229	31511	10253	181	4.03	8497	198	6163	970	1.19	1.03	0.03	1.48	**6.62**	**0.15**
10	13849	61	5698	8739	13963	18104	5694	269	6.7	9269	103	4524	422	0.88	1.09	0.04	2.13	**9.86**	**0.25**
11	25796	78	12800	19827	33022	45391	14931	219	4.08	17235	271	9188	1170	1.12	1.07	0.03	1.95	**8.00**	**0.15**
12	13494	63	9330	15502	27508	38318	14665	157	5.72	8863	158	8129	1299	1.24	1.28	0.03	1.13	**5.74**	**0.21**
13	10805	80	6990	11482	18723	25746	9116	174	5.13	7084	157	5700	971	1.15	1.21	0.04	1.32	**6.37**	**0.19**
14	32177	43	12677	20185	32383	41786	13692	295	4.94	22017	328	10275	1150	0.96	1.06	0.03	2.27	**10.80**	**0.18**
15	21485	101	12697	20013	33165	45205	16018	198	4.24	14232	440	8751	1529	1.17	1.08	0.03	1.76	**7.26**	**0.16**
16	117396	83	15991	24883	40301	52809	15659	1141	21.77	80739	219	12307	743	0.88	1.01	0.02	6.83	**41.75**	**0.80**
17	22433	97	9562	15091	25912	34845	10733	255	5.14	15268	221	7352	685	1.1	1.01	0.03	2.2	**9.34**	**0.19**
18	68704	135	31912	46519	76409	97467	32004	255	3.78	45468	518	22895	2803	0.88	1.02	0.02	2.08	**9.35**	**0.14**
19	6482	366	5146	8316	14424	19770	6409	138	4.05	4165	134	3894	768	1.09	0.98	0.04	1.13	**5.06**	**0.15**
20	13177	62	6543	10240	16811	22439	8107	239	6.37	8753	204	4965	709	1.13	1.11	0.04	1.88	**8.74**	**0.23**
21	29403	40	6574	10014	15852	20377	6379	620	16.38	20418	123	5024	345	0.91	1	0.03	4.35	**22.68**	**0.60**
22	50025	134	20791	32896	55186	74654	23620	268	4.13	33535	257	16617	1623	0.99	1.1	0.02	2.09	**9.80**	**0.15**
23	18562	113	9307	15014	25101	33260	11467	229	4.71	12332	211	7787	1229	1.08	1.12	0.03	1.69	**8.37**	**0.17**
24	20653	400	10311	16252	26757	35088	11423	219	4.04	14267	243	8426	919	0.98	1.08	0.03	1.76	**8.03**	**0.15**

TE_P7_135 (BT881)

	Natural Signal		Regeneration Points											Recycling					
	OSL	IRSL	1	2	3	4	1 Rep	ED	ED Error	N-Signal	BG-Signal	Test Signal	Residual Signal	Test Si	Ratio	Error	Ln/Tn	**ED / Gray**	**ED (error)**
1	6310	107	3850	6344	11362	14691	5545	234	7.67	6310	197	2854	893	1.49	1.07	0.04	2.42	8.58	0.28
2	4469	76	1967	3280	5573	6957	2681	335	15.2	4469	148	1550	522	1.31	1.13	0.07	3.27	12.27	0.56
3	3287	92	3788	5881	9345	11459	4610	99	4.17	3287	218	3230	1230	1.09	1.09	0.05	1.09	3.64	0.15
4	3537	36	1769	2912	4724	6107	2464	318	17.23	3537	210	1503	664	1.33	1.12	0.08	2.97	11.62	0.63
5	5305	77	3007	4470	6842	8524	3619	272	11.22	5305	204	2347	999	1.29	1.04	0.06	2.6	9.96	0.41
6	8901	70	4192	6740	10825	13271	4778	297	9.61	8901	188	3286	795	1.1	1.08	0.04	2.98	10.87	0.35
7	4017	29	2546	3705	5554	6474	2349	199	7.74	4017	139	1957	457	0.99	0.98	0.06	2.25	7.29	0.28
8	3325	168	3214	4965	8143	10093	3806	138	8.21	3325	217	2510	938	1.25	1.04	0.05	1.47	5.05	0.30
9	2234	220	1729	2717	4497	5733	2112	183	10.81	2234	133	1349	433	1.21	1.11	0.07	1.83	6.70	0.40
10	7694	918	6078	9926	17546	21401	7398	166	4.46	7694	248	4894	1313	1.17	1.11	0.04	1.71	6.09	0.16
11	11090	131	7741	11891	18162	21769	7898	183	4.43	11090	219	6262	1136	1	1.01	0.03	1.89	6.68	0.16
12	13664	38	4549	6751	10704	12416	4015	388	9.91	13664	161	3491	414	0.91	0.99	0.04	4.14	14.21	0.36
13	14022	263	8020	12632	21262	25086	7413	220	4.29	14022	238	6533	1042	0.91	1	0.03	2.29	8.06	0.16
14	12155	275	9562	14494	22810	26831	9029	149	2.98	12155	386	7468	1498	0.93	0.95	0.03	1.75	5.47	0.11
15	8044	100	5738	9184	15328	18927	7174	194	5.39	8044	312	4372	1498	1.3	1.1	0.04	2.03	7.11	0.20
16	53110	14577	35104	63054	126194	172264	48751	198	1.91	53110	1055	23968	3836	1.42	0.97	0.01	2.29	7.26	0.07
17	8996	1608	7605	12503	22854	29861	9719	152	3.76	8996	390	5833	1514	1.33	0.96	0.03	1.68	5.55	0.14
18	21452	113	8310	12539	20473	24967	9383	386	8.32	21452	318	6723	1515	1.13	0.96	0.03	3.44	14.14	0.30
19	11367	206	7911	12418	19407	22915	7882	169	3.47	11367	267	6458	1269	0.98	1.01	0.03	1.88	6.18	0.13
20	2736	179	1756	2767	4743	5731	2215	217	11.53	2736	202	1425	560	1.3	1.15	0.09	2.26	7.96	0.42
21	10461	68	5874	8694	14205	16931	6422	248	7.47	10461	230	4392	870	1.07	1.02	0.03	2.55	9.07	0.27
22	8718	242	4657	7237	12265	15577	5986	254	7.81	8718	302	3655	1127	1.25	0.97	0.04	2.65	9.29	0.29
23	10063	229	5757	8901	14857	18246	7111	267	7.47	10063	449	4435	1690	1.28	1.04	0.04	2.58	9.76	0.27
24	17026	226	7651	11680	18762	22105	7861	302	6.78	17026	432	6075	1439	1.01	0.94	0.03	3.04	11.06	0.25
25	14911	495	8490	13213	22899	28722	9948	226	4.78	14911	220	6709	1201	1.15	1.02	0.03	2.33	8.26	0.17
26	6850	108	5681	8945	14248	16966	6077	148	3.74	6850	171	4559	980	1.08	0.97	0.03	1.58	5.41	0.14

TE_P7_270 (BT882)

	Natural Signal		Regeneration Points											Recycling					
	OSL	IRSL	1	2	3	4	1 Rep	ED	ED Error	N-Signal	BG-Signal	Test Signal	Residual Signal	Test Si	Ratio	Error	Ln/Tn	**ED / Gray**	**ED (error)**
1	9678	934	15300	25074	44982	57433	19318	213	7.76	9678	2072	8413	3821	1.12	1.06	0.03	1.17	7.79	0.28
2	23176	56	9467	12939	17723	18175	6991	1274	43.78	23176	1149	5058	1986	0.6	1.08	0.04	5.24	46.63	1.60
3	1832	69	1037	1538	2673	3070	1181	806	72.06	1832	151	582	272	1.1	0.8	0.1	3.87	29.49	2.64
4	12886	313	6508	10235	17518	22019	7481	893	26.01	12886	480	3479	888	1.01	1.09	0.04	4.1	32.68	0.95
5	26878	1782	18654	32692	61077	78756	23665	591	10.66	26878	1647	9531	2604	1.15	1.04	0.02	3.09	21.65	0.39
6	314253	62	60504	66808	83100	84689	33062												
7	3362	51	6596	9707	14370	15900	6231	149	7.82	3362	263	3369	1472	0.89	1.01	0.04	1.04	5.46	0.29
8	186868	8531	96337	151691	266057	329090	94627	764	7.63	186868	13874	50918	10097	0.78	1	0.01	4.33	27.96	0.28
9	922	38	634	919	1447	1606	837	886	194.05	922	151	386	337	1.32	0.93	0.2	3.47	32.41	7.10
10	17235	1847	13521	25221	52582	73197	21299	535	10.34	17235	549	5736	1451	1.56	0.96	0.02	3.18	19.59	0.38
11	4577	64	2274	3314	5786	7648	3066	1045	69.21	4577	179	1226	607	1.38	1.06	0.08	4.46	38.25	2.53
12	1838	144	1974	2798	4321	4934	2035	396	32.32	1838	350	1345	562	1.05	0.93	0.07	1.61	14.48	1.18
13	79541	932	21363	27118	41353	52034	23549												
14	1794	5633	10898	19129	37722	56504	15374	56	5.34	1794	224	4454	1099	1.52	0.92	0.02	0.38	2.03	0.20
15	557	77	325	560	893	1272	493	768	173.88	557	73	193	133	1.28	1.09	0.29	4.1	28.12	6.36
16	18032	4239	12901	22055	43329	65569	17336	580	13.93	18032	697	5623	1222	1.21	1.03	0.03	3.42	21.22	0.51
17	3649	221	2221	3185	5063	6382	2436	896	63.62	3649	198	1140	358	1.13	1.01	0.07	3.71	32.79	2.33
18	15583	407	5455	7776	11836	15787	6074	1831	105.63	15583	384	3020	878	1.06	0.95	0.04	6.11	67.00	3.87
19	1357	89	892	1308	2256	2830	1163	794	84.24	1357	89	490	180	1.24	1.01	0.1	3.32	29.04	3.08
20	1600	204	829	1311	2199	2907	967	1208	161.96	1600	111	411	164	1.19	0.95	0.12	5.13	44.22	5.93
21	38638	678	19874	27862	39346	45701	16113	913	19.08	38638	1969	10644	3315	0.71	0.99	0.03	4	33.42	0.70
22	7292	157	6231	8797	12538	15601	5709	463	17.07	7292	500	4015	858	0.74	1.14	0.05	2.02	16.96	0.62
23	3404	720	2683	4617	7834	11207	3411	500	22.68	3404	146	1481	586	1.14	1.11	0.07	2.48	18.30	0.83
24	6295	518	5633	8328	11884	14889	5476	481	17.38	6295	267	3233	1071	0.99	1.13	0.05	2.14	17.59	0.64

TE_P8_110 (BT883)

	Natural Signal		Regeneration Points											Recycling					
	OSL	IRSL	1	2	3	4	1 Rep	ED	ED Error	N-Signal	BG-Signal	Test Signal	Residual Signal	Test Si	Ratio	Error	Ln/Tn	**ED / Gray**	**ED (error)**
1	615	13	350	460	649	748	366	1170	287.85	615	114	381	187	1.06	0.9	0.21	2.33	42.82	10.54
2	5468	20	1954	2301	3241	3491	1838												
3	10602	115	12824	18322	26981	29622	12217	211	8.29	10602	366	14140	3554	0.81	1.14	0.03	0.78	7.73	0.30
4	351	20	211	280	456	566	243	764	118.49	351	76	239	81	1.1	0.98	0.23	1.77	27.98	4.34
5	699	44	953	1221	1834	1997	1061	136	29.59	699	136	1547	441	0.86	1.29	0.1	0.43	4.97	1.08
6	22738	22	3788	5416	9303	11380	3838	2452	83.34	22738	120	3643	144	0.97	1.02	0.04	6.57	89.73	3.05
7	2732	22	1008	1449	2428	3048	1230	1083	66.46	2732	90	1136	219	1.12	1.09	0.08	2.69	39.64	2.43
8	252	12	151	158	215	274	172	353	82.86	252	55	239	59	0.67	1.24	0.42	1.15	12.94	3.03
9	177	25	373	537	820	855	465	53	16.32	177	98	351	125	1.15	1.07	0.19	0.33	1.95	0.60
10	273	25	148	211	296	328	186	886	330.92	273	64	161	80	0.88	1.3	0.44	2.38	32.42	12.11
11	1498	61	445	637	1077	1309	517	2046	482.77	1498	102	464	122	0.88	0.99	0.14	3.84	74.88	17.67
12	927	31	474	645	903	1067	581	962	141.16	927	206	563	295	1.01	1.14	0.22	2.17	35.22	5.17
13	26652	79	6271	8756	12724	15315	6843												
14	3748	35	4039	7004	12464	15377	6874	361	14.4	3748	276	4172	680	1.52	1.14	0.04	1.02	13.20	0.53
15	13007	34	6495	9908	14509	16453	6995	1204	40.32	13007	187	5197	522	1.12	1.04	0.03	2.65	44.05	1.48
16	1197	34	560	720	1207	1546	653	1157	138.69	1197	135	571	181	1.04	1.03	0.15	2.55	42.35	5.08
17	8967	31	2752	4052	6278	7359	2700	1478	47.84	8967	108	2906	382	0.85	1.11	0.05	3.25	54.10	1.75
18	1815	220	1055	1618	2796	3470	1535	792	54.7	1815	334	1411	445	1.19	1.2	0.11	1.47	28.99	2.00
19	3316	50	1987	2591	3769	4671	2160	1062	71.08	3316	222	2052	408	1.18	0.82	0.05	1.88	38.87	2.60
20	637	63	397	666	999	1278	594	760	91.31	637	87	477	224	1.35	1.06	0.2	1.92	27.83	3.34
21	2019	18	640	906	1378	1636	674	1910	214.95	2019	86	629	88	1.06	1.16	0.12	3.6	69.90	7.87
22	50347	208	31015	45847	69132	78043	34724	840	21.38	50347	4375	27681	11846	0.88	1.19	0.02	2.02	30.75	0.78
23	2945	31	1098	1484	2144	2453	1301												
24	1829	85	1008	1530	2567	3126	1253	1071	91.25	1829	151	827	225	1.27	0.88	0.08	2.61	39.20	3.34

T2_P1_200

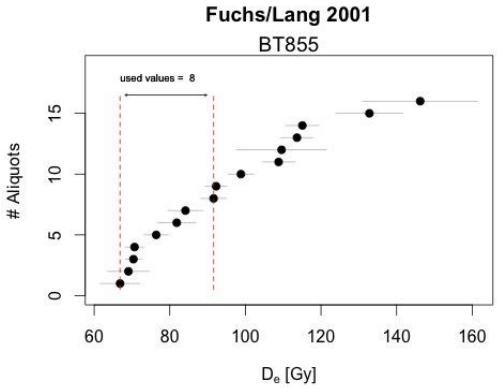

T2_P1_340

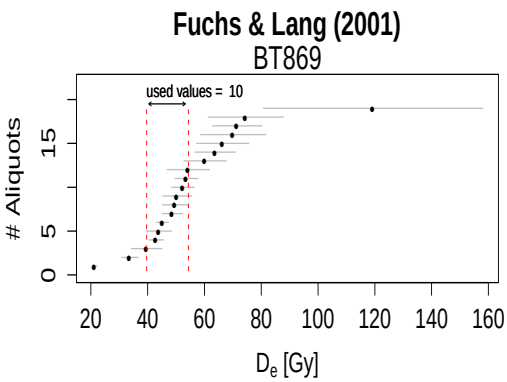

T2_P1_380

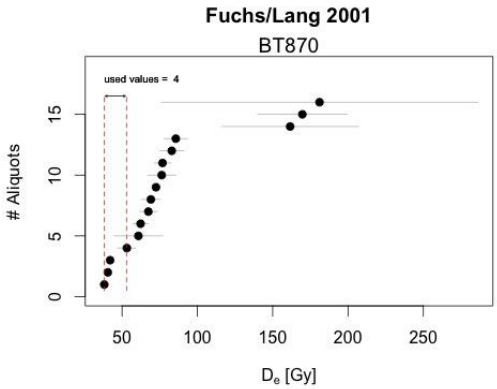

T2_P1_420

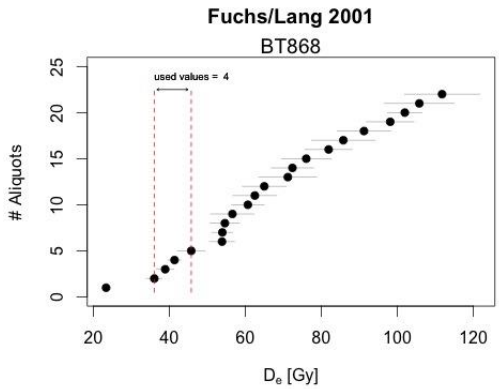

T1_P9_145

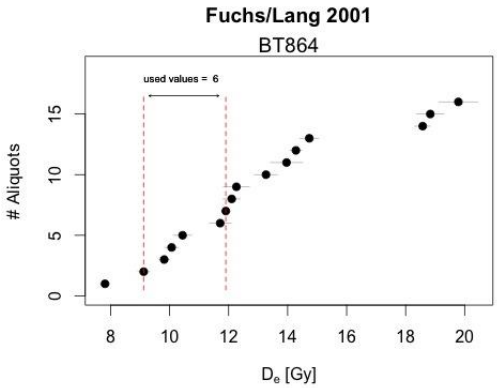

T1_P9_195

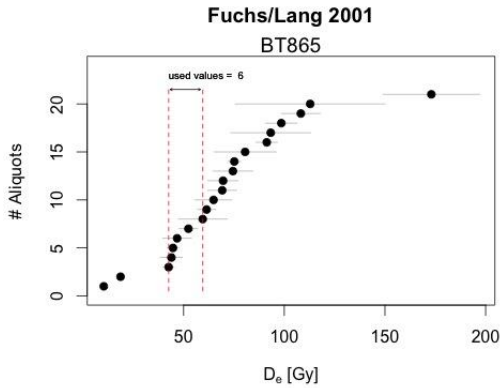

T1_P9_435

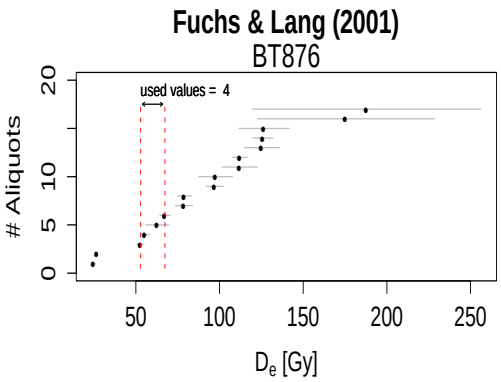

T1_P10_235

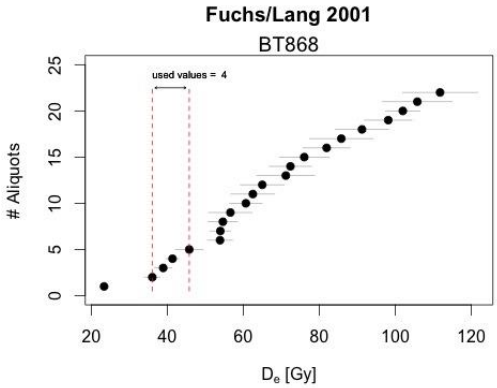

TE_P7_100

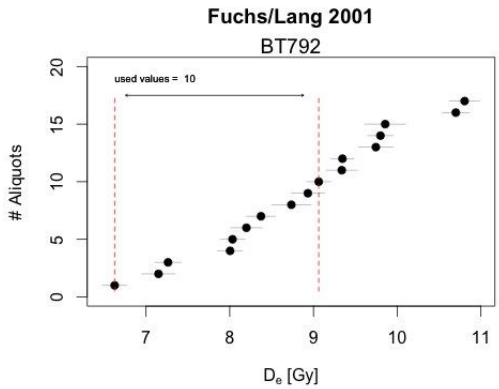

TE_P7_135

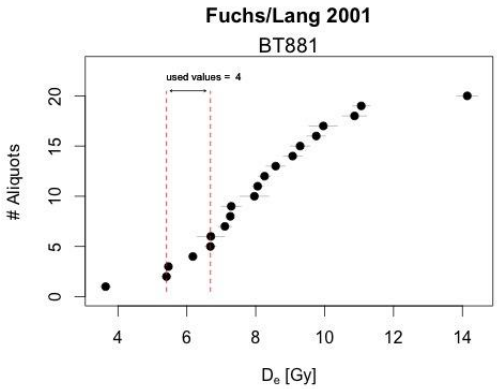

figures and calculations produced with Kreutzer et al 2012

TE_P8_110

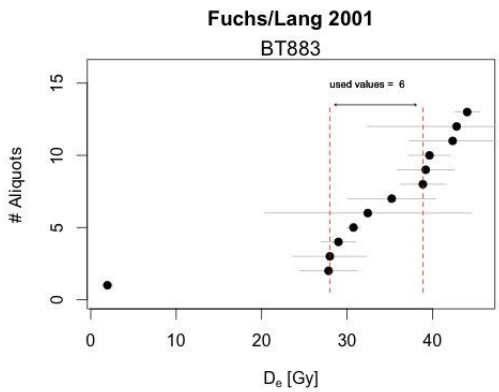

Moisture % (OSL Samples)	
Sample	**Moisture %**
T2_P1_200	**est 15%**
T2_P1_340	18.55%
T2_P1_380	20.03%
T2_P1_420	22.45%
T1_P9_145	11.41%
T1_P9_195	15.30%
T1_P9_395	15.70%
T1_P10_235	10.80%
TE_P7_100	10.68%
TE_P7_135	11.42%
TE_P7_270	23.40%
TE_P8_110	19.69%

APPENDIX D – ^{210}Pb Profiles

In the following section the XS ^{210}Pb profiles are presented. Including grain size measurements, density and CICCS deposition rate calculations.

^{210}Pb Profiles

Int. Err	Core	Depth (avg)	notes	Pb-210 DPM/g	dpm/g clay	dpm/g % < 2um	err	% Clay	%Silt	%Sand	% < 2um	notes	137Cs	Supported Background (dpm/g clay)	XS clay activity	Radon Ventillation Effect	XS Activity (CVC)
1	Cemetary	1		1.37	7.53	10.68	0.58	18.55	44.37	37.08	13.08		4.27	2.821675889	4.71	-0.79	5.49
1	Cemetary	3		1.57	6.90	9.02	0.43	23.22	43.90	32.88	17.76	na		2.448522752	4.45	-0.77	5.23
1	Cemetary	5		1.48	5.42	6.73	0.42	27.89	43.44	28.67	22.44		3.74	2.180844076	3.24	-0.76	4.00
1	Cemetary	7		1.34	4.89	6.84	0.38	28.00	42.56	29.44	20.01		1.98	2.175146473	2.72	-0.75	3.46
1	Cemetary	9		1.07	3.85	6.15	0.31	28.12	41.68	30.20	17.58		9.33	2.169487151	1.68	-0.74	2.42
1	Cemetary	11		0.82	3.09	3.85	0.25	26.93	42.30	30.78	21.61		3.23	2.229523533	0.86	-0.73	1.58
1	Cemetary	13		0.81	3.00	3.69	0.24	27.37	43.91	28.72	22.30		0.00	2.206708525	0.80	-0.71	1.51
1	Cemetary	15		0.70	2.63	3.26	0.21	26.57	44.69	28.74	21.42		0.00	2.248553342	0.38	-0.70	1.08
1	Cemetary	17		0.59	2.29	2.87	0.19	25.77	45.48	28.75	20.54		3.14	2.292510598	0.00	-0.69	0.69
1	Cemetary	19		0.59	2.28	2.83	0.19	25.98	44.80	29.22	20.98		0	2.28086605	0.00	-0.68	0.68
1	Cemetary	41		0.52	2.13	2.72	0.18	24.41	49.90	25.70	19.08		0	2.372532951	-0.25	-0.56	0.31
1	Cemetary	48		0.49	1.37	1.66	0.13	35.03	41.93	23.04	29.00		0.00	1.888263215	-0.51	-0.52	0.01

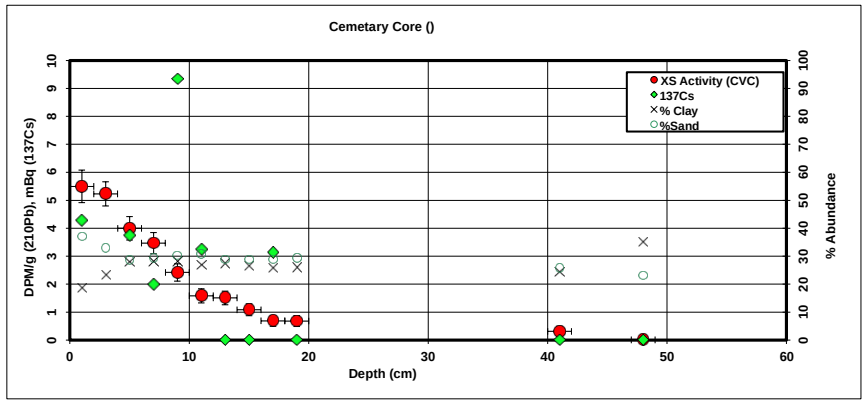

Avg. % Clay	Avg. Density
25.84	1.53

Likely to be higher bioturbation due to watering and mowing.

Found plastic buried at 20cm depth

Assumed Supported --> (DPM/ g clay)	0.00
Assumed Den (g/cc)	1.50
Assumed Area (tube cross-section)	3.70
Present activi	0.00
Confidence In	0.00
Original sedim	3.00
Background U	0.60
CIRCA Uncert	0.20
N/N_0	-0.25
S.E. (N/N_0)	-0.02
Predicted sed	#NUM!
S.E. (age)	#NUM!
minimum age	#NUM!
maximum age	#NUM!
Activity offset f	-1.5
Deposition dat	#NUM!

depth	Density (measured)	unsupported activity / g clay	US activity / gram	Trapazoidal Depth-Integration of (activity * volume * density)
0.00	1.89	5.49	1.02	
1.00	1.89	5.49	1.02	7.12
3.00	1.27	5.23	1.21	13.05
5.00	1.67	4.00	1.11	12.68
7.00	1.56	3.46	0.97	12.45
9.00	1.24	2.42	0.68	8.53
11.00	1.11	1.58	0.43	4.79
13.00	1.50	1.51	0.41	4.04
15.00	1.31	1.08	0.29	3.64
17.00	1.66	0.69	0.18	2.55
19.00	1.63	0.68	0.24	
41.00	1.66	0.31	0.00	
48.00	1.78	0.01	0.00	

68.85	--->	18.61
Total integrated US activity (integrated tube DPM)		(DPM/cm^2) US activity

collected Rolf Aalto analysed Mathias Will

^{210}Pb Profiles

Int. Err	Core	Depth (avg)	notes	Pb-210 DPM/g	dpm/g clay	dpm/g % < 2um	err	% Clay	%Silt	%Sand	% < 2um	notes
1	GL1	1		1.64	4.67		0.38	36.12				est
1	GL1	3		1.22	3.45	4.27	0.29	36.12	58.45	5.43	29.13	
1	GL1	5		1.17	4.23	5.86	0.35	28.35	61.57	10.09	20.49	
1	GL1	7		1.00	2.77	3.68	0.23	36.69	55.74	7.57	27.60	
1	GL1	9		0.89	2.41	3.09	0.21	37.27	56.27	6.46	29.04	
1	GL1	11		0.83	2.54	3.44	0.22	33.05	59.99	6.95	24.43	
1	GL1	21		0.57	2.04	2.75	0.18	27.63	60.91	11.46	20.52	
1	GL1	31		0.58	1.75	2.38	0.15	33.19	54.13	12.69	24.42	
1	GL1	41		0.61	1.82	2.45	0.16	33.52	51.06	15.42	24.93	
1	GL1	89		0.52	1.93	2.37	0.16	26.75	34.55	38.70	21.78	

Supported Background (dpm/g clay)	XS clay activity	Radon Ventillation Effect	XS Activity (CVC)
1.851973432	2.82	-0.79	3.61
1.851973432	1.59	-0.77	2.37
2.158452666	2.08	-0.76	2.84
1.833625984	0.93	-0.75	1.68
1.815654245	0.59	-0.74	1.33
1.958740792	0.58	-0.73	1.31
2.193630096	-0.16	-0.67	0.51
1.953762191	-0.20	-0.61	0.41
1.941368596	-0.12	-0.56	0.44
2.23889892	-0.31	-0.33	0.02

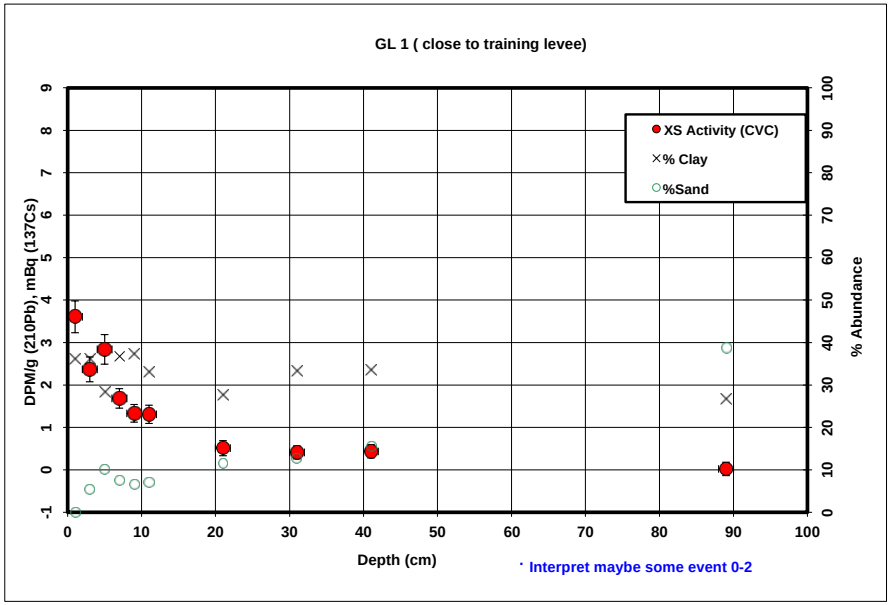

143.62	--->	38.82
Total integrated US activity (integrated tube DPM)		(DPM/cm^2) US activity
Assumed Mete (Atoms Pb-210/ M cm^2) (average 'shielded' rate of C18 & sites 41)	--->	17.76
US Activity fro (DPM/ cm^2)	--->	21.05
Input Sedimen (DPM / g clay) (from proximal grab samples)	--->	1.76
CICCS Accum (grams clay / cm^2 yr)	--->	0.37
CICCS Accum (grams / cm^2 yr)	--->	1.13
CICCS Accum (cm / yr)	--->	0.54

Avg. % Clay	Avg. Density
32.87	2.11

Assumed Supported -->	0.00
(DPM/ g clay)	
Assumed Den (g/cc)	1.50
Assumed Area (tube cross-section)	3.70

Present activi	0.34
Confidence In	0.05
Original sedim	1.76
Background US activity	
CIRCA Uncerta	0.20
N/N_o	0.19
S.E. (N/N_o)	0.04
Predicted sed	52.89
S.E. (age)	6.02
minimum age	47.41
maximum age	59.51
Activity offset f	-1.5
Deposition dat	1948.6

Present activity	
Confidence In	0.00
Original sedim	3.00
Background U	0.60
CIRCA Uncerta	0.20
N/N_o	-0.25
S.E. (N/N_o)	-0.02
Predicted sed	#NUM!
S.E. (age)	#NUM!
minimum age	#NUM!
maximum age	#NUM!
Activity offset f	-1.5
Deposition dat	#NUM!

	--->	
Additional 'cap' activity (integrated tube DPM)		(DPM/cm^2) Cap activity
Assumed Mete (Atoms Pb-210/ M cm^2) (average 'shielded' rate of C18 & sites 41)	--->	17.76
Growth time fo	--->	0
Activity offset from 2000		-2.5
Deposition date		2002.5

depth	Density (measured)	unsupported activity / g clay	US activity / gram	Trapazoidal Depth-Integration of (activity * volume * density)
0.00	1.67	3.61	1.30	
1.00	1.67	3.61	1.30	8.03
3.00	2.07	2.37	0.86	14.93
5.00	2.33	2.84	0.80	13.53
7.00	2.17	1.68	0.62	11.84
9.00	2.29	1.33	0.50	9.19
11.00	2.71	1.31	0.43	8.59
21.00	2.46	0.51	0.14	27.44
31.00	2.60	0.41	0.14	12.99
41.00	3.24	0.44	0.15	15.23
89.00	0.00	0.02	0.01	21.83

collected Rolf Aalto analysed Mathias Will

^{210}Pb Profiles

Int.	Err	Core	Depth (avg)	notes	Pb-210 DPM/g	dpm/g clay	dpm/g % < 2um	err	% Clay	%Silt	%Sand	% < 2um	notes
1	LSD	1 A	1	16.315 dpm at 5/9/	1.74	4.93	6.61	0.35	36.38	53.90	9.73	27.11	
1	LSD	1 A	3	0	1.73	5.01	6.72	0.32	34.84	44.16	21.00	25.95	
1	LSD	1 A	5	0	0.88	2.63	3.60	0.18	33.89	47.89	18.23	24.77	
1	LSD	1 A	7	0	0.70	2.04	2.68	0.14	34.52	41.45	24.04	26.25	
1	LSD	1 A	9	0	0.88	2.90	3.98	0.19	30.40	42.07	27.53	22.14	
1	LSD	1 A	11	0	0.69	1.82	2.28	0.13	38.15	42.76	19.09	30.41	
1	LSD	1 A	13	0	0.65	1.60	1.92	0.12	40.53	41.61	17.86	33.90	
1	LSD	1 A	15	0	0.62	1.69	2.07	0.13	36.64	41.51	21.85	29.90	
1	LSD	1 A	17	0	0.51	1.66	2.16	0.13	30.53	44.51	24.96	23.49	
1	LSD	1 A	19	0	0.68	2.29	2.97	0.17	29.81	41.59	28.60	22.99	
1	LSD	1 A	23	0	0.49	1.80	2.41	0.14	26.51	54.36	19.13	19.77	
1	LSD	1 A	29	0	0.53	1.62	2.04	0.12	31.93	51.27	16.80	25.31	
1	LSD	1 A	35	0	0.51	1.35	1.82	0.11	36.42	61.54	2.04	27.04	
1	LSD	1 A	41	0	0.50	2.06	2.52	0.16	24.42	18.72	56.86	19.93	
1	LSD	1 A	51	0	0.41	7.18	9.11	1.29	5.79	3.66	90.55	4.56	
1	LSD	1 A	61	0	0.40	5.33	6.59	0.76	7.56	5.55	86.89	6.12	
1	LSD	1 A	71	0	0.33	5.74	7.37	1.04	5.83	3.81	90.37	4.54	
1	LSD	1 A	85.5	0	0.47	3.03	3.67	0.26	15.36	16.64	67.99	12.69	
						1.82							
						0.259459718							

Supported Background (dpm/g clay)	XS clay activity	Radon Ventillation Effect	XS Activity (CVC)
1.843581489	3.08	-0.79	3.87
1.89464274	3.11	-0.77	3.89
1.928152633	0.70	-0.76	1.46
1.905773836	0.13	-0.75	0.88
2.065091623	0.83	-0.74	1.57
1.789069094	0.03	-0.73	0.76
1.721778103	-0.12	-0.71	0.59
1.835297105	-0.14	-0.70	0.56
2.059659689	-0.40	-0.69	0.29
2.090774464	0.20	-0.68	0.88
2.251517338	-0.46	-0.66	0.20
2.002088376	-0.38	-0.62	0.24
1.842236335	-0.49	-0.59	0.09
2.371952964	-0.32	-0.56	0.24
5.888426039	1.29	-0.51	1.80
4.974399486	0.36	-0.46	0.82
5.86491786	-0.13	-0.41	0.28
3.178714748	-0.14	-0.35	0.20

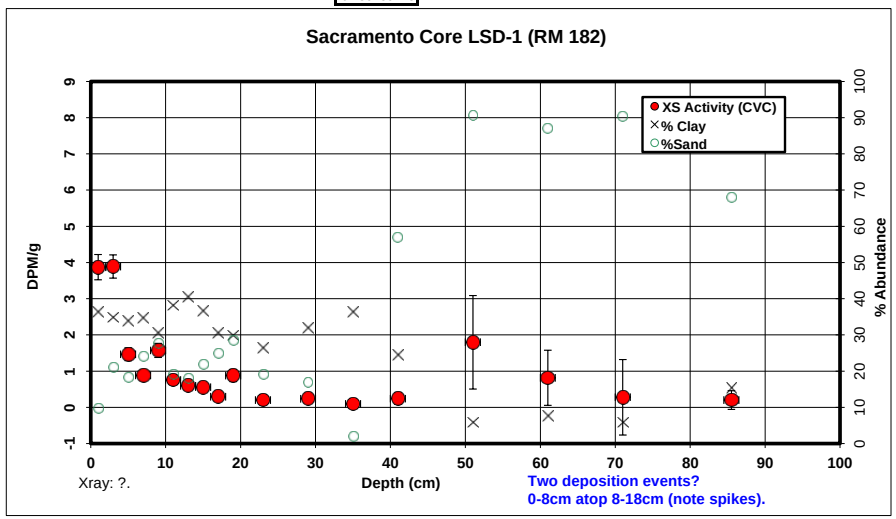

82.82	--->	22.39
Total integrated US activity (integrated tube DPM)		(DPM/cm^2) US activity
Assumed Mete (Atoms Pb-210/ M cm^2) (average 'shielded' rate of C18 & sites 41)	--->	17.76
US Activity fro (DPM/ cm^2)	--->	4.62
Input Sedimen (DPM / g clay) (from proximal grab samples)	--->	1.76
CICCS Accum (grams clay / cm^2 yr)	--->	0.08
CICCS Accum (grams / cm^2 yr)	--->	0.29
CICCS Accum (cm / yr)	--->	0.19

Avg. % Clay	Avg. Density
27.75	1.58

Assumed Supported -->	0.00
(DPM/ g clay)	
Assumed Den (g/cc)	1.50
Assumed Are (tube cross-section)	3.70

Present activi	0.20
Confidence In	0.05
Original sedin	1.76
Background US activity	
CIRCA Uncert	0.20
N/N_o	0.11
S.E. (N/N_o)	0.03
Predicted sed	69.97
S.E. (age)	8.98
minimum age	62.16
maximum age	80.29
Activity offset f	-1.5
Deposition dat	1931.5

	--->	22.39
Additional 'cap' activity (integrated tube DPM)		(DPM/cm^2) Cap activity
Assumed Mete (Atoms Pb-210/ M cm^2) (average 'shielded' rate of C18 & sites 41)	--->	17.76
Growth time fc	--->	#NUM!
Water year of sample		2002
Deposition date		#NUM!

depth	Density (measured)	unsupported activity / g clay	US activity / gram	Trapazoidal Depth-Integration of (activity * volume * density)
0.00	1.50	3.87	1.41	
1.00	1.50	3.87	1.41	7.81
3.00	1.07	3.89	1.35	13.11
5.00	1.50	1.46	0.50	8.79
7.00	1.50	0.88	0.30	4.44
9.00	1.95	1.57	0.48	4.99
11.00	1.50	0.76	0.29	4.89
13.00	1.50	0.59	0.24	2.94
15.00	1.50	0.56	0.20	2.47
17.00	1.50	0.29	0.09	1.63
19.00	1.81	0.88	0.26	2.15
23.00	2.09	0.20	0.05	4.53
29.00	2.21	0.24	0.08	3.08
35.00	1.92	0.09	0.03	2.54
41.00	1.90	0.24	0.06	1.97
51.00	2.72	1.80	0.10	6.94
61.00	1.50	0.82	0.06	6.47
71.00	1.50	0.28	0.02	2.16
85.50	1.50	0.20	0.03	1.90

collected and analysed Rolf Aalto

^{210}Pb Profiles

Int. Err	Core	Depth (avg)	notes	Pb-210 DPM/g	dpm/g clay	dpm/g % < 2um	err	% Clay	%Silt	%Sand	% < 2um	notes
1	LSD 2 A	1		1.56	3.56	4.93	0.40	44.89	43.64	11.47	32.43	
1	LSD 2 A	3		2.11	5.86	8.86	0.45	36.50	56.50	7.00	24.13	
1	LSD 2 A	5		1.30	3.23	4.92	0.27	41.03	51.23	7.73	26.98	
1	LSD 2 A	7		1.30	2.95	4.24	0.22	44.83	51.51	3.65	31.23	
1	LSD 2 A	9		1.26	3.54	5.17	0.24	35.80	62.68	1.52	24.52	
1	LSD 2 A	11		0.68	2.12	2.98	0.16	32.06	67.05	0.89	22.82	
1	LSD 2 A	13		0.57	1.75	2.28	0.14	32.47	63.90	3.63	25.00	
1	LSD 2 A	15		0.69	2.26	3.41	0.16	30.50	66.22	3.28	20.20	
1	LSD 2 A	17		0.76	1.89	2.74	0.14	40.29	58.22	1.49	27.79	
1	LSD 2 A	19		0.99	3.12	4.65	0.20	32.09	66.19	1.72	21.52	
1	LSD 2 A	23		0.62	1.60	2.16	0.13	38.06	56.29	5.65	28.25	
1	LSD 2 A	29		0.59	2.10	2.77	0.16	28.15	71.33	0.52	21.34	
1	LSD 2 A	35		0.55	1.52	2.07	0.11	35.60	59.50	4.90	26.20	
1	LSD 2 A	41		0.58	1.74	2.27	0.13	33.05	62.88	4.07	25.28	
1	LSD 2 A	51		0.67	2.12	2.85	0.15	31.74	65.48	2.78	23.67	
1	LSD 2 A	61		0.66	2.06	2.60	0.15	32.22	56.91	10.87	25.58	
1	LSD 2 A	71		0.56	1.82	2.41	0.14	30.91	51.19	17.89	23.32	
1	LSD 2 A	80		0.64	1.91	2.42	0.14	33.59	61.02	5.39	26.54	
					1.93							
					0.072598271							

Supported Background (dpm/g clay)	XS clay activity	Radon Ventillation Effect	XS Activity (CVC)
1.614197434	1.94	-0.79	2.73
1.839655211	4.02	-0.77	4.79
1.708468717	1.53	-0.76	2.29
1.615443895	1.34	-0.75	2.09
1.862442767	1.68	-0.74	2.42
1.996831315	0.12	-0.73	0.85
1.980758293	-0.23	-0.71	0.49
2.060780896	0.20	-0.70	0.90
1.728281957	0.16	-0.69	0.85
1.99572372	1.12	-0.68	1.80
1.791654215	-0.19	-0.66	0.46
2.16780194	-0.06	-0.62	0.56
1.868944658	-0.35	-0.59	0.24
1.958968698	-0.22	-0.56	0.34
2.009487889	0.11	-0.51	0.62
1.990544751	0.07	-0.46	0.53
2.043336564	-0.23	-0.41	0.18
1.938983226	-0.03	-0.37	0.34

Assumed Supported -->	0.00
(DPM/ g clay)	
Assumed Den	1.50
(g/cc)	
Assumed Area	3.70
(tube cross-section)	

Present activit	0.34
Confidence In	0.05
Original sedim	1.76
Background US activity	
CIRCA Uncert	0.20
N/N$_o$	0.19
S.E. (N/N$_o$)	0.04
Predicted sed	52.89
S.E. (age)	6.02
minimum age	47.41
maximum age	59.51
Activity offset f	-1.5
Deposition dat	1948.6

depth	Density (measured)	unsupported activity / g clay	US activity / gram	Trapazoidal Depth-Integration of (activity * volume * density)
0.00	1.50	2.73	1.23	
1.00	1.50	2.73	1.23	6.80
3.00	1.50	4.79	1.75	16.51
5.00	1.50	2.29	0.94	14.92
7.00	1.50	2.09	0.94	10.40
9.00	1.26	2.42	0.87	9.18
11.00	1.50	0.85	0.27	5.80
13.00	1.50	0.49	0.16	2.39
15.00	1.50	0.90	0.27	2.40
17.00	1.50	0.85	0.34	3.44
19.00	1.31	1.80	0.58	4.79
23.00	1.58	0.46	0.18	8.07
29.00	1.54	0.56	0.16	5.78
35.00	1.67	0.24	0.09	4.33
41.00	1.86	0.34	0.11	3.86
51.00	1.65	0.62	0.20	9.98
61.00	1.50	0.53	0.17	10.70
71.00	1.50	0.18	0.06	6.30
80.00	1.50	0.34	0.11	4.27

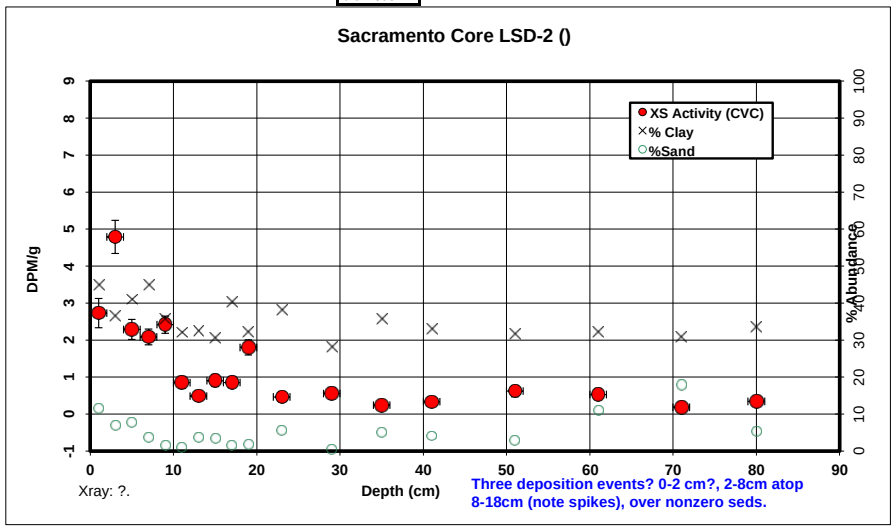

129.91	--->	35.11
Total integrated US activity (integrated tube DPM)		(DPM/cm^2) US activity
Assumed Mete	--->	17.76
(Atoms Pb-210/ M cm^2) (average 'shielded' rate of C18 & sites 41)		
US Activity fro	--->	17.35
(DPM/ cm^2)		
Input Sedimen	--->	1.76
(DPM / g clay) (from proximal grab samples)		
CICCS Accum	--->	0.31
(grams clay / cm^2 yr)		
CICCS Accum	--->	0.87
(grams / cm^2 yr)		
CICCS Accum	--->	0.59
(cm / yr)		

Avg. % Clay	Avg. Density
35.21	1.47

	--->	35.11
Additional 'cap' activity (integrated tube DPM)		(DPM/cm^2) Cap activity
Assumed Mete	--->	17.76
(Atoms Pb-210/ M cm^2) (average 'shielded' rate of C18 & sites 41)		
Growth time fc	--->	#NUM!
Water year of sample		2002
Deposition date		#NUM!

collected and analysed Rolf Aalto

^{210}Pb Profiles

Int. Err	Core	Depth (avg)	notes	Pb-210 DPM/g	dpm/g clay	dpm/g % < 2um	err	% Clay	%Silt	%Sand	% < 2um	notes	Supported Background (dpm/g clay)	XS clay activity	Radon Ventillation Effect	XS Activity (CVC)
1	LSD 3 A	1		1.29	3.78	5.36	0.28	35.05	55.50	9.46	24.71		1.887509816	1.89	-0.79	2.68
1	LSD 3 A	3		1.05	3.16	4.40	0.23	33.48	56.28	10.24	24.05		1.942908793	1.22	-0.77	1.99
1	LSD 3 A	5		0.77	1.95	2.56	0.13	39.86	51.55	8.58	30.25		1.740058004	0.21	-0.76	0.97
1	LSD 3 A	7		0.62	1.99	2.75	0.14	31.00	54.63	14.37	22.43		2.039827572	-0.05	-0.75	0.70
1	LSD 3 A	9		0.92	2.60	3.45	0.19	35.45	54.64	9.92	26.71		1.873998598	0.72	-0.74	1.46
1	LSD 3 A	11		0.61	1.81	2.51	0.13	33.59	56.22	10.20	24.20		1.938989052	-0.13	-0.73	0.60
1	LSD 3 A	13		0.61	1.55	2.02	0.11	38.72	51.75	9.52	29.77		1.772191694	-0.22	-0.71	0.49
1	LSD 3 A	15		0.62	1.83	2.50	0.13	33.48	52.15	14.37	24.53		1.942860253	-0.11	-0.70	0.59
1	LSD 3 A	17		0.66	1.61	1.99	0.12	40.71	46.47	12.82	32.87		1.716970082	-0.11	-0.69	0.58
1	LSD 3 A	19		0.74	2.19	3.09	0.16	33.76	56.99	9.26	24.00		1.932852155	0.26	-0.68	0.94
1	LSD 3 A	23		0.58	1.65	2.24	0.12	34.42	58.89	6.69	25.30		1.909219634	-0.26	-0.66	0.39
1	LSD 3 A	29		0.36	1.10	1.40	0.10	30.35	49.74	19.90	23.83		2.067085726	-0.97	-0.62	-0.35
1	LSD 3 A	35		0.37	1.17	1.47	0.10	29.41	61.86	8.73	23.26		2.108888805	-0.94	-0.59	-0.35
1	LSD 3 A	41		0.49	2.26	2.78	0.17	21.65	26.04	52.30	17.55		2.558918471	-0.30	-0.56	0.25
1	LSD 3 A	51		0.36	3.08	4.20	0.32	11.74	7.79	80.47	8.62		3.76776182	-0.68	-0.51	-0.18
1	LSD 3 A	61		0.41	3.68	4.56	0.39	11.16	7.57	81.27	9.02		3.89003311	-0.21	-0.46	0.25
1	LSD 3 A	71		0.31	4.72	6.32	0.79	6.47	2.82	90.71	4.83		5.488746225	-0.77	-0.41	-0.36
1	LSD 3 A	84		0.30	2.89	3.53	0.34	10.35	5.39	84.26	8.49		4.079688043	-1.19	-0.35	-0.84
					1.67											
					0.38723226											

Assumed Supported -->	0.00
(DPM/ g clay)	
Assumed Den	1.50
(g/cc)	
Assumed Area	3.70
(tube cross-section)	

Present activi	0.57
Confidence In	0.05
Original sedin	1.76
Background US activity	
CIRCA Uncert	0.20
N/N_o	0.32
S.E. (N/N_o)	0.05
Predicted sed	36.49
S.E. (age)	4.58
minimum age	32.22
maximum age	41.40
Activity offset f	-9.9
Deposition dat	1973.4

depth	Density (measured)	unsupported activity / g clay	US activity / gram	Trapazoidal Depth-Integration of (activity * volume * density)
0.00	1.50	2.68	0.94	
1.00	1.50	2.68	0.94	5.21
3.00	1.50	1.99	0.67	8.91
5.00	1.50	0.97	0.39	5.84
7.00	1.50	0.70	0.22	3.35
9.00	1.60	1.46	0.52	4.21
11.00	1.50	0.60	0.20	4.11
13.00	1.50	0.49	0.19	2.17
15.00	1.50	0.59	0.20	2.16
17.00	1.50	0.58	0.24	2.41
19.00	1.73	0.94	0.32	3.31
23.00	1.86	0.39	0.14	6.01
29.00	2.13	0.00	0.00	3.00
35.00	1.99	0.00	0.00	
41.00	2.48	0.25	0.05	
51.00	1.85	0.00	0.00	
61.00	1.50	0.25	0.03	
71.00	1.50	0.00	0.00	
84.00	1.50	0.00	0.00	

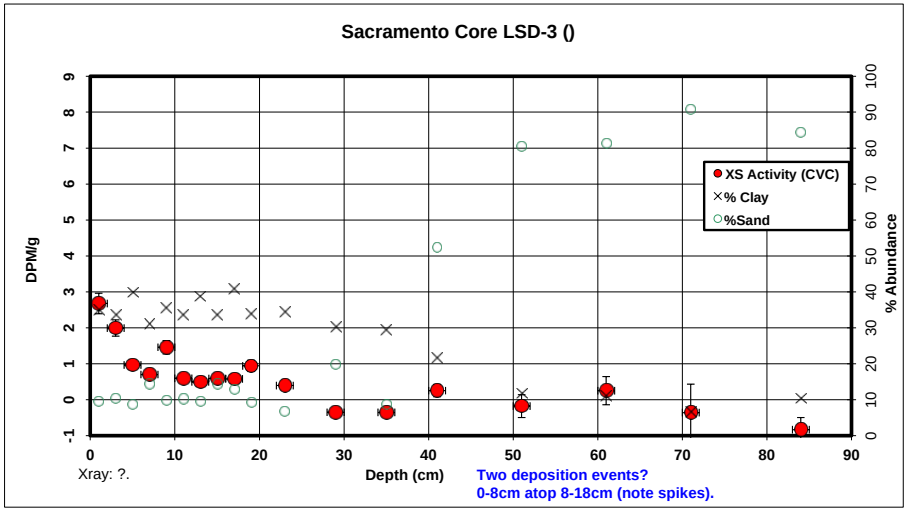

50.69	--->	13.70
Total integrated US activity (integrated tube DPM)		(DPM/cm^2) US activity
Assumed Mete	--->	17.76
(Atoms Pb-210/ M cm^2) (average 'shielded' rate of C18 & sites 41)		
US Activity fro	--->	-4.06
(DPM/ cm^2)		
Input Sedimen	--->	1.76
(DPM / g clay) (from proximal grab samples)		
CICCS Accum	--->	-0.07
(grams clay / cm^2 yr)		
CICCS Accum	--->	-0.25
(grams / cm^2 yr)		
CICCS Accum	--->	-0.16
(cm / yr)		

Avg. % Clay	Avg. Density
28.37	1.56

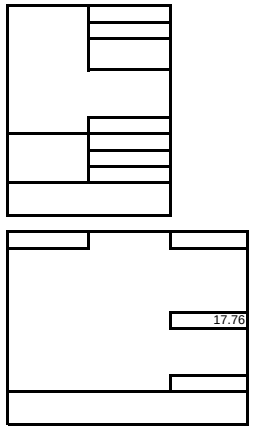

collected and analysed Rolf Aalto

^{210}Pb Profiles

Int. Err	Core	Depth (avg)	notes		Pb-210 DPM/g	dpm/g clay	dpm/g % < 2um	err	% Clay	%Silt	%Sand	% < 2um	notes	Supported Background (dpm/g clay)	XS clay activity	Radon Ventillation Effect	XS Activity (CVC)
1	lsd 4a	1		0	1.31	3.44	4.58	0.24	39.05	51.76	9.19	29.33		1.762860077	1.67	-0.79	2.46
1	lsd 4a	3		0	1.35	3.26	4.43	0.23	41.96	53.19	4.85	30.83		1.684557726	1.57	-0.77	2.35
1	lsd 4a	5		0	1.04	3.13	4.32	0.20	33.98	51.19	14.83	24.61		1.924667493	1.20	-0.76	1.96
1	lsd 4a	7		0	0.92	2.69	3.71	0.17	34.82	52.78	12.40	25.23		1.89526166	0.79	-0.75	1.54
1	lsd 4a	9		0	1.11	2.86	4.01	0.19	39.09	58.14	2.77	27.90		1.761808182	1.10	-0.74	1.84
1	lsd 4a	11		0	0.79	2.22	3.05	0.15	35.89	51.86	12.25	26.10		1.859434134	0.36	-0.73	1.08
1	lsd 4a	13		0	0.77	2.22	3.05	0.15	34.78	54.28	10.94	25.29		1.89671107	0.32	-0.71	1.03
1	lsd 4a	15		0	0.73	1.87	2.50	0.13	39.04	53.36	7.60	29.20		1.763135426	0.11	-0.70	0.81
1	lsd 4a	17		0	0.60	1.67	2.28	0.12	35.93	54.69	9.38	26.32		1.858066644	-0.18	-0.69	0.51
1	lsd 4a	19		0	0.73	1.80	2.48	0.14	40.63	56.68	2.69	29.58		1.719303647	0.09	-0.68	0.76
1	LSD-4A	23		0	0.54	1.30	1.78	0.10	40.43	55.62	3.95	29.58		1.724535011	-0.43	-0.66	0.23
1	LSD-4A	29		0	0.51	1.52	2.07	0.12	32.42	63.84	3.74	23.87		1.982853176	-0.46	-0.62	0.16
1	LSD-4A	35		0	0.44	1.45	1.84	0.12	29.08	62.94	7.98	22.90		2.123890607	-0.68	-0.59	-0.09
1	lsd 4a	41		0	0.47	1.56	2.01	0.13	29.86	64.79	5.35	23.19		2.088463852	-0.53	-0.56	0.03
1	lsd 4a	51		0	0.46	2.06	2.70	0.16	22.25	55.27	22.49	16.94		2.515615433	-0.46	-0.51	0.05
1	lsd 4a	61		0	0.44	2.30	2.95	0.18	19.08	27.40	53.52	14.90		2.771793683	-0.47	-0.46	-0.01
1	lsd 4a	71		0	0.42	2.62	3.30	0.22	16.14	21.66	62.20	12.82		3.080978558	-0.46	-0.41	-0.05
1	lsd 4a	84		0	0.50	2.49	3.16	0.19	20.14	36.75	43.11	15.84		2.679034275	-0.19	-0.35	0.16
						1.74											
						0.206321801											

Assumed Supported -->	0.00
(DPM/ g clay)	
Assumed Den	1.50
(g/cc)	
Assumed Area	3.70
(tube cross-section)	

Present activi	0.86
Confidence Interval	
Original sedin	1.76
Background US activity	
CIRCA Uncert	0.20
N/N_0	0.49
S.E. (N/N_0)	0.06
Predicted sed	23.08
S.E. (age)	3.67
minimum age	19.62
maximum age	26.97
Activity offset f	-9.9
Deposition dat	1986.8

depth	Density (measured)	unsupported activity / g clay	US activity / gram	Trapazoidal Depth-Integration of (activity * volume * density)
0.00	1.50	2.46	0.96	
1.00	1.50	2.46	0.96	5.33
3.00	1.50	2.35	0.98	10.80
5.00	1.50	1.96	0.67	9.17
7.00	1.50	1.54	0.54	6.68
9.00	1.40	1.84	0.72	6.72
11.00	1.50	1.08	0.39	5.93
13.00	1.50	1.03	0.36	4.15
15.00	1.50	0.81	0.32	3.75
17.00	1.50	0.51	0.18	2.76
19.00	1.50	0.76	0.31	2.73
23.00	1.69	0.23	0.09	4.75
29.00	1.87	0.16	0.05	2.87
35.00	1.83	0.00	0.00	1.08
41.00	1.97	0.03	0.01	
51.00	1.98	0.05	0.01	
61.00	1.50	0.00	0.00	
71.00	1.50	0.00	0.00	
84.00	1.50	0.16	0.03	

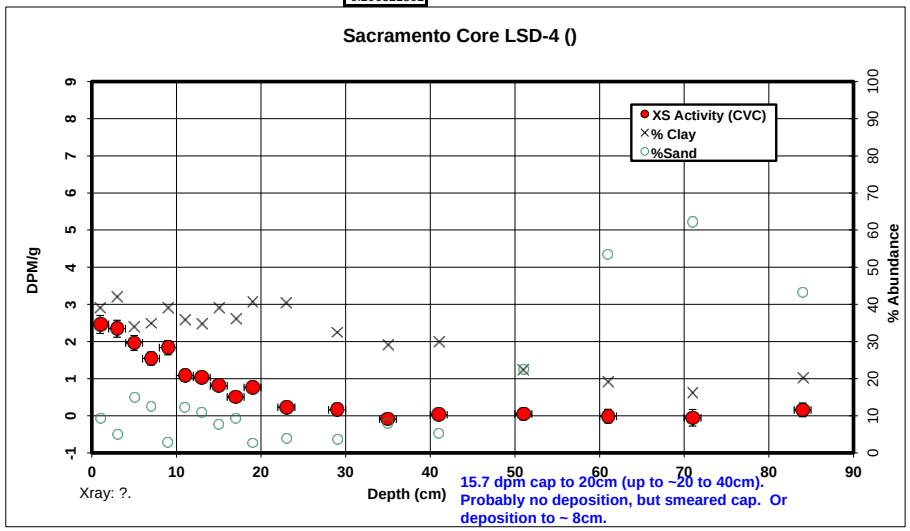

62.77	--->	16.97
Total integrated US activity (integrated tube DPM)		(DPM/cm^2) US activity
Assumed Mete	--->	17.76
(Atoms Pb-210/ M cm^2) (average 'shielded' rate of C18 & sites 41)		
US Activity fro	--->	-0.80
(DPM/ cm^2)		
Input Sedimen	--->	1.76
(DPM / g clay) (from proximal grab samples)		
CICCS Accum	--->	-0.01
(grams clay / cm^2 yr)		
CICCS Accum	--->	-0.04
(grams / cm^2 yr)		
CICCS Accum	--->	-0.03
(cm / yr)		

Avg. % Clay	Avg. Density
32.48	1.51

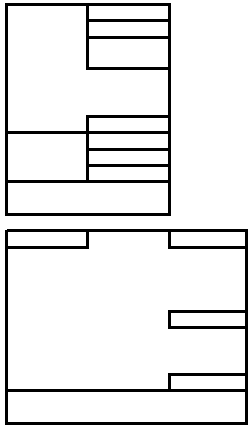

collected and analysed Rolf Aalto

^{210}Pb Profiles

Int. Err	Core	Depth (avg)	notes	Pb-210 DPM/g	dpm/g clay	dpm/g % < 2um	err	% Clay	%Silt	%Sand	% < 2um	notes
1	LSD5	1		2.18	9.41	13.15	0.91	23.94	71.02	5.04	17.13	
1	LSD5	3		2.62	7.46	9.71	0.73	36.30	60.23	3.46	27.91	
1	LSD5	5		2.28	7.17	9.71	0.58	32.88	65.50	1.62	24.29	
1	LSD5	7		1.67	4.66	6.21	0.39	36.86	64.28	-1.13	27.67	
1	LSD5	9		1.34	3.39	3.87	0.27	40.27	64.86	-5.13	35.34	
1	LSD5	11		1.35	3.40	4.59	0.28	40.76	58.94	0.30	30.18	
1	LSD5	21		0.92	2.54	3.14	0.21	36.47	62.09	1.44	29.50	
1	LSD5	31		0.67	1.97	2.53	0.18	34.11	64.39	1.50	26.50	
1	LSD5	41		0.91	2.45	3.25	0.20	37.48	63.94	-1.42	28.27	
1	LSD5	51		0.88	2.21	2.97	0.19	40.11	60.13	-0.23	29.85	
1	LSD5	61		0.71	2.01	2.60	0.17	35.57	65.23	-0.80	27.57	
1	LSD5	85.5		0.70	1.74	2.29	0.15	40.50	59.36	0.13	30.83	

Supported Background (dpm/g clay)	XS clay activity	Radon Ventillation Effect	XS Activity (CVC)
2.401468175	7.00	-0.79	7.79
1.846001837	5.62	-0.77	6.39
1.965172305	5.21	-0.76	5.97
1.828376153	2.83	-0.75	3.58
1.728840075	1.66	-0.74	2.40
1.715761762	1.68	-0.73	2.41
1.840717056	0.70	-0.67	1.37
1.920241208	0.05	-0.61	0.66
1.80920984	0.65	-0.56	1.20
1.733329107	0.47	-0.51	0.98
1.869899184	0.14	-0.46	0.60
1.722573177	0.02	-0.35	0.36

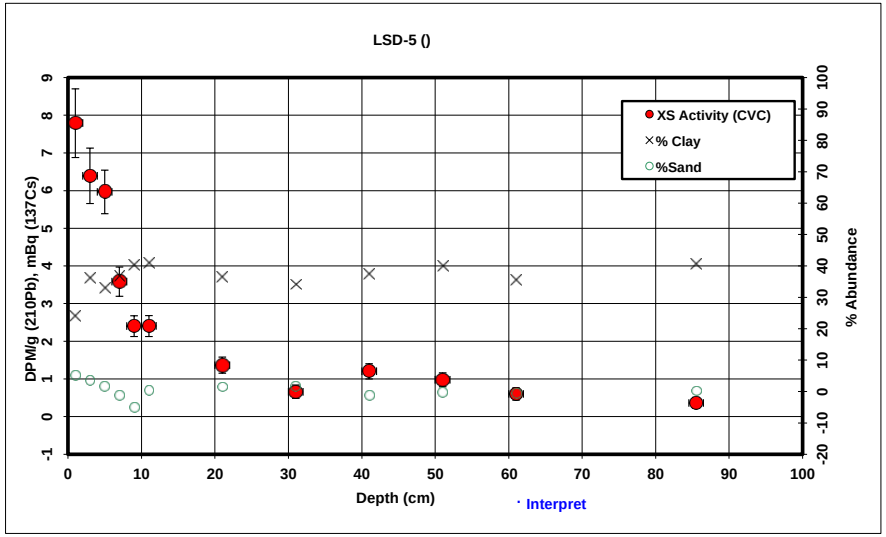

345.56	--->	93.40
Total integrated US activity (integrated tube DPM)		(DPM/cm^2) US activity
Assumed Mete (Atoms Pb-210/ M cm^2) (average 'shielded' rate of C18 & sites 41)	--->	17.76
US Activity fro (DPM/ cm^2)	--->	75.63
Input Sedimen (DPM / g clay) (from proximal grab samples)	--->	1.76
CICCS Accum (grams clay / cm^2 yr)	--->	1.34
CICCS Accum (grams / cm^2 yr)	--->	3.73
CICCS Accum (cm / yr)	--->	1.76

Avg. % Clay	Avg. Density
35.92	2.11

Assumed Supported --> (DPM/ g clay)		0.00
Assumed Den (g/cc)		1.50
Assumed Area (tube cross-section)		3.70
Present activit		0.36
Confidence In		0.00
Original sedim		1.76
Background US activity		
CIRCA Uncert		0.20
N/N_o		0.20
S.E. (N/N_o)		0.02
Predicted sed		51.06
S.E. (age)		3.67
minimum age		47.59
maximum age		54.94
Activity offset f		-9.9
Deposition dat		1958.8

Present activity		
Confidence In		0.00
Original sedim		3.00
Background U		0.60
CIRCA Uncert		0.20
N/N_o		-0.25
S.E. (N/N_o)		-0.02
Predicted sed		#NUM!
S.E. (age)		#NUM!
minimum age		#NUM!
maximum age		#NUM!
Activity offset f		-1.5
Deposition dat		#NUM!

	--->	
Additional 'cap' activity (integrated tube DPM)		(DPM/cm^2) Cap activity
Assumed Mete (Atoms Pb-210/ M cm^2) (average 'shielded' rate of C18 & sites 41)	--->	15.00
Growth time fc	--->	0
Activity offset from 2000		-2.5
Deposition date		2002.5

depth	Density (measured)	unsupported activity / g clay	US activity / gram	Trapazoidal Depth-Integration of (activity * volume * density)
0.00	1.50	7.79	1.87	
1.00	1.50	7.79	1.87	10.35
3.00	1.45	6.39	2.32	22.83
5.00	1.78	5.97	1.96	25.56
7.00	2.24	3.58	1.32	24.41
9.00	2.27	2.40	0.97	19.10
11.00	2.15	2.41	0.98	15.93
21.00	2.45	1.37	0.50	62.91
31.00	2.50	0.66	0.22	33.11
41.00	2.28	1.20	0.45	29.86
51.00	2.63	0.98	0.39	38.33
61.00	2.62	0.60	0.21	29.49
85.50	1.50	0.36	0.15	33.68

collected and analysed Rolf Aalto

Int. Err	Core	Depth (avg)	notes	Pb-210 DPM/g	dpm/g clay	dpm/g % < 2um	err	% Clay	%Silt	%Sand	% < 2um	notes
1	LSD6	1		1.60	3.60	4.64	0.34	45.42	52.39	2.19	35.26	
1	LSD6	3		1.85	5.04	6.84	0.47	37.79	59.97	2.24	27.82	
1	LSD6	5		1.52	3.65	5.18	0.36	42.59	50.71	6.70	30.00	
1	LSD6	7		1.72	4.56	5.97	0.37	38.67	58.10	3.23	29.55	
1	LSD6	9		1.18	2.96	3.79	0.24	40.73	59.22	0.05	31.81	
1	LSD6	11		1.21	2.86	3.64	0.23	43.01	57.02	-0.03	33.73	
1	LSD6	13		0.91	2.50	3.23	0.20	36.87	57.67	5.46	28.49	
1	LSD6	15		0.95	2.28	2.87	0.20	42.20	54.66	3.14	33.51	
1	LSD6	21		0.77	2.31	3.08	0.20	33.58	65.74	0.68	25.13	
1	LSD6	31		0.96	2.08	2.84	0.18	46.70	53.02	0.28	34.32	
1	LSD6	41		0.90	1.90	2.39	0.17	47.50	53.19	-0.69	37.73	
1	LSD6	66		0.76	1.57	2.02	0.14	48.50	52.14	-0.63	37.87	

Supported Background (dpm/g clay)	XS clay activity	Radon Ventillation Effect	XS Activity (CVC)
1.602212342	2.00	-0.79	**2.79**
1.799677179	3.24	-0.77	**4.01**
1.668639216	1.98	-0.76	**2.74**
1.773882191	2.79	-0.75	**3.54**
1.716419466	1.24	-0.74	**1.98**
1.658387249	1.20	-0.73	**1.92**
1.82805169	0.67	-0.71	**1.38**
1.678406763	0.60	-0.70	**1.30**
1.939364916	0.37	-0.67	**1.04**
1.574361902	0.51	-0.61	**1.12**
1.557628487	0.34	-0.56	**0.90**
1.537272632	0.04	-0.43	**0.47**

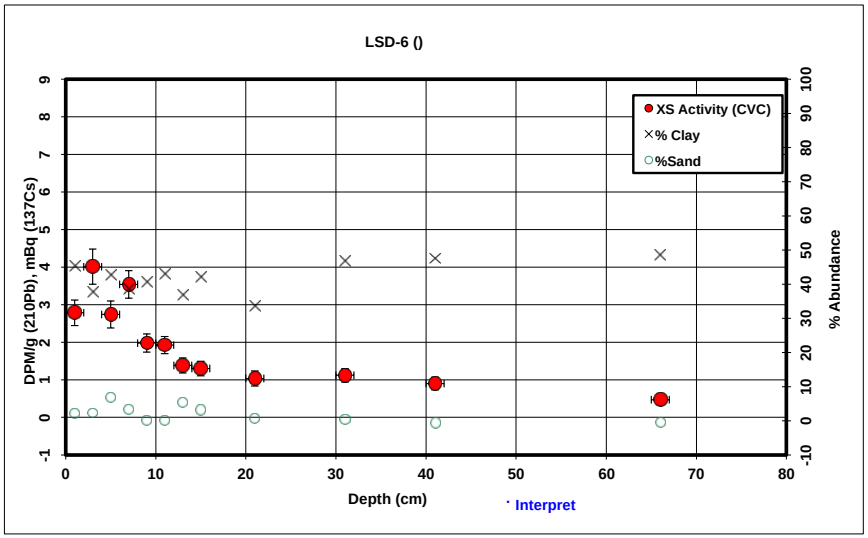

282.80	--->	76.43
Total integrated US activity (integrated tube DPM)		(DPM/cm^2) US activity
Assumed Mete (Atoms Pb-210/ M cm^2) (average 'shielded' rate of C18 & sites 41)	--->	17.76
US Activity fro (DPM/ cm^2)	--->	58.67
Input Sedimen (DPM / g clay) (from proximal grab samples)	--->	1.76
CICCS Accum (grams clay / cm^2 yr)	--->	1.04
CICCS Accum (grams / cm^2 yr)	--->	2.55
CICCS Accum (cm / yr)	--->	1.28

Avg. % Clay	Avg. Density
40.76	1.99

Assumed Supported --> (DPM/ g clay)		0.00
Assumed Den (g/cc)		1.50
Assumed Area (tube cross-section)		3.70

Present activi	0.47
Confidence In	0.00
Original sedim	1.76
Background US activity	
CIRCA Uncerta	0.20
N/N_o	0.27
S.E. (N/N_o)	0.03
Predicted sed	**42.48**
S.E. (age)	**3.67**
minimum age	39.02
maximum age	46.36
Activity offset f	-9.9
Deposition dat	**1967.4**

Present activity	
Confidence In	0.00
Original sedim	3.00
Background U	0.60
CIRCA Uncerta	0.20
N/N_o	-0.25
S.E. (N/N_o)	-0.02
Predicted sed	**#NUM!**
S.E. (age)	**#NUM!**
minimum age	#NUM!
maximum age	#NUM!
Activity offset f	-1.5
Deposition dat	**#NUM!**

	--->	
Additional 'cap' activity (integrated tube DPM)		(DPM/cm^2) Cap activity
Assumed Mete (Atoms Pb-210/ M cm^2) (average 'shielded' rate of C18 & sites 41)	--->	15.00
Growth time fo	--->	0
Activity offset from 2000		-2.5
Deposition date		**2002.5**

depth	Density (measured)	unsupported activity / g clay	US activity / gram	Trapazoidal Depth-Integration of (activity * volume * density)
0.00	1.28	2.79	1.27	
1.00	1.28	2.79	1.27	5.99
3.00	1.50	4.01	1.52	14.30
5.00	1.50	2.74	1.17	14.89
7.00	1.70	3.54	1.37	15.01
9.00	2.12	1.98	0.81	15.34
11.00	2.08	1.92	0.83	12.67
13.00	2.03	1.38	0.51	10.17
15.00	2.14	1.30	0.55	8.18
21.00	2.33	1.04	0.35	22.28
31.00	2.57	1.12	0.52	39.46
41.00	3.31	0.90	0.43	51.65
66.00	1.50	0.47	0.23	72.88

collected and analysed Rolf Aalto

^{210}Pb Profiles

Int.	Err	Core	Depth (avg)	notes	Pb-210 DPM/g	dpm/g clay	dpm/g % < 2um	err	% Clay	%Silt	%Sand	% < 2um	notes
1		lsf 1	1	x	3.13	8.58	10.24	0.58	36.86	43.27	19.86	30.89	
1		lsf 1	3		1.51	3.57	4.30	0.22	42.36	45.62	12.02	35.24	
1		lsf 2	5	x	0.82	1.78	2.10	0.13	46.21	45.48	8.32	39.01	
1		lsf 2	7		0.95	2.19	2.59	0.15	43.30	43.65	13.04	36.61	
1		lsf 3	9		0.65	1.40	1.68	0.11	46.12	45.57	8.30	38.51	
1		lsf 3	11	x	0.49	0.88	1.01	0.09	54.97	38.28	6.75	47.84	
1		lsf 4	13		0.33	0.56	0.63	0.07	59.01	34.80	6.19	52.63	
1		lsf 5	19		0.33	0.53	0.58	0.07	61.95	32.13	5.92	55.79	
1		lsf 6	31		0.34	0.56	0.63	0.08	58.98	35.08	5.94	52.77	
1		lsf 7	41		0.59	0.97	1.09	0.09	60.45	33.56	5.99	54.10	
1		lsf 8	48		0.38	1.57	2.23	0.12	23.77	67.65	8.59	16.77	

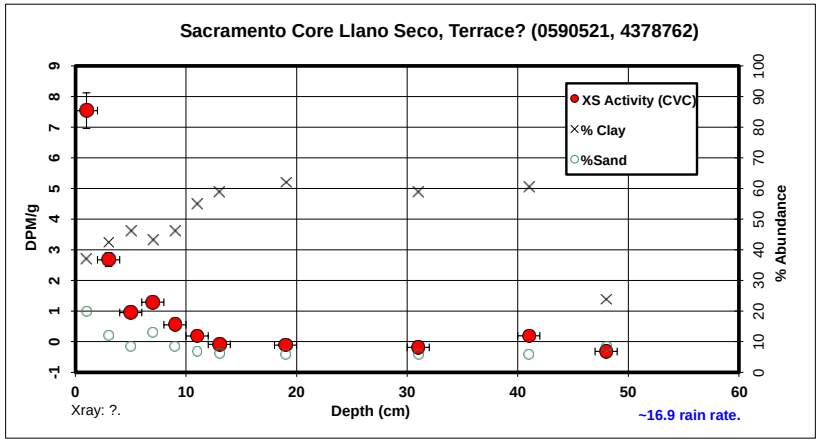

Supported Background (dpm/g clay)	XS clay activity	Radon Ventillation Effect	XS Activity (CVC)
1.828215686	6.75	-0.79	**7.54**
1.674363542	1.90	-0.77	**2.67**
1.584909677	0.19	-0.76	**0.95**
1.651296007	0.54	-0.75	**1.29**
1.586739513	-0.19	-0.74	**0.55**
1.420160161	-0.54	-0.73	**0.19**
1.358009715	-0.80	-0.71	**-0.09**
1.316821784	-0.79	-0.68	**-0.11**
1.358468411	-0.79	-0.61	**-0.18**
1.337432076	-0.37	-0.56	**0.19**
2.412653829	-0.84	-0.52	**-0.32**

Note: location is dry so likely to be underestimate

Assumed Supported --> (DPM/ g clay)	0.00
Assumed Den (g/cc)	1.50
Assumed Area (tube cross-section)	3.70

Avg. % Clay	Avg. Density
48.54	1.70

depth	Density (measured)	unsupported activity / g clay	US activity / gram	Trapazoidal Depth-Integration of (activity * volume * density)
0.00	1.50	7.65	2.82	
1.00	1.50	7.65	2.82	15.64
3.00	1.56	2.78	1.18	22.60
5.00	1.34	1.06	0.49	8.92
7.00	1.57	1.39	0.60	5.87
9.00	1.52	0.66	0.30	5.18
11.00	1.70	0.29	0.16	2.77
13.00	2.00	0.02	0.01	1.19
19.00	1.89	0.00	0.00	0.25
31.00	2.00	0.00	0.00	
41.00	2.02	0.30	0.18	
48.00	1.81	0.00	0.00	

62.42 ---> 16.87

Total integrated US activ (DPM/cm^2)

(integrated tube DPM) US activity

collected and analysed Rolf Aalto

^{210}Pb Profiles

Int. Err	Core	Depth (avg)	notes	Pb-210 DPM/g	dpm/g clay	dpm/g % < 2um	err	% Clay	%Silt	%Sand	% < 2um	notes	Supported Background (dpm/g clay)	XS clay activity	Radon Ventillation Effect	XS Activity (CVC)
1	lsl 1	1		0.64	2.98	3.66	0.19	21.50	46.01	32.49	17.55		2.570325586	0.41	-0.79	1.20
1	lsl 1	3		0.93	3.76	4.72	0.25	24.81	56.40	18.79	19.78		2.348017689	1.42	-0.77	2.19
1	lsl 1	5		0.38	3.73	4.82	0.42	10.14	28.56	61.30	7.84		4.133228427	-0.41	-0.76	0.36
1	lsl 1	7		0.29	9.69	11.68	3.28	2.99	4.37	92.64	2.48	2 - low conc	8.942810945	0.74	-0.75	1.49
1	lsl 1	9		0.40	5.94	7.52	0.94	6.72	5.04	88.24	5.31		5.361575471	0.58	-0.74	1.32
1	lsl 1	11		0.32	13.95	18.96	6.13	2.29	4.11	93.60	1.68	1 - low conc	10.59099189	3.36	-0.73	4.09
1	lsl 1	13		0.30	12.94	14.90	5.52	2.36	1.98	95.66	2.05	2 - low conc	10.39616692	2.54	-0.71	3.25
1	lsl 1	15		0.32	18.97	26.29	11.08	1.72	2.88	95.40	1.24	1 - low conc	12.69294001	6.28	-0.70	6.98
1	lsl 1	17		0.26	8.09	9.68	2.61	3.14	2.60	94.26	2.63	2 - low conc	8.663605942	-0.58	-0.69	0.11
1	lsl 1	19		0.35	6.22	7.57	1.14	5.71	4.30	90.00	4.69		5.945101453	0.28	-0.68	0.96
1	LSL-1	23	core-depths approx	0.35	1.98	2.37	0.17	16.93	31.08	51.99	14.15		2.989815428	-1.01	-0.66	-0.35
1	LSL-1	29	core-depths approx	0.49	2.82	3.52	0.21	17.18	64.71	18.11	13.78		2.962344946	-0.14	-0.62	0.48
1	LSL-1	35	core-depths approx	0.51	2.75	3.39	0.20	18.56	65.98	15.46	15.08		2.820874767	-0.07	-0.59	0.52
1	lsl 1	41		0.64	3.82	4.88	0.29	16.70	27.94	55.36	13.08		3.016033337	0.81	-0.56	1.36
1	lsl 1	51		0.36	3.52	4.12	0.41	10.29	4.32	85.39	8.79	Re-run	4.09465786	-0.58	-0.51	-0.07
1	lsl 1	61		0.55	3.19	3.99	0.24	17.17	30.66	52.17	13.73		2.963090828	0.23	-0.46	0.68
1	lsl 1	65		0.23	3.70	4.24	0.67	6.11	2.35	91.53	5.33	Re-run	5.691280102	-1.99	-0.44	-1.56
1	lsl 1	71		0.27	4.94	5.62	0.99	5.34	2.03	92.63	4.69	Re-run	6.198120894	-1.26	-0.41	-0.85

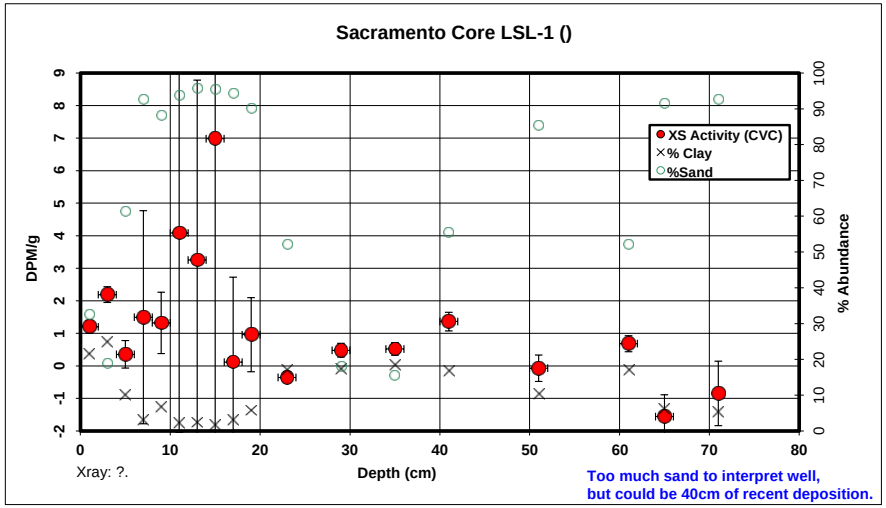

35.55	--->	9.61
Total integrated tube DPM)	US activity (integrated	(DPM/cm^2) US activity
Assumed Mete (Atoms Pb-210/ M cm^2) (average 'shielded' rate of C18 & sites 41)	--->	17.76
US Activity fro (DPM/ cm^2)	--->	-8.16
Input Sedimen (DPM / g clay) (from proximal grab samples)	--->	1.76
CICCS Accum (grams clay / cm^2 yr)	--->	-0.14
CICCS Accum (grams / cm^2 yr)	--->	-1.37
CICCS Accum (cm / yr)	--->	-0.91

Avg. % Clay	Avg. Density
10.54	1.50

Assumed Supported --> (DPM/ g clay)	0.00
Assumed Den (g/cc)	1.50
Assumed Area (tube cross-section)	3.70

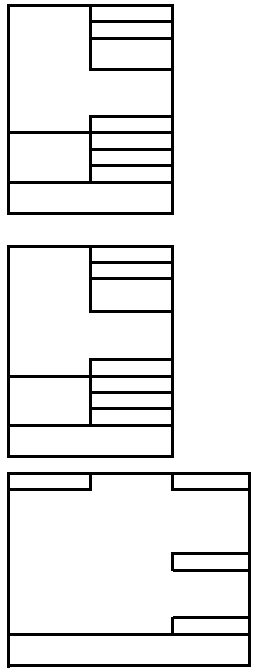

depth	Density (measured)	unsupported activity / g clay	US activity / gram	Trapazoidal Depth-Integration of (activity * volume * density)
0.00	1.50	1.20	0.26	
1.00	1.50	1.20	0.26	1.43
3.00	1.50	2.19	0.54	4.45
5.00	1.50	0.36	0.04	3.21
7.00	1.50	1.49	0.04	0.45
9.00	1.50	1.32	0.09	0.74
11.00	1.50	4.09	0.09	1.01
13.00	1.50	3.25	0.08	0.94
15.00	1.50	6.98	0.12	1.09
17.00	1.50	0.11	0.00	0.69
19.00	1.50	0.96	0.05	0.32
23.00	1.50	0.00	0.00	0.61
29.00	1.50	0.48	0.08	1.37
35.00	1.50	0.52	0.10	2.98
41.00	1.50	1.36	0.23	5.39
51.00	1.50	0.00	0.00	6.31
61.00	1.50	0.68	0.12	3.25
65.00	1.50	0.00	0.00	1.30
71.00	1.50	0.00	0.00	0.00

collected and analysed Rolf Aalto

^{210}Pb Profiles

Int. Err	Core	Depth (avg)	notes	Pb-210 DPM/g	dpm/g clay	dpm/g % < 2um	err	% Clay	%Silt	%Sand	% < 2um	notes	Supported Background (dpm/g clay)	XS clay activity	Radon Ventillation Effect	XS Activity (CVC)
1	lsl2a	1		1.44	5.17	7.03	0.36	28.68	45.42	25.90	21.08		2.14270831	3.03	-0.79	**3.81**
1	lsl 2a	3		1.06	4.12	5.43	0.29	26.01	51.06	22.92	19.73		2.278841439	1.84	-0.77	**2.61**
1	lsl2a	5		0.84	3.83	4.94	0.26	22.32	40.30	37.38	17.32		2.510027255	1.32	-0.76	**2.08**
1	lsl2a	7		1.08	3.88	4.99	0.30	28.29	49.75	21.96	22.01		2.161167496	1.72	-0.75	**2.47**
1	lsl 2a	9		1.16	3.74	5.09	0.25	31.17	59.05	9.79	22.91		2.032722604	1.71	-0.74	**2.45**
1	lsl2a	11		0.79	3.02	3.67	0.20	26.54	36.13	37.33	21.87	2 - rerun	2.24998378	0.77	-0.73	**1.50**
1	lsl2a	13		0.40	2.92	3.68	0.27	13.60	23.76	62.65	10.81		3.433966327	-0.51	-0.71	**0.20**
1	lsl2a	15		0.50	2.32	2.83	0.16	21.49	39.65	38.86	17.64		2.57106154	-0.25	-0.70	**0.45**
1	lsl2a	17		0.45	2.16	2.75	0.16	20.82	51.46	27.72	16.37		2.623540958	-0.46	-0.69	**0.23**
1	lsl 2a	19		0.47	2.27	2.96	0.17	20.84	32.67	46.49	15.97		2.621339149	-0.35	-0.68	**0.32**
1	LSL-2A	23	core-depths approx	0.47	1.67	2.06	0.13	26.95	60.02	13.02	21.88		2.228277688	-0.56	-0.66	**0.10**
1	LSL-2A	29	core-depths approx	0.52	1.69	2.14	0.13	30.19	58.54	11.27	23.81		2.073937525	-0.39	-0.62	**0.24**
1	LSL-2A	35	core-depths approx	0.48	1.69	2.05	0.12	27.27	61.96	10.77	22.48		2.211975716	-0.52	-0.59	**0.07**
1	lsl 2a	41		0.53	2.34	3.19	0.18	22.37	55.98	21.65	16.45		2.506850324	-0.16	-0.56	**0.39**
1	lsl 2a	51		0.19	0.81	1.07	0.10	22.28	48.91	28.80	16.82	averaged	2.512877877	-1.70	-0.51	**-1.20**
1	lsl 2a	61		0.29	1.29	1.67	0.12	22.20	41.84	35.96	17.18	averaged	2.518942998	-1.22	-0.46	**-0.77**
1	lsl 2a	71		0.49	2.23	2.75	0.17	22.03	27.70	50.27	17.90		2.531187463	-0.30	-0.41	**0.11**
1	lsl 2a	80		0.28	1.25	1.58	0.12	22.12	34.77	43.11	17.54	averaged	2.525046065	-1.27	-0.37	**-0.90**

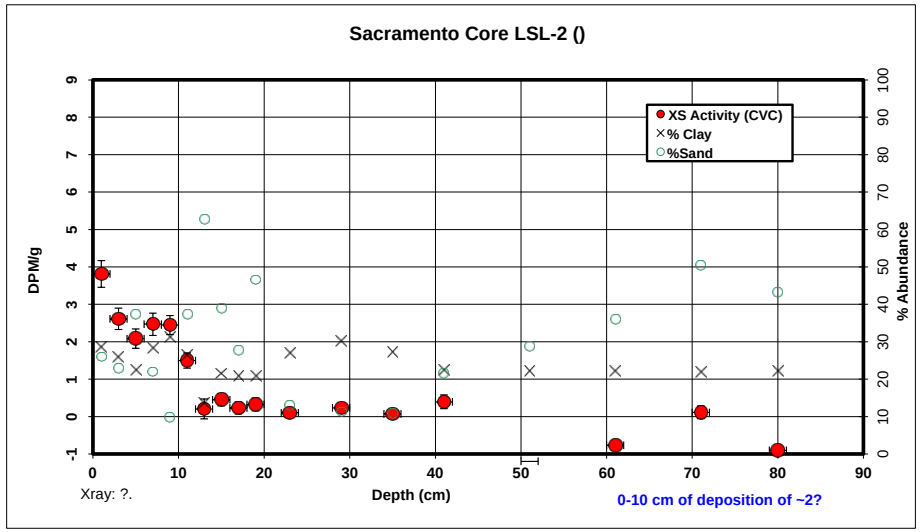

45.48	--->	12.29
Total integrated US activity (integrated tube DPM)		(DPM/cm^2) US activity
Assumed Mete	--->	17.76
(Atoms Pb-210/ M cm^2) (average 'shielded' rate of C18 & sites 41)		
US Activity fro	--->	-5.47
(DPM/ cm^2)		
Input Sedimen	--->	1.76
(DPM / g clay) (from proximal grab samples)		
CICCS Accum	--->	-0.10
(grams clay / cm^2 yr)		
CICCS Accum	--->	-0.40
(grams / cm^2 yr)		
CICCS Accum	--->	-0.27
(cm / yr)		

Avg. % Clay	Avg. Density
24.18	1.46

Assumed Supported --> (DPM/ g clay)		0.00
Assumed Den (g/cc)		1.50
Assumed Area (tube cross-section)		3.70

	--->	12.29
Additional 'cap' activity (integrated tube DPM)		(DPM/cm^2) Cap activity
Assumed Mete	--->	17.76
(Atoms Pb-210/ M cm^2) (average 'shielded' rate of C18 & sites 41)		
Growth time fc	--->	37.8755048
Activity offset from 2000		-9.9
Deposition date		1972.0

depth	Density (measured)	unsupported activity / g clay	US activity / gram	Trapazoidal Depth-Integration of (activity * volume * density)
0.00	1.50	3.81	1.09	
1.00	1.50	3.81	1.09	6.07
3.00	1.18	2.61	0.68	8.80
5.00	1.50	2.08	0.47	5.69
7.00	1.50	2.47	0.70	6.46
9.00	1.14	2.45	0.76	7.12
11.00	1.50	1.50	0.40	5.66
13.00	1.50	0.20	0.03	2.36
15.00	1.50	0.45	0.10	0.69
17.00	1.50	0.23	0.05	0.80
19.00	1.75	0.32	0.07	0.69
23.00	1.50	0.10	0.03	1.13
29.00	2.53	0.24	0.07	
35.00	1.89	0.07	0.02	
41.00	1.81	0.39	0.09	
51.00	2.35	0.00	0.00	
61.00	1.50	0.00	0.00	
71.00	1.50	0.11	0.02	
80.00	1.50	0.00	0.00	

collected and analysed Rolf Aalto

^{210}Pb Profiles

Int. Err	Core	Depth (avg)	notes	Pb-210 DPM/g	dpm/g clay	dpm/g % < 2um	err	% Clay	%Silt	%Sand	% < 2um	notes
1	LSL_3A	1		1.28	3.21		0.27	40.00		0.86		est
1	LSL_3A	3		1.20	3.01		0.27	40.00		0.74		est
1	LSL_3A	5		1.43	3.59		0.25	40.00		1.50		est
1	LSL_3A	7		1.09	2.72		0.20	40.00		0.43		est
1	LSL_3A	9		0.80	2.01		0.16	40.00		1.22		est
1	LSL_3A	11		0.62	1.45	1.74	0.14	42.87	54.78	2.35	35.60	
1	LSL_3A	21		0.33	3.82	4.72	0.36	8.60	4.89	86.50	6.96	
1	LSL_3A	31		0.35	2.59	2.97	0.23	13.32	6.53	80.15	11.61	
1	LSL_3A	41		0.57	1.58	1.92	0.14	36.12	59.52	4.36	29.84	

Supported Background (dpm/g clay)	XS clay activity	Radon Ventillation Effect	XS Activity (CVC)
1.736244671	1.48	-0.79	**2.26**
1.736244671	1.27	-0.77	**2.05**
1.736244671	1.86	-0.76	**2.62**
1.736244671	0.98	-0.75	**1.73**
1.736244671	0.27	-0.74	**1.01**
1.661745077	-0.21	-0.73	**0.51**
4.585876398	-0.77	-0.67	**-0.10**
3.479276084	-0.89	-0.61	**-0.28**
1.85190136	-0.27	-0.56	**0.29**

Assumed Supported -->	0.00
(DPM/ g clay)	
Assumed Den	1.50
(g/cc)	
Assumed Area	3.70
(tube cross-section)	

depth	Density (measured)	unsupported activity / g clay	US activity / gram	Trapazoidal Depth-Integration of (activity * volume * density)
0.00	1.03	2.26	0.91	
1.00	1.03	2.26	0.91	3.45
3.00	1.19	2.05	0.82	7.09
5.00	1.32	2.62	1.05	8.68
7.00	1.30	1.73	0.69	8.43
9.00	1.40	1.01	0.40	5.46
11.00	2.13	0.51	0.22	4.06
21.00	2.04	0.00	0.00	
31.00	1.50	0.00	0.00	
41.00	1.37	0.29	0.10	

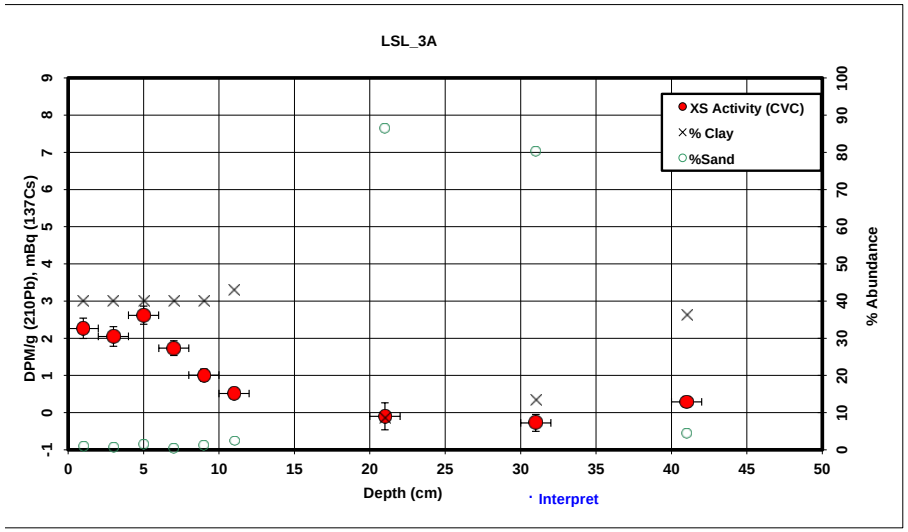

37.18	--->	10.05
Total integrated US activity (integrated tube DPM)		(DPM/cm^2) US activity
Assumed Mete (Atoms Pb-210/ M cm^2) (average 'shielded' rate of C18 & sites 41)	--->	17.76
US Activity fro (DPM/ cm^2)	--->	-7.71
Input Sedimen (DPM / g clay) (from proximal grab samples)	--->	1.76
CICCS Accum (grams clay / cm^2 yr)	--->	-0.14
CICCS Accum (grams / cm^2 yr)	--->	-0.41
CICCS Accum (cm / yr)	--->	-0.29

Avg. % Clay	Avg. Density
33.43	1.43

Present activity	
Confidence In	0.00
Original sedin	3.00
Background U	0.60
CIRCA Uncert	0.20
N/N_0	-0.25
S.E. (N/N_0)	-0.02
Predicted sed	#NUM!
S.E. (age)	#NUM!
minimum age	#NUM!
maximum age	#NUM!
Activity offset f	-1.5
Deposition dat	#NUM!

	--->	10.05
Additional 'cap' activity (integrated tube DPM)		(DPM/cm^2) Cap activity
Assumed Mete (Atoms Pb-210/ M cm^2) (average 'shielded' rate of C18 & sites 41)	--->	17.76
Growth time fc	--->	26.8343638
Activity offset from 2000		-9.9
Deposition date		1983.1

collected Rolf Aalto analysed Mathias Will

^{210}Pb Profiles

Int. Err	Core	Depth (avg)	notes	Pb-210 DPM/g	dpm/g clay	dpm/g % < 2um	err	% Clay	%Silt	%Sand	% < 2um	notes
1	LSL_4A	1		1.73	3.73	4.93	0.35	46.61	48.40	4.99	35.25	
1	LSL_4A	3		1.86	4.36	5.75	0.42	42.80	51.66	5.54	32.46	
1	LSL_4A	5		1.34	3.21	4.02	0.31	41.76	52.17	6.07	33.34	
1	LSL_4A	7		0.71	2.24	2.76	0.20	31.62	39.45	28.92	25.62	
1	LSL_4A	9		0.57	1.91	2.30	0.17	29.68	33.79	36.53	24.58	
1	LSL_4A	11		0.53	1.91	2.24	0.17	27.55	33.94	38.50	23.48	
1	LSL_4A	21		0.32	1.69	1.97	0.17	18.62	22.54	58.84	15.99	
1	LSL_4A	31		0.41	1.38	1.66	0.13	29.43	55.48	15.09	24.54	
1	LSL_4A	41		0.39	1.60	1.93	0.15	24.12	33.07	42.81	19.97	

Supported Background (dpm/g clay)	XS clay activity	Radon Ventillation Effect	XS Activity (CVC)
1.576372055	2.15	-0.79	**2.94**
1.663529375	2.70	-0.77	**3.47**
1.689554707	1.52	-0.76	**2.28**
2.014217228	0.22	-0.75	**0.97**
2.096426832	-0.19	-0.74	**0.55**
2.197420749	-0.29	-0.73	**0.44**
2.81499925	-1.12	-0.67	**-0.46**
2.107923677	-0.73	-0.61	**-0.11**
2.390247859	-0.79	-0.56	**-0.24**

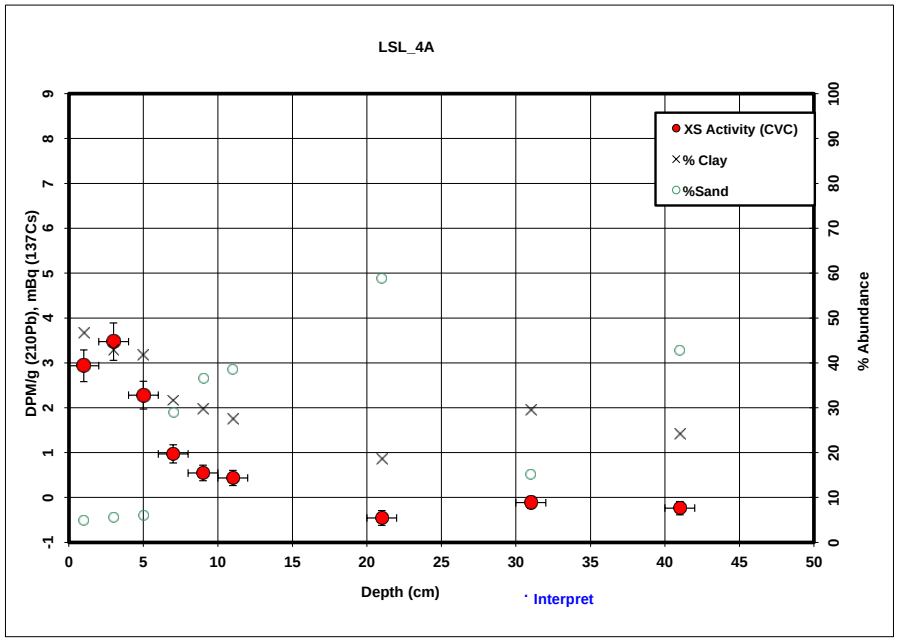

43.56	--->	11.77
Total integrated US activity (integrated tube DPM)		(DPM/cm^2) US activity
Assumed Mete	--->	17.76
(Atoms Pb-210/ M cm^2) (average 'shielded' rate of C18 & sites 41)		
US Activity fro	--->	-5.99
(DPM/ cm^2)		
Input Sedimen	--->	1.76
(DPM / g clay) (from proximal grab samples)		
CICCS Accum	--->	-0.11
(grams clay / cm^2 yr)		
CICCS Accum	--->	-0.33
(grams / cm^2 yr)		
CICCS Accum	--->	-0.20
(cm / yr)		

Avg. % Clay	Avg. Density
32.47	1.64

Assumed Supported -->	0.00
(DPM/ g clay)	
Assumed Den	1.50
(g/cc)	
Assumed Area	3.70
(tube cross-section)	

Present activity	
Confidence In	0.00
Original sedim	3.00
Background U	0.60
CIRCA Uncert	0.20
N/N_o	-0.25
S.E. (N/N_o)	-0.02
Predicted sed	#NUM!
S.E. (age)	#NUM!
minimum age	#NUM!
maximum age	#NUM!
Activity offset f	-1.5
Deposition dat	#NUM!

Present activity	
Confidence In	0.00
Original sedim	3.00
Background U	0.60
CIRCA Uncert	0.20
N/N_o	-0.25
S.E. (N/N_o)	-0.02
Predicted sed	#NUM!
S.E. (age)	#NUM!
minimum age	#NUM!
maximum age	#NUM!
Activity offset f	-1.5
Deposition dat	#NUM!

	--->	11.77
Additional 'cap' activity (integrated tube DPM)		(DPM/cm^2) Cap activity
Assumed Mete	--->	15.00
(Atoms Pb-210/ M cm^2) (average 'shielded' rate of C18 & sites 41)		
Growth time fc	--->	49.4209983
Activity offset from 2000		-2.5
Deposition date		1953.1

depth	Density (measured)	unsupported activity / g clay	US activity / gram	Trapazoidal Depth-Integration of (activity * volume * density)
0.00	1.50	2.94	1.37	
1.00	1.50	2.94	1.37	7.60
3.00	1.03	3.47	1.49	13.36
5.00	1.37	2.28	0.95	10.84
7.00	1.54	0.97	0.31	6.79
9.00	1.72	0.55	0.16	2.83
11.00	2.38	0.44	0.12	2.14
21.00	1.79	0.00	0.00	
31.00	1.91	0.00	0.00	
41.00	1.76	0.00	0.00	

collected Rolf Aalto analysed Mathias Will

^{210}Pb Profiles

Int. Err	Core	Depth (avg)	notes		Pb-210 DPM/g	dpm/g clay	dpm/g % < 2um	err	% Clay	%Silt	%Sand	% < 2um	notes
1	M_0	1		0	4.82	9.19		0.74	55.0				est
1	M_0	3		0	3.08	5.85		0.47	55.0				est
1	M_0	5	big stone		0.64	1.16		0.12	55.0				est
1	M_0	7	big stone		0.29	0.53		0.07	55.0				est
1	M_0	9	big stone		0.37	0.67		0.08	55.0				est
1	M_0	11	big stone		0.34	0.62		0.08	55.0				est
1	M_0	13	big stone		0.40	0.72		0.08	55.0				est
1	M_0	15.25	big stone		0.31	0.56		0.08	55.0				est

Supported Background (dpm/g clay)	XS clay activity	Radon Ventillation Effect	XS Activity (CVC)
1.419723008	7.77	-0.79	**8.56**
1.419723008	4.43	-0.77	**5.20**
1.419723008	-0.26	-0.76	**0.50**
1.419723008	-0.89	-0.75	**-0.14**
1.419723008	-0.75	-0.74	**-0.01**
1.419723008	-0.80	-0.73	**-0.07**
1.419723008	-0.70	-0.71	**0.02**
1.419723008	-0.86	-0.70	**-0.16**

Assumed Supported -->	0.00	
(DPM/ g clay)		
Assumed Den	1.50	
(g/cc)		
Assumed Area	3.70	
(tube cross-section)		

depth	Density (measured)	unsupported activity / g clay	US activity / gram	Trapazoidal Depth-Integration of (activity * volume * density)
0.00	1.50	8.56	4.71	
1.00	1.50	8.56	4.71	26.13
3.00	1.13	5.20	2.86	36.77
5.00	1.90	0.50	0.28	17.58
7.00	1.75	0.00	0.00	1.87
9.00	2.07	0.00	0.00	
11.00	1.82	0.00	0.00	
13.00	2.15	0.02	0.01	
15.25	1.50	0.00	0.00	

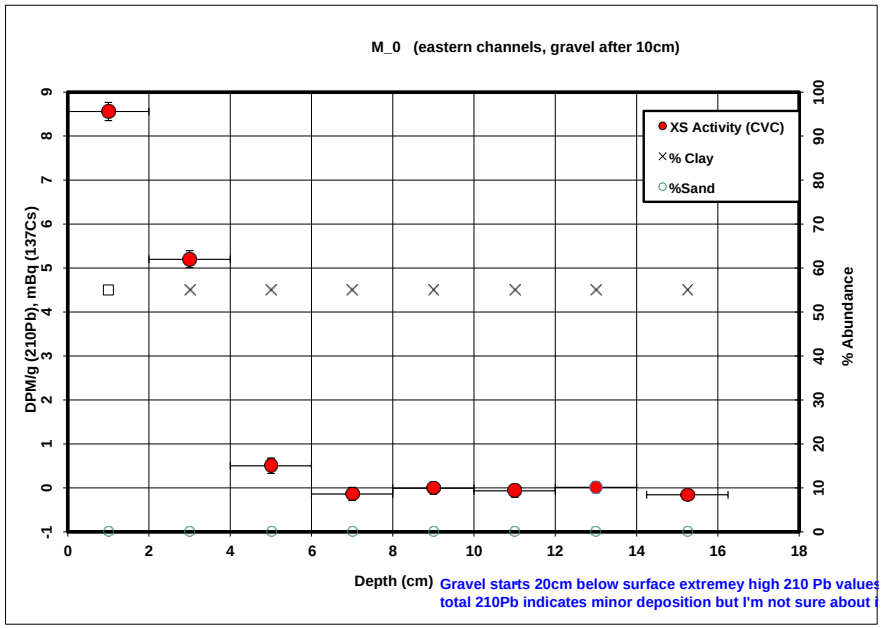

82.35	--->	22.26
Total integrated tube DPM)	US activity	(DPM/cm^2) US activity
Assumed Mete	--->	17.76
(Atoms Pb-210/ M cm^2)		
(average 'shielded' rate of C18 & sites 41)		
US Activity fro	--->	4.49
(DPM/ cm^2)		
Input Sedimen	--->	1.76
(DPM / g clay)		
(from proximal grab samples)		
CICCS Accum	--->	0.08
(grams clay / cm^2 yr)		
CICCS Accum	--->	0.14
(grams / cm^2 yr)		
CICCS Accum	--->	0.08
(cm / yr)		

Avg. % Clay	Avg. Density
55.00	1.70

Present activity		
Confidence In	#REF!	
Original sedim	3.00	
Background U	0.60	
CIRCA Uncert	0.20	
N/N_o	-0.25	
S.E. (N/N_o)	#REF!	
Predicted sed	#NUM!	
S.E. (age)	#NUM!	
minimum age	#REF!	
maximum age	#REF!	
Activity offset f	-1.5	
Deposition dat	#NUM!	

Present activity		
Confidence In	0.00	
Original sedim	3.00	
Background U	0.60	
CIRCA Uncert	0.20	
N/N_o	-0.25	
S.E. (N/N_o)	-0.02	
Predicted sed	#NUM!	
S.E. (age)	#NUM!	
minimum age	#NUM!	
maximum age	#NUM!	
Activity offset f	-1.5	
Deposition dat	#NUM!	

	--->	22.26
Additional 'cap' activity		(DPM/cm^2)
(integrated tube DPM)		Cap activity
Assumed Mete	--->	17.76
(Atoms Pb-210/ M cm^2)		
(average 'shielded' rate of C18 & sites 41)		
Growth time fc	--->	#NUM!
Activity offset from 2000		-2.5
Deposition date		#NUM!

collected Rolf Aalto analysed Mathias Will

^{210}Pb Profiles

Int. Err	Core	Depth (avg)	notes	Pb-210 DPM/g	dpm/g clay	dpm/g % < 2um	err	% Clay	%Silt	%Sand	% < 2um	notes
1	M_1	1		1.07	2.10	2.41	0.21	51.13				AVG
1	M_1	3		1.02	2.00	2.31	0.17	51.13	25.78	23.08	44.44	
1	M_1	5	big quarz 0.5cm	0.94	1.82	2.10	0.16	51.39	25.91	22.70	44.66	
1	M_1	7		0.64	1.26	1.45	0.12	51.13	25.78	23.08	44.44	
1	M_1	9		0.48	0.90	1.02	0.10	52.68	26.89	20.43	46.84	
1	M_1	11		0.53	1.09	1.24	0.11	48.79	23.73	27.47	42.68	
1	M_1	15	small stones	0.55	0.97		0.11	51.69				AVG
1	M_1	21		0.58	1.07	0.95	0.11	54.60	31.51	13.89	61.68	
1	M_1	31		0.57	0.86	0.92	0.09	66.10	15.58	18.32	61.81	
1	M_1	41		0.81	1.20	1.29	0.11	67.50	17.47	15.03	62.67	
1.15	M_1	51.15	big stones in clay	0.72	1.20	1.28	0.12	60.16	12.99	26.85	56.00	

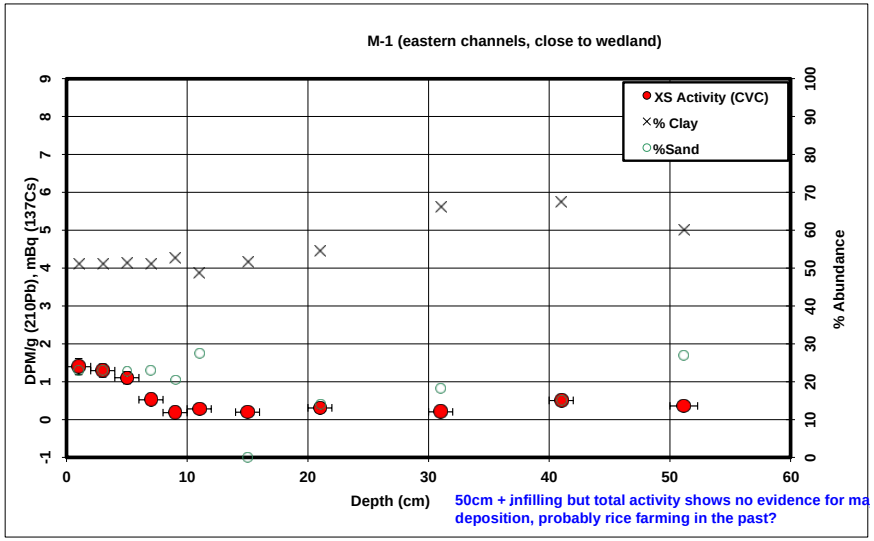

Supported Background (dpm/g clay)	XS clay activity	Radon Ventillation Effect	XS Activity (CVC)
1.486653443	0.61	-0.79	1.40
1.486653443	0.52	-0.77	1.29
1.482020839	0.34	-0.76	1.10
1.486653443	-0.23	-0.75	0.52
1.459011679	-0.55	-0.74	0.18
1.531357226	-0.45	-0.73	0.28
1.476437318	-0.51	-0.70	0.20
1.426330831	-0.36	-0.67	0.31
1.264023118	-0.41	-0.61	0.21
1.247362995	-0.05	-0.56	0.51
1.341442301	-0.15	-0.50	0.36

68.93	--->	18.63
Total integrated US activity (integrated tube DPM)		(DPM/cm^2) US activity
Assumed Mete	--->	17.76
(Atoms Pb-210/ M cm^2)		
(average 'shielded' rate of C18 & sites 41)		
US Activity fro	--->	0.87
(DPM/ cm^2)		
Input Sedimen	--->	1.76
(DPM / g clay)		
(from proximal grab samples)		
CICCS Accum	--->	0.02
(grams clay / cm^2 yr)		
CICCS Accum	--->	0.03
(grams / cm^2 yr)		
CICCS Accum	--->	0.02
(cm / yr)		

Avg. % Clay	Avg. Density
55.12	1.49

Assumed Supported -->	0.00
(DPM/ g clay)	
Assumed Den	1.50
(g/cc)	
Assumed Area	3.70
(tube cross-section)	

Present activity	
Confidence In	0.00
Original sedim	3.00
Background U	0.60
CIRCA Uncert	0.20
N/N_o	-0.25
S.E. (N/N_o)	-0.02
Predicted sed	#NUM!
S.E. (age)	#NUM!
minimum age	#NUM!
maximum age	#NUM!
Activity offset f	-1.5
Deposition dat	#NUM!

Present activity	
Confidence In	0.00
Original sedim	3.00
Background U	0.60
CIRCA Uncert	0.20
N/N_o	-0.25
S.E. (N/N_o)	-0.02
Predicted sed	#NUM!
S.E. (age)	#NUM!
minimum age	#NUM!
maximum age	#NUM!
Activity offset f	-1.5
Deposition dat	#NUM!

	--->	
Additional 'cap' activity (integrated tube DPM)		(DPM/cm^2) Cap activity
Assumed Mete	--->	17.76
(Atoms Pb-210/ M cm^2)		
(average 'shielded' rate of C18 & sites 41)		
Growth time fc	--->	0
Activity offset from 2000		-2.5
Deposition date		2002.5

depth	Density (measured)	unsupported activity / g clay	US activity / gram	Trapazoidal Depth-Integration of (activity * volume * density)
0.00	1.09	1.40	0.71	
1.00	1.09	1.40	0.71	2.88
3.00	1.28	1.29	0.66	6.02
5.00	1.37	1.10	0.57	6.02
7.00	1.86	0.52	0.27	4.99
9.00	1.63	0.18	0.17	2.82
11.00	1.51	0.28	0.17	1.97
15.00	1.50	0.20	0.17	3.77
21.00	1.65	0.31	0.17	5.90
31.00	1.77	0.21	0.14	9.62
41.00	1.62	0.51	0.34	14.95
51.15	1.50	0.36	0.00	9.99

collected Rolf Aalto analysed Mathias Will

^{210}Pb Profiles

Int. Err	Core	Depth (avg)	notes		Pb-210 DPM/g	dpm/g clay	dpm/g % < 2um	err	% Clay	%Silt	%Sand	% < 2um	notes
1	M2	1		0	1.84	3.85	4.61	0.36	47.94	48.28	3.78	39.97	AVG
1	M2	3		0	1.87	3.92	4.71	0.32	47.75				AVG
1	M2	5		0	1.26	2.63	3.16	0.22	47.75				AVG
1	M2	7	big stone 1.5cm		1.21	2.54	3.04	0.21	47.75	48.08	4.17	39.81	
1	M2	9		0	0.82	1.63	1.91	0.15	50.25	45.58	4.16	42.81	
1	M2	11	big stone 1cm		0.81	1.70	2.07	0.15	47.37	49.24	3.40	39.00	
1	M2	13		0	0.59	1.30		0.13	47.00	47.88	1.20		AVG
1	M2	15		0	0.60	1.33		0.13	47.00	46.52	0.78		AVG
1	M2	17		0	0.52	1.14		0.11	47.00	45.17	0.32		AVG
1	M2	21		0	0.45	0.83	0.97	0.09	53.68	43.81	2.51	45.88	
1	M2	31		0	0.46	0.81	0.96	0.09	56.45	42.70	0.85	47.90	
1	M2	41		0	0.47	0.85	1.00	0.09	55.15	44.30	0.55	46.45	
1	M2	76.5		0	0.59	0.96	1.10	0.10	61.94	36.25	1.81	53.71	

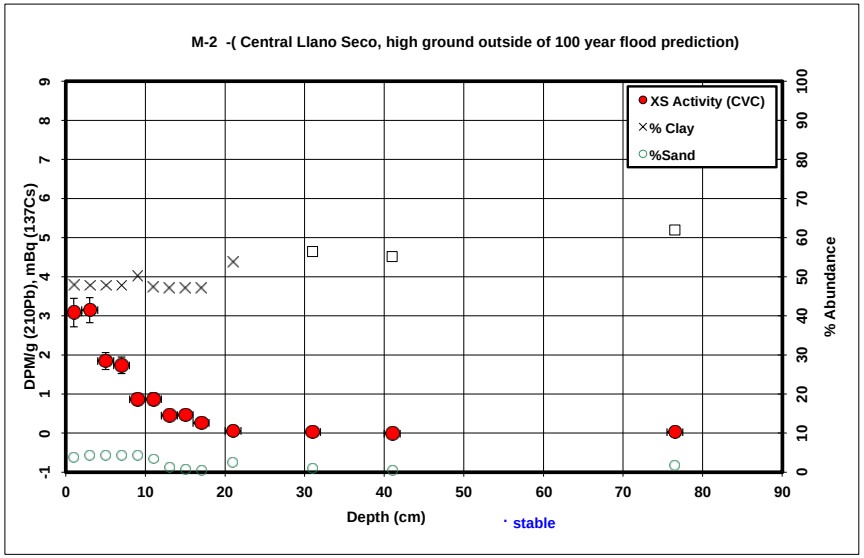

Supported Background (dpm/g clay)	XS clay activity	Radon Ventillation Effect	XS Activity (CVC)
1.548437656	2.30	-0.79	**3.08**
1.552445344	2.37	-0.77	**3.14**
1.552445344	1.08	-0.76	**1.84**
1.552445344	0.98	-0.75	**1.73**
1.503047493	0.13	-0.74	**0.86**
1.560342414	0.14	-0.73	**0.87**
1.568003378	-0.27	-0.71	**0.45**
1.568003378	-0.24	-0.70	**0.46**
1.568003378	-0.43	-0.69	**0.26**
1.441737799	-0.61	-0.67	**0.06**
1.396565233	-0.58	-0.61	**0.03**
1.417281355	-0.57	-0.56	**-0.01**
1.317038315	-0.36	-0.38	**0.02**

64.50	--->	17.43
Total integrated US activity (integrated tube DPM)		(DPM/cm^2) US activity
Assumed Mete (Atoms Pb-210/ M cm^2) (average 'shielded' rate of C18 & sites 41)	--->	17.76
US Activity fro (DPM/ cm^2)	--->	-0.33
Input Sedimen (DPM / g clay) (from proximal grab samples)	--->	1.76
CICCS Accum (grams clay / cm^2 yr)	--->	-0.01
CICCS Accum (grams / cm^2 yr)	--->	-0.01
CICCS Accum (cm / yr)	--->	-0.01

Avg. % Clay	Avg. Density
50.54	1.51

Assumed Supported --> (DPM/ g clay)	0.00
Assumed Den (g/cc)	1.20
Assumed Area (tube cross-section)	3.70

Present activity	
Confidence In	0.00
Original sedim	3.00
Background U	0.60
CIRCA Uncert	0.20
N/N_o	-0.25
S.E. (N/N_o)	-0.02
Predicted sed	#NUM!
S.E. (age)	#NUM!
minimum age	#NUM!
maximum age	#NUM!
Activity offset f	-1.5
Deposition dat	#NUM!

Present activity	
Confidence In	#REF!
Original sedim	3.00
Background U	0.60
CIRCA Uncert	0.20
N/N_o	-0.25
S.E. (N/N_o)	#REF!
Predicted sed	#NUM!
S.E. (age)	#NUM!
minimum age	#REF!
maximum age	#REF!
Activity offset f	-1.5
Deposition dat	#NUM!

	--->	17.43
Additional 'cap' activity (integrated tube DPM)		(DPM/cm^2) Cap activity
Assumed Mete (Atoms Pb-210/ M cm^2) (average 'shielded' rate of C18 & sites 41)	--->	17.76
Growth time fc	--->	128.091297
Activity offset from 2000		-2.5
Deposition date		1874.4

depth	Density (measured)	unsupported activity / g clay	US activity / gram	Trapazoidal Depth-Integration of (activity * volume * density)
0.00	1.20	3.08	1.48	
1.00	1.20	3.08	1.48	6.56
3.00	1.27	3.14	1.50	13.60
5.00	1.58	1.84	0.88	12.54
7.00	1.60	1.73	0.83	10.05
9.00	1.49	0.86	0.43	7.21
11.00	1.50	0.87	0.41	4.67
13.00	1.52	0.45	0.21	3.47
15.00	1.72	0.46	0.22	2.56
17.00	1.47	0.26	0.12	2.00
21.00	1.76	0.06	0.03	1.84
31.00	1.79	0.03	0.02	
41.00	1.94	0.00	0.00	
76.50	1.20	0.02	0.01	

collected Rolf Aalto analysed Mathias Will

^{210}Pb Profiles

Int. Err	Core	Depth (avg)	notes	Pb-210 DPM/g	dpm/g clay	dpm/g % < 2um	err	% Clay	%Silt	%Sand	% < 2um	notes
1	M3	1		2.83	6.15		0.49	48.00				est
1	M3	3		2.08	4.29		0.36	48.60				est
1	M3	5		2.05	4.22		0.35	48.60				est
1	M3	7		1.55	3.21	4.07	0.28	48.21	49.59	2.19	38.02	
1	M3	9		1.22	2.50	3.05	0.22	48.87	48.57	2.56	40.09	
1	M3	11		0.96	2.09	2.66	0.18	45.64	53.03	1.32	35.87	
1	M3	13		0.86	1.93		0.17	45.00		0.67		AVG
1	M3	15		0.78	1.74		0.15	45.00		1.15		AVG
1	M3	17		0.61	1.36		0.13	45.00		1.70		AVG
1	M3	21		0.48	0.89	1.04	0.11	52.32	44.84	2.84	44.99	
1	M3	31		0.37	0.58	0.66	0.08	64.25	32.03	3.72	56.43	
1	M3	41		0.41	0.80	0.99	0.09	51.80	42.09	6.11	41.89	
1	M3	66		0.65	1.19		0.10	55.00				

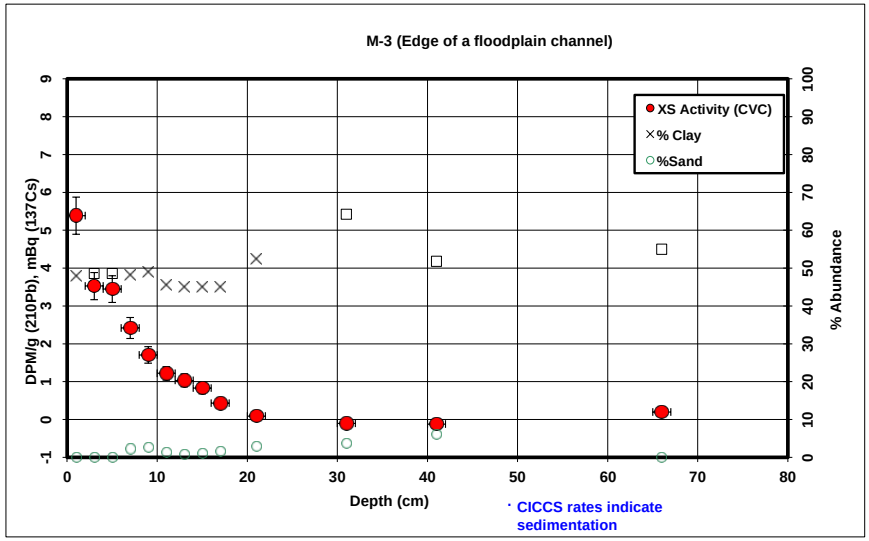

Supported Background (dpm/g clay)	XS clay activity	Radon Ventillation Effect	XS Activity (CVC)
1.547278099	4.60	-0.79	**5.38**
1.535177929	2.75	-0.77	**3.53**
1.535177929	2.69	-0.76	**3.45**
1.542936008	1.67	-0.75	**2.42**
1.529789239	0.97	-0.74	**1.71**
1.597328463	0.50	-0.73	**1.22**
1.611693786	0.32	-0.71	**1.04**
1.611693786	0.13	-0.70	**0.83**
1.611693786	-0.26	-0.69	**0.43**
1.465222971	-0.57	-0.67	**0.09**
1.286822787	-0.71	-0.61	**-0.10**
1.474556625	-0.68	-0.56	**-0.12**
1.419723008	-0.23	-0.43	**0.20**

104.56	--->	28.26
Total integrated US activity (integrated tube DPM)		(DPM/cm^2) US activity
Assumed Mete	--->	17.76
(Atoms Pb-210/ M cm^2) (average 'shielded' rate of C18 & sites 41)		
US Activity fro (DPM/ cm^2)	--->	10.49
Input Sedimen (DPM / g clay) (from proximal grab samples)	--->	1.78
CICCS Accum (grams clay / cm^2 yr)	--->	0.19
CICCS Accum (grams / cm^2 yr)	--->	0.37
CICCS Accum (cm / yr)	--->	0.25

Avg. % Clay	Avg. Density
49.72	1.49

Assumed Supported --> (DPM/ g clay)	0.00
Assumed Den (g/cc)	1.50
Assumed Area (tube cross-section)	3.70

Present activity	
Confidence In	0.00
Original sedin	3.00
Background U	0.60
CIRCA Uncert	0.20
N/N_o	-0.25
S.E. (N/N_o)	-0.02
Predicted sed	#NUM!
S.E. (age)	#NUM!
minimum age	#NUM!
maximum age	#NUM!
Activity offset f	-1.5
Deposition dat	#NUM!

Present activity	
Confidence In	#REF!
Original sedin	3.00
Background U	0.60
CIRCA Uncert	0.20
N/N_o	-0.25
S.E. (N/N_o)	#REF!
Predicted sed	#NUM!
S.E. (age)	#NUM!
minimum age	#REF!
maximum age	#REF!
Activity offset f	-1.5
Deposition dat	#NUM!

	--->	28.26
Additional 'cap' activity (integrated tube DPM)		(DPM/cm^2) Cap activity
Assumed Mete	--->	17.76
(Atoms Pb-210/ M cm^2) (average 'shielded' rate of C18 & sites 41)		
Growth time fo	--->	#NUM!
Activity offset from 2000		-2.5
Deposition date		#NUM!

depth	Density (measured)	unsupported activity / g clay	US activity / gram	Trapazoidal Depth-Integration of (activity * volume * density)
0.00	1.50	5.38	2.58	
1.00	1.50	5.38	2.58	14.34
3.00	1.50	3.53	1.71	23.86
5.00	1.27	3.45	1.68	17.38
7.00	1.42	2.42	1.17	14.13
9.00	1.45	1.71	0.83	10.62
11.00	1.47	1.22	0.56	7.52
13.00	1.49	1.04	0.47	5.60
15.00	1.55	0.83	0.37	4.73
17.00	1.73	0.43	0.20	3.46
21.00	1.50	0.09	0.05	2.92
31.00	1.50	0.00	0.00	
41.00	1.03	0.00	0.00	
66.00	1.26	0.20	0.11	

collected Rolf Aalto analysed Mathias Will

^{210}Pb Profiles

Int. Err	Core	Depth (avg)	notes	Pb-210 DPM/g	dpm/g clay	dpm/g % < 2um	err	% Clay	%Silt	%Sand	% < 2um	notes
1	M4	1		1.53	3.30	4.02	0.31	46.49	48.95	4.56	38.14	AVG
1	M4	3		1.52	3.28	4.00	0.31	46.49	48.95	4.56	38.14	
1	M4	5		1.12	2.03	2.39	0.17	55.19	42.46	2.35	46.90	
1	M4	7		0.94	1.76	2.10	0.15	53.38	43.37	3.25	44.59	
1	M4	9		0.85	1.72	2.08	0.15	49.68	46.45	3.87	40.98	
1	M4	11		0.74	1.46	1.73	0.14	50.76	44.75	4.49	42.90	
1	M4	15		0.66	1.46		0.14	50.00				AVG
1	M4	21		0.49	0.99	1.20	0.10	49.02	49.22	1.75	40.57	
1	M4	31		0.42	1.18	1.52	0.11	35.87	62.11	2.03	27.88	
1	M4	41		0.55	1.57	2.12	0.14	34.93	57.49	7.58	25.91	
1	M4	48.5		0.47	1.13	1.59	0.11	41.90	56.69	1.41	29.91	

Supported Background (dpm/g clay)	XS clay activity	Radon Ventillation Effect	XS Activity (CVC)
1.578860076	1.72	-0.79	**2.51**
1.578860076	1.70	-0.77	**2.47**
1.416651941	0.62	-0.76	**1.38**
1.446819547	0.31	-0.75	**1.06**
1.514092245	0.20	-0.74	**0.94**
1.493604902	-0.03	-0.73	**0.69**
1.507869642	-0.05	-0.70	**0.65**
1.526754896	-0.53	-0.67	**0.13**
1.860193664	-0.68	-0.61	**-0.07**
1.891513768	-0.32	-0.56	**0.24**
1.685955695	-0.55	-0.52	**-0.04**

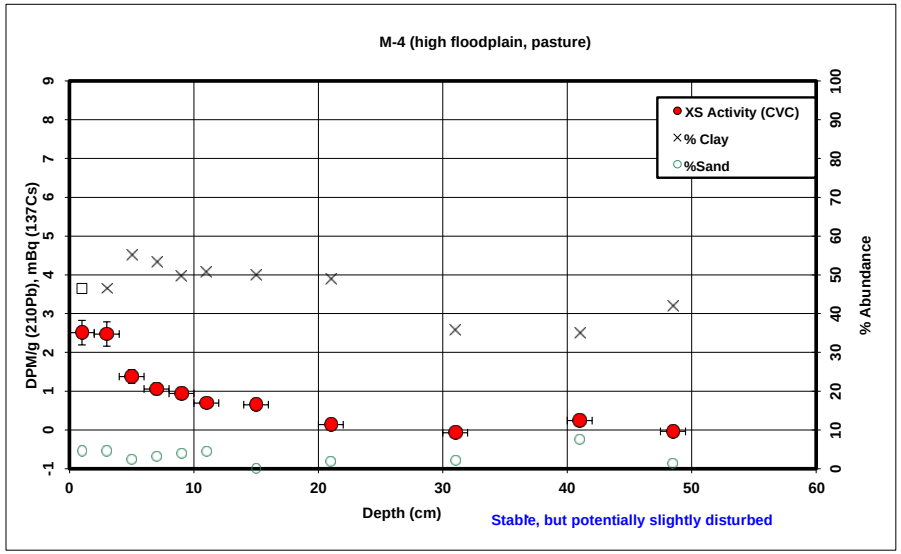

60.92	--->	16.46
Total integrated US activity (integrated tube DPM)		(DPM/cm^2) US activity
Assumed Mete (Atoms Pb-210/ M cm^2) (average 'shielded' rate of C18 & sites 41)	--->	17.76
US Activity fro (DPM/ cm^2)	--->	-1.30
Input Sedimen (DPM / g clay) (from proximal grab samples)	--->	1.76
CICCS Accum (grams clay / cm^2 yr)	--->	-0.02
CICCS Accum (grams / cm^2 yr)	--->	-0.05
CICCS Accum (cm / yr)	--->	-0.03

Avg. % Clay	Avg. Density
46.70	1.53

Assumed Supported -->	0.00
(DPM/ g clay)	
Assumed Den (g/cc)	1.50
Assumed Area (tube cross-section)	3.70

Present activity	
Confidence In	0.00
Original sedim	3.00
Background U	0.60
CIRCA Uncert	0.20
N/N_o	-0.25
S.E. (N/N_o)	-0.02
Predicted sed	#NUM!
S.E. (age)	#NUM!
minimum age	#NUM!
maximum age	#NUM!
Activity offset f	-1.5
Deposition dat	#NUM!

Present activity	
Confidence In	0.00
Original sedim	3.00
Background U	0.60
CIRCA Uncert	0.20
N/N_o	-0.25
S.E. (N/N_o)	-0.02
Predicted sed	#NUM!
S.E. (age)	#NUM!
minimum age	#NUM!
maximum age	#NUM!
Activity offset f	-1.5
Deposition dat	#NUM!

	--->	16.46
Additional 'cap' activity (integrated tube DPM)		(DPM/cm^2) Cap activity
Assumed Mete (Atoms Pb-210/ M cm^2) (average 'shielded' rate of C18 & sites 41)	--->	17.76
Growth time fc	--->	84.1441288
Activity offset from 2000		-2.5
Deposition date		1918.4

depth	Density (measured)	unsupported activity / g clay	US activity / gram	Trapazoidal Depth-Integration of (activity * volume * density)
0.00	1.03	2.51	1.17	
1.00	1.03	2.51	1.17	4.43
3.00	1.26	2.47	1.15	9.82
5.00	1.46	1.38	0.76	9.62
7.00	1.65	1.06	0.56	7.63
9.00	1.38	0.94	0.47	5.78
11.00	1.66	0.69	0.35	4.60
15.00	1.71	0.65	0.33	8.46
21.00	1.97	0.13	0.07	8.01
31.00	2.25	0.00	0.00	2.57
41.00	1.50	0.24	0.08	
48.50	1.50	0.00	0.00	

collected Rolf Aalto analysed Mathias Will

^{210}Pb Profiles

Int.	Err	Core	Depth (avg)	notes	Pb-210 DPM/g	dpm/g clay	dpm/g % < 2um	err	% Clay	%Silt	%Sand	% < 2um	notes
1		M5	1		2.47	6.11		0.57	42.00				est
1		M5	3		2.33	5.50	7.45	0.50	42.44	54.29	3.27	31.37	est
1		M5	5		2.09	4.92	6.65	0.45	42.44	54.29	3.27	31.37	
1		M5	7		1.53	3.64	4.75	0.34	41.98	56.07	1.96	32.15	
1		M5	9		1.65	3.52	4.34	0.30	46.87	51.72	1.41	38.06	
1		M5	11		1.48	3.05	3.65	0.26	48.41	49.90	1.69	40.47	
1		M5	15		0.95	2.15		0.20	45.85				AVG
1		M5	21		0.90	2.08	2.54	0.19	43.29	53.15	3.56	35.47	
1		M5	25		0.63	1.39		0.14	45.29				AVG
1		M5	31		0.50	1.06	1.23	0.11	47.28	45.34	7.38	40.69	
1		M5	41		0.44	0.65	0.75	0.08	66.52	29.39	4.09	57.75	
1		M5	55		0.45	0.71		0.09	64.31				AVG
1		M5	70		0.69	1.12	1.31	0.11	62.10	29.69	8.21	52.91	

Supported Background (dpm/g clay)	XS clay activity	Radon Ventillation Effect	XS Activity (CVC)
1.68352391	4.43	-0.79	5.21
1.672496096	3.83	-0.77	4.60
1.672496096	3.24	-0.76	4.01
1.684135684	1.96	-0.75	2.71
1.570714214	1.95	-0.74	2.69
1.539001427	1.52	-0.73	2.24
1.592738005	0.55	-0.70	1.26
1.651603569	0.43	-0.67	1.10
1.605248865	-0.22	-0.64	0.43
1.562111067	-0.51	-0.61	0.10
1.258891011	-0.61	-0.56	-0.05
1.286114857	-0.57	-0.49	-0.09
1.31491287	-0.20	-0.41	0.21

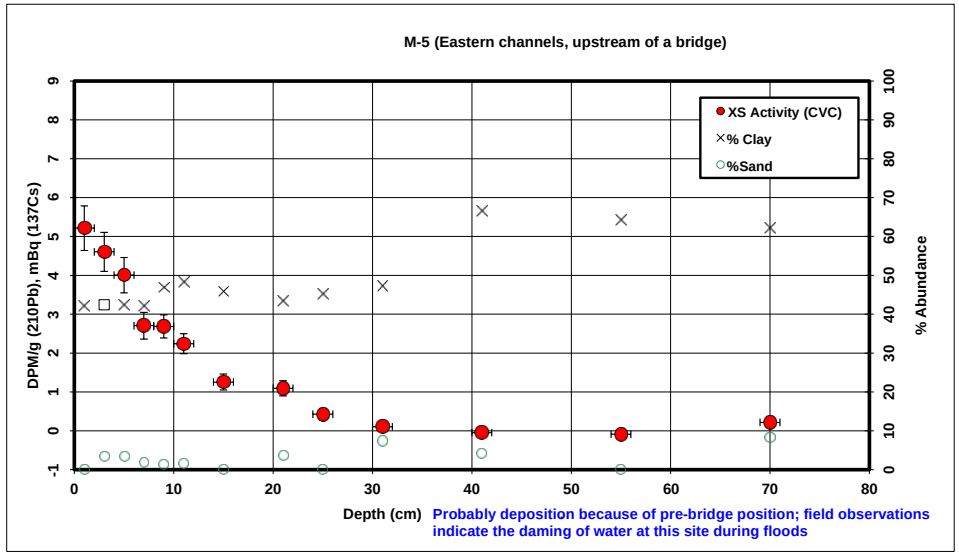

136.97	--->	37.02
Total integrated US activity (integrated tube DPM)		(DPM/cm^2) US activity
Assumed Mete	--->	17.76
(Atoms Pb-210/ M cm^2) (average 'shielded' rate of C18 & sites 41)		
US Activity fro	--->	19.25
(DPM/ cm^2)		
Input Sedimen	--->	1.76
(DPM / g clay) (from proximal grab samples)		
CICCS Accum	--->	0.34
(grams clay / cm^2 yr)		
CICCS Accum	--->	0.69
(grams / cm^2 yr)		
CICCS Accum	--->	0.49
(cm / yr)		

Avg. % Clay	Avg. Density
49.14	1.43

Assumed Supported -->	0.00
(DPM/ g clay)	
Assumed Den	1.50
(g/cc)	
Assumed Area	3.70
(tube cross-section)	

Present activity	
Confidence In	0.00
Original sedim	1.76
Background U	0.60
CIRCA Uncert	0.20
N/N$_o$	-0.52
S.E. (N/N$_o$)	-0.09
Predicted sed	#NUM!
S.E. (age)	#NUM!
minimum age	#NUM!
maximum age	#NUM!
Activity offset f	-1.5
Deposition dat	#NUM!

Present activity	
Confidence In	#REF!
Original sedim	3.00
Background U	0.60
CIRCA Uncert	0.20
N/N$_o$	-0.25
S.E. (N/N$_o$)	#REF!
Predicted sed	#NUM!
S.E. (age)	#NUM!
minimum age	#REF!
maximum age	#REF!
Activity offset f	-1.5
Deposition dat	#NUM!

	--->	37.02
Additional 'cap' activity (integrated tube DPM)		(DPM/cm^2) Cap activity
Assumed Mete	--->	17.76
(Atoms Pb-210/ M cm^2) (average 'shielded' rate of C18 & sites 41)		
Growth time fc	--->	#NUM!
Activity offset from 2000		-2.5
Deposition date		#NUM!

depth	Density (measured)	unsupported activity / g clay	US activity / gram	Trapazoidal Depth-Integration of (activity * volume * density)
0.00	1.50	5.21	2.19	
1.00	1.50	5.21	2.19	12.15
3.00	1.50	4.60	1.95	23.00
5.00	1.03	4.01	1.70	17.11
7.00	1.27	2.71	1.14	12.10
9.00	1.20	2.69	1.26	10.96
11.00	1.44	2.24	1.08	11.44
15.00	1.65	1.26	0.58	18.99
21.00	1.60	1.10	0.47	18.97
25.00	1.17	0.43	0.19	6.86
31.00	1.73	0.10	0.05	3.92
41.00	1.50	0.00	0.00	1.48
55.00	1.50	0.00	0.00	
70.00	1.13	0.21	0.13	

collected Rolf Aalto analysed Mathias Will

^{210}Pb Profiles

Int. Err	Core	Depth (avg)	notes		Pb-210 DPM/g	dpm/g clay	dpm/g % < 2um	err	% Clay	%Silt	%Sand	% < 2um	notes	Supported Background (dpm/g clay)	XS clay activity	Radon Ventillation Effect	XS Activity (CVC)	
1	MSLSF29	1		0	1.02	4.27	6.31	0.27	24.15	46.73	29.12	16.33	na	5.37	2.388248666	1.88	-0.79	2.67
1	MSLSF29	3		0	1.09	4.58	6.78	0.35	24.15	46.73	29.12	16.33		1.71	2.388248666	2.19	-0.77	2.97
1	MSLSF29	5		0	1.08	3.16	4.21	0.24	34.64	41.94	23.42	25.98		3.11	1.901541954	1.26	-0.76	2.02
1	MSLSF29	7		0	1.00	2.69	3.62	0.21	37.57	42.98	19.45	27.87		5.83	1.806334182	0.88	-0.75	1.63
1	MSLSF29	9		0	1.04	3.03	4.07	0.24	34.88	44.45	20.67	25.98		2.05	1.893146703	1.14	-0.74	1.88
1	MSLSF29	11		0	1.08	2.61	3.39	0.21	41.85	41.34	16.80	32.26		4.81	1.687208466	0.92	-0.73	1.65
1	MSLSF29	21		0	0.78	2.26	2.73	0.18	34.79	46.82	18.39	28.80		7.35	1.896417065	0.37	-0.67	1.03
1	MSLSF29	31		0	0.85	2.44	3.44	0.20	35.18	47.06	17.77	24.93		9.87	1.883164422	0.55	-0.61	1.16
1	MSLSF29	41		0	0.68	1.35	1.92	0.12	49.90	39.69	10.41	35.18		0.00	1.509713284	-0.16	-0.56	0.40
1	MSLSF29	84		0	0.63	1.77	2.62	0.15	35.83	48.90	15.27	24.18		0	1.861307956	-0.10	-0.35	0.26

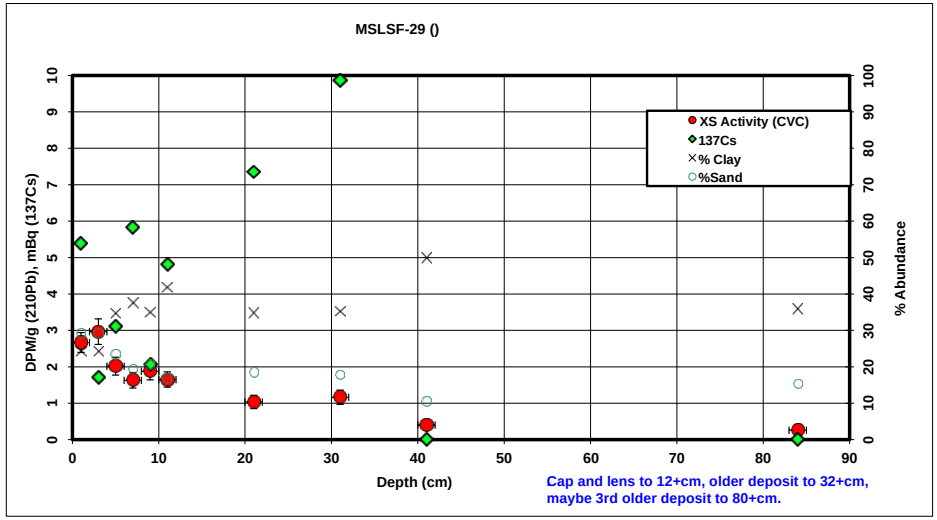

Assumed Supported --> 0.00 (DPM/ g clay)

Assumed Den 1.50 (g/cc)

Assumed Area 3.70 (tube cross-section)

depth	Density (measured)	unsupported activity / g clay	US activity / gram	Trapazoidal Depth-Integration of (activity * volume * density)	
0.00	1.89	2.67	0.64		
1.00	1.89	2.67	0.64	4.50	
3.00	1.27	2.97	0.72	7.95	
5.00	1.67	2.02	0.70	7.70	
7.00	1.56	1.63	0.61	7.83	
9.00	1.24	1.88	0.65	6.55	
11.00	1.11	1.65	0.69	5.83	
21.00	1.50	1.03	0.36	25.30	
31.00	1.31	1.16	0.41	19.95	
41.00	1.66	0.40	0.20	16.72	
84.00	1.63	0.26	0.09		

Present activit 0.26
Confidence In 0.05
Original sedim 1.76
Background US activity
CIRCA Uncerta 0.20
N/N_0 0.15
S.E. (N/N_0) 0.03
Predicted sed 61.53
S.E. (age) 7.26
minimum age 55.04
maximum age 69.66
Activity offset f -1.5
Deposition dat 1940.0

102.33 ---> 27.66
Total integrated US activity (DPM/cm^2)
(integrated tube DPM) US activity

Assumed Mete ---> 17.76
(Atoms Pb-210/ M cm^2)
(average 'shielded' rate of C18 & sites 41)

US Activity fro ---> 9.89
(DPM/ cm^2)

Input Sedimen ---> 1.76
(DPM / g clay)
(from proximal grab samples)

CICCS Accum ---> 0.18
(grams clay / cm^2 yr)

CICCS Accum ---> 0.50
(grams / cm^2 yr)

CICCS Accum ---> 0.33
(cm / yr)

Avg. % Clay	Avg. Density
35.30	1.52

Present activity
Confidence In 0.00
Original sedim 3.00
Background U 0.60
CIRCA Uncerta 0.20
N/N_0 -0.25
S.E. (N/N_0) -0.02
Predicted sed #NUM!
S.E. (age) #NUM!
minimum age #NUM!
maximum age #NUM!
Activity offset f -1.5
Deposition dat #NUM!

---> 7.00
Additional 'cap' activity (DPM/cm^2)
(integrated tube DPM) Cap activity

Assumed Mete ---> 15.00
(Atoms Pb-210/ M cm^2)
(average 'shielded' rate of C18 & sites 41)

Growth time fc ---> 20.2236
Activity offset from 2000 -2.5
Deposition date 1982.3

collected and analysed Rolf Aalto

^{210}Pb Profiles

Int. Err	Core	Depth (avg)	notes	Pb-210 DPM/g	dpm/g clay	dpm/g % < 2um	err	% Clay	%Silt	%Sand	% < 2um	notes
1	MSLSF30	1		1.18	3.34	4.00	0.29	36.02	56.23	7.75	30.10	
1	MSLSF30	3		1.24	3.78	4.86	0.31	33.44	56.40	10.16	25.98	
1	MSLSF30	5		1.12	3.34	-5.67	0.27	34.13	9.01			
1	MSLSF30	7		1.07	2.96	3.70	0.25	36.93	53.18	9.90	29.54	
1	MSLSF30	9		1.08	3.44	4.34	0.28	31.98	56.33	11.68	25.36	
1	MSLSF30	11		1.06	2.92	3.73	0.24	36.81	51.76	11.42	28.86	
1	MSLSF30	21		0.63	1.80	2.31	0.16	34.96	45.98	19.06	27.33	
1	MSLSF30	31		0.68	1.55	2.01	0.15	43.70	56.30	0.00	33.70	
1	MSLSF30	41		0.58	1.36	1.70	0.13	41.84	59.04	-0.88	33.40	
1	MSLSF30	80		0.62	0.94	2.06	0.09	64.50	27.06	8.44	29.49	

Supported Background (dpm/g clay)	XS clay activity	Radon Ventillation Effect	XS Activity (CVC)
1.855150816	1.49	-0.79	2.27
1.944389117	1.83	-0.77	2.60
1.919317186	1.43	-0.76	2.19
1.826240636	1.13	-0.75	1.88
1.999940587	1.44	-0.74	2.18
1.829737425	1.09	-0.73	1.82
1.890372574	-0.09	-0.67	0.58
1.641735633	-0.09	-0.61	0.52
1.687520733	-0.33	-0.56	0.23
1.283742822	-0.34	-0.37	0.03

Assumed Supported -->	0.00
(DPM/ g clay)	
Assumed Den	1.50
(g/cc)	
Assumed Area	3.70
(tube cross-section)	

depth	Density (measured)	unsupported activity / g clay	US activity / gram	Trapazoidal Depth-Integration of (activity * volume * density)
0.00	1.89	2.27	0.82	
1.00	1.89	2.27	0.82	5.72
3.00	1.27	2.60	0.87	9.87
5.00	1.67	2.19	0.75	8.81
7.00	1.56	1.88	0.69	8.60
9.00	1.24	2.18	0.70	7.20
11.00	1.11	1.82	0.67	5.93
21.00	1.50	0.58	0.20	21.02
31.00	1.31	0.52	0.23	11.11
41.00	1.66	0.23	0.10	8.84
80.00	1.63	0.03	0.02	13.41

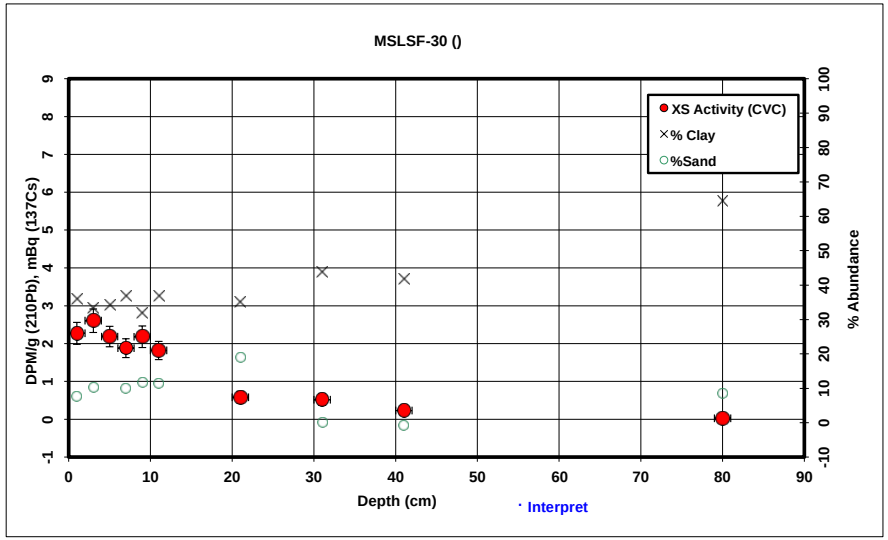

100.50	--->	27.16
Total integrated US activity (integrated tube DPM)		(DPM/cm^2) US activity
Assumed Mete (Atoms Pb-210/ M cm^2) (average 'shielded' rate of C18 & sites 41)	--->	17.76
US Activity fro (DPM/ cm^2)	--->	9.40
Input Sedimen (DPM / g clay) (from proximal grab samples)	--->	1.76
CICCS Accum (grams clay / cm^2 yr)	--->	0.17
CICCS Accum (grams / cm^2 yr)	--->	0.42
CICCS Accum (cm / yr)	--->	0.28

Present activity	
Confidence In	0.00
Original sedim	3.00
Background U	0.60
CIRCA Uncert	0.20
N/N_o	-0.25
S.E. (N/N_o)	-0.02
Predicted sed	#NUM!
S.E. (age)	#NUM!
minimum age	#NUM!
maximum age	#NUM!
Activity offset f	-1.5
Deposition dat	#NUM!

Present activity	
Confidence In	0.00
Original sedim	3.00
Background U	0.60
CIRCA Uncert	0.20
N/N_o	-0.25
S.E. (N/N_o)	-0.02
Predicted sed	#NUM!
S.E. (age)	#NUM!
minimum age	#NUM!
maximum age	#NUM!
Activity offset f	-1.5
Deposition dat	#NUM!

	--->	
Additional 'cap' activity (integrated tube DPM)		(DPM/cm^2) Cap activity
Assumed Mete (Atoms Pb-210/ M cm^2) (average 'shielded' rate of C18 & sites 41)	--->	15.00
Growth time fc	--->	0
Activity offset from 2000		-2.5
Deposition date		2002.5

Avg. % Clay	Avg. Density
39.43	1.52

collected Rolf Aalto analysed Mathias Will

^{210}Pb Profiles

Int. Err	Core	Depth (avg)	notes		Pb-210 DPM/g	dpm/g clay	dpm/g % < 2um	err	% Clay	%Silt	%Sand	% < 2um	notes
1	MSLSF31	1		0	0.95	2.69	2.80	0.25	35.92	52.24	7.48	34.47	AVG
1	MSLSF31	3		0	1.04	2.94	3.62	0.24	35.92	54.32	9.76	29.12	
1	MSLSF31	5		0	0.98	3.39	4.35	0.28	29.42	56.17	14.41	22.90	
1	MSLSF31	7		0	0.91	2.87	3.77	0.24	32.28	53.31	14.41	24.57	
1	MSLSF31	9		0	0.96	3.07		0.21	31.63				AVG
1	MSLSF31	11		0	0.84	2.68		0.19	31.63				AVG
1	MSLSF31	21		0	0.66	2.12	2.76	0.18	30.97	55.57	13.46	23.85	
1	MSLSF31	31		0	0.52	1.80	2.38	0.16	28.48	46.45	25.07	21.55	
1	MSLSF31	41		0	0.52	1.98	2.56	0.18	25.92	42.87	31.21	20.05	
1	MSLSF31	78		0	0.57	1.64	1.86	0.16	34.29	56.61	9.10	30.17	

Supported Background (dpm/g clay)	XS clay activity	Radon Ventillation Effect	XS Activity (CVC)
1.858430798	0.83	-0.79	**1.62**
1.858430798	1.08	-0.77	**1.85**
2.10831212	1.28	-0.76	**2.04**
1.988153369	0.88	-0.75	**1.63**
2.014073149	1.05	-0.74	**1.79**
2.014073149	0.66	-0.73	**1.39**
2.040883923	0.08	-0.67	**0.75**
2.152042019	-0.35	-0.61	**0.26**
2.284198939	-0.30	-0.56	**0.25**
1.913862577	-0.28	-0.38	**0.10**

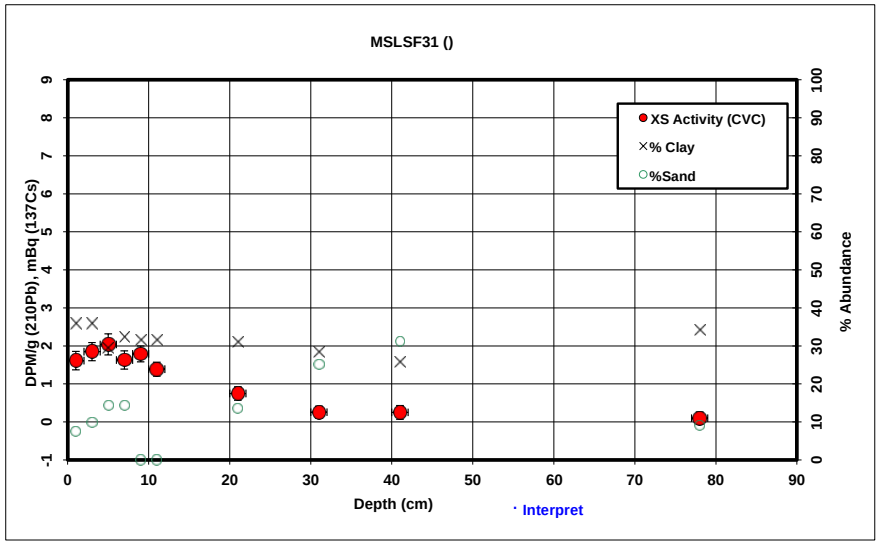

126.29	--->	34.13
Total integrated US activity (integrated tube DPM)		(DPM/cm^2) US activity
Assumed Mete (Atoms Pb-210/ M cm^2) (average 'shielded' rate of C18 & sites 41)	--->	17.76
US Activity fro (DPM/ cm^2)	--->	16.37
Input Sedimen (DPM / g clay) (from proximal grab samples)	--->	1.76
CICCS Accum (grams clay / cm^2 yr)	--->	0.29
CICCS Accum (grams / cm^2 yr)	--->	0.92
CICCS Accum (cm / yr)	--->	0.41

Avg. % Clay	Avg. Density
31.64	2.25

Assumed Supported -->	0.00
(DPM/ g clay)	
Assumed Den (g/cc)	1.50
Assumed Area (tube cross-section)	3.70

Present activi	0.10
Confidence In	0.05
Original sedim	1.76
Background US activity	
CIRCA Uncert	0.20
N/N_o	0.06
S.E. (N/N_o)	0.03
Predicted sed	92.27
S.E. (age)	17.55
minimum age	78.95
maximum age	115.40
Activity offset f	-1.5
Deposition dat	1909.2

Present activity	
Confidence In	0.00
Original sedim	3.00
Background U	0.60
CIRCA Uncert	0.20
N/N_o	-0.25
S.E. (N/N_o)	-0.02
Predicted sed	#NUM!
S.E. (age)	#NUM!
minimum age	#NUM!
maximum age	#NUM!
Activity offset f	-1.5
Deposition dat	#NUM!

	--->	
Additional 'cap' activity (integrated tube DPM)		(DPM/cm^2) Cap activity
Assumed Mete (Atoms Pb-210/ M cm^2) (average 'shielded' rate of C18 & sites 41)	--->	15.00
Growth time fo	--->	0
Activity offset from 2000		-2.5
Deposition date		2002.5

depth	Density (measured)	unsupported activity / g clay	US activity / gram	Trapazoidal Depth-Integration of (activity * volume * density)
0.00	2.12	1.62	0.58	
1.00	2.12	1.62	0.58	4.54
3.00	2.22	1.85	0.66	9.99
5.00	2.39	2.04	0.60	10.78
7.00	2.50	1.63	0.53	10.18
9.00	2.47	1.79	0.57	10.04
11.00	2.99	1.39	0.44	10.15
21.00	2.99	0.75	0.23	37.11
31.00	2.82	0.26	0.07	16.40
41.00	2.84	0.25	0.07	7.31
78.00	0.00	0.10	0.03	9.78

collected Rolf Aalto analysed Mathias Will

^{210}Pb Profiles

Int. Err	Core	Depth (avg)	notes	Pb-210 DPM/g	dpm/g clay	dpm/g % < 2um	err	% Clay	%Silt	%Sand	% < 2um	notes
1	MSLSF33	1		1.56	4.22	5.73	0.40	37.87	59.78	2.35	27.94	
1	MSLSF33	3		1.43	5.03	7.12	0.48	29.07	67.94	2.98	20.55	
1	MSLSF33	5		1.28	3.43	4.58	0.29	38.22	58.13	3.66	28.60	
1	MSLSF33	7		1.19	2.97	3.96	0.24	40.67	56.28	3.05	30.56	
1	MSLSF33	9		1.07	3.40	4.75	0.28	32.03	65.57	2.40	22.89	
1	MSLSF33	11		0.86	2.13	2.68	0.17	40.95	58.74	0.31	32.53	
1	MSLSF33	21		0.74	1.81	2.37	0.15	41.17	57.93	0.89	31.46	
1	MSLSF33	31		0.60	1.37	1.76	0.12	43.26	56.90	-0.16	33.56	
1	MSLSF33	41		0.56	1.21	1.52	0.11	45.84	53.02	1.14	36.36	
1	MSLSF33	94		0.67	1.62	1.92	0.15	41.05	52.18	6.77	34.52	

Supported Background (dpm/g clay)	XS clay activity	Radon Ventillation Effect	XS Activity (CVC)
1.797376278	2.43	-0.79	3.21
2.124074357	2.91	-0.77	3.68
1.78706563	1.64	-0.76	2.40
1.718175864	1.26	-0.75	2.00
1.997975432	1.40	-0.74	2.14
1.710726697	0.42	-0.73	1.14
1.704864274	0.10	-0.67	0.77
1.652468434	-0.29	-0.61	0.32
1.592999958	-0.39	-0.56	0.17
1.708112372	-0.09	-0.31	0.22

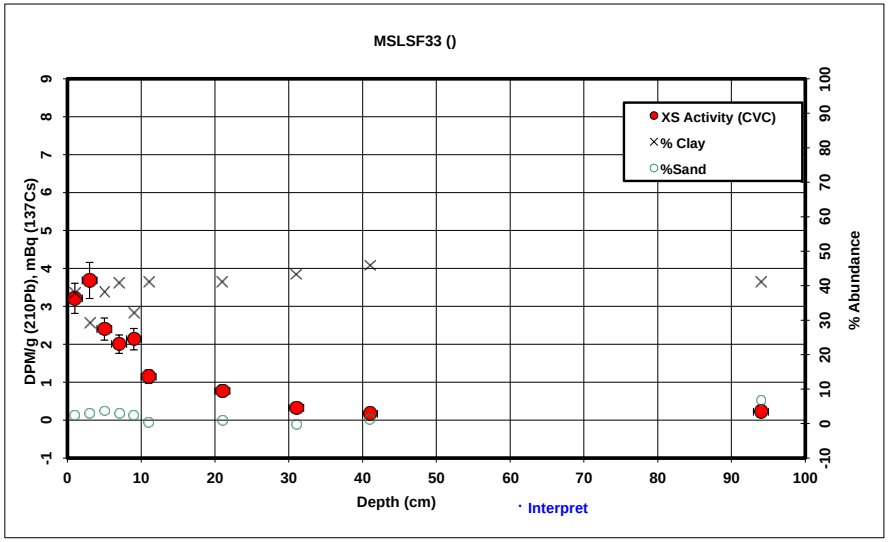

145.64	--->	39.36
Total integrated US activity (integrated tube DPM)		(DPM/cm^2) US activity

Assumed Mete (Atoms Pb-210/ M cm^2) (average 'shielded' rate of C18 & sites 41)	--->	17.76
US Activity fro (DPM/ cm^2)	--->	21.60
Input Sedimen (DPM / g clay) (from proximal grab samples)	--->	1.76
CICCS Accum (grams clay / cm^2 yr)	--->	0.38
CICCS Accum (grams / cm^2 yr)	--->	0.98
CICCS Accum (cm / yr)	--->	0.48

Avg. % Clay	Avg. Density
39.01	2.03

Assumed Supported --> (DPM/ g clay)	0.00
Assumed Den (g/cc)	1.50
Assumed Area (tube cross-section)	3.70

Present activi	0.20
Confidence In	0.05
Original sedin	1.76
Background US activity	
CIRCA Uncert	0.20
N/N$_o$	0.11
S.E. (N/N$_o$)	0.03
Predicted sed	69.97
S.E. (age)	8.98
minimum age	62.16
maximum age	80.29
Activity offset f	-1.5
Deposition dat	1931.5

Present activity	
Confidence In	0.00
Original sedin	3.00
Background U	0.60
CIRCA Uncert	0.20
N/N$_o$	-0.25
S.E. (N/N$_o$)	-0.02
Predicted sed	#NUM!
S.E. (age)	#NUM!
minimum age	#NUM!
maximum age	#NUM!
Activity offset f	-1.5
Deposition dat	#NUM!

	--->	
Additional 'cap' activity (integrated tube DPM)		(DPM/cm^2) Cap activity
Assumed Mete (Atoms Pb-210/ M cm^2) (average 'shielded' rate of C18 & sites 41)	--->	15.00
Growth time fc	--->	0
Activity offset from 2000		-2.5
Deposition date		2002.5

depth	Density (measured)	unsupported activity / g clay	US activity / gram	Trapazoidal Depth-Integration of (activity * volume * density)
0.00	1.50	3.21	1.22	
1.00	1.50	3.21	1.22	6.75
3.00	1.77	3.68	1.07	13.83
5.00	2.00	2.40	0.92	13.88
7.00	2.06	2.00	0.82	13.04
9.00	2.79	2.14	0.68	13.47
11.00	2.74	1.14	0.47	11.80
21.00	2.67	0.77	0.32	39.33
31.00	2.75	0.32	0.14	22.93
41.00	2.51	0.17	0.08	10.61
94.00	0.00	0.22	0.09	

collected and analysed Rolf Aalto

^{210}Pb Profiles

Int. Err	Core	Depth (avg)	notes	Pb-210 DPM/g	dpm/g clay	dpm/g % < 2um	err	% Clay	%Silt	%Sand	% < 2um	notes
1	RASRF_125	1		0.93	3.49	2.87	0.33	27.00	57.32	4.69	32.77	
1	RASRF_125	3		0.74	2.77		0.23	27.19				AVG
1	RASRF_125	5		0.58	2.13	2.51	0.21	27.37	48.90	23.73	23.23	
1	RASRF_125	7		0.77	2.66		0.23	29.10				AVG
1	RASRF_125	9		0.89	2.92	3.53	0.28	30.83	54.72	14.45	25.52	
1	RASRF_125	11		0.97	3.27		0.27	25.11				AVG
1	RASRF_125	15	sandy	0.83	4.36	5.03	0.45	19.39	30.66	49.96	16.79	
1	RASRF_125	21		0.57	2.46	2.93	0.24	23.03	34.35	42.62	19.33	
1	RASRF_125	31		0.51	2.64	3.17	0.26	19.22	35.21	45.57	15.99	
1	RASRF_125	41		0.36	7.14		0.93	16.39				< to sedi
1	RASRF_125	51	sandy	0.37	2.69	2.99	0.30	13.55	16.66	69.79	12.18	
1	RASRF_125	60.5		0.70	2.77	3.33	0.27	25.38	42.21	32.41	21.10	

Supported Background (dpm/g clay)	XS clay activity	Radon Ventillation Effect	XS Activity (CVC)
2.225824617	1.26	-0.79	**2.05**
2.216239541	0.56	-0.77	**1.33**
2.20676033	-0.07	-0.76	**0.69**
2.122919248	0.54	-0.75	**1.29**
2.04683798	0.87	-0.74	**1.61**
2.330427794	0.94	-0.73	**1.67**
2.744276238	1.61	-0.70	**2.32**
2.46102946	0.00	-0.67	**0.67**
2.759429209	-0.12	-0.61	**0.49**
3.051858834	4.09	-0.56	**4.64**
3.440554263	-0.75	-0.51	**-0.25**
2.314408464	0.45	-0.46	**0.91**

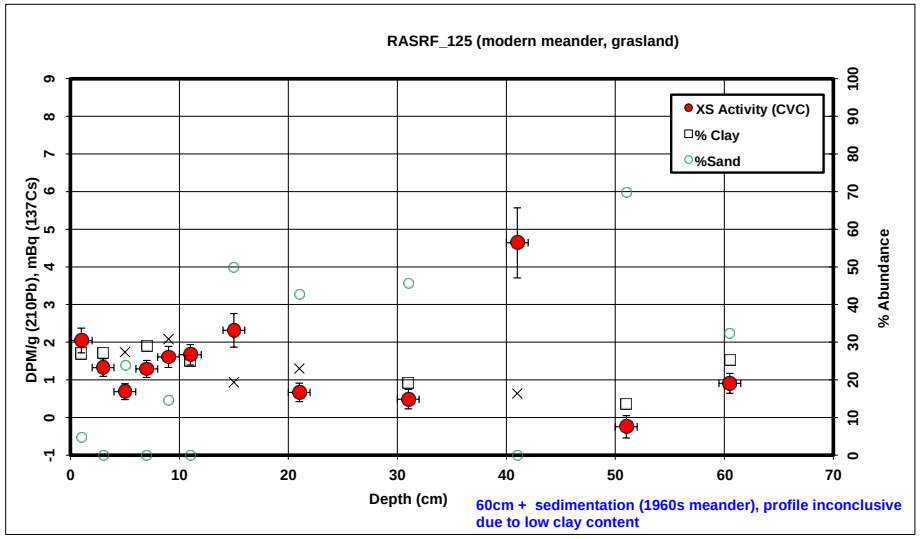

113.21	--->	30.60
Total integrated US activity (integrated tube DPM)		(DPM/cm^2) US activity
Assumed Mete (Atoms Pb-210/ M cm^2) (average 'shielded' rate of C18 & sites 41)	--->	17.76
US Activity fro (DPM/ cm^2)	--->	12.83
Input Sedimen (DPM / g clay) (from proximal grab samples)	--->	1.76
CICCS Accum (grams clay / cm^2 yr)	--->	0.23
CICCS Accum (grams / cm^2 yr)	--->	0.96
CICCS Accum (cm / yr)	--->	0.63

Avg. % Clay	Avg. Density
23.63	1.54

Assumed Supported --> (DPM/ g clay)	0.00
Assumed Den (g/cc)	1.50
Assumed Area (tube cross-section)	3.70

Present activity	
Confidence In	0.00
Original sedim	3.00
Background U	0.60
CIRCA Uncert	0.20
N/N_o	-0.25
S.E. (N/N_o)	-0.02
Predicted sed	#NUM!
S.E. (age)	#NUM!
minimum age	#NUM!
maximum age	#NUM!
Activity offset f	-1.5
Deposition dat	#NUM!

Present activity	
Confidence In	#REF!
Original sedim	3.00
Background U	0.60
CIRCA Uncert	0.20
N/N_o	-0.25
S.E. (N/N_o)	#REF!
Predicted sed	#NUM!
S.E. (age)	#NUM!
minimum age	#REF!
maximum age	#REF!
Activity offset f	-1.5
Deposition dat	#NUM!

	--->	
Additional 'cap' activity (integrated tube DPM)		(DPM/cm^2) Cap activity
Assumed Mete (Atoms Pb-210/ M cm^2) (average 'shielded' rate of C18 & sites 41)	--->	17.76
Growth time fc	--->	0
Activity offset from 2000		-2.5
Deposition date		2002.5

depth	Density (measured)	unsupported activity / g clay	US activity / gram	Trapazoidal Depth-Integration of (activity * volume * density)
0.00	1.16	2.05	0.55	
1.00	1.16	2.05	0.55	2.38
3.00	1.28	1.33	0.36	4.14
5.00	1.44	0.69	0.19	2.77
7.00	1.32	1.29	0.38	2.87
9.00	1.34	1.61	0.50	4.28
11.00	1.83	1.67	0.42	5.36
15.00	1.74	2.32	0.45	11.46
21.00	1.81	0.67	0.15	11.89
31.00	1.84	0.49	0.09	8.39
41.00	1.74	4.64	0.76	28.29
51.00	1.78	0.00	0.00	24.71
60.50	1.50	0.91	0.23	6.65

^{210}Pb Profiles

Int. Err	Core	Depth (avg)	notes	Pb-210 DPM/g	dpm/g clay	dpm/g % < 2um	err	% Clay	%Silt	%Sand	% < 2um	notes
1	RASRF_126	1		0.89	2.92	3.41	0.28	30.93	49.68	19.39	26.53	
1	RASRF_126	3		0.72	2.29		0.20	31.82				AVG
1	RASRF_126	5		1.03	3.19	3.95	0.30	32.70	53.28	14.02	26.45	
1	RASRF_126	7		1.32	4.26		0.34	31.74				AVG
1	RASRF_126	9		0.90	2.95	3.88	0.28	30.78	66.13	3.09	23.45	
1	RASRF_126	11		1.20	3.98		0.32	25.98				AVG
1	RASRF_126	21	coarse sand	0.50	2.33	2.71	0.23	21.19	45.58	33.23	18.17	
1	RASRF_126	31	coarse sand	0.31	4.37		0.49	7.00	not enouth clay/silt to sedigraph			est
1	RASRF_126	41		0.41	2.06	2.42	0.21	19.84	47.15	33.01	16.85	
1.2	RASRF_126	65.2		0.46	1.88	2.16	0.19	24.31	38.80	36.89	21.18	

Supported Background (dpm/g clay)	XS clay activity	Radon Ventillation Effect	XS Activity (CVC)
2.042691379	0.88	-0.79	**1.67**
2.006477595	0.28	-0.77	**1.05**
1.971876472	1.22	-0.76	**1.98**
2.009440009	2.25	-0.75	**3.00**
2.048908835	0.90	-0.74	**1.64**
2.280424881	1.70	-0.73	**2.43**
2.594319065	-0.27	-0.67	**0.40**
5.224092751	-0.85	-0.61	**-0.24**
2.703975895	-0.65	-0.56	**-0.09**
2.378388604	-0.50	-0.44	**-0.06**

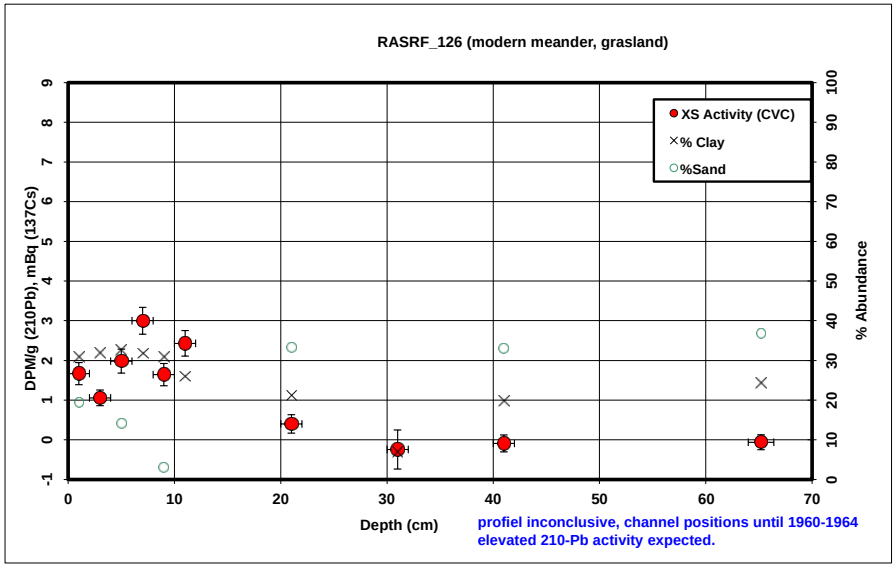

61.41	--->	16.60
Total integrated US activity (integrated tube DPM)		(DPM/cm^2) US activity
Assumed Mete (Atoms Pb-210/ M cm^2) (average 'shielded' rate of C18 & sites 41)	--->	17.76
US Activity fro (DPM/ cm^2)	--->	-1.17
Input Sedimen (DPM / g clay) (from proximal grab samples)	--->	1.76
CICCS Accum (grams clay / cm^2 yr)	--->	-0.02
CICCS Accum (grams / cm^2 yr)	--->	-0.08
CICCS Accum (cm / yr)	--->	-0.05

Avg. % Clay	Avg. Density
25.63	1.47

Assumed Supported --> (DPM/ g clay)	0.00
Assumed Den (g/cc)	1.50
Assumed Are (tube cross-section)	3.70

Present activity	
Confidence In	0.00
Original sedin	3.00
Background U	0.60
CIRCA Uncert	0.20
N/N_o	-0.25
S.E. (N/N_o)	-0.02
Predicted sed	#NUM!
S.E. (age)	#NUM!
minimum age	#NUM!
maximum age	#NUM!
Activity offset f	-1.5
Deposition dat	#NUM!

Present activity	
Confidence In	0.00
Original sedin	3.00
Background U	0.60
CIRCA Uncert	0.20
N/N_o	-0.25
S.E. (N/N_o)	-0.02
Predicted sed	#NUM!
S.E. (age)	#NUM!
minimum age	#NUM!
maximum age	#NUM!
Activity offset f	-1.5
Deposition dat	#NUM!

	--->	
Additional 'cap' activity (integrated tube DPM)		(DPM/cm^2) Cap activity
Assumed Mete (Atoms Pb-210/ M cm^2) (average 'shielded' rate of C18 & sites 41)	--->	17.76
Growth time fo	--->	0
Activity offset from 2000		-2.5
Deposition date		2002.5

depth	Density (measured)	unsupported activity / g clay	US activity / gram	Trapazoidal Depth-Integration of (activity * volume * density)
0.00	1.18	1.67	0.52	
1.00	1.18	1.67	0.52	2.25
3.00	1.20	1.05	0.34	3.75
5.00	1.18	1.98	0.65	4.34
7.00	1.26	3.00	0.95	7.23
9.00	1.29	1.64	0.51	6.86
11.00	1.79	2.43	0.63	6.47
21.00	2.34	0.40	0.08	27.31
31.00	1.77	0.00	0.00	3.21
41.00	1.44	0.00	0.00	0.00
65.20	1.50	0.00	0.00	0.00

^{210}Pb Profiles

Int. Err	Core	Depth (avg)	notes	Pb-210 DPM/g	dpm/g clay	dpm/g % < 2um	err	% Clay	%Silt	%Sand	% < 2um	notes
1	RASRF_127	1		0.85	4.57		0.44	18.62				AVG
1	RASRF_127	3		0.50	2.69	3.07	0.26	18.62	22.61	58.77	16.35	
1	RASRF_127	5		0.39	2.18		0.21	18.01				AVG
1	RASRF_127	7		0.43	2.48	2.93	0.30	17.40	16.38	66.22	14.68	
1	RASRF_127	9		0.47	2.16	2.45	0.22	21.61	16.49	61.91	19.05	
1	RASRF_127	11		0.47	3.10	3.48	0.32	15.32	18.43	66.25	13.63	
1	RASRF_127	15	silty sand	0.55	2.76		0.25	20.00				AVG
1	RASRF_127	21		0.78	2.78	3.39	0.28	28.03	52.37	19.61	22.97	
1	RASRF_127	31		0.33	4.68	5.49	0.54	6.99	5.98	87.03	5.96	
1	RASRF_127	41		0.37	2.18	2.45	0.22	16.69	10.24	73.08	14.87	
1	RASRF_127	51	sand	0.44	4.43		0.46	10.00				AVG
1	RASRF_127	65		0.34	3.49	3.99	0.35	9.70	8.77	81.52	8.50	

Supported Background (dpm/g clay)	XS clay activity	Radon Ventillation Effect	XS Activity (CVC)
2.815216901	1.75	-0.79	**2.54**
2.815216901	-0.12	-0.77	**0.65**
2.875048302	-0.70	-0.76	**0.06**
2.938277686	-0.46	-0.75	**0.29**
2.56248344	-0.40	-0.74	**0.34**
3.184520336	-0.09	-0.73	**0.64**
2.690678962	0.07	-0.70	**0.77**
2.173958166	0.60	-0.67	**1.27**
5.227600701	-0.55	-0.61	**0.06**
3.01704597	-0.83	-0.56	**-0.28**
4.169777103	0.26	-0.51	**0.76**
4.249470333	-0.76	-0.44	**-0.32**

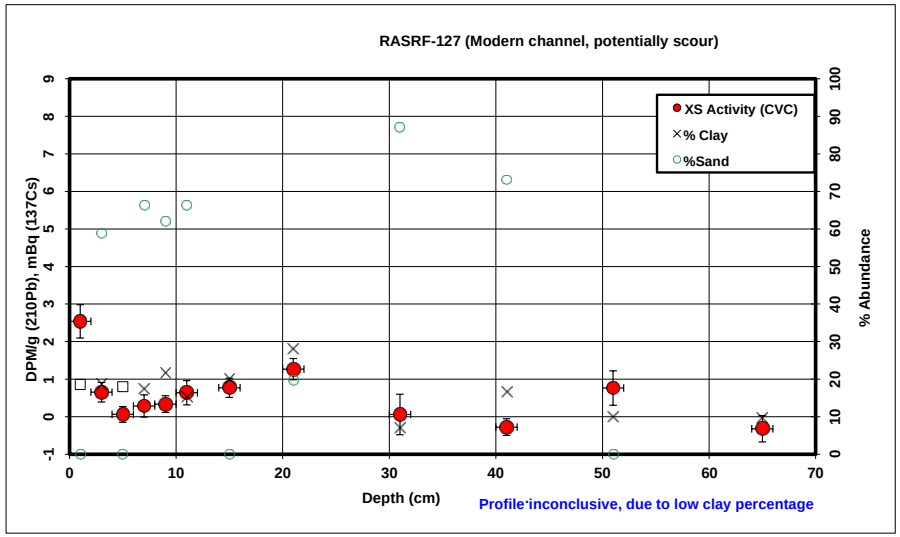

35.83	--->	9.68
Total integrated US activity (integrated tube DPM)		(DPM/cm^2) US activity
Assumed Mete (Atoms Pb-210/ M cm^2) (average 'shielded' rate of C18 & sites 41)	--->	17.76
US Activity fro (DPM/ cm^2)	--->	-8.08
Input Sedimen (DPM / g clay) (from proximal grab samples)	--->	1.76
CICCS Accum (grams clay / cm^2 yr)	--->	-0.14
CICCS Accum (grams / cm^2 yr)	--->	-0.85
CICCS Accum (cm / yr)	--->	-0.51

Avg. % Clay	Avg. Density
16.75	1.66

Assumed Supported -->	0.00
(DPM/ g clay)	
Assumed Den (g/cc)	1.50
Assumed Area (tube cross-section)	3.70

Present activity	
Confidence In	0.00
Original sedim	3.00
Background U	0.60
CIRCA Uncert	0.20
N/N$_o$	-0.25
S.E. (N/N$_o$)	-0.02
Predicted sed	#NUM!
S.E. (age)	#NUM!
minimum age	#NUM!
maximum age	#NUM!
Activity offset f	-1.5
Deposition dat	#NUM!

Present activity	
Confidence In	0.00
Original sedim	3.00
Background U	0.60
CIRCA Uncert	0.20
N/N$_o$	-0.25
S.E. (N/N$_o$)	-0.02
Predicted sed	#NUM!
S.E. (age)	#NUM!
minimum age	#NUM!
maximum age	#NUM!
Activity offset f	-1.5
Deposition dat	#NUM!

	--->	
Additional 'cap' activity (integrated tube DPM)		(DPM/cm^2) Cap activity
Assumed Mete (Atoms Pb-210/ M cm^2) (average 'shielded' rate of C18 & sites 41)	--->	17.76
Growth time fo	--->	0
Activity offset from 2000		-2.5
Deposition date		2002.5

depth	Density (measured)	unsupported activity / g clay	US activity / gram	Trapazoidal Depth-Integration of (activity * volume * density)
0.00	1.43	2.54	0.47	
1.00	1.43	2.54	0.47	2.50
3.00	1.55	0.65	0.12	3.28
5.00	1.54	0.06	0.01	0.76
7.00	1.64	0.29	0.05	0.36
9.00	1.70	0.34	0.07	0.76
11.00	1.65	0.64	0.10	1.06
15.00	1.61	0.77	0.15	3.04
21.00	2.06	1.27	0.36	10.38
31.00	2.06	0.06	0.00	13.70
41.00	1.62	0.00	0.00	
51.00	1.68	0.76	0.08	
65.00	1.50	0.00	0.00	

^{210}Pb Profiles

Int. Err	Core	Depth (avg)	notes	Pb-210 DPM/g	dpm/g clay	dpm/g % < 2um	err	% Clay	%Silt	%Sand	% < 2um	notes
1	RASRF_129	1		2.11	5.46	6.52	0.50	39.88	47.88	12.24	33.40	
1	RASRF_129	3		1.14	3.06		0.25	38.03				AVG
1	RASRF_129	5		0.77	2.15	2.55	0.21	36.18	48.37	15.45	30.51	
1	RASRF_129	7		0.66	1.75		0.15	37.83				AVG
1	RASRF_129	9		0.65	1.64	1.95	0.16	39.47	46.79	13.74	33.20	
1	RASRF_129	11		0.69	1.88		0.16	36.80				AVG
1	RASRF_129	13		0.58	1.65		0.16	36.00				AVG
1	RASRF_129	15		0.59	1.68		0.16	35.00				AVG
1	RASRF_129	17		0.57	1.62		0.16	34.50				AVG
1	RASRF_129	21		0.58	1.69	2.06	0.17	34.13	49.00	16.87	27.99	
1	RASRF_129	31		0.46	1.31	1.50	0.14	34.80	49.51	15.70	30.40	
1	RASRF_129	41		0.51	1.56	1.84	0.16	31.95	53.03	15.02	27.09	
1	RASRF_129	61		0.50	1.40		0.14	36.10				AVG
1.15	RASRF_129	85.15		0.61	1.50	1.78	0.15	40.24	53.51	6.25	33.98	

Supported Background (dpm/g clay)	XS clay activity	Radon Ventillation Effect	XS Activity (CVC)
1.739493988	3.72	-0.79	**4.50**
1.792515934	1.27	-0.77	**2.05**
1.849923122	0.30	-0.76	**1.06**
1.798639475	-0.05	-0.75	**0.70**
1.750872945	-0.11	-0.74	**0.63**
1.830139696	0.05	-0.73	**0.78**
1.855793545	-0.21	-0.71	**0.51**
1.889129963	-0.21	-0.70	**0.49**
1.906387458	-0.29	-0.69	**0.40**
1.919390124	-0.23	-0.67	**0.43**
1.896108766	-0.59	-0.61	**0.02**
2.00113253	-0.44	-0.56	**0.12**
1.852632865	-0.45	-0.46	**0.00**
1.7296079	-0.23	-0.35	**0.12**

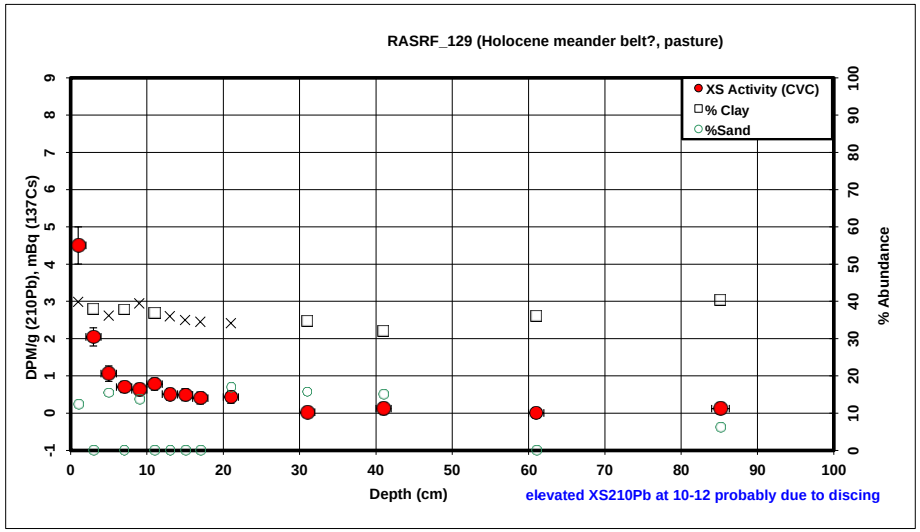

52.30	--->	14.13
Total integrated US activity (integrated tube DPM)		(DPM/cm^2) US activity
Assumed Mete (Atoms Pb-210/ M cm^2) (average 'shielded' rate of C18 & sites 41)	--->	17.76
US Activity fro (DPM/ cm^2)	--->	-3.63
Input Sedimen (DPM / g clay) (from proximal grab samples)	--->	1.76
CICCS Accum (grams clay / cm^2 yr)	--->	-0.06
CICCS Accum (grams / cm^2 yr)	--->	-0.18
CICCS Accum (cm / yr)	--->	-0.12

Avg. % Clay	Avg. Density
36.49	1.53

Assumed Supported -->	0.00
(DPM/ g clay)	
Assumed Den (g/cc)	1.50
Assumed Area (tube cross-section)	3.70

Present activi	0.66
Confidence In	0.00
Original sedim	1.76
Background US activity	
CIRCA Uncert	0.20
N/N$_o$	0.38
S.E. (N/N$_o$)	0.04
Predicted sed	31.35
S.E. (age)	3.67
minimum age	27.88
maximum age	35.24
Activity offset f	-9.9
Deposition dat	1978.5

Present activity	
Confidence In	#REF!
Original sedim	3.00
Background U	0.60
CIRCA Uncert	0.20
N/N$_o$	-0.25
S.E. (N/N$_o$)	#REF!
Predicted sed	#NUM!
S.E. (age)	#NUM!
minimum age	#REF!
maximum age	#REF!
Activity offset f	-1.5
Deposition dat	#NUM!

	--->	14.13
Additional 'cap' activity (integrated tube DPM)		(DPM/cm^2) Cap activity
Assumed Mete (Atoms Pb-210/ M cm^2) (average 'shielded' rate of C18 & sites 41)	--->	17.76
Growth time fo	--->	51.0856306
Activity offset from 2000		-9.9
Deposition date		1958.8

depth	Density (measured)	unsupported activity / g clay	US activity / gram	Trapazoidal Depth-Integration of (activity * volume * density)
0.00	1.23	4.50	1.80	
1.00	1.23	4.50	1.80	8.20
3.00	1.49	2.05	0.78	12.96
5.00	1.54	1.06	0.38	6.51
7.00	1.62	0.70	0.26	3.79
9.00	1.66	0.63	0.25	3.11
11.00	1.64	0.78	0.29	3.25
13.00	1.72	0.51	0.18	2.90
15.00	1.59	0.49	0.17	2.17
17.00	1.74	0.40	0.14	1.92
21.00	1.46	0.43	0.15	3.39
31.00	1.39	0.02	0.01	4.08
41.00	1.50	0.12	0.04	
61.00	1.41	0.00	0.00	
85.15	1.64	0.12	0.05	

^{210}Pb Profiles

Int. Err	Core	Depth (avg)	notes	Pb-210 DPM/g	dpm/g clay	dpm/g % < 2um	err	% Clay	%Silt	%Sand	% < 2um	notes
0.5	RASRF_130	0.5		2.28	5.00		0.48	46.77				AVG
0.5	RASRF_130	1.5		1.36	2.95	3.53	0.33	46.77	47.68	5.55	39.10	
0.5	RASRF_130	2.5		0.84	1.76		0.17	48.15				AVG
0.5	RASRF_130	3.5		0.66	1.32	1.53	0.15	49.52	43.42	7.05	42.79	
0.5	RASRF_130	4.5		0.85	1.85		0.17	46.33				AVG
0.5	RASRF_130	5.5		0.76	1.65		0.18	46.33		4.35		AVG
0.5	RASRF_130	6.5		0.70	1.51		0.15	46.33				AVG
0.5	RASRF_130	7.5		0.51	1.18	1.40	0.13	43.14	48.33	8.53	36.23	
0.5	RASRF_130	8.5		0.56	1.26		0.12	43.92				AVG
0.5	RASRF_130	9.5		0.56	1.23	1.42	0.14	44.69	48.96	6.35	38.70	
0.5	RASRF_130	10.5		0.54	1.23		0.12	43.33				AVG
0.5	RASRF_130	11.5		0.55	1.29	1.52	0.16	41.96	50.19	7.84	35.53	
0.5	RASRF_130	14.5		0.57	1.25		0.13	43.19				AVG
0.5	RASRF_130	20.5		0.60	1.34	1.56	0.14	44.41	49.26	6.33	38.02	
0.5	RASRF_130	30.5		0.55	1.43	1.72	0.16	38.42	50.14	11.45	31.93	
1	RASRF_130	41		0.59	1.46		0.14	39.09				AVG
0.5	RASRF_130	50		0.60	1.50	1.80	0.16	39.77	47.67	12.57	33.12	

Supported Background (dpm/g clay)	XS clay activity	Radon Ventillation Effect	XS Activity (CVC)
1.57291784	3.43	-0.79	4.22
1.57291784	1.38	-0.78	2.16
1.544327729	0.21	-0.78	0.99
1.517042061	-0.20	-0.77	0.57
1.58222664	0.27	-0.76	1.03
1.58222664	0.07	-0.76	0.83
1.58222664	-0.07	-0.75	0.68
1.655172695	-0.48	-0.75	0.27
1.636698058	-0.37	-0.74	0.37
1.618746675	-0.39	-0.73	0.34
1.650743739	-0.42	-0.73	0.30
1.684426807	-0.40	-0.72	0.33
1.654147631	-0.40	-0.70	0.30
1.625235141	-0.29	-0.67	0.38
1.781070553	-0.36	-0.61	0.26
1.76158206	-0.30	-0.56	0.25
1.742634854	-0.24	-0.51	0.27

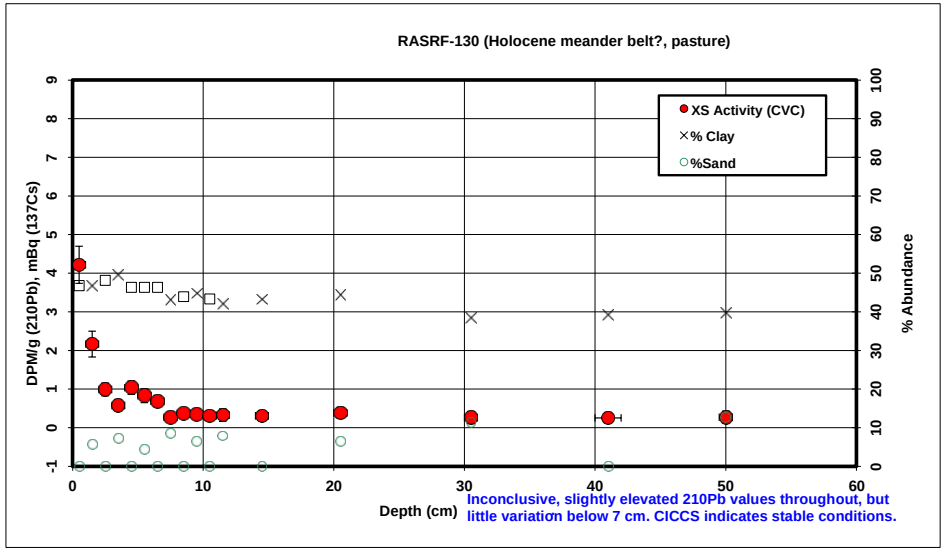

69.67	--->	18.83
Total integrated US activity (integrated tube DPM)		(DPM/cm^2) US activity
Assumed Mete (Atoms Pb-210/ M cm^2) (average 'shielded' rate of C18 & sites 41)	--->	17.76
US Activity fro (DPM/ cm^2)	--->	1.07
Input Sedimen (DPM / g clay) (from proximal grab samples)	--->	1.78
CICCS Accum (grams clay / cm^2 yr)	--->	0.02
CICCS Accum (grams / cm^2 yr)	--->	0.04
CICCS Accum (cm / yr)	--->	0.02

Avg. % Clay	Avg. Density
46.36	1.92

Assumed Supported --> (DPM/ g clay)	0.00
Assumed Den (g/cc)	1.50
Assumed Area (tube cross-section)	3.70

Present activi	0.25
Confidence In	0.00
Original sedin	1.76
Background US activity	
CIRCA Uncert	0.20
N/N_o	0.14
S.E. (N/N_o)	0.02
Predicted sed	62.73
S.E. (age)	3.67
minimum age	59.26
maximum age	66.62
Activity offset f	-1.5
Deposition dat	1938.8

Present activity	
Confidence In	1.50
Original sedin	3.00
Background U	0.60
CIRCA Uncert	0.20
N/N_o	-0.25
S.E. (N/N_o)	-0.63
Predicted sed	#NUM!
S.E. (age)	#NUM!
minimum age	#NUM!
maximum age	31.54
Activity offset f	-1.5
Deposition dat	#NUM!

	--->	18.83
Additional 'cap' activity (integrated tube DPM)		(DPM/cm^2) Cap activity
Assumed Mete (Atoms Pb-210/ M cm^2) (average 'shielded' rate of C18 & sites 41)	--->	17.76
Growth time fo	--->	#NUM!
Activity offset from 2000		-2.5
Deposition date		#NUM!

depth	Density (measured)	unsupported activity / g clay	US activity / gram	Trapazoidal Depth-Integration of (activity * volume * density)
0.00	1.54	4.22	1.97	
0.50	1.54	4.22	1.97	5.63
1.50	1.50	2.16	1.01	8.40
2.50	2.08	0.99	0.48	4.92
3.50	2.04	0.57	0.28	2.89
4.50	1.84	1.03	0.48	2.74
5.50	1.95	0.83	0.38	3.02
6.50	2.22	0.68	0.32	2.70
7.50	1.96	0.27	0.12	1.67
8.50	2.18	0.37	0.16	1.06
9.50	1.95	0.34	0.15	1.21
10.50	2.18	0.30	0.13	1.09
11.50	2.44	0.33	0.14	1.15
14.50	2.24	0.30	0.13	3.48
20.50	2.16	0.38	0.17	7.35
30.50	2.35	0.26	0.10	11.20
41.00	1.18	0.25	0.10	6.76
50.00	1.41	0.27	0.11	4.40

^{210}Pb Profiles

Int. Err	Core	Depth (avg)	notes	Pb-210 DPM/g	dpm/g clay	dpm/g % < 2um	err	% Clay	%Silt	%Sand	% < 2um	notes
0.5	RASRF_131	0.5		3.36	8.49		0.79	40.74				AVG
0.5	RASRF_131	1.5		1.83	4.59	5.87	0.49	40.74	54.75	4.51	31.85	
0.5	RASRF_131	2.5		1.35	3.43		0.35	40.01				AVG
0.5	RASRF_131	3.5		0.89	2.29	2.79	0.24	39.28	50.49	10.23	32.27	
0.5	RASRF_131	4.5		0.70	1.71		0.16	40.94				AVG
0.5	RASRF_131	5.5		0.62	1.45	1.73	0.16	42.60	47.83	9.57	35.56	
0.5	RASRF_131	6.5		0.57	1.34		0.14	41.98				AVG
0.5	RASRF_131	7.5		0.56	1.34	1.62	0.15	41.35	48.79	9.85	34.24	
0.5	RASRF_131	8.5		0.54	1.16		0.12	45.63				AVG
0.5	RASRF_131	9.5		0.53	1.04	1.21	0.12	49.91	39.23	10.87	43.20	
0.5	RASRF_131	10.5		0.58	1.20		0.12	47.31				AVG
0.5	RASRF_131	11.5		0.57	1.25	1.48	0.13	44.72	46.28	9.00	37.87	
0.5	RASRF_131	14.5		0.54	1.19		0.12	44.62				AVG
0.5	RASRF_131	20.5		0.57	1.26	1.44	0.13	44.52	44.66	10.83	38.76	
0.5	RASRF_131	30.5		0.57	1.27	1.47	0.14	44.05	45.45	10.50	38.04	
0.5	RASRF_131	45.5		0.55	1.22	1.44	0.14	44.82	43.43	11.75	37.91	

Supported Background (dpm/g clay)	XS clay activity	Radon Ventillation Effect	XS Activity (CVC)
1.716291919	6.78	-0.79	7.57
1.716291919	2.87	-0.78	3.65
1.73603809	1.69	-0.78	2.47
1.756381794	0.53	-0.77	1.30
1.710984918	0.00	-0.76	0.77
1.668499088	-0.22	-0.76	0.54
1.684100409	-0.34	-0.75	0.41
1.700084094	-0.36	-0.75	0.38
1.597579454	-0.44	-0.74	0.30
1.509647748	-0.47	-0.73	0.27
1.561430683	-0.36	-0.73	0.37
1.618064039	-0.36	-0.72	0.36
1.620404966	-0.44	-0.70	0.27
1.622754659	-0.36	-0.67	0.30
1.633529529	-0.36	-0.61	0.25
1.615806126	-0.40	-0.53	0.14

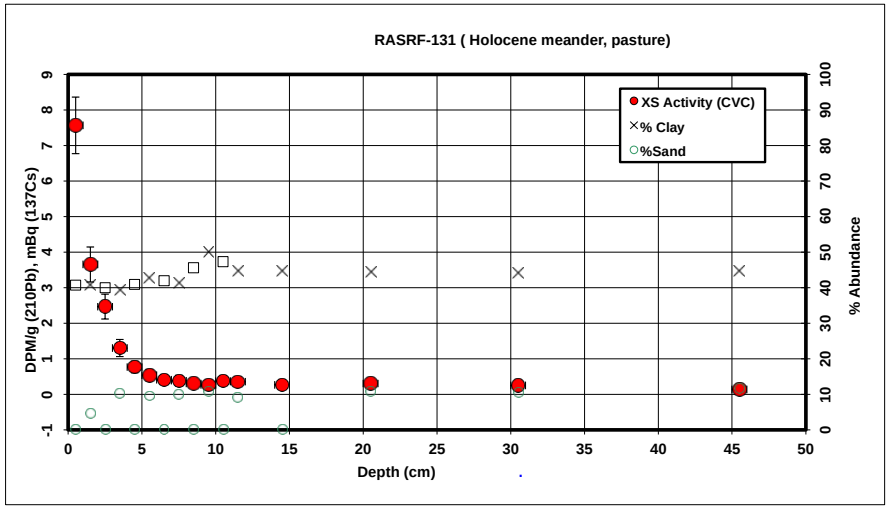

71.74	--->	19.39
Total integrated US activity (integrated tube DPM)		(DPM/cm^2) US activity
Assumed Mete	--->	17.76
(Atoms Pb-210/ M cm^2) (average 'shielded' rate of C18 & sites 41)		
US Activity fro	--->	1.62
(DPM/ cm^2)		
Input Sedimen	--->	1.76
(DPM / g clay) (from proximal grab samples)		
CICCS Accum	--->	0.03
(grams clay / cm^2 yr)		
CICCS Accum	--->	0.07
(grams / cm^2 yr)		
CICCS Accum	--->	0.04
(cm / yr)		

Avg. % Clay	Avg. Density
41.47	1.90

Assumed Supported --> (DPM/ g clay)	0.00
Assumed Den (g/cc)	1.50
Assumed Area (tube cross-section)	3.70

Present activi	0.14
Confidence In	0.05
Original sedin	1.76
Background US activity	
CIRCA Uncert	0.20
N/N_o	0.08
S.E. (N/N_o)	0.03
Predicted sed	81.44
S.E. (age)	12.44
minimum age	71.20
maximum age	96.55
Activity offset f	-1.5
Deposition dat	1920.1

Present activity	
Confidence In	1.22
Original sedin	3.00
Background U	0.60
CIRCA Uncert	0.20
N/N_o	-0.25
S.E. (N/N_o)	-0.51
Predicted sed	#NUM!
S.E. (age)	#NUM!
minimum age	#NUM!
maximum age	43.52
Activity offset f	-1.5
Deposition dat	#NUM!

	--->	19.39
Additional 'cap' activity (integrated tube DPM)		(DPM/cm^2) Cap activity
Assumed Mete	--->	17.76
(Atoms Pb-210/ M cm^2) (average 'shielded' rate of C18 & sites 41)		
Growth time fo	--->	#NUM!
Activity offset from 2000		-9.9
Deposition date		#NUM!

depth	Density (measured)	unsupported activity / g clay	US activity / gram	Trapazoidal Depth-Integration of (activity * volume * density)
0.00	1.49	7.57	3.08	
0.50	1.49	7.57	3.08	8.48
1.50	1.48	3.65	1.49	12.56
2.50	1.86	2.47	0.99	7.66
3.50	1.86	1.30	0.51	5.16
4.50	2.09	0.77	0.31	3.02
5.50	2.17	0.54	0.23	2.14
6.50	2.07	0.41	0.17	1.58
7.50	2.02	0.38	0.16	1.25
8.50	2.08	0.30	0.14	1.13
9.50	2.08	0.27	0.13	1.05
10.50	2.07	0.37	0.18	1.19
11.50	2.04	0.36	0.16	1.28
14.50	2.18	0.27	0.12	3.28
20.50	2.64	0.30	0.14	6.84
30.50	1.18	0.25	0.11	8.71
45.50	1.50	0.14	0.06	6.41

^{210}Pb Profiles

Int. Err	Core	Depth (avg)	notes	Pb-210 DPM/g	dpm/g clay	dpm/g % < 2um	err	% Clay	%Silt	%Sand	% < 2um	notes
0.5	RASRF_132	0.5		1.74	4.05		0.38	43.95				AVG
0.5	RASRF_132	1.5		1.11	2.56	3.54	0.28	43.95	40.73	15.32	31.79	
0.5	RASRF_132	2.5		0.89	2.05		0.21	43.80				AVG
0.5	RASRF_132	3.5		0.86	1.98	2.41	0.23	43.65	44.38	11.97	35.85	
0.5	RASRF_132	4.5		0.76	1.74		0.16	43.58				AVG
0.5	RASRF_132	5.5		0.73	1.68	2.11	0.17	43.52	48.16	8.32	34.57	
0.5	RASRF_132	6.5		0.76	1.64		0.15	46.72				AVG
0.5	RASRF_132	7.5		0.70	1.39	1.72	0.15	49.92	42.02	8.05	40.32	
0.5	RASRF_132	8.5		0.69	1.40		0.14	48.71				AVG
0.5	RASRF_132	9.5		0.65	1.37	1.69	0.15	47.50	45.40	7.10	38.37	
0.5	RASRF_132	10.5		0.67	1.30		0.13	50.79				AVG
0.5	RASRF_132	11.5		0.65	1.19	1.48	0.13	54.08	42.98	2.95	43.22	
0.5	RASRF_132	14.5		0.64	1.15		0.12	54.13				AVG
0.5	RASRF_132	20.5		0.63	1.16	1.57	0.13	54.18	43.87	1.95	39.84	
0.5	RASRF_132	30.5		0.73	1.23	1.66	0.15	59.70	38.45	1.85	44.10	
1	RASRF_132	41		0.73	1.33		0.13	55.00				AVG
1	RASRF_132	61		0.74	1.34		0.13	55.00				AVG
0.65	RASRF_132	81.15		0.72	1.27	1.59	0.15	56.68	40.88	2.43	45.28	

Supported Background (dpm/g clay)	XS clay activity	Radon Ventillation Effect	XS Activity (CVC)
1.635888959	2.41	-0.79	3.20
1.635888959	0.92	-0.78	1.71
1.639503506	0.41	-0.78	1.18
1.64313875	0.34	-0.77	1.11
1.644628152	0.09	-0.76	0.86
1.646121044	0.03	-0.76	0.79
1.573892718	0.06	-0.75	0.82
1.509317913	-0.12	-0.75	0.63
1.532936333	-0.13	-0.74	0.61
1.557533389	-0.19	-0.73	0.54
1.493040303	-0.19	-0.73	0.54
1.43501986	-0.25	-0.72	0.47
1.434151426	-0.28	-0.70	0.42
1.433284347	-0.28	-0.67	0.39
1.347989826	-0.12	-0.61	0.49
1.419723008	-0.09	-0.56	0.46
1.419723008	-0.08	-0.46	0.38
1.392942131	-0.13	-0.36	0.24

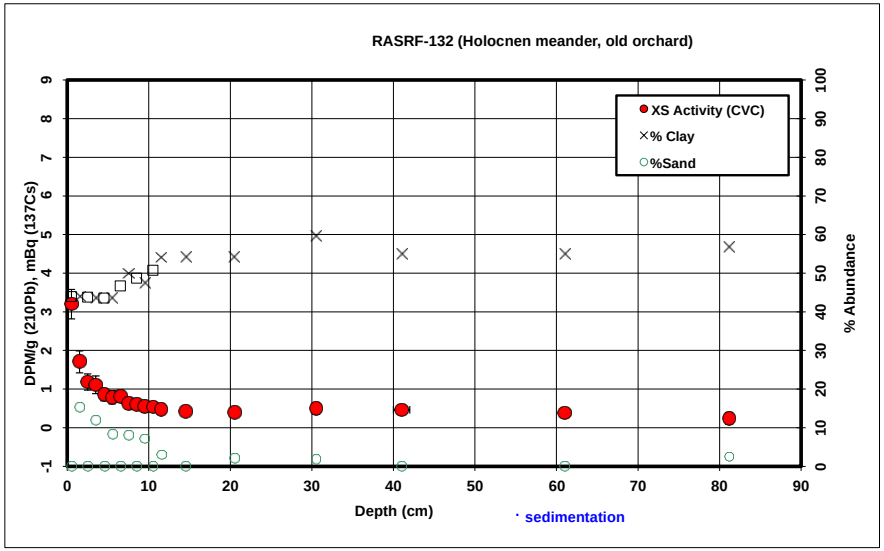

117.62	--->	31.79
Total integrated US activity (integrated tube DPM)		(DPM/cm^2) US activity
Assumed Mete (Atoms Pb-210/ M cm^2) (average 'shielded' rate of C18 & sites 41)	--->	17.76
US Activity fro (DPM/ cm^2)	--->	14.03
Input Sedimen (DPM / g clay) (from proximal grab samples)	--->	1.76
CICCS Accum (grams clay / cm^2 yr)	--->	0.25
CICCS Accum (grams / cm^2 yr)	--->	0.55
CICCS Accum (cm / yr)	--->	0.31

Avg. % Clay	Avg. Density
45.31	1.77

Assumed Supported --> (DPM/ g clay)	0.00
Assumed Den (g/cc)	1.50
Assumed Area (tube cross-section)	3.70
Present activi	0.27
Confidence In	0.05
Original sedim	1.76
Background US activity	
CIRCA Uncert	0.20
N/N_o	0.15
S.E. (N/N_o)	0.03
Predicted sed	60.31
S.E. (age)	7.06
minimum age	53.99
maximum age	68.19
Activity offset f	-1.5
Deposition dat	1941.2

Present activity	
Confidence In	1.27
Original sedim	3.00
Background U	0.60
CIRCA Uncert	0.20
N/N_o	-0.25
S.E. (N/N_o)	-0.53
Predicted sed	#NUM!
S.E. (age)	#NUM!
minimum age	#NUM!
maximum age	41.11
Activity offset f	-1.5
Deposition dat	#NUM!

	--->	
Additional 'cap' activity (integrated tube DPM)		(DPM/cm^2) Cap activity
Assumed Mete (Atoms Pb-210/ M cm^2) (average 'shielded' rate of C18 & sites 41)	--->	17.76
Growth time fo	--->	0
Activity offset from 2000		-2.5
Deposition date		2002.5

depth	Density (measured)	unsupported activity / g clay	US activity / gram	Trapazoidal Depth-Integration of (activity * volume * density)
0.00	1.41	3.20	1.41	
0.50	1.41	3.20	1.41	3.66
1.50	1.79	1.71	0.75	6.37
2.50	1.74	1.18	0.52	4.14
3.50	1.82	1.11	0.48	3.31
4.50	1.90	0.86	0.37	2.95
5.50	1.81	0.79	0.34	2.46
6.50	1.81	0.82	0.38	2.42
7.50	1.94	0.63	0.31	2.41
8.50	1.78	0.61	0.30	2.10
9.50	1.98	0.54	0.26	1.93
10.50	1.80	0.54	0.27	1.86
11.50	2.05	0.47	0.26	1.89
14.50	1.45	0.42	0.23	4.72
20.50	1.58	0.39	0.21	7.46
30.50	1.22	0.49	0.29	13.11
41.00	1.32	0.46	0.26	13.51
61.00	1.50	0.38	0.21	24.14
81.15	1.50	0.24	0.14	19.19

^{210}Pb Profiles

Int. Err	Core	Depth (avg)	notes	Pb-210 DPM/g	dpm/g clay	dpm/g % < 2um	err	% Clay	%Silt	%Sand	% < 2um	notes	Supported Background (dpm/g clay)	XS clay activity	Radon Ventillation Effect	XS Activity (CVC)
0.5	RASRF_133	0.5		1.09	2.40		0.24	46.15				AVG	1.586194072	0.81	-0.79	1.60
0.5	RASRF_133	1.5		1.02	2.23	2.70	0.25	46.15	47.45	6.40	38.19		1.586194072	0.65	-0.78	1.43
0.5	RASRF_133	2.5		0.87	1.95		0.20	45.15				AVG	1.608290638	0.34	-0.78	1.12
0.5	RASRF_133	3.5		0.80	1.81	2.16	0.21	44.15	44.76	11.09	37.15		1.631200003	0.18	-0.77	0.95
0.5	RASRF_133	4.5		0.77	1.68		0.18	45.77				AVG	1.594515174	0.09	-0.76	0.85
0.5	RASRF_133	5.5		0.79	1.67	2.00	0.19	47.39	42.52	10.09	39.45		1.559887652	0.11	-0.76	0.87
0.5	RASRF_133	6.5		0.81	1.77		0.17	45.94				AVG	1.590855274	0.18	-0.75	0.93
0.5	RASRF_133	7.5		0.78	1.77	2.10	0.20	44.48	44.58	10.94	37.51		1.623461976	0.15	-0.75	0.89
0.5	RASRF_133	8.5		0.85	1.92		0.19	44.37				AVG	1.626196091	0.29	-0.74	1.03
0.5	RASRF_133	9.5		0.81	1.83	2.26	0.20	44.25	45.28	10.47	35.83		1.628942128	0.20	-0.73	0.93
0.5	RASRF_133	10.5		0.69	1.48		0.16	46.23				AVG	1.584412013	-0.10	-0.73	0.62
0.5	RASRF_133	11.5		1.93	4.09	4.74	0.46	48.22	41.46	10.32	41.56	1st only	1.542895166	2.55	-0.72	3.27
0.5	RASRF_133	12.5		0.75	1.67		0.15	50.80				AVG	1.49280286	0.18	-0.72	0.89
0.5	RASRF_133	13.5		0.69	1.54		0.15	53.39				AVG	1.446705256	0.09	-0.71	0.80
0.5	RASRF_133	14.5		0.79	1.75		0.16	55.97				AVG	1.404112494	0.35	-0.70	1.05
0.5	RASRF_133	20.5		0.65	1.09	1.32	0.14	58.56	32.91	8.53	48.54	high error	1.364613921	-0.27	-0.67	0.40
0.5	RASRF_133	30.5		0.67	1.34	1.58	0.16	49.36	41.76	8.88	41.86		1.52027574	-0.18	-0.61	0.43
1	RASRF_133	41		0.61	1.19		0.12	50.00				AVG	1.507869642	-0.31	-0.56	0.24
1	RASRF_133	61		0.75	1.50		0.14	50.00				AVG	1.507869642	-0.01	-0.46	0.45
0.6	RASRF_133	78.6		0.73	1.21	1.54	0.15	59.66	38.39	1.95	47.08		1.348620841	-0.14	-0.38	0.24

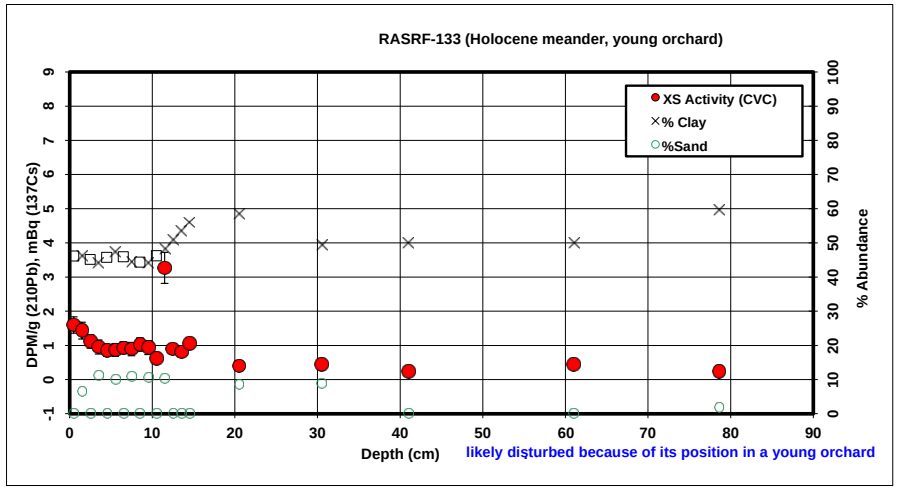

Assumed Supported -->		0.00
(DPM/ g clay)		
Assumed Den		2.00
(g/cc)		
Assumed Area		3.70
(tube cross-section)		

Present activit	0.92
Confidence In	1.50
Original sedin	1.76
Background US activity	
CIRCA Uncert	0.20
N/N_o	0.53
S.E. (N/N_o)	0.85
Predicted sed	20.73
S.E. (age)	#NUM!
minimum age	-10.36
maximum age	#NUM!
Activity offset f	-9.9
Deposition dat	1989.2

depth	Density (measured)	unsupported activity / g clay	US activity / gram	Trapazoidal Depth-Integration of (activity * volume * density)
0.00	1.78	1.60	0.74	
0.50	1.78	1.60	0.74	2.43
1.50	1.83	1.43	0.66	4.67
2.50	2.02	1.12	0.50	4.15
3.50	2.00	0.95	0.42	3.44
4.50	1.92	0.85	0.39	2.94
5.50	1.98	0.87	0.41	2.89
6.50	1.97	0.93	0.43	3.06
7.50	1.90	0.89	0.40	2.95
8.50	1.97	1.03	0.46	3.06
9.50	1.98	0.93	0.41	3.18
10.50	1.94	0.62	0.29	2.54
11.50	2.38	3.27	1.58	7.46
12.50	1.97	0.89	0.45	8.17
13.50	1.94	0.80	0.43	3.19
14.50	1.79	1.05	0.59	3.52
20.50	2.25	0.40	0.23	18.46
30.50	1.53	0.43	0.21	15.65
41.00	1.74	0.24	0.12	10.66
61.00	1.96	0.45	0.22	23.55
78.60	2.00	0.24	0.14	23.54

102.42	--->	27.68
Total integrated US activity (integrated tube DPM)		(DPM/cm^2) US activity
Assumed Mete	--->	17.76
(Atoms Pb-210/ M cm^2)		
(average 'shielded' rate of C18 & sites 41)		
US Activity fro	--->	9.92
(DPM/ cm^2)		
Input Sedimen	--->	1.76
(DPM / g clay)		
(from proximal grab samples)		
CICCS Accum	--->	0.18
(grams clay / cm^2 yr)		
CICCS Accum	--->	0.39
(grams / cm^2 yr)		
CICCS Accum	--->	0.20
(cm / yr)		

Avg. % Clay	Avg. Density
45.51	1.92

Present activity	
Confidence In	1.21
Original sedin	3.00
Background U	0.60
CIRCA Uncert	0.20
N/N_o	-0.25
S.E. (N/N_o)	-0.51
Predicted sed	#NUM!
S.E. (age)	#NUM!
minimum age	#NUM!
maximum age	43.94
Activity offset f	-1.5
Deposition dat	#NUM!

	--->	27.68
Additional 'cap' activity (integrated tube DPM)		(DPM/cm^2) Cap activity
Assumed Mete	--->	17.76
(Atoms Pb-210/ M cm^2)		
(average 'shielded' rate of C18 & sites 41)		
Growth time fc	--->	#NUM!
Activity offset from 2000		-9.9
Deposition date		#NUM!

^{210}Pb Profiles

Int. Err	Core	Depth (avg)	notes	Pb-210 DPM/g	dpm/g clay	dpm/g % < 2um	err	% Clay	%Silt	%Sand	% < 2um	notes
0.5	RASRF_134	0.5	est		5.50		1.00	43.00				est
0.5	RASRF_134	1.5		2.38	5.50	7.39	0.61	43.67	40.85	15.48	32.49	
0.5	RASRF_134	2.5		2.10	4.82	6.48	0.50	43.83	41.01	15.16	32.61	
0.5	RASRF_134	3.5		2.00	4.61	6.20	0.48	43.67	40.85	15.48	32.49	
0.5	RASRF_134	4.5		1.13	2.58		0.28	43.90				AVG
0.5	RASRF_134	5.5		0.91	2.06	2.62	0.23	44.13	35.47	20.40	34.73	
0.5	RASRF_134	6.5		0.81	1.90		0.18	42.71				AVG
0.5	RASRF_134	7.5		0.82	1.98	2.56	0.22	41.30	36.72	21.98	31.98	
0.5	RASRF_134	8.5		0.80	1.85		0.18	43.26				AVG
0.5	RASRF_134	9.5		0.85	1.87	2.34	0.20	45.22	35.69	19.08	36.15	
0.5	RASRF_134	10.5		0.77	1.73		0.17	44.62				AVG
0.5	RASRF_134	11.5		0.78	1.78	2.15	0.20	44.01	34.09	21.89	36.58	
0.5	RASRF_134	13.5		0.77	1.72		0.16	45.00				AVG
0.5	RASRF_134	15.5		0.70	1.56		0.16	45.00				AVG
0.5	RASRF_134	20.5		0.61	1.39	1.78	0.14	43.91	37.38	18.72	34.24	
0.5	RASRF_134	30.5		0.54	1.23	1.45	0.13	44.03	34.13	21.85	37.51	
0.5	RASRF_134	40.5		0.55	1.07	1.27	0.12	51.49	35.91	12.61	43.33	
0.7	RASRF_134	61.7		0.54	1.38	1.64	0.14	39.06	36.18	24.76	33.02	

Supported Background (dpm/g clay)	XS clay activity	Radon Ventillation Effect	XS Activity (CVC)
1.658673004	3.84	-0.79	**4.63**
1.642566648	3.85	-0.78	**4.64**
1.638675941	3.18	-0.78	**3.96**
1.642566648	2.97	-0.77	**3.74**
1.637167906	0.95	-0.76	**1.71**
1.631814749	0.43	-0.76	**1.19**
1.665733528	0.23	-0.75	**0.99**
1.701534879	0.28	-0.75	**1.03**
1.652370167	0.19	-0.74	**0.93**
1.606713617	0.27	-0.73	**1.00**
1.620408763	0.11	-0.73	**0.84**
1.634409471	0.15	-0.72	**0.87**
1.611693786	0.11	-0.71	**0.82**
1.611693786	-0.05	-0.70	**0.65**
1.636885986	-0.25	-0.67	**0.42**
1.634158587	-0.40	-0.61	**0.21**
1.480203628	-0.41	-0.56	**0.15**
1.762631672	-0.38	-0.45	**0.07**

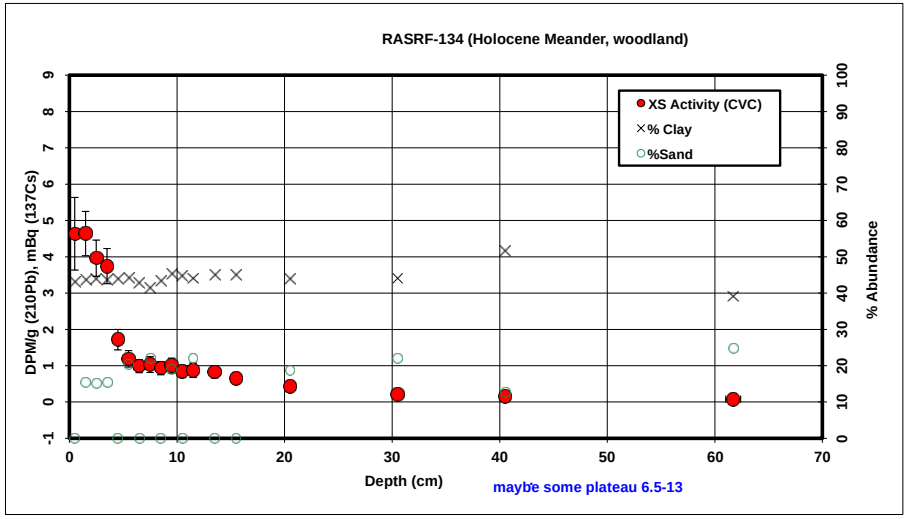

90.11	--->	24.35
Total integrated tube DPM)	US activity (integrated	(DPM/cm^2) US activity
Assumed Mete	--->	17.76
(Atoms Pb-210/ M cm^2) (average 'shielded' rate of C18 & sites 41)		
US Activity fro	--->	6.59
(DPM/ cm^2)		
Input Sedimen	--->	1.76
(DPM / g clay) (from proximal grab samples)		
CICCS Accum	--->	0.12
(grams clay / cm^2 yr)		
CICCS Accum	--->	0.27
(grams / cm^2 yr)		
CICCS Accum	--->	0.17
(cm / yr)		

Avg. % Clay	Avg. Density
43.47	1.57

Assumed Supported --> (DPM/ g clay)	0.00
Assumed Den (g/cc)	1.50
Assumed Area (tube cross-section)	3.70

Present activi	0.94
Confidence In	0.08
Original sedim	1.76
Background U	0.00
CIRCA Uncert	0.20
N/N_o	0.54
S.E. (N/N_o)	0.07
Predicted sed	20.01
S.E. (age)	4.49
minimum age	15.82
maximum age	24.82
Activity offset f	-9.9
Deposition dat	1989.9

Present activity	
Confidence In	1.38
Original sedim	3.00
Background U	0.60
CIRCA Uncert	0.20
N/N_o	-0.25
S.E. (N/N_o)	-0.58
Predicted sed	#NUM!
S.E. (age)	#NUM!
minimum age	#NUM!
maximum age	35.93
Activity offset f	-1.5
Deposition dat	#NUM!

	--->	24.35
Additional 'cap' activity (integrated tube DPM)		(DPM/cm^2) Cap activity
Assumed Mete	--->	17.76
(Atoms Pb-210/ M cm^2) (average 'shielded' rate of C18 & sites 41)		
Growth time fc	--->	#NUM!
Activity offset from 2000		-9.9
Deposition date		#NUM!

depth	Density (measured)	unsupported activity / g clay	US activity / gram	Trapazoidal Depth-Integration of (activity * volume * density)
0.00	1.50	4.63	1.99	
0.50	1.50	4.63	1.99	5.53
1.50	1.50	4.64	2.02	11.14
2.50	1.24	3.96	1.73	9.54
3.50	1.54	3.74	1.63	8.67
4.50	1.65	1.71	0.75	7.04
5.50	1.57	1.19	0.52	3.80
6.50	1.58	0.99	0.42	2.76
7.50	1.57	1.03	0.42	2.47
8.50	1.82	0.93	0.40	2.60
9.50	1.77	1.00	0.45	2.85
10.50	1.62	0.84	0.37	2.59
11.50	1.86	0.87	0.38	2.44
13.50	1.79	0.82	0.37	5.08
15.50	1.50	0.65	0.29	4.02
20.50	2.26	0.42	0.18	8.26
30.50	2.16	0.21	0.09	11.33
40.50	2.12	0.15	0.08	
61.70	1.50	0.07	0.03	

^{210}Pb Profiles

Int. Err	Core	Depth (avg)	notes	Pb-210 DPM/g	dpm/g clay	dpm/g % < 2um	err	% Clay	%Silt	%Sand	% < 2um	notes	Supported Background (dpm/g clay)	XS clay activity	Radon Ventillation Effect	XS Activity (CVC)
0.5	RASRF_135	0.5		2.13	4.77		0.43	45.00				est	1.611693786	3.16	-0.79	3.95
0.5	RASRF_135	1.5		1.78	3.97		0.36	45.00				est	1.611693786	2.36	-0.78	3.15
0.5	RASRF_135	2.5		1.55	3.47		0.32	45.00				est	1.611693786	1.85	-0.78	2.63
0.5	RASRF_135	3.5		1.49	3.33		0.31	45.00				est	1.611693786	1.72	-0.77	2.49
0.5	RASRF_135	4.5		1.31	2.92		0.28	45.00				est	1.611693786	1.31	-0.76	2.08
0.5	RASRF_135	5.5		1.01	2.24		0.22	45.00				est	1.611693786	0.63	-0.76	1.39
0.5	RASRF_135	6.5		1.09	2.43		0.23	45.00				est	1.611693786	0.82	-0.75	1.57
0.5	RASRF_135	7.5		0.86	1.93		0.20	45.00				est	1.611693786	0.31	-0.75	1.06
0.5	RASRF_135	8.5		0.94	2.09		0.20	45.00				est	1.611693786	0.48	-0.74	1.22
0.5	RASRF_135	9.5		0.77	1.71		0.18	45.00				est	1.611693786	0.10	-0.73	0.84
0.5	RASRF_135	10.5		0.91	2.02		0.20	45.00				est	1.611693786	0.41	-0.73	1.13
0.5	RASRF_135	11.5		0.87	1.94		0.17	45.00				est	1.611693786	0.33	-0.72	1.05
0.5	RASRF_135	14.5		0.78	1.75		0.17	45.00				est	1.611693786	0.14	-0.70	0.84
0.5	RASRF_135	20.5		0.68	1.52		0.14	45.00				est	1.611693786	-0.09	-0.67	0.57
0.5	RASRF_135	30.5		0.71	1.59		0.14	45.00				est	1.611693786	-0.03	-0.61	0.59
1	RASRF_135	41		0.60	1.32		0.13	45.00				est	1.611693786	-0.29	-0.56	0.27
1	RASRF_135	51		0.54	1.17		0.12	45.00				est	1.611693786	-0.44	-0.51	0.06
0.6	RASRF_135	62.6		0.55	1.23		0.11	45.00				est	1.611693786	-0.39	-0.45	0.06

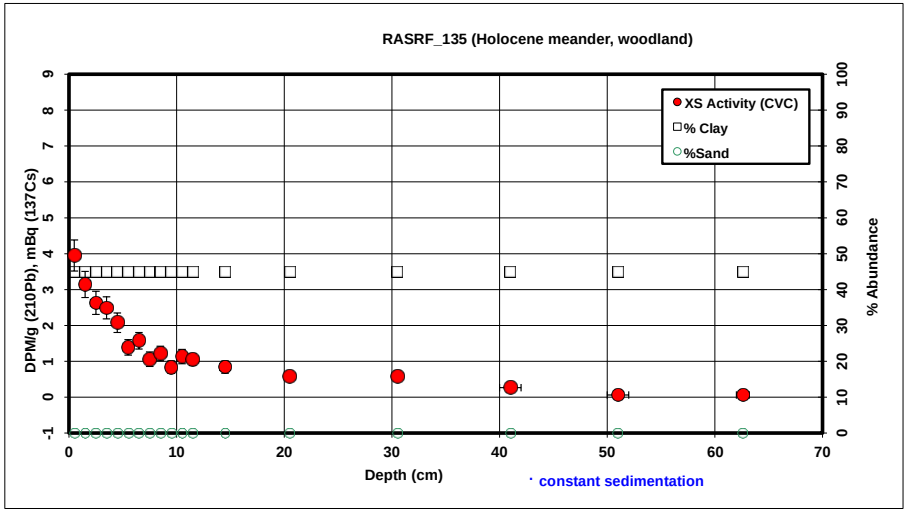

113.49	--->	30.67
Total integrated US activity (integrated tube DPM)		(DPM/cm^2) US activity
Assumed Mete (Atoms Pb-210/ M cm^2) (average 'shielded' rate of C18 & sites 41)	--->	17.76
US Activity fro (DPM/ cm^2)	--->	12.91
Input Sedimen (DPM / g clay) (from proximal grab samples)	--->	1.76
CICCS Accum (grams clay / cm^2 yr)	--->	0.23
CICCS Accum (grams / cm^2 yr)	--->	0.51
CICCS Accum (cm / yr)	--->	0.32

Avg. % Clay	Avg. Density
45.00	1.56

Assumed Supported --> (DPM/ g clay)	0.00
Assumed Den (g/cc)	1.50
Assumed Area (tube cross-section)	3.70

Present activity	
Confidence In	#REF!
Original sedim	3.00
Background U	0.60
CIRCA Uncert	0.20
N/N_o	-0.25
S.E. (N/N_o)	#REF!
Predicted sed	#NUM!
S.E. (age)	#NUM!
minimum age	#REF!
maximum age	#REF!
Activity offset f	-1.5
Deposition dat	#NUM!

Present activity	
Confidence In	1.75
Original sedim	3.00
Background U	0.60
CIRCA Uncert	0.20
N/N_o	-0.25
S.E. (N/N_o)	-0.73
Predicted sed	#NUM!
S.E. (age)	#NUM!
minimum age	#NUM!
maximum age	23.73
Activity offset f	-1.5
Deposition dat	#NUM!

	--->	
Additional 'cap' activity (integrated tube DPM)		(DPM/cm^2) Cap activity
Assumed Mete (Atoms Pb-210/ M cm^2) (average 'shielded' rate of C18 & sites 41)	--->	17.76
Growth time fc	--->	0
Activity offset from 2000		-2.5
Deposition date		2002.5

depth	Density (measured)	unsupported activity / g clay	US activity / gram	Trapazoidal Depth-Integration of (activity * volume * density)
0.00	1.50	3.95	1.78	
0.50	1.50	3.95	1.78	4.93
1.50	1.50	3.15	1.42	8.86
2.50	1.27	2.63	1.18	6.67
3.50	1.39	2.49	1.12	5.69
4.50	1.54	2.08	0.93	5.57
5.50	1.55	1.39	0.62	4.45
6.50	1.67	1.57	0.71	3.97
7.50	1.62	1.06	0.48	3.62
8.50	1.65	1.22	0.55	3.11
9.50	1.67	0.84	0.38	2.84
10.50	1.88	1.13	0.51	2.91
11.50	1.82	1.05	0.47	3.36
14.50	1.72	0.84	0.38	8.34
20.50	1.81	0.57	0.26	12.46
30.50	1.96	0.59	0.26	18.22
41.00	1.73	0.27	0.12	13.80
51.00	1.70	0.06	0.03	4.70
62.60	1.50	0.06	0.03	

^{210}Pb Profiles

Int. Err	Core	Depth (avg)	notes	Pb-210 DPM/g	dpm/g clay	dpm/g % < 2um	err	% Clay	%Silt	%Sand	% < 2um	notes
0.5	RASRF_136	0.5		2.01	4.57		0.42	45.00				est
0.5	RASRF_136	1.5		1.41	3.18		0.30	45.00				est
0.5	RASRF_136	2.5		0.98	2.20		0.22	45.00				est
0.5	RASRF_136	3.5		0.92	2.06		0.21	45.00				est
0.5	RASRF_136	4.5		0.83	1.85		0.19	45.00				est
0.5	RASRF_136	5.5		0.85	1.89		0.19	45.00				est
0.5	RASRF_136	6.5		0.85	1.90		0.20	45.00				est
0.5	RASRF_136	7.5		0.89	1.99		0.21	45.00				est
0.5	RASRF_136	8.5		0.91	2.03		0.20	45.00				est
0.5	RASRF_136	9.5		0.89	1.98		0.19	45.00				est
0.5	RASRF_136	10.5		0.85	1.90		0.19	45.00				est
0.5	RASRF_136	11.5		0.90	2.00		0.20	45.00				est
0.5	RASRF_136	14.5		0.87	1.95		0.17	45.00				est
0.5	RASRF_136	20.5		0.87	1.95		0.19	45.00				est
0.5	RASRF_136	25.5		0.69	1.54		0.15	45.00				est
0.5	RASRF_136	30.5		0.65	1.44		0.15	45.00				est
1	RASRF_136	41		0.75	1.67		0.16	45.00				est
1	RASRF_136	55		0.65	1.44		0.14	45.00				est
0.65	RASRF_136	69.65		0.67	1.49		0.16	45.00				est

Supported Background (dpm/g clay)	XS clay activity	Radon Ventillation Effect	XS Activity (CVC)
1.611693786	2.96	-0.79	3.75
1.611693786	1.57	-0.78	2.35
1.611693786	0.59	-0.78	1.37
1.611693786	0.45	-0.77	1.22
1.611693786	0.24	-0.76	1.00
1.611693786	0.28	-0.76	1.03
1.611693786	0.29	-0.75	1.04
1.611693786	0.38	-0.75	1.12
1.611693786	0.42	-0.74	1.16
1.611693786	0.37	-0.73	1.11
1.611693786	0.29	-0.73	1.02
1.611693786	0.39	-0.72	1.11
1.611693786	0.34	-0.70	1.04
1.611693786	0.34	-0.67	1.01
1.611693786	-0.08	-0.64	0.57
1.611693786	-0.17	-0.61	0.44
1.611693786	0.06	-0.56	0.61
1.611693786	-0.17	-0.49	0.32
1.611693786	-0.12	-0.42	0.29

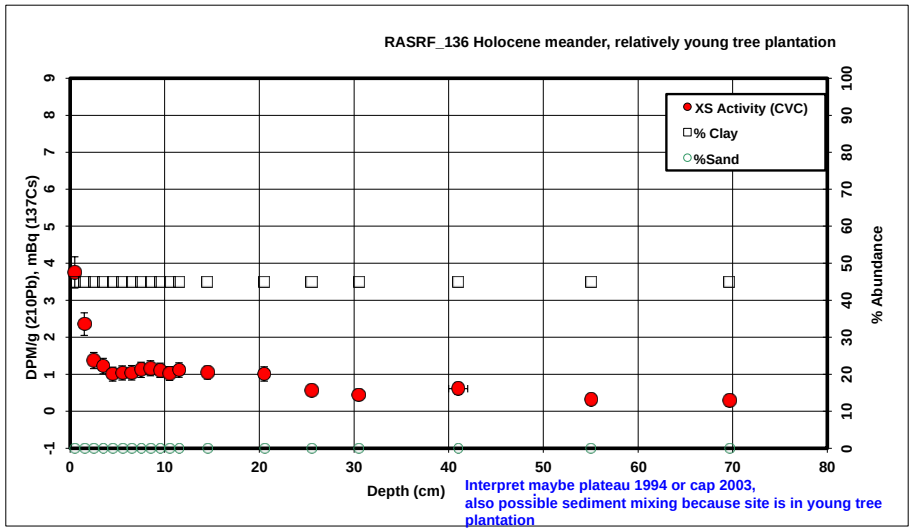

125.72	--->	33.98
Total integrated US activity (integrated tube DPM)		(DPM/cm^2) US activity
Assumed Mete (Atoms Pb-210/ M cm^2) (average 'shielded' rate of C18 & sites 41)	--->	17.76
US Activity fro (DPM/ cm^2)	--->	16.21
Input Sedimen (DPM / g clay) (from proximal grab samples)	--->	1.76
CICCS Accum (grams clay / cm^2 yr)	--->	0.29
CICCS Accum (grams / cm^2 yr)	--->	0.64
CICCS Accum (cm / yr)	--->	0.42

Avg. % Clay	Avg. Density
45.00	1.53

Assumed Supported --> (DPM/ g clay)	0.00
Assumed Den (g/cc)	1.50
Assumed Area (tube cross-section)	3.70

Present activit	0.30
Confidence In	0.06
Original sedim	1.76
Background US activity	
CIRCA Uncerta	0.20
N/N_o	0.17
S.E. (N/N_o)	0.04
Predicted sed	56.87
S.E. (age)	7.08
minimum age	50.53
maximum age	64.77
Activity offset f	-9.9
Deposition dat	1953.0

Present activity	
Confidence In	1.95
Original sedim	3.00
Background U	0.60
CIRCA Uncerta	0.20
N/N_o	-0.25
S.E. (N/N_o)	-0.81
Predicted sed	#NUM!
S.E. (age)	#NUM!
minimum age	#NUM!
maximum age	18.48
Activity offset f	-1.5
Deposition dat	#NUM!

	--->	33.98
Additional 'cap' activity (integrated tube DPM)		(DPM/cm^2) Cap activity
Assumed Mete (Atoms Pb-210/ M cm^2) (average 'shielded' rate of C18 & sites 41)	--->	17.76
Growth time fo	--->	#NUM!
Activity offset from 2000		-9.9
Deposition date		#NUM!

depth	Density (measured)	unsupported activity / g clay	US activity / gram	Trapazoidal Depth-Integration of (activity * volume * density)
0.00	1.43	3.75	1.69	
0.50	1.43	3.75	1.69	4.46
1.50	1.44	2.35	1.06	7.28
2.50	1.72	1.37	0.62	4.90
3.50	1.60	1.22	0.55	3.58
4.50	1.55	1.00	0.45	2.91
5.50	1.45	1.03	0.47	2.54
6.50	1.66	1.04	0.47	2.68
7.50	1.49	1.12	0.50	2.83
8.50	1.52	1.16	0.52	2.86
9.50	1.59	1.11	0.50	2.93
10.50	1.54	1.02	0.46	2.77
11.50	1.98	1.11	0.50	3.13
14.50	1.85	1.04	0.47	10.33
20.50	2.22	1.01	0.45	20.86
25.50	1.62	0.57	0.25	12.57
30.50	1.58	0.44	0.20	6.69
41.00	1.78	0.61	0.28	15.43
55.00	1.36	0.32	0.14	16.96
69.65	1.50	0.29	0.13	10.58

^{210}Pb Profiles

Int. Err	Core	Depth (avg	notes	Pb-210 DPM/g	dpm/g clay	dpm/g %<:err	% Clay	%Silt	%Sand	% < 2um	notes
1	RASRF_137	1		1.48	3.39	0.28	35.00				
1	RASRF_137	3		1.29	3.73	4.56	0.36	35.70	59.43	4.87	29.15
1	RASRF_137	5		1.26	3.93	0.34	33.00				
1	RASRF_137	7		1.05	3.25	0.28	33.00				
1	RASRF_137	9		0.65	1.96	0.18	33.00				
1	RASRF_137	11		0.52	1.66	1.94	0.18	30.84	43.84	25.32	26.35
1	RASRF_137	20	coarse sand	0.33	3.17	3.73	0.32	10.11	11.47	78.42	8.60
1	RASRF_137	31	fine sand	0.34	4.74	5.20	0.53	7.23	5.33	87.45	6.59
1	RASRF_137	48	fine sand	0.30	3.36	3.80	0.36	8.76	9.70	81.54	7.75

Supported Background (dpm/g clay)	XS clay activity	Radon Ventillation Effect	XS Activity (CVC)
1.889129963	1.50	-0.79	**2.28**
1.865743586	1.86	-0.77	**2.63**
1.960703979	1.97	-0.76	**2.73**
1.960703979	1.29	-0.75	**2.04**
1.960703979	0.00	-0.74	**0.74**
2.046224948	-0.39	-0.73	**0.34**
4.140944895	-0.97	-0.67	**-0.30**
5.11936518	-0.38	-0.61	**0.23**
4.534486538	-1.17	-0.52	**-0.65**

Assumed Supported -->	0.00
(DPM/ g clay)	
Assumed Den	1.50
(g/cc)	
Assumed Area	3.70
(tube cross-section)	

depth	Density (measured)	unsupported activity / g clay	US activity / gram	Trapazoidal Depth-Integration of (activity * volume * density)
0.00	1.12	2.28	0.80	
1.00	1.12	2.28	0.80	3.31
3.00	1.39	2.63	0.94	8.06
5.00	1.50	2.73	0.90	9.84
7.00	1.41	2.04	0.67	8.47
9.00	1.64	0.74	0.24	5.16
11.00	1.61	0.34	0.10	2.09
20.00	1.39	0.00	0.00	2.60
31.00	1.79	0.23	0.02	
48.00	2.09	0.00	0.00	

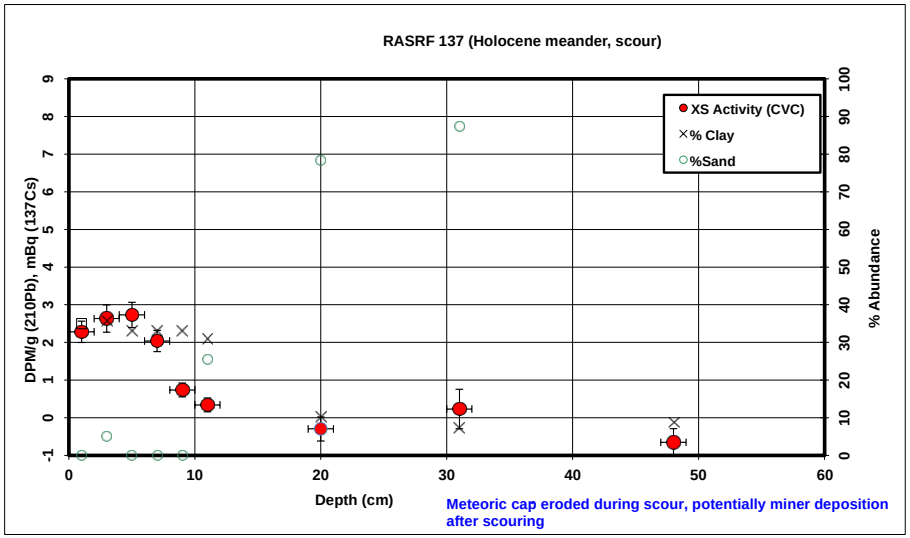

39.52	--->	10.68
Total integrated US activity (integrated tube DPM)		(DPM/cm^2) US activity
Assumed Mete	--->	17.76
(Atoms Pb-210/ M cm^2) (average 'shielded' rate of C18 & sites 41)		
US Activity fro	--->	-7.08
(DPM/ cm^2)		
Input Sedimen	--->	1.76
(DPM / g clay) (from proximal grab samples)		
CICCS Accum	--->	-0.13
(grams clay / cm^2 yr)		
CICCS Accum	--->	-0.50
(grams / cm^2 yr)		
CICCS Accum	--->	-0.33
(cm / yr)		

Avg. % Clay	Avg. Density
25.18	1.50

Present activit	0.29
Confidence In	0.05
Original sedim	1.76
Background US activity	
CIRCA Uncert	0.20
N/N_o	0.16
S.E. (N/N_o)	0.03
Predicted sed	58.01
S.E. (age)	6.70
minimum age	51.97
maximum age	65.45
Activity offset f	-1.5
Deposition dat	1943.5

Present activity	
Confidence In	0.00
Original sedim	3.00
Background U	0.60
CIRCA Uncert	0.20
N/N_o	-0.25
S.E. (N/N_o)	-0.02
Predicted sed	#NUM!
S.E. (age)	#NUM!
minimum age	#NUM!
maximum age	#NUM!
Activity offset f	-1.5
Deposition dat	#NUM!

	--->	10.68
Additional 'cap' activity (integrated tube DPM)		(DPM/cm^2) Cap activity
Assumed Mete	--->	17.76
(Atoms Pb-210/ M cm^2) (average 'shielded' rate of C18 & sites 41)		
Growth time fo	--->	29.5815874
Activity offset from 2000		-9.9
Deposition date		1980.3

^{210}Pb Profiles

Int. Err	Core	Depth (avg)	notes	Pb-210 DPM/g	dpm/g clay	dpm/g % < 2um	err	% Clay	%Silt	%Sand	% < 2um	notes
0.5	RASRF_142	0.5		1.33	2.46		0.23	55.00				AVG
0.5	RASRF_142	1.5		1.26	2.32		0.22	55.00				AVG
0.5	RASRF_142	2.5		1.33	2.45		0.23	55.00				AVG
0.5	RASRF_142	3.5		1.33	2.46		0.24	55.00				AVG
0.5	RASRF_142	4.5		1.25	2.30		0.22	55.00				AVG
0.5	RASRF_142	5.5		1.21	2.23		0.21	55.00				AVG
0.5	RASRF_142	6.5		1.16	2.14		0.20	55.00				AVG
0.5	RASRF_142	7.5		1.12	2.06		0.20	55.00				AVG
0.5	RASRF_142	8.5		1.17	2.14		0.21	55.00				AVG
0.5	RASRF_142	9.5		1.18	2.15	2.55	0.23	55.42	38.89	5.69	46.60	
0.5	RASRF_142	10.5		1.14	2.10		0.21	55.00				AVG
0.5	RASRF_142	12.5	piece of wood	0.96	2.15		0.22	55.00				AVG
0.5	RASRF_142	14.5	some wood	1.12	2.53		0.23	55.00				AVG
0.5	RASRF_142	17.5	big stones	0.60	1.31		0.13	55.00				AVG
0.5	RASRF_142	20.5		0.55	0.99		0.12	55.00				AVG
0.5	RASRF_142	26.5		0.88	1.98		0.19	55.00				AVG
0.65	RASRF_142	34.15		0.67	1.28	1.50	0.14	52.43	45.39	2.18	44.85	

Supported Background (dpm/g clay)	XS clay activity	Radon Ventillation Effect	XS Activity (CVC)
1.419723008	1.04	-0.79	1.82
1.419723008	0.90	-0.78	1.68
1.419723008	1.03	-0.78	1.80
1.419723008	1.04	-0.77	1.81
1.419723008	0.88	-0.76	1.65
1.419723008	0.81	-0.76	1.56
1.419723008	0.72	-0.75	1.47
1.419723008	0.64	-0.75	1.38
1.419723008	0.72	-0.74	1.46
1.412961014	0.73	-0.73	1.47
1.419723008	0.68	-0.73	1.41
1.419723008	0.54	-0.72	1.26
1.419723008	0.92	-0.71	1.62
1.419723008	-0.30	-0.69	0.38
1.419723008	-0.43	-0.67	0.24
1.419723008	0.37	-0.64	1.01
1.463357788	-0.18	-0.59	0.41

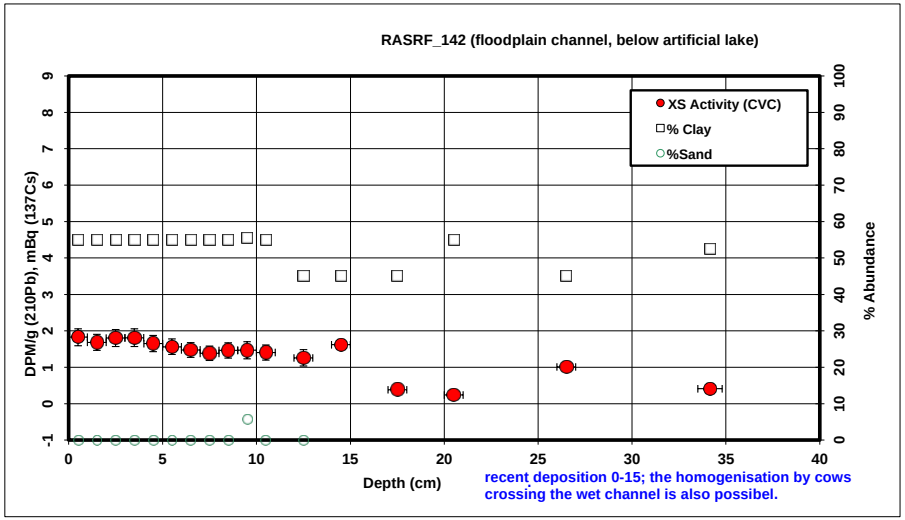

102.69	--->	27.75
Total integrated US activity (integrated tube DPM)		(DPM/cm^2) US activity
Assumed Mete (Atoms Pb-210/ M cm^2) (average 'shielded' rate of C18 & sites 41)	--->	17.76
US Activity fro (DPM/ cm^2)	--->	9.99
Input Sedimen (DPM / g clay) (from proximal grab samples)	--->	1.76
CICCS Accum (grams clay / cm^2 yr)	--->	0.18
CICCS Accum (grams / cm^2 yr)	--->	0.32
CICCS Accum (cm / yr)	--->	0.22

Avg. % Clay	Avg. Density
55.00	1.46

Assumed Supported --> (DPM/ g clay)	0.00
Assumed Den (g/cc)	1.50
Assumed Area (tube cross-section)	3.70

Present activit	0.39
Confidence In	0.05
Original sedim	1.76
Background US activity	
CIRCA Uncert	0.20
N/N_0	0.22
S.E. (N/N_0)	0.04
Predicted sed	48.48
S.E. (age)	5.55
minimum age	43.39
maximum age	54.53
Activity offset f	-1.5
Deposition dat	1953.0

Present activity	
Confidence In	2.15
Original sedim	3.00
Background U	0.60
CIRCA Uncert	0.20
N/N_0	-0.25
S.E. (N/N_0)	-0.90
Predicted sed	#NUM!
S.E. (age)	#NUM!
minimum age	#NUM!
maximum age	13.99
Activity offset f	-1.5
Deposition dat	#NUM!

	--->	
Additional 'cap' activity (integrated tube DPM)		(DPM/cm^2) Cap activity
Assumed Mete (Atoms Pb-210/ M cm^2) (average 'shielded' rate of C18 & sites 41)	--->	17.76
Growth time fo	--->	0
Activity offset from 2000		-2.5
Deposition date		2002.5

depth	Density (measured)	unsupported activity / g clay	US activity / gram	Trapazoidal Depth-Integration of (activity * volume * density)
0.00	1.50	1.82	1.00	
0.50	1.50	1.82	1.00	2.79
1.50	1.50	1.68	0.93	5.36
2.50	1.50	1.80	0.99	5.32
3.50	1.50	1.81	1.00	5.52
4.50	1.50	1.65	0.91	5.28
5.50	1.50	1.56	0.86	4.90
6.50	1.50	1.47	0.81	4.64
7.50	1.50	1.38	0.76	4.36
8.50	1.07	1.46	0.80	3.72
9.50	1.50	1.47	0.81	3.85
10.50	1.50	1.41	0.77	4.40
12.50	1.05	1.26	0.57	6.33
14.50	1.86	1.62	0.73	6.99
17.50	2.07	0.38	0.17	9.84
20.50	1.85	0.24	0.13	3.31
26.50	1.63	1.01	0.45	11.30
34.15	1.50	0.41	0.21	14.80

^{210}Pb Profiles

Int. Err	Core	Depth (avg)	notes	Pb-210 DPM/g	dpm/g clay	dpm/g % < 2um	err	% Clay	%Silt	%Sand	% < 2um	notes
0.5	RASRF_143	0.5		1.59	4.05		0.38	45.00				AVG
0.5	RASRF_143	1.5		1.36	3.12	4.00	0.33	44.35	49.00	6.65	34.62	
0.5	RASRF_143	2.5		1.23	2.59		0.25	48.00				AVG
0.5	RASRF_143	3.5		0.81	1.69		0.17	48.00				AVG
0.5	RASRF_143	4.5		0.69	1.44		0.15	48.00				AVG
0.5	RASRF_143	5.5		0.64	1.32		0.15	48.00				AVG
0.5	RASRF_143	6.5		0.67	1.38		0.15	48.00				AVG
0.5	RASRF_143	7.5		0.72	1.50		0.15	48.00				AVG
0.5	RASRF_143	8.5		0.82	1.70		0.17	48.00				AVG
0.5	RASRF_143	9.5		0.62	1.28		0.14	48.00				AVG
0.5	RASRF_143	10.5		0.54	1.10		0.13	48.00				AVG
0.5	RASRF_143	11.5		0.53	0.97	1.21	0.12	53.03	43.26	3.71	42.87	
0.5	RASRF_143	14.5		0.52	1.14		0.12	50.00				AVG
0.5	RASRF_143	20.5		0.53	1.04		0.12	50.00				AVG
0.5	RASRF_143	30.5		0.55	1.09		0.12	50.00				AVG
1	RASRF_143	41		0.53	1.15		0.12	50.00				AVG
0.55	RASRF_143	68.05		0.50	1.02	1.22	0.12	48.17	47.43	4.40	40.14	

Supported Background (dpm/g clay)	XS clay activity	Radon Ventillation Effect	XS Activity (CVC)
1.611693786	2.44	-0.79	**3.23**
1.62659828	1.50	-0.78	**2.28**
1.547278099	1.04	-0.78	**1.82**
1.547278099	0.14	-0.77	**0.91**
1.547278099	-0.10	-0.76	**0.66**
1.547278099	-0.23	-0.76	**0.53**
1.547278099	-0.16	-0.75	**0.59**
1.547278099	-0.05	-0.75	**0.69**
1.547278099	0.16	-0.74	**0.90**
1.547278099	-0.27	-0.73	**0.46**
1.547278099	-0.44	-0.73	**0.28**
1.452871515	-0.48	-0.72	**0.24**
1.507869642	-0.37	-0.70	**0.33**
1.507869642	-0.47	-0.67	**0.20**
1.507869642	-0.42	-0.61	**0.19**
1.507869642	-0.36	-0.56	**0.20**
1.543788169	-0.53	-0.42	**-0.10**

depth	Density (measured)	unsupported activity / g clay	US activity / gram	Trapazoidal Depth-Integration of (activity * volume * density)
0.00	1.42	3.23	1.45	
0.50	1.42	3.23	1.45	3.83
1.50	1.25	2.28	1.01	6.10
2.50	1.60	1.82	0.87	4.97
3.50	1.83	0.91	0.44	4.16
4.50	2.05	0.66	0.32	2.71
5.50	1.52	0.53	0.25	1.88
6.50	1.73	0.59	0.28	1.61
7.50	1.63	0.69	0.33	1.91
8.50	1.88	0.90	0.43	2.48
9.50	2.09	0.46	0.22	2.40
10.50	1.71	0.28	0.14	1.26
11.50	1.84	0.24	0.13	0.87
14.50	1.89	0.33	0.17	3.07
20.50	2.33	0.20	0.10	6.27
30.50	1.50	0.19	0.10	
41.00	1.50	0.20	0.10	
68.05	1.50	0.00	0.00	

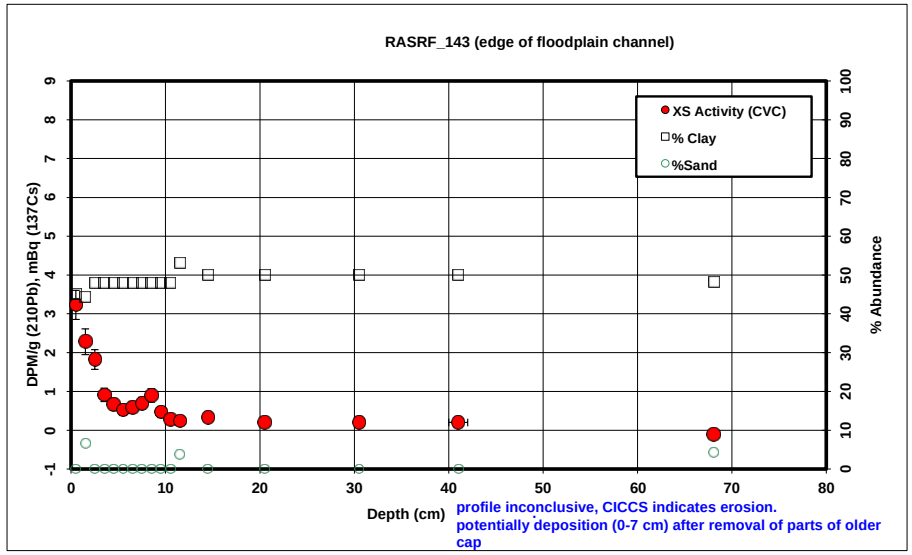

43.51	--->	11.76
Total integrated US activity (integrated tube DPM)		(DPM/cm^2) US activity
Assumed Mete	--->	17.76
(Atoms Pb-210/ M cm^2) (average 'shielded' rate of C18 & sites 41)		
US Activity fro	--->	-6.00
(DPM/ cm^2)		
Input Sedimen	--->	1.76
(DPM / g clay) (from proximal grab samples)		
CICCS Accum	--->	-0.11
(grams clay / cm^2 yr)		
CICCS Accum	--->	-0.22
(grams / cm^2 yr)		
CICCS Accum	--->	-0.13
(cm / yr)		

Avg. % Clay	Avg. Density
47.26	1.68

Assumed Supported -->	0.00
(DPM/ g clay)	
Assumed Den	1.50
(g/cc)	
Assumed Area	3.70
(tube cross-section)	

Present activi	0.56
Confidence Interval	
Original sedin	1.76
Background US activity	
CIRCA Uncert	0.20
N/N_o	0.32
S.E. (N/N_o)	0.04
Predicted sed	**36.89**
S.E. (age)	**3.67**
minimum age	33.42
maximum age	40.78
Activity offset f	-9.9
Deposition dat	1973.0

Present activity	
Confidence In	1.02
Original sedin	3.00
Background U	0.60
CIRCA Uncert	0.20
N/N_o	-0.25
S.E. (N/N_o)	-0.42
Predicted sed	#NUM!
S.E. (age)	#NUM!
minimum age	#NUM!
maximum age	56.19
Activity offset f	-1.5
Deposition dat	#NUM!

	--->	11.76
Additional 'cap' activity (integrated tube DPM)		(DPM/cm^2) Cap activity
Assumed Mete	--->	17.76
(Atoms Pb-210/ M cm^2) (average 'shielded' rate of C18 & sites 41)		
Growth time fo	--->	34.8995835
Activity offset from 2000		-9.9
Deposition date		1975.0

^{210}Pb Profiles

Int. Err	Core	Depth (avg)	notes	Pb-210 DPM/g	dpm/g clay	dpm/g % < 2um	err	% Clay	%Silt	%Sand	% < 2um	notes
0.5	RASRF_144	0.5		1.37	2.31		0.23	60.00				AVG
0.5	RASRF_144	1.5		1.58	2.48		0.24	65.00				AVG
0.5	RASRF_144	2.5		1.65	2.55	3.17	0.28	65.98	32.28	1.74	53.06	
0.5	RASRF_144	3.5		1.46	2.47		0.24	60.00				AVG
0.5	RASRF_144	4.5		1.21	2.03		0.21	60.00				AVG
0.5	RASRF_144	5.5		1.25	2.10		0.21	60.00				AVG
0.5	RASRF_144	6.5		1.28	2.16		0.22	60.00				AVG
0.5	RASRF_144	7.5		1.32	2.24		0.22	60.00				AVG
0.5	RASRF_144	8.5		1.39	2.36		0.23	60.00				AVG
0.5	RASRF_144	9.5		1.31	2.22		0.22	60.00				AVG
0.5	RASRF_144	10.5		1.29	2.18		0.22	60.00				AVG
0.5	RASRF_144	11.5		1.25	2.21	2.58	0.25	57.48	41.16	1.37	49.17	
0.5	RASRF_144	14.5		1.19	2.69		0.24	50.00				AVG
0.5	RASRF_144	20.5		0.71	1.42		0.16	50.00				AVG
0.5	RASRF_144	30.5		0.47	0.91		0.10	50.00				AVG
1	RASRF_144	41		0.52	1.13		0.11	50.00				AVG
0.5	RASRF_144	49.5		0.48	1.07	1.17	0.12	44.45	23.18	32.37	40.53	

Supported Background (dpm/g clay)	XS clay activity	Radon Ventillation Effect	XS Activity (CVC)
1.343758579	0.97	-0.79	**1.76**
1.277472615	1.20	-0.78	**1.98**
1.265462671	1.28	-0.78	**2.06**
1.343758579	1.12	-0.77	**1.89**
1.343758579	0.69	-0.76	**1.45**
1.343758579	0.76	-0.76	**1.52**
1.343758579	0.82	-0.75	**1.57**
1.343758579	0.89	-0.75	**1.64**
1.343758579	1.02	-0.74	**1.76**
1.343758579	0.88	-0.73	**1.61**
1.343758579	0.84	-0.73	**1.57**
1.380713683	0.83	-0.72	**1.55**
1.507869642	1.19	-0.70	**1.89**
1.507869642	-0.09	-0.67	**0.58**
1.507869642	-0.59	-0.61	**0.02**
1.507869642	-0.38	-0.56	**0.18**
1.624283666	-0.56	-0.51	**-0.05**

Assumed Supported -->	0.00
(DPM/ g clay)	
Assumed Den	1.25
(g/cc)	
Assumed Area	3.70
(tube cross-section)	

Present activity	
Confidence In	#REF!
Original sedim	3.00
Background U	0.60
CIRCA Uncerta	0.20
N/N_o	-0.25
S.E. (N/N_o)	#REF!
Predicted sed	#NUM!
S.E. (age)	#NUM!
minimum age	#REF!
maximum age	#REF!
Activity offset f	-1.5
Deposition dat	#NUM!

depth	Density (measured)	unsupported activity / g clay	US activity / gram	Trapazoidal Depth-Integration of (activity * volume * density)
0.00	1.25	1.76	1.06	
0.50	1.25	1.76	1.06	2.44
1.50	1.25	1.98	1.29	5.42
2.50	1.25	2.06	1.36	6.13
3.50	1.25	1.89	1.14	5.77
4.50	1.25	1.45	0.87	4.64
5.50	1.25	1.52	0.91	4.12
6.50	1.25	1.57	0.94	4.29
7.50	1.25	1.64	0.98	4.46
8.50	1.05	1.76	1.05	4.33
9.50	1.25	1.61	0.97	4.29
10.50	1.13	1.57	0.94	4.19
11.50	1.20	1.55	0.89	3.94
14.50	2.27	1.89	0.95	17.67
20.50	2.47	0.58	0.29	32.52
30.50	1.25	0.02	0.01	10.35
41.00	1.25	0.18	0.09	
49.50	1.25	0.00	0.00	

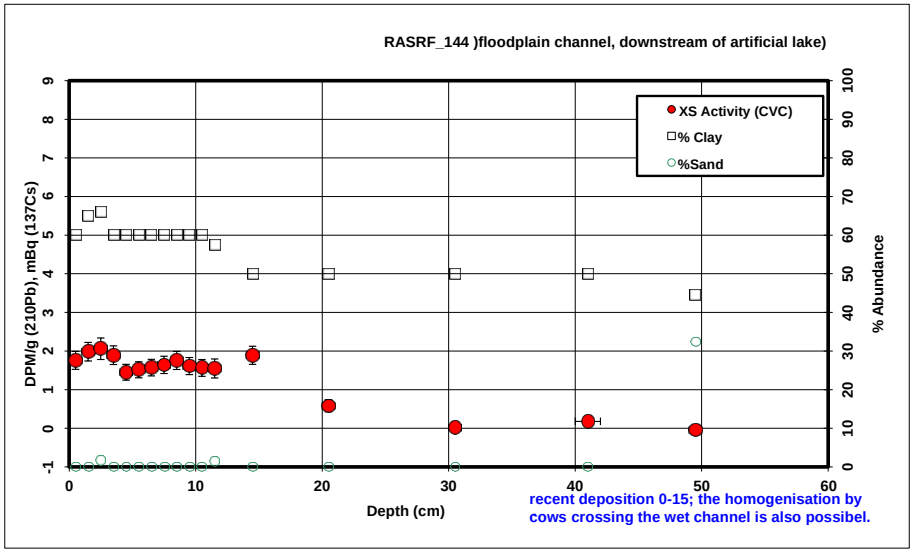

114.56	--->	30.96
Total integrated tube DPM)		(DPM/cm^2) US activity
Assumed Mete	--->	17.76
(Atoms Pb-210/ M cm^2)		
(average 'shielded' rate of C18 & sites 41)		
US Activity fro	--->	13.20
(DPM/ cm^2)		
Input Sedimen	--->	1.76
(DPM / g clay)		
(from proximal grab samples)		
CICCS Accum	--->	0.23
(grams clay / cm^2 yr)		
CICCS Accum	--->	0.38
(grams / cm^2 yr)		
CICCS Accum	--->	0.31
(cm / yr)		

Avg. % Clay	Avg. Density
61.22	1.22

Present activity	
Confidence In	1.07
Original sedim	3.00
Background U	0.60
CIRCA Uncerta	0.20
N/N_o	-0.25
S.E. (N/N_o)	-0.44
Predicted sed	#NUM!
S.E. (age)	#NUM!
minimum age	#NUM!
maximum age	52.66
Activity offset f	-1.5
Deposition dat	#NUM!

	--->	
Additional 'cap' activity		(DPM/cm^2)
(integrated tube DPM)		Cap activity
Assumed Mete	--->	17.76
(Atoms Pb-210/ M cm^2)		
(average 'shielded' rate of C18 & sites 41)		
Growth time fo	--->	0
Activity offset from 2000		-2.5
Deposition date		2002.5

^{210}Pb Profiles

Int. Err	Core	Depth (avg)	notes	Pb-210 DPM/g	dpm/g clay	dpm/g % < 2um	err	% Clay	%Silt	%Sand	% < 2um	notes
1	RASRF_146	1		2.88	6.69		0.54	45.00				est
0.5	RASRF_146	2.5		2.05	4.27		0.40	49.10				est
0.5	RASRF_146	3.5		1.95	4.06	5.33	0.43	49.10	48.61	2.30	37.39	
0.5	RASRF_146	4.5		1.94	3.87		0.36	51.14				AVG
0.5	RASRF_146	5.5		1.85	3.55	4.42	0.38	53.17	45.25	1.57	42.73	
0.5	RASRF_146	6.5		1.56	3.14		0.30	50.50				AVG
0.5	RASRF_146	7.5		1.33	2.83	3.55	0.31	47.82	50.05	2.13	38.11	
0.5	RASRF_146	8.5		1.22	2.45		0.24	50.67				AVG
0.5	RASRF_146	9.5		1.08	2.04	2.51	0.23	53.53	45.60	0.87	43.62	
0.5	RASRF_146	10.5		0.90	1.55		0.16	58.02				AVG
0.5	RASRF_146	11.5		0.86	1.37	1.67	0.16	62.52	31.48	6.00	51.56	
0.5	RASRF_146	14.5		0.86	1.57		0.15	55.00				AVG
0.5	RASRF_146	16.5		0.77	1.40		0.14	55.00				AVG
0.5	RASRF_146	20.5		0.40	0.82	0.96	0.11	47.13	41.61	11.26	40.55	
0.5	RASRF_146	30.5		0.35	0.60	0.68	0.09	55.10	29.97	14.93	48.98	
1	RASRF_146	41		0.52	0.91		0.10	56.60				AVG
0.5	RASRF_146	55.5		0.41	0.68	0.78	0.09	58.10	29.41	12.49	51.14	

Supported Background (dpm/g clay)	XS clay activity	Radon Ventillation Effect	XS Activity (CVC)
1.611693786	5.08	-0.79	5.87
1.525310702	2.74	-0.78	3.52
1.525310702	2.53	-0.77	3.30
1.486612359	2.38	-0.76	3.15
1.450351579	2.10	-0.76	2.86
1.498467246	1.64	-0.75	2.39
1.550933631	1.28	-0.75	2.03
1.495149267	0.95	-0.74	1.69
1.444267595	0.60	-0.73	1.33
1.372530835	0.18	-0.73	0.91
1.309326105	0.07	-0.72	0.79
1.419723008	0.15	-0.70	0.86
1.419723008	-0.02	-0.69	0.68
1.565182685	-0.74	-0.67	-0.07
1.41812092	-0.82	-0.61	-0.20
1.394270959	-0.48	-0.56	0.07
1.371429946	-0.69	-0.48	-0.21

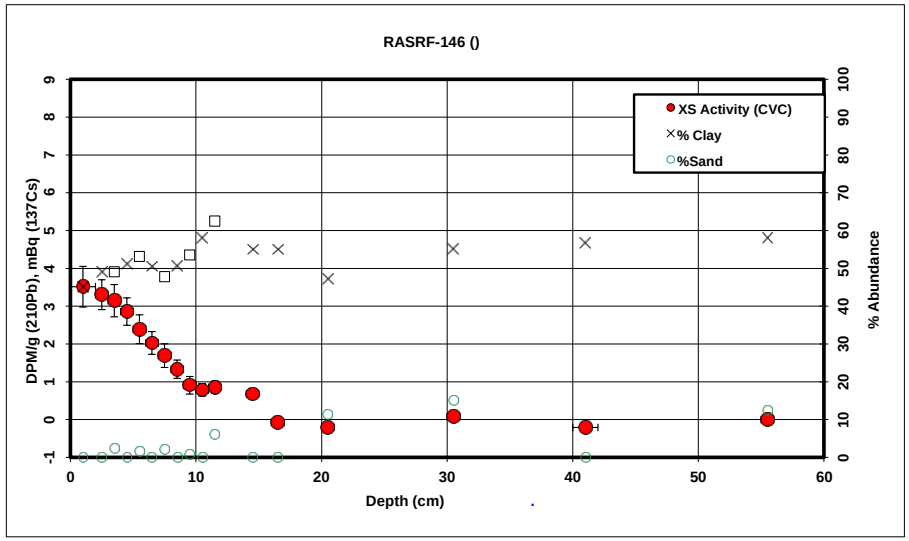

90.71	--->	24.52
Total integrated US activity (integrated tube DPM)		(DPM/cm^2) US activity
Assumed Mete (Atoms Pb-210/ M cm^2) (average 'shielded' rate of C18 & sites 41)	--->	17.76
US Activity fro (DPM/ cm^2)	--->	6.75
Input Sedimen (DPM / g clay) (from proximal grab samples)	--->	1.76
CICCS Accum (grams clay / cm^2 yr)	--->	0.12
CICCS Accum (grams / cm^2 yr)	--->	0.24
CICCS Accum (cm / yr)	--->	0.17

Avg. % Clay	Avg. Density
49.56	1.38

Assumed Supported --> (DPM/ g clay)	0.00
Assumed Den (g/cc)	1.50
Assumed Area (tube cross-section)	3.70
Present activit	0.82
Confidence In	0.05
Original sedim	1.76
Background US activity	
CIRCA Uncert	0.20
N/N_o	0.47
S.E. (N/N_o)	0.06
Predicted sed	24.45
S.E. (age)	4.14
minimum age	20.57
maximum age	28.87
Activity offset f	-9.9
Deposition dat	1985.4

Present activity	
Confidence In	0.68
Original sedim	3.00
Background U	0.60
CIRCA Uncert	0.20
N/N_o	-0.25
S.E. (N/N_o)	-0.29
Predicted sed	#NUM!
S.E. (age)	#NUM!
minimum age	#NUM!
maximum age	107.57
Activity offset f	-1.5
Deposition dat	#NUM!

	--->	24.52
Additional 'cap' activity (integrated tube DPM)		(DPM/cm^2) Cap activity
Assumed Mete (Atoms Pb-210/ M cm^2) (average 'shielded' rate of C18 & sites 41)	--->	17.76
Growth time fc	--->	#NUM!
Activity offset from 2000		-9.9
Deposition date		#NUM!

depth	Density (measured)	unsupported activity / g clay	US activity / gram	Trapazoidal Depth-Integration of (activity * volume * density)
0.00	1.08	5.87	2.64	
1.00	1.08	5.87	2.64	10.59
2.50	1.11	3.52	1.73	13.32
3.50	1.08	3.30	1.62	6.81
4.50	1.28	3.15	1.61	7.06
5.50	1.39	2.86	1.52	7.72
6.50	1.49	2.39	1.21	7.27
7.50	1.56	2.03	0.97	6.14
8.50	1.42	1.69	0.86	5.04
9.50	1.39	1.33	0.71	4.09
10.50	1.55	0.91	0.53	3.38
11.50	2.17	0.79	0.49	3.51
14.50	1.72	0.86	0.47	10.39
16.50	1.75	0.68	0.37	5.41
20.50	1.96	0.00	0.00	
30.50	2.07	0.00	0.00	
41.00	2.44	0.07	0.04	
55.50	1.50	0.00	0.00	

^{210}Pb Profiles

Int. Err	Core	Depth (avg)	notes	Pb-210 DPM/g	dpm/g clay	dpm/g % < 2um	err	% Clay	%Silt	%Sand	% < 2um	notes
0.5	RASRF_147	0.5		2.11	4.29		0.41	50.00				AVG
0.5	RASRF_147	1.5		1.22	2.39	3.01	0.27	51.58	45.83	2.59	40.93	
0.5	RASRF_147	2.5		1.23	2.25		0.23	55.00				AVG
0.5	RASRF_147	3.5		1.22	2.23		0.23	55.00				AVG
0.5	RASRF_147	4.5		0.86	1.57		0.17	55.00				AVG
0.5	RASRF_147	5.5		0.63	1.14		0.14	55.00				AVG
0.5	RASRF_147	6.5		0.76	1.37		0.16	55.00				AVG
0.5	RASRF_147	7.5		0.85	1.54		0.17	55.00				AVG
0.5	RASRF_147	8.5		0.94	1.71		0.18	55.00				AVG
0.5	RASRF_147	9.5		0.55	0.99		0.12	55.00				AVG
0.5	RASRF_147	10.5		0.48	0.86		0.10	55.00				AVG
0.5	RASRF_147	11.5		0.40	0.58	0.65	0.09	66.39	29.13	4.49	59.33	
0.5	RASRF_147	14.5		0.46	0.99		0.11	45.00				AVG
0.5	RASRF_147	20.5		0.48	0.73		0.09	65.00				AVG
0.5	RASRF_147	30.5		0.50	0.75		0.09	65.00				AVG
0.7	RASRF_147	43.7		0.48	0.73	0.84	0.09	63.77	31.40	4.83	55.85	

Supported Background (dpm/g clay)	XS clay activity	Radon Ventillation Effect	XS Activity (CVC)
1.507869642	2.79	-0.79	**3.57**
1.478530109	0.91	-0.78	**1.70**
1.419723008	0.83	-0.78	**1.61**
1.419723008	0.81	-0.77	**1.58**
1.419723008	0.15	-0.76	**0.92**
1.419723008	-0.28	-0.76	**0.48**
1.419723008	-0.05	-0.75	**0.70**
1.419723008	0.12	-0.75	**0.87**
1.419723008	0.29	-0.74	**1.03**
1.419723008	-0.43	-0.73	**0.30**
1.419723008	-0.55	-0.73	**0.17**
1.260533203	-0.68	-0.72	**0.04**
1.611693786	-0.62	-0.70	**0.08**
1.277472615	-0.55	-0.67	**0.12**
1.277472615	-0.53	-0.61	**0.09**
1.292983657	-0.56	-0.54	**-0.02**

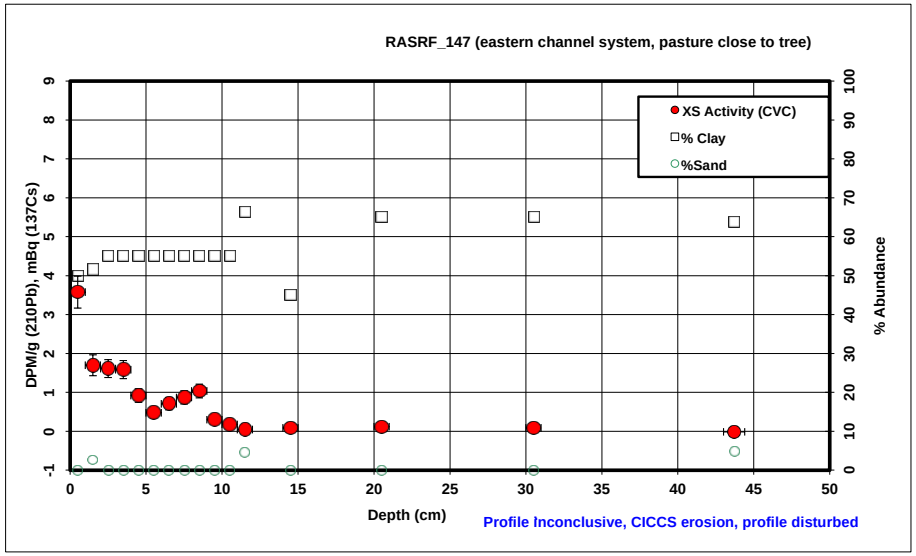

38.97	--->	10.53
Total integrated US activity (integrated tube DPM)		(DPM/cm^2) US activity
Assumed Mete (Atoms Pb-210/ M cm^2) (average 'shielded' rate of C18 & sites 41)	--->	17.76
US Activity fro (DPM/ cm^2)	--->	-7.23
Input Sedimen (DPM / g clay) (from proximal grab samples)	--->	1.76
CICCS Accum (grams clay / cm^2 yr)	--->	-0.13
CICCS Accum (grams / cm^2 yr)	--->	-0.24
CICCS Accum (cm / yr)	--->	-0.15

Avg. % Clay	Avg. Density
54.06	1.60

Assumed Supported --> (DPM/ g clay)	0.00
Assumed Den (g/cc)	1.50
Assumed Area (tube cross-section)	3.70

Present activit	1.63
Confidence In	0.06
Original sedim	1.76
Background US activity	
CIRCA Uncert	0.20
N/N_o	0.93
S.E. (N/N_o)	0.11
Predicted sed	**2.41**
S.E. (age)	**3.85**
minimum age	-1.22
maximum age	6.51
Activity offset f	-9.9
Deposition dat	**2007.5**

Present activity	
Confidence In	0.73
Original sedim	3.00
Background U	0.60
CIRCA Uncert	0.20
N/N_o	-0.25
S.E. (N/N_o)	-0.31
Predicted sed	**#NUM!**
S.E. (age)	**#NUM!**
minimum age	#NUM!
maximum age	92.29
Activity offset f	-1.5
Deposition dat	**#NUM!**

	--->	10.53
Additional 'cap' activity (integrated tube DPM)		(DPM/cm^2) Cap activity
Assumed Mete (Atoms Pb-210/ M cm^2) (average 'shielded' rate of C18 & sites 41)	--->	17.76
Growth time fc	--->	28.9176195
Activity offset from 2000		-9.9
Deposition date		**1981.0**

depth	Density (measured)	unsupported activity / g clay	US activity / gram	Trapazoidal Depth-Integration of (activity * volume * density)
0.00	1.42	3.57	1.79	
0.50	1.42	3.57	1.79	4.70
1.50	1.20	1.70	0.88	6.45
2.50	1.32	1.61	0.89	4.10
3.50	1.62	1.58	0.87	4.77
4.50	1.73	0.92	0.50	4.26
5.50	1.74	0.48	0.26	2.46
6.50	1.54	0.70	0.39	1.97
7.50	1.59	0.87	0.48	2.51
8.50	1.74	1.03	0.57	3.22
9.50	1.80	0.30	0.16	2.40
10.50	2.05	0.17	0.10	0.93
11.50	2.02	0.04	0.03	0.47
14.50	1.94	0.08	0.04	0.74
20.50	2.25	0.12	0.08	
30.50	1.50	0.09	0.06	
43.70	1.50	0.00	0.00	

^{210}Pb Profiles

Int. Err	Core	Depth (avg)	notes	Pb-210 DPM/g	dpm/g clay	dpm/g % < 2um	err	% Clay	%Silt	%Sand	% < 2um	notes	Supported Background (dpm/g clay)	XS clay activity	Radon Ventillation Effect	XS Activity (CVC)
0.5	RASRF_148	0.5		2.18	4.12		0.38	55.00				AVG	1.419723008	2.70	-0.79	3.49
0.5	RASRF_148	1.5		2.11	3.74	4.64	0.40	57.33	33.59	9.08	46.25		1.382936676	2.36	-0.78	3.14
0.5	RASRF_148	2.5		1.80	3.14		0.30	58.00				AVG	1.372860306	1.77	-0.78	2.54
0.5	RASRF_148	3.5		1.76	3.07		0.29	58.00				AVG	1.372860306	1.69	-0.77	2.46
0.5	RASRF_148	4.5		1.69	2.95		0.27	58.00				AVG	1.372860306	1.58	-0.76	2.34
0.5	RASRF_148	5.5		1.88	3.29		0.30	58.00				AVG	1.372860306	1.91	-0.76	2.67
0.5	RASRF_148	6.5		1.97	3.44		0.33	58.00				AVG	1.372860306	2.07	-0.75	2.82
0.5	RASRF_148	7.5		1.00	1.73		0.18	58.00				AVG	1.372860306	0.36	-0.75	1.11
0.5	RASRF_148	8.5		0.89	1.54		0.16	58.00				AVG	1.372860306	0.16	-0.74	0.90
0.5	RASRF_148	9.5		0.95	1.64		0.18	58.00				AVG	1.372860306	0.27	-0.73	1.01
0.5	RASRF_148	10.5		0.90	1.56		0.16	58.00				AVG	1.372860306	0.19	-0.73	0.92
0.5	RASRF_148	11.5		0.66	1.11	1.27	0.13	58.99	32.31	8.70	51.44		1.358280822	-0.25	-0.72	0.47
0.5	RASRF_148	14.5	stone 2cm	0.56	1.23		0.13	45.00				AVG	1.611693786	-0.38	-0.70	0.32
0.5	RASRF_148	20.5		0.48	0.87		0.09	55.00				AVG	1.419723008	-0.55	-0.67	0.12
0.5	RASRF_148	30.5		0.57	1.02		0.10	55.00				AVG	1.419723008	-0.40	-0.61	0.21
1	RASRF_148	41		0.56	1.23		0.12	45.00				AVG	1.611693786	-0.38	-0.56	0.18
0.65	RASRF_148	61.15		0.55	1.04	1.18	0.12	52.86	40.19	6.96	46.40		1.455856509	-0.42	-0.46	0.04

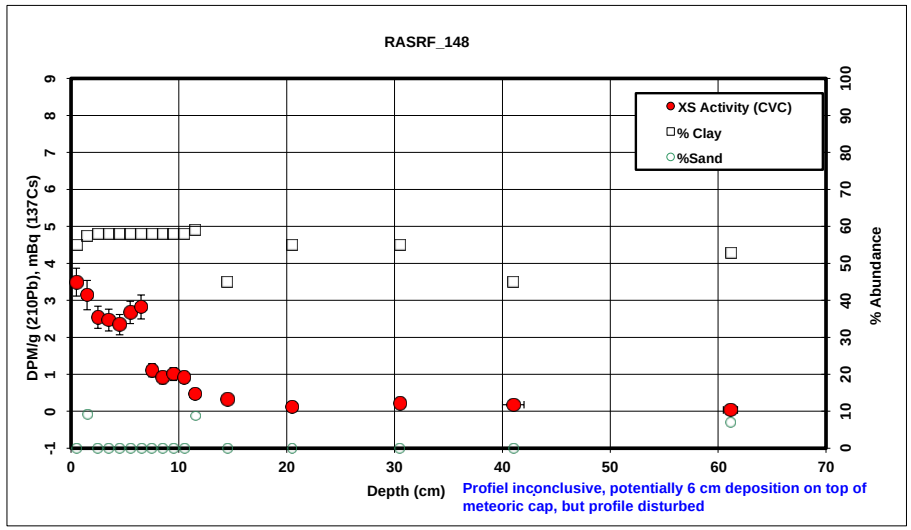

74.82	--->	20.22
Total integrated US activity (integrated tube DPM)		(DPM/cm^2) US activity

Assumed Mete (Atoms Pb-210/ M cm^2) (average 'shielded' rate of C18 & sites 41)	--->	17.76
US Activity fro (DPM/ cm^2)	--->	2.46
Input Sedimen (DPM / g clay) (from proximal grab samples)	--->	1.76
CICCS Accum (grams clay / cm^2 yr)	--->	0.04
CICCS Accum (grams / cm^2 yr)	--->	0.08
CICCS Accum (cm / yr)	--->	0.06

Avg. % Clay	Avg. Density
57.59	1.36

Assumed Supported --> (DPM/ g clay)	0.00
Assumed Den (g/cc)	1.50
Assumed Area (tube cross-section)	3.70

Present activi	0.98
Confidence In	0.10
Original sedin	1.76
Background US activity	
CIRCA Uncert	0.20
N/N_o	0.56
S.E. (N/N_o)	0.09
Predicted sed	18.66
S.E. (age)	4.93
minimum age	14.09
maximum age	23.99
Activity offset f	-9.9
Deposition dat	1991.2

Present activity	
Confidence In	1.04
Original sedin	3.00
Background U	0.60
CIRCA Uncert	0.20
N/N_o	-0.25
S.E. (N/N_o)	-0.43
Predicted sed	#NUM!
S.E. (age)	#NUM!
minimum age	#NUM!
maximum age	54.79
Activity offset f	-1.5
Deposition dat	#NUM!

	--->	20.22
Additional 'cap' activity (integrated tube DPM)		(DPM/cm^2) Cap activity
Assumed Mete (Atoms Pb-210/ M cm^2) (average 'shielded' rate of C18 & sites 41)	--->	17.76
Growth time fo	--->	#NUM!
Activity offset from 2000		-9.9
Deposition date		#NUM!

depth	Density (measured)	unsupported activity / g clay	US activity / gram	Trapazoidal Depth-Integration of (activity * volume * density)
0.00	1.50	3.49	1.92	
0.50	1.50	3.49	1.92	5.33
1.50	1.06	3.14	1.80	8.82
2.50	1.13	2.54	1.47	6.63
3.50	1.26	2.46	1.43	6.40
4.50	1.12	2.34	1.36	6.14
5.50	1.17	2.67	1.55	6.16
6.50	1.31	2.82	1.64	7.30
7.50	1.49	1.11	0.64	5.91
8.50	1.54	0.90	0.52	3.27
9.50	1.62	1.01	0.58	3.23
10.50	1.68	0.92	0.53	3.40
11.50	1.98	0.47	0.28	2.74
14.50	1.92	0.32	0.15	4.57
20.50	2.28	0.12	0.06	4.90
30.50	1.65	0.21	0.12	
41.00	1.73	0.18	0.08	
61.15	1.50	0.04	0.02	

^{210}Pb Profiles

Int. Err	Core	Depth (avg)	notes		Pb-210 DPM/g	dpm/g clay	dpm/g % < 2um	err	% Clay	%Silt	%Sand	% < 2um	notes
0.5	RASRF149	0.5		0	3.54	7.04	8.76	0.74	50.77	46.25	2.98	40.84	
0.5	RASRF149	1.5		0	1.81	3.55	4.46	0.37	51.32	45.31	3.37	40.84	
0.5	RASRF149	2.5		0	1.57	3.07	3.87	0.33	51.52	44.75	3.73	40.88	
0.5	RASRF149	3.5		0	1.62	3.16	4.00	0.34	51.42	44.69	3.89	40.66	
0.5	RASRF149	4.5		0	1.42	2.70	3.37	0.29	52.76	42.34	4.89	42.30	
0.5	RASRF149	5.5		0	1.58	2.95	3.64	0.31	53.84	40.91	5.25	43.76	
0.5	RASRF149	6.5		0	0.94	1.76	2.15	0.20	53.53	41.13	5.34	43.88	
0.5	RASRF149	7.5		0	0.70	1.32	1.60	0.15	53.20	41.40	5.40	43.95	
0.5	RASRF149	8.5		0	0.63	1.15	1.38	0.14	54.57	40.58	4.85	45.64	
0.5	RASRF149	9.5		0	0.59	1.06	1.25	0.13	55.68	39.55	4.77	47.16	
0.5	RASRF149	10.5		0	0.44	0.78	0.91	0.11	56.76	37.36	5.89	48.26	
0.5	RASRF149	11.5		0	0.57	1.00	1.17	0.11	56.86	34.52	8.62	48.62	
0.5	RASRF149	12.5		0	0.53	0.94		0.11	56.59				AVG
0.5	RASRF149	20.5		0	0.52	0.91	1.09	0.11	56.32	37.13	6.55	47.28	
0.5	RASRF149	30.5		0	0.43	0.70	0.81	0.10	60.69	31.90	7.41	52.36	
0.8	RASRF149	43.8		0	0.51	0.79	0.90	0.10	64.83	31.72	3.45	56.60	

Supported Background (dpm/g clay)	XS clay activity	Radon Ventillation Effect	XS Activity (CVC)
1.493294022	5.55	-0.79	6.34
1.483321229	2.07	-0.78	2.85
1.47960636	1.59	-0.78	2.37
1.481345308	1.68	-0.77	2.45
1.457497257	1.24	-0.76	2.01
1.439008006	1.52	-0.76	2.27
1.444313511	0.32	-0.75	1.07
1.449812453	-0.13	-0.75	0.61
1.426788837	-0.27	-0.74	0.47
1.408817219	-0.35	-0.73	0.39
1.391790076	-0.62	-0.73	0.11
1.390236543	-0.39	-0.72	0.34
1.394412127	-0.46	-0.72	0.26
1.398620251	-0.49	-0.67	0.18
1.334069748	-0.63	-0.61	-0.02
1.279603886	-0.49	-0.54	0.05

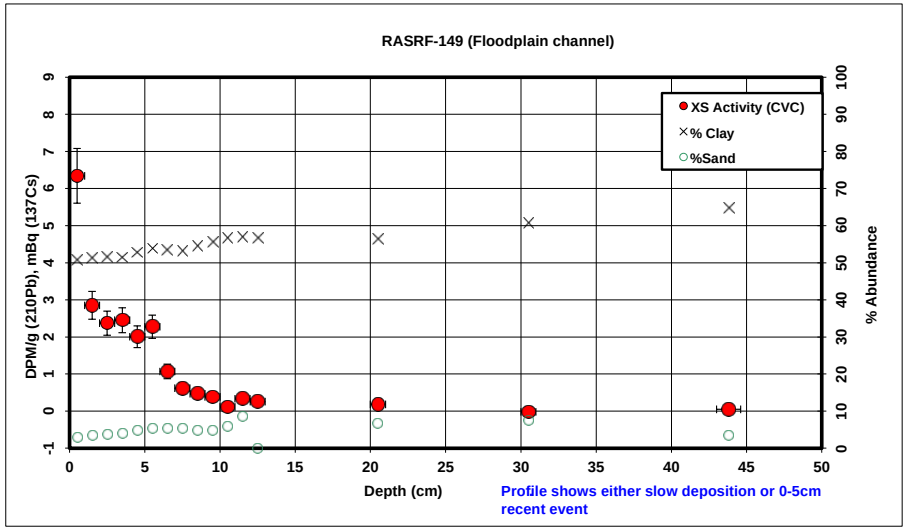

72.30	--->	19.54
Total integrated tube DPM)	US activity (integrated	(DPM/cm^2) US activity
Assumed Mete (Atoms Pb-210/ M cm^2) (average 'shielded' rate of C18 & sites 41)	--->	17.76
US Activity fro (DPM/ cm^2)	--->	1.78
Input Sedimen (DPM / g clay) (from proximal grab samples)	--->	1.76
CICCS Accum (grams clay / cm^2 yr)	--->	0.03
CICCS Accum (grams / cm^2 yr)	--->	0.06
CICCS Accum (cm / yr)	--->	0.04

Avg. % Clay	Avg. Density
52.86	1.67

Assumed Supported --> (DPM/ g clay)	0.00
Assumed Den (g/cc)	1.50
Assumed Area (tube cross-section)	3.70

Present activity	
Confidence In	0.00
Original sedim	3.00
Background U	0.60
CIRCA Uncert	0.20
N/N_o	-0.25
S.E. (N/N_o)	-0.02
Predicted sed	#NUM!
S.E. (age)	#NUM!
minimum age	#NUM!
maximum age	#NUM!
Activity offset f	-1.5
Deposition dat	#NUM!

Present activity	
Confidence In	0.94
Original sedim	3.00
Background U	0.60
CIRCA Uncert	0.20
N/N_o	-0.25
S.E. (N/N_o)	-0.39
Predicted sed	#NUM!
S.E. (age)	#NUM!
minimum age	#NUM!
maximum age	63.16
Activity offset f	-1.5
Deposition dat	#NUM!

	--->	19.54
Additional 'cap' activity (integrated tube DPM)		(DPM/cm^2) Cap activity
Assumed Mete (Atoms Pb-210/ M cm^2) (average 'shielded' rate of C18 & sites 41)	--->	17.76
Growth time fc	--->	#NUM!
Activity offset from 2000		-2.5
Deposition date		#NUM!

depth	Density (measured)	unsupported activity / g clay	US activity / gram	Trapazoidal Depth-Integration of (activity * volume * density)
0.00	1.55	6.34	3.22	
0.50	1.55	6.34	3.22	9.23
1.50	1.58	2.85	1.46	13.57
2.50	1.56	2.37	1.22	7.80
3.50	1.65	2.45	1.26	7.36
4.50	1.68	2.01	1.06	7.13
5.50	1.70	2.27	1.22	7.14
6.50	1.70	1.07	0.57	5.65
7.50	1.71	0.61	0.33	2.83
8.50	1.82	0.47	0.26	1.90
9.50	2.07	0.39	0.22	1.69
10.50	1.50	0.11	0.06	0.92
11.50	1.59	0.34	0.19	0.73
12.50	1.50	0.26	0.15	0.96
20.50	1.43	0.18	0.10	5.39
30.50	1.55	0.00	0.00	
43.80	1.50	0.05	0.03	

^{210}Pb Profiles

Int. Err	Core	Depth (avg)	notes	Pb-210 DPM/g	dpm/g clay	dpm/g % < 2um	err	% Clay	%Silt	%Sand	% < 2um	notes
1	RASRF_150	1		2.22	4.86	6.47	0.51	46.09	50.28	3.63	34.63	
0.5	RASRF_150	2.5		1.82	4.01	5.34	0.43	45.76	49.92	4.32	34.38	
0.5	RASRF_150	3.5		1.63	3.58	4.77	0.38	45.92	50.10	3.97	34.50	
0.5	RASRF_150	4.5		1.53	3.32	4.31	0.35	46.32	50.78	2.90	35.67	
0.5	RASRF_150	5.5		1.41	3.07	3.88	0.32	46.17	50.92	2.92	36.46	
0.5	RASRF_150	6.5		1.32	2.91	3.73	0.31	45.47	52.26	2.27	35.53	
0.5	RASRF_150	7.5		1.25	2.82	3.65	0.30	44.36	53.14	2.50	34.36	
0.5	RASRF_150	8.5		0.99	2.22	2.82	0.24	44.82	52.78	2.40	35.18	
0.5	RASRF_150	9.5		1.00	2.24	2.81	0.25	44.65	51.79	3.56	35.64	
0.5	RASRF_150	10.5		1.02	2.41	3.04	0.26	42.48	54.15	3.38	33.63	
0.5	RASRF_150	11.5		0.87	2.19	2.79	0.24	39.88	56.20	3.92	31.35	
1	RASRF_150	15		0.64	1.41		0.13	43.61				AVG
0.5	RASRF_150	20.5		0.64	1.34	1.62	0.14	47.34	45.71	6.94	39.20	
1	RASRF_150	25		0.49	0.95		0.10	51.03				AVG
0.5	RASRF_150	30.5		0.51	0.93	1.11	0.11	54.72	40.20	5.08	45.79	
1	RASRF_150	41		0.66	1.31		0.13	54.32				AVG
0.9	RASRF_150	54.9		0.47	0.87	1.03	0.10	53.93	37.94	8.13	45.53	

Supported Background (dpm/g clay)	XS clay activity	Radon Ventillation Effect	XS Activity (CVC)
1.587510239	3.27	-0.79	4.06
1.594770914	2.42	-0.78	3.19
1.591129882	1.99	-0.77	2.76
1.58259649	1.74	-0.76	2.50
1.585857989	1.48	-0.76	2.24
1.601154697	1.31	-0.75	2.06
1.626287051	1.20	-0.75	1.94
1.615767309	0.60	-0.74	1.34
1.61961388	0.62	-0.73	1.36
1.671568677	0.74	-0.73	1.46
1.739536905	0.45	-0.72	1.17
1.643948856	-0.23	-0.70	0.47
1.560841922	-0.22	-0.67	0.45
1.488546781	-0.54	-0.64	0.10
1.424309283	-0.50	-0.61	0.12
1.430876947	-0.12	-0.56	0.43
1.437523387	-0.56	-0.49	-0.08

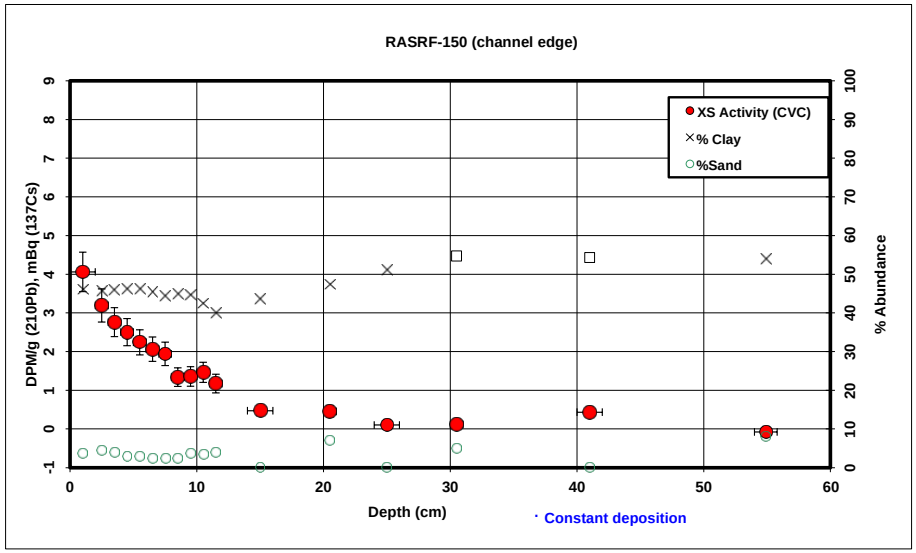

106.23	--->	28.71
Total integrated tube DPM)	US activity	(DPM/cm^2) US activity

Assumed Mete	--->	17.76
(Atoms Pb-210/ M cm^2)		
(average 'shielded' rate of C18 & sites 41)		

US Activity fro	--->	10.95
(DPM/ cm^2)		

Input Sedimen	--->	1.76
(DPM / g clay)		
(from proximal grab samples)		

CICCS Accum	--->	0.19
(grams clay / cm^2 yr)		
CICCS Accum	--->	0.43
(grams / cm^2 yr)		
CICCS Accum	--->	0.22
(cm / yr)		

Avg. % Clay	Avg. Density
45.51	1.97

Assumed Supported -->	0.00
(DPM/ g clay)	
Assumed Den	1.50
(g/cc)	
Assumed Area	3.70
(tube cross-section)	

Present activity	
Confidence In	0.00
Original sedim	3.00
Background U	0.60
CIRCA Uncert	0.20
N/N$_o$	-0.25
S.E. (N/N$_o$)	-0.02
Predicted sed	#NUM!
S.E. (age)	#NUM!
minimum age	#NUM!
maximum age	#NUM!
Activity offset f	-1.5
Deposition dat	#NUM!

Present activity	
Confidence In	1.41
Original sedim	3.00
Background U	0.60
CIRCA Uncert	0.20
N/N$_o$	-0.25
S.E. (N/N$_o$)	-0.59
Predicted sed	#NUM!
S.E. (age)	#NUM!
minimum age	#NUM!
maximum age	34.74
Activity offset f	-1.5
Deposition dat	#NUM!

	--->	
Additional 'cap' activity		(DPM/cm^2)
(integrated tube DPM)		Cap activity
Assumed Mete	--->	17.76
(Atoms Pb-210/ M cm^2)		
(average 'shielded' rate of C18 & sites 41)		
Growth time fc	--->	0
Activity offset from 2000		-2.5
Deposition date		2002.5

depth	Density (measured)	unsupported activity / g clay	US activity / gram	Trapazoidal Depth-Integration of (activity * volume * density)
0.00	1.56	4.06	1.87	
1.00	1.56	4.06	1.87	10.79
2.50	1.85	3.19	1.46	15.78
3.50	2.07	2.76	1.27	9.90
4.50	1.98	2.50	1.16	9.08
5.50	2.00	2.24	1.03	8.06
6.50	2.04	2.06	0.94	7.36
7.50	1.86	1.94	0.86	6.49
8.50	1.96	1.34	0.60	5.17
9.50	2.26	1.36	0.61	4.71
10.50	2.31	1.46	0.62	5.19
11.50	2.25	1.17	0.47	4.59
15.00	1.71	0.47	0.21	8.64
20.50	1.50	0.45	0.21	6.86
25.00	1.74	0.10	0.05	3.60
30.50	1.50	0.12	0.06	
41.00	1.11	0.43	0.24	
54.90	1.50	0.00	0.00	

^{210}Pb Profiles

Int. Err	Core	Depth (avg)	notes	Pb-210 DPM/g	dpm/g clay	dpm/g % < 2um	err	% Clay	%Silt	%Sand	% < 2um	notes
0.5	RASRF_151	0.5		1.29	2.81		0.27	46.59				AVG
0.5	RASRF_151	1.5		2.38	5.22		0.50	46.59				AVG
0.5	RASRF_151	2.5		2.28	5.01		0.48	46.59				AVG
0.5	RASRF_151	3.5		2.43	5.34	7.02	0.55	46.59	43.11	10.30	35.44	
0.5	RASRF_151	4.5		1.65	3.84		0.36	43.68				AVG
0.5	RASRF_151	5.5		1.06	2.63	3.36	0.29	40.76	54.82	4.41	31.89	
0.5	RASRF_151	6.5		0.93	2.26		0.22	41.68				AVG
0.5	RASRF_151	7.5		0.90	2.14	2.78	0.24	42.60	54.30	3.09	32.73	
0.5	RASRF_151	8.5		0.84	1.95		0.20	43.19				AVG
0.5	RASRF_151	9.5		0.74	1.70	2.11	0.19	43.78	51.88	4.33	35.13	
0.5	RASRF_151	10.5		0.71	1.67		0.17	42.85				AVG
0.5	RASRF_151	11.5		0.70	1.66	2.01	0.19	41.91	55.55	2.54	34.62	
0.5	RASRF_151	14.5		0.74	1.65		0.15	46.71				AVG
0.5	RASRF_151	20.5		0.69	1.33	1.64	0.16	51.51	42.69	5.80	41.81	
0.5	RASRF_151	30.5		0.58	1.30	1.57	0.15	44.25	49.64	6.11	36.72	
1	RASRF_151	41	small stones	0.63	1.24		0.12	49.84				AVG
0.65	RASRF_151	51.15		0.57	1.02	1.20	0.11	55.43	32.17	12.40	47.16	

Supported Background (dpm/g clay)	XS clay activity	Radon Ventillation Effect	XS Activity (CVC)
1.576689393	1.23	-0.79	2.02
1.576689393	3.64	-0.78	4.43
1.576689393	3.44	-0.78	4.21
1.576689393	3.76	-0.77	4.54
1.642358845	2.20	-0.76	2.96
1.71559066	0.92	-0.76	1.67
1.691573154	0.57	-0.75	1.32
1.668405095	0.47	-0.75	1.22
1.654001345	0.29	-0.74	1.03
1.63991438	0.06	-0.73	0.79
1.662427784	0.01	-0.73	0.73
1.685757035	-0.03	-0.72	0.69
1.574106012	0.07	-0.70	0.78
1.479744004	-0.15	-0.67	0.52
1.628937839	-0.33	-0.61	0.29
1.510916498	-0.27	-0.56	0.28
1.412711568	-0.39	-0.50	0.11

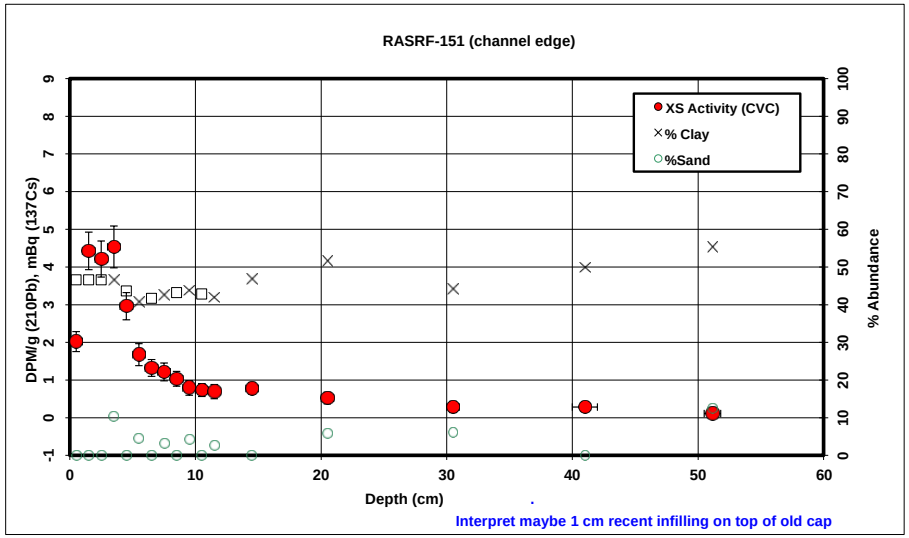

110.95	--->	29.99
Total integrated US activity (integrated tube DPM)		(DPM/cm^2) US activity
Assumed Mete (Atoms Pb-210/ M cm^2) (average 'shielded' rate of C18 & sites 41)	--->	17.76
US Activity fro (DPM/ cm^2)	--->	12.22
Input Sedimen (DPM / g clay) (from proximal grab samples)	--->	1.78
CICCS Accum (grams clay / cm^2 yr)	--->	0.22
CICCS Accum (grams / cm^2 yr)	--->	0.49
CICCS Accum (cm / yr)	--->	0.31

Avg. % Clay	Avg. Density
44.25	1.56

Assumed Supported --> (DPM/ g clay)	0.00
Assumed Den (g/cc)	1.50
Assumed Area (tube cross-section)	3.70
Present activit	0.10
Confidence In	0.05
Original sedim	1.76
Background US activity	
CIRCA Uncert	0.20
N/N_o	0.06
S.E. (N/N_o)	0.03
Predicted sed	92.21
S.E. (age)	17.55
minimum age	78.89
maximum age	115.34
Activity offset f	-9.9
Deposition dat	1917.7

Present activity	
Confidence In	1.02
Original sedim	3.00
Background U	0.60
CIRCA Uncert	0.20
N/N_o	-0.25
S.E. (N/N_o)	-0.42
Predicted sed	#NUM!
S.E. (age)	#NUM!
minimum age	#NUM!
maximum age	56.15
Activity offset f	-1.5
Deposition dat	#NUM!

	--->	
Additional 'cap' activity (integrated tube DPM)		(DPM/cm^2) Cap activity
Assumed Mete (Atoms Pb-210/ M cm^2) (average 'shielded' rate of C18 & sites 41)	--->	17.76
Growth time fo	--->	0
Activity offset from 2000		-2.5
Deposition date		2002.5

depth	Density (measured)	unsupported activity / g clay	US activity / gram	Trapazoidal Depth-Integration of (activity * volume * density)
0.00	1.50	2.02	0.94	
0.50	1.50	2.02	0.94	2.61
1.50	1.50	4.43	2.06	8.34
2.50	1.50	4.21	1.96	11.17
3.50	1.24	4.54	2.11	10.32
4.50	1.41	2.96	1.29	8.34
5.50	1.53	1.67	0.68	5.37
6.50	1.53	1.32	0.55	3.50
7.50	1.75	1.22	0.52	3.24
8.50	1.77	1.03	0.45	3.13
9.50	1.68	0.79	0.35	2.53
10.50	1.80	0.73	0.31	2.13
11.50	1.81	0.69	0.29	2.02
14.50	1.73	0.78	0.36	6.42
20.50	1.76	0.52	0.27	12.23
30.50	1.89	0.29	0.13	13.31
41.00	1.90	0.28	0.14	9.84
51.15	1.50	0.11	0.06	6.45

^{210}Pb Profiles

Int. Err	Core	Depth (avg)	notes	Pb-210 DPM/g	dpm/g clay	dpm/g % < 2um	err	% Clay	%Silt	%Sand	% < 2um	notes
0.5	RASRF_152	0.5		3.17	8.56		0.78	38.09				AVG
0.5	RASRF_152	1.5		2.68	7.21		0.67	38.09				AVG
0.5	RASRF_152	2.5		2.18	5.88	7.55	0.61	38.09	47.41	14.50	29.65	
0.5	RASRF_152	3.5		1.86	4.50	5.61	0.47	42.32	51.48	6.21	33.92	
0.5	RASRF_152	4.5		1.30	3.06		0.29	43.22				AVG
0.5	RASRF_152	5.5		0.97	2.22	2.64	0.24	44.11	52.01	3.88	37.16	
0.5	RASRF_152	6.5		0.96	2.19		0.22	44.32				AVG
0.5	RASRF_152	7.5		0.93	2.10	2.58	0.23	44.52	52.85	2.63	36.34	
0.5	RASRF_152	8.5		0.91	1.98		0.20	46.23				AVG
0.5	RASRF_152	9.5		0.97	2.05	2.46	0.22	47.95	50.45	1.60	39.95	
0.5	RASRF_152	10.5		0.87	1.78		0.19	49.01				AVG
0.5	RASRF_152	11.5		0.74	1.49	1.79	0.17	50.08	47.60	2.32	41.50	
0.5	RASRF_152	13.5		0.59	1.16		0.12	50.00				AVG
0.5	RASRF_152	15.5		0.65	1.28		0.12	50.00				AVG
0.5	RASRF_152	20.5		0.65	1.35	1.64	0.16	47.60	49.88	2.53	39.12	
0.5	RASRF_152	30.5		0.66	1.28	1.58	0.15	51.48	47.50	1.02	41.87	
1	RASRF_152	41		0.59	1.17		0.12	51.73				AVG
0.55	RASRF_152	56.05		0.57	1.09	1.31	0.14	51.98	47.05	0.97	43.17	A

Supported Background (dpm/g clay)	XS clay activity	Radon Ventillation Effect	XS Activity (CVC)
1.790866261	6.77	-0.79	7.56
1.790866261	5.42	-0.78	6.21
1.790866261	4.09	-0.78	4.86
1.675577601	2.82	-0.77	3.59
1.653452807	1.40	-0.76	2.17
1.632066975	0.59	-0.76	1.35
1.627348921	0.56	-0.75	1.31
1.622665927	0.48	-0.75	1.23
1.584355971	0.40	-0.74	1.14
1.54829759	0.50	-0.73	1.23
1.52697586	0.26	-0.73	0.99
1.506396188	-0.02	-0.72	0.70
1.507869642	-0.34	-0.71	0.37
1.507869642	-0.22	-0.70	0.48
1.555552343	-0.20	-0.67	0.47
1.480291979	-0.20	-0.61	0.42
1.475769229	-0.31	-0.56	0.25
1.47128199	-0.39	-0.48	0.09

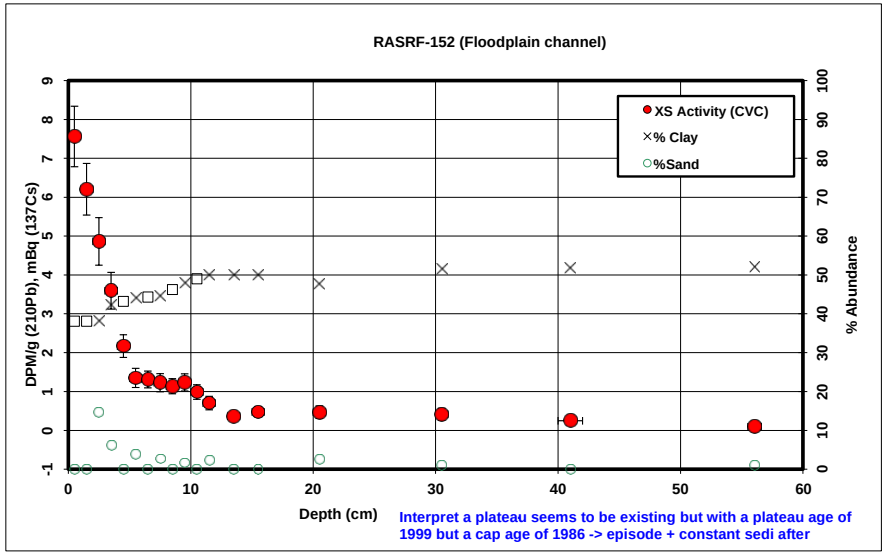

114.92	--->	31.06
Total integrated US activity (integrated tube DPM)		(DPM/cm^2) US activity
Assumed Mete	--->	17.76
(Atoms Pb-210/ M cm^2) (average 'shielded' rate of C18 & sites 41)		
US Activity fro	--->	13.30
(DPM/ cm^2)		
Input Sedimen	--->	1.76
(DPM / g clay) (from proximal grab samples)		
CICCS Accum	--->	0.24
(grams clay / cm^2 yr)		
CICCS Accum	--->	0.56
(grams / cm^2 yr)		
CICCS Accum	--->	0.36
(cm / yr)		

Avg. % Clay	Avg. Density
42.11	1.54

Assumed Supported --> (DPM/ g clay)	0.00
Assumed Den (g/cc)	1.20
Assumed Area (tube cross-section)	3.70

Present activi	1.25
Confidence In	0.08
Original sedin	1.76
Background US activity	
CIRCA Uncert	0.20
N/N_o	0.71
S.E. (N/N_o)	0.09
Predicted sed	10.92
S.E. (age)	4.24
minimum age	6.94
maximum age	15.45
Activity offset f	-9.9
Deposition dat	1999.0

Present activi	0.45
Confidence Interval	
Original sedin	1.76
Background US activity	
CIRCA Uncert	0.20
N/N_o	0.26
S.E. (N/N_o)	0.03
Predicted sed	43.69
S.E. (age)	3.67
minimum age	40.22
maximum age	47.58
Activity offset f	-9.9
Deposition dat	1966.2

	--->	31.06
Additional 'cap' activity (integrated tube DPM)		(DPM/cm^2) Cap activity
Assumed Mete	--->	17.76
(Atoms Pb-210/ M cm^2) (average 'shielded' rate of C18 & sites 41)		
Growth time fc	--->	#NUM!
Activity offset from 2000		-9.9
Deposition date		#NUM!

depth	Density (measured)	unsupported activity / g clay	US activity / gram	Trapazoidal Depth-Integration of (activity * volume * density)
0.00	1.20	7.56	2.88	
0.50	1.20	7.56	2.88	6.39
1.50	1.20	6.21	2.36	11.64
2.50	1.23	4.86	1.85	9.46
3.50	1.49	3.59	1.52	8.46
4.50	1.49	2.17	0.94	6.77
5.50	1.87	1.35	0.59	4.77
6.50	1.71	1.31	0.58	3.90
7.50	1.70	1.23	0.55	3.55
8.50	1.69	1.14	0.53	3.36
9.50	1.81	1.23	0.59	3.62
10.50	1.86	0.99	0.48	3.66
11.50	2.23	0.70	0.35	3.16
13.50	2.13	0.37	0.18	4.30
15.50	1.86	0.48	0.24	3.10
20.50	2.38	0.47	0.22	9.01
30.50	2.04	0.42	0.21	17.82
41.00	1.55	0.25	0.13	11.93
56.05	1.47	0.09	0.05	

^{210}Pb Profiles

Int. Err	Core	Depth (avg)	notes		Pb-210 DPM/g	dpm/g clay	dpm/g % < 2um	err	% Clay	%Silt	%Sand	% < 2um	notes
1	RASRF_153	1		0	3.11	7.36		0.69	43.00				AVG
0.5	RASRF_153	2.5		0	2.56	6.06	7.86	0.65	42.96	44.06	12.98	33.11	
0.5	RASRF_153	3.5		0	2.59	5.85		0.55	45.00				AVG
0.5	RASRF_153	4.5		0	2.79	6.31		0.60	45.00				AVG
0.5	RASRF_153	5.5		0	1.43	3.20		0.30	45.00				AVG
0.5	RASRF_153	6.5		0	1.06	2.36		0.23	45.00				AVG
0.5	RASRF_153	7.5		0	1.04	2.33		0.24	45.00				AVG
0.5	RASRF_153	8.5		0	1.08	2.42		0.21	45.00				AVG
0.5	RASRF_153	9.5		0	0.89	2.00		0.21	45.00				AVG
0.5	RASRF_153	10.5		0	0.60	1.33		0.14	45.00				AVG
0.5	RASRF_153	11.5		0	0.56	1.08	1.26	0.12	51.01	42.20	6.79	43.78	
1	RASRF_153	15		0	0.53	1.15		0.12	45.00				AVG
0.5	RASRF_153	20.5		0	0.55	1.09		0.11	50.00				AVG
1	RASRF_153	25		0	0.54	1.19		0.12	45.00				AVG
0.5	RASRF_153	30.5		0	0.51	1.01		0.10	50.00				AVG
1	RASRF_153	41		0	0.60	1.31		0.12	45.00				AVG
0.75	RASRF_153	65.75		0	0.84	1.53	1.82	0.15	54.76	41.83	3.41	46.12	

Supported Background (dpm/g clay)	XS clay activity	Radon Ventillation Effect	XS Activity (CVC)
1.658673004	5.70	-0.79	6.49
1.65972422	4.40	-0.78	5.18
1.611693786	4.24	-0.77	5.01
1.611693786	4.70	-0.76	5.47
1.611693786	1.59	-0.76	2.35
1.611693786	0.75	-0.75	1.50
1.611693786	0.72	-0.75	1.47
1.611693786	0.80	-0.74	1.54
1.611693786	0.39	-0.73	1.12
1.611693786	-0.28	-0.73	0.45
1.488883301	-0.40	-0.72	0.32
1.611693786	-0.46	-0.70	0.24
1.507869642	-0.42	-0.67	0.25
1.611693786	-0.43	-0.64	0.22
1.507869642	-0.50	-0.61	0.12
1.611693786	-0.30	-0.56	0.25
1.423609568	0.11	-0.43	0.54

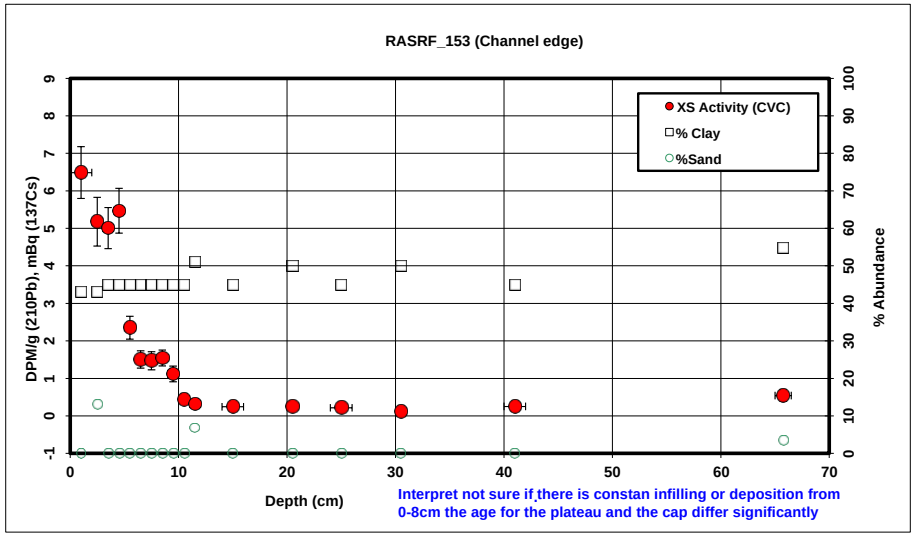

103.37	--->	27.94
Total integrated (integrated tube DPM)		US activity (DPM/cm^2) US activity
Assumed Mete (Atoms Pb-210/ M cm^2) (average 'shielded' rate of C18 & sites 41)	--->	17.76
US Activity fro (DPM/ cm^2)	--->	10.17
Input Sedimen (DPM / g clay) (from proximal grab samples)	--->	1.76
CICCS Accum (grams clay / cm^2 yr)	--->	0.18
CICCS Accum (grams / cm^2 yr)	--->	0.40
CICCS Accum (cm / yr)	--->	0.25

Avg. % Clay	Avg. Density
44.49	1.61

Assumed Supported --> (DPM/ g clay)	0.00
Assumed Den (g/cc)	1.50
Assumed Area (tube cross-section)	3.70

Present activi	0.20
Confidence In	0.04
Original sedim	1.76
Background US activity	
CIRCA Uncert	0.20
N/N_o	0.11
S.E. (N/N_o)	0.03
Predicted sed	69.91
S.E. (age)	7.16
minimum age	63.51
maximum age	77.91
Activity offset f	-9.9
Deposition dat	1940.0

Present activity	
Confidence In	1.53
Original sedim	3.00
Background U	0.60
CIRCA Uncert	0.20
N/N_o	-0.25
S.E. (N/N_o)	-0.64
Predicted sed	#NUM!
S.E. (age)	#NUM!
minimum age	#NUM!
maximum age	30.45
Activity offset f	-1.5
Deposition dat	#NUM!

	--->	27.94
Additional 'cap' activity (integrated tube DPM)		(DPM/cm^2) Cap activity
Assumed Mete (Atoms Pb-210/ M cm^2) (average 'shielded' rate of C18 & sites 41)	--->	17.76
Growth time fo	--->	#NUM!
Activity offset from 2000		-9.9
Deposition date		#NUM!

depth	Density (measured)	unsupported activity / g clay	US activity / gram	Trapazoidal Depth-Integration of (activity * volume * density)
0.00	1.50	6.49	2.79	
1.00	1.50	6.49	2.79	15.48
2.50	1.50	5.18	2.22	20.87
3.50	1.01	5.01	2.25	10.38
4.50	1.35	5.47	2.46	10.29
5.50	1.76	2.35	1.06	10.12
6.50	1.71	1.50	0.68	5.57
7.50	1.96	1.47	0.66	4.55
8.50	1.64	1.54	0.69	4.52
9.50	1.84	1.12	0.50	3.86
10.50	1.83	0.45	0.20	2.40
11.50	1.72	0.32	0.16	1.19
15.00	1.80	0.24	0.11	3.10
20.50	1.95	0.25	0.12	4.47
25.00	1.86	0.22	0.10	3.52
30.50	1.97	0.12	0.06	3.05
41.00	1.71	0.25	0.11	
65.75	1.50	0.54	0.30	

^{210}Pb Profiles

Int. Err	Core	Depth (avg)	notes	Pb-210 DPM/g	dpm/g clay	dpm/g % < 2um	err	% Clay	%Silt	%Sand	% < 2um	notes
1	RASRF_154	1		1.88	5.16		0.52	36.92				AVG
0.5	RASRF_154	2.5		1.99	5.46		0.53	36.92				AVG
0.5	RASRF_154	3.5		1.73	4.76	6.08	0.50	36.92	57.58	5.50	28.93	
0.5	RASRF_154	4.5		1.67	4.30		0.40	39.33				AVG
0.5	RASRF_154	5.5		1.80	4.38	5.67	0.49	41.73	55.97	2.30	32.24	
0.5	RASRF_154	6.5		1.67	4.14		0.41	40.91				AVG
0.5	RASRF_154	7.5		1.30	3.29	4.08	0.37	40.10	58.83	1.08	32.31	
0.5	RASRF_154	8.5		1.37	3.45		0.33	40.00				AVG
0.5	RASRF_154	9.5		1.26	3.19	4.17	0.34	39.91	58.96	1.13	30.54	
0.5	RASRF_154	10.5		1.12	2.74		0.23	41.44				AVG
0.5	RASRF_154	11.5		1.19	2.79	3.56	0.30	42.97	54.93	2.10	33.69	
1	RASRF_154	15		0.96	2.43		0.21	44.10				AVG
0.5	RASRF_154	20.5		0.70	1.56	1.91	0.17	45.22	53.99	0.79	36.80	
1	RASRF_154	25		0.66	1.66		0.15	45.54				AVG
0.5	RASRF_154	30.5		0.60	1.29	1.65	0.15	45.85	52.25	1.90	36.05	
1	RASRF_154	41		0.60	1.33		0.13	45.00				AVG
1	RASRF_154	51		0.64	1.40		0.13	45.00				AVG
1	RASRF_154	61		0.59	1.29		0.13	45.00				AVG
0.55	RASRF_154	67.55		0.59	1.13	1.45	0.14	51.97	46.12	1.91	40.61	

Supported Background (dpm/g clay)	XS clay activity	Radon Ventillation Effect	XS Activity (CVC)
1.826377389	3.33	-0.79	4.12
1.826377389	3.63	-0.78	4.41
1.826377389	2.94	-0.77	3.71
1.754956584	2.55	-0.76	3.31
1.690328342	2.69	-0.76	3.45
1.711629924	2.43	-0.75	3.18
1.733638814	1.55	-0.75	2.30
1.736131815	1.72	-0.74	2.46
1.738634095	1.45	-0.73	2.19
1.697777985	1.04	-0.73	1.77
1.659312278	1.13	-0.72	1.85
1.632437287	0.80	-0.70	1.50
1.606658244	-0.05	-0.67	0.62
1.599662798	0.06	-0.64	0.70
1.592745466	-0.30	-0.61	0.31
1.611693786	-0.28	-0.56	0.27
1.611693786	-0.21	-0.51	0.30
1.611693786	-0.32	-0.46	0.14
1.47148055	-0.34	0.00	-0.34

Assumed Supported --> (DPM/ g clay)	0.00	
Assumed Den (g/cc)	1.50	
Assumed Area (tube cross-section)	3.70	

Present activity	
Confidence In	0.00
Original sedim	3.00
Background U	0.60
CIRCA Uncert	0.20
N/N_o	-0.25
S.E. (N/N_o)	-0.02
Predicted sed	#NUM!
S.E. (age)	#NUM!
minimum age	#NUM!
maximum age	#NUM!
Activity offset f	-1.5
Deposition dat	#NUM!

depth	Density (measured)	unsupported activity / g clay	US activity / gram	Trapazoidal Depth-Integration of (activity * volume * density)
0.00	1.50	4.12	1.52	
1.00	1.50	4.12	1.52	8.43
2.50	1.50	4.41	1.63	13.10
3.50	1.13	3.71	1.37	7.29
4.50	1.13	3.31	1.30	5.59
5.50	1.35	3.45	1.44	6.31
6.50	1.32	3.18	1.30	6.76
7.50	1.27	2.30	0.92	5.31
8.50	1.46	2.46	0.98	4.80
9.50	1.52	2.19	0.87	5.11
10.50	1.63	1.77	0.73	4.68
11.50	1.81	1.85	0.80	4.87
15.00	1.84	1.50	0.66	17.24
20.50	1.85	0.62	0.28	17.69
25.00	1.75	0.70	0.32	8.99
30.50	2.07	0.31	0.14	9.00
41.00	1.73	0.27	0.12	9.85
51.00	1.79	0.30	0.13	8.36
61.00	1.50	0.14	0.06	5.97
67.55	1.50	0.00	0.00	

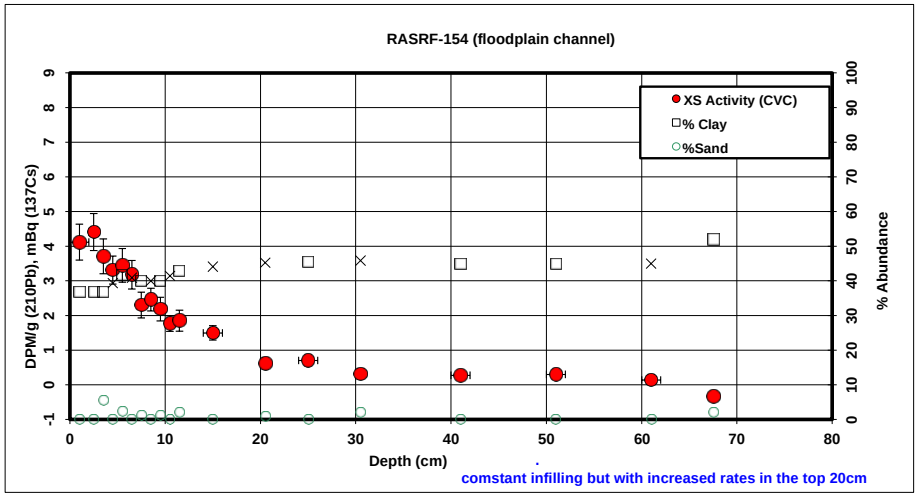

149.36	---> Total integrated US activity (integrated tube DPM)	40.37 (DPM/cm^2) US activity
	Assumed Mete (Atoms Pb-210/ M cm^2) (average 'shielded' rate of C18 & sites 41)	17.76
	US Activity fro (DPM/ cm^2)	22.60
	Input Sedimen (DPM / g clay) (from proximal grab samples)	1.76
	CICCS Accum (grams clay / cm^2 yr)	0.40
	CICCS Accum (grams / cm^2 yr)	1.02
	CICCS Accum (cm / yr)	0.72

Avg. % Clay	Avg. Density
39.10	1.43

Present activity	
Confidence In	1.13
Original sedim	3.00
Background U	0.60
CIRCA Uncert	0.20
N/N_o	-0.25
S.E. (N/N_o)	-0.47
Predicted sed	#NUM!
S.E. (age)	#NUM!
minimum age	#NUM!
maximum age	48.36
Activity offset f	-1.5
Deposition dat	#NUM!

	---> Additional 'cap' activity (integrated tube DPM)	40.37 (DPM/cm^2) Cap activity
	Assumed Mete (Atoms Pb-210/ M cm^2) (average 'shielded' rate of C18 & sites 41)	17.76
	Growth time fo	#NUM!
	Activity offset from 2000	-2.5
	Deposition date	#NUM!

^{210}Pb Profiles

Int.	Err	Core	Depth (avg)	notes	Pb-210 DPM/g	dpm/g clay	dpm/g % < 2um	err	% Clay	%Silt	%Sand	% < 2um	notes
0.5		RASRF_155	0.5		2.78	5.96		0.64	47.42		NA		AVG
0.5		RASRF_155	1.5		2.09	4.48	5.60	0.49	47.42	49.31		3.27	37.90
0.5		RASRF_155	2.5		2.00	4.41		0.49	46.14		NA		AVG
0.5		RASRF_155	3.5		1.43	3.22	4.00	0.36	44.85	54.36		0.79	36.19
0.5		RASRF_155	4.5		1.13	2.48		0.27	45.74		NA		AVG
0.5		RASRF_155	5.5		1.01	2.17	2.59	0.24	46.63	52.65		0.71	39.02
0.5		RASRF_155	6.5		0.90	1.93		0.23	46.90		NA		AVG
0.5		RASRF_155	7.5		0.83	1.76	2.05	0.21	47.17	50.29		2.54	40.37
0.5		RASRF_155	8.5		1.17	2.53		0.27	46.53		NA		AVG
0.5		RASRF_155	9.5		1.39	3.06	3.82	0.33	45.90	51.05		3.05	36.70
0.5		RASRF_155	10.5		0.92	2.11		0.21	43.84		NA		AVG
0.5		RASRF_155	11.5		0.71	1.69	2.05	0.19	41.78	54.97		3.25	34.56
1		RASRF_155	13		0.70	1.56		0.14	44.16		NA		AVG
1		RASRF_155	15		0.67	1.48		0.14	44.16		NA		AVG
0.5		RASRF_155	16.5		0.79	1.85		0.17	44.16		NA		AVG
0.5		RASRF_155	17.5		0.76	1.68		0.16	44.16		NA		AVG
0.5		RASRF_155	18.5		0.87	2.05		0.19	44.16		NA		AVG
0.5		RASRF_155	19.5		0.83	1.96		0.18	44.16		NA		AVG
0.5		RASRF_155	20.5		0.65	1.40	1.65	0.15	46.55	53.20		0.25	39.60
0.5		RASRF_155	21.5		0.59	1.33		0.13	46.98		NA		AVG
0.5		RASRF_155	22.5		0.60	1.33		0.13	46.98		NA		AVG
0.5		RASRF_155	23.5		0.68	1.53		0.14	46.98		NA		AVG
1		RASRF_155	25		0.73	1.63		0.15	46.98		NA		AVG
0.5		RASRF_155	26.5		0.68	1.43		0.14	46.98		NA		AVG
0.5		RASRF_155	27.5		0.61	1.34		0.13	46.98		NA		AVG
0.5		RASRF_155	28.5		0.55	1.24		0.12	46.98		NA		AVG
0.5		RASRF_155	29.5		0.57	1.25		0.12	46.98		NA		AVG
0.5		RASRF_155	30.5		0.53	1.12	1.27	0.13	47.40	50.90		1.70	41.60
0.5		RASRF_155	34.5		0.70	1.56		0.15	48.90		NA		AVG
1		RASRF_155	41		0.75	1.68		0.15	48.90		NA		AVG
1		RASRF_155	51		0.66	1.39		0.13	48.90		NA		AVG
0.5		RASRF_155	65.5		0.62	1.22	1.43	0.14	50.40	47.57		2.04	43.15

Supported Background (dpm/g clay)	XS clay activity	Radon Ventillation Effect	XS Activity (CVC)
1.559198707	4.40	-0.79	5.19
1.559198707	2.92	-0.78	3.70
1.586477502	2.82	-0.78	3.60
1.615023816	1.61	-0.77	2.38
1.595106046	0.89	-0.76	1.65
1.575810457	0.59	-0.76	1.35
1.570130053	0.36	-0.75	1.11
1.564502226	0.19	-0.75	0.94
1.577924739	0.96	-0.74	1.70
1.591648715	1.46	-0.73	2.20
1.638555415	0.47	-0.73	1.20
1.689206635	0.01	-0.72	0.73
1.630924275	-0.07	-0.71	0.64
1.630924275	-0.15	-0.70	0.55
1.630924275	0.22	-0.69	0.91
1.630924275	0.05	-0.69	0.74
1.630924275	0.42	-0.68	1.10
1.630924275	0.33	-0.68	1.00
1.577566223	-0.18	-0.67	0.49
1.568530723	-0.24	-0.66	0.43
1.568530723	-0.24	-0.66	0.42
1.568530723	-0.03	-0.65	0.62
1.568530723	0.06	-0.64	0.71
1.568530723	-0.13	-0.64	0.50
1.568530723	-0.23	-0.63	0.40
1.568530723	-0.32	-0.62	0.30
1.568530723	-0.32	-0.62	0.30
1.559627658	-0.44	-0.61	0.17
1.529255	0.03	-0.59	0.62
1.529255	0.15	-0.56	0.71
1.529255	-0.14	-0.51	0.36
1.500364107	-0.28	-0.43	0.16

depth	Density (measured)	unsupported activity / g clay	US activity / gram	Trapazoidal Depth-Integration of (activity * volume * density)
0.00	1.50	5.19	2.46	
0.50	1.50	5.19	2.46	6.83
1.50	1.50	3.70	1.76	11.70
2.50	1.38	3.60	1.66	9.08
3.50	1.60	2.38	1.07	7.51
4.50	1.59	1.65	0.76	5.39
5.50	1.73	1.35	0.63	4.26
6.50	1.79	1.11	0.52	3.75
7.50	1.80	0.94	0.44	3.19
8.50	1.78	1.70	0.79	4.08
9.50	1.57	2.20	1.01	5.58
10.50	1.77	1.20	0.52	4.73
11.50	2.08	0.73	0.30	2.94
13.00	1.86	0.64	0.28	3.20
15.00	1.64	0.55	0.24	3.42
16.50	1.92	0.91	0.40	3.19
17.50	1.82	0.74	0.33	2.52
18.50	1.44	1.10	0.48	2.45
19.50	0.00	1.00	0.44	1.23
20.50	1.89	0.49	0.23	1.18
21.50	1.96	0.43	0.20	1.53
22.50	1.81	0.42	0.20	1.38
23.50	1.59	0.62	0.29	1.53
25.00	1.56	0.71	0.33	2.72
26.50	1.89	0.50	0.24	2.72
27.50	2.07	0.40	0.19	1.55
28.50	1.89	0.30	0.14	1.20
29.50	1.61	0.30	0.14	0.91
30.50	1.92	0.17	0.08	0.72
34.50	1.60	0.62	0.31	5.05
41.00	1.71	0.71	0.35	12.96
51.00	1.58	0.36	0.18	15.93
65.50	1.50	0.16	0.08	10.57

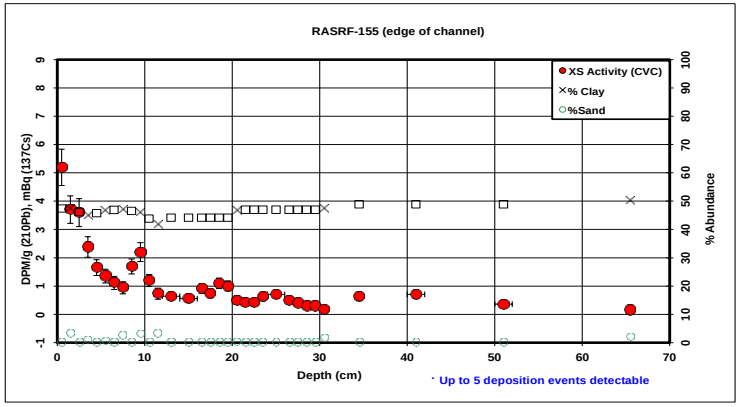

145.00	--->	39.19
Total integrated US activity (integrated tube DPM)		(DPM/cm^2) US activity
Assumed Mete (Atoms Pb-210/ M cm^2) (average 'shielded' rate of C18 & sites 41)	--->	17.76
US Activity fro (DPM/ cm^2)	--->	21.42
Input Sedimen (DPM / g clay) (from proximal grab samples)	--->	1.76
CICCS Accum (grams clay / cm^2 yr)	--->	0.38
CICCS Accum (grams / cm^2 yr)	--->	0.81
CICCS Accum (cm / yr)	--->	0.50

Avg. % Clay	Avg. Density
46.53	1.63

Present activi	0.94
Confidence In	0.05
Original sedim	1.76
Background U	0.00
CIRCA Uncert	0.20
N/N$_o$	0.53
S.E. (N/N$_o$)	0.07
Predicted sed	20.19
S.E. (age)	4.06
minimum age	16.38
maximum age	24.51
Collection Yea	2009.4
Deposition dat	1989.2

	--->	8.75
Additional 'cap' activity (integrated tube DPM)		(DPM/cm^2) Cap activity
Assumed Mete (Atoms Pb-210/ M cm^2)	--->	17.76
Growth time fo	--->	21.8
Collection Year		2009.4
Deposition date		1987.6

Present activi	0.44
Confidence In	0.02
Original sedim	1.76
Background U	0.00
CIRCA Uncert	0.20
N/N$_o$	0.25
S.E. (N/N$_o$)	0.03
Predicted sed	44.20
S.E. (age)	4.09
minimum age	40.36
maximum age	48.56
Collection Yea	2009.4
Deposition dat	1965.2

	--->	1.07
Buried 'cap' activity		(DPM/cm^2)
Back-correcte	--->	2.77
Assumed Mete	--->	17.76
Growth time fo	--->	5.4
Years Meteoric Cap is buried		30.5
Collection Year		2009.4
Deposition date		1973.4

Present activi	0.60
Confidence In	0.04
Original sedim	1.76
Background U	0.00
CIRCA Uncert	0.20
N/N$_o$	0.34
S.E. (N/N$_o$)	0.05
Predicted sed	34.74
S.E. (age)	4.34
minimum age	30.69
maximum age	39.38
Collection Yea	2009.4
Deposition dat	1974.7

	--->	2.14
Buried 'cap' activity		(DPM/cm^2)
Back-correcte	--->	4.22
Assumed Mete	--->	17.76
Growth time fo	--->	8.7
Years Meteoric Cap is buried		21.8
Collection Year		2009.4
Deposition date		1978.9

Present activi	0.26
Confidence In	0.07
Original sedim	1.76
Background U	0.00
CIRCA Uncert	0.20
N/N$_o$	0.15
S.E. (N/N$_o$)	0.04
Predicted sed	61.96
S.E. (age)	10.02
minimum age	53.39
maximum age	73.67
Collection Yea	2009.4
Deposition dat	1947.4

	--->	2.86
Buried 'cap' activity		(DPM/cm^2)
Back-correcte	--->	9.93
Assumed Mete	--->	17.76
Growth time fo	--->	26.3
Years Meteoric Cap is buried		40.0
Collection Year		2009.4
Deposition date		1943.1

^{210}Pb Profiles

Int. Err	Core	Depth (avg)	notes		Pb-210 DPM/g	dpm/g clay	dpm/g % < 2um	err	% Clay	%Silt	%Sand	% < 2um	notes
0.5	RASRF_156	0.5		0	1.49	3.73	4.70	0.39	40.64	56.00	3.36	32.24	
0.5	RASRF_156	1.5		0	0.94	2.50		0.24	38.00				AVG
0.5	RASRF_156	2.5		0	0.88	2.34		0.24	38.00				AVG
0.5	RASRF_156	3.5		0	1.07	2.85		0.27	38.00				AVG
0.5	RASRF_156	4.5		0	0.97	2.59		0.25	38.00				AVG
0.5	RASRF_156	5.5		0	0.96	2.55		0.24	38.00				AVG
0.5	RASRF_156	6.5		0	0.91	2.41		0.23	38.00				AVG
0.5	RASRF_156	7.5		0	0.94	2.50		0.24	38.00				AVG
0.5	RASRF_156	8.5		0	0.85	2.26		0.23	38.00				AVG
0.5	RASRF_156	9.5		0	0.85	2.27		0.23	38.00				AVG
0.5	RASRF_156	10.5		0	0.77	2.04		0.20	38.00				AVG
0.5	RASRF_156	11.5		0	0.69	1.93	2.43	0.22	36.04	62.28	1.68	28.63	
1	RASRF_156	15		0	0.76	1.70		0.16	45.00				AVG
0.5	RASRF_156	20.5		0	0.77	1.83		0.19	42.00				AVG
1	RASRF_156	25		0	0.68	1.50		0.14	45.00				AVG
0.5	RASRF_156	30.5		0	0.61	1.39		0.15	44.00				AVG
1	RASRF_156	41		0	0.53	1.17		0.12	45.00				AVG
1	RASRF_156	51		0	0.53	1.24		0.12	42.00				AVG
0.65	RASRF_156	62.15		0	0.52	1.07	1.29	0.13	48.21	47.43	4.36	39.83	

Supported Background (dpm/g clay)	XS clay activity	Radon Ventillation Effect	XS Activity (CVC)
1.718997587	2.01	-0.79	2.80
1.793451379	0.71	-0.78	1.49
1.793451379	0.54	-0.78	1.32
1.793451379	1.06	-0.77	1.83
1.793451379	0.80	-0.76	1.56
1.793451379	0.76	-0.76	1.52
1.793451379	0.62	-0.75	1.37
1.793451379	0.71	-0.75	1.46
1.793451379	0.47	-0.74	1.21
1.793451379	0.47	-0.73	1.21
1.793451379	0.24	-0.73	0.97
1.85438456	0.07	-0.72	0.80
1.611693786	0.09	-0.70	0.79
1.68352391	0.15	-0.67	0.82
1.611693786	-0.11	-0.64	0.54
1.634747752	-0.25	-0.61	0.36
1.611693786	-0.44	-0.56	0.11
1.68352391	-0.45	-0.51	0.06
1.543041474	-0.48	-0.45	-0.02

Assumed Supported -->	0.00	(DPM/ g clay)
Assumed Den	1.50	(g/cc)
Assumed Area	3.70	(tube cross-section)

Present activit	1.32	
Confidence Interval		
Original sedim	1.76	
Background US activity		
CIRCA Uncerta	0.20	
N/N_o	0.75	
S.E. (N/N_o)	0.09	
Predicted sed	9.22	
S.E. (age)	3.67	
minimum age	5.75	
maximum age	13.11	
Activity offset f	-9.9	
Deposition dat	2000.7	

depth	Density (measured)	unsupported activity / g clay	US activity / gram	Trapazoidal Depth-Integration of (activity * volume * density)
0.00	1.45	2.80	1.14	
0.50	1.45	2.80	1.14	3.05
1.50	1.47	1.49	0.57	4.61
2.50	1.74	1.32	0.50	3.18
3.50	1.80	1.83	0.70	3.92
4.50	1.74	1.56	0.59	4.22
5.50	1.61	1.52	0.58	3.63
6.50	1.73	1.37	0.52	3.39
7.50	1.74	1.46	0.55	3.46
8.50	1.80	1.21	0.46	3.32
9.50	1.73	1.21	0.46	3.00
10.50	1.82	0.97	0.37	2.72
11.50	1.55	0.80	0.29	2.05
15.00	1.67	0.79	0.35	6.69
20.50	1.75	0.82	0.34	12.13
25.00	1.76	0.54	0.24	8.55
30.50	1.77	0.36	0.16	7.22
41.00	2.06	0.11	0.05	7.84
51.00	1.50	0.06	0.02	
62.15	1.50	0.00	0.00	

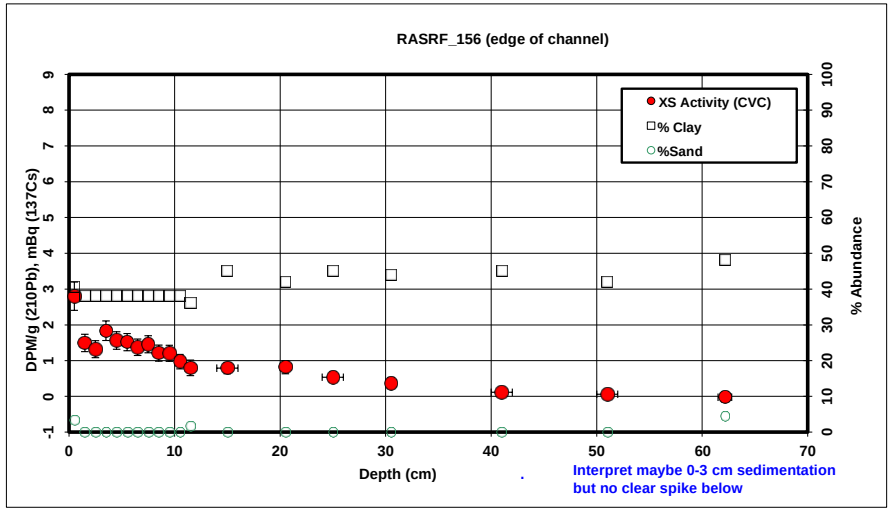

82.95	--->	22.42
Total integrated US activity (integrated tube DPM)		(DPM/cm^2) US activity
Assumed Mete (Atoms Pb-210/ M cm^2) (average 'shielded' rate of C18 & sites 41)	--->	17.76
US Activity fro (DPM/ cm^2)	--->	4.66
Input Sedimen (DPM / g clay) (from proximal grab samples)	--->	1.76
CICCS Accum (grams clay / cm^2 yr)	--->	0.08
CICCS Accum (grams / cm^2 yr)	--->	0.22
CICCS Accum (cm / yr)	--->	0.13

Avg. % Clay	Avg. Density
38.29	1.67

Present activity		
Confidence In	1.07	
Original sedim	3.00	
Background U	0.60	
CIRCA Uncerta	0.20	
N/N_o	-0.25	
S.E. (N/N_o)	-0.45	
Predicted sed	#NUM!	
S.E. (age)	#NUM!	
minimum age	#NUM!	
maximum age	52.53	
Activity offset f	-1.5	
Deposition dat	#NUM!	

	--->	22.42
Additional 'cap' activity (integrated tube DPM)		(DPM/cm^2) Cap activity
Assumed Mete (Atoms Pb-210/ M cm^2) (average 'shielded' rate of C18 & sites 41)	--->	17.76
Growth time fo	--->	#NUM!
Activity offset from 2000		-9.9
Deposition date		#NUM!

^{210}Pb Profiles

Int. Err	Core	Depth (avg)	notes	Pb-210 DPM/g	dpm/g clay	dpm/g % < 2um	err	% Clay	%Silt	%Sand	% < 2um	notes
0.5	RASRF_157	0.5		2.38	5.38	6.34	0.58	45.36	39.27	15.37	38.48	
0.5	RASRF_157	1.5		1.04	2.10		0.22	50.00				AVG
0.5	RASRF_157	2.5		0.76	1.52		0.16	50.00				AVG
0.5	RASRF_157	3.5		0.61	1.22		0.14	50.00				AVG
0.5	RASRF_157	4.5		0.69	1.38		0.16	50.00				AVG
0.5	RASRF_157	5.5		0.67	1.33		0.15	50.00				AVG
0.5	RASRF_157	6.5		0.57	1.14		0.13	50.00				AVG
0.5	RASRF_157	7.5		0.55	1.09		0.13	50.00				AVG
0.5	RASRF_157	8.5		0.54	1.08		0.13	50.00				AVG
0.5	RASRF_157	9.5		0.52	1.03		0.12	50.00				AVG
0.5	RASRF_157	10.5		0.48	0.95		0.11	50.00				AVG
0.5	RASRF_157	11.5		0.57	1.03	1.27	0.13	54.61	40.63	4.76	44.48	
0.5	RASRF_157	12.5		0.55	0.99		0.11	55.00				AVG
0.5	RASRF_157	20.5		0.38	0.66		0.10	55.00				AVG
0.5	RASRF_157	30.5		0.50	0.90		0.12	55.00				AVG
0.5	RASRF_157	37.5		0.46	0.74	0.82	0.11	60.20	34.02	5.78	54.22	

Supported Background (dpm/g clay)	XS clay activity	Radon Ventillation Effect	XS Activity (CVC)
1.603660139	3.77	-0.79	**4.56**
1.507869642	0.59	-0.78	**1.37**
1.507869642	0.01	-0.78	**0.79**
1.507869642	-0.29	-0.77	**0.48**
1.507869642	-0.13	-0.76	**0.64**
1.507869642	-0.17	-0.76	**0.58**
1.507869642	-0.37	-0.75	**0.38**
1.507869642	-0.42	-0.75	**0.32**
1.507869642	-0.43	-0.74	**0.31**
1.507869642	-0.48	-0.73	**0.26**
1.507869642	-0.56	-0.73	**0.17**
1.426075927	-0.39	-0.72	**0.33**
1.419723008	-0.43	-0.72	**0.28**
1.419723008	-0.76	-0.67	**-0.09**
1.419723008	-0.52	-0.61	**0.09**
1.340929363	-0.60	-0.58	**-0.02**

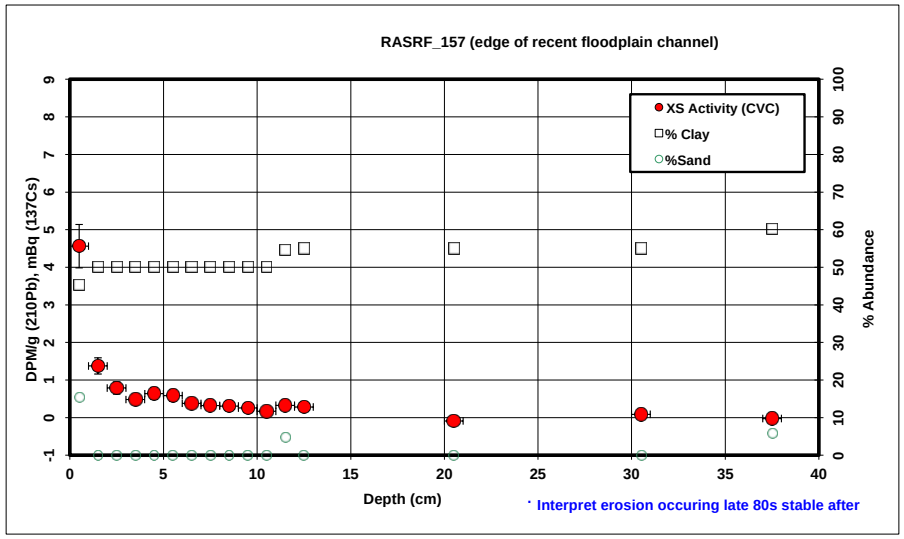

30.82	--->	8.33
Total integrated US activity (integrated tube DPM)		(DPM/cm^2) US activity
Assumed Mete (Atoms Pb-210/ M cm^2) (average 'shielded' rate of C18 & sites 41)	--->	17.76
US Activity fro (DPM/ cm^2)	--->	-9.43
Input Sedimen (DPM / g clay) (from proximal grab samples)	--->	1.76
CICCS Accum (grams clay / cm^2 yr)	--->	-0.17
CICCS Accum (grams / cm^2 yr)	--->	-0.34
CICCS Accum (cm / yr)	--->	-0.18

Avg. % Clay	Avg. Density
49.48	1.89

Assumed Supported --> (DPM/ g clay)	0.00
Assumed Den (g/cc)	1.50
Assumed Area (tube cross-section)	3.70

Present activity	
Confidence In	0.00
Original sedin	3.00
Background U	0.60
CIRCA Uncert	0.20
N/N$_o$	-0.25
S.E. (N/N$_o$)	-0.02
Predicted sed	#NUM!
S.E. (age)	#NUM!
minimum age	#NUM!
maximum age	#NUM!
Activity offset f	-1.5
Deposition dat	#NUM!

Present activity	
Confidence In	0.74
Original sedin	3.00
Background U	0.60
CIRCA Uncert	0.20
N/N$_o$	-0.25
S.E. (N/N$_o$)	-0.31
Predicted sed	#NUM!
S.E. (age)	#NUM!
minimum age	#NUM!
maximum age	90.69
Activity offset f	-1.5
Deposition dat	#NUM!

	--->	8.33
Additional 'cap' activity (integrated tube DPM)		(DPM/cm^2) Cap activity
Assumed Mete (Atoms Pb-210/ M cm^2) (average 'shielded' rate of C18 & sites 41)	--->	17.76
Growth time fo	--->	20.3625339
Activity offset from 2000		-9.9
Deposition date		1989.5

depth	Density (measured)	unsupported activity / g clay	US activity / gram	Trapazoidal Depth-Integration of (activity * volume * density)
0.00	1.50	4.56	2.07	
0.50	1.50	4.56	2.07	5.74
1.50	1.58	1.37	0.69	7.84
2.50	1.98	0.79	0.39	3.56
3.50	1.85	0.48	0.24	2.25
4.50	1.94	0.64	0.32	1.96
5.50	2.10	0.58	0.29	2.29
6.50	1.93	0.38	0.19	1.80
7.50	2.08	0.32	0.16	1.31
8.50	2.11	0.31	0.15	1.22
9.50	2.04	0.26	0.13	1.08
10.50	2.05	0.17	0.08	0.80
11.50	1.93	0.33	0.18	0.96
12.50	2.20	0.28	0.16	
20.50	2.13	0.00	0.00	
30.50	1.90	0.09	0.05	
37.50	1.50	0.00	0.00	

^{210}Pb Profiles

Int. Err	Core	Depth (avg)	notes	Pb-210 DPM/g	dpm/g clay	dpm/g % < 2um	err	% Clay	%Silt	%Sand	% < 2um	notes
0.5	RASRF_158	0.5		3.77	7.08		0.65	54.70				AVG
0.5	RASRF_158	1.5		1.35	2.51	2.89	0.28	54.71	35.85	9.44	47.43	
0.5	RASRF_158	2.5		0.44	0.77		0.10	56.10				AVG
0.5	RASRF_158	3.5		0.45	0.78		0.10	56.10				AVG
0.5	RASRF_158	4.5		0.46	0.79		0.10	56.10				AVG
0.5	RASRF_158	5.5		0.42	0.73		0.10	56.10				AVG
0.5	RASRF_158	6.5		0.46	0.80		0.10	56.10				AVG
0.5	RASRF_158	7.5		0.42	0.73		0.10	56.10				AVG
0.5	RASRF_158	8.5		0.46	0.80		0.11	56.10				AVG
0.5	RASRF_158	9.5		0.44	0.76		0.10	56.10				AVG
0.5	RASRF_158	10.5		0.43	0.74		0.10	56.10				AVG
0.5	RASRF_158	11.5		0.46	0.76	0.86	0.10	58.89	33.04	8.07	52.16	
0.5	RASRF_158	20.5		0.50	0.89		0.11	55.50				AVG
0.5	RASRF_158	30.5		0.50	0.89		0.11	55.50				AVG
0.5	RASRF_158	60.5		0.55	1.04	1.19	0.14	52.11	33.99	13.91	45.61	

Supported Background (dpm/g clay)	XS clay activity	Radon Ventillation Effect	XS Activity (CVC)
1.424639069	5.65	-0.79	6.44
1.424464298	1.08	-0.78	1.87
1.402065529	-0.63	-0.78	0.15
1.402065529	-0.63	-0.77	0.15
1.402065529	-0.61	-0.76	0.16
1.402065529	-0.67	-0.76	0.09
1.402065529	-0.60	-0.75	0.15
1.402065529	-0.67	-0.75	0.08
1.402065529	-0.60	-0.74	0.14
1.402065529	-0.65	-0.73	0.09
1.402065529	-0.66	-0.73	0.07
1.359768312	-0.60	-0.72	0.12
1.411626085	-0.52	-0.67	0.15
1.411626085	-0.52	-0.61	0.09
1.469032554	-0.43	-0.46	0.03

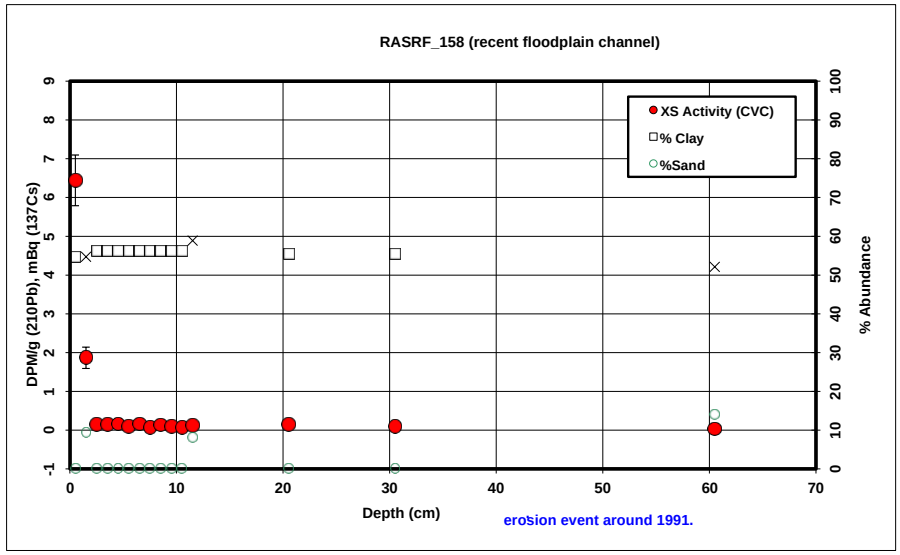

30.69	--->	8.30
Total integrated US activity (integrated tube DPM)		(DPM/cm^2) US activity
Assumed Mete (Atoms Pb-210/ M cm^2) (average 'shielded' rate of C18 & sites 41)	--->	17.76
US Activity fro (DPM/ cm^2)	--->	-9.47
Input Sedimen (DPM / g clay) (from proximal grab samples)	--->	1.76
CICCS Accum (grams clay / cm^2 yr)	--->	-0.17
CICCS Accum (grams / cm^2 yr)	--->	-0.30
CICCS Accum (cm / yr)	--->	-0.13

Avg. % Clay	Avg. Density
55.79	2.24

Assumed Supported --> (DPM/ g clay)	0.00
Assumed Den (g/cc)	2.10
Assumed Area (tube cross-section)	3.70

Present activity	
Confidence In	0.00
Original sedim	3.00
Background U	0.60
CIRCA Uncert	0.20
N/N_o	-0.25
S.E. (N/N_o)	-0.02
Predicted sed	#NUM!
S.E. (age)	#NUM!
minimum age	#NUM!
maximum age	#NUM!
Activity offset f	-1.5
Deposition dat	#NUM!

Present activity	
Confidence In	1.04
Original sedim	3.00
Background U	0.60
CIRCA Uncert	0.20
N/N_o	-0.25
S.E. (N/N_o)	-0.43
Predicted sed	#NUM!
S.E. (age)	#NUM!
minimum age	#NUM!
maximum age	54.54
Activity offset f	-1.5
Deposition dat	#NUM!

	--->	8.30
Additional 'cap' activity (integrated tube DPM)		(DPM/cm^2) Cap activity
Assumed Mete (Atoms Pb-210/ M cm^2) (average 'shielded' rate of C18 & sites 41)	--->	17.76
Growth time fo	--->	20.2437489
Activity offset from 2000		-9.9
Deposition date		1989.7

depth	Density (measured)	unsupported activity / g clay	US activity / gram	Trapazoidal Depth-Integration of (activity * volume * density)
0.00	1.63	6.44	3.52	
0.50	1.63	6.44	3.52	10.65
1.50	2.11	1.87	1.02	15.75
2.50	2.10	0.15	0.08	4.30
3.50	2.10	0.15	0.08	
4.50	2.05	0.16	0.09	
5.50	2.28	0.09	0.05	
6.50	3.10	0.15	0.09	
7.50	2.45	0.08	0.04	
8.50	2.35	0.14	0.08	
9.50	1.92	0.09	0.05	
10.50	3.10	0.07	0.04	
11.50	1.87	0.12	0.07	
20.50	2.27	0.15	0.08	
30.50	4.10	0.09	0.05	
60.50	2.10	0.03	0.01	

^{210}Pb Profiles

Int. Err	Core	Depth (avg)	notes	Pb-210 DPM/g	dpm/g clay	dpm/g % < 2um	err	% Clay	%Silt	%Sand	% < 2um	notes	Supported Background (dpm/g clay)	XS clay activity	Radon Ventillation Effect	XS Activity (CVC)
0.5	RASRF_159	0.5		4.12	9.43		0.84	45.00				est	1.611693786	7.81	-0.79	8.60
0.5	RASRF_159	1.5		2.02	4.59		0.42	45.00				est	1.611693786	2.98	-0.78	3.76
0.5	RASRF_159	2.5		1.50	3.40		0.32	45.00				est	1.611693786	1.79	-0.78	2.57
0.5	RASRF_159	3.5		1.08	2.43		0.24	45.00				est	1.611693786	0.82	-0.77	1.59
0.5	RASRF_159	4.5		1.60	3.63		0.34	45.00				est	1.611693786	2.02	-0.76	2.78
0.5	RASRF_159	5.5		1.38	3.11		0.30	45.00				est	1.611693786	1.50	-0.76	2.26
0.5	RASRF_159	6.5		0.85	1.90		0.19	45.00				est	1.611693786	0.29	-0.75	1.04
0.5	RASRF_159	7.5		0.69	1.52		0.16	45.00				est	1.611693786	-0.09	-0.75	0.66
0.5	RASRF_159	8.5		0.53	1.17		0.13	45.00				est	1.611693786	-0.44	-0.74	0.30
0.5	RASRF_159	9.5		0.74	1.64		0.17	45.00				est	1.611693786	0.03	-0.73	0.77
0.5	RASRF_159	10.5		0.59	1.29		0.12	45.00				est	1.611693786	-0.32	-0.73	0.41
0.5	RASRF_159	11.5		0.79	1.77		0.18	45.00				est	1.611693786	0.15	-0.72	0.88
1	RASRF_159	15		0.69	1.53		0.14	45.00				est	1.611693786	-0.09	-0.70	0.62
1	RASRF_159	21		0.56	1.23		0.12	45.00				est	1.611693786	-0.38	-0.67	0.28
0.5	RASRF_159	25.5		0.60	1.32		0.14	45.00				est	1.611693786	-0.29	-0.64	0.35

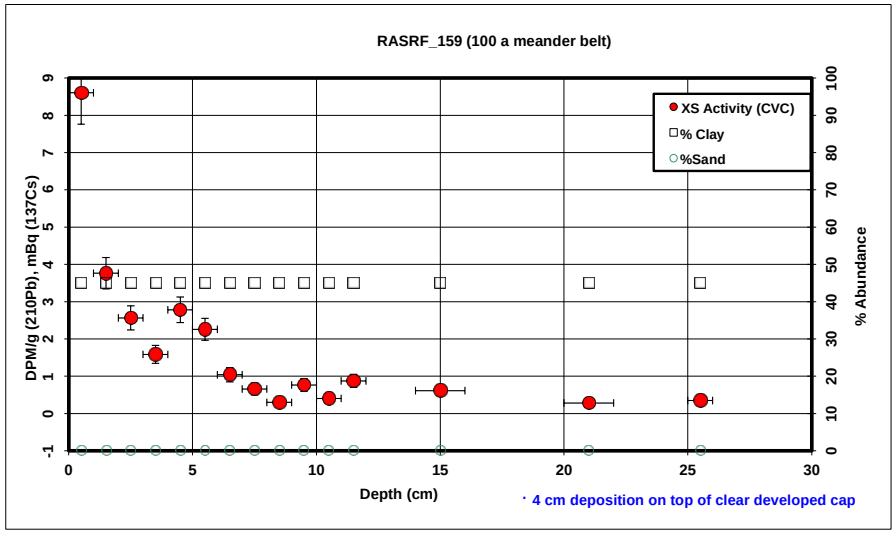

· 4 cm deposition on top of clear developed cap

78.59	--->	21.24
Total integrated US activity (integrated tube DPM)		(DPM/cm^2) US activity

Assumed Mete	--->	17.78
(Atoms Pb-210/ M cm^2)		
(average 'shielded' rate of C18 & sites 41)		

US Activity fro	--->	3.48
(DPM/ cm^2)		

Input Sedimen	--->	1.78
(DPM / g clay)		
(from proximal grab samples)		

CICCS Accum	--->	0.06
(grams clay / cm^2 yr)		
CICCS Accum	--->	0.14
(grams / cm^2 yr)		
CICCS Accum	--->	0.09
(cm / yr)		

Avg. % Clay	Avg. Density
45.00	1.55

Assumed Supported -->	0.00
(DPM/ g clay)	
Assumed Den	1.50
(g/cc)	
Assumed Area	3.70
(tube cross-section)	

Present activi	0.35
Confidence In	0.28
Original sedin	1.76
Background US activity	
CIRCA Uncert	0.20
N/N_o	0.20
S.E. (N/N_o)	0.16
Predicted sed	51.91
S.E. (age)	31.36
minimum age	32.98
maximum age	103.85
Activity offset f	-9.9
Deposition dat	1958.0

Present activity	
Confidence In	0.00
Original sedin	3.00
Background U	0.60
CIRCA Uncert	0.20
N/N_o	-0.25
S.E. (N/N_o)	-0.02
Predicted sed	#NUM!
S.E. (age)	#NUM!
minimum age	#NUM!
maximum age	#NUM!
Activity offset f	-1.5
Deposition dat	#NUM!

	--->	21.24
Additional 'cap' activity (integrated tube DPM)		(DPM/cm^2) Cap activity
Assumed Mete	--->	17.76
(Atoms Pb-210/ M cm^2)		
(average 'shielded' rate of C18 & sites 41)		
Growth time fo	--->	#NUM!
Activity offset from 2000		-2.5
Deposition date		#NUM!

depth	Density (measured)	unsupported activity / g clay	US activity / gram	Trapazoidal Depth-Integration of (activity * volume * density)
0.00	1.50	8.60	3.87	
0.50	1.50	8.60	3.87	10.74
1.50	1.19	3.76	1.69	13.84
2.50	1.28	2.57	1.15	6.51
3.50	1.55	1.59	0.71	4.89
4.50	1.54	2.78	1.25	5.61
5.50	1.74	2.26	1.02	6.89
6.50	1.39	1.04	0.47	4.30
7.50	1.71	0.66	0.30	2.19
8.50	1.67	0.30	0.13	1.35
9.50	1.89	0.77	0.35	1.58
10.50	1.59	0.41	0.18	1.70
11.50	1.69	0.88	0.39	1.75
15.00	1.50	0.62	0.28	6.94
21.00	1.50	0.28	0.13	6.74
25.50	1.50	0.35	0.16	3.56

^{210}Pb Profiles

Int. Err	Core	Depth (avg)	notes	Pb-210 DPM/g	dpm/g clay	dpm/g % < 2um	err	% Clay	%Silt	%Sand	% < 2um	notes
1	RASRF_160	1		2.51	6.52	8.78	0.68	39.54	56.18	4.28	29.35	
1	RASRF_160	3		1.67	4.02	5.15	0.38	42.44	55.34	2.22	33.12	
1	RASRF_160	5		1.02	2.78	3.54	0.28	36.99	61.02	1.98	29.07	
1	RASRF_160	7		0.91	2.23	2.85	0.22	41.10	57.40	1.50	32.14	
1	RASRF_160	9		0.67	1.69	2.19	0.17	39.45	59.55	1.00	30.55	
1	RASRF_160	11		0.54	1.33	1.64	0.14	40.51	57.90	1.59	32.74	
0.5	RASRF_160	20.5		0.47	1.05	1.27	0.14	43.40	56.25	0.35	36.00	
0.5	RASRF_160	30.5		0.54	1.17	1.48	0.14	45.35	53.55	1.10	35.95	
0.5	RASRF_160	49.5		0.44	1.32	1.61	0.14	32.43	47.79	19.78	26.56	

Supported Background (dpm/g clay)	XS clay activity	Radon Ventillation Effect	XS Activity (CVC)
1.748946601	4.77	-0.79	5.56
1.67235193	2.35	-0.77	3.12
1.824150485	0.96	-0.76	1.72
1.706632235	0.52	-0.75	1.27
1.751503992	-0.06	-0.74	0.68
1.722351349	-0.39	-0.73	0.33
1.648994971	-0.60	-0.67	0.07
1.603821356	-0.43	-0.61	0.18
1.982439254	-0.66	-0.51	-0.15

Assumed Supported -->	0.00
(DPM/ g clay)	
Assumed Dens	1.50
(g/cc)	
Assumed Area	3.70
(tube cross-section)	

depth	Density (measured)	unsupported activity / g clay	US activity / gram	Trapazoidal Depth-Integration of (activity * volume * density)
0.00	1.32	5.56	2.20	
1.00	1.32	5.56	2.20	10.74
3.00	1.49	3.12	1.32	18.32
5.00	1.46	1.72	0.64	10.69
7.00	1.56	1.27	0.52	6.47
9.00	1.62	0.68	0.27	4.66
11.00	1.77	0.33	0.13	2.52
20.50	1.69	0.07	0.03	5.04
30.50	1.71	0.18	0.08	
49.50	1.50	0.00	0.00	

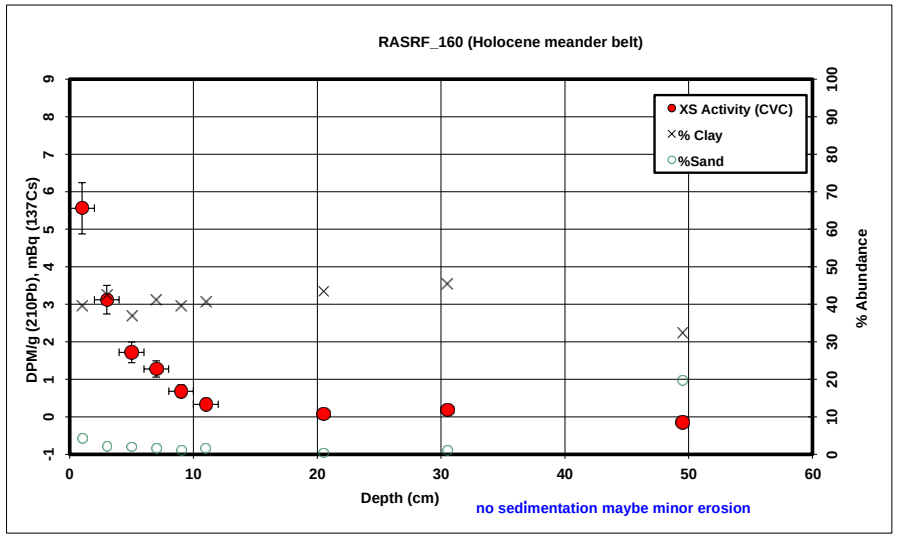

58.44	--->	15.79
Total integrated US activity (integrated tube DPM)		(DPM/cm^2) US activity
Assumed Mete (Atoms Pb-210/ M cm^2) (average 'shielded' rate of C18 & sites 41)	--->	17.76
US Activity fro (DPM/ cm^2)	--->	-1.97
Input Sedimen (DPM / g clay) (from proximal grab samples)	--->	1.76
CICCS Accum (grams clay / cm^2 yr)	--->	-0.03
CICCS Accum (grams / cm^2 yr)	--->	-0.09
CICCS Accum (cm / yr)	--->	-0.06

Avg. % Clay	Avg. Density
40.14	1.54

Present activity	
Confidence In	0.00
Original sedin	3.00
Background U	0.60
CIRCA Uncert	0.20
N/N_o	-0.25
S.E. (N/N_o)	-0.02
Predicted sed	#NUM!
S.E. (age)	#NUM!
minimum age	#NUM!
maximum age	#NUM!
Activity offset f	-1.5
Deposition dat	#NUM!

Present activity	
Confidence In	0.00
Original sedin	3.00
Background U	0.60
CIRCA Uncert	0.20
N/N_o	-0.25
S.E. (N/N_o)	-0.02
Predicted sed	#NUM!
S.E. (age)	#NUM!
minimum age	#NUM!
maximum age	#NUM!
Activity offset f	-1.5
Deposition dat	#NUM!

	--->	15.79
Additional 'cap' activity (integrated tube DPM)		(DPM/cm^2) Cap activity
Assumed Mete (Atoms Pb-210/ M cm^2) (average 'shielded' rate of C18 & sites 41)	--->	17.76
Growth time fo	--->	70.7446406
Activity offset from 2000		-2.5
Deposition date		1931.8

^{210}Pb Profiles

Int. Err	Core	Depth (avg)	notes	Pb-210 DPM/g	dpm/g clay	dpm/g % < 2um	err	% Clay	%Silt	%Sand	% < 2um	notes
0.5	RASRF_161	0.5		1.62	2.86		0.30	57.25				AVG
0.5	RASRF_161	1.5		2.12	3.75		0.38	57.25				AVG
0.5	RASRF_161	2.5		1.45	2.56	3.33	0.30	57.25	42.60	0.15	44.00	
0.5	RASRF_161	3.5		1.31	2.25		0.24	58.53				AVG
0.5	RASRF_161	4.5		1.37	2.36		0.26	58.53				AVG
0.5	RASRF_161	5.5		1.83	3.10	3.86	0.36	59.81	38.93	1.26	48.07	
0.5	RASRF_161	6.5		1.07	1.90		0.21	56.58				AVG
0.5	RASRF_161	7.5		1.42	2.69	3.43	0.30	53.35	44.26	2.39	41.91	
0.5	RASRF_161	8.5		1.67	3.18		0.32	53.07				AVG
0.5	RASRF_161	9.5		1.32	2.52	3.17	0.29	52.78	43.45	3.77	41.94	
0.5	RASRF_161	10.5		0.77	1.48		0.17	51.74				AVG
0.5	RASRF_161	11.5		0.61	1.17		0.13	51.74		9.75		failed
0.5	RASRF_161	14.5		0.57	1.11		0.12	50.00				AVG
0.5	RASRF_161	20.5		0.57	1.10		0.13	51.74		7.00		failed
0.5	RASRF_161	25.5		0.44	0.84		0.09	50.00				AVG
0.5	RASRF_161	30.5		0.53	1.04	1.21	0.12	50.70	42.50	6.80	43.47	
1	RASRF_161	41		0.58	1.13		0.11	50.00				AVG
0.65	RASRF_161	54.65		0.59	1.15		0.13	50.70		1.94		failed

Supported Background (dpm/g clay)	XS clay activity	Radon Ventillation Effect	XS Activity (CVC)
1.384199634	1.48	-0.79	2.27
1.384199634	2.36	-0.78	3.15
1.384199634	1.18	-0.78	1.95
1.364997885	0.89	-0.77	1.66
1.364997885	0.99	-0.76	1.76
1.346469209	1.76	-0.76	2.51
1.394515239	0.51	-0.75	1.26
1.447253822	1.25	-0.75	1.99
1.452196784	1.73	-0.74	2.47
1.457183579	1.06	-0.73	1.80
1.475602832	0.01	-0.73	0.73
1.475602832	-0.30	-0.72	0.42
1.507869642	-0.40	-0.70	0.31
1.475602832	-0.38	-0.67	0.29
1.507869642	-0.67	-0.64	-0.03
1.494635582	-0.46	-0.61	0.15
1.507869642	-0.37	-0.56	0.18
1.494635582	-0.34	-0.49	0.14

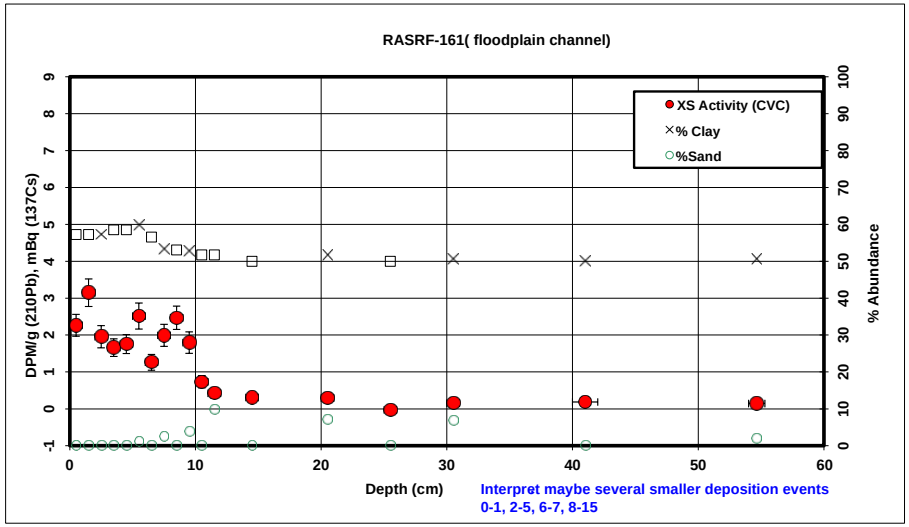

78.71	--->	21.27
Total integrated tube DPM)	US activity (integrated	(DPM/cm^2) US activity
Assumed Mete (Atoms Pb-210/ M cm^2) (average 'shielded' rate of C18 & sites 41)	--->	17.76
US Activity fro (DPM/ cm^2)	--->	3.51
Input Sedimen (DPM / g clay) (from proximal grab samples)	--->	1.76
CICCS Accum (grams clay / cm^2 yr)	--->	0.06
CICCS Accum (grams / cm^2 yr)	--->	0.11
CICCS Accum (cm / yr)	--->	0.07

Avg. % Clay	Avg. Density
56.85	1.49

Assumed Supported --> (DPM/ g clay)	0.00
Assumed Dens (g/cc)	1.50
Assumed Area (tube cross-section)	3.70

Present activity	
Confidence In	0.84
Original sedim	3.00
Background U	0.60
CIRCA Uncerta	0.20
N/N_o	-0.25
S.E. (N/N_o)	-0.35
Predicted sed	#NUM!
S.E. (age)	#NUM!
minimum age	#NUM!
maximum age	74.15
Activity offset f	-1.5
Deposition dat	#NUM!

Present activity	
Confidence In	1.15
Original sedim	3.00
Background U	0.60
CIRCA Uncerta	0.20
N/N_o	-0.25
S.E. (N/N_o)	-0.48
Predicted sed	#NUM!
S.E. (age)	#NUM!
minimum age	#NUM!
maximum age	47.29
Activity offset f	-1.5
Deposition dat	#NUM!

	--->	
Additional 'cap' activity (integrated tube DPM)		(DPM/cm^2) Cap activity
Assumed Mete (Atoms Pb-210/ M cm^2) (average 'shielded' rate of C18 & sites 41)	--->	17.76
Growth time fo	--->	0
Activity offset from 2000		-2.5
Deposition date		2002.5

depth	Density (measured)	unsupported activity / g clay	US activity / gram	Trapazoidal Depth-Integration of (activity * volume * density)
0.00	1.50	2.27	1.30	
0.50	1.50	2.27	1.30	3.60
1.50	1.08	3.15	1.80	7.39
2.50	1.50	1.95	1.12	6.95
3.50	1.37	1.66	0.97	5.53
4.50	1.31	1.76	1.03	4.95
5.50	1.56	2.51	1.50	6.71
6.50	1.50	1.26	0.71	6.28
7.50	1.14	1.99	1.06	4.35
8.50	1.67	2.47	1.31	6.18
9.50	1.81	1.80	0.95	7.28
10.50	1.90	0.73	0.38	4.56
11.50	1.97	0.42	0.22	2.13
14.50	1.70	0.31	0.15	3.77
20.50	2.16	0.29	0.15	6.51
25.50	1.45	0.00	0.00	2.52
30.50	2.11	0.15	0.08	
41.00	1.87	0.18	0.09	
54.65	1.50	0.14	0.07	

^{210}Pb Profiles

Int. Err	Core	Depth (avg)	notes	Pb-210 DPM/g	dpm/g clay	dpm/g % < 2um	err	% Clay	%Silt	%Sand	% < 2um	notes
1	RASRF_162	1		1.69	4.27		0.40	40.00				AVG
0.5	RASRF_162	2.5		1.46	3.63	4.80	0.39	40.44	55.37	4.20	30.63	
0.5	RASRF_162	3.5		1.42	3.17		0.30	45.00				AVG
0.5	RASRF_162	4.5		1.41	3.16		0.30	45.00				AVG
0.5	RASRF_162	5.5		1.12	2.49		0.24	45.00				AVG
0.5	RASRF_162	6.5		1.27	2.83		0.28	45.00				AVG
0.5	RASRF_162	7.5		1.26	2.81		0.27	45.00				AVG
0.5	RASRF_162	8.5		1.25	2.80		0.27	45.00				AVG
0.5	RASRF_162	9.5		1.26	2.83		0.27	45.00				AVG
0.5	RASRF_162	10.5		0.80	1.78		0.18	45.00				AVG
0.5	RASRF_162	11.5		0.70	1.45	1.78	0.17	47.91	48.60	3.50	39.07	
1	RASRF_162	15		0.50	0.98		0.11	50.00				AVG
0.5	RASRF_162	20.5		0.66	1.31		0.12	50.00				AVG
1	RASRF_162	25		0.64	1.26		0.13	50.00				AVG
0.5	RASRF_162	30.5		0.48	0.95		0.11	50.00				AVG
0.7	RASRF_162	39.7		6.24	11.55	14.00	1.07	54.67	38.68	6.65	45.11	

Supported Background (dpm/g clay)	XS clay activity	Radon Ventillation Effect	XS Activity (CVC)
1.736244671	2.53	-0.79	3.32
1.724370665	1.91	-0.78	2.69
1.611693786	1.56	-0.77	2.33
1.611693786	1.55	-0.76	2.31
1.611693786	0.88	-0.76	1.64
1.611693786	1.22	-0.75	1.97
1.611693786	1.20	-0.75	1.94
1.611693786	1.19	-0.74	1.93
1.611693786	1.21	-0.73	1.95
1.611693786	0.16	-0.73	0.89
1.549205765	-0.10	-0.72	0.62
1.507869642	-0.53	-0.70	0.17
1.507869642	-0.20	-0.67	0.47
1.507869642	-0.24	-0.64	0.40
1.507869642	-0.56	-0.61	0.05
1.425130438	10.13	-0.56	10.69

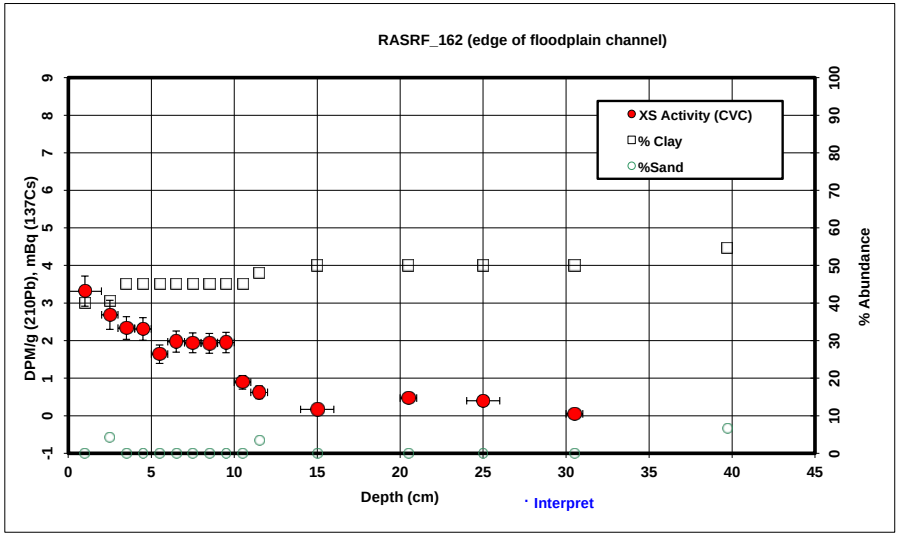

73.37	--->	19.83
Total integrated US activity (integrated tube DPM)		(DPM/cm^2) US activity
Assumed Mete (Atoms Pb-210/ M cm^2) (average 'shielded' rate of C18 & sites 41)	--->	17.76
US Activity fro (DPM/ cm^2)	--->	2.07
Input Sedimen (DPM / g clay) (from proximal grab samples)	--->	1.76
CICCS Accum (grams clay / cm^2 yr)	--->	0.04
CICCS Accum (grams / cm^2 yr)	--->	0.08
CICCS Accum (cm / yr)	--->	0.06

Avg. % Clay	Avg. Density
43.94	1.47

Assumed Supported --> (DPM/ g clay)	0.00
Assumed Den (g/cc)	1.50
Assumed Area (tube cross-section)	3.70

Present activity	
Confidence In	0.00
Original sedim	3.00
Background U	0.60
CIRCA Uncert	0.20
N/N$_o$	-0.25
S.E. (N/N$_o$)	-0.02
Predicted sed	#NUM!
S.E. (age)	#NUM!
minimum age	#NUM!
maximum age	#NUM!
Activity offset f	-1.5
Deposition dat	#NUM!

Present activity	
Confidence In	0.98
Original sedim	3.00
Background U	0.60
CIRCA Uncert	0.20
N/N$_o$	-0.25
S.E. (N/N$_o$)	-0.41
Predicted sed	#NUM!
S.E. (age)	#NUM!
minimum age	#NUM!
maximum age	59.57
Activity offset f	-1.5
Deposition dat	#NUM!

	--->	
Additional 'cap' activity (integrated tube DPM)		(DPM/cm^2) Cap activity
Assumed Mete (Atoms Pb-210/ M cm^2) (average 'shielded' rate of C18 & sites 41)	--->	17.76
Growth time fc	--->	0
Activity offset from 2000		-2.5
Deposition date		2002.5

depth	Density (measured)	unsupported activity / g clay	US activity / gram	Trapazoidal Depth-Integration of (activity * volume * density)
0.00	1.11	3.32	1.33	
1.00	1.11	3.32	1.33	5.47
2.50	1.35	2.69	1.09	8.26
3.50	1.36	2.33	1.05	5.36
4.50	1.52	2.31	1.04	5.57
5.50	1.48	1.64	0.74	4.94
6.50	1.47	1.97	0.89	4.44
7.50	1.36	1.94	0.87	4.62
8.50	1.52	1.93	0.87	4.63
9.50	1.68	1.95	0.88	5.16
10.50	1.64	0.89	0.40	3.93
11.50	2.06	0.62	0.30	2.40
15.00	1.74	0.17	0.08	4.71
20.50	1.42	0.47	0.24	5.14
25.00	1.50	0.40	0.20	5.29
30.50	1.50	0.05	0.03	3.44
39.70	1.50	10.69	5.84	

^{210}Pb Profiles

Int. Err	Core	Depth (avg)	notes	Pb-210 DPM/g	dpm/g clay	dpm/g % < 2um	err	% Clay	%Silt	%Sand	% < 2um	notes	Supported Background (dpm/g clay)	XS clay activity	Radon Ventillation Effect	XS Activity (CVC)
0.5	RASRF_163	0.5		1.48	3.31		0.34	45.00				AVG	1.611693786	1.70	-0.79	**2.49**
0.5	RASRF_163	1.5		1.57	3.52		0.34	45.00				AVG	1.611693786	1.91	-0.78	**2.69**
0.5	RASRF_163	2.5		1.37	3.08		0.30	45.00				AVG	1.611693786	1.47	-0.78	**2.24**
0.5	RASRF_163	3.5		1.04	2.33		0.24	45.00				AVG	1.611693786	0.71	-0.77	**1.49**
0.5	RASRF_163	4.5		0.98	2.18		0.23	45.00				AVG	1.611693786	0.57	-0.76	**1.34**
0.5	RASRF_163	5.5		0.84	1.87		0.20	45.00				AVG	1.611693786	0.26	-0.76	**1.02**
0.5	RASRF_163	6.5		0.90	2.00		0.21	45.00				AVG	1.611693786	0.38	-0.75	**1.14**
0.5	RASRF_163	7.5		0.51	1.14		0.13	45.00				AVG	1.611693786	-0.48	-0.75	**0.27**
0.5	RASRF_163	8.5		0.44	0.97		0.11	45.00				AVG	1.611693786	-0.64	-0.74	**0.10**
0.5	RASRF_163	9.5		0.36	0.79		0.10	45.00				AVG	1.611693786	-0.82	-0.73	**-0.09**
0.5	RASRF_163	10.5		0.45	0.99		0.10	45.00				AVG	1.611693786	-0.62	-0.73	**0.11**
0.5	RASRF_163	11.5		0.42	0.92		0.10	45.00				AVG	1.611693786	-0.69	-0.72	**0.03**
0.5	RASRF_163	15	small stones	0.41	0.88		0.10	45.00				AVG	1.611693786	-0.47	-0.67	**0.20**
0.5	RASRF_163	20.5		0.52	1.14		0.11	45.00				AVG	1.611693786	-0.74	-0.61	**-0.12**
0.7	RASRF_163	25		0.50	1.08		0.11	45.00				AVG	1.611693786	-0.38	-0.46	**0.08**
1	RASRF_163	30.5		0.40	0.87		0.10	45.00				AVG	1.611693786	-0.73	-0.70	**-0.03**
1	RASRF_163	60.2		0.56	1.23		0.12	45.00				AVG	1.611693786	-0.53	-0.64	**0.11**

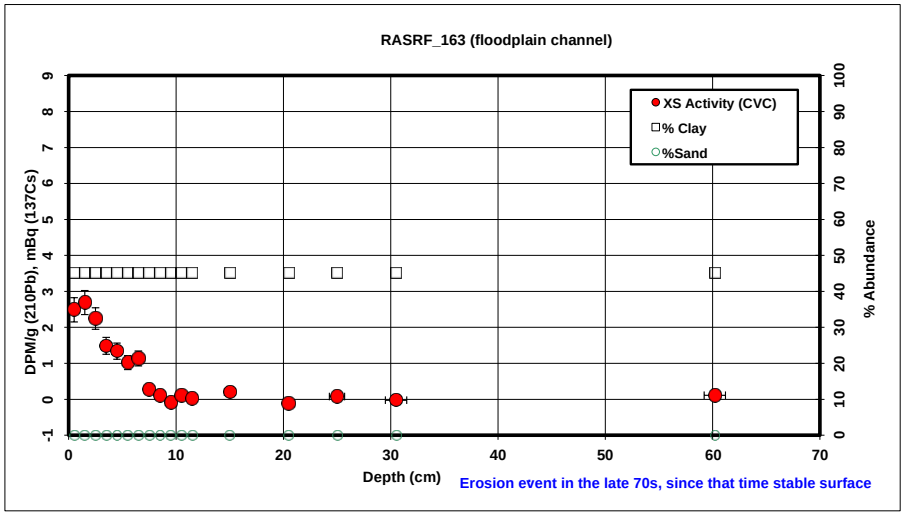

36.67	--->	9.91
Total integrated US activity (integrated tube DPM)		(DPM/cm^2) US activity
Assumed Mete	--->	17.76
(Atoms Pb-210/ M cm^2) (average 'shielded' rate of C18 & sites 41)		
US Activity fro	--->	-7.85
(DPM/ cm^2)		
Input Sedimen	--->	1.76
(DPM / g clay) (from proximal grab samples)		
CICCS Accum	--->	-0.14
(grams clay / cm^2 yr)		
CICCS Accum	--->	-0.31
(grams / cm^2 yr)		
CICCS Accum	--->	-0.17
(cm / yr)		

Avg. % Clay	Avg. Density
45.00	1.86

Assumed Supported --> (DPM/ g clay)	0.00
Assumed Den (g/cc)	1.50
Assumed Area (tube cross-section)	3.70

Present activity	
Confidence In	#REF!
Original sedim	3.00
Background U	0.60
CIRCA Uncerta	0.20
N/N_o	-0.25
S.E. (N/N_o)	#REF!
Predicted sed	#NUM!
S.E. (age)	#NUM!
minimum age	#REF!
maximum age	#REF!
Activity offset f	-1.5
Deposition dat	#NUM!

Present activity	
Confidence In	1.23
Original sedim	3.00
Background U	0.60
CIRCA Uncerta	0.20
N/N_o	-0.25
S.E. (N/N_o)	-0.51
Predicted sed	#NUM!
S.E. (age)	#NUM!
minimum age	#NUM!
maximum age	43.00
Activity offset f	-1.5
Deposition dat	#NUM!

	--->	9.91
Additional 'cap' activity (integrated tube DPM)		(DPM/cm^2) Cap activity
Assumed Mete	--->	17.76
(Atoms Pb-210/ M cm^2) (average 'shielded' rate of C18 & sites 41)		
Growth time fc	--->	26.2640641
Activity offset from 2000		-9.9
Deposition date		1983.6

depth	Density (measured)	unsupported activity / g clay	US activity / gram	Trapazoidal Depth-Integration of (activity * volume * density)
0.00	1.18	2.49	1.12	
0.50	1.18	2.49	1.12	2.45
1.50	1.61	2.69	1.21	6.02
2.50	1.80	2.24	1.01	7.02
3.50	1.81	1.49	0.67	5.62
4.50	1.98	1.34	0.60	4.45
5.50	1.71	1.02	0.46	3.62
6.50	2.43	1.14	0.51	3.71
7.50	2.29	0.27	0.12	2.76
8.50	2.04	0.10	0.05	0.67
9.50	2.03	0.00	0.00	0.17
10.50	2.25	0.11	0.05	0.19
11.50	2.43	0.03	0.01	
15.00	2.36	0.20	0.09	
20.50	2.04	0.00	0.00	
25.00	1.73	0.08	0.03	
30.50	2.19	0.00	0.00	
60.20	1.50	0.11	0.05	

^{210}Pb Profiles

Int. Err	Core	Depth (avg)	notes	Pb-210 DPM/g	dpm/g clay	dpm/g % < 2um	err	% Clay	%Silt	%Sand	% < 2um	notes	Supported Background (dpm/g clay)	XS clay activity	Radon Ventillation Effect	XS Activity (CVC)
1	RASRF_165	1		0.98	1.80	2.13	0.20	54.47	29.84	15.69	45.89	0.00	1.428458665	0.37	-0.79	1.16
0.5	RASRF_165	2.5		0.94	1.76	1.98	0.20	53.77	29.58	16.66	47.95		1.440183789	0.32	-0.78	1.10
0.5	RASRF_165	3.5		1.33	2.65	2.81	0.28	50.55	27.90	21.55	47.58		1.497568286	1.15	-0.77	1.92
0.5	RASRF_165	4.5		0.73	1.40	1.59	0.17	51.85	26.42	21.73	45.75		1.473644781	-0.07	-0.76	0.69
0.5	RASRF_165	5.5		0.60	1.17	1.42	0.13	50.84	24.02	25.14	42.00		1.491993545	-0.32	-0.76	0.44
0.5	RASRF_165	6.5		0.64	1.26	1.50	0.13	50.48	24.02	25.50	42.55		1.498764364	-0.24	-0.75	0.51
0.5	RASRF_165	7.5		0.52	0.87	1.02	0.10	58.70	28.33	12.98	50.39		1.362537687	-0.49	-0.75	0.26
0.5	RASRF_165	8.5		0.52	0.85	0.98	0.10	60.79	26.85	12.36	52.72		1.332698254	-0.49	-0.74	0.25
0.5	RASRF_165	9.5		0.49	0.74	0.84	0.10	66.02	26.57	7.41	57.75		1.26494596	-0.53	-0.73	0.20
0.5	RASRF_165	10.5		0.48	0.73	0.80	0.09	65.27	27.23	7.50	58.87		1.27414203	-0.55	-0.73	0.18
0.5	RASRF_165	11.5		0.47	0.71	0.77	0.09	65.27	28.18	6.54	60.70		1.274096858	-0.56	-0.72	0.16
1	RASRF_165	15		0.51	0.76		0.09	62.09				AVG	1.315048168	-0.56	-0.70	0.14
0.5	RASRF_165	20.5		0.48	0.81	0.92	0.10	58.90	32.99	8.11	51.91		1.359580794	-0.55	-0.67	0.12
1	RASRF_165	25	stones	0.39	1.06		0.11	35.00				AVG	1.889129963	-0.83	-0.64	-0.19
0.5	RASRF_165	30.5		0.38	1.06	1.20	0.12	35.92	20.12	43.96	31.65		1.858486114	-0.80	-0.61	-0.19
1	RASRF_165	37	stones	0.35	1.30	1.47	0.15	25.79	6.38	67.83	22.76		2.291299664	-0.99	-0.58	-0.41
1.15	RASRF_165	39.15		0.27	1.57	1.79	0.17	16.77	9.39	73.83	14.78		3.007301858	-1.43	-0.57	-0.87

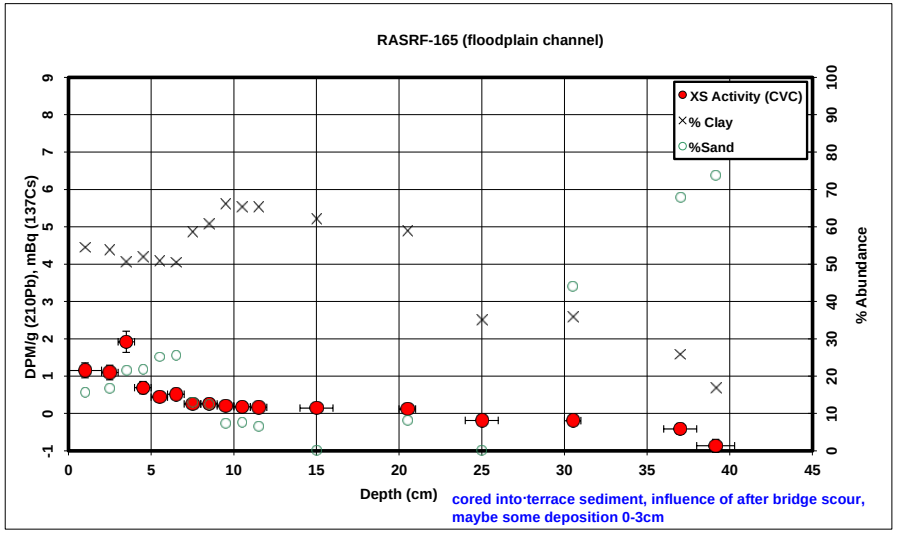

30.39	--->	8.21
Total integrated US activity (integrated tube DPM)		(DPM/cm^2) US activity
Assumed Mete	--->	17.76
(Atoms Pb-210/ M cm^2) (average 'shielded' rate of C18 & sites 41)		
US Activity fro	--->	-9.55
(DPM/ cm^2)		
Input Sedimen	--->	1.76
(DPM / g clay) (from proximal grab samples)		
CICCS Accum	--->	-0.17
(grams clay / cm^2 yr)		
CICCS Accum	--->	-0.31
(grams / cm^2 yr)		
CICCS Accum	--->	-0.17
(cm / yr)		

Avg. % Clay	Avg. Density
55.27	1.76

Assumed Supported --> (DPM/ g clay)	0.00
Assumed Den (g/cc)	1.50
Assumed Area (tube cross-section)	3.70

Present activit	1.13
Confidence In	0.00
Original sedim	1.76
Background US activity	
CIRCA Uncert	0.20
N/N$_o$	0.64
S.E. (N/N$_o$)	0.07
Predicted sed	14.20
S.E. (age)	3.67
minimum age	10.73
maximum age	18.09
Activity offset f	-1.5
Deposition dat	1987.3

Present activity	
Confidence In	0.76
Original sedim	3.00
Background U	0.60
CIRCA Uncert	0.20
N/N$_o$	-0.25
S.E. (N/N$_o$)	-0.32
Predicted sed	#NUM!
S.E. (age)	#NUM!
minimum age	#NUM!
maximum age	87.55
Activity offset f	-1.5
Deposition dat	#NUM!

	--->	
Additional 'cap' activity (integrated tube DPM)		(DPM/cm^2) Cap activity
Assumed Mete	--->	17.76
(Atoms Pb-210/ M cm^2) (average 'shielded' rate of C18 & sites 41)		
Growth time fo	--->	0
Activity offset from 2000		-2.5
Deposition date		2002.5

depth	Density (measured)	unsupported activity / g clay	US activity / gram	Trapazoidal Depth-Integration of (activity * volume * density)
0.00	1.13	1.16	0.63	
1.00	1.13	1.16	0.63	2.64
2.50	1.24	1.10	0.59	4.02
3.50	1.56	1.92	0.97	4.05
4.50	1.85	0.69	0.36	4.19
5.50	2.07	0.44	0.22	2.11
6.50	1.98	0.51	0.26	1.80
7.50	2.00	0.26	0.15	1.51
8.50	2.04	0.25	0.15	1.14
9.50	1.86	0.20	0.14	1.04
10.50	1.96	0.18	0.12	0.89
11.50	2.26	0.16	0.11	0.87
15.00	1.99	0.14	0.09	2.68
20.50	2.31	0.12	0.07	3.45
25.00	2.38	0.00	0.00	
30.50	2.25	0.00	0.00	
37.00	1.88	0.00	0.00	
39.15	1.50	0.00	0.00	

^{210}Pb Profiles

Int. Err	Core	Depth (avg)	notes	Pb-210 DPM/g	dpm/g clay	dpm/g % < 2um	err	% Clay	%Silt	%Sand	% < 2um	notes
0.5	RASRF_166	0.5		1.36	2.90		0.27	47.39				AVG
0.5	RASRF_166							47.39				AVG
0.5	RASRF_166	2.5		1.68	3.59	4.27	0.38	47.39	41.00	11.62	39.78	
0.5	RASRF_166	3.5		1.48	2.85	3.38	0.30	52.29	41.40	6.31	44.09	
0.5	RASRF_166	4.5		1.32	2.56		0.28	51.91				AVG
0.5	RASRF_166	5.5		1.15	2.25	2.68	0.24	51.54	42.55	5.91	43.27	
0.5	RASRF_166	6.5		1.11	2.29		0.22	49.01				AVG
0.5	RASRF_166	7.5		1.00	2.15	2.62	0.23	46.48	45.43	8.09	38.17	
0.5	RASRF_166	8.5		0.99	2.09		0.22	47.39				AVG
0.5	RASRF_166	9.5		0.91	1.90	2.30	0.22	48.30	42.72	8.98	39.93	
0.5	RASRF_166	10.5		0.93	1.91		0.22	48.82				AVG
0.5	RASRF_166	11.5		0.86	1.74	2.06	0.18	49.35	41.40	9.25	41.78	
1	RASRF_166	15		0.64	1.41		0.13	46.13				AVG
0.5	RASRF_166	20.5		0.57	1.33	1.58	0.14	42.91	45.12	11.97	35.92	
1	RASRF_166	25		0.46	0.99		0.11	45.34				AVG
0.5	RASRF_166	30.5		0.49	1.02	1.24	0.12	47.78	38.48	13.74	39.48	
1	RASRF_166	41		0.50	1.08		0.11	46.49				AVG
0.6	RASRF_166	65.1		0.50	1.09	1.30	0.13	45.19	43.78	11.03	37.84	

Supported Background (dpm/g clay)	XS clay activity	Radon Ventillation Effect	XS Activity (CVC)
1.559939664	1.34	-0.79	**2.13**
1.559939664			
1.559939664	2.03	-0.78	**2.80**
1.465782125	1.38	-0.77	**2.15**
1.472483962	1.09	-0.76	**1.85**
1.479265503	0.77	-0.76	**1.53**
1.527083058	0.76	-0.75	**1.51**
1.579107606	0.57	-0.75	**1.32**
1.559885869	0.53	-0.74	**1.27**
1.541256916	0.36	-0.73	**1.09**
1.530725519	0.38	-0.73	**1.11**
1.520377959	0.22	-0.72	**0.94**
1.586670827	-0.17	-0.70	**0.53**
1.660982409	-0.34	-0.67	**0.33**
1.603957546	-0.61	-0.64	**0.03**
1.551728121	-0.53	-0.61	**0.09**
1.578941312	-0.50	-0.56	**0.05**
1.607422094	-0.52	-0.44	**-0.08**

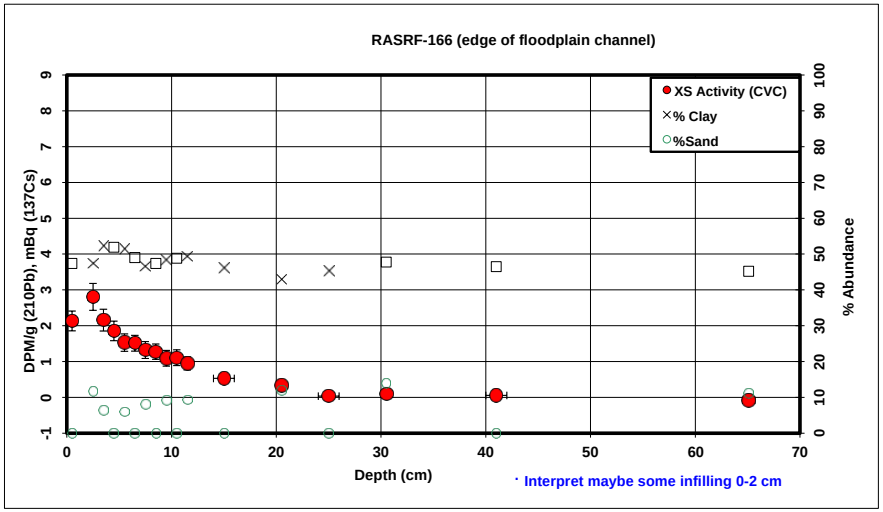

70.88	--->	19.16
Total integrated US activity (integrated tube DPM)		(DPM/cm^2) US activity
Assumed Mete (Atoms Pb-210/ M cm^2) (average 'shielded' rate of C18 & sites 41)	--->	17.76
US Activity fro (DPM/ cm^2)	--->	1.39
Input Sedimen (DPM / g clay) (from proximal grab samples)	--->	1.76
CICCS Accum (grams clay / cm^2 yr)	--->	0.02
CICCS Accum (grams / cm^2 yr)	--->	0.05
CICCS Accum (cm / yr)	--->	0.03

Avg. % Clay	Avg. Density
48.97	1.51

Assumed Supported --> (DPM/ g clay)	0.00
Assumed Den (g/cc)	1.50
Assumed Area (tube cross-section)	3.70

Present activity	
Confidence In	0.00
Original sedim	3.00
Background U	0.60
CIRCA Uncert	0.20
N/N_o	-0.25
S.E. (N/N_o)	-0.02
Predicted sed	#NUM!
S.E. (age)	#NUM!
minimum age	#NUM!
maximum age	#NUM!
Activity offset f	-1.5
Deposition dat	#NUM!

Present activity	
Confidence In	1.09
Original sedim	3.00
Background U	0.60
CIRCA Uncert	0.20
N/N_o	-0.25
S.E. (N/N_o)	-0.45
Predicted sed	#NUM!
S.E. (age)	#NUM!
minimum age	#NUM!
maximum age	51.12
Activity offset f	-1.5
Deposition dat	#NUM!

	--->	
Additional 'cap' activity (integrated tube DPM)		(DPM/cm^2) Cap activity
Assumed Mete (Atoms Pb-210/ M cm^2) (average 'shielded' rate of C18 & sites 41)	--->	17.76
Growth time fo	--->	0
Activity offset from 2000		-2.5
Deposition date		2002.5

depth	Density (measured)	unsupported activity / g clay	US activity / gram	Trapazoidal Depth-Integration of (activity * volume * density)
0.00	1.50	2.13	1.01	
0.50	1.50	2.13	1.01	2.80
1.50	1.50		1.01	5.61
2.50	1.15	2.80	1.33	5.72
3.50	1.30	2.15	1.13	5.56
4.50	1.61	1.85	0.96	5.62
5.50	1.62	1.53	0.79	5.22
6.50	1.37	1.51	0.74	4.22
7.50	1.65	1.32	0.61	3.78
8.50	1.60	1.27	0.60	3.66
9.50	1.58	1.09	0.53	3.33
10.50	1.78	1.11	0.54	3.32
11.50	1.82	0.94	0.47	3.35
15.00	1.83	0.53	0.24	8.38
20.50	2.12	0.33	0.14	7.79
25.00	1.72	0.03	0.01	2.52
30.50	1.95	0.09	0.04	
41.00	1.89	0.05	0.03	
65.10	1.50	0.00	0.00	

^{210}Pb Profiles

Int. Err	Core	Depth (avg)	notes	Pb-210 DPM/g	dpm/g clay	dpm/g % < 2um	err	% Clay	%Silt	%Sand	% < 2um	notes
0.5	RASRF_167	0.5		1.60	3.30		0.35	48.75				AVG
0.5	RASRF_167	1.5		1.62	3.34	4.02	0.36	48.75	37.07	14.18	40.45	
0.5	RASRF_167	2.5		1.21	2.45		0.27	49.81				AVG
0.5	RASRF_167	3.5		1.43	2.83	3.34	0.31	50.86	36.30	12.84	43.10	
0.5	RASRF_167	4.5		1.27	2.66		0.29	47.90				AVG
0.5	RASRF_167	5.5		1.63	3.66	4.33	0.40	44.95	35.80	19.25	38.01	
0.5	RASRF_167	6.5		1.94	4.18		0.45	46.77				AVG
0.5	RASRF_167	7.5		1.68	3.48	4.08	0.37	48.58	39.02	12.40	41.40	
0.5	RASRF_167	8.5		1.44	3.24		0.31	44.83				AVG
0.5	RASRF_167	9.5		1.20	2.94	3.59	0.32	41.08	37.02	21.90	33.56	
0.5	RASRF_167	10.5		0.80	2.11		0.22	37.90				AVG
0.5	RASRF_167	11.5		0.72	2.07	2.34	0.21	34.71	23.69	41.59	30.63	
1	RASRF_167	15		0.58	1.75		0.16	33.00				AVG
1	RASRF_167	21		0.64	1.95		0.18	33.00				AVG
0.5	RASRF_167	23.5		0.61	1.89	2.21	0.22	32.45	25.85	41.70	27.72	

Supported Background (dpm/g clay)	XS clay activity	Radon Ventillation Effect	XS Activity (CVC)
1.532108605	1.76	-0.79	2.55
1.532108605	1.81	-0.78	2.59
1.511556592	0.93	-0.78	1.71
1.491701698	1.34	-0.77	2.11
1.549247064	1.11	-0.76	1.88
1.612898346	2.05	-0.76	2.81
1.572977946	2.61	-0.75	3.36
1.53551294	1.94	-0.75	2.69
1.615533254	1.63	-0.74	2.37
1.707292571	1.23	-0.73	1.96
1.796547587	0.32	-0.73	1.04
1.898941722	0.17	-0.72	0.89
1.960703979	-0.21	-0.70	0.49
1.960703979	-0.01	-0.67	0.66
1.98178144	-0.09	-0.65	0.56

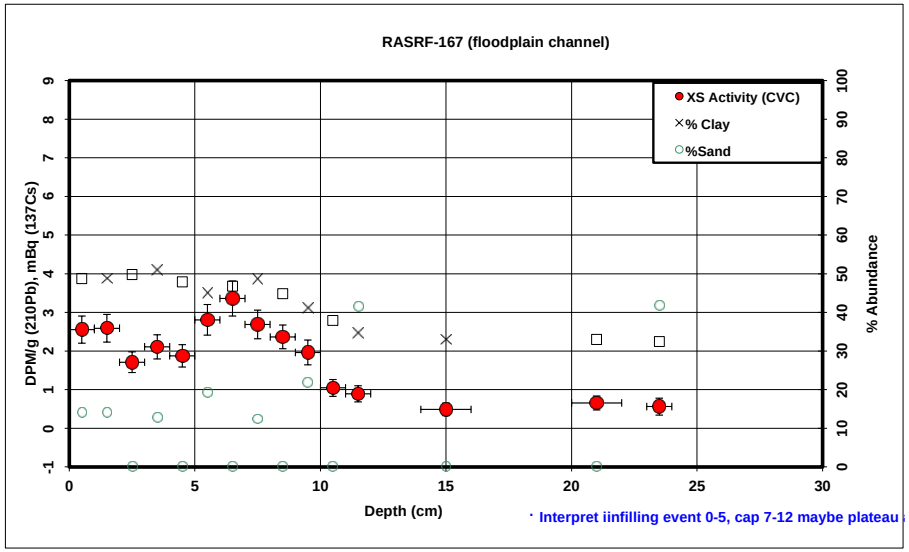

75.19	--->	20.32
Total integrated US activity (integrated tube DPM)		(DPM/cm^2) US activity
Assumed Mete (Atoms Pb-210/ M cm^2) (average 'shielded' rate of C18 & sites 41)	--->	17.76
US Activity fro (DPM/ cm^2)	--->	2.56
Input Sedimen (DPM / g clay) (from proximal grab samples)	--->	1.76
CICCS Accum (grams clay / cm^2 yr)	--->	0.05
CICCS Accum (grams / cm^2 yr)	--->	0.09
CICCS Accum (cm / yr)	--->	0.07

Avg. % Clay	Avg. Density
47.91	1.37

Assumed Supported --> (DPM/ g clay)	0.00
Assumed Den (g/cc)	1.50
Assumed Area (tube cross-section)	3.70

Present activi	0.57
Confidence In	0.08
Original sedin	1.76
Background US activity	
CIRCA Uncert	0.20
N/N_o	0.32
S.E. (N/N_o)	0.06
Predicted sed	36.32
S.E. (age)	6.08
minimum age	30.79
maximum age	42.99
Activity offset f	-9.9
Deposition dat	1973.6

Present activity	
Confidence In	1.95
Original sedin	3.00
Background U	0.60
CIRCA Uncert	0.20
N/N_o	-0.25
S.E. (N/N_o)	-0.81
Predicted sed	#NUM!
S.E. (age)	#NUM!
minimum age	#NUM!
maximum age	18.49
Activity offset f	-1.5
Deposition dat	#NUM!

	--->	
Additional 'cap' activity (integrated tube DPM)		(DPM/cm^2) Cap activity
Assumed Mete (Atoms Pb-210/ M cm^2) (average 'shielded' rate of C18 & sites 41)	--->	17.76
Growth time fo	--->	0
Activity offset from 2000		-2.5
Deposition date		2002.5

depth	Density (measured)	unsupported activity / g clay	US activity / gram	Trapazoidal Depth-Integration of (activity * volume * density)
0.00	1.50	2.55	1.25	
0.50	1.50	2.55	1.25	3.46
1.50	1.50	2.59	1.26	6.96
2.50	1.11	1.71	0.85	5.11
3.50	1.20	2.11	1.07	4.12
4.50	1.02	1.88	0.90	4.05
5.50	1.02	2.81	1.26	4.07
6.50	1.20	3.36	1.57	5.82
7.50	1.24	2.69	1.31	6.49
8.50	1.60	2.37	1.06	6.22
9.50	1.76	1.96	0.81	5.80
10.50	1.84	1.04	0.40	4.00
11.50	1.90	0.89	0.31	2.44
15.00	1.88	0.49	0.16	5.75
21.00	1.85	0.66	0.22	7.82
23.50	1.50	0.56	0.18	3.09

^{210}Pb Profiles

Int. Err	Core	Depth (avg)	notes	Pb-210 DPM/g	dpm/g clay	dpm/g % < 2um	err	% Clay	%Silt	%Sand	% < 2um	notes
0.5	RASRF168	0.5		2.07	5.55	7.10	0.59	37.67	54.43	7.91	29.47	
0.5	RASRF168	1.5		2.11	5.64	7.21	0.61	37.67	54.43	7.91	29.47	
0.5	RASRF168	2.5		1.78	4.62	5.63	0.48	38.84	53.06	8.11	31.84	
0.5	RASRF168	3.5		1.75	4.40	5.13	0.48	40.16	51.97	7.87	34.40	
0.5	RASRF168	4.5		1.37	3.33	3.96	0.37	41.52	49.68	8.81	34.91	
0.5	RASRF168	5.5		1.39	3.20	3.86	0.37	43.84	48.68	7.49	36.31	
0.5	RASRF168	6.5		1.05	2.51	3.11	0.28	42.08	49.07	8.85	34.06	
0.5	RASRF168	7.5		0.86	2.12	2.68	0.25	40.63	49.79	9.58	32.07	
0.5	RASRF168	8.5		0.66	1.52	1.84	0.17	43.74	46.62	9.63	36.07	
0.5	RASRF168	9.5		0.69	1.48	1.74	0.16	46.47	43.00	10.52	39.67	
0.5	RASRF168	10.5		0.66	1.49	1.75	0.16	44.19	47.05	8.77	37.66	
0.5	RASRF168	11.5		0.66	1.69	1.99	0.18	39.15	48.23	12.62	33.29	
1	RASRF168	15		0.54	1.19		0.12	44.58				AVG
0.5	RASRF168	20.5		0.56	1.12	1.29	0.12	50.01	43.17	6.82	43.17	
1	RASRF168	25		0.54	1.17		0.12	48.50				AVG
0.5	RASRF168	30.5		0.49	1.05	1.22	0.12	47.00	48.23	4.77	40.28	
1	RASRF168	41		0.57	1.25		0.13	45.00				AVG
1	RASRF168	51		0.68	1.50		0.14	45.00				AVG
0.7	RASRF168	61.7		0.53	1.17	1.33	0.12	45.41	46.10	8.49	40.01	

Supported Background (dpm/g clay)	XS clay activity	Radon Ventillation Effect	XS Activity (CVC)
1.803465742	3.75	-0.79	4.54
1.803465742	3.84	-0.78	4.62
1.768953925	2.85	-0.78	3.62
1.731867381	2.66	-0.77	3.44
1.695898239	1.63	-0.76	2.39
1.638598517	1.56	-0.76	2.32
1.681516989	0.83	-0.75	1.59
1.719207399	0.40	-0.75	1.15
1.640839781	-0.13	-0.74	0.61
1.579191488	-0.10	-0.73	0.64
1.630400028	-0.14	-0.73	0.59
1.760073956	-0.07	-0.72	0.66
1.621337232	-0.43	-0.70	0.27
1.507717793	-0.39	-0.67	0.28
1.537126963	-0.37	-0.64	0.28
1.568064674	-0.52	-0.61	0.09
1.611693786	-0.36	-0.56	0.19
1.611693786	-0.11	-0.51	0.39
1.602387225	-0.43	-0.45	0.02

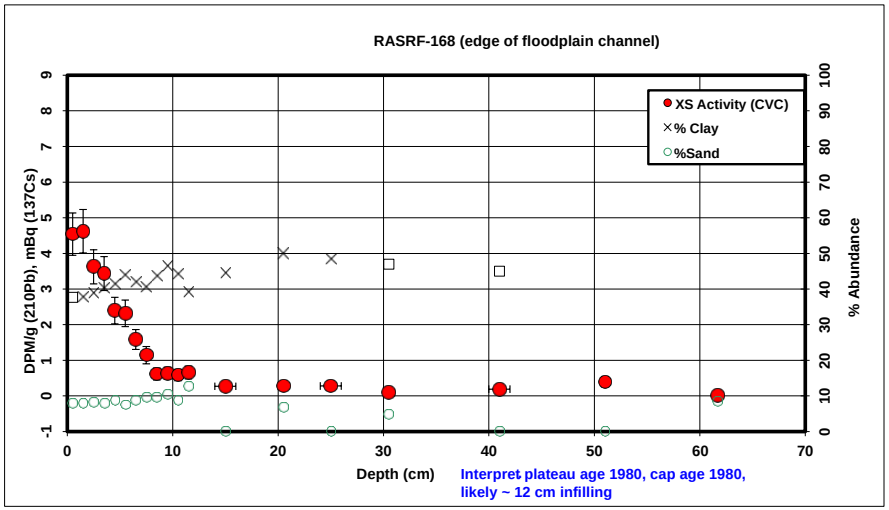

81.50	--->	22.03
Total integrated US activity (integrated tube DPM)		(DPM/cm^2) US activity

Assumed Mete ---> 17.76
(Atoms Pb-210/ M cm^2)
(average 'shielded' rate of C18 & sites 41)

US Activity fro ---> 4.26
(DPM/ cm^2)

Input Sedimen ---> 1.76
(DPM / g clay)
(from proximal grab samples)

CICCS Accum ---> 0.08
(grams clay / cm^2 yr)

CICCS Accum ---> 0.18
(grams / cm^2 yr)

CICCS Accum ---> 0.13
(cm / yr)

Avg. % Clay	Avg. Density
41.26	1.46

Assumed Supported -->	0.00
(DPM/ g clay)	
Assumed Den	1.50
(g/cc)	
Assumed Area	3.70
(tube cross-section)	

Present activi	0.62
Confidence In	0.03
Original sedin	1.76
Background US activity	
CIRCA Uncert	0.20
N/N_o	0.36
S.E. (N/N_o)	0.04
Predicted sed	33.32
S.E. (age)	3.98
minimum age	29.58
maximum age	37.55
Activity offset f	-9.9
Deposition dat	1976.6

Present activity	
Confidence In	1.19
Original sedin	3.00
Background U	0.60
CIRCA Uncert	0.20
N/N_o	-0.25
S.E. (N/N_o)	-0.50
Predicted sed	#NUM!
S.E. (age)	#NUM!
minimum age	#NUM!
maximum age	45.08
Activity offset f	-1.5
Deposition dat	#NUM!

	--->	22.03
Additional 'cap' activity (integrated tube DPM)		(DPM/cm^2) Cap activity

Assumed Mete ---> 17.76
(Atoms Pb-210/ M cm^2)
(average 'shielded' rate of C18 & sites 41)

Growth time fo ---> #NUM!

Activity offset from 2000	-9.9
Deposition date	#NUM!

depth	Density (measured)	unsupported activity / g clay	US activity / gram	Trapazoidal Depth-Integration of (activity * volume * density)
0.00	1.01	4.54	1.71	
0.50	1.01	4.54	1.71	3.19
1.50	1.03	4.62	1.74	6.51
2.50	1.40	3.62	1.41	7.09
3.50	1.35	3.44	1.38	7.08
4.50	1.51	2.39	0.99	6.26
5.50	1.58	2.32	1.02	5.73
6.50	1.57	1.59	0.67	4.90
7.50	1.57	1.15	0.47	3.29
8.50	1.78	0.61	0.27	2.27
9.50	1.84	0.64	0.30	1.89
10.50	1.87	0.59	0.26	1.91
11.50	2.08	0.66	0.26	1.89
15.00	1.80	0.27	0.12	4.74
20.50	1.82	0.28	0.14	4.76
25.00	1.76	0.28	0.13	4.07
30.50	1.81	0.09	0.04	3.23
41.00	1.71	0.19	0.09	4.43
51.00	1.69	0.39	0.18	8.25
61.70	1.50	0.02	0.01	5.81

^{210}Pb Profiles

Int. Err	Core	Depth (avg)	notes	Pb-210 DPM/g	dpm/g clay	dpm/g % < 2um	err	% Clay	%Silt	%Sand	% < 2um	notes
0.5	RASRF_169	0.5		0.94	2.96	3.71	0.32	32.01	41.20	26.79	25.55	
0.5	RASRF_169	1.5		1.37	4.06	5.04	0.42	33.95	50.28	15.77	27.39	
0.5	RASRF_169	2.5		1.19	3.51		0.33	34.17				AVG
0.5	RASRF_169	3.5		1.09	3.18	3.92	0.34	34.38	53.89	11.73	27.89	
0.5	RASRF_169	4.5		1.03	3.02		0.29	34.39				AVG
0.5	RASRF_169	5.5		0.90	2.63	3.28	0.28	34.39	54.74	10.87	27.61	
0.5	RASRF_169	6.5		0.88	2.58		0.28	34.07				AVG
0.5	RASRF_169	7.5		1.16	3.45	4.20	0.38	33.75	56.78	9.47	27.72	
0.5	RASRF_169	8.5		1.02	2.92		0.30	35.31				AVG
0.5	RASRF_169	9.5		0.97	2.64	3.32	0.30	36.87	59.77	3.36	29.30	
0.5	RASRF_169	10.5		0.94	2.60		0.27	36.36				AVG
0.5	RASRF_169	11.5		0.73	2.04	2.62	0.21	35.86	55.43	8.71	27.93	
1	RASRF_169	15		0.74	2.13		0.19	35.00				AVG
0.5	RASRF_169	17.5		0.76	2.18		0.20	35.00				AVG
0.5	RASRF_169	20.5		0.58	1.50	1.80	0.17	38.63	48.01	13.36	32.13	
1	RASRF_169	25		0.59	1.67		0.16	38.00				est
0.5	RASRF_169	30.5		0.59	1.67		0.16	38.00		5.42		est
1	RASRF_169	41		0.63	1.78		0.16	38.00				est
1	RASRF_169	51		0.56	1.57		0.15	38.00				est
0.6	RASRF_169	55.6		0.44	1.24		0.13	38.00		10.64		est

Supported Background (dpm/g clay)	XS clay activity	Radon Ventillation Effect	XS Activity (CVC)
1.99886507	0.96	-0.79	1.75
1.92589135	2.14	-0.78	2.92
1.91817105	1.59	-0.78	2.37
1.910530164	1.27	-0.77	2.04
1.910380281	1.11	-0.76	1.87
1.910230427	0.72	-0.76	1.48
1.921502728	0.66	-0.75	1.41
1.932948416	1.52	-0.75	2.26
1.878631255	1.04	-0.74	1.78
1.828087974	0.81	-0.73	1.55
1.844110062	0.75	-0.73	1.48
1.860499865	0.18	-0.72	0.90
1.889129963	0.25	-0.70	0.95
1.889129963	0.29	-0.69	0.98
1.774951846	-0.28	-0.67	0.39
1.793451379	-0.12	-0.64	0.52
1.793451379	-0.12	-0.61	0.49
1.793451379	-0.01	-0.56	0.55
1.793451379	-0.22	-0.51	0.28
1.793451379	-0.56	-0.48	-0.08

Assumed Supported -->	0.00
(DPM/ g clay)	
Assumed Den	1.50
(g/cc)	
Assumed Area	3.70
(tube cross-section)	

Present activi	0.94
Confidence In	0.04
Original sedim	1.76
Background US activity	
CIRCA Uncerta	0.20
N/N_o	0.54
S.E. (N/N_o)	0.06
Predicted sed	20.01
S.E. (age)	3.90
minimum age	16.34
maximum age	24.15
Activity offset f	-9.9
Deposition dat	1989.9

depth	Density (measured)	unsupported activity / g clay	US activity / gram	Trapazoidal Depth-Integration of (activity * volume * density)
0.00	1.50	1.75	0.56	
0.50	1.50	1.75	0.56	1.55
1.50	1.02	2.92	0.99	3.61
2.50	1.28	2.37	0.81	3.82
3.50	1.30	2.04	0.70	3.59
4.50	1.36	1.87	0.64	3.31
5.50	1.50	1.48	0.51	3.06
6.50	1.47	1.41	0.48	2.72
7.50	1.48	2.26	0.76	3.39
8.50	1.57	1.78	0.63	3.92
9.50	1.57	1.55	0.57	3.48
10.50	1.80	1.48	0.54	3.46
11.50	1.58	0.90	0.32	2.69
15.00	1.74	0.95	0.33	7.04
17.50	1.55	0.98	0.34	5.14
20.50	1.97	0.39	0.15	4.84
25.00	1.75	0.52	0.20	5.44
30.50	1.59	0.49	0.19	6.55
41.00	1.70	0.55	0.21	12.59
51.00	1.94	0.28	0.11	10.60
55.60	1.75	0.00	0.00	1.68

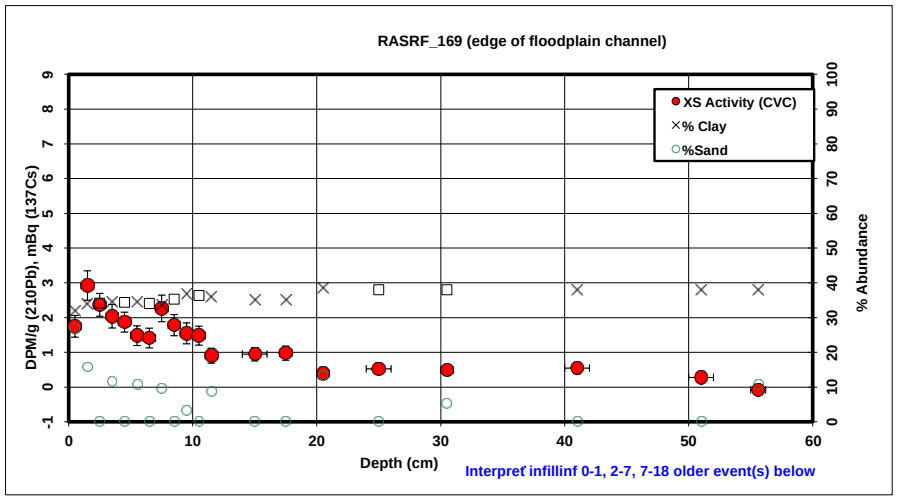

92.49	--->	25.00
Total integrated tube DPM)		US activity (DPM/cm^2)
Assumed Mete	--->	17.76
(Atoms Pb-210/ M cm^2)		
(average 'shielded' rate of C18 & sites 41)		
US Activity fro	--->	7.23
(DPM/ cm^2)		
Input Sedimen	--->	1.76
(DPM / g clay)		
(from proximal grab samples)		
CICCS Accum	--->	0.13
(grams clay / cm^2 yr)		
CICCS Accum	--->	0.37
(grams / cm^2 yr)		
CICCS Accum	--->	0.26
(cm / yr)		

Avg. % Clay	Avg. Density
34.33	1.44

Present activi	0.49
Confidence In	0.07
Original sedim	3.00
Background US activity	
CIRCA Uncerta	0.20
N/N_o	0.16
S.E. (N/N_o)	0.03
Predicted sed	58.39
S.E. (age)	4.97
minimum age	53.79
maximum age	63.77
Activity offset f	-9.9
Deposition dat	1951.5

	--->	25.00
Additional 'cap' activity (integrated tube DPM)		(DPM/cm^2) Cap activity
Assumed Mete	--->	17.76
(Atoms Pb-210/ M cm^2)		
(average 'shielded' rate of C18 & sites 41)		
Growth time fo	--->	#NUM!
Activity offset from 2000		-7
Deposition date		#NUM!

^{210}Pb Profiles

Int. Err	Core	Depth (avg)	notes	Pb-210 DPM/g	dpm/g clay	dpm/g % < 2um	err	% Clay	%Silt	%Sand	% < 2um	notes
1	T2_P1	1		1.27	2.59		0.21	50.00				AVG
1	T2_P1	3		1.04	2.03	2.38	0.20	51.92	43.97	4.11	44.16	
1	T2_P1	5		0.93	1.80	2.10	0.18	52.08	45.06	2.86	44.81	
1	T2_P1	7		0.81	1.51	1.71	0.15	54.17	42.62	3.21	47.79	
1	T2_P1	9		0.72	1.32	1.52	0.14	54.22	42.78	2.99	47.05	
1	T2_P1	11		0.77	1.42	1.65	0.15	54.38	42.38	3.24	46.83	
1	T2_P1	13	no stones	0.69	1.25		0.12	56.02				AVG
1	T2_P1	15	several big stones	0.67	1.21		0.12	57.66				AVG
1	T2_P1	17	no stones	0.55	0.97		0.11	59.30				AVG
1	T2_P1	19	heavily weathered s	0.52	0.92		0.10	60.93				AVG
1	T2_P1	21		0.49	0.76	0.84	0.09	62.57	36.40	1.03	56.86	
1	T2_P1	23		0.53	0.95		0.10	61.20				AVG
1	T2_P1	31		0.56	0.91	1.02	0.10	59.83	38.56	1.60	53.32	
1	T2_P1	41		0.53	0.84	0.94	0.10	61.71	36.85	1.44	55.17	
1.05	T2_P1	62.55		0.59	0.96	1.07	0.11	60.11	38.19	1.70	53.96	

Supported Background (dpm/g clay)	XS clay activity	Radon Ventillation Effect	XS Activity (CVC)
1.507869642	1.09	-0.79	**1.87**
1.472327432	0.55	-0.77	**1.33**
1.469539463	0.33	-0.76	**1.10**
1.433386922	0.07	-0.75	**0.82**
1.432517907	-0.11	-0.74	**0.62**
1.429951744	-0.01	-0.73	**0.72**
1.403368504	-0.15	-0.71	**0.56**
1.378024967	-0.17	-0.70	**0.53**
1.353830483	-0.38	-0.69	**0.31**
1.330703304	-0.41	-0.68	**0.27**
1.308569492	-0.54	-0.67	**0.12**
1.32699845	-0.38	-0.66	**0.28**
1.346112898	-0.44	-0.61	**0.17**
1.320073353	-0.48	-0.56	**0.08**
1.342185728	-0.38	-0.45	**0.06**

Assumed Supported -->		0.00
(DPM/ g clay)		
Assumed Dens		1.50
(g/cc)		
Assumed Area		3.70
(tube cross-section)		

Present activity	
Confidence In	#REF!
Original sedim	3.00
Background U	0.60
CIRCA Uncert	0.20
N/N_o	-0.25
S.E. (N/N_o)	#REF!
Predicted sed	#NUM!
S.E. (age)	#NUM!
minimum age	#REF!
maximum age	#REF!
Activity offset f	-1.5
Deposition dat	#NUM!

Present activity	
Confidence In	0.00
Original sedim	3.00
Background U	0.60
CIRCA Uncert	0.20
N/N_o	-0.25
S.E. (N/N_o)	-0.02
Predicted sed	#NUM!
S.E. (age)	#NUM!
minimum age	#NUM!
maximum age	#NUM!
Activity offset f	-1.5
Deposition dat	#NUM!

depth	Density (measured)	unsupported activity / g clay	US activity / gram	Trapazoidal Depth-Integration of (activity * volume * density)
0.00	1.12	1.87	0.94	
1.00	1.12	1.87	0.94	3.88
3.00	1.39	1.33	0.69	7.53
5.00	1.50	1.10	0.57	6.73
7.00	1.41	0.82	0.45	5.47
9.00	1.64	0.62	0.34	4.42
11.00	1.61	0.72	0.39	4.39
13.00	1.50	0.56	0.31	4.05
15.00	1.79	0.53	0.31	3.78
17.00	2.09	0.31	0.18	3.52
19.00	1.62	0.27	0.16	2.37
21.00	1.50	0.12	0.08	1.38
23.00	1.50	0.28	0.17	1.36
31.00	1.18	0.17	0.10	5.39
41.00	1.50	0.08	0.05	3.75
62.55	1.50	0.06	0.04	

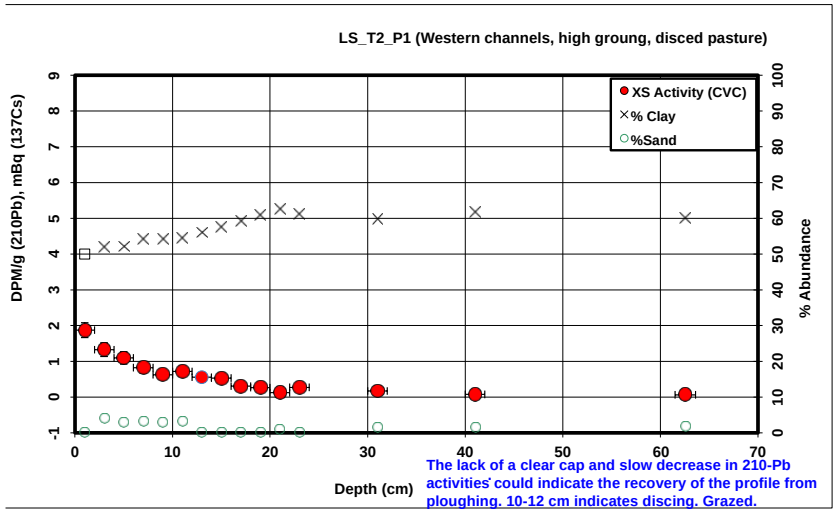

58.03	--->	15.68
Total integrated US activity (integrated tube DPM)		(DPM/cm^2) US activity
Assumed Mete (Atoms Pb-210/ M cm^2) (average 'shielded' rate of C18 & sites 41)	--->	17.76
US Activity fro (DPM/ cm^2)	--->	-2.08
Input Sedimen (DPM / g clay) (from proximal grab samples)	--->	1.76
CICCS Accum (grams clay / cm^2 yr)	--->	-0.04
CICCS Accum (grams / cm^2 yr)	--->	-0.06
CICCS Accum (cm / yr)	--->	-0.04

Avg. % Clay	Avg. Density
57.07	1.52

	--->	15.68
Additional 'cap' activity (integrated tube DPM)		(DPM/cm^2) Cap activity
Assumed Mete (Atoms Pb-210/ M cm^2) (average 'shielded' rate of C18 & sites 41)	--->	17.76
Growth time fc	--->	69.0088615
Activity offset from 2000		-2.5
Deposition date		1933.5

^{210}Pb Profiles

Int. Err	Core	Depth (avg)	notes	Pb-210 DPM/g	dpm/g clay	dpm/g % < 2um	err	% Clay	%Silt	%Sand	% < 2um	notes	Supported Background (dpm/g clay)	XS clay activity	Radon Ventillation Effect	XS Activity (CVC)
1	T2_P2	1		1.80	3.96		0.50	47.00				AVG	1.568003378	2.39	-0.79	**3.18**
1	T2_P2	3		1.11	2.32		0.20	47.80		1.27		first run didn't	1.551435164	0.76	-0.77	**1.54**
1	T2_P2	5		0.98	2.05	2.56	0.18	47.80	49.88	2.32	38.28		1.551435164	0.50	-0.76	**1.26**
1	T2_P2	7		0.90	1.70	2.09	0.15	53.04	47.68	-0.72	42.97		1.45270558	0.24	-0.75	**0.99**
1	T2_P2	9		0.81	1.55	1.96	0.14	52.57	48.70	-1.28	41.46		1.460807417	0.09	-0.74	**0.83**
1	T2_P2	11		0.82	1.64	2.10	0.16	49.96	50.60	-0.56	38.94		1.508667421	0.13	-0.73	**0.86**
1	T2_P2	13		0.90	1.82		0.16	51.11				AVG	1.487177869	0.34	-0.71	**1.05**
1	T2_P2	17		0.81	1.62		0.15	52.25				AVG	1.466461337	0.16	-0.69	**0.85**
1	T2_P2	21		0.66	1.23	1.51	0.13	53.40	46.87	-0.27	43.49		1.446473948	-0.22	-0.67	**0.45**
1	T2_P2	25		0.63	1.24		0.12	53.00				AVG	1.453411575	-0.21	-0.64	**0.43**
1	T2_P2	31		0.52	0.99	1.25	0.10	52.59	48.06	-0.66	41.44		1.460435783	-0.47	-0.61	**0.14**
1	T2_P2	41		0.49	0.95	1.17	0.10	51.93	47.75	0.32	42.22		1.472223045	-0.52	-0.56	**0.03**
1	T2_P2	65		0.65	1.28		0.13	50.97				AVG	1.489741998	-0.21	-0.44	**0.23**
1	T2_P2	89		0.62	1.24	1.55	0.13	50.00	47.42	2.57	40.13		1.507809615	-0.27	-0.33	**0.06**

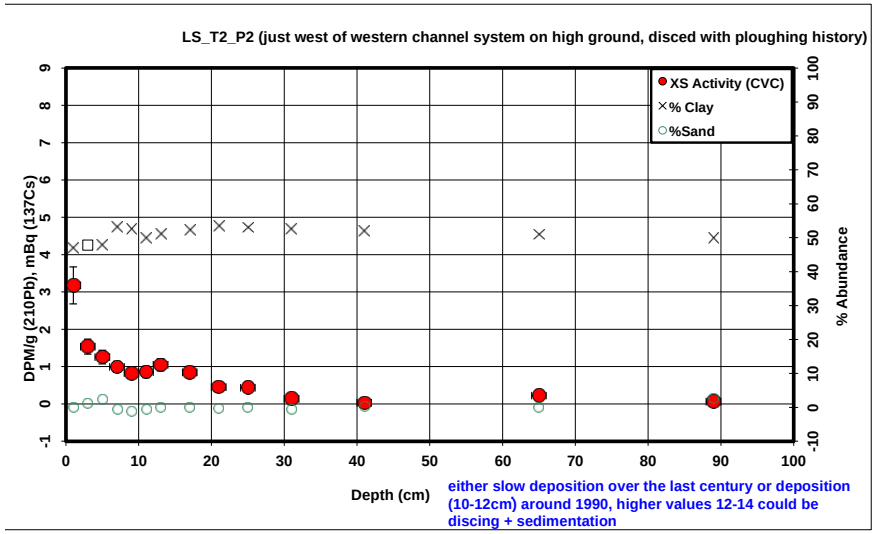

81.17	--->	21.94
Total integrated US activity (integrated tube DPM)		(DPM/cm^2) US activity
Assumed Mete (Atoms Pb-210/ M cm^2) (average 'shielded' rate of C18 & sites 41)	--->	17.76
US Activity fro (DPM/ cm^2)	--->	4.17
Input Sedimen (DPM / g clay) (from proximal grab samples)	--->	1.76
CICCS Accum (grams clay / cm^2 yr)	--->	0.07
CICCS Accum (grams / cm^2 yr)	--->	0.14
CICCS Accum (cm / yr)	--->	0.10

Avg. % Clay	Avg. Density
50.96	1.51

Assumed Supported -->	0.00
(DPM/ g clay)	
Assumed Den (g/cc)	1.50
Assumed Area (tube cross-section)	3.70

Present activi	0.84
Confidence In	0.02
Original sedim	1.76
Background US activity	
CIRCA Uncert	0.20
N/N$_0$	0.48
S.E. (N/N$_0$)	0.06
Predicted sed	23.74
S.E. (age)	3.77
minimum age	20.18
maximum age	27.74
Activity offset f	-9.5
Deposition dat	1985.8

Present activity	
Confidence In	1.28
Original sedim	3.00
Background U	0.60
CIRCA Uncert	0.20
N/N$_0$	-0.25
S.E. (N/N$_0$)	-0.53
Predicted sed	#NUM!
S.E. (age)	#NUM!
minimum age	#NUM!
maximum age	40.58
Activity offset f	-1.5
Deposition dat	#NUM!

	--->	21.94
Additional 'cap' activity (integrated tube DPM)		(DPM/cm^2) Cap activity
Assumed Mete (Atoms Pb-210/ M cm^2) (average 'shielded' rate of C18 & sites 41)	--->	17.76
Growth time fc	--->	#NUM!
Activity offset from 2000		-9.5
Deposition date		#NUM!

depth	Density (measured)	unsupported activity / g clay	US activity / gram	Trapazoidal Depth-Integration of (activity * volume * density)
0.00	1.12	3.18	1.49	
1.00	1.12	3.18	1.49	6.19
3.00	1.39	1.54	0.74	10.33
5.00	1.50	1.26	0.60	7.14
7.00	1.41	0.99	0.53	6.07
9.00	1.64	0.83	0.43	5.42
11.00	1.61	0.86	0.43	5.18
13.00	1.39	1.05	0.54	5.34
17.00	1.79	0.85	0.44	11.49
21.00	2.09	0.45	0.24	9.80
25.00	1.62	0.43	0.23	6.46
31.00	1.50	0.14	0.07	5.24
41.00	1.50	0.03	0.02	2.51
65.00	1.18	0.23	0.12	
89.00	1.50	0.06	0.03	

^{210}Pb Profiles

Int. Err	Core	Depth (avg)	notes	Pb-210 DPM/g	dpm/g clay	dpm/g % < 2um	err	% Clay	%Silt	%Sand	% < 2um	notes
1	T2_P3	1		1.01	2.09	2.70	0.22	48.17	45.23	6.60	37.30	
1	T2_P3	3		0.97	1.96	2.54	0.17	49.31	45.03	5.66	37.98	
1	T2_P3	5		0.87	1.71	2.18	0.15	51.01	43.65	5.35	39.99	
1	T2_P3	7		0.88	1.78	2.30	0.15	49.53	45.20	5.26	38.49	
1	T2_P3	9		0.86	1.78	2.33	0.16	48.22	46.70	5.09	36.84	
1	T2_P3	11		0.87	1.69	2.20	0.15	51.38	43.73	4.89	39.49	
1	T2_P3	21	sediment from side	0.71	1.48	1.91	0.13	47.90	47.94	4.16	37.07	
1	T2_P3	31		0.59	1.25	1.65	0.12	47.42	48.26	4.32	35.99	
1	T2_P3	41		0.55	1.11	1.42	0.11	49.94	46.21	3.85	39.04	
1	T2_P3	61		0.56	1.11		0.11	47.32				AVG
1	T2_P3	86		0.59	1.31	1.62	0.13	44.70	46.04	9.26	36.25	

Supported Background (dpm/g clay)	XS clay activity	Radon Ventillation Effect	XS Activity (CVC)
1.543913132	0.55	-0.79	1.34
1.521204991	0.44	-0.77	1.21
1.488956408	0.22	-0.76	0.98
1.516828032	0.27	-0.75	1.02
1.542878119	0.24	-0.74	0.98
1.482100365	0.21	-0.73	0.94
1.549419155	-0.07	-0.67	0.60
1.559118991	-0.31	-0.61	0.30
1.509028583	-0.40	-0.56	0.15
1.618521548	-0.30	-0.34	0.04
1.561301337	-0.46	-0.46	0.00

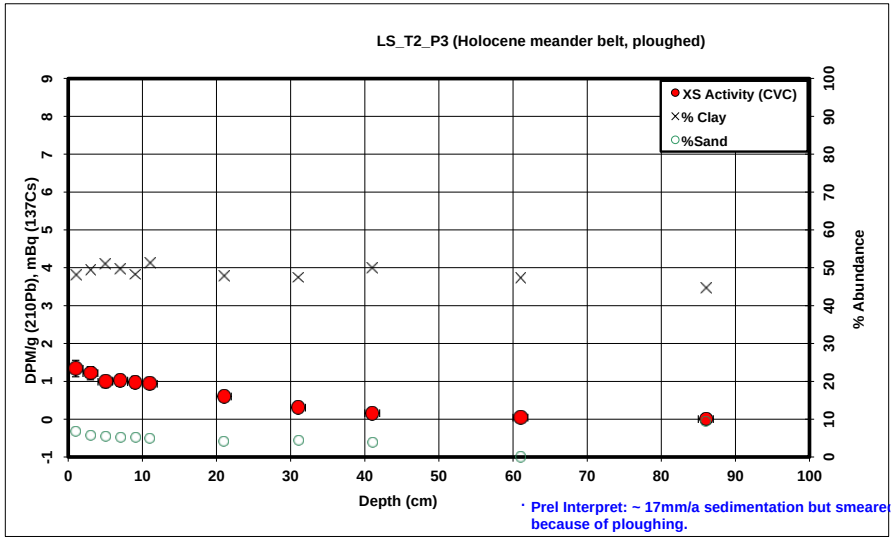

· Prel Interpret: ~ 17mm/a sedimentation but smeared because of ploughing.

85.84	--->	23.20
Total integrated US activity (integrated tube DPM)		(DPM/cm^2) US activity
Assumed Mete	--->	17.76
(Atoms Pb-210/ M cm^2) (average 'shielded' rate of C18 & sites 41)		
US Activity fro	--->	5.44
(DPM/ cm^2)		
Input Sedimen	--->	1.76
(DPM / g clay) (from proximal grab samples)		
CICCS Accum	--->	0.10
(grams clay / cm^2 yr)		
CICCS Accum	--->	0.20
(grams / cm^2 yr)		
CICCS Accum	--->	0.12
(cm / yr)		

Avg. % Clay	Avg. Density
48.63	1.67

Assumed Supported -->	0.00
(DPM/ g clay)	
Assumed Den	1.50
(g/cc)	
Assumed Area	3.70
(tube cross-section)	

Present activi	0.98
Confidence In	0.00
Original sedin	1.00
Background U	0.60
CIRCA Uncert	0.20
N/N_o	0.95
S.E. (N/N_o)	0.48
Predicted sed	1.65
S.E. (age)	17.06
minimum age	-11.39
maximum age	23.95
Activity offset f	-9.5
Deposition dat	2007.8

Present activity	
Confidence In	0.00
Original sedin	3.00
Background U	0.60
CIRCA Uncert	0.20
N/N_o	-0.25
S.E. (N/N_o)	-0.02
Predicted sed	#NUM!
S.E. (age)	#NUM!
minimum age	#NUM!
maximum age	#NUM!
Activity offset f	-1.5
Deposition dat	#NUM!

	--->	23.20
Additional 'cap' activity (integrated tube DPM)		(DPM/cm^2) Cap activity
Assumed Mete	--->	17.76
(Atoms Pb-210/ M cm^2) (average 'shielded' rate of C18 & sites 41)		
Growth time fc	--->	#NUM!
Activity offset from 2000		-9.5
Deposition date		#NUM!

depth	Density (measured)	unsupported activity / g clay	US activity / gram	Trapazoidal Depth-Integration of (activity * volume * density)
0.00	1.50	1.34	0.64	
1.00	1.50	1.34	0.64	3.57
3.00	1.41	1.21	0.60	6.68
5.00	1.48	0.98	0.50	5.89
7.00	1.61	1.02	0.50	5.76
9.00	1.62	0.98	0.47	5.82
11.00	1.56	0.94	0.48	5.60
21.00	2.14	0.60	0.29	26.28
31.00	2.31	0.30	0.14	17.72
41.00	1.86	0.15	0.08	8.52
61.00	1.52	0.04	0.02	
86.00	1.50	0.00	0.00	

^{210}Pb Profiles

Int. Err	Core	Depth (avg)	notes	Pb-210 DPM/g	dpm/g clay	dpm/g % < 2um	err	% Clay	%Silt	%Sand	% < 2um	notes
1	T2_P4	1		1.19	2.66		0.25	48.00				AVG
1	T2_P4	3		1.19	2.70		0.23	48.00				AVG
1	T2_P4	5		1.10	2.33	3.10	0.23	47.40	41.98	10.63	35.65	
1	T2_P4	7		0.92	1.90	2.51	0.18	48.45	39.37	12.18	36.65	
1	T2_P4	9		1.05	2.11	2.75	0.20	50.00	39.14	10.86	38.41	
1	T2_P4	11		1.02	2.10	2.80	0.20	48.87	42.56	8.56	36.54	
1	T2_P4	15	small stone in acid	0.99	2.02		0.18	49.63				AVG
1	T2_P4	21		0.88	1.75	2.32	0.17	50.39	42.14	7.47	37.99	
1	T2_P4	31		0.84	1.62	2.19	0.16	51.89	45.47	2.64	38.57	
1	T2_P4	41		0.81	1.73	2.46	0.17	46.57	51.24	2.19	32.82	
1	T2_P4	51		0.72	1.43		0.14	49.39				AVG
1	T2_P4	65		0.71	1.42		0.14	52.21				AVG
1	T2_P4	80		0.73	1.33	1.85	0.14	55.03	43.76	1.22	39.73	

Supported Background (dpm/g clay)	XS clay activity	Radon Ventillation Effect	XS Activity (CVC)
1.547278099	1.11	-0.79	**1.90**
1.547278099	1.16	-0.77	**1.93**
1.559699963	0.77	-0.76	**1.53**
1.538262499	0.36	-0.75	**1.11**
1.507869642	0.60	-0.74	**1.34**
1.529800429	0.57	-0.73	**1.29**
1.514959938	0.50	-0.70	**1.20**
1.500485592	0.25	-0.67	**0.92**
1.472980492	0.15	-0.61	**0.76**
1.577070147	0.15	-0.56	**0.71**
1.519575497	-0.09	-0.51	**0.41**
1.46719873	-0.04	-0.44	**0.39**
1.419243076	-0.09	-0.37	**0.28**

Assumed Supported --> (DPM/ g clay)	0.00	
Assumed Den (g/cc)	1.20	
Assumed Area (tube cross-section)	3.70	

Present activit	0.28
Confidence In	0.10
Original sedim	1.76
Background US activity	
CIRCA Uncert	0.20
N/N_o	0.16
S.E. (N/N_o)	0.06
Predicted sed	**59.14**
S.E. (age)	**12.44**
minimum age	48.90
maximum age	74.25
Activity offset f	-1.5
Deposition dat	**1942.4**

Present activity		
Confidence In		#REF!
Original sedim		3.00
Background U		0.60
CIRCA Uncert		0.20
N/N_o		-0.25
S.E. (N/N_o)		#REF!
Predicted sed		**#NUM!**
S.E. (age)		**#NUM!**
minimum age		#REF!
maximum age		#REF!
Activity offset f		-1.5
Deposition dat		**#NUM!**

depth	Density (measured)	unsupported activity / g clay	US activity / gram	Trapazoidal Depth-Integration of (activity * volume * density)
0.00	1.20	1.90	0.91	
1	1.20	1.90	0.91	4.04
3	1.19	1.93	0.93	8.13
5	1.33	1.53	0.73	7.71
7	1.34	1.11	0.54	6.24
9	1.33	1.34	0.67	5.96
11	1.56	1.29	0.63	6.96
15	1.55	1.20	0.60	14.14
21	1.52	0.92	0.46	18.02
31	1.40	0.76	0.40	23.16
41	1.31	0.71	0.33	18.21
51	1.43	0.41	0.20	13.58
65	1.57	0.39	0.21	15.94
80	1.20	0.28	0.16	13.88

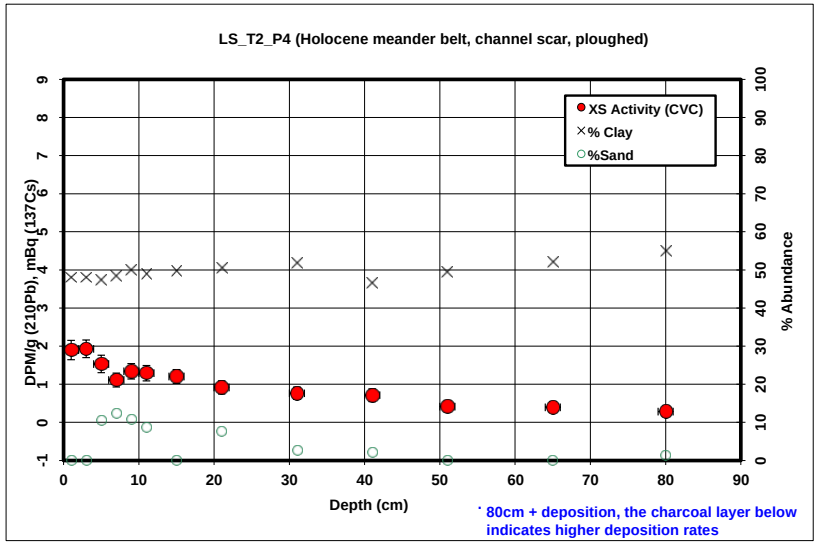

155.97	--->	42.15
Total integrated US activity (integrated tube DPM)		(DPM/cm^2) US activity
Assumed Mete (Atoms Pb-210/ M cm^2) (average 'shielded' rate of C18 & sites 41)	--->	17.76
US Activity fro (DPM/ cm^2)	--->	24.39
Input Sedimen (DPM / g clay) (from proximal grab samples)	--->	1.76
CICCS Accum (grams clay / cm^2 yr)	--->	0.43
CICCS Accum (grams / cm^2 yr)	--->	0.87
CICCS Accum (cm / yr)	--->	0.64

Avg. % Clay	Avg. Density
49.68	1.36

	--->	
Additional 'cap' activity (integrated tube DPM)		(DPM/cm^2) Cap activity
Assumed Mete (Atoms Pb-210/ M cm^2) (average 'shielded' rate of C18 & sites 41)	--->	17.76
Growth time fo	--->	0
Activity offset from 2000		-2.5
Deposition date		**2002.5**

^{210}Pb Profiles

Int. Err	Core	Depth (avg)	notes	Pb-210 DPM/g	dpm/g clay	dpm/g % < 2um	err	% Clay	%Silt	%Sand	% < 2um	notes
1	T2_P5	1		1.44	3.28	4.21	0.36	44.74	48.86	6.40	34.84	
1	T2_P5	3		1.24	2.89		0.25	43.51		2.90		AVG
1	T2_P5	5		1.04	2.48	3.21	0.25	42.28	52.63	5.10	32.62	
1	T2_P5	7		1.07	2.39		0.21	45.03		0.80		AVG
1	T2_P5	9		0.93	1.95	2.45	0.20	47.79	49.91	2.30	38.10	
1	T2_P5	11		0.94	1.90		0.17	49.74		0.66		AVG
1	T2_P5	15		0.79	1.57		0.15	50.71				AVG
1	T2_P5	21		0.71	1.37	1.76	0.15	51.69	47.18	1.13	40.43	
1	T2_P5	31		0.53	1.06	1.31	0.12	49.05	50.45	0.50	39.50	
1	T2_P5	41		0.53	1.25	1.52	0.14	41.70	58.05	0.25	34.50	
1	T2_P5	84		0.60	1.35	1.78	0.15	44.05	55.60	0.35	33.45	

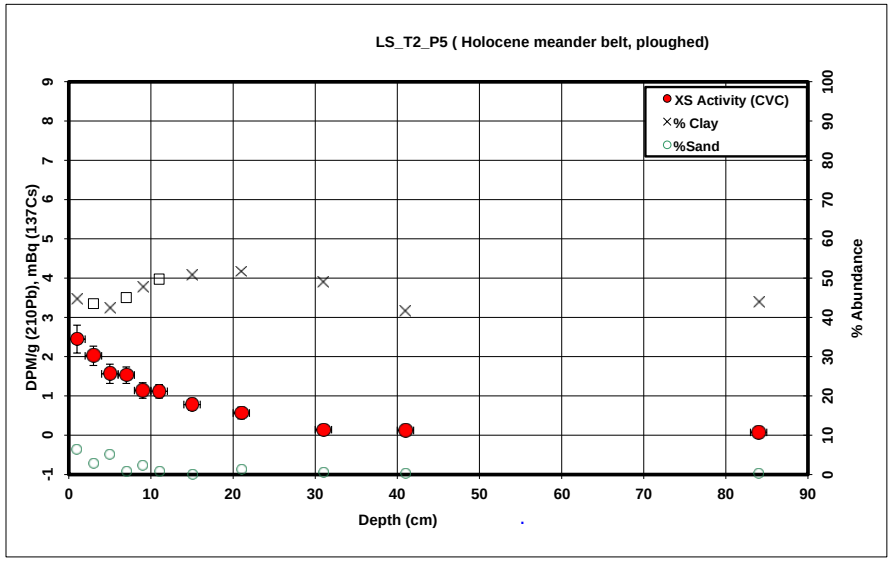

Supported Background (dpm/g clay)	XS clay activity	Radon Ventillation Effect	XS Activity (CVC)
1.617579194	1.66	-0.79	2.45
1.646374632	1.25	-0.77	2.02
1.676532156	0.80	-0.76	1.56
1.610955501	0.78	-0.75	1.53
1.551616989	0.40	-0.74	1.14
1.512869733	0.39	-0.73	1.12
1.494412752	0.08	-0.70	0.78
1.476526229	-0.10	-0.67	0.56
1.526261625	-0.47	-0.61	0.14
1.691168394	-0.44	-0.56	0.12
1.633574793	-0.28	-0.35	0.07

85.18	--->	23.02
Total integrated US activity (integrated tube DPM)		(DPM/cm^2) US activity
Assumed Mete (Atoms Pb-210/ M cm^2) (average 'shielded' rate of C18 & sites 41)	--->	17.76
US Activity fro (DPM/ cm^2)	--->	5.26
Input Sedimen (DPM / g clay) (from proximal grab samples)	--->	1.76
CICCS Accum (grams clay / cm^2 yr)	--->	0.09
CICCS Accum (grams / cm^2 yr)	--->	0.20
CICCS Accum (cm / yr)	--->	0.10

Avg. % Clay	Avg. Density
46.62	2.10

Assumed Supported -->	0.00
(DPM/ g clay)	
Assumed Den (g/cc)	1.50
Assumed Area (tube cross-section)	3.70

Present activi	1.13
Confidence In	0.00
Original sedin	1.30
Background US activity	
CIRCA Uncert	0.20
N/N$_o$	0.87
S.E. (N/N$_o$)	0.13
Predicted sed	4.51
S.E. (age)	4.97
minimum age	-0.10
maximum age	9.88
Activity offset f	-9.5
Deposition dat	2005.0

Present activity	
Confidence In	0.00
Original sedin	3.00
Background U	0.60
CIRCA Uncert	0.20
N/N$_o$	-0.25
S.E. (N/N$_o$)	-0.02
Predicted sed	#NUM!
S.E. (age)	#NUM!
minimum age	#NUM!
maximum age	#NUM!
Activity offset f	-1.5
Deposition dat	#NUM!

	--->	23.02
Additional 'cap' activity (integrated tube DPM)		(DPM/cm^2) Cap activity
Assumed Mete (Atoms Pb-210/ M cm^2) (average 'shielded' rate of C18 & sites 41)	--->	17.76
Growth time fc	--->	#NUM!
Activity offset from 2000		-9.5
Deposition date		#NUM!

depth	Density (measured)	unsupported activity / g clay	US activity / gram	Trapazoidal Depth-Integration of (activity * volume * density)
0.00	1.50	1.56	0.70	
1.00	1.50	1.56	0.70	3.88
3.00	1.23	1.56	0.68	6.96
5.00	1.36	1.56	0.66	6.41
7.00	1.26	1.14	0.51	5.68
9.00	1.38	1.14	0.54	5.15
11.00	1.45	0.78	0.39	4.87
15.00	1.47	0.78	0.40	8.46
21.00	9.87	0.12	0.06	28.82
31.00	1.15	0.12	0.06	12.28
41.00	1.50	0.12	0.05	2.66
84.00	1.50	0.00	0.00	

^{210}Pb Profiles

Int. Err	Core	Depth (avg)	notes	Pb-210 DPM/g	dpm/g clay	dpm/g % < 2um	err	% Clay	%Silt	%Sand	% < 2um	notes
1	T2_P6	1		2.75	6.37		0.59	45.00				AVG
1	T2_P6	3		2.01	4.11	5.46	0.39	48.88	49.42	1.70	36.77	
1	T2_P6	5		1.49	3.09	4.16	0.26	48.38	49.97	1.66	35.99	
1	T2_P6	7		1.19	2.39	3.15	0.21	49.95	49.15	0.90	37.85	
1	T2_P6	9		0.81	1.68	2.22	0.16	48.00	50.34	1.66	36.34	
1	T2_P6	11		0.83	1.76	2.36	0.16	46.97	52.15	0.88	35.02	
1	T2_P6	15		0.75	1.67		0.16	48.80				AVG
1	T2_P6	21		0.78	1.54	2.01	0.14	50.64	47.32	2.04	38.77	
1	T2_P6	31		0.70	1.29	1.69	0.13	54.54	52.92		41.60	
1	T2_P6	35		0.56	1.22		0.12	58.28				AVG
1	T2_P6	41		0.54	0.87	1.24	0.09	62.02	37.74	0.24	43.47	
1	T2_P6	61		0.64	1.14		0.12	55.00				AVG
1	T2_P6	86		0.53	1.42	1.83	0.14	37.09	62.41	0.50	28.86	

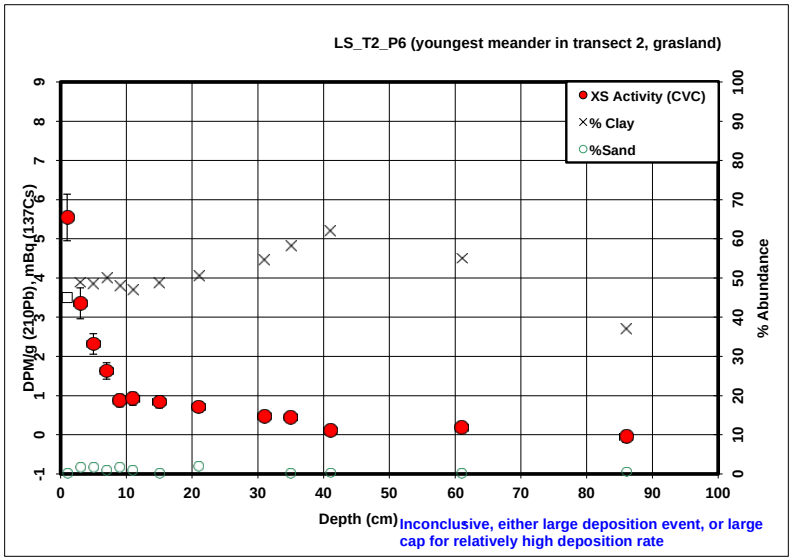

Supported Background (dpm/g clay)	XS clay activity	Radon Ventillation Effect	XS Activity (CVC)
1.611693786	4.76	-0.79	5.54
1.52962567	2.58	-0.77	3.35
1.539600087	1.55	-0.76	2.32
1.508819591	0.88	-0.75	1.63
1.547234131	0.13	-0.74	0.87
1.568592443	0.19	-0.73	0.92
1.531120356	0.14	-0.70	0.84
1.495875745	0.04	-0.67	0.71
1.427239062	-0.14	-0.61	0.47
1.368672323	-0.14	-0.59	0.44
1.315933823	-0.45	-0.56	0.11
1.419723008	-0.28	-0.46	0.18
1.821242565	-0.40	-0.34	-0.05

113.81	--->	30.76
Total integrated US activity (integrated tube DPM)		(DPM/cm^2) US activity
Assumed Mete	--->	17.76
(Atoms Pb-210/ M cm^2) (average 'shielded' rate of C18 & sites 41)		
US Activity fro	--->	13.00
(DPM/ cm^2)		
Input Sedimen	--->	1.76
(DPM / g clay) (from proximal grab samples)		
CICCS Accum	--->	0.23
(grams clay / cm^2 yr)		
CICCS Accum	--->	0.46
(grams / cm^2 yr)		
CICCS Accum	--->	0.33
(cm / yr)		

Avg. % Clay	Avg. Density
50.27	1.37

Assumed Supported --> (DPM/ g clay)	0.00
Assumed Den (g/cc)	1.50
Assumed Area (tube cross-section)	3.70
Present activit	0.84
Confidence In	0.09
Original sedin	1.76
Background US activity	
CIRCA Uncert	0.20
N/N_o	0.48
S.E. (N/N_o)	0.07
Predicted sed	23.93
S.E. (age)	5.03
minimum age	19.28
maximum age	29.37
Activity offset f	-9.5
Deposition dat	1985.6

Present activity	
Confidence In	#REF!
Original sedin	3.00
Background U	0.60
CIRCA Uncert	0.20
N/N_o	-0.25
S.E. (N/N_o)	#REF!
Predicted sed	#NUM!
S.E. (age)	#NUM!
minimum age	#REF!
maximum age	#REF!
Activity offset f	-9.5
Deposition dat	#NUM!

	--->	30.76
Additional 'cap' activity (integrated tube DPM)		(DPM/cm^2) Cap activity
Assumed Mete	--->	17.76
(Atoms Pb-210/ M cm^2) (average 'shielded' rate of C18 & sites 41)		
Growth time fo	--->	#NUM!
Activity offset from 2000		-9.5
Deposition date		#NUM!

depth	Density (measured)	unsupported activity / g clay	US activity / gram	Trapazoidal Depth-Integration of (activity * volume * density)
0.00	1.01	5.54	2.49	
1.00	1.01	5.54	2.49	9.34
3.00	1.29	3.35	1.64	17.60
5.00	1.41	2.32	1.12	13.76
7.00	1.49	1.63	0.81	10.37
9.00	1.47	0.87	0.42	6.75
11.00	1.72	0.92	0.43	5.01
15.00	1.70	0.84	0.41	10.64
21.00	1.67	0.71	0.36	14.42
31.00	1.17	0.47	0.26	16.24
35.00	1.50	0.44	0.26	5.10
41.00	1.03	0.11	0.07	4.58
61.00	1.19	0.18	0.10	
86.00	1.32	0.00	0.00	

^{210}Pb Profiles

Int. Err	Core	Depth (avg)	notes	Pb-210 DPM/g	dpm/g clay	dpm/g % < 2um	err	% Clay	%Silt	%Sand	% < 2um	notes
1	TE_P7	1		3.89	8.65		0.68	45.00				AVG
1	TE_P7	3		0.93	1.96	2.34	0.18	47.63	47.78	4.59	39.86	
1	TE_P7	5		0.77	1.46	1.75	0.14	52.39	40.93	6.67	43.87	
1	TE_P7	7		0.45	0.92	1.08	0.10	49.29	44.11	6.60	41.91	
1	TE_P7	9		0.47	0.92	1.05	0.10	50.93	41.38	7.69	44.61	
1	TE_P7	11		0.65	1.28	1.51	0.12	50.56	42.65	6.80	42.98	
1	TE_P7	13		0.51	0.90		0.10	52.29		3.38		AVG
1	TE_P7	15		0.43	0.75		0.09	54.02		5.35		AVG
1	TE_P7	17		0.39	0.68		0.09	55.75				AVG
1	TE_P7	19		0.33	0.57		0.08	57.48				AVG
1	TE_P7	21		0.37	0.62	0.71	0.08	59.21	36.07	4.72	51.90	
1	TE_P7	31		0.40	0.69	0.77	0.08	58.58	34.54	6.88	52.46	
1	TE_P7	41		0.37	0.62	0.70	0.08	59.31	34.19	6.50	52.52	
1	TE_P7	87.7		0.45	0.79	0.89	0.09	57.25	32.83	9.93	50.85	

Supported Background (dpm/g clay)	XS clay activity	Radon Ventillation Effect	XS Activity (CVC)
1.611693786	7.04	-0.79	**7.83**
1.554792151	0.40	-0.77	**1.18**
1.463962044	0.00	-0.76	**0.76**
1.521554823	-0.60	-0.75	**0.14**
1.490425062	-0.57	-0.74	**0.16**
1.497333877	-0.21	-0.73	**0.51**
1.465823784	-0.57	-0.71	**0.15**
1.43597088	-0.68	-0.70	**0.02**
1.40763899	-0.73	-0.69	**-0.04**
1.380706913	-0.81	-0.68	**-0.13**
1.355066384	-0.73	-0.67	**-0.06**
1.364238973	-0.68	-0.61	**-0.07**
1.353604585	-0.73	-0.56	**-0.17**
1.384243836	-0.60	-0.34	**-0.26**

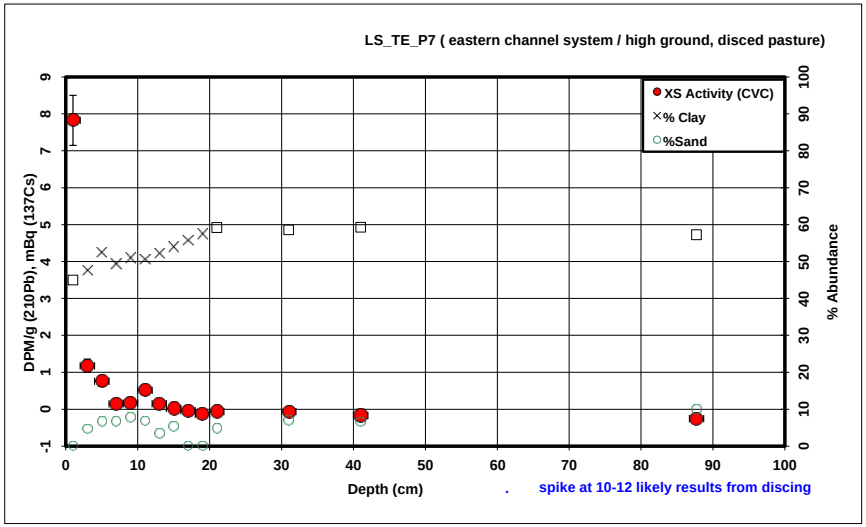

52.51	--->	14.19
Total integrated US activity (integrated tube DPM)		(DPM/cm^2) US activity
Assumed Mete (Atoms Pb-210/ M cm^2) (average 'shielded' rate of C18 & sites 41)	--->	17.76
US Activity fro (DPM/ cm^2)	--->	-3.57
Input Sedimen (DPM / g clay) (from proximal grab samples)	--->	1.76
CICCS Accum (grams clay / cm^2 yr)	--->	-0.06
CICCS Accum (grams / cm^2 yr)	--->	-0.12
CICCS Accum (cm / yr)	--->	-0.07

Avg. % Clay	Avg. Density
53.55	1.68

Assumed Supported --> (DPM/ g clay)	0.00
Assumed Den (g/cc)	1.50
Assumed Area (tube cross-section)	3.70

Present activi	0.15
Confidence In	0.00
Original sedin	0.20
Background US activity	
CIRCA Uncerta	0.20
N/N$_0$	0.75
S.E. (N/N$_0$)	0.75
Predicted sed	9.26
S.E. (age)	#NUM!
minimum age	-13.04
maximum age	#NUM!
Activity offset f	9.5
Deposition dat	1981.2

Present activity	
Confidence In	#REF!
Original sedim	3.00
Background U	0.60
CIRCA Uncerta	0.20
N/N$_0$	-0.25
S.E. (N/N$_0$)	#REF!
Predicted sed	#NUM!
S.E. (age)	#NUM!
minimum age	#REF!
maximum age	#REF!
Activity offset f	-1.5
Deposition dat	#NUM!

	--->	14.19
Additional 'cap' activity (integrated tube DPM)		(DPM/cm^2) Cap activity
Assumed Mete (Atoms Pb-210/ M cm^2) (average 'shielded' rate of C18 & sites 41)	--->	17.76
Growth time fo	--->	51.6114918
Activity offset from 2000		-9.5
Deposition date		1957.9

	depth	Density (measured)	unsupported activity / g clay	US activity / gram	Trapazoidal Depth-Integration of (activity * volume * density)	
	0.00	7.83	1.21	7.83	3.52	
1.21	1.00	7.83	1.21	7.83	3.52	15.83
1.59	3.00	1.18	1.59	1.18	0.56	21.18
1.82	5.00	0.76	1.82	0.76	0.40	6.03
1.62	7.00	0.14	1.62	0.14	0.07	2.98
1.66	9.00	0.16	1.66	0.16	0.08	0.94
2.26	11.00	0.51	2.26	0.51	0.26	2.48
1.71	13.00	0.15	1.71	0.15	0.08	2.47
2.04	15.00	0.02	2.04	0.02	0.01	0.60
1.74	17.00	-0.04	1.74	0.00	0.00	
1.36	19.00	-0.13	1.36	0.00	0.00	
1.98	21.00	-0.06	1.98	0.00	0.00	
1.86	31.00	-0.07	1.86	0.00	0.00	
1.71	41.00	-0.17	1.71	0.00	0.00	
	87.70	-0.26	1.50	0.00	0.00	

^{210}Pb Profiles

Int. Err	Core	Depth (avg)	notes	Pb-210 DPM/g	dpm/g clay	dpm/g % < 2um	err	% Clay	%Silt	%Sand	% < 2um	notes
1	TE_P8	1			3.16		1.00	57.62				reconstr
1	TE_P8	3		1.86	3.16	3.78	0.26	58.90	34.90	6.19	49.27	
1	TE_P8	5		1.67	2.97	3.63	0.25	56.35	38.30	5.35	46.14	
1	TE_P8	7		1.24	2.20	2.68	0.19	56.27	39.67	4.05	46.29	
1	TE_P8	9		0.85	1.59	1.91	0.15	53.34	41.73	4.92	44.50	
1	TE_P8	11		0.61	1.19	1.44	0.12	51.30	43.46	5.23	42.30	
1	TE_P8	13		0.56	1.24		0.12	52.32		3.60		AVG
1	TE_P8	15		0.60	1.33		0.13	53.34		4.42		AVG
1	TE_P8	17		0.55	0.97		0.11	54.36				AVG
1	TE_P8	19	small stones in acic	0.38	0.64		0.08	55.38				AVG
1	TE_P8	21		0.49	0.87	1.01	0.09	56.39	34.73	8.88	48.39	
1	TE_P8	31		0.47	0.72	0.82	0.09	62.10	28.09	9.81	54.89	
1	TE_P8	41		0.52	0.78	0.86	0.10	64.52	24.58	10.90	58.22	
1	TE_P8	74.5	stones	0.58	0.85	0.93	0.10	66.59	23.73	9.68	61.26	

Supported Background (dpm/g clay)	XS clay activity	Radon Ventillation Effect	XS Activity (CVC)
1.378523259	1.78	-0.79	2.57
1.359539951	1.80	-0.77	2.58
1.398206513	1.58	-0.76	2.34
1.399336572	0.80	-0.75	1.55
1.447418397	0.14	-0.74	0.88
1.483533183	-0.29	-0.73	0.43
1.465225066	-0.23	-0.71	0.48
1.447489217	-0.12	-0.70	0.58
1.430297329	-0.46	-0.69	0.23
1.413622993	-0.77	-0.68	-0.09
1.397441536	-0.53	-0.67	0.14
1.314825917	-0.59	-0.61	0.02
1.283411799	-0.50	-0.56	0.05
1.258120332	-0.41	-0.39	-0.01

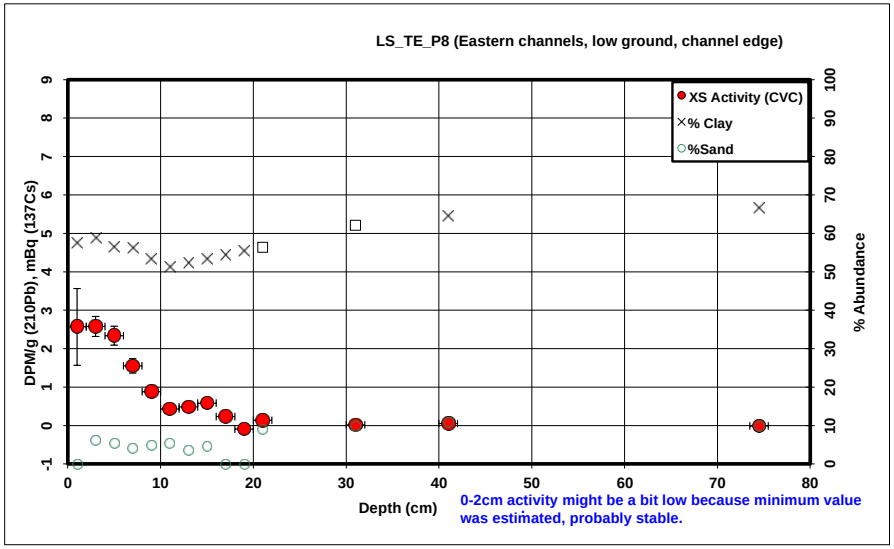

61.28	--->	16.56
Total integrated US activity (integrated tube DPM)		(DPM/cm^2) US activity
Assumed Mete (Atoms Pb-210/ M cm^2) (average 'shielded' rate of C18 & sites 41)	--->	17.76
US Activity fro (DPM/ cm^2)	--->	-1.20
Input Sedimen (DPM / g clay) (from proximal grab samples)	--->	1.76
CICCS Accum (grams clay / cm^2 yr)	--->	-0.02
CICCS Accum (grams / cm^2 yr)	--->	-0.04
CICCS Accum (cm / yr)	--->	-0.03

Avg. % Clay	Avg. Density
57.06	1.39

Assumed Supported -->	0.00	
(DPM/ g clay)		
Assumed Den (g/cc)	1.50	
Assumed Area (tube cross-section)	3.70	

Present activity		
Confidence In	0.00	
Original sedin	3.00	
Background U	0.60	
CIRCA Uncert	0.20	
N/N_o	-0.25	
S.E. (N/N_o)	-0.02	
Predicted sed	#NUM!	
S.E. (age)	#NUM!	
minimum age	#NUM!	
maximum age	#NUM!	
Activity offset f	-1.5	
Deposition dat	#NUM!	

Present activity		
Confidence In	0.00	
Original sedin	3.00	
Background U	0.60	
CIRCA Uncert	0.20	
N/N_o	-0.25	
S.E. (N/N_o)	-0.02	
Predicted sed	#NUM!	
S.E. (age)	#NUM!	
minimum age	#NUM!	
maximum age	#NUM!	
Activity offset f	-1.5	
Deposition dat	#NUM!	

	--->	16.56
Additional 'cap' activity (integrated tube DPM)		(DPM/cm^2) Cap activity
Assumed Mete (Atoms Pb-210/ M cm^2) (average 'shielded' rate of C18 & sites 41)	--->	17.76
Growth time fc	--->	86.6377623
Activity offset from 2000		-2.5
Deposition date		1915.9

depth	Density (measured)	unsupported activity / g clay	US activity / gram	Trapazoidal Depth-Integration of (activity * volume * density)
0.00	1.15	2.57	1.48	
1.00	1.15	2.57	1.48	6.32
3.00	1.12	2.58	1.52	12.60
5.00	1.20	2.34	1.32	12.17
7.00	1.24	1.55	0.87	9.91
9.00	1.43	0.88	0.47	6.63
11.00	1.61	0.43	0.22	3.88
13.00	1.44	0.48	0.25	2.68
15.00	1.65	0.58	0.31	3.22
17.00	1.69	0.23	0.13	2.69
19.00	1.50	0.00	0.00	0.75
21.00	1.50	0.14	0.08	0.44
31.00	1.27	0.02	0.01	
41.00	1.44	0.05	0.03	
74.50	1.59	0.00	0.00	

^{210}Pb Profiles

Int. Err	Core	Depth (avg)	notes	Pb-210 DPM/g	dpm/g clay	dpm/g % < 2um	err	% Clay	%Silt	%Sand	% < 2um	notes
1	T1_P9	1		1.26	2.79		0.25	46.00				AVG
1	T1_P9	3		1.45	3.18	3.98	0.32	46.62	49.20	4.18	37.24	
1	T1_P9	5		1.05	2.26		0.20	46.85				AVG
1	T1_P9	7		1.03	2.23		0.20	46.85				AVG
1	T1_P9	9		0.93	2.01		0.18	46.85				AVG
1	T1_P9	11		0.81	1.73	2.15	0.18	47.08	49.98	2.94	37.77	
1	T1_P9	15		0.73	1.55		0.15	47.00				AVG
1	T1_P9	17		0.72	1.52		0.14	47.00				AVG
1	T1_P9	21		0.61	1.15		0.12	52.00				AVG
1	T1_P9	25		0.47	0.97		0.11	47.00				AVG
1	T1_P9	31		0.47	0.88		0.10	52.00				AVG
1	T1_P9	41		0.53	0.99		0.11	52.00				AVG
1	T1_P9	61		0.57	1.01		0.11	55.00				AVG
1.25	T1_P9	80.25		0.56	0.93	1.04	0.11	59.80	36.85	3.35	53.17	

Supported Background (dpm/g clay)	XS clay activity	Radon Ventillation Effect	XS Activity (CVC)
1.589461053	1.20	-0.79	**1.98**
1.575997846	1.61	-0.77	**2.38**
1.571155145	0.69	-0.76	**1.46**
1.571155145	0.66	-0.75	**1.41**
1.571155145	0.44	-0.74	**1.17**
1.566350685	0.16	-0.73	**0.89**
1.568003378	-0.02	-0.70	**0.68**
1.568003378	-0.04	-0.69	**0.65**
1.470952765	-0.32	-0.67	**0.35**
1.568003378	-0.59	-0.64	**0.05**
1.470952765	-0.59	-0.61	**0.02**
1.470952765	-0.48	-0.56	**0.07**
1.419723008	-0.41	-0.46	**0.04**
1.346584885	-0.42	-0.37	**-0.05**

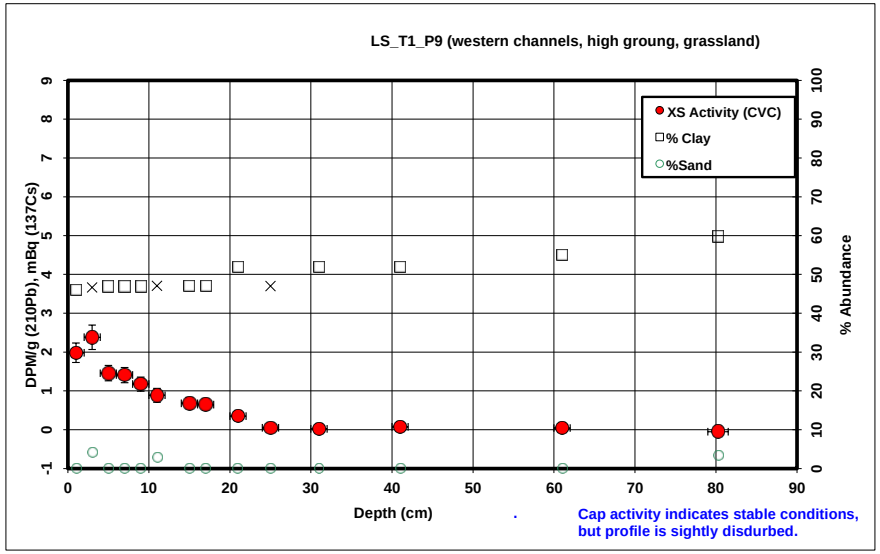

61.53	--->	16.63
Total integrated (integrated tube DPM)		US activity (DPM/cm^2) US activity

Assumed Mete (Atoms Pb-210/ M cm^2) (average 'shielded' rate of C18 & sites 41)	--->	17.76
US Activity fro (DPM/ cm^2)	--->	-1.13
Input Sedimen (DPM / g clay) (from proximal grab samples)	--->	1.76
CICCS Accum (grams clay / cm^2 yr)	--->	-0.02
CICCS Accum (grams / cm^2 yr)	--->	-0.04
CICCS Accum (cm / yr)	--->	-0.03

Avg. % Clay	Avg. Density
49.43	1.46

Assumed Supported --> (DPM/ g clay)	0.00
Assumed Den (g/cc)	1.50
Assumed Area (tube cross-section)	3.70

Present activity	
Confidence In	0.00
Original sedin	3.00
Background U	0.60
CIRCA Uncerta	0.20
N/N_o	-0.25
S.E. (N/N_o)	-0.02
Predicted sed	#NUM!
S.E. (age)	#NUM!
minimum age	#NUM!
maximum age	#NUM!
Activity offset f	-1.5
Deposition dat	#NUM!

Present activity	
Confidence In	#REF!
Original sedin	3.00
Background U	0.60
CIRCA Uncerta	0.20
N/N_o	-0.25
S.E. (N/N_o)	#REF!
Predicted sed	#NUM!
S.E. (age)	#NUM!
minimum age	#REF!
maximum age	#REF!
Activity offset f	-1.5
Deposition dat	#NUM!

	--->	16.63
Additional 'cap' activity (integrated tube DPM)		(DPM/cm^2) Cap activity
Assumed Mete (Atoms Pb-210/ M cm^2) (average 'shielded' rate of C18 & sites 41)	--->	17.76
Growth time fo	--->	88.5003362
Activity offset from 2000		-2.5
Deposition date		1914.0

depth	Density (measured)	unsupported activity / g clay	US activity / gram	Trapazoidal Depth-Integration of (activity * volume * density)
0.00	1.08	1.98	0.91	
1.00	1.08	1.98	0.91	3.64
3.00	1.17	2.38	1.11	8.41
5.00	1.45	1.46	0.68	8.66
7.00	1.54	1.41	0.66	7.40
9.00	1.46	1.17	0.55	6.70
11.00	1.57	0.89	0.42	5.42
15.00	1.71	0.68	0.32	8.93
17.00	1.33	0.65	0.30	3.50
21.00	2.10	0.35	0.18	6.15
25.00	1.50	0.05	0.02	2.72
31.00	1.50	0.02	0.01	
41.00	1.50	0.07	0.04	
61.00	1.50	0.04	0.02	
80.25	1.50	0.00	0.00	

^{210}Pb Profiles

Int. Err	Core	Depth (avg)	notes	Pb-210 DPM/g	dpm/g clay	dpm/g % < 2um	err	% Clay	%Silt	%Sand	% < 2um	notes	Supported Background (dpm/g clay)	XS clay activity	Radon Ventillation Effect	XS Activity (CVC)
1	T1_P10	1		1.91	4.29		0.41	46.00				AVG	1.589461053	2.70	-0.79	3.48
1	T1_P10	3		2.06	4.42	5.54	0.42	46.62	44.38	9.00	37.18		1.576171382	2.84	-0.77	3.62
1	T1_P10	5		1.87	3.95	4.98	0.38	47.31	47.89	4.80	37.56	1st run didn't v	1.561434263	2.39	-0.76	3.15
1	T1_P10	7		1.69	3.50	4.45	0.29	48.27	48.96	2.76	38.05	2nd run didn't	1.541705963	1.96	-0.75	2.71
1	T1_P10	9		1.49	3.19	4.12	0.27	46.79	51.39	1.82	36.23		1.572343432	1.62	-0.74	2.36
1	T1_P10	11		1.09	2.15	2.83	0.19	50.87	49.98	-0.85	38.62		1.491591532	0.66	-0.73	1.38
1	T1_P10	13		0.98	1.98		0.18	50.98		1.48		AVG	1.48948589	0.49	-0.71	1.20
1	T1_P10	15		0.74	1.48		0.14	51.09				AVG	1.487387907	-0.01	-0.70	0.70
1	T1_P10	21		0.70	1.37	1.81	0.13	51.21	48.46	0.33	38.85		1.485297538	-0.11	-0.67	0.56
1	T1_P10	31		0.65	1.28	1.67	0.13	50.86	46.93	2.21	39.09		1.491766211	-0.21	-0.61	0.40
1	T1_P10	41		0.58	1.05	1.32	0.12	55.70	45.09	-0.79	44.14		1.408407778	-0.36	-0.56	0.20
1	T1_P10	51		0.53	0.95		0.10	55.00				AVG	1.419723008	-0.47	-0.51	0.03
1	T1_P10	61		0.59	1.30		0.13	55.00				AVG	1.419723008	-0.12	-0.46	0.34
1	T1_P10	71		0.76	1.49		0.14	55.00				AVG	1.489115859	0.00	-0.41	0.41
1	T1_P10	86		0.62	1.21		0.11	55.00		0.75		AVG	1.489115859	-0.28	-0.34	0.06

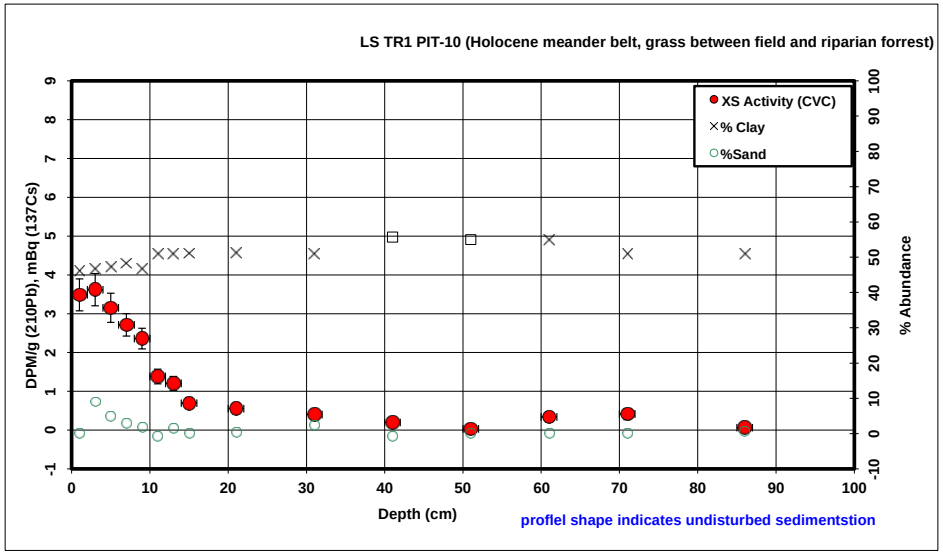

143.76	--->	38.85
Total integrated US activity (integrated tube DPM)		(DPM/cm^2) US activity
Assumed Mete (Atoms Pb-210/ M cm^2) (average 'shielded' rate of C18 & sites 41)	--->	17.76
US Activity fro (DPM/ cm^2)	--->	21.09
Input Sedimen (DPM / g clay) (from proximal grab samples)	--->	1.76
CICCS Accum (grams clay / cm^2 yr)	--->	0.37
CICCS Accum (grams / cm^2 yr)	--->	0.74
CICCS Accum (cm / yr)	--->	0.54

Avg. % Clay	Avg. Density
50.51	1.36

Assumed Supported -->	0.00	
(DPM/ g clay)		
Assumed Den (g/cc)	1.50	
Assumed Area (tube cross-section)	3.70	
Present activi	0.00	
Confidence In	0.00	
Original sedim	5.00	
Background US activity		
CIRCA Uncert	0.20	
N/N_o	0.00	
S.E. (N/N_o)	#DIV/0!	
Predicted sed	#NUM!	
S.E. (age)	#NUM!	
minimum age	#DIV/0!	
maximum age	#DIV/0!	
Activity offset f	-9.5	
Deposition dat	#NUM!	

Present activity	
Confidence In	#REF!
Original sedim	3.00
Background U	0.60
CIRCA Uncert	0.20
N/N_o	-0.25
S.E. (N/N_o)	#REF!
Predicted sed	#NUM!
S.E. (age)	#NUM!
minimum age	#REF!
maximum age	#REF!
Activity offset f	-1.5
Deposition dat	#NUM!

	--->	38.85
Additional 'cap' activity (integrated tube DPM)		(DPM/cm^2) Cap activity
Assumed Mete (Atoms Pb-210/ M cm^2) (average 'shielded' rate of C18 & sites 41)	--->	17.76
Growth time fc	--->	#NUM!
Activity offset from 2000		-9.5
Deposition date		#NUM!

depth	Density (measured)	unsupported activity / g clay	US activity / gram	Trapazoidal Depth-Integration of (activity * volume * density)
0.00	1.50	3.48	1.60	
1.00	1.50	3.48	1.60	8.90
3.00	1.06	3.62	1.69	15.57
5.00	1.15	3.15	1.49	12.96
7.00	1.20	2.71	1.31	12.18
9.00	1.31	2.36	1.10	11.22
11.00	1.51	1.38	0.70	9.43
13.00	1.24	1.20	0.61	6.69
15.00	1.59	0.70	0.36	5.07
21.00	1.54	0.56	0.28	11.13
31.00	1.44	0.40	0.20	13.47
41.00	1.27	0.20	0.11	7.88
51.00	1.42	0.03	0.02	3.17
61.00	1.69	0.34	0.19	5.85
71.00	1.28	0.41	0.21	10.87
86.00	1.50	0.06	0.03	9.36
86.00	1.50	0.00	0.00	
13.00	1.50	0.00	0.00	

^{210}Pb Profiles

Int. Err	Core	Depth (avg)	notes	Pb-210 DPM/g	dpm/g clay	dpm/g % < 2um	err	% Clay	%Silt	%Sand	% < 2um	notes
1	T1_P11	1		3.49	8.08		0.73	45.00				AVG
1	T1_P11	3		1.80	3.95	5.33	0.37	45.55	53.82	0.63	33.79	
1	T1_P11	5		1.14	2.49	3.19	0.21	45.92	53.69	0.39	35.86	
1	T1_P11	7		0.97	2.18		0.19	47.00				AVG
1	T1_P11	9		0.89	1.84	2.42	0.17	48.07	52.23	-0.31	36.69	
1	T1_P11	11		0.86	1.82	2.35	0.16	47.45	55.23	-2.68	36.69	
1	T1_P11	15		0.86	1.94		0.18	48.32				AVG
1	T1_P11	21		0.78	1.58	2.05	0.14	49.18	52.31	-1.50	37.76	
1	T1_P11	31		0.66	1.18	1.55	0.11	55.72	46.37	-2.09	42.70	
1	T1_P11	41		0.69	1.23	1.72	0.12	55.69	46.05	-1.74	39.99	
1	T1_P11	51		0.60	1.08		0.11	55.00				AVG
1	T1_P11	61		0.64	1.15		0.11	55.00				AVG
1	T1_P11	71		0.57	1.01		0.11	55.00				AVG
1	T1_P11	83		0.57	1.04		0.09	55.00		12.75		AVG

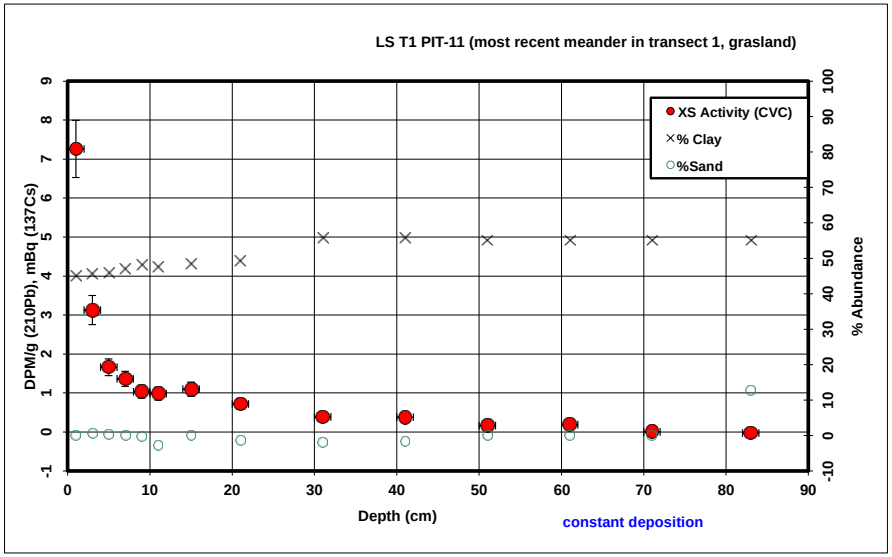

Supported Background (dpm/g clay)	XS clay activity	Radon Ventillation Effect	XS Activity (CVC)
1.611693786	6.47	-0.79	7.26
1.599416424	2.35	-0.77	3.13
1.591280153	0.90	-0.76	1.66
1.568099932	0.61	-0.75	1.36
1.54577203	0.30	-0.74	1.03
1.558524732	0.26	-0.73	0.98
1.54082648	0.40	-0.70	1.10
1.523638051	0.05	-0.67	0.72
1.408127505	-0.22	-0.61	0.39
1.40856912	-0.17	-0.56	0.38
1.419723008	-0.34	-0.51	0.16
1.419723008	-0.27	-0.46	0.19
1.419723008	-0.41	-0.41	0.00
1.419723008	-0.38	-0.36	-0.03

134.78	--->	36.43
Total integrated US activity (integrated tube DPM)		(DPM/cm^2) US activity
Assumed Mete (Atoms Pb-210/ M cm^2) (average 'shielded' rate of C18 & sites 41)	--->	17.76
US Activity fro (DPM/ cm^2)	--->	18.66
Input Sedimen (DPM / g clay) (from proximal grab samples)	--->	1.76
CICCS Accum (grams clay / cm^2 yr)	--->	0.33
CICCS Accum (grams / cm^2 yr)	--->	0.65
CICCS Accum (cm / yr)	--->	0.46

Avg. % Clay	Avg. Density
50.56	1.43

Assumed Supported -->	0.00
(DPM/ g clay)	
Assumed Den (g/cc)	1.50
Assumed Area (tube cross-section)	3.70

Present activi	1.01
Confidence In	0.00
Original sedim	1.76
Background US activity	
CIRCA Uncert	0.20
N/N$_o$	0.57
S.E. (N/N$_o$)	0.07
Predicted sed	17.87
S.E. (age)	3.67
minimum age	14.40
maximum age	21.76
Activity offset f	-9.5
Deposition dat	1991.6

Present activity	
Confidence In	#REF!
Original sedim	3.00
Background U	0.60
CIRCA Uncert	0.20
N/N$_o$	-0.25
S.E. (N/N$_o$)	#REF!
Predicted sed	#NUM!
S.E. (age)	#NUM!
minimum age	#REF!
maximum age	#REF!
Activity offset f	-1.5
Deposition dat	#NUM!

	--->	36.43
Additional 'cap' activity (integrated tube DPM)		(DPM/cm^2) Cap activity
Assumed Mete (Atoms Pb-210/ M cm^2) (average 'shielded' rate of C18 & sites 41)	--->	17.76
Growth time fc	--->	#NUM!
Activity offset from 2000		-9.5
Deposition date		#NUM!

depth	Density (measured)	unsupported activity / g clay	US activity / gram	Trapazoidal Depth-Integration of (activity * volume * density)
0.00	1.01	7.26	3.27	
1.00	1.01	7.26	3.27	12.17
3.00	1.36	3.13	1.42	20.56
5.00	1.31	1.66	0.76	10.80
7.00	1.31	1.36	0.64	6.79
9.00	1.42	1.03	0.50	5.75
11.00	1.71	0.98	0.47	5.58
15.00	1.79	1.10	0.53	12.89
21.00	1.68	0.72	0.35	17.02
31.00	1.63	0.39	0.22	17.42
41.00	1.35	0.38	0.21	11.79
51.00	1.55	0.16	0.09	8.14
61.00	1.70	0.19	0.10	5.84
71.00	1.52	0.00	0.00	
83.00	1.65	0.00	0.00	

^{210}Pb Profiles

Int. Err	Core	Depth (avg)	notes	Pb-210 DPM/g	dpm/g clay	dpm/g % < 2um	err	% Clay	%Silt	%Sand	% < 2um	notes
1	T3_P13	1		2.76	6.37		0.58	45.00				AVG
1	T3_P13	3		2.44	5.13	6.90	0.48	47.63	46.77	5.61	35.39	
1	T3_P13	5		1.61	3.20	4.06	0.27	50.38	45.54	4.07	39.67	
1	T3_P13	7		1.20	2.80	3.64	0.24	42.95	53.92	3.13	33.06	
1	T3_P13	9		0.74	1.63	1.97	0.15	45.40	47.60	6.99	37.49	
1	T3_P13	11		0.66	1.51	1.81	0.14	43.76	46.53	9.71	36.39	
1	T3_P13	15		0.53	1.15		0.12	43.65				AVG
1	T3_P13	17		0.55	1.19		0.12	43.55				AVG
1	T3_P13	19		0.51	1.10		0.11	43.44				AVG
1	T3_P13	21		0.05	0.12	0.14	0.06	43.33	50.85	5.82	36.11	
1	T3_P13	23		0.50	1.07		0.11	37.66				AVG
1	T3_P13	31		0.42	1.31	1.56	0.13	31.98	51.78	16.24	26.80	
1	T3_P13	41		0.44	1.54	1.80	0.14	28.45	46.98	24.56	24.37	
1	T3_P13	51		0.45	1.47		0.14	28.36				AVG
1	T3_P13	61	fine sand	0.43	1.50	1.73	0.16	28.28	44.70	27.03	24.39	
1	T3_P13	77		0.35	1.78	2.04	0.16	19.89	15.00	65.11	17.39	

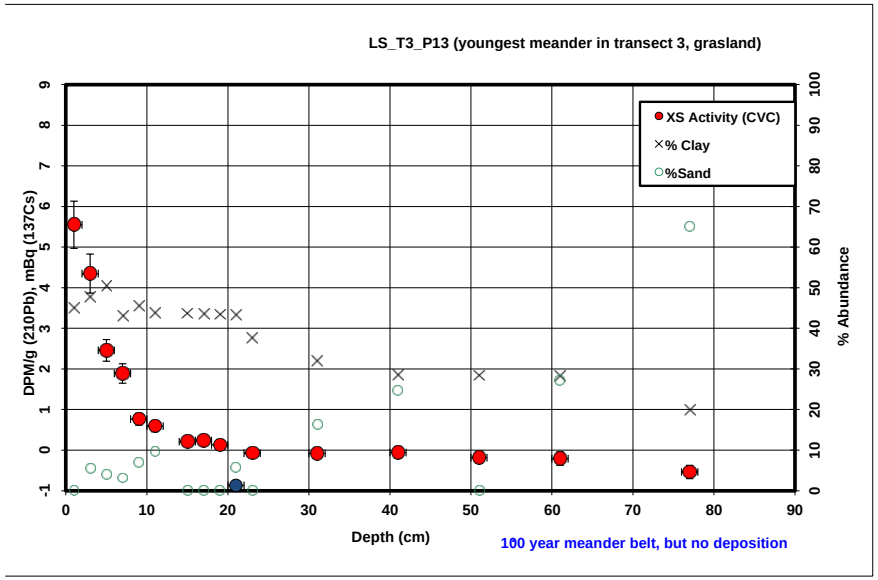

Supported Background (dpm/g clay)	XS clay activity	Radon Ventillation Effect	XS Activity (CVC)
1.611693786	4.76	-0.79	**5.55**
1.554927431	3.57	-0.77	**4.35**
1.500598228	1.69	-0.76	**2.46**
1.65994957	1.14	-0.75	**1.89**
1.602604387	0.03	-0.74	**0.76**
1.640398994	-0.14	-0.73	**0.59**
1.642936609	-0.49	-0.70	**0.21**
1.645484385	-0.45	-0.69	**0.23**
1.648042389	-0.55	-0.68	**0.13**
1.650610687	-1.53	-0.67	**-0.87**
1.803804548	-0.73	-0.66	**-0.08**
2.00007172	-0.69	-0.61	**-0.08**
2.153419725	-0.61	-0.56	**-0.06**
2.157537862	-0.69	-0.51	**-0.18**
2.161676398	-0.67	-0.46	**-0.21**
2.700409711	-0.92	-0.38	**-0.54**

72.77	--->	19.67
Total integrated US activity (integrated tube DPM)		(DPM/cm^2) US activity
Assumed Mete (Atoms Pb-210/ M cm^2) (average 'shielded' rate of C18 & sites 41)	--->	17.76
US Activity fro (DPM/ cm^2)	--->	1.90
Input Sedimen (DPM / g clay) (from proximal grab samples)	--->	1.76
CICCS Accum (grams clay / cm^2 yr)	--->	0.03
CICCS Accum (grams / cm^2 yr)	--->	0.09
CICCS Accum (cm / yr)	--->	0.06

Avg. % Clay	Avg. Density
38.98	1.48

Assumed Supported --> (DPM/ g clay)	0.00
Assumed Den (g/cc)	1.50
Assumed Area (tube cross-section)	3.70

Present activit	0.26
Confidence In	0.00
Original sedim	3.20
Background US activity	
CIRCA Uncert	0.20
N/N_0	0.08
S.E. (N/N_0)	0.01
Predicted sed	**80.76**
S.E. (age)	**2.01**
minimum age	78.81
maximum age	82.84
Activity offset f	-9.9
Deposition dat	1929.1

Present activity	
Confidence In	#REF!
Original sedim	3.00
Background U	0.60
CIRCA Uncert	0.20
N/N_0	-0.25
S.E. (N/N_0)	#REF!
Predicted sed	**#NUM!**
S.E. (age)	**#NUM!**
minimum age	#REF!
maximum age	#REF!
Activity offset f	-1.5
Deposition dat	#NUM!

	--->	19.67
Additional 'cap' activity (integrated tube DPM)		(DPM/cm^2) Cap activity
Assumed Mete (Atoms Pb-210/ M cm^2) (average 'shielded' rate of C18 & sites 41)	--->	17.76
Growth time fo	--->	#NUM!
Activity offset from 2000		-9.9
Deposition date		#NUM!

depth	Density (measured)	unsupported activity / g clay	US activity / gram	Trapazoidal Depth-Integration of (activity * volume * density)
0.00	1.08	5.55	2.50	
1.00	1.08	5.55	2.50	9.97
3.00	1.17	4.35	2.07	18.99
5.00	1.45	2.46	1.24	15.99
7.00	1.54	1.89	0.81	11.30
9.00	1.46	0.76	0.35	6.41
11.00	1.57	0.59	0.26	3.39
15.00	1.71	0.21	0.09	4.24
17.00	1.33	0.23	0.10	1.09
19.00	2.10	0.13	0.06	1.01
21.00	1.50	0.00	0.00	0.37
23.00	1.78	0.00	0.00	0.00
31.00	1.80	0.00	0.00	
41.00	1.86	0.00	0.00	
51.00	1.71	0.00	0.00	
61.00	1.84	0.00	0.00	
77.00	1.75	0.00	0.00	

^{210}Pb Profiles

Int. Err	Core	Depth (avg)	notes	Pb-210 DPM/g	dpm/g clay	dpm/g % < 2um	err	% Clay	%Silt	%Sand	% < 2um	notes	Supported Background (dpm/g clay)	XS clay activity	Radon Ventillation Effect	XS Activity (CVC)
0.5	T3_P14	0.5		0.97	2.29		0.23	43.00				AVG	1.658673004	0.63	-0.79	1.42
0.5	T3_P14	1.5		0.90	2.08	2.52	0.23	43.54	49.29	7.18	36.05		1.645744355	0.44	-0.78	1.22
0.5	T3_P14	2.5		0.91	2.03		0.20	45.10				AVG	1.609434349	0.42	-0.78	1.20
0.5	T3_P14	3.5		0.98	2.18		0.21	45.10				AVG	1.609434349	0.57	-0.77	1.34
0.5	T3_P14	4.5		0.87	1.94		0.20	45.10				AVG	1.609434349	0.33	-0.76	1.09
0.5	T3_P14	5.5		0.93	2.08		0.21	45.10				AVG	1.609434349	0.47	-0.76	1.23
0.5	T3_P14	6.5		0.99	2.22		0.21	45.10				AVG	1.609434349	0.61	-0.75	1.37
0.5	T3_P14	7.5		0.87	1.94		0.20	45.10				AVG	1.609434349	0.33	-0.75	1.08
0.5	T3_P14	8.5		0.83	1.85		0.19	45.10				AVG	1.609434349	0.24	-0.74	0.98
0.5	T3_P14	9.5		0.80	1.77		0.18	45.10				AVG	1.609434349	0.16	-0.73	0.90
0.5	T3_P14	10.5		0.76	1.69		0.17	45.10				AVG	1.609434349	0.08	-0.73	0.81
0.5	T3_P14	11.5		0.69	1.47	1.76	0.17	46.77	49.66	3.57	39.14		1.572875959	-0.10	-0.72	0.62
1	T3_P14	15		0.58	1.27		0.13	45.00				AVG	1.611693786	-0.34	-0.70	0.36
1	T3_P14	17		0.61	1.35		0.13	45.00				AVG	1.611693786	-0.26	-0.69	0.43
0.5	T3_P14	20.5		0.62	1.34		0.14	46.20				AVG	1.585108927	-0.25	-0.67	0.42
1	T3_P14	25	big red stone not ro	0.51	1.11		0.11	45.00				AVG	1.611693786	-0.51	-0.64	0.14
0.5	T3_P14	30.5		0.55	1.17		0.13	46.20				AVG	1.585108927	-0.42	-0.61	0.19
1	T3_P14	41		0.60	1.33		0.13	45.00				AVG	1.611693786	-0.29	-0.56	0.27
1	T3_P14	61		0.62	1.37		0.14	45.00				AVG	1.611693786	-0.24	-0.46	0.21
0.65	T3_P14	79.15		0.67	1.47	1.73	0.17	45.44	49.39	5.17	38.58		1.601781618	-0.14	-0.37	0.24

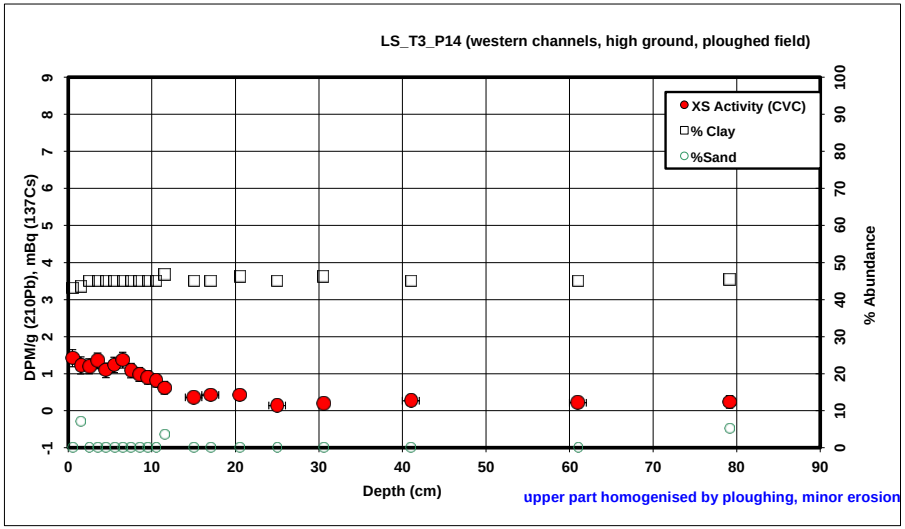

59.47	--->	16.07
Total integrated US activity (integrated tube DPM)		(DPM/cm^2) US activity
Assumed Mete (Atoms Pb-210/ M cm^2) (average 'shielded' rate of C18 & sites 41)	--->	17.76
US Activity fro (DPM/ cm^2)	--->	-1.69
Input Sedimen (DPM / g clay) (from proximal grab samples)	--->	1.76
CICCS Accum (grams clay / cm^2 yr)	--->	-0.03
CICCS Accum (grams / cm^2 yr)	--->	-0.07
CICCS Accum (cm / yr)	--->	-0.04

Avg. % Clay	Avg. Density
44.69	1.66

Assumed Supported -->	0.00
(DPM/ g clay)	
Assumed Den (g/cc)	1.50
Assumed Area (tube cross-section)	3.70

Present activi	0.24
Confidence In	0.05
Original sedim	1.76
Background US activity	
CIRCA Uncert	0.20
N/N_o	0.14
S.E. (N/N_o)	0.03
Predicted sed	64.10
S.E. (age)	7.73
minimum age	57.25
maximum age	72.82
Activity offset f	-1.5
Deposition dat	1937.4

Present activity	
Confidence In	1.47
Original sedim	3.00
Background U	0.60
CIRCA Uncert	0.20
N/N_o	-0.25
S.E. (N/N_o)	-0.61
Predicted sed	#NUM!
S.E. (age)	#NUM!
minimum age	#NUM!
maximum age	32.77
Activity offset f	-1.5
Deposition dat	#NUM!

	--->	16.07
Additional 'cap' activity (integrated tube DPM)		(DPM/cm^2) Cap activity
Assumed Mete (Atoms Pb-210/ M cm^2) (average 'shielded' rate of C18 & sites 41)	--->	17.76
Growth time fc	--->	75.666188
Activity offset from 2000		-2.5
Deposition date		1926.8

depth	Density (measured)	unsupported activity / g clay	US activity / gram	Trapazoidal Depth-Integration of (activity * volume * density)
0.00	1.58	1.42	0.61	
0.50	1.58	1.42	0.61	1.78
1.50	1.43	1.22	0.53	3.18
2.50	1.49	1.20	0.54	2.90
3.50	1.60	1.34	0.61	3.28
4.50	1.74	1.09	0.49	3.40
5.50	1.83	1.23	0.56	3.46
6.50	1.68	1.37	0.62	3.81
7.50	1.68	1.08	0.49	3.43
8.50	1.72	0.98	0.44	2.92
9.50	1.59	0.90	0.40	2.59
10.50	1.97	0.81	0.36	2.53
11.50	2.15	0.62	0.29	2.49
15.00	2.21	0.36	0.16	6.38
17.00	1.46	0.43	0.19	2.40
20.50	1.15	0.42	0.19	3.26
25.00	1.45	0.14	0.06	2.78
30.50	1.47	0.19	0.09	2.26
41.00	1.74	0.27	0.12	6.62
61.00	1.80	0.21	0.10	14.31
79.15	1.74	0.24	0.11	12.15

^{210}Pb Profiles

Int. Err	Core	Depth (avg)	notes	Pb-210 DPM/g	dpm/g clay	dpm/g % < 2um	err	% Clay	%Silt	%Sand	% < 2um	notes	Supported Background (dpm/g clay)	XS clay activity	Radon Ventillation Effect	XS Activity (CVC)
1	TE_P15	1		1.97	4.74		0.38	43.00				reconstr	1.658673004	3.09	-0.79	**3.87**
1	TE_P15	3		1.40	3.21	3.88	0.32	43.73	48.30	7.96	36.27		1.641030457	1.57	-0.77	**2.35**
1	TE_P15	5		0.93	1.71	2.04	0.15	54.47	42.16	3.37	45.59	B / graph off	1.428520175	0.28	-0.76	**1.04**
1	TE_P15	7		0.91	2.13	2.61	0.18	42.60	52.83	4.57	34.78		1.668418376	0.46	-0.75	**1.21**
1	TE_P15	9		0.86	2.15	2.68	0.19	40.00	54.91	5.09	32.16		1.736158949	0.42	-0.74	**1.16**
1	TE_P15	11		0.87	2.16	2.62	0.18	40.11	55.79	4.10	33.04		1.733254612	0.43	-0.73	**1.15**
1	TE_P15	13		0.87	1.94		0.17	40.04				AVG	1.735052503	0.20	-0.71	**0.92**
1	TE_P15	15		0.70	1.56		0.14	39.98				AVG	1.736855218	-0.18	-0.70	**0.52**
1	TE_P15	17		0.69	1.53		0.14	39.91		2.73		AVG	1.738662777	-0.21	-0.69	**0.48**
1	TE_P15	21		0.66	1.65	2.01	0.17	39.85	57.48	2.67	32.66		1.740475202	-0.09	-0.67	**0.58**
1	TE_P15	31		0.62	1.74	2.17	0.17	35.50	62.74	1.76	28.43		1.872332372	-0.13	-0.61	**0.48**
1	TE_P15	41		0.60	1.60		0.14	35.00				AVG	1.803298278	-0.21	-0.56	**0.35**
1	TE_P15	51		0.67	1.92		0.18	35.00					1.889129963	0.03	-0.51	**0.54**
1	TE_P15	71		0.75	2.15		0.20	35.00					1.889129963	0.26	-0.41	**0.67**
1	TE_P15	85.5		0.74	1.96		0.17	35.00				AVG	1.803298278	0.15	-0.35	**0.50**

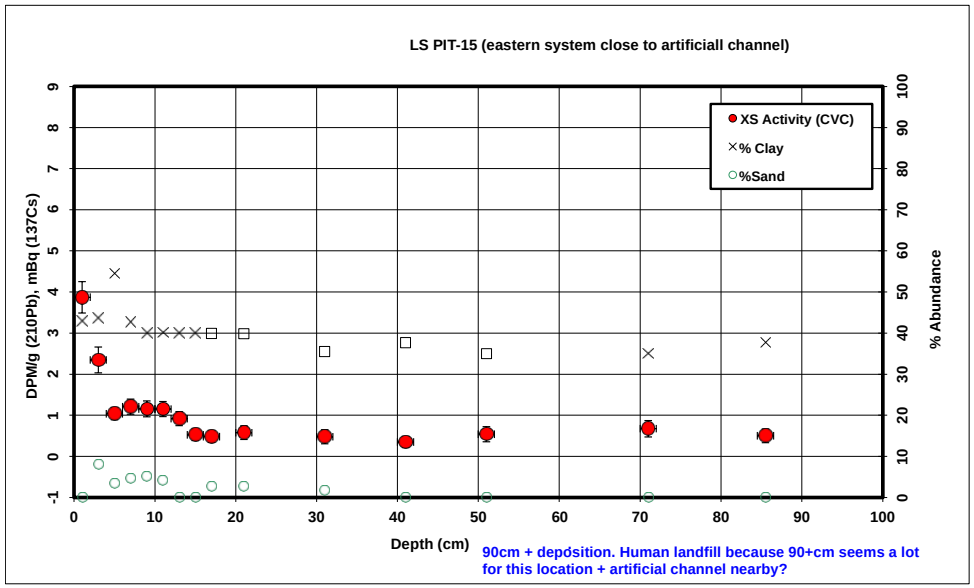

135.06	--->	36.50
Total integrated US activity (integrated tube DPM)		(DPM/cm^2) US activity
Assumed Mete (Atoms Pb-210/ M cm^2) (average 'shielded' rate of C18 & sites 41)	--->	17.76
US Activity fro (DPM/ cm^2)	--->	18.74
Input Sedimen (DPM / g clay) (from proximal grab samples)	--->	1.76
CICCS Accum (grams clay / cm^2 yr)	--->	0.33
CICCS Accum (grams / cm^2 yr)	--->	0.82
CICCS Accum (cm / yr)	--->	0.53

Avg. % Clay	Avg. Density
40.30	1.54

Assumed Supported -->		0.00
(DPM/ g clay)		
Assumed Den (g/cc)		1.50
Assumed Area (tube cross-section)		3.70

Present activit	1.17
Confidence In	0.03
Original sedin	1.76
Background US activity	
CIRCA Uncert	0.20
N/N_o	0.67
S.E. (N/N_o)	0.08
Predicted sed	13.01
S.E. (age)	3.79
minimum age	9.44
maximum age	17.02
Activity offset f	-9.5
Deposition dat	1996.5

Present activity	
Confidence In	#REF!
Original sedim	3.00
Background U	0.60
CIRCA Uncert	0.20
N/N_o	-0.25
S.E. (N/N_o)	#REF!
Predicted sed	#NUM!
S.E. (age)	#NUM!
minimum age	#REF!
maximum age	#REF!
Activity offset f	-1.5
Deposition dat	#NUM!

	--->	36.50
Additional 'cap' activity (integrated tube DPM)		(DPM/cm^2) Cap activity
Assumed Mete (Atoms Pb-210/ M cm^2) (average 'shielded' rate of C18 & sites 41)	--->	17.76
Growth time fc	--->	#NUM!
Activity offset from 2000		9.5
Deposition date		#NUM!

depth	Density (measured)	unsupported activity / g clay	US activity / gram	Trapazoidal Depth-Integration of (activity * volume * density)
0.00	1.05	3.87	1.66	
1.00	1.05	3.87	1.66	6.47
3.00	1.68	2.35	1.03	13.61
5.00	1.56	1.04	0.57	9.54
7.00	1.53	1.21	0.52	6.18
9.00	1.57	1.16	0.46	5.60
11.00	2.03	1.15	0.46	6.15
13.00	1.71	0.92	0.37	5.75
15.00	1.67	0.52	0.21	3.61
17.00	1.44	0.48	0.19	2.32
21.00	1.61	0.58	0.23	4.76
31.00	1.60	0.48	0.17	11.86
41.00	1.25	0.35	0.13	7.94
51.00	1.83	0.54	0.19	9.13
71.00	1.42	0.67	0.24	25.52
85.50	1.50	0.50	0.19	16.62

^{210}Pb Profiles

Int. Err	Core	Depth (avg)	notes	Pb-210 DPM/g	dpm/g clay	dpm/g % < 2um	err	% Clay	%Silt	%Sand	% < 2um	notes	Supported Background (dpm/g clay)	XS clay activity	Radon Ventillation Effect	XS Activity (CVC)
1	TE_P16	1		3.34	6.82	8.21	0.64	49.07	41.94	8.98	40.79		1.525830438	5.30	-0.79	**6.08**
1	TE_P16	3		1.49	3.16	3.80	0.27	47.34	47.92	4.74	39.28		1.560960009	1.59	-0.77	**2.37**
1	TE_P16	5		0.84	1.78	2.15	0.18	47.15	47.64	5.21	38.94		1.564818685	0.21	-0.76	**0.98**
1	TE_P16	7		0.82	1.67	1.92	0.16	48.84	46.79	4.38	42.39	1st run didn't v	1.530461151	0.14	-0.75	**0.89**
1	TE_P16	9		0.70	1.28	1.47	0.13	54.53	40.13	5.34	47.52		1.427456599	-0.15	-0.74	**0.59**
1	TE_P16	11		0.64	1.28	1.51	0.13	50.02	47.26	2.72	42.39		1.50751788	-0.23	-0.73	**0.50**
1	TE_P16	13		0.59	1.29		0.12	51.61				AVG	1.47803765	-0.19	-0.71	**0.53**
1	TE_P16	15		0.47	1.02		0.11	53.19				AVG	1.450001461	-0.43	-0.70	**0.27**
1	TE_P16	17		0.40	0.85		0.10	54.78				AVG	1.423298561	-0.58	-0.69	**0.11**
1	TE_P16	21		0.36	0.64	0.73	0.08	56.37	40.42	3.21	49.47		1.397829584	-0.76	-0.67	**-0.09**
1	TE_P16	31		0.40	0.69	0.80	0.09	57.54	38.87	3.59	50.04		1.379787694	-0.69	-0.61	**-0.08**
1	TE_P16	41		0.37	0.58	0.64	0.08	63.40	35.69	0.91	57.30		1.297734102	-0.72	-0.56	**-0.16**
1	TE_P16	86		0.45	0.77	0.86	0.09	58.72	37.25	4.03	52.40		1.362211128	-0.59	-0.34	**-0.25**

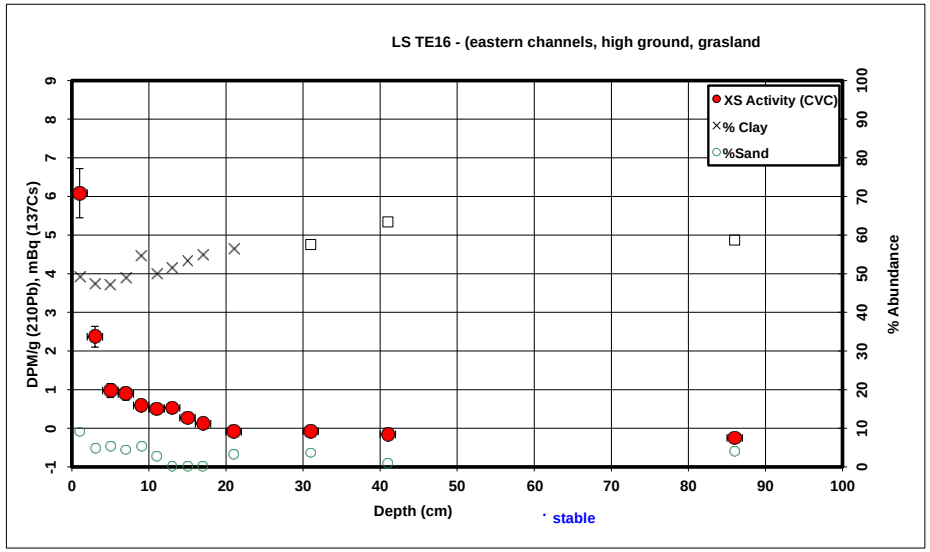

67.17	--->	18.15
Total integrated US activity (integrated tube DPM)		(DPM/cm^2) US activity
Assumed Mete (Atoms Pb-210/ M cm^2) (average 'shielded' rate of C18 & sites 41)	--->	17.76
US Activity fro (DPM/ cm^2)	--->	0.39
Input Sedimen (DPM / g clay) (from proximal grab samples)	--->	1.76
CICCS Accum (grams clay / cm^2 yr)	--->	0.01
CICCS Accum (grams / cm^2 yr)	--->	0.01
CICCS Accum (cm / yr)	--->	0.01

Avg. % Clay	Avg. Density
53.27	1.57

Assumed Supported -->	0.00
(DPM/ g clay)	
Assumed Den (g/cc)	1.50
Assumed Area (tube cross-section)	3.70

Present activity	
Confidence In	0.00
Original sedim	3.00
Background U	0.60
CIRCA Uncert	0.20
N/N_o	-0.25
S.E. (N/N_o)	-0.02
Predicted sed	#NUM!
S.E. (age)	#NUM!
minimum age	#NUM!
maximum age	#NUM!
Activity offset f	-1.5
Deposition dat	#NUM!

Present activity	
Confidence In	#REF!
Original sedim	3.00
Background U	0.60
CIRCA Uncert	0.20
N/N_o	-0.25
S.E. (N/N_o)	#REF!
Predicted sed	#NUM!
S.E. (age)	#NUM!
minimum age	#REF!
maximum age	#REF!
Activity offset f	-1.5
Deposition dat	#NUM!

	--->	18.15
Additional 'cap' activity (integrated tube DPM)		(DPM/cm^2) Cap activity
Assumed Mete (Atoms Pb-210/ M cm^2) (average 'shielded' rate of C18 & sites 41)	--->	17.76
Growth time fc	--->	#NUM!
Activity offset from 2000		-2.5
Deposition date		#NUM!

depth	Density (measured)	unsupported activity / g clay	US activity / gram	Trapazoidal Depth-Integration of (activity * volume * density)
0.00	1.50	6.08	2.99	
1.00	1.50	6.08	2.99	16.57
3.00	1.51	2.37	1.12	22.85
5.00	1.31	0.98	0.46	8.26
7.00	1.48	0.89	0.43	4.62
9.00	1.45	0.59	0.32	4.08
11.00	1.53	0.50	0.25	3.13
13.00	1.59	0.53	0.27	3.00
15.00	1.74	0.27	0.14	2.56
17.00	1.68	0.11	0.06	1.30
21.00	1.78	0.00	0.00	0.80
31.00	1.77	0.00	0.00	
41.00	2.01	0.00	0.00	
86.00	1.79	0.00	0.00	

^{210}Pb Profiles

Int. Err	Core	Depth (avg)	notes	Pb-210 DPM/g	dpm/g clay	dpm/g % < 2um	err	% Clay	%Silt	%Sand	% < 2um	notes
0.5	TEP17	0.5		2.34	5.21		0.48	46.00				AVG
0.5	TEP17	1.5		1.96	4.36		0.40	46.00				AVG
0.5	TEP17	2.5		1.64	3.64		0.34	46.00				AVG
0.5	TEP17	3.5		1.51	3.35	4.14	0.36	46.01	39.33	14.67	37.14	
0.5	TEP17	4.5		1.42	3.06		0.29	47.36				AVG
0.5	TEP17	5.5		1.32	2.83		0.28	47.40				AVG
0.5	TEP17	6.5		1.03	2.20		0.22	47.40				AVG
0.5	TEP17	7.5		0.90	1.91		0.20	47.40				AVG
0.5	TEP17	8.5		0.89	1.90		0.20	47.40				AVG
0.5	TEP17	9.5		0.85	1.81		0.19	47.40				AVG
0.5	TEP17	10.5		0.86	1.82		0.19	47.40				AVG
0.5	TEP17	11.5		0.81	1.66	1.98	0.19	48.72	38.24	13.05	40.87	
0.5	TEP17	12.5		0.76	1.58		0.15	48.00				AVG
0.5	TEP17	13.5		0.61	1.24		0.12	48.00				AVG
0.5	TEP17	14.5		0.64	1.33		0.13	48.00				AVG
0.5	TEP17	20.5		0.63	1.23		0.12	50.59				AVG
0.5	TEP17	30.5		0.43	0.82		0.09	50.60				AVG
1	TEP17	51	Outlier ?	0.80	1.61		0.15	50.00				
0.5	TEP17	81.5		0.52	0.98	1.16	0.13	52.47	41.84	5.69	44.64	

Supported Background (dpm/g clay)	XS clay activity	Radon Ventillation Effect	XS Activity (CVC)
1.589461053	3.62	-0.79	4.41
1.589461053	2.77	-0.78	3.55
1.589461053	2.05	-0.78	2.83
1.589295915	1.76	-0.77	2.53
1.560431371	1.50	-0.77	2.27
1.559627658	1.27	-0.76	2.03
1.559627658	0.64	-0.75	1.39
1.559627658	0.35	-0.75	1.10
1.559627658	0.34	-0.74	1.08
1.559627658	0.25	-0.74	0.98
1.559627658	0.26	-0.73	0.99
1.53288276	0.13	-0.72	0.85
1.547278099	0.04	-0.72	0.75
1.547278099	-0.30	-0.71	0.41
1.547278099	-0.22	-0.71	0.49
1.496710419	-0.27	-0.67	0.40
1.49654477	-0.67	-0.62	-0.06
1.507869642	0.10	-0.51	0.61
1.462663008	-0.48	-0.36	-0.11

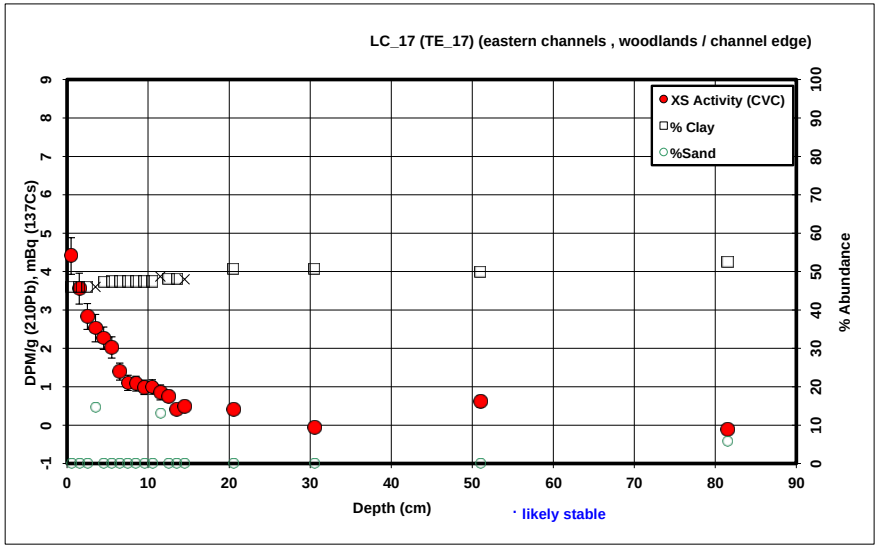

64.65	--->	17.47
Total integrated tube DPM)	US activity (integrated	(DPM/cm^2) US activity
Assumed Mete (Atoms Pb-210/ M cm^2) (average 'shielded' rate of C18 & sites 41)	--->	17.76
US Activity fro (DPM/ cm^2)	--->	-0.29
Input Sedimen (DPM / g clay) (from proximal grab samples)	--->	1.76
39.01	CICCS Accum (grams clay / cm^2 yr) --->	-0.01
	CICCS Accum (grams / cm^2 yr) --->	-0.01
	CICCS Accum (cm / yr) --->	-0.01

Avg. % Clay	Avg. Density
46.77	1.35

Assumed Supported -->	0.00
(DPM/ g clay)	
Assumed Den (g/cc)	1.50
Assumed Area (tube cross-section)	3.70

Present activit	1.04
Confidence In	0.00
Original sedin	1.76
Background US activity	
CIRCA Uncert	0.20
N/N_o	0.59
S.E. (N/N_o)	0.07
Predicted sed	16.87
S.E. (age)	3.67
minimum age	13.40
maximum age	20.76
Activity offset f	-9.5
Deposition dat	1992.6

Present activity	
Confidence In	0.98
Original sedin	3.00
Background U	0.60
CIRCA Uncert	0.20
N/N_o	-0.25
S.E. (N/N_o)	-0.41
Predicted sed	#NUM!
S.E. (age)	#NUM!
minimum age	#NUM!
maximum age	58.86
Activity offset f	-1.5
Deposition dat	#NUM!

	--->	17.47
Additional 'cap' activity (integrated tube DPM)		(DPM/cm^2) Cap activity
Assumed Mete (Atoms Pb-210/ M cm^2) (average 'shielded' rate of C18 & sites 41)	--->	17.76
Growth time fc	--->	132.154513
Activity offset from 2000		-9.5
Deposition date		1877.3

depth	Density (measured)	unsupported activity / g clay	US activity / gram	Trapazoidal Depth-Integration of (activity * volume * density)
0.00	1.50	4.41	2.03	
0.50	1.50	4.41	2.03	5.63
1.50	1.11	3.55	1.63	8.86
2.50	1.28	2.83	1.30	6.49
3.50	1.00	2.53	1.16	5.20
4.50	1.12	2.27	0.47	3.20
5.50	1.37	2.03	0.47	2.15
6.50	1.39	1.39	0.47	2.38
7.50	1.52	1.10	0.47	2.51
8.50	1.45	1.08	0.47	2.56
9.50	1.46	0.98	0.47	2.51
10.50	1.55	0.99	0.20	1.86
11.50	2.08	0.85	0.20	1.36
12.50	1.63	0.75	0.20	1.40
13.50	1.71	0.41	0.20	1.26
14.50	1.65	0.49	0.20	1.26
20.50	2.29	0.40	0.20	8.89
30.50	1.50	0.00	0.00	7.12
51.00	1.55	0.61	0.00	
81.50	1.50	0.00	0.00	

Profile Descriptions

Below the profiles used in this thesis to reconstruct the evolution of the Sacramento River are described. A map of the profile locations is presented in chapter 3 (Figure 22, Figure 23), coordinates of the sites can be found in appendix A, profile graphs can be found in appendix B and C.

Composite Profiles

Composite profiles are profiles where a superficial profile description on deep (2 – 5 m) pits has been conducted in the field, and OSL and 14C samples for dating purposes have been collected. Parallel to these cores for ^{210}Pb analysis have been collected at the same sites.

T2P1

The site of the 5 m deep pit and the 64 cm long core T2P1 is located ~ 7000 m from the next potential flood source on an elevated improved pasture within the western ephemeral floodplain channel system at an elevation of 33.03 m a.s.l.. On the surface silty loams are situated down to ~ 2.2 m depth. In these silts secondary carbonate precipitations are present from ~ 1.1 m. The carbonate precipitations are limited to vertical dry cracks in the sediment profile. At the bottom of this silty section in the transition towards sandier sediments (~ 2.2 – 2.25 m) a soil has developed with large plant macrofossils preserved in it. This soil is not fully preserved because solid calcite/gypsum/silica precipitations are superimposing prior characteristic (2.25 – 2.6 m). This precipitation is located in the uppermost part of a complex of more or less silt rich sands extending down to 4.8 m below surface. From 2.6 m Mn-Fe precipitations are visible, as well as clay filled pipe like features that might possibly be linked to burrowing animal activity. Below 4.8 m gravel are present. There is little organic (< 1.5 %) present in the sediment. A monotonic decline in organic matter can be observed from the surface up to 2.2 m. Below 2.3 m organic matter remains extremely low (< 0.1 %). Except for the calcite precipitation in vertical cracks, there is no calcium carbonate present in the upper 1.7 m – 2.3 m of the profile. Below 2.3 m below surface the calcium carbonate content increases to 1.6 % and stays above 1.5 % until 2.6 m before it gradually drops to not detectable levels at 3.6 m below surface. The profile's XS ^{210}Pb inventory is 15.68 DPM/$g_{(clay),}$ what would result in an CICCS erosion rate of - 0.03 cm/a. It shows

a monotonic decline in XS ^{210}Pb activities up to 10 cm a slight increase in XS ^{210}Pb activities between 10 - 12 cm and a monotonic decline below, reaching background levels at 20 cm.

T2P2

The site of the 5 m deep pit and the 90 cm long core T2P2 is located ~ 7000 m from the next potential flood source on an elevated formerly ploughed improved pasture at the western edge of the western ephemeral floodplain channel system at an elevation of 32.42 m a.s.l.. Its XS ^{210}Pb inventory is 21.94 DPM/g$_{(clay)}$ what would result in an CICCS sedimentation rate of 0.1 cm/a. It shows a monotonic decline in XS ^{210}Pb activities up to 12 cm a slight increase in XS ^{210}Pb activities between 12 - 14 cm and a monotonic decline below, reaching background levels at 30 cm. The profile mostly consist of homogeneous silty clays. At around 4 m depth the silty clay is slowly transitioning to sandy silt / silty sand.

T2P3

The site of the 3.8 m deep pit and the 87 cm long core T2P3 is located ~ 1500 m from the next potential flood source in a ploughed field in the Holocene meander belt at an elevation of 32.83 m a.s.l.. The core shows elevated XS ^{210}Pb activities at the surface with a slow monotonic decline up to 40 cm with background activities below. Its XS ^{210}Pb inventory is 23.20 DPM/g$_{(clay)}$ what would result in an CICCS sedimentation rate of 0.12 cm/a. The profile shows silts to sandy silts at the top, sandy silts from 1.5 m to 3.2 m with a sand layer at 2.2 – 2.35 cm below surface. From 3.2 m gravel are present in the profile.

T2P4

The site of the 3.2 m deep pit and the 81 cm long core T2P4 is located ~ 1500 m from the next potential flood source in a ploughed field at a low point in a meander scar in the Holocene meander belt at an elevation of 30.67 m a.s.l.. Its XS ^{210}Pb inventory is 54.38 DPM/g$_{(clay)}$ what would result in an CICCS sedimentation rate of 0.64 cm/a. It shows elevated XS ^{210}Pb activities up to the bottom of the core, thus a CIRCACS sedimentation rate has been calculated to 1.33 cm/a. The top of the profile to 1.2 cm consists of homogeneous clay rich silts. From 0.9 m reworked silt/clay conglomerates that show clear indications of

burning are present. At 1.2 – 1.25 m below surface a layer of strongly in situ burned clay and silt is present. Below 1.25 the profile shows alternating layers of silt and organic rich silts respectively.

T2P5

The site of the 4.0 m deep pit and the 85 cm long core T2P5 is located ~ 1500 m from the next potential flood source in a ploughed field in the Holocene meander belt at an elevation of 33.03 m a.s.l.. The core shows elevated XS ^{210}Pb activities at the surface with a slow monotonic decline up to 30 cm with background activities below. Its XS ^{210}Pb inventory is 23.03 DPM/g$_{(clay)}$ what would result in an CICCS sedimentation rate of 0.10 cm/a. The profile shows clay rich silts from the top to 3.1 m below surface. Indications of burning (increased amounts of charcoal) can be found at 1.0 m, 2.0 m, and 2.2 m below surface. From 3.1 m – 3.5 m sandy silts are present. Below 3.5 m the profile consist of sand.

T2P6

The site of the 2.6 m deep pit and the 87 cm long core T2P6 is located ~ 1000 m from the next potential flood source in the Holocene meander belt in a little used natural grassland with bushy vegetation at an elevation of 31.79 m a.s.l.. The core shows high XS ^{210}Pb activities at the surface with a monotonic decline up to 40 cm with background activities below. Its XS ^{210}Pb inventory is 30.76 DPM/g$_{(clay)}$ what would result in an CICCS sedimentation rate of 0.34 cm/a. In this profile just in the top 0.1 m a significant clay content can be observed. From 0.1 m – 1.6 m silty sand is present, below 1.6 m the profile consists of sand.

TEP7

The site of the 2.8 m deep pit and the 89 cm long core TEP7 is located ~ 7000 m from the next potential flood source in an improved pasture with discing taking place at an elevation of 33.44 m a.s.l.. The profile consist of sily clay from the surface to 1.7 m depth. From 1.0 m calcite precipitations are present in vertical dry cracks. Between 1.7 m and 1.9 m below surface a duric layer is developed. Below 1.9 m silty sands have been deposited. From approximately 3.5 m below surface gravel are present in this profile. The whole core is low in

organic carbon content (< 1.4 %) with a monotonic decline in organic carbon throughout the core. Calcium carbonate is not present in the first 0.8 m below surface. From 0.9 m below surface there is a slight increase in calcium carbonate. Calcium carbonate is present in the profile to the depth of 1.7 m. The core showing high XS ^{210}Pb at the surface that are monotonically declining until 10 cm below surface with increased XS ^{210}Pb values between 10 - 12 cm and monotonically declining thereafter until reaching background values at 15 cm. The profile's XS ^{210}Pb inventory is 14.19 DPM/$g_{(clay)}$ what would result in an CICCS sedimentation rate of - 0.07 cm/a.

TEP8

The site of the 1.4 m deep pit and the 76 cm long core TEP8 is located ~ 10000 m from the next potential flood source within one of the shallow eastern channels at an elevation of 30.70 m a.s.l.. The XS ^{210}Pb activity for the first 2 cm below surface had to be estimated because of a lack of mineral material present. It can be assumed that it is higher than the activity at 2 - 4 cm, but the XS ^{210}Pb activity from 2 - 4 cm has been used with an added error of 1 DPM/$g_{(clay)}$. Below 4 cm the core shows a monotonic decrease in XS ^{210}Pb activities up to 12 cm, a slight increase in XS ^{210}Pb activities up to 16 cm and a decrease thereafter, reaching background at 18 cm. Its XS ^{210}Pb inventory is 16.56 DPM/$g_{(clay)}$ what would result in an CICCS erosion rate of - 0.03 cm/a. The profile shows silty clay for the first meter below surface with sands below that shows a petrocalcic layer from 1.0 m – 1.2 m below surface. Below the sand at approximately 2 m below surface gravel deposits start.

T1P9

The site of the 4.2 m deep pit and the 82 cm long core T1P9 is located ~ 3000 m from the next potential flood source at the edge of the westernmost ephemeral floodplain channel at an elevation of 30.74 m a.s.l.. Little time was spend on the profile description, because water entered the pit early on, making it unsafe to work in. In the upper part of the profile a silty loam is present (0 – 1.5 m). Below the profile consists of silty sands. A strong palaeo soil is visible in the upper part of the sandy complex (1.5 – 1.7 m) that is superimposed in its lower part by calcite precipitations that could be described as petrocalcic layer (1.7 – 1.9 m). It shows slightly lower XS ^{210}Pb activities from 0 – 2 cm, a slight

increase in XS ^{210}Pb activities from 2 – 4 cm and a monotonic decrease in XS ^{210}Pb activities below, reaching background XS ^{210}Pb activity at 24 cm below surface. Its XS ^{210}Pb inventory is 16.66 DPM/$g_{(clay)}$ what would result in an CICCS erosion rate of - 0.03 cm/a.

T1P10

The site of the 4.5 m deep pit and the 87 cm long core T1P10 is located ~ 2000 m from the next potential flood source in a forested area with bushy undergrowth at the inner bend of Eddie Lake, an oxbow lake connected to the western ephemeral floodplain channels at an elevation of 30.78 m a.s.l.. The profile shows homogeneous XS ^{210}Pb activities for the first 4 cm and a monotonic decline in XS ^{210}Pb activities below, reaching background levels at 50 cm Its XS ^{210}Pb inventory is 38.85 DPM/$g_{(clay)}$ what would result in an CICCS sedimentation rate of 0.54 cm/a. The profile shows clay rich silt from the surface to 1.2 m below surface. From 1.2 m to 2.6 m the sand content is steadily increasing with little clay present. Below 2.6 m silty sand is present with an initial soil developed at 3.3 m below surface. From 4.0 m below surface hardly any silt is left in the sediment and it can be described as sand.

T1P11

The site of the 3.2 m deep pit and the 84 cm long core T1P11 is located ~ 2000 m from the next potential flood source at the inner bend of an oxbow lake with a grassland/bush vegetation at an elevation of 29.14 m a.s.l.. The profile shows a monotonic decline in XS ^{210}Pb activity throughout the core reaching background activities at ~ 50 cm below surface. Its XS ^{210}Pb inventory is 36.43 DPM/$g_{(clay)}$ what would result in an CICCS sedimentation rate of 0.45 cm/a. In the profile from the surface to 0.9 m clay rich silt with a noticeable sand content is present. From 0.9 m to 1.8 m below surface an increasing gravel content in silty matrix can be observed. The silt matrix is replaced by a sand matrix from 1.8 m to 2.1 m below surfaced. From 2.1 m to 2.6 m below surface sand without gravel can be observed. Below 2.6 m the profile consists of gravel.

T3P12

The site of the 2.9 m deep pit T3P12 is located ~ 800 m from the next potential flood source in a ploughed field on a second order meander at an

elevation of 34.25 m a.s.l.. No core has been collected at this location. The sedimentation rate for the site has been reconstructed using a 1980 horizon at a depth of 1 m below surface, thus the average sedimentation rate since 1980 has been calculated to 0.33 cm/a. In this profile from the surface to 1.0 m below surface clay rich silts with a noticeable sand content is present. From 0.5 m reworked sediment showing clear indications of intense burning can be observed. At 1.0 m below surface a layer showing intense in situ burning is present. In this layer a pit with filled with burned material is visible. Below the burned layer sandy to clay rich silts are present to 2.3 m below surface. From 2.3 m sandy sediment can be observed.

T3P13

The site of the 2.5 m deep pit and the 78 cm long core T3P13 is located ~ 300 m from the next potential flood source that has been abandoned between 1896 and 1908 in the Holocene meander belt, with natural grassland vegetation at an elevation of 33.92 m a.s.l.. The core shows a high XS ^{210}Pb activities at the surface with a monotonic decline up to 20 cm with background activities below. Its XS ^{210}Pb inventory is 19.67 DPM/g$_{(clay)}$ what would result in an CICCS sedimentation rate of 0.06 cm/a.

T3P14

The site of the 4.7 m deep pit and the 80 cm long core T3P14 is located ~ 5000 m from the next potential flood source at an elevated ploughed field in the centre of the western ephemeral floodplain channels at an elevation of 33.92 m a.s.l.. The core shows homogeneous XS ^{210}Pb activities in the uppermost 7 cm with a monotonic decline in activities from 7 to 14 cm and homogeneous XS ^{210}Pb activities from 14 – 20 cm reaching background levels at 25 cm. Its XS ^{210}Pb inventory is 16.07 DPM/g$_{(clay)}$ what would result in an CICCS erosion rate of - 0.04 cm/a.

TEP15

The site of the 4 m deep pit and the 87 cm long core TEP15 is located ~ 4000 m from the next potential flood source at the edge of an artificial channel at an elevation of 35.02 m a.s.l.. It shows a monotonic decline in XS ^{210}Pb values from the surface down to 4 cm, heterogeneous XS ^{210}Pb activities from 4

– 12 cm, a steep decline thereafter, but elevated activities throughout the core. Its XS ^{210}Pb inventory is 36.50 DPM/g$_{(clay)}$ what would result in an CICCS sedimentation rate of 0.53 cm/a. The position close to the artificial channel and profile disturbances visible in a profile pit nearby indicate that the profile is potentially the result of a human landfill.

Profiles for XS ^{210}Pb analysis

The reference profiles

The natural fallout inventory was calculated by locating undisturbed sites outside the recently flooded area that are unlikely to have received sediment within the last century from natural or anthropogenic processes. Three of these sites are within the research area (M2, TE_P16, LSF-T) and one has been collected outside or the immediate research area (Cemetery).

LSL-Terrace

The 49 cm long profile LSL-Terrace has been collected at an undisturbed location well outside the area of natural flooding at an elevation of 31.94 m a.s.l.. The core LC-17 shows high XS ^{210}Pb activities at the top of the core and a mostly monotonic decline in XS ^{210}Pb activities with only a minor increase in XS ^{210}Pb activities from 6 – 8 cm. with reaching background levels at ~ 12 cm below surface. Its XS ^{210}Pb inventory is 16.87 DPM/g$_{(clay)}$.

M-2

The 77.5 cm long core M-2 has been collected at an undisturbed location on high ground (elevation) outside the area of natural flooding (Fig) at an elevation of 33.38 m a.s.l.. It shows a monotonic decline in XS ^{210}Pb activities up to 20 cm depth. There is no sign of post sedimentary profile reworking. Its XS ^{210}Pb inventory is 17.43 DPM/g$_{(clay)}$.

TE_P16

The profile TE_P16 is located on an elevated part of the floodplain at the far southern end of Llano Seco on an unimproved pasture, at an elevation of 32.08 m a.s.l.. The 87 cm long core shows a monotonic decline in XS ^{210}Pb

activities up to 20 cm below surface, staying at background level thereafter. Its XS ^{210}Pb inventory is 18.15 DPM/g$_{(clay)}$.

Cemetery

The 49 cm long core was collected outside the premise of Llano Seco and the research area in an historic cemetery close to a 19th century gravestone. For this site it is assumed that the age of the grave is an indication that the side was probably not disturbed within the last century. It shows a monotonic decline of XS ^{210}Pb activities up to 20 cm below surface. Its XS ^{210}Pb inventory is 18.60 DPM/g$_{(clay)}$.

The average inventory of the four undisturbed reference profiles that have been used to establish the natural meteoric fallout inventory was calculated to 17.76 ± 0.77 DPM/cm^2. Cores with CICCS inventories below or above that activity are deemed eroding or infilling, respectively.

Core descriptions of floodplain cores

GL-1

The 90 cm long core GL-1 has been collected ~ 2500 m from the next potential flood source on an unimproved pasture, close to an artificial training levee at an elevation of 29.24 m a.s.l.. It shows declining XS ^{210}Pb activities for the first 4 cm, followed by a peak below and declining activities thereafter. Its XS ^{210}Pb inventory is 38.82 DPM/$g_{(clay)}$ what would result in an CICCS sedimentation rate of 0.54 cm/a

LC-17

The 82 cm long core LC-17 has been collected ~ 4000 m from the next potential flood source in a naturally forested area with some brambles as undergrowth within the eastern floodplain channel system close to Little Chico Creek at an elevation of 34.00 m a.s.l.. The core shows high XS ^{210}Pb activity at the top with a monotonic decline until reaching background between 22 and 30 cm below surface. Its XS ^{210}Pb inventory is 17.47 DPM/$g_{(clay)}$ what would result in an CICCS erosion rate of - 0.01 cm/a.

LSD-1

The 87 cm ling core LSD-1 has been collected ~ 50 m from the next potential flood source in a little used natural grassland with some bushy vegetation at an elevation of 33.23 m a.s.l.. The XS ^{210}Pb activities in core LSD-1 show a monotonic decline from the surface to 8 cm, a peak followed by a monotonic decline from 10 – 18 cm and a peak at 18 – 20 cm, before reaching background levels of XS ^{210}Pb. The core shows elevated XS ^{210}Pb activities with high sand and low clay content from 50 – 70 cm. Its XS ^{210}Pb inventory is 22.39 DPM/$g_{(clay)}$ what would result in an CICCS sedimentation rate of 0.19 cm/a.

LSD-2

The 81 cm long core LSD-2 has been collected ~ 350 m from the next potential flood source on the edge of a shallow ephemeral channel in a little used natural grassland with bushy vegetation at an elevation of 32.95 m a.s.l.. In core LSD-2 the upper 2 cm show a XS ^{210}Pb activity of ~ 3 DPM/$g_{(clay)}$, a

peak with a monotonic decline below from 2 - 8cm, a peak followed by a monotonic decline from 10 – 18 cm and a peak at 18 – 20 cm. Background levels of XS ^{210}Pb are not reached in this core. Its XS ^{210}Pb inventory is 35.11 DPM/$g_{(clay)}$ what would result in an CICCS sedimentation rate of 0.59 cm/a.

LSD-3

The 85 cm long core LSD-3 has been collected ~ 600 m from the next potential flood source in a little used natural grassland with bushy vegetation at an elevation of 33.65 m a.s.l.. The XS ^{210}Pb activities in core LSD-3 show a monotonic decline from the surface to 8 cm, a peak followed by a monotonic decline from 10 – 18 cm and a peak at 18 – 20 cm, before reaching background levels of XS ^{210}Pb at ~ 25 cm below surface. Its XS ^{210}Pb inventory is 13.70 DPM/$g_{(clay)}$ what would result in an CICCS erosion rate of - 0.16 cm/a.

LSD-4

The 85 cm long core LSD-4 has been collected ~ 800 m from the next potential flood source in a little used natural grassland with bushy vegetation at an elevation of 33.28 m a.s.l.. The XS ^{210}Pb activities in core LSD-4 show a monotonic decline from the surface to 8 cm, a peak followed by a monotonic decline from 10 – 18 cm and a peak at 18 – 20 cm, before reaching background levels of XS ^{210}Pb at ~ 24 cm below surface. Its XS ^{210}Pb inventory is 16.97 DPM/$g_{(clay)}$ what would result in an CICCS erosion rate of - 0.03 cm/a.

LSD-5

The 87 cm long core LSD-5 has been collected ~ 1000 m from the next potential flood source in a 1st order channel scar vegetated with large trees and thick undergrowth at an elevation of 39.75 m a.s.l.. The XS ^{210}Pb activities in core LSD-5 show a slow monotonic decline to the bottom of the core without reaching background levels. Its XS ^{210}Pb inventory is 93.40 DPM/$g_{(clay)}$ what would result in an CICCS sedimentation rate of 1.76 cm/a. It shows elevated XS ^{210}Pb activities up to the bottom of the core.

LSD-6

The 87 cm long core LSD-5 has been collected ~ 1000 m from the next potential flood source in a 1st order channel scar vegetated with large trees and

thick undergrowth at an elevation of 39.59 m a.s.l.. Core LSD-5 shows variable XS ^{210}Pb activities in the upper 10 cm with a slow monotonic decline to the bottom of the core without reaching background levels. Its XS ^{210}Pb inventory is 76.43 DPM/$g_{(clay)}$ what would result in an CICCS sedimentation rate of 1.28 cm/a. It shows elevated XS ^{210}Pb activities up to the bottom of the core, thus a CIRCACS sedimentation rate has been calculated to 1.89 cm/a.

LSL-1

The 72 cm long core LSL-1 has been collected ~ 200 m from the next potential flood source at the site of a young point bar at an elevation of 32.54 m a.s.l.. Its XS ^{210}Pb inventory is 7.64 DPM/$g_{(clay)}$ what would result in an CICCS erosion rate of - 1.13 cm/a. The core shows elevated XS ^{210}Pb levels throughout the core with high XS ^{210}Pb activities between 6 – 20 cm, but the low clay content and therefore high XS ^{210}Pb error does not lent itself for further interpretation. It shows elevated XS ^{210}Pb activities up to the bottom of the core, thus a CIRCACS sedimentation rate has been calculated to 1.44 cm/a.

LSL-2

The 81 cm long core LSL-2 has been collected ~ 300 m from the next potential flood source at the site of a young point bar at an elevation of 34.06 m a.s.l.. The XS ^{210}Pb activities in core LSL-2 show high values at to surface with a rather monotonic decline from the surface to ~ 12 cm with background levels thereafter. Its XS ^{210}Pb inventory is 14.76 DPM/$g_{(clay)}$ what would result in an CICCS erosion rate of -0.15 cm/a.

LSL-3A

The 42 cm long core LSL-3 has been collected ~ 400 m from the next potential flood source at the site of a young point bar at an elevation of 32.54 m a.s.l.. The XS ^{210}Pb activities are homogeneous from the surface to 6 cm with a monotonic decline thereafter reaching background levels between 10 and 20 cm. Its XS ^{210}Pb inventory is 13.58 DPM/$g_{(clay)}$ what would result in an CICCS erosion rate of - 0.15 cm/a.

LSL-4A

The 42 cm long core LSL-4 has been collected ~ 400 m from the next potential flood source at the in a slightly elevated position in a grassland / bush at an elevation of 34.13 m a.s.l.. The XS ^{210}Pb activities are homogeneous from the surface to 4 cm with a monotonic decline thereafter reaching background levels between 10 and 20 cm. Its XS ^{210}Pb inventory is 13.91 DPM/$g_{(clay)}$ what would result in an CICCS erosion rate of - 0.14 cm/a.

M-0

The 16 cm long core M-0 has been collected ~ 10000 m from the next potential flood source at the edge of a floodplain channel to the east of the extent of the eastern ephemeral channels at an elevation of 31.65 m a.s.l.. The core shows high XS ^{210}Pb activities at the surface with a monotonic decline up to 6 cm below surface with reaching background levels thereafter. Its XS ^{210}Pb inventory is 22.26 DPM/$g_{(clay)}$ what would result in an CICCS sedimentation rate of 0.08 cm/a.

M-1

The 52 cm long core M-1 has been collected ~ 9000 m from the next potential flood source within the eastern ephemeral channel system at an elevation of 31.70 m a.s.l.. The XS ^{210}Pb activities in core M-1 show a slow monotonic decline from the surface to 8 cm, before reaching background levels in XS ^{210}Pb. Its XS ^{210}Pb inventory is 18.63 DPM/$g_{(clay)}$ what would result in an CICCS sedimentation rate of 0.02 cm/a.

M-3

The 67 cm long core M-3 has been collected ~ 8000 m from the next potential flood source at the edge of one of the major channels of the western ephemeral channel system at an elevation of 30.37 m a.s.l.. The XS ^{210}Pb activities show high values at the surface (5.38 DPM/$g_{(clay)}$) with a monotonic decline before reaching background levels at 20 cm. Its XS ^{210}Pb inventory is 28.26 DPM/$g_{(clay)}$ what would result in an CICCS sedimentation rate of 0.25 cm/a.

M-4

The 50 cm long core M-4 has been collected ~ 4000 m from the next potential flood source at the far southern end of Llano Seco at the edge of one of the western ephemeral floodplain channels at an elevation of 28.66 m a.s.l.. The XS ^{210}Pb activities in core M-4 show a slow monotonic decline from the surface to 20 cm, before reaching background levels in XS ^{210}Pb. Its XS ^{210}Pb inventory is 16.46 DPM/g$_{(clay)}$ what would result in an CICCS erosion rate of -0.01 cm/a.

M-5

The 71 cm long core M-5 has been collected ~ 3500 m from the next potential flood source within the eastern channels system close to Little Chico Creek at an elevation of 33.66 m a.s.l.. Its location is close to one of the major passing roads and a wire fence is separating the grassland the core was taken from the road at the downstream end. At the fence loads of grass and debris was observed potentially creating an artificial dam with just a small bridge tunnel as an outlet. The XS ^{210}Pb activities in core M-5 show a slow monotonic decline from the surface to 30 cm, before reaching background levels in XS ^{210}Pb. Its XS ^{210}Pb inventory is 37.02 DPM/g$_{(clay)}$ what would result in an CICCS sedimentation rate of 0.49 cm/a.

MLSLF-29

The 85 cm long core MLSLF-29 has been collected ~ 500 m from the next potential flood source in a grassland/field at an elevation of 31.38 m a.s.l.. Its XS ^{210}Pb inventory is 27.66 DPM/g$_{(clay)}$ what would result in an CICCS sedimentation rate of 0.33 cm/a. It shows elevated XS ^{210}Pb activities up to the bottom of the core, thus a CIRCACS sedimentation rate has been calculated to 1.40 cm/a.

MLSLF-30

The 81 cm long core MLSLF-30 has been collected ~ 500 m from the next potential flood source in a grassland at an elevation of 31.88 m a.s.l.. The core shows similar XS ^{210}Pb activities from 0 – 10 cm, before monotonically decreasing, reaching background levels of XS ^{210}Pb below 40 cm. Its XS ^{210}Pb

inventory is 27.16 DPM/$g_{(clay)}$ what would result in an CICCS sedimentation rate of 0.28 cm/a.

MLSLF-31

The 79 cm long core MLSLF-31 has been collected ~ 800 m from the next potential flood source in a grassland at an elevation of 31.93 m a.s.l.. The core shows similar XS ^{210}Pb activities from 0 – 10 cm, before monotonically decreasing, reaching background levels of XS ^{210}Pb below 40 cm. Its XS ^{210}Pb inventory is 17.84 DPM/$g_{(clay)}$ what would result in an CICCS sedimentation rate of 0.00 cm/a.

MLSLF-33

The 95 cm long core MLSLF-33 has been collected ~ 3000 m from the next potential flood source in a grassland at an elevation of 31.65 m a.s.l.. The XS ^{210}Pb activities in core MLSLF-33 show a monotonic decline from the surface to 40 cm, before reaching background levels in XS ^{210}Pb. Its XS ^{210}Pb inventory is 25.77 DPM/$g_{(clay)}$ what would result in an CICCS sedimentation rate of 0.24 cm/a.

RASRF_125

The 61.5 cm long core RASRF_125 has been collected ~ 40 m from the next potential flood source on a recent meander in the Holocene meander belt at an elevation of 38.66 m a.s.l.. It was collected on a small (ca 10m diameter) meadow surrounded by trees and bushes. The core shows a monotonic decline in XS ^{210}Pb valued above 6 cm with an increase from 6 – 15 cm declining again until ~ 30 cm with a strong increase in XS ^{210}Pb values at 40 cm, and not reaching background levels in the core. Its XS ^{210}Pb inventory is 30.60 DPM/$g_{(clay)}$ what would result in an CICCS sedimentation rate of 0.63 cm/a. It shows elevated XS ^{210}Pb activities up to the bottom of the core, thus a CIRCACS sedimentation rate has been calculated to 1.20 cm/a.

RASRF_126

The 66.5 cm long core RASRF_126 has been collected ~ 50 m from the next potential flood source on a recent meander that has been abandoned between 1960 and 1964 in the Holocene meander belt at an elevation of 40.70

m a.s.l.. The core's XS ^{210}Pb activity shows decreasing values above 4 cm and higher activities from 4 – 12 cm before decreasing after 12 cm reaching background around 30 cm below surface. Its XS ^{210}Pb inventory is 16.60 DPM/$g_{(clay)}$ what would result in an CICCS sedimentation rate of - 0.05 cm/a. It shows elevated XS ^{210}Pb activities up to the bottom of the core, thus a CIRCACS sedimentation rate has been calculated to 1.3 cm/a.

RASRF_127

The 66 cm long core RASRF_127 has been collected ~ 100 m from the next potential flood on a recent meander that has been abandoned between 1960 and 1964 in the Holocene meander belt at an elevation of 39.97 m a.s.l.. The core's XS ^{210}Pb activity shows decreasing values up to 6 cm and a monotonic increase up to 20 cm, reaching background values around 30 cm. Its XS ^{210}Pb inventory is 9.68 DPM/$g_{(clay)}$ what would result in an CICCS erosion rate of - 0.51 cm/a. It shows elevated XS ^{210}Pb activities up to the bottom of the core, thus a CIRCACS sedimentation rate has been calculated to 0.72 cm/a.

RASRF_129

The 86 cm long core RASRF_129 has been collected ~ 1000 m from the next potential flood in an improved pasture with discing taking place at an elevation of 38.38 m a.s.l.. The core showing a high XS ^{210}Pb activity at the surface (4.50 DPM/$g_{(clay)}$) that are monotonically declining until 10 cm below surface with increased XS ^{210}Pb values between 10 – 12 cm and monotonically declining thereafter until reaching background values at 30 cm. Its XS ^{210}Pb inventory is 14.13 DPM/$g_{(clay)}$ what would result in an CICCS erosion rate of - 0.12 cm/a.

RASRF_130

The 51 cm long core RASRF_130 with a total depth of 50 cm has been collected ~ 1500 m from the next potential flood in a pasture bar at an elevation of 37.54 m a.s.l.. The core shows high XS ^{210}Pb activity at the surface (4.22 DPM/$g_{(clay)}$) with a monotonically decline up to 4 cm. Below there is a second monotonically declining cap between 4 – 8 cm and homogeneous activity throughout the core below (~ 0.3 DPM/$g_{(clay)}$), without reaching background values in the core. Its XS ^{210}Pb inventory is 18.83 DPM/$g_{(clay)}$ what would result

in an CICCS sedimentation rate of 0.02 cm/a. It shows elevated XS ^{210}Pb activities up to the bottom of the core, thus a CIRCACS sedimentation rate has been calculated to 0.77 cm/a.

RASRF_131

The 46 cm long core RASRF_131 has been collected ~ 1500 m from the next potential flood source in a pasture at an elevation of 37.73 m a.s.l.. The core shows high XS ^{210}Pb activities at the surface (7.57 DPM/$g_{(clay)}$) with a monotonically decline up to 8 cm, homogeneous levels up to 30 cm reaching background levels below. Its XS ^{210}Pb inventory is 21.82 DPM/$g_{(clay)}$ what would result in an CICCS sedimentation rate of 0.09 cm/a. It shows elevated XS ^{210}Pb activities up to the bottom of the core, thus a CIRCACS sedimentation rate has been calculated to 0.56 cm/a.

RASRF_132

The 82 cm long core RASRF_132 has been collected ~ 1000 m from the next potential flood source in an old walnut orchard at an elevation of 34.39 m a.s.l.. The core shows high XS ^{210}Pb values at the surface (3.20 DPM/$g_{(clay)}$) with a monotonically decline up to ~ 12 cm, homogeneous activities below without reaching background levels below. Its XS ^{210}Pb inventory is 31.79 DPM/$g_{(clay)}$ what would result in an CICCS sedimentation rate of 0.31 cm/a. It shows elevated XS ^{210}Pb activities up to the bottom of the core, thus a CIRCACS sedimentation rate has been calculated to 1.33 cm/a.

RASRF_133

The 79 cm long core RASRF_133 has been collected ~ 1500 m from the next potential flood source in a relatively young orchard at an elevation of 35.31 m a.s.l.. Its XS ^{210}Pb inventory is 27.68 DPM/$g_{(clay)}$ what would result in an CICCS sedimentation rate of 0.20 cm/a. It shows a slight decline in XS ^{210}Pb activites from 0 – 4 cm, a plateau of XS ^{210}Pb activities from 4 – 10 cm at around 0.8 DPM/$g_{(clay)}$, slightly lower values at 11 cm, high XS ^{210}Pb activities at 12 cm (1.9 DPM/$g_{(clay)}$) and plateau like values from 12 – 15 cm at around 0.75 DPM/$g_{(clay)}$. Below there is a slow monotonic decline thereafter without reching background activity at the bottom of the core.

RASRF_134

The 62.5 cm long core RASRF_134 has been collected ~ 1500 m from the next potential flood source in a woodland with some bushy vegetation at an elevation of 29.60 m a.s.l.. The core shows high XS ^{210}Pb values at the surface (4.64 DPM/$g_{(clay)}$) with a monotonically decline up to ~ 7 cm, homogeneous activity between 7 and 14 cm (~ 0.95 DPM/$g_{(clay)}$), and monotonic decrease from 14 – 40 cm, reaching background activity below 40 cm. Its XS ^{210}Pb inventory is 24.35 DPM/$g_{(clay)}$ what would result in an CICCS sedimentation rate of 0.17 cm/a.

RASRF_135

The 63 cm long core RASRF_135 has been collected ~ 3000 m from the next potential flood source in a forest with sparse undergrowth but some deadwood at an elevation of 30.84 m a.s.l.. The core shows high XS ^{210}Pb values at the surface with a monotonically decline up to ~ 50 cm, showing background levels below. Its XS ^{210}Pb inventory is 30.67 DPM/$g_{(clay)}$ what would result in an CICCS sedimentation rate of 0.32 cm/a.

RASRF_136

The 70.5 cm long core RASRF_136 has been collected ~ 1500 m from the next potential flood source at the in a woodland with some bushy vegetation at an elevation of 30.61 m a.s.l.. The core shows monotonically decreasing XS ^{210}Pb activities from the surface to 5 cm and homogeneous activities from 5 – 20 cm (~ 1.10 DPM/$g_{(clay)}$) with a slight decrease in activity below 21 cm. XS ^{210}Pb activity remains low (~ 0.5 DPM/$g_{(clay)}$), but never reaching background within the core. Its XS ^{210}Pb inventory is 33.98 DPM/$g_{(clay)}$ what would result in an CICCS sedimentation rate of 0.42 cm/a. It shows elevated XS ^{210}Pb activities up to the bottom of the core, thus a CIRCACS sedimentation rate has been calculated to 1.17 cm/a.

RASRF_137

The 49 cm long core RASRF_137 has been collected ~ 1000 m from the next potential flood source at the site of a major early 90s scour in an area with young trees at an elevation of 30.49 m a.s.l.. The core shows homogeneous elevated XS ^{210}Pb activities in the first 8 cm below the surface with a monotonic

decline below reaching background levels between 12 and 20 cm. Its XS ^{210}Pb inventory is 10.68 DPM/$g_{(clay)}$ what would result in an CICCS erosion rate of -0.33 cm/a. The meteoric cap has been dated to an erosion event around 1991.

RASRF_142

The 35 cm long core RASRF_142 has been collected ~ 7000 m from the next potential flood source within the westernmost of the western ephemeral channels in thick reed grass at an elevation of 29.75 m a.s.l.. The site is located downstream of a major body of standing water and heavily trotted by cattle. The core shows homogeneous XS ^{210}Pb activities from the surface to 15 cm with a decline thereafter. XS ^{210}Pb activities increase around 25 cm again without reaching background values in the core. Its XS ^{210}Pb inventory is 27.76 DPM/$g_{(clay)}$ what results in an CICCS sedimentation rate of 0.22 cm/a. It shows elevated XS ^{210}Pb activities up to the bottom of the core, thus a CIRCACS sedimentation rate has been calculated to 0.8 cm/a.

RASRF_143

The 68.5 cm long core RASRF_143 has been collected ~ 7000 m from the next potential flood source at the edge of the westernmost of the western ephemeral channels at an elevation of 31.21 m a.s.l.. The site is located downstream of a major body of standing water. The core was collected close to a couple of small trees to ensure that the site has not disturbed by agricultural activity. Its XS ^{210}Pb inventory is 11.76 DPM/$g_{(clay)}$ what would result in an CICCS erosion rate of - 0.13 cm/a.

RASRF_144

The 50 cm long core RASRF_144 has been collected ~ 7000 m from the next potential flood source within the westernmost of the western ephemeral channels in thick reed grass at an elevation of 29.70 m a.s.l.. The core shows homogeneous XS ^{210}Pb activities from the surface to 15 cm with a decline thereafter, reaching background levels between 22 and 30 cm. The site is located downstream a major body of standing water and heavily trotted by cattle. Its XS ^{210}Pb inventory is 30.96 DPM/$g_{(clay)}$ what would result in an CICCS sedimentation rate of 0.31 cm/a.

RASRF_146

The 56 cm long core RASRF_146 has been collected ~ 4000 m from the next potential flood source in a wood with bramble undergrowth at the edge of Little Chico Creek in the eastern part of the research area at an elevation of 33.54 m a.s.l.. The core shows a high XS ^{210}Pb activities at the surface with a monotonic decline up to 10 cm with homogeneous activities from 10 – 15 cm reaching background activity at 16 cm. Its XS ^{210}Pb inventory is 24.52 DPM/$g_{(clay)}$ what would result in an CICCS sedimentation rate of 0.17 cm/a.

RASRF_147

The 44.4 cm long core RASRF_147 has been collected ~ 4500 m from the next potential flood source in a non-improved pasture at the edge of Little Chico Creek at an elevation of 32.99 m a.s.l.. There are high XS ^{210}Pb activities at the top of the core (4.29 DPM/$g_{(clay)}$), a plateau from 1 – 4 cm (1.22 DPM/$g_{(clay)}$), a monotonic decline from 4 – 6 cm and a subsequent monotonic increase in XS ^{210}Pb activities from 4 – 9 cm. Below there are low XS ^{210}Pb activities, before reaching background at 11 cm. Its XS ^{210}Pb inventory is 10.53 DPM/$g_{(clay)}$ what would result in an CICCS erosion rate of - 0.15 cm/a.

RASRF_148

The 62 cm long core RASRF_148 has been collected ~ 4500 m from the next potential flood source in an elevated area at the edge of Little Chico Creek close to a large tree in an non-improved pasture at an elevation of 33.71 m a.s.l.. There is a monotonic decline in XS ^{210}Pb activitiesfrom the top of the core (4.12 DPM/$g_{(clay)}$) to 5 cm (2.95 DPM/$g_{(clay)}$), a slight increase to 7 cm (3.44 DPM/$g_{(clay)}$). From 7 – 11 cm there is a XS ^{210}Pb activity plateau at 1.6 DPM/$g_{(clay)}$. Below XS ^{210}Pb activities are monotonically declining before reaching background at 20 cm. Its XS ^{210}Pb inventory is 20.22 DPM/$g_{(clay)}$ what would result in an CICCS sedimentation rate of 0.06 cm/a.

RASRF_149

The 44.5 cm long core RASRF_149 has been collected ~ 5000 m from the next potential flood source within one of the major ephemeral channels with little vegetation at an elevation of 30.93 m a.s.l.. XS ^{210}Pb activities are monotonically declining from the top of the profile down to 11 cm. From 11 cm

XS ^{210}Pb activities stay low before reaching background at ~ 30 cm. Its XS ^{210}Pb inventory is 19.54 DPM/$g_{(clay)}$ what would result in an CICCS sedimentation rate of 0.04 cm/a.

RASRF_150

The 56 cm long core RASRF_150 has been collected ~ 5000 m from the next potential flood source at the edge of one of the major ephemeral channels with sparse bushy vegetation at an elevation of 31.69 m a.s.l.. The core shows a high XS ^{210}Pb activities at the surface with a monotonic decline up to 25 cm reaching background activities below. Its XS ^{210}Pb inventory is 28.71 DPM/$g_{(clay)}$ what would result in an CICCS sedimentation rate of 0.22 cm/a.

RASRF_151

The 52 cm long core RASRF_151 has been collected ~ 4500 m from the next potential flood source within one of the major ephemeral channels at an elevation of 31.98 m a.s.l.. The XS ^{210}Pb activity profile shows relatively low activity (2.0 dpm/$g_{(clay)}$) at the surface, high and homogeneous activity from 1 – 4 cm (~ 4.3 dpm/$g_{(clay)}$) and monotonically decreasing activities below 4 cm throughout the core. Its XS ^{210}Pb inventory is 29.99 DPM/$g_{(clay)}$ what would result in an CICCS sedimentation rate of 0.31 cm/a.

RASRF_152

The 57 cm long core RASRF_152 has been collected ~ 4500 m from the next potential flood source at the side of one of the major ephemeral channels at an elevation of 34.25 m a.s.l.. The profile shows high XS ^{210}Pb activity (7.56 dpm/$g_{(clay)}$) at the surface with a monotonic decrease to 6 cm. From 6 to 10 cm XS ^{210}Pb activities are homogeneous (~ 1.2 dpm/$g_{(clay)}$), showing a monotonic decrease from 10 to 15 cm and elevated activities (~ 0.5 dpm/$g_{(clay)}$) throughout the rest of the core. Its XS ^{210}Pb inventory is 31.06 DPM/$g_{(clay)}$ what would result in an CICCS sedimentation rate of 0.36 cm/a.

RASRF_153

The 66.5 cm long core RASRF_153 has been collected ~ 5000 m from the next potential flood source within one of the major ephemeral channels at an elevation of 31.49 m a.s.l.. The XS ^{210}Pb activity profile shows a declining

trend from the surface to 7 cm, followed by homogeneous activity from 7 to 9 cm and a monotonic decrease in activity from 9 to 15 cm. From 15 cm XS ^{210}Pb activity is very low but above background (0.2 dpm/$g_{(clay)}$) throughout the core. Its XS ^{210}Pb inventory is 27.94 DPM/$g_{(clay)}$ what would result in an CICCS sedimentation rate of 0.25 cm/a. It shows elevated XS ^{210}Pb activities up to the bottom of the core, thus a CIRCACS sedimentation rate has been calculated to 0.93 cm/a.

RASRF_154

The 68 cm long core RASRF_154 has been collected ~ 5000 m from the next potential flood source at the side of one of the major ephemeral channels at an elevation of 34.21 m a.s.l.. The core shows a high XS ^{210}Pb activity (4.12 dpm/$g_{(clay)}$) at the surface with a monotonic decline up to 60 cm with background activities below. Its XS ^{210}Pb inventory is 40.37 DPM/$g_{(clay)}$ what would result in an CICCS sedimentation rate of 0.72 cm/a.

RASRF_155

The 66 cm long core RASRF_155 has been collected ~ 5500 m from the next potential flood source in a low position in an undulating part of the floodplain ~ 10 m from Little Chico Creek / Angle Slough with large trees and thick undergrowth an elevation of 32.90 m a.s.l.. The profile shows high XS ^{210}Pb activities at the surface (5.19 dpm/$g_{(clay)}$) monotonically decreasing to 8 cm, followed by an increase in activity (8 - 10 cm). XS ^{210}Pb activity decreases monotonically from 10 to 16 cm. From 16 to 19 cm XS ^{210}Pb activities are variable. XS ^{210}Pb activity shows a monotonic decrease from 19 to 23 cm, an increase from 23 to 26 cm and a monotonic decrease from 26 to 30 cm. Below 31 cm XS ^{210}Pb activities remain variable. Its XS ^{210}Pb inventory is 27.12 DPM/$g_{(clay)}$ what would result in an CICCS sedimentation rate of 0.13 cm/a.

RASRF_156

The 63 cm long core RASRF_156 has been collected ~ 5500 m from the next potential flood source in an elevated position in an undulating part of the floodplain ~ 10 m from Little Chico Creek / Angle Slough with large trees and thick undergrowth at an elevation of 33.34 m a.s.l.. The profile shows elevated XS ^{210}Pb activity at the surface (2.8 dpm/$g_{(clay)}$) followed by a monotonic decline

to 3 cm. At 3 cm there is a slight increase in activity followed by a monotonic decline up to 40 cm, reaching background thereafter. Its XS ^{210}Pb inventory is 22.42 DPM/$g_{(clay)}$ what would result in an CICCS sedimentation rate of 0.13 cm/a.

RASRF_157

The 38 cm long core RASRF_157 has been collected ~ 3500 m from the next potential flood source at the shoulder of an ephemeral channel in an unimproved pasture an elevation of 30.03 m a.s.l.. The core shows a high XS ^{210}Pb activity at the surface (4.56 dpm/$g_{(clay)}$) with a monotonic decline up to 13 cm reaching background activities between 13 and 20 cm. Its XS ^{210}Pb inventory is 8.33 DPM/$g_{(clay)}$ what would result in an CICCS erosion rate of -0.18 cm/a.

RASRF_158

The 61 cm long core RASRF_158 has been collected ~ 3500 m from the next potential flood source at the bottom of an ephemeral channel in an unimproved pasture at an elevation of 29.47 m a.s.l.. The core shows a high XS ^{210}Pb activity at the surface (6.44 dpm/$g_{(clay)}$) with a monotonic decline up to 2 cm with background activities below. Its XS ^{210}Pb inventory is calculated to 8.26 DPM/$g_{(clay)}$ what would result in an CICCS erosion rate of - 0.13 cm/a.

RASRF_159

The 26 cm long core RASRF_159 has been collected ~ 800 m from the next potential flood source on a point bar of a former meander of the Sacramento River main stem that has been abandoned between 1960 and 1964 at an elevation of 30.76 m a.s.l.. It shows high XS ^{210}Pb activity at the surface (8.60 dpm/$g_{(clay)}$) and a monotonic decrease in activity up to 4 cm. At 4 cm the XS ^{210}Pb increases and shows a monotonic decrease from 4 to 9 cm. Below 9 cm the core shows low, but varying XS ^{210}Pb activities throughout the rest of the profile. Its XS ^{210}Pb inventory is 21.24 DPM/$g_{(clay)}$ what would result in an CICCS sedimentation rate of 0.09 cm/a. It shows elevated XS ^{210}Pb activities up to the bottom of the core, thus a CIRCACS sedimentation rate has been calculated to 0.5 cm/a.

RASRF_160

The 50 cm long core RASRF_160 has been collected ~ 700 m from the next potential flood source in the Holocene meander belt at an elevation of 32.09 m a.s.l.. The core shows a high XS ^{210}Pb activity at the surface (5.56 dpm/$g_{(clay)}$) with a monotonic decline up to 12 cm reaching background activities between 12 and 20 cm. Its XS ^{210}Pb inventory is 15.79 DPM/$g_{(clay)}$ what would result in an CICCS erosion rate of - 0.06 cm/a.

RASRF_161

The 55 cm long core RASRF_161 has been collected ~ 5000 m from the next potential flood source at the bottom of an ephemeral channel with some bushy undergrowth at an elevation of 31.11 m a.s.l.. The XS ^{210}Pb activity profile is highly variable from 0 - 8 cm with a monotonic decline from 8 – 15 cm reaching background activities between 21 and 25 cm. Its XS ^{210}Pb inventory is 21.27 DPM/$g_{(clay)}$ what would result in an CICCS sedimentation rate of 0.07 cm/a.

RASRF_162

The 40.5 cm long core RASRF_162 has been collected ~ 5000 m from the next potential flood source at the flank of an ephemeral channel with slight bushy undergrowth, and some brambles at an elevation of 32.61 m a.s.l.. The profile shows a monotonic decrease in XS ^{210}Pb activity from 0 to 6 cm, homogeneous XS ^{210}Pb activities from 6 to 10 cm, a monotonic decrease in activities from 10 to 15 cm and low XS ^{210}Pb activities below 15 cm, reaching background at ~ 30 cm. Its XS ^{210}Pb inventory is 19.83 DPM/$g_{(clay)}$ what would result in an CICCS sedimentation rate of 0.06 cm/a.

RASRF_163

The 61 cm long core RASRF_163 has been collected ~ 3000 m from the next potential flood source at the bottom of an ephemeral channel with little bushy undergrowth at an elevation of 33.01 m a.s.l.. The site is located downstream of a road bridge. The core shows a high XS ^{210}Pb activities at the surface with a monotonic decline up to 9 cm with background activities below. Its XS ^{210}Pb inventory is 9.91 DPM/$g_{(clay)}$ what would result in an CICCS erosion rate of - 0.17 cm/a.

RASRF_165

The 40 cm long core RASRF_165 has been collected ~ 2500 m from the next potential flood source at the bottom of an ephemeral channel with low grass vegetation at an elevation of 32.29 m a.s.l.. The site is located downstream of a road bridge. The XS ^{210}Pb profile shows low and homogeneous activities from 0 to 4 cm, an increase at 4 cm and a monotonic decrease thereafter, reaching background between 20 and 25 cm. Its XS ^{210}Pb inventory is 8.21 DPM/g$_{(clay)}$ what would result in an CICCS erosion rate of -0.17 cm/a.

RASRF_166

The 66 cm long core RASRF_166 has been collected ~ 3000 m from the next potential flood source on an elevated grassland within the western ephemeral channels at an elevation of 35.15 m a.s.l.. It shows moderate XS ^{210}Pb activity at the surface, an increase in activity at 3 cm and a monotonic decline in activities below 3 cm, reaching background activities at 24 cm. Its XS ^{210}Pb inventory is 19.16 DPM/g$_{(clay)}$ what would result in an CICCS sedimentation rate of 0.03 cm/a.

RASRF_167

The 24 cm long core RASRF_167 has been collected ~ 3000 m from the next potential flood source within one of the channels that was densely vegetated by trees and bushed in the western ephemeral channel system. The core was collected close to a large bush with fresh sedimentation visible around its roots at an elevation of 31.95 m a.s.l.. The XS ^{210}Pb profile shows highly variable activities from 0 – 6 cm, a monotonic decline in XS ^{210}Pb activities from 6 – 14 cm and homogeneous activities from 14 cm to the bottom of the core at 24 cm. Its XS ^{210}Pb inventory is 20.32 DPM/g$_{(clay)}$ what would result in an CICCS sedimentation rate of 0.07 cm/a. It shows elevated XS ^{210}Pb activities up to the bottom of the core, thus a CIRCACS sedimentation rate has been calculated to 0.63 cm/a.

RASRF_168

The 63 cm long core RASRF_168 has been collected ~ 3000 m from the next potential flood source at the edge of a channel of the western ephemeral

channel system at an elevation of 35.49 m a.s.l.. The XS ^{210}Pb profile shows a monotonic decline from the surface to 8 cm, homogeneous XS ^{210}Pb activities between 8 and 12 cm and between 14 and 26 cm before reaching background level at 30 cm. Its XS ^{210}Pb inventory is 22.03 DPM/$g_{(clay)}$ what would result in an CICCS sedimentation rate of 0.13 cm/a.

RASRF_169

The 56 cm long core RASRF_169 has been collected ~ 3000 m from the next potential flood source at the edge of a channel in the western ephemeral channel system at an elevation of 35.60 m a.s.l.. The XS ^{210}Pb activity profile shows low values for the first 1 cm, two clearly visible meteoric fallout caps below (1 – 7 cm, 7 – 12 cm). Below the 2nd meteoric cap there are homogeneous XS ^{210}Pb activities from 11 – 18 cm. Below XS ^{210}Pb activities stay elevated throughout the core, reaching background levels just at the very bottom at 55 cm. Its XS ^{210}Pb inventory is 24.00 DPM/$g_{(clay)}$ what would result in an CICCS sedimentation rate of 0.26 cm/a.

7. REFERENCES

A

Aalto, R. E. & Dietrich, W. E., (2005). Sediment accumulation determined with 210Pb geochronology for Strickland River flood plains, Papua New Guinea. Sediment Budgets I, pp.303–309.

Aalto, R. E. & Nittrouer, C. A., (2012). 210Pb geochronology of flood events in large tropical river systems. Philosophical Transactions of the Royal Society A: Mathematical, Physical and Engineering Sciences, 370(1966), pp.2040–2074.

Aalto, R. E., Maurice-Bourgoin, L., Dunne, T., Montgomery, D. R., Nittrouer, C. A., & Guyot, J. L., (2003). Episodic sediment accumulation on Amazonian flood plains influenced by El Nino/Southern Oscillation. Nature, 425(6957), pp.493–497.

Aalto, R. E., Lauer, J. W. & Dietrich, W. E., (2008). Spatial and temporal dynamics of sediment accumulation and exchange along Strickland River floodplains (Papua New Guinea) over decadal-to-centennial timescales. Journal of Geophysical Research, 113, F01S04.

Adam, D. P. & West, G. J., (1983). Temperature and precipitation estimates through the last glacial cycle from Clear Lake, California, pollen data. Science, 219(4581), pp.168–170.

Aitken, M. J. (1998). Introduction to Optical Dating: The Dating of Quaternary Sediments by the Use of Photon-stimulated Luminescence. Oxford University Press.

Allison, M. A., Kuehl, S. A., Martin, T. C., & Hassan, A. (1998). Importance of flood-plain sedimentation for river sediment budgets and terrigenous input to the oceans: Insights from the Brahmaputra-Jamuna River. Geology, 26, pp.175–178.

Anders, M. D., Pederson, J. L., Rittenour, T. M., Sharp, W. D., Gosse, J. C., Karlstrom, K. E., Crossey, L. J., Goble, R. J., Stockli, L., & Yang, G., (2005). Pleistocene geomorphology and geochronology of eastern Grand Canyon: linkages of landscape components during climate changes. Quaternary Science Reviews, 24, pp.2428–2448.

Appleby, P. G., (2008). Three decades of dating recent sediments by fallout radionuclides: a review. The Holocene, 18(1), pp.83–93.

Arcement, G. J. & Schneider, V. R., (1989). Guide for Selecting Manning's Roughness Coefficients for Natural Channels and Flood Plains. U.S. Geological Survey Water-Supply Paper 2339. 67 p.

Arnold J. R. & Libby, W. F., (1949). Age Determinations by Radiocarbon Content – Checks with Samples of Known Age. Science, 110, pp.678-680.

Aslan, A. & Autin, W. J., (1999). Evolution of the Holocene Mississippi River floodplain, Ferriday, Louisiana: insights on the origin of fine-grained floodplains. Journal of Sedimentary Research, 69(4), pp.800–815.

Aslan, A., Autin, W. J. & Blum, M. D., (2005). Causes of River Avulsion: Insights from the Late Holocene Avulsion History of the Mississippi River, U.S.A. Journal of Sedimentary Research, 75(4), pp.650–664.

Aslani, M. A. A., Akyil, S., Aytas, S., Gurboga, G. & Eral, M., (2005). Activity concentration of ^{210}Pb (^{210}Po) in soils taken from cultivated lands. Radiation Measurements. 39(2), pp.139-135.

B

Bacon, S. N., Burke, R. M., Pezzopane, S. K. & Jayko, A. S., (2006). Last glacial maximum and Holocene lake levels of Owens Lake, eastern California, USA. Quaternary Science Reviews, 25(11-12), pp.1264–1282.

Bard, E., Hamelin, B., Fairbanks, R. G., & Zindler, A., (1990). Calibration of the 14C timescale over the past 30,000 years using mass spectrometric U-Th ages from Barbados corals. Nature, 345, pp.406–410.

Barron, J. A., Heusser, L., Herbert, T., & Lyle, M., (2003). High-resolution climatic evolution of coastal northern California during the past 16,000 years. Paleoceanography, 18(1), 1020. doi:10.1029/2002PA000768

Bartlein, P. J., Anderson, K. H., Anderson, P. M., Edwards, M. E., Mock, C. J., Thompson, R. S., Webb, R. S., Webb III, T., & Whitlock, C. (1998). Paleoclimate simulations for North America over the past 21,000 years features of the simulated climate and comparisons with paleoenvironmental data. Quaternary Science Reviews, 17(6-7), pp.549–585.

Bateman, J. C., & Wahrhaftig, C., (1966). Geology of the Sierra Nevada. California Division of Mines and Geology, Bulletin, 190, pp.107-172.

Benmansour, M., Mabit, L., Nouira, A., Moussadek, R., Bouksirate, H., Duchemin, M., & Benkdad, A., (2013). Assessment of soil erosion and deposition rates in a Moroccan agricultural field using fallout ^{137}Cs and $^{210}Pb_{ex}$. Journal of Environmental Radioactivity, 115, pp.97–106.

Benson, L., Kashgarian, M., Rye, R., Lund, S., Paillet, F., Smoot, J., Kesler, C., Mensing, S., Meko, D., & Lindström, S. (2002). Holocene multidecadal and multicentennial droughts affecting Northern California and Nevada. Quaternary Science Reviews, 21(4-6), pp.659–682.

Benson, L., Kashgarian, M. & Rubin, M., (1995). Carbonate deposition, Pyramid Lake subbasin, Nevada: 2. Lake levels and polar jet stream positions reconstructed from radiocarbon ages and elevations of carbonates (tufas) deposited in the Lahontan basin. Palaeogeography, Palaeoclimatology, Palaeoecology, 117(1-2), pp.1–30.

Benson, M. A. & Dalrymple, T., (1967). General field and office procedures for indirect discharge measurements: U.S. Geological Survey Techniques of Water-Resources Investigations, book 3, chap. A1, 30 p.

Blodgett, J. C., & Stiehr, P. L. (1974): Hydraulic analysis of floodflows in Butte Basin at State Highway 162, Glenn and Butte Counties, California. U.S. Geological Survey Open File Report 74 – 198, 48 p.

Blum, M., Martin, J., Milliken, K., & Garvin, M., (2013). Paleovalley systems: Insights from Quaternary analogs and experiments. Earth Science Reviews, 116(C), pp.128–169.

Blum, M. D. & Aslan, A., (2006). Signatures of climate vs. sea-level change within incised valley-fill successions: Quaternary examples from the Texas Gulf Coast. Sedimentary Geology, 190(1), pp.177–211.

Blum, M. D. & Törnqvist, T. E., (2000). Fluvial responses to climate and sea-level change: a review and look forward. Sedimentology, 47(s1), pp.2–48.

Blum, M. D. & Valastro, Jr, S., (1994). Late Quaternary sedimentation, lower Colorado River, Gulf Coastal Plain of Texas. Geological Society of America Bulletin, 106(8), pp.1002–1016.

Boenigk, W. & Frechen, M., (2006). The Pliocene and Quaternary fluvial archives of the Rhine system. Quaternary Science Reviews, 25(5-6), pp.550–574.

Bradbury, J. P., (1992). Late Cenozoic lacustrine and climatic environments at Tule Lake, northern Great Basin, USA. Climate Dynamics, 6(3-4), pp.275–285.

Bradbury, J. P., Colman, S. M. & Dean, W. E., (2004). Limnological and climatic environments at Upper Klamath Lake, Oregon during the past 45 000 years. Journal of Paleolimnology, 31(2), pp.167–188.

Brathauer, U., Brauer, A., Negendank, J. F. W., Zolitschka, B., (1999). Rasche Klimaänderungen am Beginn der heutigen Warmzeit. Zweijahresbericht, Geo Forschungs Zentrum, Potsdam, pp.29–33.

Brice, J., (1977). Lateral Migration of the Middle Sacramento River, California. U.S. Geological Survey Water-Resources Investigations 77-43. 51 p.

Bridgland, D. & Westaway, R., (2008). Climatically controlled river terrace staircases: a worldwide Quaternary phenomenon. Geomorphology, 98(3-4), pp.285–315.

C

Cabezas, Á., Angulo-Martínez, M., González-Sanchis, M., Jiménez, J. J., & Comín, F. A., (2010). Spatial variability in floodplain sedimentation: the use of generalized linear mixed-effects models. Hydrology and Earth System Sciences, 14(8), pp.1655–1668.

Cammeraat, C., van Beek, R. & Kooijman, A., (2005). Vegetation succession and its consequences for slope stability in SE Spain. Plant and Soil, 278(1), pp.135-147.

Caroll, J. & Lerche, I., edt. (2003). Sedimentary Processes: Quantification Using Radionuclides. Elsevier, Qxford, 272 p.

Chambers, J. M., Cleveland, W. S., Kleiner, B. & Tukey, P. A. (1983). Graphical Methods for Data Analysis. Duxbury Press, Boston, 336 p.

Chorley, R. J., (1962). Geomorphology and General Systems Theory, U.S. Geological Survey Professional Paper 500-1B, 14 p.

Chow, V. T., (1959). Open-channel hydraulics. McGraw-Hill, New York, 680 p.

Church, M., (2006). Bed material transport and the morphology of alluvial river channels. Annu. Rev. Earth Planet. Sci., 34, pp.325–354.

Clark, P. U. & Bartlein, P. J., (1995). Correlation of late Pleistocene glaciation in the western United States with North Atlantic Heinrich events. Geology, 23(6), pp.483–486.

Constantine, J. A. & Dunne, T., (2008). Meander cutoff and the controls on the production of oxbow lakes. Geology, 36(1), pp.23–26.

Constantine, J. A., McLean, S. R. & Dunne, T., (2010). A mechanism of chute cutoff along large meandering rivers with uniform floodplain topography. Geological Society of America Bulletin, 122(5-6), pp.855–869.

Cowen, W. L. (1956): Estimating hydraulic roughness coefficients: Agricultural Engineering, 37(7), pp.473–475.

Culling, W. E. H. (1957). Multicyle streams and the equilibrium theory of grade, Journal of Geology, 65, pp.259–274.

CVJV (2013). Central Valley Joined Venture http://www.centralvalleyjointventure.org/our-history/archives/news/cvjv-flagship-project-llano-seco-rancho- (Last accessed 15.02.2015).

D

Damnati, B., Ibrahimi, S. & Radakovitch, O., (2013). Quantifying erosion using 137Cs and 210Pb in cultivated soils in three Mediterranean watershed: Synthesis study from El Hachef, Raouz and Nakhla (North West Morocco). Journal of African Earth Sciences, 79, pp.50–57.

Daniels, M. L., Anderson, R. S. & Whitlock, C., (2005). Vegetation and fire history since the Late Pleistocene from the Trinity Mountains, northwestern California, USA. Holocene, 15(7), pp.1062–1071.

Dansgaard, W., Johnsen, S. J., Clausen, H. B., Dahl-Jensen, D., Gundestrup, N. S., Hammer, C. U., Hvidberg, C. S., Steffensen, J. P. Sveinbjörnsdottir, A. E., Jouzel, J., & Bond, G., (1993). Evidence for general instability of past climate from a 250-kyr ice-core record. Nature, 364, pp.218–220.

Davis, L. G., (2006). Geoarchaeological insights from Indian Sands, a Late Pleistocene site on the southern northwest coast, USA. Geoarchaeology, 21(4), pp.351–361.

Day, G., Dietrich, W. E., Rowland, J. E., & Marshall, A., (2008). The depositional web on the floodplain of the Fly River, Papua New Guinea. Journal of Geophysical Research, 113, F01S02.

Dettinger, M. D., (2004). Fifty-Two Years of Pineapple-Express Storms across the West Coast of North America; California Energy Commission PIER Energy-Related Environmental Research Report CEC-500-2005-004; California Energy Commission: Sacramento, CA, USA, 2004, 15 p.

Dettinger, M. D., (2011), Climate Change, Atmospheric Rivers, and Floods in California - A Multimodel Analysis of Storm Frequency and Magnitude

Changes. JAWRA Journal of the American Water Resources Association, 47(3), pp.514–523.

Dietrich, W. E., Day, G. & Parker, G., (1999). The Fly River, Papua New Guinea: inferences about river dynamics, floodplain sedimentation, and fate of sediment. In A. J. Miller & A. Gupta, eds. Varieties in Fluvial Form. New York: John Wiley, pp.345–376.

Doering, C., Akber, R. & Heijnis, H., (2006). Vertical distributions of ^{210}Pb excess, ^{7}Be and ^{137}Cs in selected grass covered soils in Southeast Queensland, Australia. J. Environ. Radioact. 87, pp.135–147.

Dorr H. & Munnich K. O., (1989). Downward movement of soil organic matter and its influence on trace-element transport (210-Pb, 137-Cs) in the soil. Radiocarbon, 31, pp.655–663.

Dreibrodt, S., Lomax, J., Nelle, O., Lubos, C., Fischer, P., Mitusov, A., Reiss, S., Radtke, U., Nadeau, M., Grootes, P. M., Bork, H.-R., (2010). Are mid-latitude slopes sensitive to climatic oscillations? Implications from an Early Holocene sequence of slope deposits and buried soils from eastern Germany. Geomorphology. 122, pp.351-369.

Dunne, T. & Aalto, R. E., (2013). Large River Floodplains. In J. F. Shroder, ed. Treatise on Geomorphology. San Diego: Academic Press, pp.645–678.

Dunne, T., Mertes, L. A. K., Meade, R. H., Richey, J. E. & Forsberg, B. R., (1998). Exchanges of sediment between the flood plain and channel of the Amazon River in Brazil. Geological Society of America Bulletin, 110, pp.450–467.

Dyke, A. S., (2004). An outline of North American deglaciation with emphasis on central and northern Canada. In J. Ehlers & P. L. Gibbard, eds. Quaternary Glaciations-Extent and Chronology, Part II: North America. Amsterdam: Elsevier, pp.373–424.

E

Ehlers, J., Gibbard, P. L., Huges, P. D., (edt.) (2011). Quaternary Glaciations - Extent and Chronology A Closer Look. Developments in Quaternary Sciences, 15, 1108 p.

F

Fairbanks, R. G., Mortlock, R. A., Chui, T.-C., Cao, L, Kaplan, A, Guilderson, T. P., Fairbanks, T. W., Bloom, A. L., Grootes, P. M., Nadeau, M.-J. (2005): Radiocarbon calibration curve spanning 0 to 50,000 years BP based on paired 230Th/234U/238U and 14C dates on pristine corals. Quaternary Science Reviews, 24, pp.1781-1796.

FEMA map, http://msc.fema.gov/portal

Fisher, K. J., (1994). Fluvial geomorphology and flood control strategies: Sacramento River, California. In: Schumm, S. A. & Winkley, B. R. (eds.). The variability of large alluvial rivers. New York: ASCE Press, pp.115–138.

Fischer, M., (2009). Arbeitsanweisungen für das Lumineszenzlabor. Unpublished laboratory notes. 19 p.

Fuchs, M. & Lang, A., (2001). OSL dating of coarse-grain fluvial quartz using single-aliquot protocols on sediments from NE Peloponnese, Greece. Quaternary Science Reviews, 20, pp.783–787.

Fuchs, M. & Wagner, G., (2003). Recognition of insufficient bleaching by small aliquots of quartz for reconstructing soil erosion in Greece. Quaternary Science Reviews, 22(10-13), pp.1161–1167.

Fuchs, M., Will, M., Kunert, E., Kreutzer, S., Fischer, M., & Reverman, R., (2011). The temporal and spatial quantification of Holocene sediment dynamics in a meso-scale catchment in northern Bavaria, Germany. The Holocene, 21(7), pp.1093–1104.

Fuchs, M., Fischer, M. & Reverman, R., (2010). Colluvial and alluvial sediment archives temporally resolved by OSL dating: Implications for reconstructing soil erosion. Quaternary Geochronology, 5(2-3), pp.269–273.

G

Garvin, M., (2008). Late Quaternary Geochronologic, Stratigraphic, and Sedimentologic Framework of the Trinity River Incised Valley, East Texas Coast. Unpublished Masters Thesis, Louisiana State University.

Gaspar, L., Nava, A., Walling, D. E., Machín, J., Gómez Arozamena, J., (2013). Using ^{137}Cs and $^{210}Pb_{ex}$ to assess soil redistribution on slopes at different temporal scales. Catena, 102, pp.46–54.

Gilbert, G.K., (1917). Hydraulic mining debris in the Sierra Nevada. U.S. Geological Survey Professional Paper 105.

Gillespie, A. & Zehfuss, P., (2004). Glaciations of the Sierra Nevada, California, USA. Developments in Quaternary Sciences, 2, pp.51–62.

Goldberg, D. E., (1963). Geochronology with lead-210. In: Radioactive dating. I.A.E.A. Vienna. pp.121-131

Goodbred, Jr., S. L., & Kuehl, S. A., (1998). Floodplain processes in the Bengal Basin and the storage of Ganges-Brahmaputra river sediment: an accretion study using 137Cs and 210Pb geochronology. Sedimentary Geology, (121), pp.239–258.

Goodwin, H. (1962): Half-Life of Radiocarbon. – Nature, 195: 984.

Greco, S. E. & Alford, C. A., (2003a). Historical Channel Mapping of the Sacramento River from Historical Maps, Colusa to Red Bluff, California: 1870 - 1920. Technical Report prepared for California Department of Water Resources, Northern District, Red Bluff, California. Landscape Analysis and Systems Research Laboratory, Department of Environmental Design, University of California.

Greco, S. E. & Alford, C. A., (2003b). Historical Channel Mapping of the Sacramento River from Historical Maps, Colusa to Red Bluff, California: 1937 - 1997. Technical Report prepared for California Department of Water Resources, Northern District, Red Bluff, California. Landscape Analysis and Systems Research Laboratory, Department of Environmental Design, University of California.

Grigg, L. D. & Whitlock, C., (1998). Late-Glacial Vegetation and Climate Change in Western Oregon. Quaternary Research, 49(3), pp.287–298.

Grigg, L. D., Whitlock, C. & Dean, W. E., (2001). Evidence for Millennial-Scale Climate Change During Marine Isotope Stages 2 and 3 at Little Lake, Western Oregon, U.S.A. Quaternary Research, 56(1), pp.10–22.

H

Haines-Young, R. H., & Petch, J. R., (1983). Multiple working hypotheses: equifinality and the study of landforms, Transactions of the Institute of British Geographers, 8, pp.458–466.

Hajdas, I., (2008). Radiocarbon dating and its applications in Quaternary studies. Eiszeitalter und Gegenwart Quaternary Science Journal, 57(1-2), pp.2–24.

Hajdas, I., (2009). Applications of radiocarbon dating method. Radiocarbon, 51(1), pp.79-90.

Hajdas, I., Ivy, S. D., Beer, J., Bonani, G., Imboden, D., Lotter, A. F., Sturm, M. & Suter, M., (1993). AMS radiocarbon dating and varve chronology of Lake Soppensee: 6000 to 12000 14C years BP. Climate Dynamics, 9(3), pp.107–116.

Hakala, K. J. & Adam, D. P., (2004). Late Pleistocene Vegetation and Climate in the Southern Cascade Range and the Modoc Plateau Region. Journal of Paleolimnology, 31(2), pp.189–215.

Harmon, J. G., (1994). Flood data for the Sacramento River and Butte Basin, Sacramento Valley, California, 1980-90. US-Geological Survey. Open-File Report 93-68. 30 p.

Harvey, A. M., (2002). Effective timescales of coupling within fluvial systems. Geormorphology, 44, pp.175–201.

Harvey, E. N., (1957). A history of luminescence. Memoirs of the American Philosophical Society, 44, pp.1–351.

Harwood, D. S. & Helley, E. J., (1987). Late Cenozoic tectonism of the Sacramento Valley, California. U.S. Geological Survey Professional Paper 1359.

Harwood, D. S. & Helley, E. J., (1982). Preliminary structure contour map of the Sacramento Valley, California showing major late cenezoic structural features and depth to basement. U.S. Geological Survey Open-File Report 82-737.

He, Q. & Walling, D. E., (1996). Interpreting particle size effects in the adsorption of 137Cs and unsupported 210Pb by mineral soils and sediments. Journal of Environmental Radioactivity, 30(2), pp.117–137.

He, Q., Walling, D.E., (1996b). Use fallout Pb-210 measurements to investigate longer-term rates and patterns of overbank sediment deposition on the floodplains of lowland rivers. Earth and Surface Processes and Landforms, 21, pp.141–154.

He, Q. & Walling, D. E., (1997). The distribution of fallout 137Cs and 210Pb in undisturbed and cultivated soils. Applied Radiation and Isotopes, 48(5), pp.677–690.

Helley, E. J. & Harwood, D. S., (1985). Geologic Map of the Late Cenozoic deposits of the Sacramento Valley and northern Sierra Nevada Foodhills, California. U.S. Geological Survey Miscellaneous Field Studies Map MF–1790, 24 p. scale 1:62,500.

Helley EJ and C Jaworowski. 1985. The Red Bluff pediment, a datum plane for locating Quaternary structures in the Sacramento Valley, California. U.S. Geological Survey Bulletin 1628. 13 p.

Henderson F. M., (1963). Stability of alluvial channels. Trans Am Soc Civ Eng 128, pp.657–686.

Herbert, T. D., Schuffert, J. D., Andreasen, D., Heusser, L., Lyle, M, Mix, A., Ravelo, A. C., Stott, L. D., Herguera, J. D., (2001). Collapse of the California Current During Glacial Maxima Linked to Climate Change on Land. Science, 293(5527), pp.71–76.

Higgins, R. W., Schemm, J. K. E., Shi, W., Leetmaa, A., (2000). Extreme precipitation events in the western United States related to tropical forcing. J. Climate, 13, pp.793–820.

Houben, P., (2007). Geomorphological facies reconstruction of Late Quaternary alluvia by the application of fluvial architecture concepts. Geomorphology, 86(1-2), pp.94–114.

Houben, P., (2003). Spatio-temporally variable response of fluvial systems to Late Pleistocene climate change: a case study from central Germany. Quaternary Science Reviews, 22(20), pp.2125–2140.

Hudson, P. F. & Colditz, R. R., (2003). Flood delineation in a large and complex alluvial valley, lower Pánuco basin, Mexico. Journal of Hydrology, 280(1-4), pp.229–245.

Huijzer, A. S. & Vandenberghe, J., (1998). Climatic reconstruction of the Weichselian Pleniglacial in north-western and central Europe. Journal of Quaternary Science, 13, pp.391–417.

Huisink, M., (2000). Changing river styles in response to Weichselian climate changes in the Vecht valley, eastern Netherlands. Sedimentary Geology, 133(1-2), pp.115–134.

Huisink, M., (1997). Late-glacial sedimentological and morphological changes in a lowland river in response to climatic change: the Maas, southern Netherlands. Journal of Quaternary Science, 12(3), pp.209–223.

Huntley, D. J., Godfrey-Smith, D. I. & Thewalt, M. L. W. (1985). Optical dating of sediments. Nature, 313, pp.105–107.

I

Ibarra, D. E., Egger, A. E., Weaver, K. L., Harris, C. R. & Maher, K., (2014): Rise and fall of late Pleistocene pluvial lakes in response to reduced evaporation and precipitation: Evidence from Lake Surprise, California. Geological Society of America Bulletin; 126(11-12), pp.1387–1415.

Ingram, B. L. & Lin, J. C., (2002). Geochemical tracers of sediment sources to San Francisco Bay. Geology, 30(6), pp.575–578.

J

Jain, M. & Tandon, S. K., (2003). Fluvial response to Late Quaternary climate changes, western India. Quaternary Science Reviews, 22(20), pp.2223–2235.

James, L. A., (1991). Incision and morphologic evolution of an alluvial channel recovering from hydraulic mining sediment. Geological Society of America Bulletin, 103(6), pp.723–736.

James, L. A., Harbor, J., Fabel, D., Dahms, D., & Elmore, D., (2002). Late Pleistocene glaciations in the northwestern Sierra Nevada, California. Quaternary Research, 57(3), pp.409–419.

Jenkins, O. P., (1938). Geomorphic Map of California. (1:2000000).

Jostes, B. D., (1972). John Parrott, Consul, 1811–1884; Selected Papers of a Western Pioneer, San Francisco, CA.

Julien, P. Y., (2010). Erosion and Sedimentation. New York. Cambridge University Press. 2nd ed., 371 p.

K

Kasse, C., Hoek, W. Z., Bohncke, S. J. P., Konert, M., Weijers, J. W. H., Cassee, M. L., & Van der Zee, R. M., (2005). Late Glacial fluvial response of the Niers-Rhine (western Germany) to climate and vegetation change. Journal of Quaternary Science, 20(4), pp.377–394.

Kato, H., Onda, Y. & Tanaka, Y., (2010). Using ^{137}Cs and $^{210}Pb_{ex}$ measurements to estimate soil redistribution rates on semi-arid grassland in Mongolia. Geomorphology, 114(4), pp.508–519.

Kesel, R. H., (2008). A revised Holocene geochronology for the Lower Mississippi valley. Geomorphology, 101(1-2), pp.78–89.

Kim, S.-J., Crowley, T. J., Erickson, D. J., Govindasamy, B., Duffy, P. B., & Lee, B. Y., (2008). High-resolution climate simulation of the last glacial maximum. Climate Dynamics, 31(1), pp.1–16.

Knighton, A. D., & Nanson, G. C. (1993). Anastomosis and the continuum of channel pattern. Earth Surf. Process. Landforms, 18, pp.613–625.

Knox, J. C., (1995). Fluvial systems since 20,000 yrs BP. In K. J. Gregory, L. Starkel, & V. R. Baker, eds. Global Continental Palaeohydrology. John Wiley & Sons (Chichester), pp.87–108.

Knox, J. C., (1996). Late Quaternary Upper Mississippi River alluvial episodes and their significance to the Lower Mississippi River system. Engineering geology, 45, pp.263–285.

Koide, M., Soutar, A, & Goldberg, E. D., (1972). Marine geochronology with 210Pb. Earth and Planetary Science Letters, 14, pp.442–446.

Kreutzer, S., Schmidt, C., Fuchs, M. C., Dietze, M., Fischer, M., & Fuchs, M. (2012). Introducing an R package for luminescence dating analysis. Ancient TL, 30(1), pp.1–8.

Krishnaswami, S., Lal, D., Martin, J. M., & Meybeck, M., (1971). Geochronology of Lake Sediments. Earth and Planetary Science Letters, 11, pp.407–414.

Kulig, G., (2005). Erstellung einer Auswertesoftware zur Altersbestimmung mittels Lumineszenzverfahren unter spezieller Beru¨cksichtigung des Einflusses radio- aktiver Ungleichgewichte in der 238U-Zerfallsreihe. Unpublished BSc thesis. Technical University Bergakademie Freiberg.

L

Lane E. W., (1957). A study of the shape of channels formed by natural streams flowing in erodible material. United States Army Engineer Division, Missouri River Division, Corps of Engineers, Omaha.

Larsen, E. W., (2007). Sacramento River Ecological Flows Study: Meander Migration Modeling Final Report. Prepared for The Nature Conservancy, Chico, CA. Davis, CA.

Larsen, E. W., and S. E. Greco. 2002. Modeling channel management impacts on river migration: A case study of Woodson Bridge State Recreation Area, Sacramento River, California, USA. Environmental Management, 30, pp.209–224.

Larsen, E. W., Fremier, A. K. & Girvetz, E. H., (2006), Modeling the effects of variable annual flow on river channel meander migration patterns, Sacramento River, California, USA. JAWRA Journal of the American Water Resources Association, 42, pp.1063–1075.

Larsen, E. W., Girvetz, E. H. & Fremier, A. K. (2006)b, Assessing the Effects of Alternative Setback Channel Constraint Scenarios Employing a River Meander Migration Model. Environmental Management, 37(6), pp.880–897.

Larsen, W. E., Anderson, E., Avery, E. & Dole, K., (2002). The controls on and evolution of channel morphology of the Sacramento River: A case study of River Miles 201-185, Davis: Report to the Nature Conservancy.

Leigh, D. S., (2008). Late Quaternary climates and river channels of the Atlantic Coastal Plain, Southeastern USA. Geomorphology, 101(1-2), pp.90–108.

Leigh, D. S., (2006). Terminal Pleistocene braided to meandering transition in rivers of the Southeastern USA. Catena, 66(1-2), pp.155–160.

Leopold, L.B. and Wolman, M.G., (1957). River channel pattern: braided, meandering and straight. U.S. Geological Survey Professional Papers, 282, pp.1–84.

Lian, O. B. & Hickin, E. J., (1996). Early Postglacial Sedimentation of Lower Seymour Valley, Southwestern British Columbia. Géographie physique et Quaternaire, 50(1), pp.95–102.

Libby, W. F.; Anderson, E. C.; Arnold, J. R., (1949). Age Determination by Radiocarbon Content - World-Wide Assay of Natural Radiocarbon. – Science, 109, pp.227–228.

Libby, W. F., (1967): History of Radiocarbon Dating. In: Radioactive Dating and Methods of Low-level Counting. Proceedings of a Symposium Held in Monaco, 2–10 Mar 1967. International Atomic Energy Agency, Vienna (Austria), pp.3–25.

Licciardi, J. M., Teller, J. T. & Clark, P. U., (1999). Freshwater Routing by the Laurentide Ice Sheet During the Last Deglaciation. In P. U. Clark, R. S. Webb, & L. D. Keigwin, eds. Mechanisms of Global Climate Change at Millennial Time Scales. Washington, DC: American Geophysical Union Geophysical Monograph 112, pp.177–201.

Lund, J. R., (2012). Flood management in California. Water, 4, pp.157–169.

Lydon P. A., (1968). Geology and lahars of the Tuscan Formation, Northern California. in Coats, R. R., Hay, R. L. & Anderson, C. A., eds., Studies in Volcanology, a memoir in honor of Howell Williams. Geological Society of America Memoir, 116, pp.441–475.

M

Mabit, L., Benmansour, M. & Walling, D., (2008). Comparative advantages and limitations of the fallout radionuclides 137Cs, 210Pbex and 7Be for assessing soil erosion and sedimentation. Journal of Environmental Radioactivity, 99(12), pp.1799–1807.

Maher, K., Wooden, J. L., Paces, J. B., Miller, D. M., (2007). 230Th–U dating of surficial deposits using the ion microprobe (SHRIMP-RG): A microstratigraphic perspective. Quaternary International, 166(1), pp.15–28.

Makaske, B., (2001). Anastomosing rivers: a review of their classification, origin and sedimentary products. Earth Science Reviews, 53(3-4), pp.149–196.

Marchand, D. E. & Allwardt, A., (1981). Late Cenozoic stratigraphic units, Northeastern San Joaquin Valley, California. U.S. Geological Survey Bulletin 1470.

Medeiros S. C., Scott C. Hagen, S. C., Weishampel, J. F., (2012): Comparison of floodplain surface roughness parameters derived from land cover data and field measurements. Journal of Hydrology 452-453, pp.139–149.

Mejdahl, V., (1985). Thermoluminescence dating of partially bleached sediments. Nuclear Tracks and Radiation Measurements (1982), 10(4-6), pp.711–715.

Meisel, S., Gerzabek, M. H. & Müller, H. K., (1991). Influence of ploughing on the depth distribution of various radionuclides in the soil. Zeitschrift für Pflanzenernährung und Bodenkunde, 154(2), pp.211–215.

Mertes, L. A. K., (1994). Rates of flood-plain sedimentation on the central Amazon River. Geology, 22, pp.171–174.

Meyer, J., (2013). A Geoarchaeological Overview and Assessment of Northeast California. Cultural Resources Inventory of Caltrans District 2 Rural Conventional Highways: Lassen, Modoc, Plumas, Shasta, Siskiyou, Tehama, and Trinity Counties. Volume 1: Report. Far Western Anthropological Research Group, Inc., Davis. 196 p.

Meyer, J. & Rosenthal, J. S., (2008). A Geoarchaeological Overview and Assessment of Caltrans District 3 Cultural Resources Inventory of Caltrans District 3 Rural Conventional Highways. Far Western Anthropological Research Group, Inc., Davis. 376 p.

Miall, A. D. (2014): Fluvial depositional systems: Springer-Verlag, Berlin. 316 p.

Michalková, M., Piégay, H., Kondolf, G. & Greco, S., (2011). Lateral erosion of the Sacramento River, California (1942 - 1999), and responses of channel and floodplain lake to human influences. Earth Surface Processes and Landforms, 36(2), pp.257–272.

Micheli, E. R. & Larsen, E. W., (2011), River channel cutoff dynamics, Sacramento River, California, USA. River Res. Applic., 27, pp.328–344.

Middelkoop, H. & Asselman, N. E. M., (1998). Spatial variability of floodplain sedimentation at the event scale in the Rhine–Meuse delta, The Netherlands. Earth Surface Processes and Landforms, 23(6), pp.561–573.

Mihailović, A., Vasić, M. V., Todorović, N., Hansman, J. , Vasin, J. & Krmar, M. (2014). Potential factors affecting accumulation of unsupported ^{210}Pb in soil. Radiation Physics and Chemistry, 99. pp.74–78.

Miller, C. D., (1980). Potential Hazards from Future Eruptions in the Vicinity of Mount Shasta Volcano, Northern California. U.S. Geological Survey Bulletin 1503.

Murray, A. S. & Wintle, A. G., (2000). Luminescence dating of quartz using an improved single-aliquot regenerative-dose protocol. Radiation Measurements, 32(1), pp.57–73.

Murray, A. S., & Wintle, A. G., (2003). The single aliquot regenerative dose protocol: potential for improvements in reliability. Radiation Measurements, 37(4), pp.377–381.

N

Nanson, G. & Croke, J., (1992). A genetic classification of floodplains. Geomorphology, 4(6), pp.459–486.

Narayana, Y., Shetty, P.K. & Siddappa, K., (2006). Behavior of ^{210}Po and ^{210}Pb in high background areas of coastal Kerala on the south west coast of India. Applied Radiation and Isotopes, 64, pp.396–401.

Nittrouer, C. A., Sternberg, R. W., Carpenter, R. & Bennett, J. T., (1979). Use of Pb-210 geochronology as a sedimentological tool – application to the Washington continental-shelf. Mar. Geol., 31, pp.297–316.

North Greenland Ice Core Project members (NGCIP-members); Andersen, K. K., Azuma, N., Barnola, J.-M., Bigler, M., Biscaye, P., Caillon, N., Chappellaz, J., Clausen, H. B., Dahl-Jensen, D., Fischer, H., Flückiger, J., Fritzsche, D., Fujii, Y., Goto-Azuma, K., Grønvold, K., Gundestrup, N. S., Hansson, M., Huber, C., Hvidberg, C. S.; Johnsen, S. J., Jonsell, U., Jouzel, J., Kipfstuhl, S., Landais, A., Leuenberger, M., Lorrain, R., Masson-Delmotte, V., Miller, H., Motoyama, H., Narita, H., Popp, T., Rasmussen, S. O., Raynaud, D., Röthlisberger, R., Ruth, U., Samyn, D., Schwander, J., Shoji, H., Andersen, M. L. S., Steffensen, J. P., Stocker, T., Sveinbjörnsdóttir, A. E., Svensson, A.,

Takata, M., Tison, J.-L., Thorsteinsson, Th., Watanabe, O., Wilhelms, F., White, J. W. C., (2004). High-resolution record of Northern Hemisphere climate extending into the last interglacial period. Nature, 431(7005), pp.147–151.

O

Olmsted, F. H. & Davis, G. H., (1961). Geologic Features and Ground-Water Storage of the Sacramento Valley California. U.S. Geological Survey Water-Supply Paper, 1497.

Olson, I. U., (2009). Radiocarbon Dating History: Early Days, Questions, and Problems met, Radiocarbon, 51(1), pp.1–43

Özden, B., Uğur, A., Esetlili, T., Esetlili, B.Ç. & Kurucu, Y., (2013). Assessment of the effects of physical–chemical parameters on ^{210}Po and ^{210}Pb concentrations in cultivated and uncultivated soil from different areas. Geoderma, 192, pp.7–11.

P

Pastre, J. F., Limondin-Lozouet, N., Leroyer, C., Ponel, P., & Fontugne, M., (2003). River system evolution and environmental changes during the Lateglacial in the Paris Basin (France). Quaternary Science Reviews, 22(20), pp.2177–2188.

Peakall, J., Leeder, M., Best, J., Ashworth, P., (2000). River response to lateral ground tilting: a synthesis and some implications for the modelling of alluvial architecture in extensional basins. Basin Research, 12(3-4), pp.413–424.

Pearson, G. W., Pilcher, J. R., Baillie, M. G. L., Corbett, D. M. & Qua, F. (1986) High-precicion C-14 measurement of Irish oaks to show the natural C-14 variations from AD 1840 to 5210 BC. Radiocarbon, 28, pp.911–934.

Penck, A. & Brückner, E., (1909). Die Alpen im Eiszeitalter, Leipzig: Tauchnitz.

Perreault, L. M., Yager, E. M., & Aalto, R., (2012). Application of $^{210}Pb_{ex}$ inventories to measure net hillslope erosion at burned sites. Earth Surface Processes and Landforms, 38 (2), pp.133–145.

Phillips, F. M., Zreda, M. G., Benson, L. V., Plummer, M. A., Elmore, D., Sharma, P., (1996). Chronology for Fluctuations in Late Pleistocene Sierra Nevada Glaciers and Lakes. Science, 274(5288), pp.748–751.

Phillips, J. D., (2009). Avulsion regimes in southeast Texas rivers. Earth Surface Processes and Landforms, 34(1), pp.75–87.

Phillips, J. V., & Ingersoll, T. L. (1998): Verification of roughness coefficients for selected and natural channels in Arizona: U.S. Geological Survey Professional Paper 1584, 77 p.

Phillips, J. V., & Tadayon, S. (2006): Selection of Manning's roughness coefficient for natural and constructed vegetated and non-vegetated channels, and vegetation maintenance plan guidelines for vegetated channels in central Arizona: U.S. Geological Survey Scientific Investigations Report 2006–5108, 41 p.

Porto, P. & Walling, D. E., (2012). Using plot experiments to test the validity of mass balance models employed to estimate soil redistribution rates from ^{137}Cs and $^{210}Pb_{ex}$ measurements. Applied Radiation and Isotopes, 70(10), pp.2451–2459.

Preusser, F., Degering, D., Fuchs, M., Hilgers, A., Kadereit, A., Klasen, N., Krbetschek, M, Richter, D. & Spencer, J. Q., (2008). Luminescence dating: basics, methods and applications. Quaternary Science Journal, 57(1-2), pp.95–149.

PRISM Climate Group, Oregon State University, http://prism.oregonstate.edu, created 30 June 2014.

R

Ralph, F. M., and Dettinger, M. D., (2011). Storms, floods, and the science of atmospheric rivers. Eos, Transactions American Geophysical Union, 92(32), pp.265–266

Reimer P. J., Baillie M. G. L., Bard E., Bayliss A., Beck J. W., Bertrand, C. J. H., Blackwell, P. G., Buck, C. E., Burr, G. S., Cutler, K. B., Damon, P. E., Edwards, R. L., Fairbanks, R. G., Friedrich, M., Guilderson, T. P., Hogg, A. G., Hughen, K. A., Kromer, B., McCormac, G., Manning, S., Ramsey, C. B., Reimer, R. W., Remmele, S., Southon, J. R., Stuiver, M., Talamo, S., Taylor, F. W., van der Plicht, J., Weyhenmeyer, C. E., (2004). IntCal04 Terrestrial Radiocarbon Age Calibration, 0–26 cal kyr BP. Radiocarbon, 46(3), pp.1029-1058

Reimer P. J., Baillie M. G. L., Bard E., Bayliss A., Beck J. W., Blackwell P. G., Bronk Ramsey C., Buck C. E., Burr G. S., Edwards R. L., Friedrich M., Grootes P. M., Guilderson T. P., Hajdas I., Heaton T. J., Hogg A. G., Hughen K. A., Kaiser K. F., Kromer B., McCormac F. G., Manning S. W., Reimer R. W., Richards D. A., Southon J. R., Talamo S., Turney C. S. M., van der Plicht J., Weyhenmeyer C. E., (2009). IntCal09 and Marine09 radiocarbon age calibration curves, 0–50,000 years cal BP. Radiocarbon, 51(4), pp.1111–1150.

Reimer P. J., Bard E., Bayliss A., Beck J. W., Blackwell P. G., Bronk Ramsey C., Buck C. E., Cheng H., Edwards R. L., Friedrich M., Grootes P. M., Guilderson T. P., Haflidason H., Hajdas I., Hatté C., Heaton T. J., Hoffmann D. L., Hogg A. G., Hughen K. A., Kaiser K. F., Kromer B., Manning S. W., Niu M., Reimer R. W., Richards D. A., Scott E. M., Southon J. R., Staff R. A., Turney C. S. M., van der Plicht J., (2013). IntCal13 and Marine13 radiocarbon age calibration curves 0–50,000 years cal BP. Radiocarbon, 55(4), pp.1869–1887.

Renfrew, C (1973): Before Civilisation: The Radiocarbon Revolution and Prehistoric Europe, London: Jonathan Cape.

Resner, K., Yoo, K., Hale, C., Aufdenkampe, A., Blum, A., & Sebestyen, S., (2011). Elemental and mineralogical changes in soils due to bioturbation along an earthworm invasion chronosequence in Northern Minnesota. Applied Geochemistry, 26(S), pp.127–131.

Rittenour, T. M., (2008). Luminescence dating of fluvial deposits: applications to geomorphic, palaeoseismic and archaeological research. Boreas, 37(4), pp.613–635.

Rittenour, T. M., Blum, M. D. & Goble, R. J., (2007). Fluvial evolution of the lower Mississippi River valley during the last 100 ky glacial cycle: Response

to glaciation and sea-level change. Geological Society of America Bulletin, 119(5-6), pp.586–608.

Rittenour, T. M., Goble, R. J. & Blum, M. D., (2005). Development of an OSL chronology for Late Pleistocene channel belts in the lower Mississippi valley, USA. Quaternary Science Reviews, 24(23-24), pp.2539–2554.

Robertson, K. G., (1987). Paleochannels and recent evolution of the Sacramento River, California. Davis, California: Unpublished Masters Thesis, University of California, Davis.

Rosenbaum, J. G. & Reynolds, R. L., (2004a). Basis for paleoenvironmental interpretation of magnetic properties of sediment from Upper Klamath Lake (Oregon): effects of weathering and mineralogical sorting. Journal of Paleolimnology, 31(2), pp.253–265.

Rosenbaum, J. G. & Reynolds, R. L., (2004b). Record of Late Pleistocene glaciation and deglaciation in the southern Cascade Range. II. Flux of glacial flour in a sediment core from Upper Klamath Lake, Oregon. Journal of Paleolimnology, 31(2), pp.235–252.

Rosgen, David L., (1994): A classification of natural rivers. Catena (22), pp.169–199.

Rowland, J. C., Lepper, K., Dietrich, W. E., Wilson, C. J., & Sheldon, R., (2005). Tie channel sedimentation rates, oxbow formation age and channel migration rate from optically stimulated luminescence (OSL) analysis of floodplain deposits. Earth Surface Processes and Landforms, 30(9), pp.1161–1179.

S

sacramentoriver.org, (http://www.sacramentoriver.org/forum/index.php?id=data)

San Miguel, E.G., Bolivar, J.P. & Garcia-Tenorio, R., (2004). Vertical distribution of Th-isotope ratios, ^{210}Pb, ^{226}Ra and ^{137}Cs in sediment cores from an estuary affected by anthropogenic releases. Sci. Total Environ. 318, pp.143–157.

Saucier, R. T., (1994). Geomorphology and Quaternary Geologic History of the lower Mississippi Valley. Vicksburg: Mississippi River Commission.

Schumm, S. A., (1981). Evolution and response of the fluvial system, sedimentologic implications. Society of Economic Paleontologists and Mineralogists, Special Publication, 1, pp.19–29.

seamless.usgs.gov, now redirected to http://nationalmap.gov/viewer.html

Shimazaki, H., & Shinomoto, S. (2010). Kernel bandwidth optimization in spike rate estimation. Journal of computational neuroscience, 29(1-2), pp.171–182.

Simpson, R. G., (1978). Flood hydrology of Butte Basin, 1973-77 water years, Sacramento Valley, California, U. S. Geological Survey Water-Resources Investigations 78-86.

Singer, M. B., (2007). The Influence of major dams on the hydrology through the drainage network of the Sacramento River basin, California. River Research and Applications, 22, pp.55–72.

Singer, M. B., (2008). Downstream patterns of bed material grain size in a large, lowland alluvial river subject to low sediment supply. Water Resources Research, 44(12), W12202.

Singer, M. B. (2015-In Press), Fluvial responses to management along the Sacramento River, California, USA: Transience v. Persistence, in Hudson, P.F. & H. Middlekoop (eds.), Geomorphic Approaches to Integrated Floodplain Management of Lowland Fluvial Systems in North America and Europe, Springer.

Singer, M. B. & Aalto, R. E., (2009). Floodplain development in an engineered setting. Earth Surface Processes and Landforms, 34(2), pp.291–304.

Singer, M. B., Aalto, R. E. & James, L. A., (2008). Status of the lower Sacramento Valley flood-control system within the context of its natural geomorphic setting. Natural Hazards Review, 9, pp.104–115.

Singer, M. B. & Dunne, T., (2001). Identifying eroding and depositional reaches of valley by analysis of suspended sediment transport in the Sacramento River, California. Water Resources Research, 40, W03302.

Singer, M. B. & Dunne, T., (2004). An empirical-stochastic, event-based model for simulating inflow from a tributary network: theoretical framework and application to the Sacramento River basin, California. Water Resources Research 40: W075066.

Slingerland, R. & Smith, N. D., (2004). River Avulsions and their Deposits. Annual Review of Earth and Planetary Sciences, 32(1), pp.257–285.

Smith, N. D., Cross, T. A., Dufficy, J. P., Clough, S. R., (1989). Anatomy of an avulsion. Sedimentology, 36(1), pp.1–23.

Steele, W., C., (1980). Quaternary stream terraces in the northwestern Sacramento Valley, Glenn, Tehama, and Shasta Counties, California. U. S. Geological Survey Open-File Report 80-512. 167 p.

Stuiver M., Reimer P. J., Bard E., Beck J. W., Burr G. S., Hughen K. A., Kromer B., McCormac G., van der Plicht J., Spurk M., (1998). IntCal98 radiocarbon age calibration, 24,000–0 cal BP. Radiocarbon, 40(3), pp.1041–83.

Stuiver, M., Reimer, P. J., and Reimer, R. W., (2005). CALIB v. 6.1.0. [WWW program and documentation]

Sullivan, D. G., (1982). Prehistoric Flooding in the Sacramento Valley: Stratigraphic Evidence from Little Packer Lake, Glenn County, California. Unpublished Masters Thesis, University of California, Berkeley.

Swanson, K. M., Watson, E., Aalto, R. E., Lauer, J., Bera, M. T., Marshall, A., Taylor, M. P., Apte, S. C. & Dietrich, W. E., (2008). Sediment load and floodplain deposition rates: Comparison of the Fly and Strickland rivers, Papua New Guinea. Journal of Geophysical Research, 113, F01S03.

T

Tanton, L. T. E., Grove, T. L. & Donnelly-Nolan, J., (2001). Hot, shallow mantle melting under the Cascades volcanic arc. Geology, 29(7), pp.631–634.

Tebbens, L. A., Veldkamp, A., Westerhoff, W. & Kroonenberg, S. B., (1999). Fluvial incision and channel downcutting as a response to Late-glacial and Early Holocene climate change: the lower reach of the River Meuse (Maas), The Netherlands. Journal of Quaternary Science, 14(1), pp.59–75.

Thonon, I., Middelkoop, H. & Van der Perk, M., (2007). The influence of floodplain morphology and river works on spatial patterns of overbank deposition. Netherlands Journal of Geosciences, 86(1), pp.63–75.

Törnqvist, T. E. & Bridge, J. S., (2002). Spatial variation of overbank aggradation rate and its influence on avulsion frequency. Sedimentology, 49(5), pp.891–905.

U

U.S. Army Corps of Engineers (USACE), (1998). Post-Flood Assessment for 1983, 1986, 1995, and 1997 Central Valley, California, Sacramento, California.

U.S. Geological Survey and California Division of Mines and Geology (USGS), (1966). Geologic map of California. U.S. Geological Survey Miscellaneous Geologic Investigations Map, (1:2,500,000).

V

Vaaramaa, K., Aro, L., Solatie, D. & Lehto, J., (2010). Distribution of ^{210}Pb and ^{210}Po in boreal forest soil. Sci. Total Environ. 408, pp.6165–6171.

Vandenberghe, J., (1995). Timescales, climate and river development. Quaternary Science Reviews, 14(6), pp.631–638.

Vandenberghe, J., (2003). Climate forcing of fluvial system development: an evolution of ideas. Quaternary Science Reviews, 22(20), pp.2053–2060.

Vandenberghe, J., (2008). The fluvial cycle at cold-warm-cold transitions in lowland regions: A refinement of theory. Geomorphology, 98(3-4), pp.275–284.

W

Wagner, G. A., (1998). Age Determination of Young Rocks and Artifacts: physical and chemical clocks in Quaternary geology and archaeology. Springer. Heidelberg, 460 p.

Wahrhaftig, C. & Birman, J. H., (1965). The Quaternary of the Pacific mountain system in California. In: Wright, H. E., Jr. & Frey D. G., eds. The Quaternary of the United States. Princeton University Press, Princeton, pp.299–340.

Wakiyama, Y., Onda, Y., Mizugaki, S., Asai, H., & Hiramatsu, S., (2010). Soil erosion rates on forested mountain hillslopes estimated using ^{137}Cs and $^{210}Pb_{ex}$. Geoderma, 159(1-2), pp.39–52.

Walker, Mike J. C., (2005): Quaternary Dating Methods. John Wiley & Sons, Chicester. 286 p.

Walling, D. E., (1999): Linking land use, erosion and sediment yields in river basins.

Walling, D. E., (2005): Tracing suspended sediment sources in catchments and river systems. Science of the total environment. 344, pp.159–184.

Walling, D. E., Quine, T. A. & He, Q. (1992): Investigating contemporary rates of floodplain sedimentation. In: Carling, P. A. & Petts, G. E., eds. Lowland Floodplain Rivers: Geomorphological Perspectives. John Wiley & Sons, Chichester, pp.165–184

Walling, D. E. & He, Q., (1994). Rates of overbank sedimentation on the flood plains of several British rivers during the past 100 years. IAHS Publications-Series of Proceedings and Reports-Intern Assoc Hydrological Sciences, 224, pp.203–210.

Walling, D. E. & He, Q., (1997). Investigating spatial patterns of overbank sedimentation on river floodplains. Water, Air, and Soil Pollution, 99, pp.9–20.

Walling, D. E. & He, Q., (1998). The spatial variability of overbank sedimentation on river floodplains. Geomorphology, 24(2), pp.209–223.

Walling, D. E., Collins, A. L. & Sichingabula, H. M., (2003). Using unsupported lead-210 measurements to investigate soil erosion and sediment delivery in a small Zambian catchment. Geomorphology, 52(3-4), pp.193–213.

Water Engineering & Technology Inc. (WET), (1990). Geomorphic Analysis of Sacramento River Geomorphic Analysis of Reach from Colusa to Red Bluff Diversion Dam, River Mile 143 to River Mile 243. Final Phase II Report, prepared for the U.S. Army Corps of Engineers, Sacramento District.

Water Engineering & Technology Inc. (WET), (1994). Geomorphic Analysis of the Sacramento River. Geomorphic Analysis of Butte Basin Reach River Mile 174 to River Mile 194. Final Phase I Report, prepared for the U.S Army Corps of Engineers.

Weaver, R. L., (1962) Meteorology of Hydrologically Critical Storms in California; U.S. Department of Commerce Hydrometeorology Report No. 37; Department of Commerce Hydrometeorology: Washington, DC, 207 p.

Weninger, B., Jöris, O., (2009). A ^{14}C age calibration curve for the last 60 ka: the Greenland-Hulu U/Th timescale and its impact on understanding the Middle to Upper Paleolithic transition in Western Eurasia. Journal of Human Evolution, 55(5), pp.772–781

Wessa, P. (2015), Free Statistics Software, Office for Research Development and Education, version 1.1.23-r7, URL:http://www.wessa.net/

Worona, M. A. & Whitlock, C., (1995). Late quaternary vegetation and climate history near Little Lake, central Coast Range, Oregon. Geological Society of America Bulletin, 107(7), pp.867–876.

Y

Yukihara, E. G. & McKeever S. W. S., (2011). Optically stimulated luminescence: fundamentals and applications. John Wiley & Sons Ltd. Chichester. 362 p.

Z

Zaborska, A., Carroll, J., Papucci, C., & Pempkowiak, J., (2007). Intercomparison of alpha and gamma spectrometry techniques used in 210 Pb geochronology. Journal of Environmental Radioactivity, 93(1), pp.38–50.

Zolitschka, B. & Negendank, J. F. W., (1998). A high resolution record of Holocene palaeohydrological changes from Lake Holzmaar (Germany). In: Frenzel, B. (Ed.), Palaeohydrology as reflected in lake-level changes as climatic evidence for Holocene times: European Palaeoclimate and Man, 17, pp.37–52